ΕΘΝΙΚΟ ΜΕΤΣΟΒΙΟ ΠΟΛΥΤΕΧΝΕΙΟ

ΣΧΟΛΗ ΕΦΑΡΜΟΣΜΕΝΩΝ ΜΑΘΗΜΑΤΙΚΩΝ
ΚΑΙ ΦΥΣΙΚΩΝ ΕΠΙΣΤΗΜΩΝ

ΑΥΘΟΡΜΗΤΟ ΚΑΙ ΤΑΥΤΟΧΡΟΝΟ ΣΠΑΣΙΜΟ ΤΗΣ ΕΣΩΤΕΡΙΚΗΣ ΣΥΜΜΕΤΡΙΑΣ ΚΑΙ ΤΗΣ ΣΥΜΜΕΤΡΙΑΣ ΚΛΙΜΑΚΑΣ ΣΕ ΕΝΕΡΓΕΣ ΘΕΩΡΙΕΣ ΠΕΔΙΟΥ, ΠΡΟΕΡΧΟΜΕΝΕΣ ΑΠΟ ΜΙΑ ΕΞΤΡΑ ΔΙΑΣΤΑΣΗ, ΕΝΙΣΧΥΜΕΝΕΣ ΜΕ ΤΕΛΕΣΤΕΣ ΔΙΑΣΤΑΣΗΣ ΜΕΓΑΛΥΤΕΡΗΣ ΤΟΥ ΤΕΣΣΕΡΑ:

ΜΙΑ ΝΕΑ ΠΡΟΣΕΓΓΙΣΗ ΣΤΟ ΠΡΟΒΛΗΜΑ ΤΗΣ ΙΕΡΑΡΧΙΑΣ

ΔΙΔΑΚΤΟΡΙΚΗ ΔΙΑΤΡΙΒΗ

ΦΩΤΙΟΥ Λ. ΚΟΥΤΡΟΥΛΗ

ΕΠΙΒΛΕΠΩΝ:

ΝΙΚΟΛΑΟΣ ΗΡΓΕΣ

Αναπληρωτής Καθηγητής
ΕΜΠ

Αθήνα, Ιούνιος 2021

ΕΘΝΙΚΟ ΜΕΤΣΟΒΙΟ ΠΟΛΥΤΕΧΝΕΙΟ

ΣΧΟΛΗ ΕΦΑΡΜΟΣΜΕΝΩΝ ΜΑΘΗΜΑΤΙΚΩΝ
ΚΑΙ ΦΥΣΙΚΩΝ ΕΠΙΣΤΗΜΩΝ

ΑΥΘΟΡΜΗΤΟ ΚΑΙ ΤΑΥΤΟΧΡΟΝΟ ΣΠΑΣΙΜΟ ΤΗΣ ΕΣΩΤΕΡΙΚΗΣ ΣΥΜΜΕΤΡΙΑΣ ΚΑΙ ΤΗΣ ΣΥΜΜΕΤΡΙΑΣ ΚΛΙΜΑΚΑΣ ΣΕ ΕΝΕΡΓΕΣ ΘΕΩΡΙΕΣ ΠΕΔΙΟΥ, ΠΡΟΕΡΧΟΜΕΝΕΣ ΑΠΟ ΜΙΑ ΕΞΤΡΑ ΔΙΑΣΤΑΣΗ, ΕΝΙΣΧΥΜΕΝΕΣ ΜΕ ΤΕΛΕΣΤΕΣ ΔΙΑΣΤΑΣΗΣ ΜΕΓΑΛΥΤΕΡΗΣ ΤΟΥ ΤΕΣΣΕΡΑ:

ΜΙΑ ΝΕΑ ΠΡΟΣΕΓΓΙΣΗ ΣΤΟ ΠΡΟΒΛΗΜΑ ΤΗΣ ΙΕΡΑΡΧΙΑΣ

ΔΙΔΑΚΤΟΡΙΚΗ ΔΙΑΤΡΙΒΗ

ΦΩΤΙΟΥ Λ. ΚΟΥΤΡΟΥΛΗ

Διπλωματούχου Τμήματος Φυσικής Πανεπιστημίου
Πατρών

ΤΡΙΜΕΛΗΣ ΣΥΜΒΟΥΛΕΥΤΙΚΗ ΕΠΙΤΡΟΠΗ:

1. Νικόλαος Ήργες, Αν. Καθ. ΕΜΠ (Επιβλέπων)
2. Αλέξανδρος Κεχαγιάς, Καθ. ΕΜΠ
3. Claudio Coriano, Αν. Καθ. Παν. Salento, Lecce

ΕΠΤΑΜΕΛΗΣ ΣΥΜΒΟΥΛΕΥΤΙΚΗ ΕΠΙΤΡΟΠΗ:

1. Νικόλαος Ήργες, Αν. Καθ. ΕΜΠ (Επιβλέπων)
2. Αλέξανδρος Κεχαγιάς, Καθ. ΕΜΠ
3. Claudio Coriano, Αν. Καθ. Παν. Salento, Lecce
4. Κωνσταντίνος Φαράκος, Καθ. ΕΜΠ
5. Γεώργιος Κουτσούμπας, Καθ. ΕΜΠ
6. Νικόλαος Τράκας, Καθ. ΕΜΠ
7. Χριστόφορος Κούβαρης, Καθ. ΕΜΠ

Αθήνα, Ιούνιος 2021

ΛΙΣΤΑ ΔΗΜΟΣΙΕΥΣΕΩΝ

Τα Κεφάλαια της παρούσας διδακτορικής διατριβής προέρχονται από τα ακόλουθα ερευνητικά/δημοσιευμένα πρότζεκτς:

- Nikos Irges and Fotis Koutroulis, *RG flows in Non-Perturbative Gauge-Higgs Unification II. Effective action for the Higgs phase near the quantum phase transition*, Eur. Phys. J. C **81** (2021) 2, 187

- Nikos Irges, Fotis Koutroulis and Dimosthenis Theofilopoulos, *The conformal N-point scalar correlator in coordinate space*, arXiv: 2001.07171 [hep-th]

- Nikos Irges and Fotis Koutroulis, *On RG flows in Generalized Effective Field Theory*, Nucl. Phys. B **950** (2020) 114833

- Nikos Irges and Fotis Koutroulis, *Symmetry breaking and renormalization group flows with higher dimensional operators*, Phys. Rev. D **100** (2019) 6, 065004

- Nikos Irges and Fotis Koutroulis, *RG flows in Non-Perturbative Gauge-Higgs Unification I*, Nucl. Phys. B **937** (2018) 135-195

- Nikos Irges and Fotis Koutroulis, *Renormalization of the Abelian–Higgs model in the Rξ and Unitary gauges and the physicality of its scalar potential*, Nucl. Phys. B **924** (2017) 178-278

ΠΕΡΙΛΗΨΗ

Πολύ πριν από την πρόσφατη ανακάλυψη του μποζονίου Higgs, ο συσχετιζόμενος μηχανισμός ήταν υπό συνεχή διερεύνηση λόγω μιας βασικής θεωρητικής ασυνέπειας που φαινόταν να έχει, γνωστή ως το πρόβλημα της ιεραρχίας του Higgs. Η ασυνέπεια αυτή αναφέρεται στην ευαισθησία της μάζας του μποζονίου Higgs στις υπεριώδεις κβαντικές συνεισφορές που έχει ως αποτέλεσμα την ανάγκη ενός πολύ ισχυρού συντονισμού των φυσικών παραμέτρων προκειμένου να παραμένει η συγκεκριμένη μάζα σχεδόν ανεπηρέαστη από τις κβαντικές διορθώσεις. Παραδοσιακά, οι πιο βιώσιμες προτάσεις για την επίλυση του προβλήματος συντονισμού της μάζας του μποζονίου Higgs είναι η εισαγωγή νέων συμμετριών, όπως η υπερσυμμετρία, που προστατεύουν τη αντίστοιχη μάζα από τις διορθώσεις UV ή την εισαγωγή επιπλέον χωρικών διαστάσεων, μαζί με τα αποτελέσματα της συμπαγοποίησης (όπως οι Kaluza-Klein καταστάσεις, …, κλπ), οι οποίες καθιστούν τις τετραγωνικές αποκλίσεις λιγότερο επιβλαβείς. Κατά τη διάρκεια των τελευταίων ετών έχουν προταθεί πολλές λύσεις προς αυτές τις κατευθύνσεις, ωστόσο καμία από αυτές δεν επιβεβαιώθηκε πειραματικά. Σε αυτή τη διατριβή προτείνουμε μια νέα λύση στο πρόβλημα της ιεραρχίας του Higgs, κατασκευάζοντας ένα μοντέλο στο πλαίσιο ενός πενταδιάστατου χωροχρόνου. Τα βασικά χαρακτηριστικά που διακρίνουν την προσέγγισή μας από τις άλλες του αντίστοιχου είδους είναι ότι στην περίπτωσή μας το σύστημα υφίσταται διαστατική μείωση μέσω εντοπιότητας όπως επίσης και το γεγονός ότι υπάρχει μη-διαταρακτική πληροφορία που κληρονομεί το συνεχές μας μοντέλο περιορίζοντας σε μεγάλο βαθμό τη συσχετιζόμενη φυσική. Συγκεκριμένα, το κύριο συστατικό της λύσης μας είναι η κατασκευή μιας 4-d ενεργής δράσης στο συνεχές η οποία προέρχεται από ένα συγκεκριμένο, έξτρα-διαστατικό, μη-διαταρακτικό, μοντέλο με πολύ ειδικές οριακές συνθήκες και με τελεστές διάστασης μεγαλύτερης του τέσσερα. Αυτό είναι το επονομαζόμενο και ως Μοντέλο Μη-Διαταρακτική Ενοποίησης Βαθμίδας-Higgs, ένα 5-d και $SU(2)$ μοντέλο που αναπτύχθηκε στο πλέγμα με συνοριακές συνθήκες orbifold που οδηγούν σε ένα τετραδιάστατο σύνορο μειωμένης συμμετρίας βαθμίδας. Στο τελευταίο, στο συνεχές, ζει ένα μοντέλο τύπου Abelian Higgs το οποίο όμως φέρει επιπλέον περιορισμούς λόγω της μη-διαταρακτικής προέλευσής του, το αποτέλεσμα των οποίων καθιστά σχεδόν αμελητέο το πρόβλημα του συντονισμού της μάζας του μποζονίου Higgs. Ένα τέτοιο μοντέλο στο σύνορο αποτελεί μια ιδανική περίπτωση για το σκοπό μας, δεδομένου ότι διαθέτει ένα μη-τετριμμένο ενεργό δυναμικό, ευαίσθητο στις διορθώσεις UV με την πρώτη ματιά, ωστόσο απαλλαγμένο από την πολυπλοκότητα της συνεισφορας των υψηλότερων ομάδων βαθμίδας που φέρει το Καθιερωμένο Πρότυπο των σωματιδίων. Καθοριστικό ρόλο για την κατασκευή του μοντέλου μας παίζει η φυσικότητα του τετραδιάστατου δυναμικού, η μη-τετριμμένη σύνδεση μεταξύ συνόρου και bulk όπως επίσης και η επίδραση των τελεστών διάστασης μεγαλύτερης του τέσσερα. Επομένως, το πρώτο μας βήμα είναι να ασχοληθούμε με το συνηθισμένο μοντέλο Abelian-Higgs σε τέσσερις χωροχρονικές διαστάσεις όπου αποδεικνύουμε ότι το αντίστοιχο ενεργό δυναμικό είναι μια αναλλοίωτη, εξ ου και φυσική, κάτω από μετασχηματισμούς βαθμίδας ποσότητα που δίνει συνεπή αποτελέσματα κάτω από διαφορετικές επιλογές βαθμίδας. Για το δεύτερο βήμα μας επικεντρωνόμαστε στο Μοντέλο Μη-Διαταρακτική Ενοποίησης Βαθμίδας-Higgs με την υπόθεση ότι bulk και το σύνορο έχουν αποσυνδεθεί εντελώς. Παρόλο που αυτή η υπόθεση δίνει συνεπή αποτελέσματα, δεν λύνει το πρόβλημα της ιεραρχίας στην μάζα του μποζονίου Higgs και η ανάγκη να εξεταστεί η σύνδεση μεταξύ bulk και συνόρου καθίσταται επείγουσα. Ως συνέπεια αυτού είναι ότι η εισαγωγή τελεστών μεγαλύτερης διάστασης είναι αναπόφευκτη. Επομένως, πριν επιστρέψουμε στο αρχικό μας μοντέλο, εξετάζουμε το ενεργό δυναμικό ενός πραγματικού και βαθμωτού πεδίου ενισχυμένου με τελεστές διαστάσεις έξι και οκτώ. Ως εκ τούτου δείχνουμε ποιες είναι οι διάφορες περιπτώσεις κατά τις οποίες ένα τέτοιο δυναμικό είναι σταθερό και διακατέχεται από αυθόρμητο και ταυτόχρονο σπάσιμο της εσωτερικής του συμμετρίας και της συμμετρίας κλίμακας καθώς φθάνει σε ένα αλληλεπιδρών ή ένα Γκαουσιανό σταθερό σημείο. Τέλος, με βάση τα προηγούμενα συμπεράσματα στο χέρι μας, επιστρέφουμε στο πενταδιάστατο μοντέλο λαμβάνοντας υπόψιν μας τη σύνδεση μεταξύ bulk και συνόρου η οποία παράγει στο 4-d σύνορο, στο συνεχές, μια ενεργό δράση ενισχυμένη με τελεστές διάστασης μεγαλύτερης του τέσσερα. Οι τελευταίοι είναι κβαντικής φύσεως και περιλαμβάνουν μη-διαταρακτική πληροφορία που οδηγεί σε μια κβαντική, πρώτης τάξης, αλλαγή φάσης η οποία διαχωρίζει τη φάση Higgs από την Υβριδική φάση. Η ροή της Ομάδας Επανακανονικοποίησης (ΟΕ) που ξεκινάει από τη μία φάση περιορίζει ισχυρά τη ροή της ΟΕ που ξεκινά από την άλλη και φτάνουν ταυτόχρονα στη αλλαγή φάσης πρώτης τάξης στο UV. Κάτω από αυτές τις συνθήκες, η ενεργός δράση στο σύνορο αποκτά μια πεπερασμένη κλίμακα αποκοπής η οποία είναι πολύ χαμηλή και ως αποτέλεσμα ο συντονισμός της μάζας του βαθμωτού πεδίου είναι σχεδόν αμελητέος.

ABSTRACT

Way before the very recent discovery of the Higgs boson the associated mechanism was under speculation due to a theoretical inconsistency, the well known Higgs hierarchy problem. The inconsistency refers to the sensitivity of the Higgs mass to the ultra violet contributions which results in the need of a very strong fine tuning of the physical parameters in order to leave the mass almost unaffected by the quantum corrections. Traditionally, the most viable proposals in order to solve the Higgs mass fine-tuning problem is the introduction of new symmetries, like supersymmetry, which protect the Higgs mass from the UV corrections or the introduction of extra spacial dimensions, along with their compactification effects (Kaluza-Klein states,..., etc), which make the quadratic divergencies less severe. Many solutions towards these directions have been proposed during the past years, however, none of them has given a confirmation signal. In this dissertation we propose a novel solution to the Higgs hierarchy problem constructing a model under the framework of a five-dimensional spacetime. The main features that distinguish our approach from the others of the sort is that in our case the system undergoes dimensional reduction through localization and the fact that there is non-perturbative information inherited in our continuum model which highly constrains the associated physics. In particular, the main ingredient of our solution is the construction of a 4-d continuum effective action which originates from a specific extra dimensional, non-perturbative, model with very special boundary conditions and higher than four dimensional operators. This is the so called Non-Perturbative Gauge Higgs Unification model, an $SU(2)$ and 5-d model developed on the lattice with orbifold boundary conditions which lead to a 4-d boundary of reduced gauge symmetry. On the latter, at the continuum, lives a kind of an Abelian Higgs model which possesses extra constraints due to its non-perturbative origin whose effect renders the Higgs mass fine-tuning problem almost negligible. Such a boundary model is an ideal case for our purpose since it possesses a non-trivial effective potential, sensitive to the UV corrections at first glance and yet relieved of the complexity of the Standard Model's higher gauge group contributions. Crucial features for the construction of our model is the physicality of the 4-d potential, the non-trivial connection between boundary and bulk and the effect of the higher than four dimensional operators Therefore, our first step is to deal with the usual Abelian Higgs model in four spacetime dimensions where we prove that the associated effective potential is a gauge invariant, hence physical, quantity which gives consistent results under different gauge choices. For our second step we focus on the Non-Perturbative Gauge Higgs Unification model under the assumption that bulk and boundary are completely disconnected. Even though this hypothesis gives consistent results, does not solve the fine tuning problem and the need to consider a connection between bulk and boundary becomes urgent. A consequence of this is that the insertion of higher dimensional operators is unavoidable. Therefore, before going back to our original model we examine the effective potential of a real scalar field enhanced with dimension six and eight operators. What we show is the various cases under which such a potential is both stable and exhibits spontaneous and simultaneous breaking of its internal and scale symmetry as it reaches an interacting or a Gaussian fixed point. Finally, with these advances in our hand we turn back to the 5-d orbifold model and take into account the bulk-boundary connection which produces at the 4-d boundary an effective continuum action enhanced with higher than four dimensional operators. The latter are of quantum nature and include non-perturbative information related to a first order and quantum phase transition which separates the Higgs phase from the Hybrid, layered, phase. The RG flow starting from the one phase constrains the RG flow which starts from the other and they reach simultaneously the first order phase transition at the UV. Under these circumstances the boundary effective action acquires a finite cut-off that is very low and the fine tuning of the scalar mass is rather mild.

ΑΦΙΕΡΩΣΗ

Στην οικογένεια μου (υπό την πιο ευρεία έννοια)

ΕΥΧΑΡΙΣΤΙΕΣ

Το μονοπάτι που πρέπει να ακολουθήσει κάποιος προκειμένου να κινείται πάνω στον επιστημονικό χάρτη είναι κατασκευασμένο από προσωπική αναζήτηση και προσπάθεια, καθώς επίσης και από ομαδική εργασία και εμπιστοσύνη στους κατάλληλους συνεργάτες. Δεδομένου ότι επέλεξα να ακολουθήσω αυτό το μονοπάτι ήδη ως μεταπτυχιακός φοιτητής, θεώρησα τον εαυτό μου πραγματικά τυχερό επειδή περιβαλλόταν από λαμπρούς δασκάλους, συναδέλφους και φίλους αλλά και λόγω της υποστήριξης από την οικογένειά μου καθόλη την διάρκεια των σπουδών μου. Φυσικά, η πραγματικότητα είναι ότι η παρούσα διατριβή δεν θα είχε ολοκληρωθεί χωρίς τη βοήθεια αυτής της ομάδας ανθρώπων και, επομένως, αυτή είναι μια μεγάλη ευκαιρία να τους ευχαριστήσω όλους.

Επιτρέψτε μου να ξεκινήσω ευχαριστώντας τον επιβλέπων καθηγητή μου, τον Αναπλ. Καθηγητή Νίκο Ήργε. Χωρίς αμφιβολία εάν δεν ήταν η ανεκτίμητη βοήθειά του, τόσο για την επιστημονική όσο και για την προσωπική μου ζωή, η ποιότητα της έρευνας μου δεν θα ήταν η ίδια. Κατά τη διάρκεια των μεταπτυχιακών μου σπουδών απέκτησα μια βαθιά κατανόηση για την Κβαντική Θεωρία Πεδίου λόγω του τρόπου με τον οποίο δίδαξε το μάθημα ενώ, όντας διδακτορικός φοιτητής υπό την επίβλεψη του εκτίμησα πραγματικά τις βαθιές του γνώσεις, τη σαφήνεια της σκέψης του και την αποφασιστικότητά με την οποία δούλευε πάνω σε μερικά από τα πιο βασικά προβλήματα της Θεωρητικής Φυσικής Υψηλών Ενεργειών. Όλα αυτά τα χαρακτηρίστηκα του έγιναν μια σταθερή πηγή έμπνευσης για μένα. Θα ήταν αδύνατο να μην αναφέρω την εκτίμησή μου για την προθυμία του να ακούσει υπομονετικά τις σκέψεις και τις ιδέες μου, παρόλο που μερικές φορές ήταν ελλιπείς σε συνέπεια. Θα ήθελα πραγματικά να τον ευχαριστήσω για την προθυμία του να αφιερώσει πολλές ώρες συζητώντας μαζί μου για τη φυσική, την επιστημονική ζωή γενικά και την καθημερινή ζωή, καθώς και για να μου δώσει πολύτιμες συμβουλές. Το γεγονός ότι ήταν αυστηρός μαζί μου και πέρασε πολύ χρόνο διορθώνοντας τα όποια λάθη μου, με βοήθησε να διατηρηθώ στον σωστό επιστημονικά δρόμο κατά τη διάρκεια των διδακτορικών μου σπουδών και είμαι πραγματικά ευγνώμων για αυτό. Τέλος, θαύμαζα ιδιαίτερα την επιμονή του να παραμένει επιστημονικά ακριβής και συνεπής κάθε φορά που έχουμε ένα ερευνητικό έργο στα χέρια μας, καθώς και την προθυμία του να ασχοληθεί με λιγότερο οικείους αλλά συνάμα πολύ συναρπαστικούς τομείς έρευνας. Τα ανωτέρω έπαιξαν καθοριστικό ρόλο στη δημιουργία του επιστημονικού μου χαρακτήρα και σίγουρα θα με ακολουθούν καθώς συνεχίζω την ερευνητική μου καριέρα.

Ο κατάλογος των ανθρώπων στους οποίους είμαι πραγματικά ευγνώμων συνεχίζεται με τον καθηγητή Αλέξανδρο Κεχαγιά, τον Αναπλ. Καθηγητή Κωνσταντίνο Αναγνωστόπουλο και τον Αναπλ. Καθηγητή Claudio Coriano. Πρόσφατα, αφού το διδακτορικό μου τελείωσε ουσιαστικά, σταμάτησα για λίγο την έρευνά μου πάνω στην σωματιδιακή φυσική για να ασχοληθώ με το πεδίο της Κβαντικής Κοσμολογίας. Τότε, ο καθηγητής Αλέξανδρος Κεχαγιάς ήταν περισσότερο από πρόθυμος να συζητήσει μαζί μου για τις βασικές ιδέες του πεδίου αυτού κάτι που βελτίωσε κατα πολύ την κατανόησή μου, οπότε θα ήθελα να τον ευχαριστήσω για τον χρόνο και τις συμβουλές του. Κατά τη διάρκεια των πρώτων μου βημάτων ως μεταπτυχιακός φοιτητής, θεώρησα τον εαυτό μου αρκετά τυχερό να παρακολουθήσω σπουδαίες διαλέξεις πάνω στην Κβαντική Θεωρία Πεδίου από τον Αναπλ. Καθηγητή Κωνσταντίνο Αναγνωστόπουλο οι οποίες με βοήθησαν να εμβαθύνω τις γνώσεις μου πάνω στο θέμα και γι 'αυτό τον ευχαριστώ πολύ. Όταν έφτασε η ώρα να υποβάλω αιτήσεις για να συνεχίσω στον χώρο ως μεταδιδάκτορας, ζήτησα από τον Αλέξανδρο Κεχαγιά και τον Κωνσταντίνο Αναγνωστόπουλο να γράψουν μια συστατική επιστολή για μένα, το οποίο το έκαναν χωρίς δεύτερη σκέψη και ως εκ τούτου είμαι πολύ ευγνώμων και στους δύο. Παρόλο που είχα την ευκαιρία να συνεργαστώ με τον Αναπλ. Καθ. Claudio Coriano μόνο για μικρό χρονικό διάστημα, είναι αδύνατο να μην αναφέρω την επιρροή του στα επιστημονικά μου βήματα. Ως νεαρός μεταπτυχιακός φοιτητής απήλαυσα τη ζεστή φιλοξενία του κατά τη διάρκεια μιας όχι και τόσο σύντομης επίσκεψής μου στο Λέτσε (αν θυμάμαι σωστά, ήμουν ο πρώτος φυσικός, μετά από αυτόν εννοείται, που έμεινε στο νεόκτιστο σπίτι του) όπου είχαμε αμέτρητες ώρες συζήτησης για την φυσική και την επιστημονική ζωή εν γένει. Θα ήθελα να τον ευχαριστήσω πολύ αφού οι συμβουλές του έπαιξαν καθοριστικό ρόλο για την πορεία μου στον τομέα της Θεωρητικής Φυσικής Υψηλών Ενεργειών.

Είναι γνωστό ότι το περιβάλλον στο οποίο κάποιος κάνει το διδακτορικό του διαδραματίζει πολύ σημαντικό ρόλο κατά τη διάρκεια των σπουδών του. Για μένα αυτό δεν ήταν πρόβλημα αφού ήμουν πραγματικά τυχερός που μοιράστηκα το γραφείο μου με σπουδαίους συναδέλφους και φίλους από τους οποίους έμαθα πολλά. Θέλω να ευχαριστήσω πολύ τον Γιάννη Νταλιάνη, τον Γιάννη Τάσκα και τον Γιώργο Τρίγγα για τις εξαιρετικά ενδιαφέρουσες και ενημερωτικές συζητήσεις μας σχετικά με τη φυσική όπως επίσης και άλλους επιστημονικούς τομείς, τη μουσική, τον αθλητισμό και τις ανησυχίες μας για το κοινωνικό γίγνεσθαι. Όσον αφορά τους συναδέλφους μου, η λίστα μου δεν θα ολοκληρωθεί ποτέ εάν δεν ευχαριστήσω τους πιο πρόσφατους συνεργάτες και φίλους μου, τον Δημοσθένη Θεοφιλόπουλο και τον Αντώνη Καλογείρου. Ο Δημοσθένης Θεοφιλόπουλος και εγώ αναπτύξαμε μια δυνατή φιλία σχεδόν από την στιγμή που συναντηθήκαμε για πρώτη φορά. Σχετικά πρόσφατα συνεργαστήκαμε σε ένα έργο σχετικά με τους correlators της Σύμμορφη Θεωρίας Πεδικού μέσω του χώρου εμβάπτισης για το οποίο είχαμε μια πολύ καρποφόρα συνεργασία. Θα ήθελα να τον ευχαριστήσω για τις αμέτρητες συζητήσεις μας τόσο σε επιστημονικό όσο και σε προσωπικό επίπεδο και για τη συνεργασία μας. Το ερευνητικό μου ταξίδι στη Κβαντική Κοσμολογία απέχει πολύ από το να είναι σόλο καθώς με τον Αντώνης Καλογείρου έχουμε αναπτύξει μια πολύ στενή συνεργασία. Θα ήθελα να τον ευχαριστήσω τόσο για την σχεδόν καθημερινή επικοινωνία μας, η οποία με έχει βοηθήσει στο να σημειώσω μεγάλη πρόοδο όσον αφορά την δουλειά μου πάνω στο ερευνητικό μας θέμα, αλλά και για τις πολλές ενδιαφέρουσες και ενημερωτικές συζητήσεις μας.

Κανένα από τα παραπάνω δεν θα ήταν δυνατό χωρίς τη γενναιόδωρη υποστήριξη, την άνευ όρων αγάπη και τη φροντίδα της οικογένειάς μου. Και οι δύο γονείς μου ήταν κοντά μου καθώς μεγάλωνα υποστηρίζοντας και ενισχύοντας το όνειρό μου να γίνω επιστήμονας. Όταν αποφάσισα ότι το πραγματικό μου όνειρο ήταν να γίνω Φυσικός και ειδικότερα ερευνητής στον τομέα της Θεωρητικής Φυσικής Υψηλών Ενεργειών, στάθηκαν δίπλα μου χωρίς καμία δεύτερη σκέψη τόσο πνευματικά όσο και οικονομικά, οπότε θα τους είμαι πάντα ευγνώμων. Θα ήθελα επίσης να ευχαριστήσω την αδερφή μου, Μικαέλα, γιατί έχουμε αναπτύξει μια τόσο υγιή και ισχυρή προσωπική και επιστημονική σχέση. Η Μικαέλα ακολουθεί τα δικά της επιστημονικά βήματα ως Βιολόγος και πιο συγκεκριμένα ως ερευνητής στο τομέα της Βιοπληροφορικής (μια σοφή επιλογή αφού δεν πιστεύω ότι οι γονείς μου θα ανέχονται έναν άλλο Φυσικό στην οικογένεια), οπότε και έχουμε περάσει πολλές ώρες να την διδάσκω φυσική και εκείνη να με μυεί στην βιολογία και την βιοπληροφορική. Φυσικά μετράω ως μέλος της οικογένειάς μου και τη Σταυρούλα που είναι η κοπέλα μου και τον Άρη που είναι ο καλύτερος μου φίλος. Η Σταυρούλα, μια μαθηματικός που εργάζεται επαγγελματικά σε κουζίνες υψηλής γαστρονομίας, κατάφερε να ανεχτεί την εμμονή μου με την επιστήμη και ιδιαίτερα με τη φυσική όλα αυτά τα χρόνια, ήταν δίπλα μου συνεχώς και ήταν πάντα πρόθυμη να ακούσει τις ανησυχίες μου. Ως εκ τούτου, είμαι πραγματικά ευγνώμων για την άνευ όρων υποστήριξή της κατά τη διάρκεια των διδακτορικών μου σπουδών. Τέλος, πολλές ευχαριστίες ανήκουν στον καλύτερό μου φίλο Άρη, που ήταν πάντα κοντά μου ήδη από την παιδική μας ηλικία, για το αδιαμφισβήτητο ταλέντο του να διασκεδάζει σε οποιαδήποτε δεδομένη ευκαιρία και για την υποστήριξη και την προθυμία του να με ακούει να μιλάω για φυσική, παρόλο που είναι εκτός της επιστημονικής κοινότητα.

Ως υπότροφος του ΕΛΚΕ, θα ήθελα να ευχαριστήσω τον ΕΛΚΕ του ΕΜΠ για την οικονομική υποστήριξη των διδακτορικών μου σπουδών, διευκολύνοντας κατ΄αυτό τον τρόπο το επιστημονικό μου ταξίδι.

National Technical University of Athens
School of Applied Mathematical and Physical Sciences
Department of Physics

On the Spontaneous and Simultaneous Breaking of Internal and Scale symmetry in Effective Field Theories of extra dimensional origin enhanced with Higher Dimensional Operators: A New Approach to the Hierarchy Problem

by

Fotis Koutroulis

A dissertation presented for the degree of
Philosophiae Doctor

The Advisory Committee:
Nikos Irges, Assoc. Prof., NTU of Athens (Supervisor)
Alexandros Kehagias, Prof., NTU of Athens
Claudio Coriano, Assoc. Prof., Un. of Salento, Lecce

Greece, June 2021

© Copyright by
Fotis Koutroulis
2021

Acknowledgement

The path that leads towards and keeps someone alongside the scientific world is constructed out of personal quest and effort as well as of team work and trust on the appropriate collaborators. Since I chose to follow that path, already as a MSc student, I considered my self really fortunate to be surrounded by brilliant teachers, colleagues and friends and to be supported by my family all the way down the line. Of course it is an inevitable truth that the current thesis would not have been completed without the assistance of this group of people and therefore this is a great opportunity to thank all of them.

Let me start by thanking my supervisor, Assoc. Prof. Nikos Irges. Without any doubt if it were not for his priceless assistance, regarding both my scientific and personal life, my research quality would not have been the same. During my years as his master student I obtained a deep understanding for Quantum Field Theory due to the way that he taught the subject and becoming his PhD student I really appreciated his deep insights, clarity of thought and determination to attack some of the fundamental problems of the High Energy Theoretical Physics. All these qualities became a constant source of inspiration for me. It would be impossible not to mention my appreciation for his willingness to patiently listen to my thoughts and ideas even though some times they were lacking in consistency. I would really like to thank him for his willingness to spent many hours discussing with me about physics, scientific life in general and every day life as well and for giving me very valuable pieces of advice. With the fact that he was strict on me and spent a lot of time correcting my mistakes I managed to keep myself on the correct track during my PhD studies and I am really grateful about that. Finally, I especially admired his persistence on staying scientifically accurate and consistent every time we had a research project in our hands as well as his eagerness to deal with less familiar but yet very exciting areas of research. The above qualities played a crucial role in creating my scientific character and they will definitely follow me as I continue my research career.

The list of people that I am really thankful to continues with Prof. Alexandros Kehagias, Assoc. Prof. Konstantinos Anagnostopoulos and Assoc. Prof. Claudio Coriano. Recently, after my PhD was essentially finished, I paused for a moment my research on Particle Physics

in order to jump into the field of Quantum Cosmology. Then, Prof. Alexandros Kehagias was more than eager to discuss with me about its core ideas enhancing my understanding, so I would like to thank him for his time and advice. During my first steps as a graduate student I considered my self fortunate enough to attend great lectures on Quantum Field Theory given by Assoc. Prof. Konstantinos Anagnostopoulos which helped me to deepen my knowledge on the subject and for that reason I am grateful to him. When the time to apply to a PostDoc position had came, I asked Alexandros Kehagias and Konstantinos Anagnostopoulos to write a letter of recommendations for me, which they did it without any second thoughts and hence I am greatly indebted to both of them. Even though I had the chance to collaborating with Assoc. Prof. Claudio Coriano only for a short period of time, It is impossible not to mention his influence on my scientific steps. As a young graduate student I enjoyed his warm hospitality during my not so short visit to Lecce (if I remember correctly I was the first physicist, after him of course, who stayed at his newly built house) where we had countless hours of discussion about physics and scientific life. I would like to thank him since his advice played a key role for my trajectory through the field of High Energy Theoretical Physics.

It is well-known that the environment at which someone does his PhD plays very important role during his studies. For me this was not a problem since I was really fortunate to have great office-mates and friends from whom I learned a lot. Many thanks to Yiannis Dalianis, John Taskas and George Tringas for our extremely interesting and informative discussions regarding physics and various other scientific fields as well, music, sports and our worries about the social anxiety. Regarding the colleagues of mine, my list will never be completed if I do not thank my most recent collaborators and friends, Dimosthenis Theofilopoulos and Antonis Kalogirou. Dimosthenis Theofilopoulos and I developed a strong friendship almost by the time we had first met. More recently, him and I worked together on a project regarding the Conformal Field Theory correlators and the embeding space for which we had one very fruitful collaboration. I would like to thank him for our countless discussions on both scientific and personal level and for our collaboration. My research journey at Quantum Cosmology is far from being a solo one since Antonis Kalogirou and I have developed a very close collaboration. I would like to thank him for our almost daily communication which has helped me making a lot of progress on my project and for our many interesting and informative discussions.

None of this would have been possible without the generous support, unconditional love, and care of my family. Both my parents were close to me as I was growing up supporting and enhancing my dream about becoming a scientist. When I decided that my actual dream was to become a Physicist and in particular a researcher on the field of High Energy Theoretical Physics, they stood by me without any second thoughts both mentally and economically so I will always be grateful to them. I would also like to thank my sister, Mikaela, for having such a healthy and strong personal and scientific relationship with me. Mikaela follows her own scientific steps as a Biologist and more precisely as a researcher on Bioinformatics (a wise choice since I do not believe that my parents would tolerate an other Physicist in the family) so we have spent many hours teaching her physics while I was being taught biology and bioinformatics

by her. Of course I count as a member of my family also Stavroula who is my girlfriend and Aris who is my best friend. Stavroula, a mathematician who works professionally at a haute cuisine, managed to tolerate my obsession with science and particularly with physics all these years, she stood by me constantly and was always eager to listen to my concerns. Hence I am really grateful for hers unconditional support during my graduate studies. Finally, many thanks go to my best friend Aris, who was always close to me already from our childhood, for his undoubtable talent to have fun in any given opportunity and for his support and willingness to listen to me even though he is outside the scientific community.

As an ELKE's Fellow I would like to thank ELKE of NTU of Athens for economically supporting my graduate studies, making in this way my scientific journey easier.

Dedication

To my family (taken in its widest sense)

List of Publications

The chapters of the current dissertation originate from the following research/published projects:

- Nikos Irges and Fotis Koutroulis, *RG flows in Non-Perturbative Gauge-Higgs Unification II. Effective action for the Higgs phase near the quantum phase transition*, Eur. Phys. J. C **81** (2021) 2, 187
- Nikos Irges, Fotis Koutroulis and Dimosthenis Theofilopoulos, *The conformal N-point scalar correlator in coordinate space*, arXiv: 2001.07171 [hep-th]
- Nikos Irges and Fotis Koutroulis, *On RG flows in Generalized Effective Field Theory*, Nucl. Phys. B **950** (2020) 114833
- Nikos Irges and Fotis Koutroulis, *Symmetry breaking and renormalization group flows with higher dimensional operators*, Phys. Rev. D **100** (2019) 6, 065004
- Nikos Irges and Fotis Koutroulis, *RG flows in Non-Perturbative Gauge-Higgs Unification I*, Nucl. Phys. B **937** (2018) 135-195
- Nikos Irges and Fotis Koutroulis, *Renormalization of the Abelian–Higgs model in the R_ξ and Unitary gauges and the physicality of its scalar potential*, Nucl. Phys. B **924** (2017) 178-278

Contents

Acknowledgement i

Dedication iv

List of Publications v

1 Introduction **7**

2 Rendering the scalar potential of the Abelian-Higgs model a physical quantity **13**

2.1 Introduction 13

2.2 The classical theory and some basics 14

2.3 R_ξ gauge 18

2.3.1 Tadpoles 21

2.3.2 Corrections to the gauge boson mass 22

2.3.3 Corrections to the Higgs mass 24

2.3.4 Corrections to the Higgs cubic vertex 28

2.3.5 Corrections to the quartic coupling 35

2.4 Unitary Gauge 45

2.4.1 Tadpoles 46

2.4.2 Corrections to the gauge boson mass 47

2.4.3 Corrections to the Higgs mass 49

2.4.4 Corrections to the Higgs cubic vertex 51

2.4.5 Corrections to the quartic coupling 54

2.5 Renormalization 58

2.5.1 Counter-terms 59

2.5.2 Physical quantities and the β-functions 63

2.6 The one-loop Higgs potential 65

2.7 Lines of Constant Physics 71

Appendices **76**

2.A One-loop integrals . . . 76

2.B Passarino -Veltman . . . 77

2.B.1 Scalars . . . 77

2.B.2 Tensors . . . 79

2.C U-integrals . . . 82

2.C.1 U-integrals in Tadpoles . . . 82

2.C.2 U-integrals in mass corrections . . . 83

2.C.3 U-integrals in Triangles . . . 84

2.C.4 U-integrals in Boxes . . . 85

2.D Explicit calculation of the diagrams . . . 86

2.D.1 R_ξ-diagrams . . . 87

2.D.2 Unitary gauge diagrams . . . 94

2.E Finite parts . . . 98

2.E.1 R_ξ gauge . . . 98

2.E.2 Unitary gauge . . . 106

2.F On-shell results . . . 107

3 Is the leading order truncation enough to develop a Higgs mechanism? **111**

3.1 Introduction . . . 111

3.2 The classical continuum action from the lattice action . . . 112

3.2.1 Boundary-Hybrid action . . . 115

3.2.2 Bulk action . . . 118

3.2.3 The leading order continuum action . . . 119

3.3 Quantum effects . . . 120

3.3.1 1-loop diagrams . . . 121

3.3.2 Renormalization, β-functions and anomalous dimensions . . . 129

3.4 RG Flows and the Phase Diagram . . . 138

3.4.1 Boundary . . . 138

3.4.2 Bulk . . . 139

3.5 Scale invariance and the Stress-Energy Tensor . . . 148

3.5.1 Boundary . . . 149

3.5.2 Bulk . . . 150

Appendices **152**

3.A Couplings . . . 152

3.B Dimensional analysis . . . 152

3.C Global symmetries . . . 155

3.C.1 Parity P . . . 155

3.C.2 Charge conjugation C . . . 155

3.C.3 Stick symmetry $\mathcal{S}$ . . . 156

3.D Feynman rules . . . 156

3.E Looking at the scaleless integrals . . . 160

3.F Box Diagrams on the Boundary . . . 162

3.F.1 Four-photon Diagrams . . . 163

3.F.2 Four-scalar Diagrams . . . 166

4 Generalized effective field theory: The quantum origin of the higher dimensional operators **170**

4.1 Introduction . . . 170

4.2 GEFT β-functions and anomalous dimensions . . . 171

4.3 Inserting dimension-6 operators . . . 176

4.3.1 Ghosts induced by higher derivative operators . . . 178

4.3.2 The pure polynomial W-basis . . . 190

4.3.3 Filling a couple of remaining holes . . . 200

4.4 Dimension-8 operators . . . 201

Appendices **211**

4.A Scaleless integrals . . . 211

4.B Review of the $\mathcal{L}^{(2)} + \mathcal{L}^{(4)}$ (usual ϕ^4) theory . . . 214

5 A quantum, 1st order, phase Transition as the solution of the Higgs fine tuning problem **221**

5.1 Introduction . . . 221

5.2 Quantization with higher derivative operators . . . 224

5.2.1 The ghost-free basis of the gauge-fixed classical action . . . 226

5.2.2 One loop corrections . . . 229
5.2.3 Renormalization and β-functions . . . 238
5.3 The Higgs phase . . . 246
5.3.1 The scalar potential and a comparison to the Coleman-Weinberg model . 246
5.3.2 What if polynomial potential terms where allowed? . . . 253
5.4 The effective action near the Higgs-Hybrid phase transition . . . 254
5.4.1 Matching RG flows in the Higgs and Hybrid phases . . . 257
5.4.2 Physics in the vicinity of the phase transition . . . 262
5.4.3 Lines of Constant Physics . . . 267

Appendices **271**
5.A Review of the NPGHU model . . . 271
5.A.1 The orbifold lattice action . . . 271
5.A.2 The Boundary-Hybrid action with higher order terms . . . 274
5.A.3 The Bulk action with higher order terms . . . 280
5.B Field redefinition and gauge invariance . . . 284
5.C Feynman Rules for the Boundary-Hybrid action . . . 287
5.D Review of the Coleman-Weinberg model . . . 290

Chapter 1

Introduction

Almost a decade ago the Large Hadron Collider at CERN released undoubtable evidences regarding the existence of the Higgs boson, the predicted scalar field excitation of the Brout-Englert-Higgs (or simply Higgs) mechanism [1], which is responsible for the ElectroWeak symmetry breaking. Already before the discovery of the Higgs boson, the Higgs mechanism was considered as a key ingredient for the completeness of the Standard Model (SM) of particles since it provides a consistent mechanism to spontaneously break gauge theories. Under such a Spontaneous Symmetry Breaking (SSB) all the gauge bosons that are coupled to the Higgs field acquire a mass while essentially the associated symmetry group remains untouched. However, even though the introduction of the Higgs mechanism is of crucial importance for the clarity of the SM there is a price to be paid since it comes along with a theoretical inconsistency. After the renormalization of the SM and already at one-loop level the Higgs boson, due to its coupling with almost all the fundamental particles, acquires quantum corrections on which the Higgs mass is very sensitive. Under these circumstances, with the most severe contribution coming from the heaviest elementary particle, the top quark, the predicted Higgs mass is placed somewhere around the Planck mass $\approx 10^{19}$ GeV. To rephrase, the quantum nature of the SM gives birth to the well know quadratic corrections to the Higgs mass exposing its sensitivity to the high energy, Ultra Violet (UV), scales and results in a value much larger than the measured one at 125.1 GeV. The latter is approximately 10^{17} orders of magnitude smaller that the Planck mass and this energy mismatch is well known by the name of the Higgs Hierarchy Problem (HHP) which is part of the larger group of the naturalness problems. In a manner of speaking, the understanding behind the HHP is that for an inexplicable reason the Higgs mass should exhibit a huge amount of fine tuning, in order to matching its measured value, in the sense that somehow those quadratic, UV, contributions should cancel out. Since such a hierarchy of scales is inherited from the internal structure of the SM, the various solutions of the problem should lay beyond that structure and towards the direction of new physics.

The current thesis moves along the framework of Beyond the Standard Model (BSM) physics and its purpose is to propose a novel way in order to solve this theoretical inconsistency using as its base the above incarnation of the HHP, the Higgs mass fine-tuning problem. The playground

of our construction follows the path of extra dimensional scenarios enhanced with a non-Abelian gauge group and in particular those that refer to spacetimes with one extra spacial dimension. Regarding our approach, the core of the HHP's solution is the proposal of a novel underline Higgs mechanism, of extra dimensional origin, generating a Higgs mass which is insensitive to the UV corrections. Keep in mind the fact that the gauge symmetry of this extra dimensional model protects, essentially, the associated mass from the severe quantum corrections. More precisely, our target is the construction of a four-dimensional (4d) continuum effective action for a five-dimensional (5d) model, originally constructed on the lattice [4, 5, 6] and dubbed as a model of Non-Perturbative Gauge-Higgs Unification (NPGHU). The model in its simplest version has a pure $SU(2)$ gauge symmetry in 5d with orbifold boundary conditions along the anisotropic fifth dimension (with $\gamma = a_4/a_5$ the anisotropy parameter at tree level), that generate a 4d boundary on which a $U(1)$ gauge field coupled to a complex scalar survive. The main novel property of this model is that, at the non-perturbative level, it exhibits spontaneous breaking of its gauge symmetry in infinite fifth dimension [5, 7, 10, 11, 12], which distinguishes it from extra-dimensional models where the scalar potential is of a finite temperature type, inversely proportional to the size of the extra dimension. Its pure bosonic nature sets it apart also from similar mechanisms where the presence of fermions is necessary in order that a Higgs mechanism is triggered. The absence of any polynomial terms in the (quantum) effective scalar potential distinguishes it from models with a classical potential but also from the Coleman-Weinberg model [13] and its generalizations, where at least a quartic potential operator appears at the classical level. These features seem to point to a quantum and pure bosonic Higgs mechanism, a new class of Higgs-type mechanisms.[1] One of the main characteristics of our model lies in the fact that in the Higgs phase, the ratio of the scalar to the gauge boson mass near the 5d "bulk" or "zero-temperature" or "quantum" phase transition and not far from the triple point on the phase diagram turns out to be numerically close to the corresponding ratio of the Higgs to the Z boson mass in the Standard Model [11]. This regime is near the line of first order phase transitions that separates the Higgs phase from the "Hybrid" phase, where in the bulk the system decomposes into a weakly interacting array of 4d, confined hyperplanes. Hence, due to the fact that the zero-temperature phase transition of interest is of first order, the effective action under consideration inherits a finite cut-off and the non-trivial result is that, even though perturbatively non-renormalizable, our theory possesses a low cut-off, giving a possible resolution to the Higgs mass fine tuning problem. Being able to draw Lines of Constant Physics (LCP), that is lines on the phase diagram ending on the phase transition along which the mass spectrum remains constant, supports such a conclusion. The model that the current dissertation proposes, possesses specific characteristics three of which should be examined and developed in a separate, from our core construction, way. Indeed, our research activity during the completion of that thesis dealt with those characteristics in an independent manner.

To be more precise, the first feature of the NPGHU model that worths a separate examination is that on its 4d boundary lives a kind of an Abelian Higgs Guage (AHG) model. In principle it

[1] See [14, 15] for a recent review on that matter.

was supposed that the quantum nature of an AHG model is problematic in the sense that even though classicaly there is a simple qualitative description of its mechanism, at the quantum level where this theory is more precisely defined, ambiguities arise which are related to the question of whether one can consider the quantum scalar potential itself as a physical quantity or not. Therefore in order to consistently proceed with the NPGHU model we should first answer this question. Indeed, a part of this work is devoted to that, approaching the issue from two different angles in the context of the AHG model [2]. The one angle of approach has to do with the basis of representation for the Higgs field. In particular, instead of writing the (complex) Higgs field in a Cartesian basis[2], we choose the not so usual prescription for loop calculations, the Polar basis.[3] The other angle of our approach has to do with the quantization scheme. It is well known that there is an infinitum of possible gauge fixing functions that one can use during quantization, each one of them introducing at least one gauge fixing parameter, say ξ. A typical representative of these schemes is R_ξ gauge fixing. Any sensible quantization scheme should produce a gauge independent set of physical quantities.[4] Nevertheless, the scalar effective potential computed with the background field method on the other hand is notoriously known to be ξ-dependent already at one-loop, which renders its physicality (and the relevance of the precision triviality and instability bounds derived from it) a delicate matter [16, 62]. It is therefore an open issue how to define an unambiguous, physical, quantum potential in spontaneously broken gauge theories. For this reason, we choose the Unitary gauge [18] as our quantization scheme where only physical fields propagate demonstrating explicitly the physical spectrum of spontaneously broken gauge theories at the classical level. It is rarely used though for loop calculations, in fact we are not aware of a complete renormalization work in this gauge, while the Unitary gauge is sometimes called a non-renormalizable gauge.[5] A necessary condition therefore for a Unitary gauge calculation to make sense is that the physical quantities that are ξ-independent in the R_ξ gauge, to coincide with the corresponding quantities derived in the Unitary gauge. Here we prove that indeed this condition is fulfilled and hence, through the renormalization procedure, we automatically obtain a version of the scalar potential, the Unitary gauge scalar potential, that is by definition gauge independent. In other words the obtained potential can safely be considered as a physical quantity.

The other two features of the Non-Perturbative Gauge Higgs Unification model that need a separate examination are connected and both have to do with a technical issue and in particular with the strategy for building a continuum effective action starting from the lattice construction.

[2]This choice suggests that $H = \phi_1 + i\phi_2$ [19], where the real part of the field ϕ_1 is the physical Higgs particle, while ϕ_2 represents the unphysical Nambu-Goldstone (or simply Goldstone) boson.

[3]This choice suggests that $H = \phi e^{i\chi/v}$, where now the physical Higgs field is $\phi = \sqrt{\phi_1^2 + \phi_2^2}$ and χ is the Goldstone boson while v is some vacuum expectation value (vev).

[4]Such quantities are for sure the masses of physical fields and the independent dimensionless couplings like λ. So, gauge independence of physical quantities in a scheme like the R_ξ is then ensured if the corresponding β-functions are ξ-independent and this is indeed the case in every consistent loop calculation.

[5]A possible obstruction to completing reliably such a program may be the high momentum behaviour of the Unitary gauge boson propagator resulting in integrals that often diverge worse than quadratically with a cut-off, even in a renormalizable theory.

More precisely, the standard procedure is to start from the lattice plaquette action and expand it in small lattice spacing, a well known process that generates an infinite tower of operators of increasing classical dimension, with the ones of dimension larger than d, typically called Higher Dimensional Operators (HDO).[6] Truncating the expansion at a given order and then taking the naive continuum limit, gives us a classical, continuum effective action that may be quantized. So a fair question that naturally arises is what should be the appropriate order in the lattice spacing to truncate this expansion in order to reveal the associated Higgs phase. To answer this question we break the construction of the 4d effective action into two parts where in the first one we truncate the expansion at leading order (LO) while in the second we consider next to leading order (NLO) terms including in particular the dominant HDO.[7] Under the choice of a LO truncation, which corresponds to the one of the two features mentioned previously, we consider a certain limit in which the boundary decouples completely from the bulk. As a result, in the bulk we have a 5d $SU(2)$ Yang-Mills system and on the boundary a 4d, massless and free scalar QED (SQED) model, which does not develop any scalar potential neither in classical nor in quantum level, that can be analyzed separately. The phase diagrams for both cases is known. The boundary is expected to possess only a Gaussian fixed point while the bulk phase diagram for general γ was determined via Monte Carlo simulations (see [20]) and has only two phases, a Confined and a Coulomb phase separated again by a line of first order quantum phase transitions. Indeed we reproduce the above phase diagrams for the LO effective action using the ε-expansion, according to which the bulk driven phase transition may be re-constructed as a line of 5d Wilson-Fisher (WF) fixed points. The subtle issue with this is that a WF fixed point is usually interpreted as the sign of a second order phase transition whereas here we are after a first order transition, as well as that at LO the phase diagram is blind to the Higgs and Hybrid phases. As a consequence we have to move further, truncating at NLO the lattice spacing expansion and include HDO in order to have access to the Higgs phase and to the associated Higgs mechanism.

This brings us to our last feature which needs a separate analysis and has to do with the quantum nature of scalar field theories, enhanced with HDO. This is a necessary step in order to consistently develop the 4d effective action of the NPGHU model which, for our ultimate goal, should include HDO. Therefore, a part of the current thesis is devoted to analysing such a toy model under the framework of the Generalized Effective Field Theory (GEFT). GEFT is the non-renormalizable extension of an Effective Field Theory (EFT) where the Wilson coefficients are endowed by their own, independent scale dependence. One fair question is whether the HDO are of a classical or a quantum nature and we argue that when the suppressing scale, say Λ, is an internal scale, they must have a quantum origin.[8] In particular, we demonstrate that the

[6] At a fixed order in the power of the lattice spacing there may also be generated gauge variant operators (lattice artefacts) that we must drop in a continuum approach.

[7] In a lattice language such a process is called Symanzik's improvement and it was conducted for the first time, for a pure Yangs-Mills gauge theory, in [21]. For its application to lattice QCD, see [22].

[8] In DR for example, as we show for the boundary effective action, one can identify Λ with the regulating scale μ or alternatively with a fixed scale derived from μ, such as μ_*.

(1-loop) quantization of a Lagrangian with vertices deriving from the HDO, like

$$\mathcal{L} = -\frac{1}{2}\phi_0(\Box + m_0^2)\phi_0 - \frac{\lambda_0}{4!}\phi_0^4 + \sum_{n=3,\cdots} \frac{c_0^{(2n)}}{\Lambda^{2n-4}}\phi_0^{2n}\,, \tag{1.0.1}$$

is equivalent to the quantization of a Lagrangian without HDO but taking into account all possible operator insertions, using the Operator Insertion Method (OIM)

$$\langle O \rangle \sim \int D\phi\, O\, e^{i\int d^4x \mathcal{L}}\,. \tag{1.0.2}$$

The associated Lagrangian, $\mathcal{L}$, is already renormalized and the operator O (with an associated coupling c) develops an anomalous dimension when the arguments of the fields it contains coincide, a fact slightly beyond basic, perturbative quantum field theory.[9] The equivalence of Eq. (1.0.1) and Eq. (1.0.2), the fact that Λ is an internal to the theory scale together with the fact that in the standard renormalizable picture the HDO represent finite quantum effects, allow us to characterize the HDO as quantum corrections. This is not an unimportant detail since then, in the presence of a Higgs mechanism, scale and internal symmetry break spontaneously and simultaneously by quantum effects. This is a crucial result regarding the role that the HDO play in the continuum description of the NPGHU model.

Under all the above arguments we consistently construct the boundary effective action of the Non-Perturbative Gauge-Higgs Unification model and show that it indeed exhibits a novel Higgs mechanism where the associated Higgs mass is almost free of the fine tuning problem. The current dissertation is organised as follows:

In Chapter 2 we perform an old school, one-loop renormalization of the Abelian-Higgs model in the Unitary and R_ξ gauges, focused on the scalar potential and the gauge boson mass. Our goal is to demonstrate in this simple context the validity of the Unitary gauge at the quantum level, which could open the way for an until now (mostly) avoided framework for loop computations. We indeed find that the Unitary gauge is consistent and equivalent to the R_ξ gauge at the level of β-functions. Then we compare the renormalized, finite, one-loop Higgs potential in the two gauges and we again find equivalence. This equivalence needs not only a complete cancellation of the gauge fixing parameter ξ from the R_ξ gauge potential but also requires its ξ-independent part to be equal to the Unitary gauge result. We follow the quantum behaviour of the system by plotting Renormalization Group trajectories and Lines of Constant Physics, with the former the well known curves and with the latter, determined by the finite parts of the counter-terms, particularly well suited for a comparison with non-perturbative studies.

In chapter 3 we initiate the continuum description of a non-perturbative 5d lattice Yang-Mills model with 4d boundaries using the ε-expansion. In its simplest version classically the bulk has an $SU(2)$ gauge symmetry and on the boundary there is an Abelian-Higgs system with zero

[9] OIM allows us to use the kinetic term as the pivot Lagrangian and treat any other operator as an insertion, including the mass and quartic interactions. In other words the starting action is that of a pure scalar Conformal Field Theory (CFT) one for which, a recent closed form regarding its correlators, using the embedding space technic, is obtained in [23].

scalar potential. In part I we compute the Renormalization Group flows and related quantities in a limit where the boundary decouples from the bulk.

in Chapter 4 we deal with a pure scalar GEFT and we construct the associated effective theory quantizing a Lagrangian in the presence of all internal symmetry respecting operators of any mass dimension. The resulting theory may be practically useful in regimes of its phase diagram where the perturbative expansion and a truncation of the infinite tower of Higher Dimensional Operators (HDO) are valid. The massless limit of GEFT is especially interesting as the spontaneous breaking of internal symmetry and of scale invariance are correlated.

In Chapter 5 we construct the zero temperature (no compact dimensions) effective action for an $SU(2)$ Yang-Mills theory in five dimensions, with boundary conditions that reduce the symmetry on the four-dimensional boundary located at the origin to a $U(1)$-complex scalar system. In order to be sensitive to the Higgs phase, we need to include higher dimensional operators in the effective action, which can be naturally achieved by generating it by expanding the corresponding lattice construction in small lattice spacing, taking the naive continuum limit and then renormalizing. In addition, we build in the effective action non-perturbative information, related to a first order quantum phase transition known to exist. As a result, the effective action acquires a finite cut-off that is low and the fine tuning of the scalar mass is rather mild.

Chapter 2

Rendering the scalar potential of the Abelian-Higgs model a physical quantity

2.1 Introduction

In the first Chapter, we consider the usual, 4-dimensional, Abelian-Higgs model and perform the one-loop renormalization of the gauge boson mass and of the Higgs potential in both the R_ξ and Unitary gauges. In addition, this double computation allows us to monitor and ensure the credibility of the Unitary gauge calculation. As we have already mentioned in Chapter 4.1 the main drawback, at least seemingly, of the Unitary gauge has to do with the highly divergent loop integrals. For this reason the Unitary gauge is sometimes called a non-renormalizable gauge. We call these integrals, "U-integrals". However, we show that as far as the β-functions (determined by the divergent parts of the one-loop amplitudes) is concerned, the Unitary gauge is equally consistent, in fact equivalent to the R_ξ gauge. Such an equivalence opens a new direction in Standard Model calculations, as the number of diagrams in the Unitary gauge is significantly smaller. Apart however from simplifying already known results, computations such as done here could also render currently ambiguous results based on the dynamics of the scalar potential away from its extrema, more robust (since this work is just a demonstration of gauge independence of the Higgs potential by construction it would be certainly worth trying to construct some sort of a more formal 'proof'). Then we consider the scalar potential (determined by the finite parts of the amplitudes after renormalization) and ask whether it could also be physical. Let the finite part of the one-loop value of a quantity $\star$ be defined as $(\star)_f$ with the subscript f denoting finite part. Such quantities will be the various loop corrections entering in the renormalized Higgs potential. Then schematically we have that in general

$$\left[(\star)_f\,, \lim_{\xi\to\infty}\right] = \lim_{\xi\to\infty} g(\lambda, m_H, m_Z, \mu, \xi)\,, \tag{2.1.1}$$

where the behaviour of the function g at $\xi = \infty$ is one thing we would like to understand. The background field method in the $\overline{\text{MS}}$ scheme for example gives an effective potential where $\lim_{\xi\to\infty} g(\xi) = \infty$ for a large class of gauge fixing functions [62], rendering the Unitary gauge limit after loop integration, singular. The singularity implies that the Unitary gauge is disconnected from the space of R_ξ gauges and essentially that the Higgs potential is unphysical away from its extrema. Our calculation instead shows that $\lim_{\xi\to\infty} g(\xi) = 0$, perhaps the most striking result of this work, as it implies that the Higgs potential can be made gauge invariant, hence physical, even away from its extrema. For formal aspects of the quantization of the Abelian-Higgs model, see [36, 37].

Moreover, we analyze numerically the Higgs potential and show that the system generically behaves perturbatively until quite close to the Landau pole of λ. It becomes metastable already in the perturbative regime and only during its last steps towards the phase transition into the Coulomb phase turns non-perturbative. Finally, we constructed a couple of Lines of Constant Physics in the Unitary gauge and placed them on the Abelian-Higgs phase diagram in order to enhance the perturbative analysis by some non-perturbative input. This suggested us that in a Higgs-scalar system the cut-off can not be generically driven to the highest possible scales that the RG flow or the stability of the potential allows, if we want to keep the physics constant. This is because it is possible that way before those scales are reached, a phase transition may be encountered.

Regarding generalizations of this work, simple bosonic extensions should work in a similar way, without any surprises. In the presence of fermions some extra care may be needed to handle the U-integrals but this is expected to be a straightforward extra technical step. In this case though it is also expected that a new instability will appear at some intermediate scale and it would be interesting to work out in our framework how this modifies the bosonic system. Finally, if the observed consistency between the two gauges breaks down at higher loops then there is something about the quantum internal structure of spontaneously broken gauge theories that needs to be understood better.

2.2 The classical theory and some basics

The bare Lagrangean of the AH model is

$$\mathcal{L}_0 = -\frac{1}{4}F_{0,\mu\nu}^2 + |D_\mu H_0|^2 + m_0^2|H_0|^2 - \lambda_0|H_0|^4 \,. \tag{2.2.1}$$

Zero subscripts or superscripts denote bare quantities. As usual, the covariant derivative is $D_\mu = \partial_\mu + ig_0 A_\mu^0$ and the gauge field strength is $F_{0,\mu\nu} = \partial_\mu A_\nu^0 - \partial_\nu A_\mu^0$. The Higgs field H_0 is a complex scalar field. The Lagrangean is invariant under the $U(1)$ gauge transformations

$$\begin{aligned} A_\mu^0(x) &\to A_\mu^0(x) + \frac{1}{g_0}\partial_\mu\theta(x) \\ H_0(x) &\to H_0(x)e^{i\theta(x)} \end{aligned} \tag{2.2.2}$$

with $\theta(x)$ a gauge transformation function and the discrete, global Z_2 symmetry

$$H_0(x) \quad \rightarrow \quad -H_0(x) \tag{2.2.3}$$

We assume that both m_0 and λ_0 are positive quantities.

As it stands, the part of the Lagrangean that corresponds to a potential

$$V_0 = -m_0^2|H_0|^2 + \lambda_0|H_0|^4 \tag{2.2.4}$$

triggers SSB. Minimization yields the vev

$$\langle H_0 \rangle = \pm\frac{m_0}{\sqrt{2\lambda_0}} = \pm\frac{v_0}{\sqrt{2}}\,. \tag{2.2.5}$$

The second of the above equations defines the bare vacuum expectation value (vev) parameter v_0. The field H_0 can be expanded around its vev as

$$H_0\left(x\right) = \frac{\left(v_0 + \phi_0(x)\right) e^{i\frac{\chi_0(x)}{v_0}}}{\sqrt{2}}\,, \tag{2.2.6}$$

where now ϕ_0 is the new Higgs field fluctuation and χ_0 is a massless Goldstone boson. Eq. (2.2.6) is the so called "Polar basis" for the Higgs field, as opposed to the "Cartesian basis" $H_0(x) = 1/\sqrt{2}(v_0 + \phi_{1,0}(x) + i\phi_{2,0}(x))$. The former is typically used for demonstrating the physical spectrum while the latter for quantization. Here we will stick to the Polar basis for both. Replacing the vev into Eq.(2.2.1), the Lagrangean takes the form

$$\begin{aligned}
\mathcal{L}_0 \;=\; & -\frac{1}{4}F_{0,\mu\nu}^2 + \frac{1}{2}\left(\partial_\mu\phi_0\right)\left(\partial^\mu\phi_0\right) + \frac{1}{2}\left(\partial_\mu\chi_0\right)\left(\partial^\mu\chi_0\right) + \frac{1}{2}m_{Z_0}^2 A_\mu^0 A^{0\mu} \\
+ \; & m_{Z_0}(\partial^\mu\chi_0)A_\mu^0 + 2\frac{m_{Z_0}}{m_{H_0}}\sqrt{2\lambda_0}A_\mu^0(\partial^\mu\chi_0)\phi_0 + \frac{\sqrt{2\lambda_0}}{m_{H_0}}(\partial_\mu\chi_0)^2\phi_0 + \frac{2\lambda_0 m_{Z_0}}{m_{H_0}^2}A_\mu^0(\partial^\mu\chi_0)\phi_0^2 \\
+ \; & \frac{\lambda_0}{m_{H_0}^2}(\partial_\mu\chi_0)^2\phi_0^2 + g^{\mu\nu}\frac{\lambda_0 m_{Z_0}^2}{m_{H_0}^2}A_\mu^0 A_\nu^0\phi_0^2 + g^{\mu\nu}\frac{m_{Z_0}^2}{m_{H_0}}\sqrt{2\lambda_0}\phi_0 A_\mu^0 A_\nu^0 \\
- \; & \frac{1}{2}m_{H_0}^2\phi_0^2 - \sqrt{\frac{\lambda_0}{2}}m_{H_0}\phi_0^3 - \frac{\lambda_0}{4}\phi_0^4 + const.\,,
\end{aligned} \tag{2.2.7}$$

with $g^{\mu\nu}$ the Minkowski space metric. The bare gauge boson (Z boson) mass is defined as $m_{Z_0} = g_0 v_0$ and the bare Higgs mass as $m_{H_0} = \sqrt{2}m_0 = \sqrt{2\lambda_0}v_0$. As implied by the above expression, we have decided to use as independent parameters the masses and the quartic coupling λ_0. This means that we have eliminated the gauge coupling according to $g_0 = \frac{m_{Z_0}}{m_{H_0}}\sqrt{2\lambda_0}$ and the vev according to $v_0 = \frac{m_{H_0}}{\sqrt{2\lambda_0}}$ wherever they appear. Setting the Goldstone field χ_0 to zero, gives us the Unitary gauge Lagrangean which will be the topic of a separate section. For now we will keep the Goldstone in the spectrum. A consequence of having a Goldstone in the spectrum is a mixing term between the Z and χ_0 in Eq. (2.2.7).

We will compute all one-loop Feynman diagrams that contribute to the renormalization of the Z mass and of the scalar potential, using Dimensional Regularization (DR) [44]. We assume basic knowledge of the DR technology that we therefore do not review here, except from some

necessary basic facts that can be found in the Appendices. The renormalization scale parameter of DR is denoted by μ. The small expansion parameter ε of DR is defined via

$$\varepsilon = 4 - d\,. \tag{2.2.8}$$

Since we are using DR in our renormalization scheme, a consequence is that the trace of the metric is $g_{\mu\nu}g^{\mu\nu} = d$.

Now, each diagram comes with a symmetry factor. Consider a one-loop diagram containing n vertices with k_n lines on each vertex. These k_n lines are divided into k_n^{in} and k_n^{ext} for the internal and the external lines respectively. The procedure to obtain the correct symmetry factor is given for example in [43]:

- For each of the n vertices, count all possible ways that the k_n lines can be connected to the external legs of a given diagram. This is k_n^{ext}. Doing this for every vertex defines n_O as the product of the k_n^{ext}'s. The remaining lines belong to k_n^{in}.
- At each of the n vertices there are k_n^{in} lines. Count all the possible ways the loop can be constructed using these lines. The product of the k_n^{in}'s defines n_I.
- For each of the n vertices, count the number of k_i lines that are equivalent. This defines ℓ_i.
- Finally, for a given diagram count all the possible equivalent vertices of type j, defining v_j.

The symmetry factor of the diagram is then

$$\mathcal{S}_b^a = \frac{n_O n_I}{\prod_i \ell_i! \prod_j v_j!}\,, \tag{2.2.9}$$

where a, b are indicators specifying the diagram.

A large part of the one-loop diagram expressions is dominated by the set of basic integrals called Passarino-Veltman (PV) integrals [45]. We collect in Appendix 2.B the basics of the formulation of PV integrals, following mostly [46]. In our calculation several non-standard integrals emerge as well. The divergent ones we call collectively U-integrals and we compute them in Appendix 2.C. Finite integrals and finite parts of divergent integrals are harder to classify systematically so we will be dealing with them as we proceed.

We also introduce some useful notation. Our convention for the name of a one-loop Feynman diagram F is

$$F_E^{G,L} \tag{2.2.10}$$

$G = R_\xi, U$ specifies either the R_ξ or the Unitary gauge where the diagram is computed. L is a list containing the field(s) running in the loop in the direction of the loop momentum flow, starting from the vertex on the left side of the diagram. In case the diagram is an irreducible Box, we start the list from the upper left vertex. $E = H, Z$ specifies the external legs. In

the case $E = Z$, there may be additional Lorentz indices following E. We know that one-loop Feynman diagrams can be either finite or divergent. In the first case the corresponding integrals contain only finite terms and in the second case they include both divergent and finite parts. Furthermore, in each of the above cases, in the R_ξ gauge, the corresponding parts could be either gauge (i.e. ξ) dependent or gauge independent. In the Unitary gauge there is no such distinction. Therefore, every set of one-loop diagrams contributing to the same correlator, where the sum over the index L has been performed and the Lorentz indices (if present) have been appropriately contracted, can be expressed as

$$(4\pi)^{d/2} F_E^G = \mu^\varepsilon \left(\left[F_E^G\right]_\varepsilon + \left\{F_E^G\right\}_\varepsilon + \left[F_E^G\right]_f + \left\{F_E^G\right\}_f \right) , \tag{2.2.11}$$

where the square brackets denote ξ-independent part, the curly brackets denote ξ-dependent part and the subscripts ε and f denote divergent and finite part respectively. The $1/\varepsilon$ factor is absorbed in the definitions of $[F_E^G]_\varepsilon$ and $\left\{F_E^G\right\}_\varepsilon$. A word of caution here is that the above separation of diagrams into ξ-independent and ξ-dependent parts is clearly not unique. Nevertheless it is a very useful notation (once we get used to it) since it allows to perform algebra with diagrams easily and also facilitates the comparison with the Unitary gauge. In fact, in most cases the ξ-independent part of sums of diagrams is just the corresponding Unitary gauge result. The sum of the gauge independent and gauge dependent finite parts is denoted as

$$\left(F_E^G\right)_f = \left[F_E^G\right]_f + \left\{F_E^G\right\}_f . \tag{2.2.12}$$

Round, square and curly brackets appearing in any other context have their usual meaning. All entirely finite integrals are computed as described in Appendix 2.A. We will be giving the divergent parts and the finite parts of sums of groups of diagrams explicitly in the main text, leaving some of the (increasingly cumbersome) expressions for finite (parts of) diagrams to Appendix 2.E. There are some finite parts sitting inside the U-integrals too, which we compute together with their divergent parts and do not show explicitly, in order to avoid repetitions.

We perform renormalization away from the usual $\overline{\text{MS}}$ scheme. This means that our renormalization conditions force us to keep some non-trivial finite terms, that eventually enter in the renormalized Higgs potential. What finite terms are kept is of course not a unique choice. We have not checked if the gauge invariance of the potential could also be achieved in a pure $\overline{\text{MS}}$ scheme. If however $\overline{\text{MS}}$ (or any other scheme) would result in a gauge dependent potential, it would mean that in spontaneously broken gauge theories scheme dependence kicks in already at one loop. Recall that in QCD (a not spontaneously broken theory) scheme dependence appears at three loops. This would be strange because it would relate gauge dependence to scheme dependence. Our feeling is that any physical renormalization subtraction scheme applied to our calculation should produce a gauge invariant Higgs potential.

Furthermore, we perform renormalization off-shell, at zero external momenta. External momenta will be generically denoted by p. In 2-point, 3-point and 4-point functions zero external momenta means $p_i = 0$ with $i = 1, 2$, $i = 1, 2, 3$ and $i = 1, 2, 3, 4$ respectively. This choice, beyond being a huge simplifying factor, is justified since we are interested in terms of the Lagrangean without derivatives. It would be equally strange if after renormalization the Higgs

potential would pick up an external momentum dependence. In other words we believe that even if we had performed renormalization on-shell for example, we would have obtained the same results, alas in a more complicated way: not only individual diagrams would become much more involved, but also non-1PI diagrams may have to be added in order to arrive at gauge invariant β-functions. A physical argument for zero external momenta could be that if one is interested in the high energy limit, is entitled to set the masses of external particles equal to zero, that is $p_i^2 = 0$. But this choice, using momentum conservation in 2, 3 and 4-point functions is the same as setting the momenta themselves to zero. A subtle point of setting external momenta to zero is that in a diagram a term of the form $p_\mu p_\nu T^{\mu\nu}(p, m_i)$, with p an external momentum, m_i mass parameters and $T^{\mu\nu}$ a tensor (DR) integral, may appear. If we set $p = 0$ before integration, this term is zero. If on the other hand we do the integral first, then contract and then take the limit $p \to 0$, we may find a non-zero result. The latter procedure is the correct one. Expressions of the form of Eq. (2.2.11) in the main text will be thus given at zero external momenta. Nevertheless, for completeness and for potential future use, we collect some on-shell expressions in Appendix 2.F.

2.3 R_ξ gauge

Quantization of Eq. (2.2.7) requires gauge fixing. The gauge fixing term

$$\mathcal{L}_{\rm gf} = \frac{1}{2\xi}(\partial^\mu A^0_\mu - \xi g_0 v_0 \chi_0)^2 \tag{2.3.1}$$

that removes the Goldstone-gauge boson mixing defines the R_ξ gauge and under the standard Faddeev-Popov procedure introduces the extra ghost contribution

$$\mathcal{L}_{ghost} = (\partial_\mu \bar{c})\,(\partial^\mu c) - \xi m_{Z_0}^2 \bar{c} c\,. \tag{2.3.2}$$

The sum $\mathcal{L}_{R_\xi} = \mathcal{L}_0 + \mathcal{L}_{\rm gf} + \mathcal{L}_{ghost}$

$$\begin{aligned}
\mathcal{L}_{R_\xi} &= -\frac{1}{4}F^2_{\mu\nu} + \frac{1}{2}\left(\partial_\mu\phi_0\right)\left(\partial^\mu\phi_0\right) + \frac{1}{2}\left(\partial_\mu\chi_0\right)\left(\partial^\mu\chi_0\right) - \frac{1}{2\xi}\left(\partial^\mu A^0_\mu\right)^2 + \frac{1}{2}m^2_{Z_0}A^0_\mu A^{0\mu} \\
&+ 2\frac{m_{Z_0}}{m_{H_0}}\sqrt{2\lambda_0}A^0_\mu(\partial^\mu\chi_0)\phi_0 + \frac{\sqrt{2\lambda_0}}{m_{H_0}}(\partial_\mu\chi_0)^2\phi_0 + \frac{2\lambda_0 m_{Z_0}}{m^2_{H_0}}A^0_\mu(\partial^\mu\chi_0)\phi_0^2 + \frac{\lambda_0}{m^2_{H_0}}(\partial_\mu\chi_0)^2\phi_0^2 \\
&+ g^{\mu\nu}\frac{\lambda_0 m^2_{Z_0}}{m^2_{H_0}}A^0_\mu A^0_\nu\phi_0^2 + g^{\mu\nu}\frac{m^2_{Z_0}}{m_{H_0}}\sqrt{2\lambda_0}\phi_0 A^0_\mu A^0_\nu - \frac{1}{2}\xi m^2_{Z_0}\chi_0^2 \\
&- \frac{1}{2}m^2_{H_0}\phi_0^2 - \sqrt{\frac{\lambda_0}{2}}m_{H_0}\phi_0^3 - \frac{\lambda_0}{4}\phi_0^4 + \mathcal{L}_{ghost} + const.
\end{aligned} \tag{2.3.3}$$

yields the final expression from which the R_ξ gauge Feynman rules can be derived. Notice that the Goldstone has acquired an unphysical, gauge dependent mass $m_{\chi_0} = \sqrt{\xi} m_{Z_0}$. With this gauge fixing choice the ghost fields have apart from a kinetic term, a mass term equal to that of the Goldstone boson's but they are not coupled to the Higgs field or to the gauge boson.

The Feynman rules arising from Eq.(2.3.3) are the following:

- Gauge boson propagator

$$= \frac{i\left(-g^{\mu\nu} + \frac{(1-\xi)k^\mu k^\nu}{k^2 - \xi m_{Z_0}^2}\right)}{k^2 - m_{Z_0}^2 + i\varepsilon}$$

- Higgs propagator

$$= \frac{i}{k^2 - m_{H_0}^2 + i\varepsilon}$$

- Goldstone propagator

$$= \frac{i}{k^2 - \xi m_{Z_0}^2 + i\varepsilon}$$

- Ghost propagator

$$= \frac{i}{k^2 - \xi m_{Z_0}^2 + i\varepsilon}$$

- ϕ-χ-Z vertex

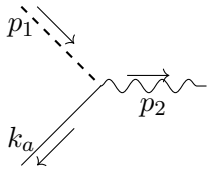

$$= -\frac{2m_{Z_0}}{m_{H_0}}\sqrt{2\lambda_0}k_a^\mu$$

- ϕ-Z-Z vertex

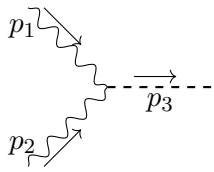

$$= 2ig^{\mu\nu}\frac{m_{Z_0}^2}{m_{H_0}}\sqrt{2\lambda_0}$$

- ϕ-ϕ-ϕ vertex

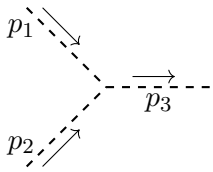

$$= -6i\sqrt{\frac{\lambda_0}{2}}m_{H_0}$$

- ϕ-χ-χ vertex

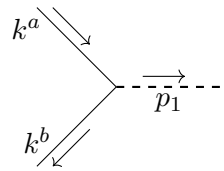

$$= 2ig^{\mu\nu}\frac{\sqrt{2\lambda_0}}{m_{H_0}}k^a_\mu k^b_\nu$$

- ϕ-ϕ-Z-Z vertex

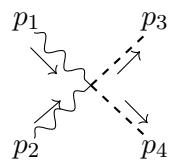

$$= 4i\frac{\lambda_0 m^2_{Z_0}}{m^2_{H_0}}g^{\mu\nu}$$

- ϕ-ϕ-ϕ-ϕ vertex

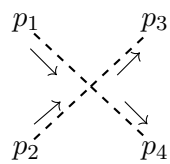

$$= -6i\lambda_0$$

- ϕ-ϕ-χ-Z vertex

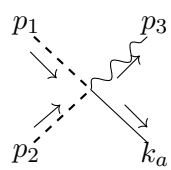

$$= -4\frac{\lambda_0 m_{Z_0}}{m^2_{H_0}}k^\mu_a$$

- ϕ-ϕ-χ-χ vertex

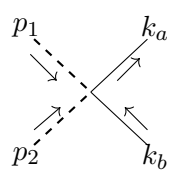

$$= 4ig^{\mu\nu}\frac{\lambda_0}{m^2_{H_0}}k^a_\mu k^b_\nu$$

In the above rules, $k_{a,b}$ denotes the momenta of the Goldstone bosons in a vertex. In the case that we have two Goldstones in a diagram, we choose the convention where one of them gets in and the other gets out of the vertex (since we will encounter the Goldstone only in loops).

The momentum dependence of the vertices including at least one Goldstone boson is a direct consequence of our choice to use the Polar instead of the Cartesian basis for the Higgs field, as in the latter case there are no such vertices. As a result, the corresponding loop integrals will have extra loop momentum factors in their numerator and this triggers the appearance of U-integrals (also) in the R_ξ gauge.

In what follows, we present only the final expressions for the divergent and finite parts of the various sectors given at zero external momenta. The explicit calculation steps that we followed are given in the Appendix 2.D.

2.3.1 Tadpoles

One-point functions are also called tadpoles. The first such diagram is

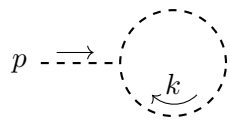

$$= i\mathcal{T}_H^{R_\xi,\phi}$$

and analytically evaluates to

$$\mathcal{T}_H^{R_\xi,\phi} = 3\sqrt{\frac{\lambda_0}{2}} m_{H_0} \mu^\varepsilon A_0(m_{H_0})\,. \tag{2.3.4}$$

The next tadpole comes with a gauge boson loop:

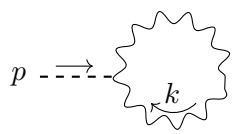

$$= i\mathcal{T}_H^{R_\xi,Z}$$

and it is equal to

$$\mathcal{T}_H^{R_\xi,Z} \quad = \quad \frac{m_{Z_0}^2}{m_{H_0}} \sqrt{2\lambda_0} \mu^\varepsilon \left\{ 3A_0(m_{Z_0}) + \xi A_0(\sqrt{\xi} m_{Z_0}) \right\}. \tag{2.3.5}$$

The last tadpole has a Goldstone loop:

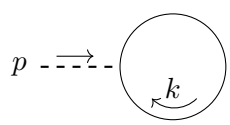

$$= i\mathcal{T}_H^{R_\xi,\chi}$$

Using Eq.(2.C.2) where $U_{\mathcal{T}}(m_{\chi_0})$ is calculated we obtain that the above diagram is equal to

$$\mathcal{T}_H^{R_\xi,\chi} = -\frac{\sqrt{2\lambda_0}}{m_{H_0}} \mu^\varepsilon m_{\chi_0}^2 A_0(m_{\chi_0})\,. \tag{2.3.6}$$

The total tadpole value is the sum of the above three contributions:

$$\mathcal{T}_H^{R_\xi} \quad = \quad \mu^\varepsilon \left(3\sqrt{\frac{\lambda_0}{2}} m_{H_0} A_0(m_H) + 3\frac{\sqrt{2\lambda_0} m_{Z_0}^2}{m_{H_0}} A_0(m_Z) \right). \tag{2.3.7}$$

Exploiting our notation it can also be expressed as

$$(4\pi)^{d/2} \mathcal{T}_H^{R_\xi} = \mu^\varepsilon \left([\mathcal{T}_H^{R_\xi}]_\varepsilon + \left\{ \mathcal{T}_H^{R_\xi} \right\}_\varepsilon + [\mathcal{T}_H^{R_\xi}]_f + \left\{ \mathcal{T}_H^{R_\xi} \right\}_f \right),$$

with

$$\varepsilon[\mathcal{T}_H^{R_\xi}]_\varepsilon \quad = \quad 6\sqrt{\frac{\lambda_0}{2}} m_{H_0}^3 + 6\frac{\sqrt{2\lambda_0} m_{Z_0}^4}{m_{H_0}}$$

$$\left\{\mathcal{T}_H^{R_\xi}\right\}_\varepsilon = 0 \tag{2.3.8}$$

and

$$\begin{aligned}
[\mathcal{T}_H^{R_\xi}]_f &= 3\sqrt{\frac{\lambda_0}{2}}m_{H_0}^3 + 3\frac{\sqrt{2\lambda_0}m_{Z_0}^4}{m_{H_0}} + 3\sqrt{\frac{\lambda_0}{2}}m_{H_0}^3 \ln\frac{\mu^2}{m_{H_0}^2} + 3\frac{\sqrt{2\lambda_0}m_{Z_0}^4}{m_{H_0}}\ln\frac{\mu^2}{m_{Z_0}^2} \\
\left\{\mathcal{T}_H^{R_\xi}\right\}_f &= 0\,. \qquad (2.3.9)
\end{aligned}$$

These expressions show that the tadpole sum is ξ-independent both in its divergent and in its finite part. Note that tadpoles are external momentum independent objects.
A detailed descriptions of the steps that we followed is presented in Appendix 2.D.1.

2.3.2 Corrections to the gauge boson mass

Starting the 2-point function calculations, before we compute the Higgs 2-point function, we first move out of the way the Z 2-point function. It will be needed for the renormalization of the Z mass.

A gauge-boson vacuum polarization amplitude can be Lorentz-covariantly split into a transverse and a longitudinal part, as we show in Appendix 2.D.1. So, following this procedure we obtain that the quantity that enters in the renormalization of the mass of the Z gauge boson is therefore

$$\mathcal{M}_Z = -\frac{1}{3}\left(g^{\mu\nu} - \frac{p^\mu p^\nu}{p^2}\right)\mathcal{M}_{Z,\mu\nu}(p)\,. \tag{2.3.10}$$

We now start computing the one-loop Feynman diagrams contributing to $\mathcal{M}_{Z,\mu\nu}^{R_\xi}$.

The first contributing diagram has a Higgs running in the loop:

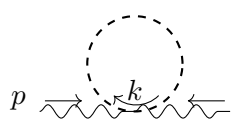

$$= i\mathcal{M}_{Z,\mu\nu}^{R_\xi,\phi}$$

and, in DR, it is equal to

$$\mathcal{M}_{Z,\mu\nu}^{R_\xi,\phi} = -2g_{\mu\nu}\frac{m_{Z_0}^2}{m_{H_0}^2}\lambda_0\mu^\varepsilon A_0(m_{H_0})\,. \tag{2.3.11}$$

Next we meet a couple of "sunset" diagrams. The first is

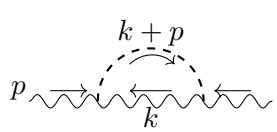

$$= i\mathcal{M}_{Z,\mu\nu}^{R_\xi,\phi Z}$$

In DR and using Eq. (2.B.35), it can be expressed as

$$\mathcal{M}_{Z,\mu\nu}^{R_\xi,\phi Z} = 8\frac{m_{Z_0}^4}{m_{H_0}^2}\lambda_0\mu^\varepsilon\left\{-g_{\mu\nu}B_0(p,m_{Z_0},m_{H_0}) + (1-\xi)C_{\mu\nu}^1(p,m_{Z_0},m_{H_0},m_{\chi_0})\right\}.$$

Notice that the C-type integral above is a special PV case, computed in Appendix 2.B as well.

The next sunset diagram is the last that contributes to the one-loop correction of the gauge boson propagator:

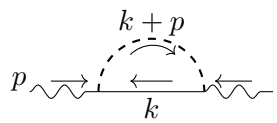

$$= i\mathcal{M}^{R_\xi,\chi\phi}_{Z,\mu\nu}$$

and its explicit form reads

$$\mathcal{M}^{R_\xi,\chi\phi}_{Z,\mu\nu} = 8\frac{m^2_{Z_0}}{m^2_{H_0}}\lambda_0\mu^\varepsilon B_{\mu\nu}(p, m_{\chi_0}, m_{H_0})\,. \tag{2.3.12}$$

Adding up all contributions we obtain

$$\begin{aligned}\mathcal{M}^{R_\xi}_{Z,\mu\nu} &= \frac{m^2_{Z_0}}{m^2_{H_0}}\lambda_0\mu^\varepsilon\Big\{-2g_{\mu\nu}A_0(m_{H_0}) - 8g_{\mu\nu}m^2_{Z_0}B_0(p, m_{Z_0}, m_{H_0}) \\ &+ 8(1-\xi)m^2_{Z_0}C^1_{\mu\nu}(m_{Z_0}, m_{H_0}, m_{\chi_0}) + 8B_{\mu\nu}(p, m_{\chi_0}, m_{H_0})\Big\}\,.\end{aligned} \tag{2.3.13}$$

The contraction that we need is Eq. (2.3.10), which for general p has the form

$$\begin{aligned}\mathcal{M}^{R_\xi}_Z(p) &= -\frac{1}{3}\frac{m^2_{Z_0}}{m^2_{H_0}}\lambda_0\frac{\mu^\varepsilon}{16\pi^2}\Bigg(\Big\{-2(d+\varepsilon)A_0(m_{H_0}) - 8(d+\varepsilon)m^2_{Z_0}B_0(p, m_{Z_0}, m_{H_0}) \\ &+ 8(1-\xi)m^2_{Z_0}g^{\mu\nu}C^1_{\mu\nu}(p, m_{Z_0}, m_{H_0}, m_{\chi_0}) + 8g^{\mu\nu}B_{\mu\nu}(p, m_{\chi_0}, m_{H_0})\Big\} \\ &- \Big\{-2A_0(m_H) - 8m^2_{Z_0}B_0(p, m_{Z_0}, m_{H_0}) \\ &+ 8(1-\xi)m^2_{Z_0}\frac{p^\mu p^\nu}{p^2}C^1_{\mu\nu}(p, m_{Z_0}, m_{H_0}, m_{\chi_0}) + 8\frac{p^\mu p^\nu}{p^2}B_{\mu\nu}(p, m_{\chi_0}, m_{H_0})\Big\}\Bigg)\,.\end{aligned} \tag{2.3.14}$$

Specializing now to $p = 0$, we can express the result as

$$(4\pi)^{d/2}\mathcal{M}^{R_\xi}_Z = \mu^\varepsilon\left([\mathcal{M}^{R_\xi}_Z]_\varepsilon + \left\{\mathcal{M}^{R_\xi}_Z\right\}_\varepsilon + [\mathcal{M}^{R_\xi}_Z]_f + \left\{\mathcal{M}^{R_\xi}_Z\right\}_f\right)\,, \tag{2.3.15}$$

with

$$\begin{aligned}\varepsilon[\mathcal{M}^{R_\xi}_Z]_\varepsilon &= 12\frac{\lambda_0 m^4_{Z_0}}{m^2_{H_0}} \\ \left\{\mathcal{M}^{R_\xi}_Z\right\}_\varepsilon &= 0\,.\end{aligned} \tag{2.3.16}$$

The anomalous dimension of Z can be also determined now, through the relation

$$\delta A^{R_\xi} = -\left.\frac{d\mathcal{M}^{R_\xi}_Z(p)}{dp^2}\right|_{p^2=0} = \frac{\mu^\varepsilon}{(4\pi)^{d/2}}\left([\delta A^{R_\xi}]_\varepsilon + \left\{\delta A^{R_\xi}\right\}_\varepsilon + [\delta A^{R_\xi}]_f + \left\{\delta A^{R_\xi}\right\}_f\right)\,,$$

(2.3.17)

with

$$\begin{aligned}\varepsilon[\delta A^{R_\xi}]_\varepsilon &= -\frac{4}{3}\lambda_0\frac{m_{Z_0}^2}{m_{H_0}^2}\\ \left\{\delta A^{R_\xi}\right\}_\varepsilon &= 0\,.\end{aligned} \tag{2.3.18}$$

Evidently, all divergent parts in this sector are ξ-independent.

Regarding the finite parts, we have

$$\begin{aligned}(\mathcal{M}_Z^{R_\xi})_f &= -\frac{\lambda_0 m_{Z_0}^4(\xi-19)}{3m_{H_0}^2}+\frac{8\lambda_0 m_{Z_0}^6(\xi-1)\xi\ln\frac{m_{Z_0}^2}{m_{H_0}^2}}{3\left(m_{H_0}^2-m_{Z_0}^2\right)\left(m_{H_0}^2-m_{Z_0}^2\xi\right)}\\ &+\frac{2\lambda_0 m_{Z_0}^4\ln\left(m_{H_0}^2\right)\left(m_{H_0}^2(\xi-9)+4m_{Z_0}^2\xi(\xi+1)\right)}{3\left(m_{H_0}^2-m_{Z_0}^2\right)\left(m_{H_0}^2-m_{Z_0}^2\xi\right)}\\ &-\frac{2\lambda_0 m_{Z_0}^4\ln\left(m_{Z_0}^2\right)\left(m_{Z_0}^4\xi+m_{H_0}^2m_{Z_0}^2\left(4\xi^2-5\xi-9\right)+9m_{Z_0}^4\xi\right)}{3m_{H_0}^2\left(m_{H_0}^2-m_{Z_0}^2\right)\left(m_{H_0}^2-m_{Z_0}^2\xi\right)}\\ &+\frac{6\lambda_0 m_{Z_0}^4\ln\mu^2}{m_{H_0}^2}+\frac{8\lambda_0 m_{Z_0}^4}{3m_{H_0}^2}-\frac{2\lambda_0 m_{Z_0}^4\xi\ln\xi}{3m_{H_0}^2-3m_{Z_0}^2\xi}-\frac{4\lambda_0 m_{Z_0}^2}{3}\end{aligned} \tag{2.3.19}$$

and

$$(\delta A^{R_\xi})_f = -\frac{2}{3}\frac{m_{Z_0}^2\lambda_0}{(m_{H_0}^2-m_{Z_0}^2\xi)}\left(\left(1+\ln\frac{\mu^2}{m_{H_0}^2}\right)-\frac{m_{Z_0}^2}{m_{H_0}^4}\left(1+\xi\ln\frac{\mu^2}{\xi m_{Z_0}^2}\right)\right)\,. \tag{2.3.20}$$

The finite parts here are gauge dependent and we do not separate them further to ξ-independent and ξ-dependent parts. The limit $\xi\to\infty$ is divergent.

2.3.3 Corrections to the Higgs mass

We move on to the Higgs propagator. The first diagram we encounter is

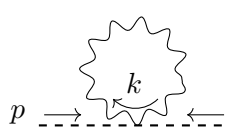

$$= i\mathcal{M}_H^{R_\xi,Z}$$

and after reductions performed in Appendix 2.D.1, finally the above integral is written as

$$\mathcal{M}_H^{R_\xi,Z} = \frac{m_{Z_0}^2}{m_{H_0}^2}\lambda_0\mu^\varepsilon\left\{6A_0(m_{Z_0})+2\xi A_0(m_{\chi_0})\right\}. \tag{2.3.21}$$

The next contribution comes from the diagram

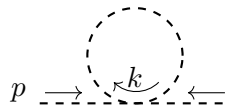

$$= i\mathcal{M}_H^{R_\xi,\phi}$$

and its explicit form is given by

$$\mathcal{M}_H^{R_\xi,\phi} = 3\lambda_0\mu^\varepsilon A_0(m_{H_0}) \tag{2.3.22}$$

in DR.

Next comes the Goldstone loop

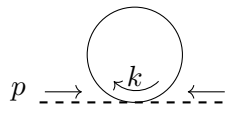

$$= i\mathcal{M}_H^{R_\xi,\chi}$$

which, following Appendix 2.D.1, is equal to

$$\mathcal{M}_H^{R_\xi,\chi} = -\frac{2\lambda_0}{m_{H_0}^2}\mu^\varepsilon m_{\chi_0}^2 A_0(m_{\chi_0})\,. \tag{2.3.23}$$

It is easy to check that all of the above three diagrams are reducible Tadpoles corresponding to the three Tadpoles of Section 2.3.1.

A few vacum polarization diagrams are in order. The first is

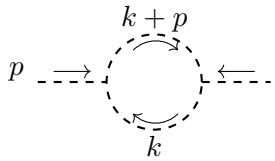

$$= i\mathcal{M}_H^{R_\xi,\phi\phi}$$

and in DR, is equal to

$$\mathcal{M}_H^{R_\xi,\phi\phi} \quad = \quad 9\lambda_0 m_{H_0}^2\mu^\varepsilon B_0(p, m_{H_0}, m_{H_0})\,. \tag{2.3.24}$$

The Goldstone loop contribution

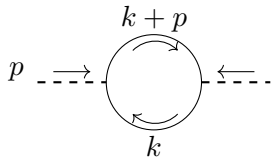

$$= i\mathcal{M}_H^{R_\xi,\chi\chi}$$

which, following Appendix 2.D.1, takes in DR the final form

$$\mathcal{M}_H^{R_\xi,\chi\chi} \quad = \quad 4\frac{\lambda_0}{m_{H_0}^2}\mu^\varepsilon\left\{m_{\chi_0}^2 A_0(m_{\chi_0}) + (m_{\chi_0}^2 - p^2)g_{\mu\nu}B^{\mu\nu}(p, m_{\chi_0}, m_{\chi_0}) + p_\mu p_\nu B^{\mu\nu}(p, m_{\chi_0}, m_{\chi_0})\right\}. \tag{2.3.25}$$

Slightly more complicated is the gauge boson loop

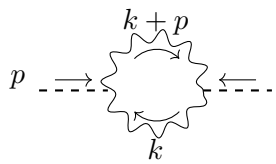

$$= i\mathcal{M}_H^{R_\xi,ZZ}$$

and expressing it by standard steps in terms of PV integrals, it becomes

$$\begin{aligned}
\mathcal{M}_H^{R_\xi,ZZ} &= 4\frac{m_{Z_0}^4}{m_{H_0}^2}\lambda_0\mu^\varepsilon\Bigg\{dB_0(p,m_{Z_0},m_{Z_0}) - (1-\xi)\Big\{g_{\mu\nu}C^{1\mu\nu}(p,m_{Z_0},m_{Z_0},m_{\chi_0}) \\
&+ g_{\mu\nu}C^{\mu\nu}(p,p,m_{Z_0},m_{Z_0},m_{\chi_0})\Big\} \\
&+ (1-\xi)^2\Big\{g_{\mu\nu}C^{1\mu\nu}(p,m_{Z_0},m_{Z_0},m_{\chi_0}) \\
&+ (m_{Z_0}^2-p^2)g_{\mu\nu}D^{\mu\nu}(p,m_{Z_0},m_{Z_0},m_{\chi_0},m_{\chi_0}) + p_\mu p_\nu D^{\mu\nu}(p,m_{Z_0},m_{Z_0},m_{\chi_0},m_{\chi_0})\,,\Big\}\Bigg\}
\end{aligned} \tag{2.3.26}$$

where the $a = 1,2,3$ superscripts on the C_0-integrals correspond to the different combinations of the denominators according to Eq. (2.B.12) of Appendix 2.B. The $D^{\mu\nu}$ integrals are defined in Eq. (2.B.39).

The last contribution to the one-loop correction of the Higgs mass comes from the sunset

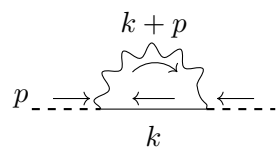

$$= i\mathcal{M}_H^{R_\xi,\chi Z}$$

where using again the standard steps, we are allowed to write this as

$$\begin{aligned}
\mathcal{M}_H^{R_\xi,\chi Z} &= 8\lambda_0\frac{m_{Z_0}^2}{m_{H_0}^2}\mu^\varepsilon\Bigg\{-g_{\mu\nu}B^{\mu\nu}(p,m_{\chi_0},m_{Z_0}) \\
&+ (1-\xi)\Big\{g_{\mu\nu}B^{\mu\nu}(p,m_{\chi_0},m_{\chi_0}) + (m_{Z_0}^2-p^2)g_{\mu\nu}C^{1\mu\nu}(p,m_{Z_0},m_{\chi_0},m_{Z_0}) \\
&+ p_\mu p_\nu C^{1\mu\nu}(p,m_{\chi_0},m_{Z_0},m_{\chi_0})\Big\}\Bigg\}\,,
\end{aligned} \tag{2.3.27}$$

where $C^1_{\mu\nu}$ is defined in Eq. (2.B.34) in Appendix 2.B.

Finally, summing up all contributions into $\mathcal{M}_H^{R_\xi}$ we obtain

$$\begin{aligned}
\mathcal{M}_H^{R_\xi}(p) &= \mu^\varepsilon\Bigg\{3\lambda_0A_0(m_{H_0}) + 6\frac{m_{Z_0}^2}{m_{H_0}^2}\lambda_0A_0(m_{Z_0}) + 2\xi\frac{m_{Z_0}^2}{m_{H_0}^2}\lambda_0A_0(m_{\chi_0}) \\
&- 2\frac{\lambda_0}{m_{H_0}^2}m_{\chi_0}^2A_0(m_{\chi_0}) + 9\lambda_0m_{H_0}^2B_0(p,m_{H_0},m_{H_0}) \\
&+ 4\frac{\lambda_0}{m_{H_0}^2}\left(m_{\chi_0}^2A_0(m_{\chi_0}) + (m_{\chi_0}^2-p^2)g_{\mu\nu}B^{\mu\nu}(p,m_{\chi_0},m_{\chi_0}) + p_\mu p_\nu B^{\mu\nu}(p,m_{\chi_0},m_{\chi_0})\right)
\end{aligned}$$

$$
\begin{aligned}
&+ \quad 4d\frac{m_{Z_0}^4}{m_{H_0}^2}\lambda_0 B_0(p,m_{Z_0},m_{Z_0}) - 8\lambda_0\frac{m_{Z_0}^2}{m_{H_0}^2}g_{\mu\nu}B^{\mu\nu}(p,m_{\chi_0},m_{Z_0}) \\
&+ \quad \frac{m_{Z_0}^2}{m_{H_0}^2}\lambda_0(1-\xi)\Big\{-4m_{Z_0}^2 g_{\mu\nu}C^{1\mu\nu}(p,m_{Z_0},m_{Z_0},m_{\chi_0}) - 4m_{Z_0}^2 g_{\mu\nu}C^{\mu\nu}(p,p,m_{Z_0},m_{Z_0},m_{\chi_0}) \\
&+ \quad 8g_{\mu\nu}B^{\mu\nu}(p,m_{\chi_0},m_{\chi_0}) + 8(m_{Z_0}^2-p^2)g_{\mu\nu}C^{1\mu\nu}(p,m_{\chi_0},m_{Z_0},m_{\chi_0}) \\
&+ \quad 8p_\mu p_\nu C^{1\mu\nu}(p,m_{\chi_0},m_{Z_0},m_{\chi_0})\Big\} \\
&+ \quad 4\frac{m_{Z_0}^4}{m_{H_0}^2}\lambda_0(1-\xi)^2\Big\{g_{\mu\nu}C^{1\mu\nu}(p,m_{Z_0},m_{Z_0},m_{\chi_0}) \\
&+ \quad (m_{Z_0}^2-p^2)g_{\mu\nu}D^{\mu\nu}(p,m_{Z_0},m_{Z_0},m_{\chi_0},m_{\chi_0}) + p_\mu p_\nu D^{\mu\nu}(p,m_{Z_0},m_{Z_0},m_{\chi_0},m_{\chi_0})\Big\}\Bigg\}\,.
\end{aligned}
\tag{2.3.28}
$$

Note that the reduction of the $g_{\mu\nu}D^{\mu\nu}$ and $p_\mu p_\nu D^{\mu\nu}$ terms give only C_0 and D_0 contributions which are finite. We then have that

$$
(4\pi)^{d/2}\mathcal{M}_H^{R_\xi} = \mu^\varepsilon\left([\mathcal{M}_H^{R_\xi}]_\varepsilon + \left\{\mathcal{M}_H^{R_\xi}\right\}_\varepsilon + [\mathcal{M}_H^{R_\xi}]_f + \left\{\mathcal{M}_H^{R_\xi}\right\}_f\right) \tag{2.3.29}
$$

with

$$
\begin{aligned}
\varepsilon[\mathcal{M}_H^{R_\xi}]_\varepsilon &= 24\lambda_0 m_{H_0}^2 + 36\frac{\lambda_0 m_{Z_0}^4}{m_{H_0}^2} \\
\left\{\mathcal{M}_H^{R_\xi}\right\}_\varepsilon &= 0
\end{aligned}
\tag{2.3.30}
$$

and

$$
\begin{aligned}
[\mathcal{M}_H^{R_\xi}]_f &= 3\lambda_0 m_{H_0}^2 + 6\frac{\lambda_0 m_{Z_0}^4}{m_{H_0}^2} + 12\lambda_0 m_{H_0}^2\ln\frac{\mu^2}{m_{H_0}^2} + 18\frac{\lambda_0 m_{Z_0}^4}{m_{H_0}^2}\ln\frac{\mu^2}{m_{Z_0}^2} \\
\left\{\mathcal{M}_H^{R_\xi}\right\}_f &= 0
\end{aligned}
\tag{2.3.31}
$$

at $p=0$.

We are also able to compute the anomalous dimension of the Higgs, determined by

$$
\delta\phi^{R_\xi} = -\frac{d\mathcal{M}_H^{R_\xi}(p)}{dp^2}\bigg|_{p^2=0} = \frac{\mu^\varepsilon}{(4\pi)^{d/2}}\left([\delta\phi^{R_\xi}]_\varepsilon + \left\{\delta\phi^{R_\xi}\right\}_\varepsilon + [\delta\phi^{R_\xi}]_f + \left\{\delta\phi^{R_\xi}\right\}_f\right)
$$

with

$$
\begin{aligned}
\varepsilon[\delta\phi^{R_\xi}]_\varepsilon &= 12\lambda_0\frac{m_{Z_0}^2}{m_{H_0}^2} \\
\left\{\delta\phi^{R_\xi}\right\}_\varepsilon &= 0\,.
\end{aligned}
\tag{2.3.32}
$$

and

$$
\begin{aligned}
[\delta\phi^{R_\xi}]_f &= 2\lambda_0\frac{m_{Z_0}^2}{m_{H_0}^2} + 6\lambda_0\frac{m_{Z_0}^2}{m_{H_0}^2}\ln\frac{\mu^2}{m_{Z_0}^2} \\
\left\{\delta\phi^{R_\xi}\right\}_f &= 0\,.
\end{aligned}
\tag{2.3.33}
$$

This sector turns out to be ξ-independent.

2.3.4 Corrections to the Higgs cubic vertex

Triangle diagrams with Higgs external legs yield corrections to the Higgs cubic vertex. Such corrections will play a crucial role in the definition of the one-loop scalar potential. The external momenta are taken to be all inflowing, thus satisfying $p_1 + p_2 + p_3 = 0$. Triangle diagrams can be split in "reducible" and "irreducible" kinds. Reducible are those that are expressible in terms of 2-point function diagrams and irreducible are those that are not.

Reducible Triangles

The first reducible Triangle diagram is:

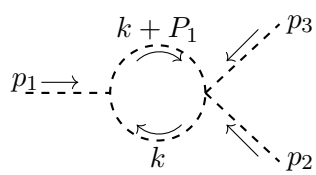

$$= \; i\mathcal{K}_H^{R_\xi,\phi\phi}$$

As anticipated, it is not an independent diagram. It is the same loop-diagram as in Eq. (2.D.35) (with the same symmetry factor), divided by v_0. We can therefore write directly the result:

$$\mathcal{K}_H^{R_\xi,\phi\phi} \;=\; 3 \cdot 18 \frac{\lambda_0^{3/2}}{\sqrt{2}} m_{H_0} \mu^\varepsilon B_0(P_1, m_{H_0}, m_{H_0})\,. \tag{2.3.34}$$

The factor of 3 is due to two additional diagrams, obtained from the above by cyclically permuting the external momenta. These contributions however, evaluated at either $p_1 = p_2 = p_3 = 0$ or $p_1^2 = p_2^2 = p_3^2 = m_H^2$ give an identical result.

The next diagram is one with a Goldstone in the loop:

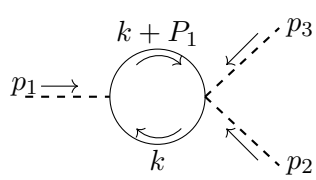

$$= \; i\mathcal{K}_H^{R_\xi,\chi\chi}$$

and it is equal to Eq. (2.D.37) divided by v_0:

$$\mathcal{K}_H^{R_\xi,\chi\chi} = \\ 3 \cdot 8 \frac{\lambda_0^{3/2}}{m_{H_0}^3} \mu^\varepsilon \left\{ m_{\chi_0}^2 A_0(m_{\chi_0}) + (m_{\chi_0}^2 - P_1^2) g_{\mu\nu} B^{\mu\nu}(P_1, m_{\chi_0}, m_{\chi_0}) + P_{1\mu} P_{1\nu} B^{\mu\nu}(P_1, m_{\chi_0}, m_{\chi_0}) \right\}. \tag{2.3.35}$$

The factor of 3 has a similar origin as before.

The diagram with a gauge boson loop

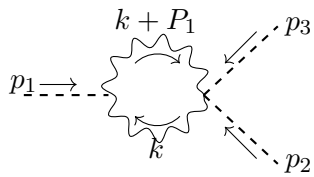

$$= \; i\mathcal{K}_H^{R_\xi,ZZ}$$

is equal to Eq. (2.D.40) divided by v_0:

$$\begin{aligned}
\mathcal{K}_H^{R_\xi,ZZ} &= 3\cdot\frac{8}{\sqrt{2}}\frac{m_{Z_0}^4}{m_{H_0}^3}\lambda_0^{3/2}\mu^\varepsilon\Bigg\{dB_0(P_1,m_{Z_0},m_{Z_0})-(1-\xi)\Big\{g_{\mu\nu}C^{1\mu\nu}(p,m_{Z_0},m_{Z_0},m_{\chi_0}) \\
&+ g_{\mu\nu}C^{1\mu\nu}(P_1,m_{Z_0},m_{Z_0},m_{\chi_0})\Big\} \\
&+ (1-\xi)^2\Big\{g_{\mu\nu}C^{1\mu\nu}(P_1,m_{Z_0},m_{Z_0},m_{\chi_0}) \\
&+ (m_{Z_0}^2-P_1^2)g_{\mu\nu}D^{\mu\nu}(P_1,m_{Z_0},m_{Z_0},m_{\chi_0},m_{\chi_0})+P_{1\mu}P_{1\nu}D^{\mu\nu}(P_1,m_{Z_0},m_{Z_0},m_{\chi_0},m_{\chi_0})\,,\Big\}\Bigg\}.
\end{aligned} \tag{2.3.36}$$

The last reducible Triangle is:

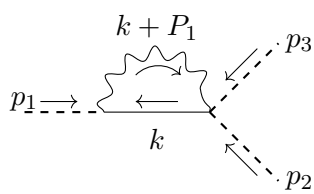

$$= \; i\mathcal{K}_H^{R_\xi,\chi Z}$$

It is the same as Eq. (2.D.42) divided by v_0:

$$\begin{aligned}
\mathcal{K}_H^{R_\xi,\chi Z} &= 3\cdot\frac{16}{\sqrt{2}}\lambda_0^{3/2}\frac{m_{Z_0}^2}{m_{H_0}^3}\mu^\varepsilon\Bigg\{-g_{\mu\nu}B^{\mu\nu}(P_1,m_{\chi_0},m_{Z_0}) \\
&+ (1-\xi)\Big\{g_{\mu\nu}B^{\mu\nu}(P_1,m_{\chi_0},m_{\chi_0})+(m_{Z_0}^2-P_1^2)g_{\mu\nu}C^{1\mu\nu}(P_1,m_{Z_0},m_{\chi_0},m_{Z_0}) \\
&+ P_{1\mu}P_{1\nu}C^{1\mu\nu}(P_1,m_{\chi_0},m_{Z_0},m_{\chi_0})\Big\}\Bigg\}.
\end{aligned} \tag{2.3.37}$$

Let us collect all reducible Triangle contributions by adding Eq. (2.3.34), Eq. (2.3.35), Eq. (2.3.36) and Eq. (2.3.37). At zero external momenta, we obtain

$$(4\pi)^{d/2}\mathcal{K}_H^{R_\xi,\text{red.}} = \mu^\varepsilon\left([\mathcal{K}_H^{R_\xi,\text{red.}}]_\varepsilon+\left\{\mathcal{K}_H^{R_\xi,\text{red.}}\right\}_\varepsilon+[\mathcal{K}_H^{R_\xi,\text{red.}}]_f+\left\{\mathcal{K}_H^{R_\xi,\text{red.}}\right\}_f\right), \tag{2.3.38}$$

with

$$\begin{aligned}
\varepsilon[\mathcal{K}_H^{R_\xi,\text{red.}}]_\varepsilon &= \frac{m_{H_0}}{\sqrt{2\lambda_0}}\left(108\lambda_0^2+144\frac{\lambda_0^2 m_{Z_0}^4}{m_{H_0}^4}\right) \\
\left\{\mathcal{K}_H^{R_\xi,\text{red.}}\right\}_\varepsilon &= 0.
\end{aligned} \tag{2.3.39}$$

and

$$
\begin{aligned}
[\mathcal{K}_H^{R_\xi,\text{red.}}]_f &= \frac{m_{H_0}}{\sqrt{2\lambda_0}}\Big(54\lambda_0^2 \ln\frac{\mu^2}{m_{H_0}^2} + 72\frac{\lambda_0^2 m_{Z_0}^4}{m_{H_0}^4}\ln\frac{\mu^2}{m_{Z_0}^2}\Big) \\
\Big\{\mathcal{K}_H^{R_\xi,\text{red.}}\Big\}_f &= 0\,. \qquad (2.3.40)
\end{aligned}
$$

Irreducible Triangles

We now turn to the irreducible Triangles. All irreducible Triangle diagrams can be labelled by the momenta $P_1 = p_1$ and $P_2 = p_1 + p_3$. A simplifying consequence of renormalizing at $p_i = 0$ is that we can set $P_i = 0$, hence we can extract both divergent and finite parts, using

$$
\lim_{P_i\to 0} \mathcal{K}_H^{R_\xi,\cdots}(P_1,P_2) \equiv \mathcal{K}_H^{R_\xi,\cdots}(0,0). \qquad (2.3.41)
$$

The limit should be carefully taken, as explained in Sect. 2.2. Regarding denominators, from now on, we start following the notation of Eq. (2.A.3). Here, apart from finite integrals of the E-type, we will also see the appearance of several divergent U-integrals. All finite integrals and U-integrals here and in the following are computed (sometimes without further notice) in Appendices 2.E and 2.C respectively. Finite diagrams do not play a role in the renormalization program but they contribute to the scalar potential.

The first contribution to the irreducible Triangle class involves a Higgs loop and it is finite. It is the diagram

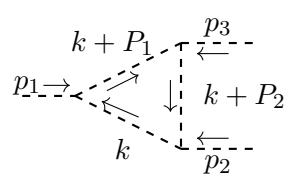

$$
= i\mathcal{K}_H^{R_\xi,\phi\phi\phi}.
$$

It is equal to[1]

$$
\mathcal{K}_H^{R_\xi,\phi\phi\phi} = \frac{108}{\sqrt{2}}\lambda_0^{3/2} m_{H_0}^3 \int \frac{d^4k}{(2\pi)^4}(-i)\frac{1}{D_1 D_2 D_3} \qquad (2.3.42)
$$

with a symmetry factor $S^5_{K_H} = 1$. In DR it can be expressed as

$$
\mathcal{K}_H^{R_\xi,\phi\phi\phi}(P_1,P_2) = \frac{108}{\sqrt{2}}\lambda_0^{3/2} m_{H_0}^3 \mu^\varepsilon C_0(P_1,P_2,m_{H_0},m_{H_0},m_{H_0}). \qquad (2.3.43)
$$

As explained,

$$
\lim_{P_i\to 0} \mathcal{K}_H^{R_\xi,\phi\phi\phi}(P_1,P_2) \equiv \mathcal{K}_H^{R_\xi,\phi\phi\phi}(0,0). \qquad (2.3.44)
$$

There is another finite diagram, the one with a gauge boson loop:

[1] We thank A. Chatziagapiou for pointing out a factor of 2 in this diagram that was missing in the previous version of the paper.

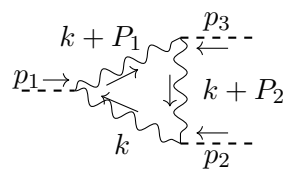

$$= \; i\mathcal{K}_H^{R_\xi,ZZZ}$$

It is equal to

$$\begin{aligned}\mathcal{K}_H^{R_\xi,ZZZ} &= -16\sqrt{2}\frac{m_{Z_0}^6\lambda_0^{3/2}}{m_{H_0}^3}g^{\mu\nu}g^{\alpha\beta}g^{\gamma\delta}\int\frac{d^4k}{(2\pi)^4}\frac{-i\left(-g_{\mu\gamma}+\frac{(1-\xi)k_\mu k_\gamma}{k^2-\xi m_{Z_0}^2}\right)}{D_1}\frac{\left(-g_{\nu\alpha}+\frac{(1-\xi)(k+P_1)_\nu(k+P_1)_\alpha}{(k+P_1)^2-\xi m_{Z_0}^2}\right)}{D_2}\\ &\times\frac{\left(-g_{\delta\beta}+\frac{(1-\xi)(k+P_2)_\delta(k+P_2)_\beta}{(k+P_2)^2-\xi m_{Z_0}^2}\right)}{D_3}\end{aligned} \tag{2.3.45}$$

with a symmetry factor $\mathcal{S}^6_{\mathcal{K}_H}=1$. Its expression in DR is

$$\mathcal{K}_H^{R_\xi,ZZZ}(P_1,P_2) \;=\; (K_H^{R_\xi,ZZZ}(P_1,P_2))_f\,, \tag{2.3.46}$$

where we have used the notation for finite (parts of) diagrams, explained in Eq. (2.2.12). Following again previous arguments, at zero momentum we obtain

$$\lim_{P_i\to 0}\mathcal{K}_H^{R_\xi,ZZZ}(P_1,P_2)\equiv\mathcal{K}_H^{R_\xi,ZZZ}(0,0)\,. \tag{2.3.47}$$

This is the first of several irreducible diagrams whose explicit form is not particularly illuminating, so we directly transfer it to Appendix 2.E.

Now, let us move on to diagrams that have both an infinite and a finite part. The first such diagram is

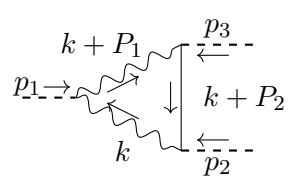

$$= \; i\mathcal{K}_H^{R_\xi,Z\chi Z}$$

It is equal to

$$\begin{aligned}\mathcal{K}_H^{R_\xi,Z\chi Z} &= 32v_0\lambda_0^2\frac{m_{Z_0}^4}{m_{H_0}^4}g^{\mu\nu}\int\frac{d^4k}{(2\pi)^4}\frac{-i\left(-g_{\mu\alpha}+\frac{(1-\xi)k_\mu k_\alpha}{k^2-\xi m_{Z_0}^2}\right)}{D_1}\frac{\left(-g_{\nu\beta}+\frac{(1-\xi)(k+P_1)_\nu(k+P_1)_\beta}{(k+P_1)^2-\xi m_{Z_0}^2}\right)}{D_2}\\ &\times\frac{(k+P_2)^\alpha(k+P_2)^\beta}{D_3}\,,\end{aligned} \tag{2.3.48}$$

with a symmetry factor $\mathcal{S}^7_{\mathcal{K}_H}=1$. In DR it becomes

$$\mathcal{K}_H^{R_\xi,Z\chi Z}(P_1,P_2) \;=\; -32v_0\lambda_0^2\frac{m_{Z_0}^4}{m_{H_0}^4}\mu^\varepsilon\Big\{B_0(P_1,m_{Z_0},m_{Z_0})+m_{\chi_0}^2C_0(P_1,m_{Z_0},m_{Z_0},m_{\chi_0})$$

$$
\begin{aligned}
&- \quad (1-\xi)\Big\{2B_0(P_1, m_{Z_0}, m_{Z_0}) + 2m_{\chi_0}^2 C_0(P_1, m_{Z_0}, m_{Z_0}, m_{\chi_0}) \\
&+ \quad m_{\chi_0}^4 D_0(P_1, P_2, m_{Z_0}, m_{Z_0}, m_{\chi_0}, m_{\chi_0}) + P_2^\mu P_2^\nu D_{\mu\nu}(P_1, P_2, m_{Z_0}, m_{Z_0}, m_{\chi_0}, m_{\chi_0})\Big\} \\
&+ \quad (1-\xi)^2\Big\{D_{\mathcal{B}4}(P_1, P_2, m_{Z_0}, m_{Z_0}, m_{\chi_0}, m_{\chi_0}) \\
&+ \quad m_{\chi_0}^2 E_4(D_1, D_2, D_3, D_4(0, m_{\chi_0}), D_5(P_1, m_{\chi_0})) \\
&+ \quad 2P_{2\mu} E_5^\mu(D_1, D_2, D_3, D_4(0, m_{\chi_0}), D_5(P_1, m_{\chi_0})) \\
&+ \quad P_{2\mu} P_{2\nu} E_4^{\mu\nu}(D_1, D_2, D_3, D_4(0, m_{\chi_0}), D_5(P_1, m_{\chi_0}))\Big\}\Bigg\}, \qquad (2.3.49)
\end{aligned}
$$

where the mass arguments of the $D_{1,2,3}$ denominators are easily recovered from the $Z\chi Z$ superscript structure of the diagram: $D_1(m_Z)$, $D_2(m_\chi)$ and $D_3(m_Z)$. We are not done yet since there are three different ways to insert the Goldstone propagator in the loop. Therefore, there are two more contributing diagrams of the same kind as $\mathcal{K}_H^{R_\xi, Z\chi Z}$. These are the diagrams

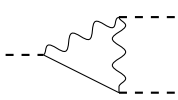

$= i\mathcal{K}_H^{R_\xi, ZZ\chi}(P_1, P_2)$

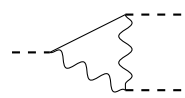

$= i\mathcal{K}_H^{R_\xi, \chi ZZ}(P_1, P_2)$

Performing the calculations at zero external momenta, the above diagrams have identical divergent and finite parts with $\mathcal{K}_H^{R_\xi, Z\chi Z}$, that is

$$
\mathcal{K}_H^{R_\xi, Z\chi Z}(0,0) = \mathcal{K}_H^{R_\xi, ZZ\chi}(0,0) = \mathcal{K}_H^{R_\xi, \chi ZZ}(0,0). \qquad (2.3.50)
$$

Next, we have the diagram with two Goldstones and one gauge boson in the loop:

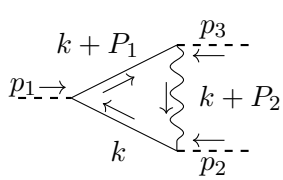

$= i\mathcal{K}_H^{R_\xi, \chi Z\chi}$

It is given by the relation

$$
\mathcal{K}_H^{R_\xi, \chi Z\chi} = -32 v_0 \lambda_0^2 \frac{m_{Z_0}^2}{m_{H_0}^4} \int \frac{d^4k}{(2\pi)^4} \frac{-i\left(-g_{\mu\nu} + \frac{(1-\xi)(k+P_2)_\mu (k+P_2)_\nu}{(k+P_2)^2 - \xi m_{Z_0}^2}\right)}{D_1 D_2 D_3} k^\mu (k+P_1)^\nu (k+P_1)\cdot k \qquad (2.3.51)
$$

with symmetry factor $\mathcal{S}_{\mathcal{K}_H}^8 = 1$. In DR it reads

$$
\begin{aligned}
\mathcal{K}_H^{R_\xi, \chi Z\chi}(P_1, P_2) &= 32 v_0 \lambda_0^2 \frac{m_{Z_0}^2}{m_{H_0}^4} \mu^\varepsilon \Big\{ U_{K4}(P_1, P_2, m_{Z_0}, m_{\chi_0}, m_{\chi_0}) \\
&+ 2(P_1 + P_2)_\mu C_{\mathcal{K}3}^\mu(P_1, P_2, m_{Z_0}, m_{\chi_0}, m_{\chi_0}) \\
&+ (P_{1\mu} P_{1\nu} + 2P_{1\mu} P_{2\nu} + P_{2\mu} P_{2\nu}) C^{\mu\nu}(P_1, P_2, m_{Z_0}, m_{\chi_0}, m_{\chi_0}) \\
&+ 2P_1 \cdot P_2 g_{\mu\nu} C^{\mu\nu}(P_1, P_2, m_{Z_0}, m_{\chi_0}, m_{\chi_0})
\end{aligned}
$$

$$
\begin{aligned}
&- \quad (1-\xi)\Big\{U_{K4}(P_1,P_2,m_{Z_0},m_{\chi_0},m_{\chi_0}) + m_{\chi_0}^2 g_{\mu\nu}C^{\mu\nu}(P_1,P_2,m_{Z_0},m_{\chi_0},m_{\chi_0}) \\
&+ \quad 2(P_1+P_2)_\mu C^\mu_{\mathcal{K}3}(P_1,P_2,m_{Z_0},m_{\chi_0},m_{\chi_0}) \\
&+ \quad (P_{1\mu}P_{1\nu} + 3P_{1\mu}P_{2\nu} + P_{2\mu}P_{2\nu})C^{\mu\nu}(P_1,P_2,m_{Z_0},m_{\chi_0},m_{\chi_0}) \\
&+ \quad P_1\cdot P_2 g_{\mu\nu}C^{\mu\nu}(P_1,P_2,m_{Z_0},m_{\chi_0},m_{\chi_0}) \\
&+ \quad P_1\cdot P_2 P_{1\mu}P_{2\nu}D^{\mu\nu}(P_1,P_2,P_3 m_{Z_0},m_{\chi_0},m_{\chi_0},m_{\chi_0})\Big\}\Bigg\}. \qquad (2.3.52)
\end{aligned}
$$

Now, similarly to the previous case there are three ways to insert the gauge boson in the loop, which means that there are two more diagrams of the same kind as $\mathcal{K}_H^{R_\xi,\chi Z\chi}$:

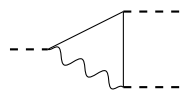

$$= i\mathcal{K}_H^{R_\xi,\chi\chi Z}(P_1,P_2)$$

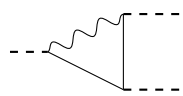

$$= i\mathcal{K}_H^{R_\xi,Z\chi\chi}(P_1,P_2).$$

Again here, at zero external momenta all three diagrams have the same divergent and finite parts:

$$\mathcal{K}_H^{R_\xi,\chi Z\chi}(0,0) = \mathcal{K}_H^{R_\xi,\chi\chi Z}(0,0) = \mathcal{K}_H^{R_\xi,Z\chi\chi}(0,0). \qquad (2.3.53)$$

The last one-loop correction to the three-point vertex comes from the irreducible Triangle

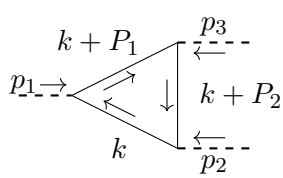

$$= i\mathcal{K}_H^{R_\xi,\chi\chi\chi}$$

given by the expression

$$\mathcal{K}_H^{R_\xi,\chi\chi\chi} = -32v_0\frac{\lambda_0^2}{m_{H_0}^4}\int\frac{d^4k}{(2\pi)^4}\frac{-ik\cdot(k+P_1)}{D_1D_2D_3}(k+P_1)\cdot(k+P_2)(k+P_2)\cdot k\,, \qquad (2.3.54)$$

with symmetry factor $\mathcal{S}^9_{\mathcal{K}_H} = 1$. There is only one diagram of this kind and its explicit form in DR reads

$$
\begin{aligned}
\mathcal{K}_H^{R_\xi,\chi\chi\chi}(P_1,P_2) &= -32v_0\frac{\lambda_0^2}{m_{H_0}^4}\mu^\varepsilon\Big\{U_{K6}(P_1,P_2,m_{\chi_0},m_{\chi_0},m_{\chi_0}) \\
&+ \quad 2(P_1+P_2)_\mu U^\mu_{K5}(P_1,P_2,m_{\chi_0},m_{\chi_0},m_{\chi_0}) \\
&+ \quad (P_{1\mu}P_{1\nu} + 3P_{1\mu}P_{2\nu} + P_{2\mu}P_{2\nu})U^{\mu\nu}_{K4}(P_1,P_2,m_{\chi_0},m_{\chi_0},m_{\chi_0}) \\
&+ \quad P_1\cdot P_2 U_{K4}(P_1,P_2,m_{\chi_0},m_{\chi_0},m_{\chi_0}) \\
&+ \quad (P_{1\mu}P_{1\nu}P_{2\alpha} + P_{1\mu}P_{2\nu}P_{2\alpha})C^{\mu\nu\alpha}(P_1,P_2,m_{\chi_0},m_{\chi_0},m_{\chi_0}) \\
&+ \quad P_1\cdot P_2(P_{1\mu}+P_{2\mu})C^\mu_{\mathcal{K}3}(P_1,P_2,m_{\chi_0},m_{\chi_0},m_{\chi_0}) \\
&+ \quad P_1\cdot P_2 P_{1\mu}P_{2\nu}C^{\mu\nu}(P_1,P_2,m_{\chi_0},m_{\chi_0},m_{\chi_0})\Big\}. \qquad (2.3.55)
\end{aligned}
$$

Summing up all the irreducible Triangles, we find that at zero external momenta

$$(4\pi)^{d/2}\mathcal{K}_H^{R_\xi,\text{irred.}} = \mu^\varepsilon\left([\mathcal{K}_H^{R_\xi,\text{irred.}}]_\varepsilon + \left\{\mathcal{K}_H^{R_\xi,\text{irred.}}\right\}_\varepsilon + [\mathcal{K}_H^{R_\xi,\text{irred.}}]_f + \left\{\mathcal{K}_H^{R_\xi,\text{irred.}}\right\}_f\right) \tag{2.3.56}$$

with

$$\begin{aligned}[\mathcal{K}_H^{R_\xi,\text{irred.}}]_\varepsilon &= 0\\ \left\{\mathcal{K}_H^{R_\xi,\text{irred.}}\right\}_\varepsilon &= 0\end{aligned} \tag{2.3.57}$$

and

$$\begin{aligned}[\mathcal{K}_H^{R_\xi,\text{irred.}}]_f &= -\frac{m_{H_0}}{\sqrt{2\lambda_0}}\Big(54\lambda_0^2 + 48\frac{\lambda_0^2 m_{Z_0}^4}{m_{H_0}^4}\Big)\\ \left\{\mathcal{K}_H^{R_\xi,\text{irred.}}\right\}_f &= 0\,.\end{aligned} \tag{2.3.58}$$

We see that the irreducible Triangles do not contribute to the divergent part of the 3-point function.

It is worth looking a bit closer at the cancellation of the gauge fixing parameter ξ from the finite part of this sector. The finite parts, collected according to the loop propagators, are

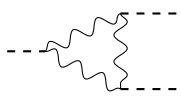
$= \frac{m_{H_0}}{\sqrt{2\lambda_0}}\Big(-\frac{48\lambda_0^2 m_{Z_0}^4}{m_{H_0}^4} - \frac{16\lambda_0^2 m_{Z_0}^4\xi^2}{m_{H_0}^4}\Big)$

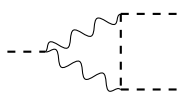
$= \frac{m_{H_0}}{\sqrt{2\lambda_0}}\Big(\frac{48\lambda_0^2 m_{Z_0}^4\xi^2}{m_{H_0}^4} - \frac{96\lambda_0^2 m_{Z_0}^4\xi^2}{m_{H_0}^4}\ln\frac{\mu^2}{m_{Z_0}^2\xi}\Big)$

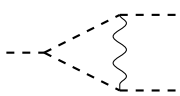
$= \frac{m_{H_0}}{\sqrt{2\lambda_0}}\Big(\frac{48\lambda_0^2 m_{Z_0}^4\xi^2}{m_{H_0}^4} + \frac{288\lambda_0^2 m_{Z_0}^4\xi^2}{m_{H_0}^4}\ln\frac{\mu^2}{m_{Z_0}^2\xi}\Big)$

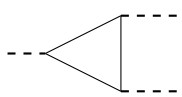
$= \frac{m_{H_0}}{\sqrt{2\lambda_0}}\Big(\frac{-80\lambda_0^2 m_{Z_0}^4\xi^2}{m_{H_0}^4} - \frac{192\lambda_0^2 m_{Z_0}^4\xi^2}{m_{H_0}^4}\ln\frac{\mu^2}{m_{Z_0}^2\xi}\Big)$

It is easy to see the cancellation of ξ in the sum.

We now add reducible and irreducible contributions into $\mathcal{K}_H^{R_\xi} = \mathcal{K}_H^{R_\xi,\text{red.}} + \mathcal{K}_H^{R_\xi,\text{irred.}}$ and we have

$$(4\pi)^{d/2}\mathcal{K}_H^{R_\xi} = \mu^\varepsilon\left([\mathcal{K}_H^{R_\xi}]_\varepsilon + \left\{\mathcal{K}_H^{R_\xi}\right\}_\varepsilon + [\mathcal{K}_H^{R_\xi}]_f + \left\{\mathcal{K}_H^{R_\xi}\right\}_f\right) \tag{2.3.59}$$

where

$$\begin{aligned}\varepsilon[\mathcal{K}_H^{R_\xi}]_\varepsilon &= \frac{m_{H_0}}{\sqrt{2\lambda_0}}\left(108\lambda_0^2 + 144\frac{\lambda_0^2 m_{Z_0}^4}{m_{H_0}^4}\right)\\ \left\{\mathcal{K}_H^{R_\xi}\right\}_\varepsilon &= 0\end{aligned} \tag{2.3.60}$$

and

$$\begin{aligned}[\mathcal{K}_H^{R_\xi}]_f &= \frac{m_{H_0}}{\sqrt{2\lambda_0}}\Big(-54\lambda_0^2 - 24\frac{\lambda_0^2 m_{Z_0}^4}{m_{H_0}^4} + 54\lambda_0^2\ln\frac{\mu^2}{m_{H_0}^2} + 72\frac{\lambda_0^2 m_{Z_0}^4}{m_{H_0}^4}\ln\frac{\mu^2}{m_{Z_0}^2}\Big)\\ \left\{\mathcal{K}_H^{R_\xi}\right\}_f &= 0\,.\end{aligned} \tag{2.3.61}$$

2.3.5 Corrections to the quartic coupling

Diagrams with four external Higgs fields contribute through their divergent parts to the running of the Higgs quartic self coupling λ and through their finite parts they contribute to the one-loop scalar potential. They are collectively called "Box diagrams", denoted as $\mathcal{B}_H$ and come in three classes. The first two of these classes contain reducible diagrams and the third class contains irreducible Box diagrams, called "Square (S)-Boxes". The reducible class is further split in two subclasses, called "Candy (C)-Boxes" and "Triangular (T)-Boxes". They have the following structure:

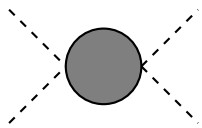 $= \mathcal{B}_H^C,$ 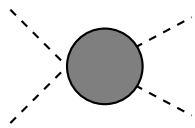 $= \mathcal{B}_H^T,$ 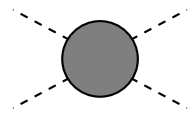 $= \mathcal{B}_H^S$

Regarding the momentum flow, we take all four external momenta $p_i = 1, 2, 3, 4$ to be inflowing and satisfying $p_1 + p_2 + p_3 + p_4 = 0$. Candies and S-Boxes come in three versions, corresponding to the usual s, t and u channels, where

$$s = (p_1 + p_2)^2, \qquad t = (p_1 + p_3)^2, \qquad u = (p_1 + p_4)^2 \tag{2.3.62}$$

T-Boxes come in six versions instead because they are not invariant under a reflection with respect to the axis passing through the centre of the loop in the diagram. There are two inequivalent topologies and each topology comes with s, t and u channels. Any U-integral that may appear is dealt with in Appendix 2.C and finite integrals of the E, F, G and H-type in Appendix 2.E.

Reducible Boxes

Candies have the generic momentum dependence $\mathcal{B}_H^{R_\xi,C}(P_1)$, where $P_1 = \sqrt{s}$, $\sqrt{t}$ and $\sqrt{u}$ for the three channels. Their total contribution is then a sum over P_1.

The first Candy is the famous diagram

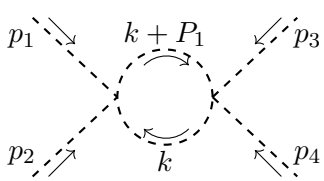

$= i\mathcal{B}_H^{R_\xi,\phi\phi}, \quad S^1_{\mathcal{B}_H^C} = \frac{1}{2}$

which solely determines the β-function in pure scalar theories, in the case where the Higgs is expressed in the Cartesian basis, all other diagrams being finite. Here in the Polar basis we will see that this is still the case alas in a non-trivial way. The result for this diagram can be obtained from Eq. (2.3.34) (without the factor of 3) divided by v_0 and evaluated at P_1:

$$\mathcal{B}_H^{R_\xi,\phi\phi} \quad = \quad 18\lambda_0^2\mu^\varepsilon B_0(P_1, m_{H_0}, m_{H_0})\,. \tag{2.3.63}$$

The Goldstone Candy

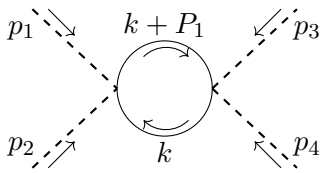

$$= i\mathcal{B}_H^{R_\xi,\chi\chi}, \quad S^2_{\mathcal{B}_H^C} = \tfrac{1}{2}$$

is analogously equal to Eq. (2.3.35) divided by v_0 (without the factor of 3), evaluated at P_1:

$$\begin{aligned}\mathcal{B}_H^{R_\xi,\chi\chi} &= 8\frac{\lambda_0^2}{m_{H_0}^4}\mu^\varepsilon\Big\{m_{\chi_0}^2 A_0(m_{\chi_0}) + (m_{\chi_0}^2 - P_1^2)g_{\mu\nu}B^{\mu\nu}(P_1, m_{\chi_0}, m_{\chi_0}) \\ &+ P_{1\mu}P_{1\nu}B^{\mu\nu}(P_1, m_{\chi_0}, m_{\chi_0})\Big\}. \end{aligned} \tag{2.3.64}$$

The gauge Candy

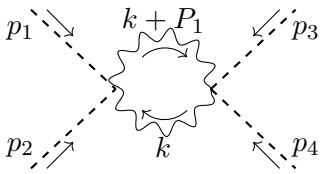

$$= i\mathcal{B}_H^{R_\xi,ZZ}, \quad S^3_{\mathcal{B}_H^C} = \tfrac{1}{2}$$

is obtained from Eq. (2.3.36):

$$\begin{aligned}\mathcal{B}_H^{R_\xi,ZZ} &= 8\frac{m_{Z_0}^4}{m_{H_0}^4}\lambda_0^2\mu^\varepsilon\Big\{dB_0(P_1, m_{Z_0}, m_{Z_0}) - (1-\xi)\Big\{g_{\mu\nu}C^{1\mu\nu}(P_1, m_{Z_0}, m_{Z_0}, m_{\chi_0}) \\ &+ g_{\mu\nu}C^{1\mu\nu}(P_1, m_{Z_0}, m_{Z_0}, m_{\chi_0})\Big\} \\ &+ (1-\xi)^2\Big\{g_{\mu\nu}C^{1\mu\nu}(P_1, m_{Z_0}, m_{Z_0}, m_{\chi_0}) \\ &+ (m_{Z_0}^2 - P_1^2)g_{\mu\nu}D^{\mu\nu}(P_1, m_{Z_0}, m_{Z_0}, m_{\chi_0}, m_{\chi_0}) + P_{1\mu}P_{1\nu}D^{\mu\nu}(P_1, m_{Z_0}, m_{Z_0}, m_{\chi_0}, m_{\chi_0}),\Big\}\Big\}. \end{aligned} \tag{2.3.65}$$

Finally, there is a mixed Candy

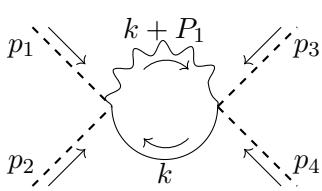

$$= i\mathcal{B}_H^{R_\xi,Z\chi}, \quad S^4_{\mathcal{B}_H^C} = 1$$

obtained easily from Eq. (2.3.37):

$$\begin{aligned}\mathcal{B}_H^{R_\xi,Z\chi} &= 16\lambda_0^2\frac{m_{Z_0}^2}{m_{H_0}^4}\mu^\varepsilon\Big\{-g_{\mu\nu}B^{\mu\nu}(P_1, m_{\chi_0}, m_{Z_0}) \\ &+ (1-\xi)\Big\{g_{\mu\nu}B^{\mu\nu}(P_1, m_{\chi_0}, m_{\chi_0}) + (m_{Z_0}^2 - P_1^2)g_{\mu\nu}C^{1\mu\nu}(P_1, m_{Z_0}, m_{\chi_0}, m_{Z_0})\end{aligned}$$

$$+ \quad P_{1\mu}P_{1\nu}C^{1\mu\nu}(P_1, m_{\chi_0}, m_{Z_0}, m_{\chi_0})\Big\}\Big\}. \tag{2.3.66}$$

The full contribution of the Candies is obtained by adding Eq. (2.3.63), Eq. (2.3.64), Eq. (2.3.65) and Eq. (2.3.66) (summed over the three channels) and can be expressed as

$$(4\pi)^{d/2}\mathcal{B}_H^{R_\xi,C} = \mu^\varepsilon \left([\mathcal{B}_H^{R_\xi,C}]_\varepsilon + \left\{\mathcal{B}_H^{R_\xi,C}\right\}_\varepsilon + [\mathcal{B}_H^{R_\xi,C}]_f + \left\{\mathcal{B}_H^{R_\xi,C}\right\}_f \right) \tag{2.3.67}$$

where

$$\begin{aligned} \varepsilon[\mathcal{B}_H^{R_\xi,C}]_\varepsilon &= 108\lambda_0^2 + 144\frac{\lambda_0^2 m_{Z_0}^4}{m_{H_0}^4} + 4\frac{s^2\lambda_0^2}{m_{H_0}^4} + 4\frac{t^2\lambda_0^2}{m_{H_0}^4} + 4\frac{u^2\lambda_0^2}{m_{H_0}^4} \\ \left\{\mathcal{B}_H^{R_\xi,C}\right\}_\varepsilon &= 0. \end{aligned} \tag{2.3.68}$$

and

$$\begin{aligned} [\mathcal{B}_H^{R_\xi,C}]_f &= 54\lambda_0^2 \ln\frac{\mu^2}{m_{H_0}^2} + 72\frac{\lambda_0^2 m_{Z_0}^4}{m_{H_0}^4}\ln\frac{\mu^2}{m_{Z_0}^2} \\ \left\{\mathcal{B}_H^{R_\xi,C}\right\}_f &= 0 \end{aligned} \tag{2.3.69}$$

for $p_i = 0$. We now turn to the T-Boxes that have three propagators in the loop. Each of the six channels of a given T-Box is determined by two linear combinations of the external momenta that we call P_1 and P_2. A consistent choice for (P_1, P_2) for the channels $T_{1,\cdots,6}$ is for example $T_1 : (\sqrt{s}, p_1 + p_2 + p_3)$, $T_2 : (\sqrt{t}, p_1 + p_3 + p_4)$, $T_3 : (\sqrt{u}, p_1 + p_3 + p_4)$, $T_4 : (\sqrt{s}, p_2 + p_3 + p_4)$, $T_5 : (p_1, \sqrt{t})$, $T_6 : (p_1, \sqrt{u})$. The generic form of a T-Box is therefore $\mathcal{B}_H^{R_\xi,T}(P_1, P_2)$ and the total contribution is obtained by a sum over the six different pairs (P_1, P_2). Note that the Mandelstam variables enter also via the inner products

$$\begin{aligned} p_1 \cdot p_2 &= p_3 \cdot p_4 = \frac{s}{2} \\ p_1 \cdot p_3 &= p_2 \cdot p_4 = \frac{t}{2} \\ p_1 \cdot p_4 &= p_2 \cdot p_3 = \frac{u}{2} \end{aligned} \tag{2.3.70}$$

All T-Boxes can be obtained from their corresponding irreducible Triangles. They share a common symmetry factor and analytical structure with all the difference encoded in the values that the pair (P_1, P_2) can take. Hence, in this sector we give directly the formal expression in order to avoid unnecessary repetitions. To begin, we have two finite diagrams:

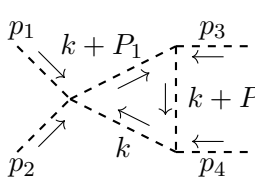

$$= i\mathcal{B}_H^{R_\xi,\phi\phi\phi} = \sum_{(P_1,P_2)} \tfrac{1}{v_0} i\mathcal{K}_H^{R_\xi,\phi\phi\phi}(P_1, P_2)$$

and

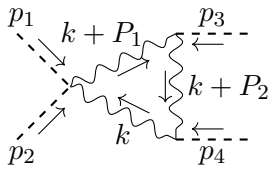

$$= i\mathcal{B}_H^{R_\xi,ZZZ} = \sum_{(P_1,P_2)} \frac{1}{v_0} i\mathcal{K}_H^{R_\xi,ZZZ}(P_1,P_2)$$

There are diagrams that have both divergent and finite parts. There are three with one Goldstone and two gauge bosons in the loop:

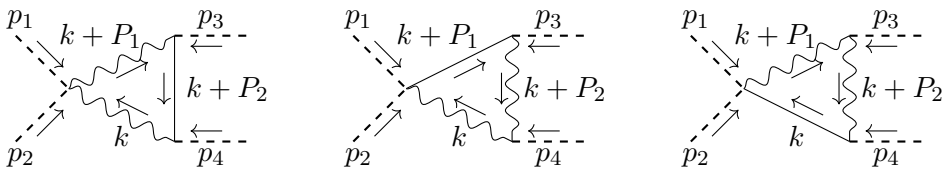

which are equal to $i\mathcal{B}_H^{R_\xi,Z\chi Z} = \sum_{(P_1,P_2)} \frac{1}{v_0} i\mathcal{K}_H^{R_\xi,Z\chi Z}(P_1,P_2)$, $i\mathcal{B}_H^{R_\xi,\chi ZZ} = \sum_{(P_1,P_2)} \frac{1}{v_0} i\mathcal{K}_H^{R_\xi,\chi ZZ}(P_1,P_2)$ and $i\mathcal{B}_H^{R_\xi,ZZ\chi} = \sum_{(P_1,P_2)} \frac{1}{v_0} i\mathcal{K}_H^{R_\xi,ZZ\chi}(P_1,P_2)$ respectively.
And there are three with one gauge boson and two Goldstones in the loop:

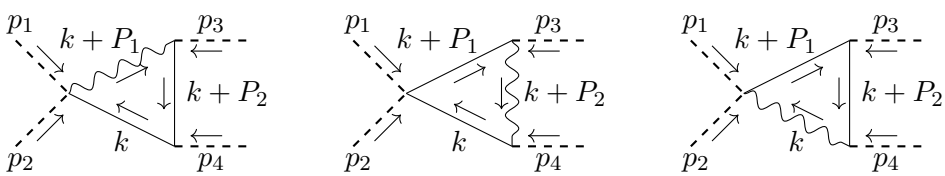

which are equal to $i\mathcal{B}_H^{R_\xi,Z\chi\chi} = \sum_{(P_1,P_2)} \frac{1}{v_0} i\mathcal{K}_H^{R_\xi,Z\chi\chi}(P_1,P_2)$, $i\mathcal{B}_H^{R_\xi,\chi Z\chi} = \sum_{(P_1,P_2)} \frac{1}{v_0} i\mathcal{K}_H^{R_\xi,\chi Z\chi}(P_1,P_2)$ and $i\mathcal{B}_H^{R_\xi,\chi\chi Z} = \sum_{(P_1,P_2)} \frac{1}{v_0} i\mathcal{K}_H^{R_\xi,\chi\chi Z}(P_1,P_2)$ respectively.
We finally have the Goldstone T-Box

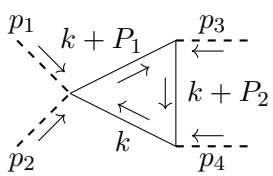

$$= i\mathcal{B}_H^{R_\xi,\chi\chi\chi} = \sum_{(P_1,P_2)} \frac{1}{v_0} i\mathcal{K}_H^{R_\xi,\chi\chi\chi}(P_1,P_2)$$

Adding up all the T-Boxes we find that at zero external momenta

$$(4\pi)^{d/2}\mathcal{B}_H^{R_\xi,T} = \mu^\varepsilon \left([\mathcal{B}_{HR_\xi}^T]_\varepsilon + \left\{\mathcal{B}_{HR_\xi}^T\right\}_\varepsilon + [\mathcal{B}_{HR_\xi}^T]_f + \left\{\mathcal{B}_{HR_\xi}^T\right\}_f \right) \tag{2.3.71}$$

where

$$\begin{aligned} \varepsilon[\mathcal{B}_H^{R_\xi,T}]_\varepsilon &= -28\frac{s^2\lambda_0^2}{m_{H_0}^4} - 40\frac{s\cdot t\lambda_0^2}{m_{H_0}^4} - 28\frac{t^2\lambda_0^2}{m_{H_0}^4} - 40\frac{s\cdot u\lambda_0^2}{m_{H_0}^4} - 40\frac{t\cdot u\lambda_0^2}{m_{H_0}^4} - 28\frac{u^2\lambda_0^2}{m_{H_0}^4} \\ \left\{\mathcal{B}_{HR_\xi}^T\right\}_\varepsilon &= 0. \end{aligned} \tag{2.3.72}$$

and

$$\begin{aligned} [\mathcal{B}_H^{R_\xi,T}]_f &= -162\lambda_0^2 - 288\frac{\lambda_0^2 m_{Z_0}^4}{m_{H_0}^4} \\ \left\{\mathcal{B}_H^{R_\xi,T}\right\}_f &= 0\,. \end{aligned} \tag{2.3.73}$$

Irreducible Boxes

Irreducible, or S-Boxes, have a channel structure determined by three linear combinations of momenta, called P_1, P_2 and P_3. The resulting three independent channels are the usual s, t and u channels

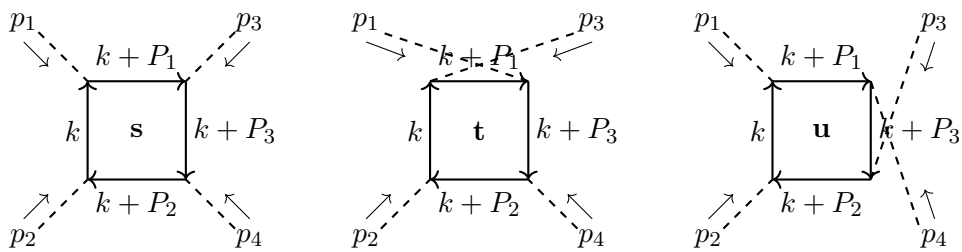

with the momenta $P_{1,2,3}$ determined easily from the above figure:

$$\begin{aligned} s\ -\text{channel}: &\quad P_1 = p_1,\ P_2 = p_1 + p_3 + p_4,\ P_3 = p_1 + p_3 \\ t\ -\text{channel}: &\quad P_1 = p_3,\ P_2 = p_1 + p_3 + p_4,\ P_3 = p_1 + p_3 \\ u\ -\text{channel}: &\quad P_1 = p_1,\ P_2 = p_1 + p_3 + p_4,\ P_3 = p_1 + p_4 \end{aligned} \tag{2.3.74}$$

Irreducible Boxes have therefore the generic form $\mathcal{B}_H^{R_\xi,S}(P_1, P_2, P_3)$ and receive a contribution from the s, t and u channels. In order to take into account all channels, after considering the different diagram topologies, we sum over the (P_1, P_2, P_3) according to the above rule. All S-Boxes have symmetry factor 1. Several annoying for the eye expressions for finite terms $(B_H^{R_\xi,\cdots})_f$ are moved to Appendix 2.E.

We start the computation of the S-Boxes with the finite Higgs loop diagram

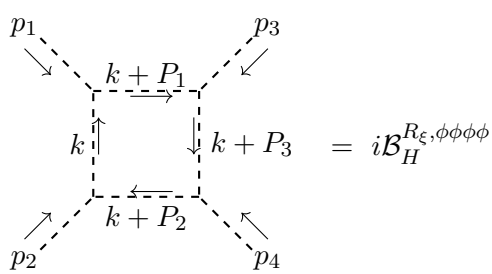

given by the expression

$$\mathcal{B}_H^{R_\xi,\phi\phi\phi\phi} \quad = \quad 324\lambda_0^2 m_{H_0}^2 \int \frac{d^4k}{(2\pi)^4} \frac{(-i)}{D_1 D_2 D_3 D_4}\,, \tag{2.3.75}$$

with the D_i in the denominator defined in Appendix 2.A. This is just a finite D_0 PV integral:

$$\mathcal{B}_H^{R_\xi,\phi\phi\phi\phi} = 324\lambda_0^2 m_{H_0}^2 \mu^\varepsilon D_0(P_1, P_2, P_3, m_{H_0}, m_{H_0}, m_{H_0}, m_{H_0})\,. \tag{2.3.76}$$

The next diagram is also finite. It is

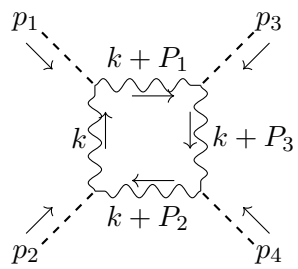

$$= i\mathcal{B}_H^{R_\xi,ZZZZ}$$

and is equal to

$$\begin{aligned}\mathcal{B}_H^{R_\xi,ZZZZ} &= 64\frac{m_{Z_0}^8\lambda_0^2}{m_{H_0}^4}g^{\mu\nu}g^{\alpha\beta}g^{\gamma\delta}g^{\epsilon\zeta}\int\frac{d^4k}{(2\pi)^4}\frac{-i\left(-g_{\mu\zeta}+\frac{(1-\xi)k_\mu k_\zeta}{k^2-\xi m_{Z_0}^2}\right)}{D_1}\frac{\left(-g_{\nu\alpha}+\frac{(1-\xi)(k+P_1)_\nu(k+P_1)_\alpha}{(k+P_1)^2-\xi m_{Z_0}^2}\right)}{D_2}\\ &\times\frac{\left(-g_{\delta\beta}+\frac{(1-\xi)(k+P_2)_\delta(k+P_2)_\beta}{(k+P_2)^2-\xi m_{Z_0}^2}\right)}{D_3}\frac{\left(-g_{\epsilon\gamma}+\frac{(1-\xi)(k+P_3)_\epsilon(k+P_3)_\gamma}{(k+P_3)^2-\xi m_{Z_0}^2}\right)}{D_4}\,. \end{aligned} \tag{2.3.77}$$

In DR it takes the form

$$\mathcal{B}_H^{R_\xi,ZZZZ} = (B_H^{R_\xi,ZZZZ})_f\,. \tag{2.3.78}$$

Another finite diagram is

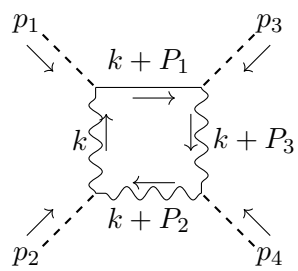

$$= i\mathcal{B}_H^{R_\xi,\chi ZZZ}$$

which is equal to

$$\begin{aligned}\mathcal{B}_H^{R_\xi,\chi ZZZ} &= 64\frac{m_{Z_0}^6\lambda_0^2}{m_{H_0}^4}g^{\mu\nu}g^{\gamma\delta}\int\frac{d^4k}{(2\pi)^4}\frac{-i\left(-g_{\mu\delta}+\frac{(1-\xi)k_\mu k_\delta}{k^2-\xi m_{Z_0}^2}\right)}{D_1}\frac{\left(-g_{\nu\alpha}+\frac{(1-\xi)(k+P_2)_\nu(k+P_2)_\alpha}{(k+P_2)^2-\xi m_{Z_0}^2}\right)}{D_3}\\ &\times\frac{(k+P_1)^\alpha(k+P_1)^\beta}{D_2}\frac{\left(-g_{\gamma\beta}+\frac{(1-\xi)(k+P_3)_\gamma(k+P_3)_\beta}{(k+P_3)^2-\xi m_{Z_0}^2}\right)}{D_4} \end{aligned} \tag{2.3.79}$$

and in DR to

$$\mathcal{B}_H^{R_\xi,\chi ZZZ} = (B_H^{R_\xi,\chi ZZZ})_f\,. \tag{2.3.80}$$

Now, there are three additional diagrams of this type, $\mathcal{B}_H^{R_\xi,Z\chi ZZ}$, $\mathcal{B}_H^{R_\xi,ZZ\chi Z}$ and $\mathcal{B}_H^{R_\xi,ZZZ\chi}$, giving different, but finite result. The total contribution of these diagrams too is obtained by summing over the three possible channels (P_1, P_2, P_3), i.e. the s, t and u channels, according to Eq. (2.3.74).

We turn to the S-Boxes which have both infinite and finite parts. The first one of this type is

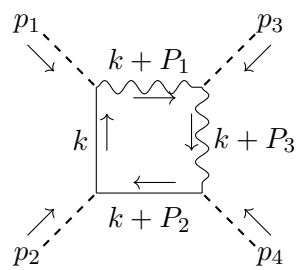

$$= i\mathcal{B}_H^{R_\xi,ZZ\chi\chi}$$

and is given by the expression

$$\begin{aligned}\mathcal{B}_H^{R_\xi,ZZ\chi\chi} &= 64\frac{m_{Z_0}^4\lambda_0^2}{m_{H_0}^4}g^{\mu\beta}\int\frac{d^4k}{(2\pi)^4}\frac{-i\left(-g_{\nu\beta}+\frac{(1-\xi)(k+P_1)_\nu(k+P_1)_\beta}{(k+P_1)^2-\xi m_{Z_0}^2}\right)}{D_1D_2D_3D_4}\cdot \\ &\left(-g_{\mu\alpha}+\frac{(1-\xi)\,(k+P_3)_\mu\,(k+P_3)_\alpha}{(k+P_3)^2-\xi m_{Z_0}^2}\right)k^\nu(k+P_2)^\alpha k\cdot(k+P_2).\end{aligned} \tag{2.3.81}$$

Its DR form is

$$\begin{aligned}\mathcal{B}_H^{R_\xi,ZZ\chi\chi} &= 64\frac{\lambda_0^2m_{Z_0}^4}{m_{H_0}^4}\mu^\varepsilon\Big\{D_{\mathcal{B}4}(P_1,P_2,P_3,m_{Z_0},m_{Z_0},m_{\chi_0},m_{\chi_0}) \\ &+ (1-\xi)\Big\{2D_{\mathcal{B}4}(P_1,P_2,P_3,m_{\chi_0},m_{Z_0},m_{\chi_0},m_{\chi_0})\Big\} \\ &+ (1-\xi)^2\Big\{D_{\mathcal{B}4}(P_1,P_2,P_3,m_{\chi_0},m_{Z_0},m_{\chi_0},m_{\chi_0})\Big\}\Big\} \\ &+ (B_H^{R_\xi,ZZ\chi\chi})_{f,1}+(1-\xi)(B_H^{R_\xi,ZZ\chi\chi})_{f,2}+(1-\xi)^2(B_H^{R_\xi,ZZ\chi\chi})_{f,3}\,.\end{aligned} \tag{2.3.82}$$

A portion of the finite part of the above diagram is actually built in the $D_{\mathcal{B}4}$-integrals (defined at the end of Sect. 2.B.2) while the rest of it is given in Appendix 2.E. There are in total six different topologies for this diagram corresponding to the different ways the two Goldstones can be distributed in the loop. All these diagrams have exactly the same divergent part as $\mathcal{B}_H^{R_\xi,ZZ\chi\chi}$ but not the same finite part.

Next, we have

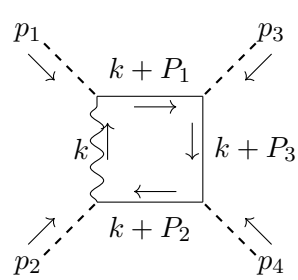

$$= i\mathcal{B}_H^{R_\xi,\chi\chi\chi Z}$$

together with $\mathcal{B}_H^{R_\xi,Z\chi\chi\chi}$, $\mathcal{B}_H^{R_\xi,\chi Z\chi\chi}$ and $\mathcal{B}_H^{R_\xi,\chi\chi Z\chi}$ that have also identical divergent parts but different finite parts. $\mathcal{B}_H^{R_\xi,\chi\chi\chi Z}$ is equal to

$$\begin{aligned}\mathcal{B}_H^{R_\xi,\chi\chi\chi Z} &= 64\frac{m_{Z_0}^2\lambda_0^2}{m_{H_0}^4}\int\frac{d^4k}{(2\pi)^4}\frac{-i\left(-g_{\mu\nu}+\frac{(1-\xi)k_\mu k_\nu}{k^2-\xi m_{Z_0}^2}\right)}{D_1D_2D_3D_4}(k+P_1)^\mu(k+P_2)^\nu \\ &\times\ (k+P_1)\cdot(k+P_3)(k+P_3)\cdot(k+P_2) \end{aligned} \tag{2.3.83}$$

and in DR evaluates to

$$\begin{aligned}\mathcal{B}_H^{R_\xi,\chi\chi\chi Z} &= -64\frac{\lambda_0^2 m_{Z_0}^2}{m_{H_0}^4}\mu^\varepsilon\Big\{U_{B6}(P_1,P_2,P_3,m_{Z_0},m_{\chi_0},m_{\chi_0},m_{\chi_0}) \\ &+\ 2(P_1+P_2+P_3)_\mu U_{B5}^\mu(P_1,P_2,P_3,m_{Z_0},m_{\chi_0},m_{\chi_0},m_{\chi_0}) \\ &+\ (P_{1\mu}P_{1\nu}+3P_{1\mu}P_{2\nu}+P_{2\mu}P_{2\nu} \\ &+\ 3P_{1\mu}P_{3\nu}+3P_{2\mu}P_{3\nu}+P_{3\mu}P_{3\nu})D_{B4}^{\mu\nu}(P_1,P_2,P_3,m_{Z_0},m_{\chi_0},m_{\chi_0},m_{\chi_0}) \\ &+\ (P_1\cdot P_2+P_1\cdot P_3+P_2\cdot P_3)D_{B4}(P_1,P_2,P_3,m_{Z_0},m_{\chi_0},m_{\chi_0},m_{\chi_0}) \\ &-\ (1-\xi)\Big\{U_{B6}(P_1,P_2,P_3,m_{Z_0},m_{\chi_0},m_{\chi_0},m_{\chi_0}) \\ &+\ m_{\chi_0}^2U_{B4}(P_1,P_2,P_3,m_{Z_0},m_{\chi_0},m_{\chi_0},m_{\chi_0}) \\ &+\ 2(P_1+P_2+P_3)_\mu U_{B5}^\mu(P_1,P_2,P_3,m_{Z_0},m_{\chi_0},m_{\chi_0},m_{\chi_0}) \\ &+\ (P_{1\mu}P_{1\nu}+3P_{1\mu}P_{2\nu}+P_{2\mu}P_{2\nu} \\ &+\ 4P_{1\mu}P_{3\nu}+3P_{2\mu}P_{3\nu}+P_{3\mu}P_{3\nu})D_{B4}^{\mu\nu}(P_1,P_2,P_3,m_{Z_0},m_{\chi_0},m_{\chi_0},m_{\chi_0}) \\ &+\ (P_1\cdot P_2+P_2\cdot P_3)D_{B4}(P_1,P_2,P_3,m_{Z_0},m_{\chi_0},m_{\chi_0},m_{\chi_0})\Big\}\Big\} \\ &+\ (B_H^{R_\xi,\chi\chi\chi Z})_{f,1}+(1-\xi)(B_H^{R_\xi,\chi\chi\chi Z})_{f,2}\,, \end{aligned} \tag{2.3.84}$$

where $(B_H^{R_\xi,\chi\chi\chi Z})_{f,1}$ and $(B_H^{R_\xi,\chi\chi\chi Z})_{f,2}$ are entirely finite, given in Appendix 2.E. The rest of the finite part is encoded in the PV and U-integrals.

The last divergent S-Box is the one with only Goldstone bosons inside the loop:

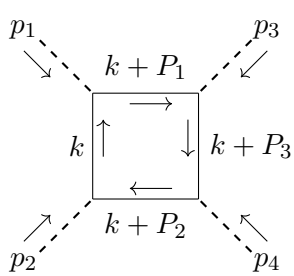

$$= i\mathcal{B}_H^{R_\xi,\chi\chi\chi\chi}$$

and is equal to

$$\mathcal{B}_H^{R_\xi,\chi\chi\chi\chi} = 64\frac{\lambda_0^2}{m_{H_0}^4}\int\frac{d^4k}{(2\pi)^4}\frac{-ik\cdot(k+P_1)}{D_1D_2D_3D_4}(k+P_1)\cdot(k+P_3)\times(k+P_3)\cdot(k+P_2)\times(k+P_2)\cdot k. \tag{2.3.85}$$

Its DR form is

$$
\begin{aligned}
\mathcal{B}_H^{R_\xi,\chi\chi\chi\chi} &= 64\frac{\lambda_0^2 m_{Z_0}^2}{m_{H_0}^4}\mu^\varepsilon\Big\{U_{B8}(P_1,P_2,P_3,m_{\chi_0},m_{\chi_0},m_{\chi_0},m_{\chi_0}) \\
&+ 2(P_1+P_2+P_3)_\mu U_{B7}^\mu(P_1,P_2,P_3,m_{\chi_0},m_{\chi_0},m_{\chi_0},m_{\chi_0}) \\
&+ \Big\{P_{1\mu}P_{1\nu}+3P_{1\mu}P_{2\nu}+P_{2\mu}P_{2\nu} \\
&+ 4P_{1\mu}P_{3\nu}+3P_{2\mu}P_{3\nu}+P_{3\mu}P_{3\nu}\Big\}U_{B6}^{\mu\nu}(P_1,P_2,P_3,m_{\chi_0},m_{\chi_0},m_{\chi_0},m_{\chi_0}) \\
&+ (P_1\cdot P_2+P_2\cdot P_3)U_{B6}(P_1,P_2,P_3,m_{\chi_0},m_{\chi_0},m_{\chi_0},m_{\chi_0}) \\
&+ \Big\{P_{1\mu}P_{1\nu}P_{2\alpha}+P_{1\mu}P_{2\nu}P_{2\alpha}+2P_{1\mu}P_{1\nu}P_{3\alpha}+4P_{1\mu}P_{2\nu}P_{3\alpha} \\
&+ P_{2\mu}P_{2\nu}P_{3\alpha}+2P_{1\mu}P_{3\nu}P_{3\alpha}+P_{2\mu}P_{3\nu}P_{3\alpha}\Big\}U_{B5}^{\mu\nu\alpha}(P_1,P_2,P_3,m_{\chi_0},m_{\chi_0},m_{\chi_0},m_{\chi_0}) \\
&+ \Big\{P_1\cdot P_2(P_1+P_2+2P_3)_\mu \\
&+ P_2\cdot P_3(2P_1+P_2+P_3)_\mu\Big\}U_{B5}^{\mu}(P_1,P_2,P_3,m_{\chi_0},m_{\chi_0},m_{\chi_0},m_{\chi_0}) \\
&+ \Big\{P_{1\mu}P_{1\nu}P_{2\alpha}P_{3\beta}+P_{1\mu}P_{2\nu}P_{2\alpha}P_{3\beta} \\
&+ P_{1\mu}P_{1\nu}P_{3\alpha}P_{3\beta}+P_{1\mu}P_{2\nu}P_{3\alpha}P_{3\beta}\Big\}D^{\mu\nu\alpha\beta}(P_1,P_2,P_3,m_{\chi_0},m_{\chi_0},m_{\chi_0},m_{\chi_0}) \\
&+ \Big\{P_1\cdot P_2[P_{1\mu}P_{1\nu}+2P_{1\mu}P_{3\nu}+P_{2\mu}P_{3\nu}+P_{3\mu}P_{3\nu}] \\
&+ P_2\cdot P_3[P_{1\mu}P_{1\nu}+P_{1\mu}P_{2\nu}+2P_{1\mu}P_{3\nu}+P_{2\mu}P_{3\nu}]\Big\}D_{B4}^{\mu\nu}(P_1,P_2,P_3,m_{\chi_0},m_{\chi_0},m_{\chi_0},m_{\chi_0}) \\
&+ (P_1\cdot P_2\times P_2\cdot P_3)D_{B4}(P_1,P_2,P_3,m_{\chi_0},m_{\chi_0},m_{\chi_0},m_{\chi_0})\Big\}. \qquad (2.3.86)
\end{aligned}
$$

Summing up all topologies and channels, at zero external momenta, we find for the S-Boxes the relations

$$
\begin{aligned}
\varepsilon[\mathcal{B}_H^{R_\xi,S}]_\varepsilon &= 24\frac{s^2\lambda_0^2}{m_{H_0}^4}+40\frac{s\cdot t\lambda_0^2}{m_{H_0}^4}+24\frac{t^2\lambda_0^2}{m_{H_0}^4}+40\frac{s\cdot u\lambda_0^2}{m_{H_0}^4}+40\frac{t\cdot u\lambda_0^2}{m_{H_0}^4}+24\frac{u^2\lambda_0^2}{m_{H_0}^4} \\
\Big\{\mathcal{B}_H^{R_\xi,S}\Big\}_\varepsilon &= 0 \qquad (2.3.87)
\end{aligned}
$$

and

$$
\begin{aligned}
[\mathcal{B}_H^{R_\xi,S}]_f &= 162\lambda_0^2+96\frac{\lambda_0^2 m_{Z_0}^4}{m_{H_0}^4} \\
\Big\{\mathcal{B}_H^{R_\xi,S}\Big\}_f &= 0 \qquad (2.3.88)
\end{aligned}
$$

We note the interesting facts that $\mathcal{B}_H^{R_\xi,ZZ\chi\chi}$ has only a $\{\cdots\}_\varepsilon$ part and that

$$
\Big\{\mathcal{B}_H^{R_\xi,ZZ\chi\chi}+\mathcal{B}_H^{R_\xi,\chi\chi\chi Z}+\mathcal{B}_H^{R_\xi,\chi\chi\chi\chi}\Big\}_\varepsilon = 0\,, \qquad (2.3.89)
$$

while $[\mathcal{B}_H^{R_\xi,\chi\chi\chi Z}]_\varepsilon \sim \frac{\lambda_0^2 m_{Z_0}^2}{m_{H_0}^2}$ and $[\mathcal{B}_H^{R_\xi,\chi\chi\chi\chi}]_\varepsilon \sim \lambda_0^2$.

The cancellation of ξ from the finite parts is more illuminating when results from individual

loop structures are shown:

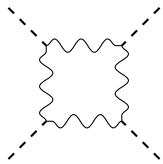

$$= \frac{96\lambda_0^2 m_{Z_0}^4}{m_{H_0}^4} + \frac{32\lambda_0^2 m_{Z_0}^4 \xi^2}{m_{H_0}^4}$$

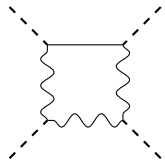

$$= \frac{256\lambda_0^2 m_{Z_0}^4 \xi^2}{m_{H_0}^4}$$

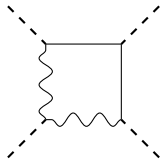

$$= -\frac{960\lambda_0^2 m_{Z_0}^4 \xi^2}{m_{H_0}^4} + \frac{1152\lambda_0^2 m_{Z_0}^4 \xi^2}{m_{H_0}^4} \ln \frac{\mu^2}{m_{Z_0}^2 \xi}$$

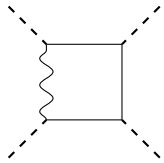

$$= \frac{256\lambda_0^2 m_{Z_0}^4 \xi^2}{m_{H_0}^4} - \frac{3072\lambda_0^2 m_{Z_0}^4 \xi^2}{m_{H_0}^4} \ln \frac{\mu^2}{m_{Z_0}^2 \xi}$$

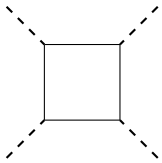

$$= \frac{416\lambda_0^2 m_{Z_0}^4 \xi^2}{m_{H_0}^4} + \frac{1920\lambda_0^2 m_{Z_0}^4 \xi^2}{m_{H_0}^4} \ln \frac{\mu^2}{m_{Z_0}^2 \xi}.$$

The cancellation of ξ is now evident.

The final step here is to collect all Boxes and sum them up. Adding Eq.(2.3.68), Eq.(2.3.72) and Eq.(2.3.87), we obtain at $p_i = 0$:

$$\begin{aligned} \varepsilon[\mathcal{B}_H^{R_\xi}]_\varepsilon &= 108\lambda_0^2 + 144\frac{\lambda_0^2 m_{Z_0}^4}{m_{H_0}^4} \\ \left\{\mathcal{B}_H^{R_\xi}\right\}_\varepsilon &= 0. \end{aligned} \tag{2.3.90}$$

and

$$\begin{aligned} [\mathcal{B}_H^{R_\xi}]_f &= -168\frac{\lambda_0^2 m_{Z_0}^4}{m_{H_0}^4} + 54\lambda_0^2 \ln\frac{\mu^2}{m_{H_0}^2} + 72\frac{\lambda_0^2 m_{Z_0}^4}{m_{H_0}^4} \ln\frac{\mu^2}{m_{Z_0}^2} \\ \left\{\mathcal{B}_H^{R_\xi}\right\}_f &= 0\,. \end{aligned} \tag{2.3.91}$$

A couple of final comments are in order. First, each block of box diagrams, Candies, T and S-Boxes is by itself ξ-independent. Moreover, looking at the results from the three sectors, one notices that they have an explicit s, t and u-dependence. So, one would expect that $[\mathcal{B}_H^{R_\xi}]_\varepsilon$ could also be channel dependent. Nevertheless, Eq.(2.3.90) shows that the s, t and u-dependence cancels when the full contribution of the box diagrams is taken into account.

2.4 Unitary Gauge

In the previous section, we computed one-loop processes in the Abelian Higgs model when the gauge symmetry is broken using an R_ξ gauge fixing term. However one of our main goals here is to investigate this model in the Unitary gauge. This is interesting since, in the Unitary gauge only physical degrees of freedom are present, in contrast to the R_ξ gauge. Moreover, there are statements in the literature that argue that the Unitary gauge may be problematic at the quantum level, so by comparing it to the R_ξ gauge, we will try to clarify the correctness of these arguments.

In the Unitary gauge, no gauge fixing is needed, therefore there is no need for ghosts. The Unitary gauge Lagrangean can be simply obtained from Eq. (2.3.3) by removing gauge fixing and ghost terms and setting $\chi_0 = 0$ in the remaining. Doing so, we obtain the Unitary gauge Lagrangean

$$\begin{aligned}\mathcal{L}_{AH} &= -\frac{1}{4}F_{0,\mu\nu}^2 + \frac{1}{2}\left(\partial_\mu\phi_0\right)\left(\partial^\mu\phi_0\right) + \frac{1}{2}m_{Z_0}^2 A_\mu^0 A^{0\mu} + g^{\mu\nu}\frac{\lambda_0 m_{Z_0}^2}{m_{H_0}^2}\phi_0^2 A_\mu^0 A_\nu^0 \\ &+ g^{\mu\nu}\frac{\sqrt{2\lambda_0}m_{Z_0}^2}{m_{H_0}}\phi_0 A_\mu^0 A_\nu^0 - \frac{1}{2}m_{H_0}^2\phi_0^2 - \sqrt{\frac{\lambda_0}{2}}m_{H_0}\phi_0^3 - \frac{\lambda_0}{4}\phi_0^4 + const. \qquad (2.4.1)\end{aligned}$$

from which the Feynman rules can be derived:

- Gauge boson propagator

$$= \frac{i\left(-g^{\mu\nu} + \frac{k^\mu k^\nu}{m_{Z_0}^2}\right)}{k^2 - m_{Z_0}^2 + i\varepsilon}$$

- Higgs propagator

$$= \frac{i}{k^2 - m_{H_0}^2 + i\varepsilon}$$

- ϕ-Z-Z vertex

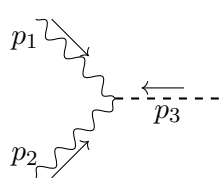

$$= 2ig^{\mu\nu}\frac{m_{Z_0}^2}{m_{H_0}}\sqrt{2\lambda_0}$$

- ϕ-ϕ-ϕ vertex

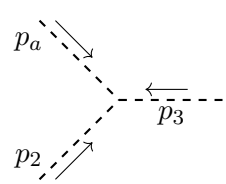

$$= -6i\sqrt{\frac{\lambda_0}{2}}m_{H_0}$$

- ϕ-ϕ-Z-Z vertex

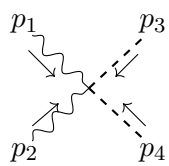

$$= 4i\frac{\lambda_0 m_{Z_0}^2}{m_{H_0}^2}g^{\mu\nu}$$

- ϕ-ϕ-ϕ-ϕ vertex

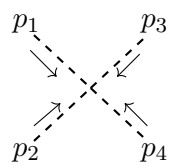

$$= -6i\lambda_0$$

In the Unitary gauge, integrals of the U-type are ubiquitous. But such integrals we have already seen in the R_ξ gauge due to the momentum dependent vertices of the Polar basis for the Higgs field. In the Unitary gauge we do not have momentum dependent vertices, the U-integrals arise only because of the form of the propagators.

In the following sections we compute one-loop diagrams, setting the external momenta to zero at the end, as in the R_ξ gauge. Again for completeness, we present some on-shell results in Appendix 2.F. We will directly insert symmetry factors here since they are the same as in the corresponding R_ξ calculation. In the Unitary gauge, since there is no gauge fixing parameter, we have trivially $\{\star\}_\varepsilon = \{\star\}_f \equiv 0$. As before, we will consistently move nasty expressions for finite parts to Appendix 2.E.

2.4.1 Tadpoles

The Higgs tadpole is

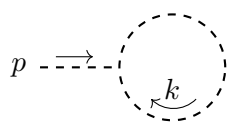

$$= i\mathcal{T}_H^{U,\phi}$$

$$\mathcal{T}_H^{U,\phi} = -6\frac{1}{2}\sqrt{\frac{\lambda_0}{2}}m_{H_0}\int\frac{d^4k}{(2\pi)^4}\frac{i}{\left(k^2-m_{H_0}^2\right)} \tag{2.4.2}$$

and in DR reads

$$\mathcal{T}_H^{U,\phi} = 3\sqrt{\frac{\lambda_0}{2}}m_{H_0}\mu^\varepsilon A_0(m_{H_0}). \tag{2.4.3}$$

The gauge tadpole is

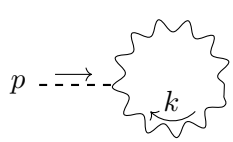

$$= i\mathcal{T}_H^{U,Z}$$

and following Appendix 2.D.2, this becomes

$$\mathcal{T}_H^U = \mu^\varepsilon \left(3\sqrt{\frac{\lambda_0}{2}} m_{H_0} A_0(m_{H_0}) + 3\frac{\sqrt{2\lambda_0} m_{Z_0}^2}{m_{H_0}} A_0(m_{Z_0}) \right). \tag{2.4.4}$$

Adding up the two results, we have

$$(4\pi)^{d/2} \mathcal{T}_H^U = \mu^\varepsilon \left([\mathcal{T}_H^U]_\varepsilon + [\mathcal{T}_H^U]_f \right) \tag{2.4.5}$$

with

$$\varepsilon [\mathcal{T}_H^U]_\varepsilon = 6\sqrt{\frac{\lambda_0}{2}} m_{H_0}^3 + 6\frac{\sqrt{2\lambda_0} m_{Z_0}^4}{m_{H_0}} \tag{2.4.6}$$

and

$$[\mathcal{T}_H^U]_f = 3\sqrt{\frac{\lambda_0}{2}} m_{H_0}^3 + 3\frac{\sqrt{2\lambda_0} m_{Z_0}^4}{m_{H_0}} + 3\sqrt{\frac{\lambda_0}{2}} m_{H_0}^3 \ln\frac{\mu^2}{m_{H_0}^2} + 3\frac{\sqrt{2\lambda_0} m_{Z_0}^4}{m_{H_0}} \ln\frac{\mu^2}{m_{Z_0}^2} . \tag{2.4.7}$$

The above expressions are identical to the R_ξ expressions Eq. (2.3.8) and Eq. (2.3.9).

2.4.2 Corrections to the gauge boson mass

The Z boson mass receives its first correction from

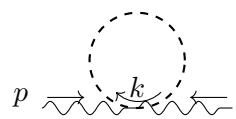

$$= i\mathcal{M}_{Z,\mu\nu}^{U,\phi}$$

which is equal to

$$\mathcal{M}_{Z,\mu\nu}^{U,\phi} = -2g_{\mu\nu}\frac{m_{Z_0}^2}{m_{H_0}^2}\lambda_0 \mu^\varepsilon A_0(m_{H_0}) . \tag{2.4.8}$$

Next is the Higgs sunset

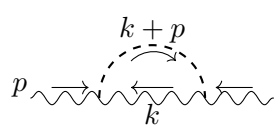

$$= i\mathcal{M}_{Z,\mu\nu}^{U,\phi Z}$$

translating in DR to

$$\mathcal{M}_{Z,\mu\nu}^{U,\phi Z} = -8g_{\mu\nu}\frac{m_{Z_0}^4}{m_{H_0}^2}\lambda_0 \mu^\varepsilon B_0(p, m_{Z_0}, m_{H_0}) + 8\frac{m_{Z_0}^2}{m_{H_0}^2}\lambda_0 \mu^\varepsilon B_{\mu\nu}(p, m_{Z_0}, m_{H_0}) . \tag{2.4.9}$$

The sum of these two corrections is

$$\mathcal{M}_{Z,\mu\nu}^{U} = \frac{m_{Z_0}^2}{m_{H_0}^2}\lambda_0 \mu^\varepsilon \Big\{ -8g_{\mu\nu} m_{Z_0}^2 B_0(p, m_{Z_0}, m_{H_0}) - 2g_{\mu\nu} A_0(m_{H_0})$$

$$+ \quad 8B_{\mu\nu}(p, m_{Z_0}, m_{H_0})\Bigg\}. \tag{2.4.10}$$

As before, the proper contraction we are after is

$$\mathcal{M}_Z^U = \frac{1}{3}\left(-g^{\mu\nu} + \frac{p^\mu p^\nu}{p^2}\right)\mathcal{M}_{Z,\mu\nu}^U(p) \tag{2.4.11}$$

which can be easily shown to be equal to

$$\begin{aligned}\mathcal{M}_Z^U(p) &= -\frac{1}{3}\frac{m_{Z_0}^2}{m_{H_0}^2}\lambda_0\mu^\varepsilon\Bigg\{\Big\{-8(d+\varepsilon)m_{Z_0}^2 B_0(p, m_{Z_0}, m_{H_0}) - 2(d+\varepsilon)A_0(m_{H_0}) \\ &+ 8g^{\mu\nu}B_{\mu\nu}(p, m_{Z_0}, m_{H_0})\Big\} - 8m_{Z_0}^2 B_0(p, m_{Z_0}, m_{H_0}) - 2A_0(m_{H_0}) \\ &+ 8\frac{p^\mu p^\nu}{p^2}B_{\mu\nu}(p, m_{Z_0}, m_{H_0})\Bigg\}. \end{aligned} \tag{2.4.12}$$

At $p = 0$, we have

$$(4\pi)^{d/2}\mathcal{M}_Z^U = \mu^\varepsilon\left([\mathcal{M}_Z^U]_\varepsilon + [\mathcal{M}_Z^U]_f\right) \tag{2.4.13}$$

with

$$\varepsilon[\mathcal{M}_Z^U]_\varepsilon = 12\frac{\lambda_0 m_{Z_0}^4}{m_{H_0}^2}. \tag{2.4.14}$$

The wave function renormalization factor is now straightforward to compute:

$$\delta A^U = -\left.\frac{d\mathcal{M}_Z^U(p)}{dp^2}\right|_{p^2=0} = \frac{\mu^\varepsilon}{(4\pi)^{d/2}}\left([\delta A^U]_\varepsilon + [\delta A^U]_f\right) \tag{2.4.15}$$

with

$$\varepsilon[\delta A^U]_\varepsilon = -\frac{4}{3}\lambda_0\frac{m_{Z_0}^2}{m_{H_0}^2}. \tag{2.4.16}$$

Glancing back on Sect.2.3.2 we see the first sign of the consistency of the calculation by noticing that $\mathcal{M}_Z^U$ and $\mathcal{M}_Z^{R_\xi}$ have the same gauge-independent divergent parts and divergent parts of their respective anomalous dimensions.

Regarding the finite parts we have

$$\begin{aligned}[\mathcal{M}_Z^U]_f &= -\frac{4}{3}\frac{m_{H_0}^2 m_{Z_0}^2\lambda_0}{(m_{H_0}^2 - m_{Z_0}^2)} + \frac{10}{3}\frac{m_{Z_0}^4\lambda_0}{(m_{H_0}^2 - m_{Z_0}^2)} - \frac{26}{3}\frac{m_{Z_0}^6\lambda_0}{m_{H_0}^2(m_{H_0}^2 - m_{Z_0}^2)} \\ &+ \frac{16}{3}\frac{m_{Z_0}^4\lambda_0}{m_{H_0}^2(m_{H_0}^2 - m_{Z_0}^2)}\ln\frac{\mu^2}{m_{H_0}^2} + \frac{2}{3}\frac{m_{Z_0}^4\lambda_0}{(m_{H_0}^2 - m_{Z_0}^2)}\ln\frac{\mu^2}{m_{Z_0}^2} - 6\frac{m_{Z_0}^6\lambda_0}{m_{H_0}^2(m_{H_0}^2 - m_{Z_0}^2)}\ln\frac{\mu^2}{m_{Z_0}^2}\end{aligned} \tag{2.4.17}$$

and

$$[\delta A^U]_f = -\frac{2}{3}\frac{m_{Z_0}^2\lambda_0}{(m_{H_0}^2 - m_{Z_0}^2)}\left(\left(1 + \ln\frac{\mu^2}{m_{H_0}^2}\right) - \frac{m_{Z_0}^2}{m_{H_0}^4}\left(1 + \ln\frac{\mu^2}{m_{Z_0}^2}\right)\right). \tag{2.4.18}$$

It is interesting to notice that the last two expressions for the finite parts can be obtained from the corresponding R_ξ gauge expressions in Eq. (2.3.19) and Eq. (2.3.20) for $\xi = 1$ and not for $\xi \to \infty$.

2.4.3 Corrections to the Higgs mass

The first correction to the Higgs mass comes from

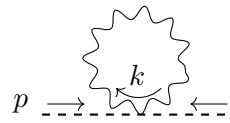

$$= \; i\mathcal{M}_H^{U,Z}$$

and in DR it becomes

$$\begin{aligned}\mathcal{M}_H^{U,Z} &= \mu^\varepsilon\Big\{2d\frac{\lambda_0 m_{Z_0}^2}{m_{H_0}^2}A_0(m_{Z_0}) - 2\frac{\lambda_0}{m_{H_0}^2}U_{\mathcal{T}}(1,m_{Z_0})\Big\} \\ &= \mu^\varepsilon 6\frac{\lambda_0 m_{Z_0}^2}{m_{H_0}^2}A_0(m_{Z_0})\,. \end{aligned} \tag{2.4.19}$$

Next is

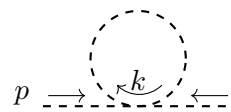

$$= \; i\mathcal{M}_H^{U,\phi}$$

In DR it reads,

$$\mathcal{M}_H^{U,\phi} = 3\lambda_0\mu^\varepsilon A_0(m_{H_0}). \tag{2.4.20}$$

The Higgs vacuum polarization diagram

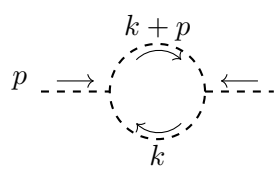

$$= \; i\mathcal{M}_H^{U,\phi\phi}$$

which in DR is equal to

$$\mathcal{M}_H^{U,\phi\phi} = 9\lambda_0 m_{H_0}^2\mu^\varepsilon B_0(p,m_{H_0},m_{H_0})\,. \tag{2.4.21}$$

The corresponding gauge loop is

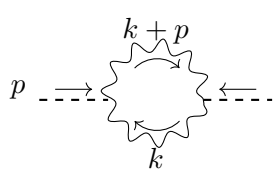

$$= \; i\mathcal{M}_H^{U,ZZ}$$

and in DR

$$\begin{aligned}
\mathcal{M}_H^{U,ZZ} &= \mu^\varepsilon \Bigg\{ 4d \frac{\lambda_0 m_{Z_0}^4}{m_{H_0}^2} B_0(p, m_{Z_0}, m_{Z_0}) \\
&- 4 \frac{\lambda_0 m_{Z_0}^2}{m_{H_0}^2} g_{\mu\nu} B_{k+p}^{\mu\nu}(p, m_{Z_0}, m_{Z_0}) + 4 \frac{\lambda_0}{m_{H_0}^2} m_{Z_0}^2 A_0(m_{Z_0}) + 4 \frac{\lambda_0}{m_{H_0}^2} m_{Z_0}^4 \\
&- 4 \frac{\lambda_0}{m_{H_0}^2} p^2 g_{\mu\nu} B^{\mu\nu}(p, m_{Z_0}, m_{Z_0}) + 4 \frac{\lambda_0}{m_{H_0}^2} p_\mu p_\nu B^{\mu\nu}(p, m_{Z_0}, m_{Z_0}) \Bigg\} , \qquad (2.4.22)
\end{aligned}$$

where we have defined

$$g_{\mu\nu} B_{k+p}^{\mu\nu}(p, m_{Z_0}, m_{Z_0}) = \int \frac{d^4 k}{(2\pi)^4} \frac{-i(k+p)^2}{\left(k^2 - m_{Z_0}^2\right)\left((k+p)^2 - m_{Z_0}^2\right)} . \qquad (2.4.23)$$

Adding up Eq. (2.4.19), Eq. (2.4.20), Eq. (2.4.21) and Eq. (2.4.22) we obtain

$$\begin{aligned}
\mathcal{M}_H^U(p) &= \mu^\varepsilon \Bigg\{ 6 \frac{\lambda m_{Z_0}^2}{m_{H_0}^2} A_0(m_{Z_0}) + \frac{2\lambda m_{Z_0}^4}{m_{H_0}^2} + 3\lambda_0 A_0(m_{H_0}) \\
&+ 9\lambda_0 m_{H_0}^2 B_0(p, m_{H_0}, m_{H_0}) + \frac{\lambda_0 m_{Z_0}^2}{m_{H_0}^2} \Big\{ 4d m_{Z_0}^2 B_0(p, m_{Z_0}, m_{Z_0}) \\
&- 4 g_{\mu\nu} B_{k+p}^{\mu\nu}(p, m_{Z_0}, m_{Z_0}) + 4 A_0(m_{Z_0}) - 4 \frac{p^2}{m_{Z_0}^2} g_{\mu\nu} B^{\mu\nu}(p, m_{Z_0}, m_{Z_0}) \\
&+ 4 m_{Z_0}^2 + 4 \frac{p_\mu p_\nu}{m_{Z_0}^2} B^{\mu\nu}(p, m_{Z_0}, m_{Z_0}) \Big\} \Bigg\} . \qquad (2.4.24)
\end{aligned}$$

Using the reduction formulae in Appendix 2.B and summing up all contributions we can extract

$$(4\pi)^{d/2} \mathcal{M}_H^U = \mu^\varepsilon \left([\mathcal{M}_H^U]_\varepsilon + [\mathcal{M}_H^U]_f \right) \qquad (2.4.25)$$

with

$$\varepsilon [\mathcal{M}_H^U]_\varepsilon = 24 \lambda_0 m_{H_0}^2 + 36 \frac{\lambda_0 m_{Z_0}^4}{m_{H_0}^2} \qquad (2.4.26)$$

and

$$[\mathcal{M}_H^U]_f = 3\lambda_0 m_{H_0}^2 + 6 \frac{\lambda_0 m_{Z_0}^4}{m_{H_0}^2} + 12 \lambda_0 m_{H_0}^2 \ln \frac{\mu^2}{m_{H_0}^2} + 18 \frac{\lambda_0 m_{Z_0}^4}{m_{H_0}^2} \ln \frac{\mu^2}{m_{Z_0}^2} . \qquad (2.4.27)$$

The anomalous dimension is then

$$\delta\phi^U = - \frac{d\mathcal{M}_H^U(p)}{dp^2} \bigg|_{p^2=0} = \frac{\mu^\varepsilon}{(4\pi)^{d/2}} \left([\delta\phi^U]_\varepsilon + [\delta\phi^U]_f \right) \qquad (2.4.28)$$

with

$$\varepsilon [\delta\phi^U]_\varepsilon = 12 \lambda_0 \frac{m_{Z_0}^2}{m_{H_0}^2} . \qquad (2.4.29)$$

and

$$[\delta\phi^U]_f \quad = \quad 2\lambda_0 \frac{m_{Z_0}^2}{m_{H_0}^2} + 6\lambda_0 \frac{m_{Z_0}^4}{m_{H_0}^2} \ln \frac{\mu^2}{m_{Z_0}^2} \,. \tag{2.4.30}$$

Comparing to the result of Sect. 2.3.3 we can see that Eq. (2.4.26) and Eq. (2.4.27) of $\mathcal{M}_H^U$ are identical to Eq. (2.3.30) and Eq. (2.3.31) of $\mathcal{M}_H^{R_\xi}$ and (the ξ-independent) anomalous dimension of the R_ξ gauge is equal to $\delta\phi^U$.

2.4.4 Corrections to the Higgs cubic vertex

As before we split the diagrams in two classes. The first class consists of the reducible Triangle diagrams, while the second one consists of the irreducible Triangles. The contribution of the various topologies and channels is contained in their P_1 and (P_1, P_2) dependence respectively, exactly as in the R_ξ-gauge calculation.

Reducible Triangles

The first reducible Triangle is

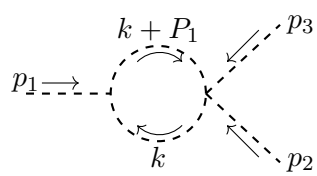

$$= \; i\mathcal{K}_H^{U,\phi\phi}$$

and it is the same loop as in Eq. (2.4.21) with $p \to P_1$, with the same symmetry factor, divided by v_0:

$$\mathcal{K}_H^{U,\phi\phi} \quad = \quad 18 \frac{\lambda_0^{3/2}}{\sqrt{2}} m_{H_0} \mu^\varepsilon B_0(P_1, m_{H_0}, m_{H_0}) \,, \tag{2.4.31}$$

where the three different channels are obtained by summing over P_1, with $P_1 = p_1, p_2, p_3$ (resulting to an overall factor of 3, as in the R_ξ-gauge).

Next is the gauge loop

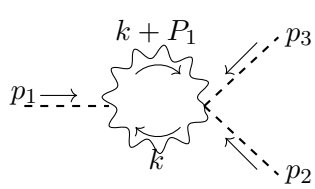

$$= \; i\mathcal{K}_H^{U,ZZ}$$

which is Eq. (2.4.22), divided by v_0:

$$\mathcal{K}_H^{U,ZZ} \quad = \quad \frac{1}{v_0} \frac{4\lambda_0}{m_{H_0}^2} \mu^\varepsilon \Bigg\{ d m_{Z_0}^4 B_0(P_1, m_{Z_0}, m_{Z_0})$$

$$
\begin{aligned}
&- \quad m_{Z_0}^2 g_{\mu\nu} B^{\mu\nu}_{k+P_1}(P_1, m_{Z_0}, m_{Z_0}) + m_{Z_0}^2 A_0(m_{Z_0}) + 4m_{Z_0}^2 \\
&- \quad P_1^2 g_{\mu\nu} B^{\mu\nu}(P_1, m_{Z_0}, m_{Z_0}) + P_{1\mu} P_{1\nu} B^{\mu\nu}(P_1, m_{Z_0}, m_{Z_0}) \Big\}. \qquad (2.4.32)
\end{aligned}
$$

There are again two more channels with $P_1 = p_2$ and $P_1 = p_3$, yielding identical contributions.

Adding up all the reducible Triangles, we have

$$
(4\pi)^{d/2} \mathcal{K}_H^{U,\text{red.}} = \mu^\varepsilon \left([\mathcal{K}_H^{U,\text{red.}}]_\varepsilon + [\mathcal{K}_H^{U,\text{red.}}]_f \right) \qquad (2.4.33)
$$

with

$$
\varepsilon [\mathcal{K}_H^{U,\text{red.}}]_\varepsilon = \frac{m_{H_0}}{\sqrt{2\lambda_0}} \left(108\lambda_0^2 + 144 \frac{\lambda_0^2 m_{Z_0}^4}{m_{H_0}^4} \right) \qquad (2.4.34)
$$

and

$$
[\mathcal{K}_H^{U,\text{red.}}]_f = \frac{m_{H_0}}{\sqrt{2\lambda}} \Big(54\lambda_0^2 \ln \frac{\mu^2}{m_{H_0}^2} + 72 \frac{\lambda_0^2 m_{Z_0}^4}{m_{H_0}^4} \ln \frac{\mu^2}{m_{Z_0}^2} \Big) \qquad (2.4.35)
$$

at $p_i = 0$.

Irreducible Triangles

The first irreducible Triangle is

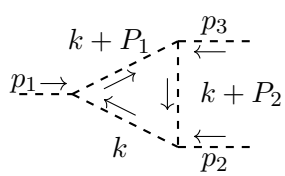

$$
= i\mathcal{K}_H^{U,\phi\phi\phi}
$$

$$
\mathcal{K}_H^{U,\phi\phi\phi} = \frac{108}{\sqrt{2}} \lambda_0^{3/2} m_{H_0}^3 \int \frac{d^4k}{(2\pi)^4} (-i) \frac{1}{D_1 D_2 D_3}. \qquad (2.4.36)
$$

and in DR

$$
\mathcal{K}_H^{U\phi\phi\phi} = \frac{108}{\sqrt{2}} \lambda_0^{3/2} m_{H_0}^3 \mu^\varepsilon C_0(P_1, P_2, m_{H_0}, m_{H_0}, m_{H_0}). \qquad (2.4.37)
$$

In the Unitary gauge there is only one more divergent irreducible Triangle, which is

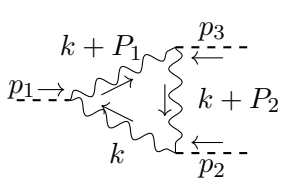

$$
= i\mathcal{K}_H^{U,ZZZ}
$$

$$
\begin{aligned}
\mathcal{K}_H^{U,ZZZ} &= -16\sqrt{2}\frac{m_{Z_0}^6\lambda_0^{3/2}}{m_{H_0}^3}g^{\mu\nu}g^{\alpha\beta}g^{\gamma\delta}\int\frac{d^4k}{(2\pi)^4}\frac{-i\left(-g_{\mu\gamma}+\frac{k_\mu k_\gamma}{m_{Z_0}^2}\right)}{D_1D_2D_3}\left(-g_{\nu\alpha}+\frac{(k+P_1)_\nu(k+P_1)_\alpha}{m_{Z_0}^2}\right)\\
&\times\left(-g_{\delta\beta}+\frac{(k+P_2)_\delta(k+P_2)_\beta}{m_{Z_0}^2}\right) \qquad (2.4.38)
\end{aligned}
$$

and in DR

$$
\begin{aligned}
\mathcal{K}_H^{U,ZZZ} &= -32v_0\frac{m_{Z_0}^6\lambda_0^2}{m_{H_0}^4}\mu^\varepsilon\Bigg\{-dC_0(P_1,P_2,m_{Z_0},m_{Z_0},m_{Z_0})\\
&+ \frac{1}{m_{Z_0}^2}\Big\{(3m_{Z_0}^2+P_1\cdot P_1+P_2\cdot P_2)C_0(P_1,P_2,m_{Z_0},m_{Z_0},m_{Z_0})+3B_0(P_1,m_{Z_0},m_{Z_0})\Big\}\\
&+ \frac{1}{m_{Z_0}^4}\Big\{3U_{K4}(P_1,P_2,m_{Z_0},m_{Z_0},m_{Z_0})+4(P_1+P_2)_\mu C_{\mathcal{K}3}^\mu(P_1,P_2,m_{Z_0},m_{Z_0},m_{Z_0})\\
&+ 2(P_{1\mu}P_{1\nu}+P_{1\mu}P_{2\nu}+P_{2\mu}P_{2\nu})C^{\mu\nu}(P_1,P_2,m_{Z_0},m_{Z_0},m_{Z_0})+2P_1\cdot P_2B_0(p_1,m_{Z_0},m_{Z_0})\\
&+ 2P_1\cdot P_2(P_1+P_2)_\mu C^\mu(P_1,P_2,m_{Z_0},m_{Z_0},m_{Z_0})+P_1\cdot P_2C_0(P_1,P_2,m_{Z_0},m_{Z_0},m_{Z_0})\Big\}\\
&+ \frac{1}{m_{Z_0}^6}\Big\{U_{K6}(P_1,P_2,m_{Z_0},m_{Z_0},m_{Z_0})+2(P_1+P_2)_\mu U_{K5}^\mu(P_1,P_2,m_{Z_0},m_{Z_0},m_{Z_0})\\
&+ (P_{1\mu}P_{1\nu}+3P_{1\mu}P_{2\nu}+P_{2\mu}P_{2\nu})U_{K4}^{\mu\nu}(P_1,P_2,m_{Z_0},m_{Z_0},m_{Z_0})\\
&+ P_1\cdot P_2U_{K4}(P_1,P_2,m_{Z_0},m_{Z_0},m_{Z_0})\\
&+ (P_{1\mu}P_{1\nu}P_{2\alpha}+P_{1\mu}P_{2\nu}P_{2\alpha})C^{\mu\nu\alpha}(P_1,P_2,m_{Z_0},m_{Z_0},m_{Z_0})\\
&+ P_1\cdot P_2(P_{1\mu}+P_{2\mu})C_{\mathcal{K}3}^\mu(P_1,P_2,m_{Z_0},m_{Z_0},m_{Z_0})\\
&+ P_1\cdot P_2P_{1\mu}P_{2\nu}C^{\mu\nu}(P_1,P_2,m_{Z_0},m_{Z_0},m_{Z_0})\Big\}\Bigg\}, \qquad (2.4.39)
\end{aligned}
$$

where in this case $P_1 = p_1$ and $P_2 = p_1 + p_3$. The contracted PV integral $C_{\mathcal{K}3}^\mu$ is defined in Appendix 2.B.2.

In total, we find for the irreducible Triangles

$$
(4\pi)^{d/2}\mathcal{K}_H^{U,\text{irred.}} = \mu^\varepsilon\left([\mathcal{K}_H^{U,\text{irred.}}]_\varepsilon+[\mathcal{K}_H^{U,\text{irred.}}]_f\right) \qquad (2.4.40)
$$

with

$$
[\mathcal{K}_H^{U,\text{irred.}}]_\varepsilon = 0 \qquad (2.4.41)
$$

and

$$
[\mathcal{K}_H^{U,\text{irred.}}]_f = -\frac{m_{H_0}}{\sqrt{2\lambda}}\left(54\lambda_0^2+48\frac{\lambda_0^2m_{Z_0}^4}{m_{H_0}^4}\right). \qquad (2.4.42)
$$

Finally, adding reducible and irreducible contributions, we have

$$
(4\pi)^{d/2}\mathcal{K}_H^U = \mu^\varepsilon\left([\mathcal{K}_H^U]_\varepsilon+[\mathcal{K}_H^U]_f\right) \qquad (2.4.43)
$$

where

$$
\varepsilon[\mathcal{K}_H^U]_\varepsilon = \frac{m_{H_0}}{\sqrt{2\lambda_0}}\left(108\lambda_0^2+144\frac{\lambda_0^2m_{Z_0}^4}{m_{H_0}^4}\right) \qquad (2.4.44)
$$

and

$$[\mathcal{K}_H^U]_f \quad = \quad \frac{m_{H_0}}{\sqrt{2\lambda}}\Big(-54\lambda_0^2 - 24\frac{\lambda_0^2 m_{Z_0}^4}{m_{H_0}^4} + 54\lambda_0^2 \ln\frac{\mu^2}{m_{H_0}^2} + 72\frac{\lambda_0^2 m_{Z_0}^4}{m_{H_0}^4}\ln\frac{\mu^2}{m_{Z_0}^2}\Big). \tag{2.4.45}$$

These are the same results as the ones found in Eq. (2.3.60) and Eq. (2.3.61) in the R_ξ-gauge.

2.4.5 Corrections to the quartic coupling

The separation of the Box diagrams into C, T and S-Boxes in the Unitary gauge holds exactly like in the R_ξ gauge. The same goes for the labelling of the various channels by the momenta P_1 (for Candies), (P_1, P_2) for T-Boxes and (P_1, P_2, P_3) for S-Boxes.

Reducible Boxes

The Higgs Candy

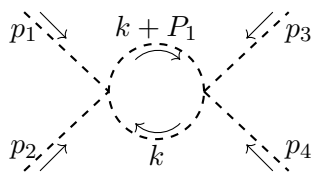

$$= \; i\mathcal{B}_H^{U,\phi\phi}$$

has been computed already in the R_ξ gauge with the result

$$\mathcal{B}_H^{U,\phi\phi} \quad = \quad 18\lambda_0^2\mu^\varepsilon B_0(P_1, m_{H_0}, m_{H_0})\,. \tag{2.4.46}$$

The gauge Candy is slightly different due to the different gauge boson propagator. The diagram is

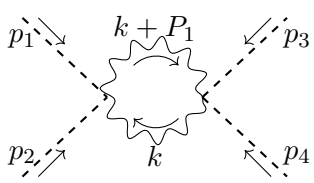

$$= \; i\mathcal{B}_H^{U,ZZ}$$

It evaluates in DR to

$$\begin{aligned}(4\pi)^{d/2}\mathcal{B}_H^{U,ZZ} \quad &= \quad 8\frac{m_{Z_0}^2}{m_{H_0}^4}\lambda_0^2\mu^\varepsilon\Big\{dm_{Z_0}^2 B_0(P_1, m_{Z_0}, m_{Z_0}) \\ &- \quad g_{\mu\nu}B_{k+P_1}^{\mu\nu}(P_1, m_{Z_0}, m_{Z_0}) + A_0(m_{Z_0}) + 2m_{Z_0}^2 \\ &- \quad \frac{P_1^2}{m_{Z_0}^2}g_{\mu\nu}B^{\mu\nu}(P_1, m_{Z_0}, m_{Z_0}) + \frac{P_{1\mu}P_{1\nu}}{m_{Z_0}^2}B^{\mu\nu}(P_1, m_{Z_0}, m_{Z_0})\Big\}\,. \end{aligned} \tag{2.4.47}$$

These are the only two contributions in this sector and adding them up, we have

$$(4\pi)^{d/2}\mathcal{B}_H^{U,C} = \mu^\varepsilon\left([\mathcal{B}_H^{U,C}]_\varepsilon + [\mathcal{B}_H^{U,C}]_f\right) \tag{2.4.48}$$

where

$$\varepsilon[\mathcal{B}_H^{U,C}]_\varepsilon = 108\lambda_0^2 + 144\frac{\lambda_0^2 m_{Z_0}^4}{m_{H_0}^4} + 4\frac{s^2\lambda_0^2}{m_{H_0}^4} + 4\frac{t^2\lambda_0^2}{m_{H_0}^4} + 4\frac{u^2\lambda_0^2}{m_{H_0}^4} \tag{2.4.49}$$

and

$$[\mathcal{B}_H^{U,C}]_f = 54\lambda_0^2 \ln\frac{\mu^2}{m_{H_0}^2} + 72\frac{\lambda_0^2 m_{Z_0}^4}{m_{H_0}^4}\ln\frac{\mu^2}{m_{Z_0}^2}. \tag{2.4.50}$$

We turn to the T-Boxes. In the Unitary gauge we have only two contributing diagrams, one finite and one divergent. The finite diagram is

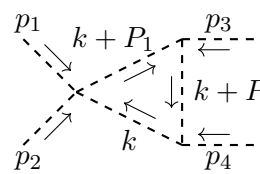

$$= i\mathcal{B}_H^{U,\phi\phi\phi}$$

The s channel contribution is equal to

$$\mathcal{B}_H^{U,\phi\phi\phi} = 108\lambda_0^2 m_{H_0}^2 \mu^\varepsilon C_0(P_1, m_{H_0}, m_{H_0}, m_{H_0}). \tag{2.4.51}$$

The t and u channels can be obtained as explained in the R_ξ-gauge calculation. The divergent diagram in this sector is

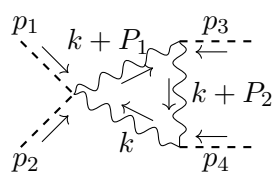

$$= i\mathcal{B}_H^{U,ZZZ}$$

and can be easily be obtained from Eq.(2.4.39) by dividing by v_0:

$$\begin{aligned}
\mathcal{B}_H^{U,ZZZ} &= -32\frac{m_{Z_0}^6\lambda_0^2}{m_{H_0}^4}\mu^\varepsilon\Big\{-dC_0(P_1,P_2,m_{Z_0},m_{Z_0},m_{Z_0}) \\
&+ \frac{1}{m_{Z_0}^2}\Big\{(3m_{Z_0}^2 + P_1\cdot P_1 + P_2\cdot P_2)C_0(P_1,P_2,m_{Z_0},m_{Z_0},m_{Z_0}) + 3B_0(P_1,m_{Z_0},m_{Z_0})\Big\} \\
&+ \frac{1}{m_{Z_0}^4}\Big\{3U_{K4}(P_1,P_2,m_{Z_0},m_{Z_0},m_{Z_0}) + 4(P_1+P_2)_\mu C_{\mathcal{K}3}^\mu(P_1,P_2,m_{Z_0},m_{Z_0},m_{Z_0}) \\
&+ 2(P_{1\mu}P_{1\nu} + P_{1\mu}P_{2\nu} + P_{2\mu}P_{2\nu})C^{\mu\nu}(P_1,P_2,m_{Z_0},m_{Z_0},m_{Z_0}) + 2P_1\cdot P_2 B_0(p_1,m_{Z_0},m_{Z_0}) \\
&+ 2P_1\cdot P_2(P_1+P_2)_\mu C^\mu(P_1,P_2,m_{Z_0},m_{Z_0},m_{Z_0}) + P_1\cdot P_2 C_0(P_1,P_2,m_{Z_0},m_{Z_0},m_{Z_0})\Big\} \\
&+ \frac{1}{m_{Z_0}^6}\Big\{U_{K6}(P_1,P_2,m_{Z_0},m_{Z_0},m_{Z_0}) + 2(P_1+P_2)_\mu U_{K5}^\mu(P_1,P_2,m_{Z_0},m_{Z_0},m_{Z_0}) \\
&+ (P_{1\mu}P_{1\nu} + 3P_{1\mu}P_{2\nu} + P_{2\mu}P_{2\nu})U_{K4}^{\mu\nu}(P_1,P_2,m_{Z_0},m_{Z_0},m_{Z_0}) \\
&+ P_1\cdot P_2 U_{K4}(P_1,P_2,m_{Z_0},m_{Z_0},m_{Z_0})
\end{aligned}$$

$$
\begin{aligned}
&+ \quad (P_{1\mu}P_{1\nu}P_{2\alpha} + P_{1\mu}P_{2\nu}P_{2\alpha})C^{\mu\nu\alpha}(P_1, P_2, m_{Z_0}, m_{Z_0}, m_{Z_0}) \\
&+ \quad P_1 \cdot P_2(P_{1\mu} + P_{2\mu})C^{\mu}_{\mathcal{K}3}(P_1, P_2, m_{Z_0}, m_{Z_0}, m_{Z_0}) \\
&+ \quad P_1 \cdot P_2 P_{1\mu}P_{2\nu}C^{\mu\nu}(P_1, P_2, m_{Z_0}, m_{Z_0}, m_{Z_0})\Big\}\Bigg\}. \qquad (2.4.52)
\end{aligned}
$$

After summing over all channels by summing over all (P_1, P_2), we obtain

$$
(4\pi)^{d/2}\mathcal{B}_H^{U,T} = \mu^{\varepsilon}\left([\mathcal{B}_H^{U,T}]_{\varepsilon} + [\mathcal{B}_H^{U,T}]_f\right) \qquad (2.4.53)
$$

where

$$
\varepsilon[\mathcal{B}_H^{U,T}]_{\varepsilon} = -28\frac{s^2\lambda_0^2}{m_{H_0}^4} - 40\frac{s\cdot t\lambda_0^2}{m_{H_0}^4} - 28\frac{t^2\lambda_0^2}{m_{H_0}^4} - 40\frac{s\cdot u\lambda_0^2}{m_{H_0}^4} - 40\frac{t\cdot u\lambda_0^2}{m_{H_0}^4} - 28\frac{u^2\lambda_0^2}{m_{H_0}^4} \qquad (2.4.54)
$$

and

$$
[\mathcal{B}_H^{U,T}]_f = -162\lambda_0^2 - 288\frac{\lambda_0^2 m_{Z_0}^4}{m_{H_0}^4} \qquad (2.4.55)
$$

at $p_i = 0$.

Irreducible Boxes

The irreducible, S-Boxes in the Unitary gauge are only two, one finite and one divergent. The finite diagram is the Higgs S-Box

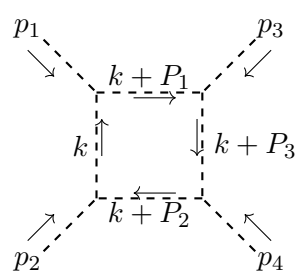

$$
= i\mathcal{B}_H^{U,\phi\phi\phi\phi}
$$

$$
\mathcal{B}_H^{U,\phi\phi\phi\phi} = 324\lambda_0^2 m_{H_0}^2 \int \frac{d^4k}{(2\pi)^4}\frac{-i}{D_1D_2D_3D_4}. \qquad (2.4.56)
$$

In DR

$$
\mathcal{B}_H^{U,\phi\phi\phi\phi} = 324\lambda_0^2 m_{H_0}^2 \mu^{\varepsilon} D_0(P_1, P_2, P_3, m_{H_0}, m_{H_0}, m_{H_0}, m_{H_0}). \qquad (2.4.57)
$$

The divergent S-Box is the one with a gauge loop

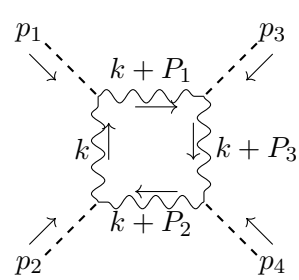

$$
= i\mathcal{B}_H^{U,ZZZZ}
$$

which is equal to

$$\begin{aligned}
\mathcal{B}_H^{U,ZZZZ} &= 64\frac{m_{Z_0}^8\lambda_0^2}{m_{H_0}^4}g^{\mu\nu}g^{\alpha\beta}g^{\gamma\delta}g^{\epsilon\zeta}\int\frac{d^4k}{(2\pi)^4}\frac{-i\left(-g_{\zeta\mu}+\frac{k_\zeta k_\mu}{m_{Z_0}^2}\right)}{D_1D_2D_3D_4}\left(-g_{\nu\alpha}+\frac{(k+P_1)_\nu(k+P_1)_\alpha}{m_{Z_0}^2}\right)\\
&\times\left(-g_{\beta\gamma}+\frac{(k+P_2)_\beta(k+P_2)_\gamma}{m_{Z_0}^2}\right)\left(-g_{\delta\epsilon}+\frac{(k+P_3)_\delta(k+P_3)_\epsilon}{m_{Z_0}^2}\right), \qquad (2.4.58)
\end{aligned}$$

and in DR

$$\begin{aligned}
\mathcal{B}_H^{U,ZZZZ} &= 64\frac{\lambda_0^2m_{Z_0}^8}{m_{H_0}^4}\mu^\varepsilon\Big\{dD_0(P_1,P_2,P_3,m_{Z_0},m_{Z_0},m_{Z_0},m_{Z_0})\\
&- \frac{1}{m_{Z_0}^2}\Big\{4g_{\mu\nu}D^{\mu\nu}(P_1,P_2,P_3,m_{Z_0},m_{Z_0},m_{Z_0},m_{Z_0})\\
&+ 2(P_1+P_2+P_3)_\mu D^\mu(P_1,P_2,P_3,m_{Z_0},m_{Z_0},m_{Z_0},m_{Z_0})\\
&+ (P_1^2+P_2^2+P_3^2)D_0(P_1,P_2,P_3,m_{Z_0},m_{Z_0},m_{Z_0},m_{Z_0})\Big\}\\
&+ \frac{1}{m_{Z_0}^4}\Big\{6D_{\mathcal{B}4}(P_1,P_2,P_3,m_{Z_0},m_{Z_0},m_{Z_0},m_{Z_0})\Big\}\\
&- \frac{1}{m_{Z_0}^6}\Big\{4U_{B_6}(P_1,P_2,P_3,m_{Z_0},m_{Z_0},m_{Z_0},m_{Z_0})\\
&+ 6(P_1+P_2+P_3)_\mu U_{B_5}^\mu(P_1,P_2,P_3,m_{Z_0},m_{Z_0},m_{Z_0},m_{Z_0})\\
&+ 3(2P_{1\mu}P_{2\nu}+P_{2\mu}P_{2\nu}+2P_{1\mu}P_{3\nu}+2P_{2\mu}P_{3\nu}\\
&+ P_{3\mu}P_{3\nu}+P_{1\mu}P_{1\nu})D_{\mathcal{B}4}^{\mu\nu}(P_1,P_2,P_3,m_{Z_0},m_{Z_0},m_{Z_0},m_{Z_0})\\
&+ 2(P_1\cdot P_2+P_1\cdot P_3+P_2\cdot P_3)D_{\mathcal{B}4}(P_1,P_2,P_3,m_{Z_0},m_{Z_0},m_{Z_0},m_{Z_0})\Big\}\\
&+ \frac{1}{m_{Z_0}^8}\Big\{U_{B8}(P_1,P_2,P_3,m_{Z_0},m_{Z_0},m_{Z_0},m_{Z_0})\\
&+ 2(P_1+P_2+P_3)_\mu U_{B7}^\mu(P_1,P_2,P_3,m_{Z_0},m_{Z_0},m_{Z_0},m_{Z_0})\\
&+ \Big\{P_{1\mu}P_{1\nu}+3P_{1\mu}P_{2\nu}+P_{2\mu}P_{2\nu}\\
&+ 4P_{1\mu}P_{3\nu}+3P_{2\mu}P_{3\nu}+P_{3\mu}P_{3\nu}\Big\}U_{B6}^{\mu\nu}(P_1,P_2,P_3,m_{Z_0},m_{\chi_0},m_{Z_0},m_{Z_0})\\
&+ (P_1\cdot P_2+P_2\cdot P_3)U_{B6}(P_1,P_2,P_3,m_{Z_0},m_{Z_0},m_{Z_0},m_{Z_0})\\
&+ \Big\{P_{1\mu}P_{1\nu}P_{2\alpha}+P_{1\mu}P_{2\nu}P_{2\alpha}+2P_{1\mu}P_{1\nu}P_{3\alpha}+4P_{1\mu}P_{2\nu}P_{3\alpha}\\
&+ P_{2\mu}P_{2\nu}P_{3\alpha}+2P_{1\mu}P_{3\nu}P_{3\alpha}+P_{2\mu}P_{3\nu}P_{3\alpha}\Big\}U_{B5}^{\mu\nu\alpha}(P_1,P_2,P_3,m_{Z_0},m_{Z_0},m_{Z_0},m_{Z_0})\\
&+ \Big\{P_1\cdot P_2[P_1+P_2+2P_3]_\mu+P_2\cdot P_3[2P_1+P_2+P_3]_\mu\Big\}U_{B5}^\mu(P_1,P_2,P_3,m_{Z_0},m_{Z_0},m_{Z_0},m_{Z_0})\\
&+ \Big\{P_{1\mu}P_{1\nu}P_{2\alpha}P_{3\beta}+P_{1\mu}P_{2\nu}P_{2\alpha}P_{3\beta}\\
&+ P_{1\mu}P_{1\nu}P_{3\alpha}P_{3\beta}+P_{1\mu}P_{2\nu}P_{3\alpha}P_{3\beta}\Big\}D^{\mu\nu\alpha\beta}(P_1,P_2,P_3,m_{Z_0},m_{Z_0},m_{Z_0},m_{Z_0})\\
&+ \Big\{P_1\cdot P_2[P_{1\mu}P_{1\nu}+2P_{1\mu}P_{3\nu}+P_{2\mu}P_{3\nu}+P_{3\mu}P_{3\nu}]\\
&+ P_2\cdot P_3[P_{1\mu}P_{1\nu}+P_{1\mu}P_{2\nu}+2P_{1\mu}P_{3\nu}+P_{2\mu}P_{3\nu}]\Big\}D_{\mathcal{B}4}^{\mu\nu}(P_1,P_2,P_3,m_{Z_0},m_{Z_0},m_{Z_0},m_{Z_0})\\
&+ (P_1\cdot P_2\times P_2\cdot P_3)D_{\mathcal{B}4}(P_1,P_2,P_3,m_{Z_0},m_{Z_0},m_{Z_0},m_{Z_0})\Big\}\Big\}
\end{aligned}$$

$$+ \quad (B_H^{U,ZZZZ})_{f,1} + (B_H^{U,ZZZZ})_{f,2} + (B_H^{U,ZZZZ})_{f,3}\,. \tag{2.4.59}$$

The $(B_H^{U,ZZZZ})_{f,1}$, $(B_H^{U,ZZZZ})_{f,2}$ and $(B_H^{U,ZZZZ})_{f,3}$ are finite integrals, moved to Appendix 2.E. The U-integrals are dealt with in Appendix 2.C. The s, t and u channels are taken into account by summing over the (P_1, P_2, P_3) as in the R_ξ gauge. The divergence structure of the sum of the S-Boxes at zero external momenta is revealed through the relation

$$(4\pi)^{d/2}\mathcal{B}_H^{U,S} \quad = \quad \mu^\varepsilon \left([\mathcal{B}_H^{U,S}]_\varepsilon + [\mathcal{B}_H^{U,S}]_f\right) \tag{2.4.60}$$

where

$$\varepsilon[\mathcal{B}_H^{U,S}]_\varepsilon \quad = \quad 24\frac{s^2\lambda_0^2}{m_{H_0}^4} + 40\frac{s\cdot t\lambda_0^2}{m_{H_0}^4} + 24\frac{t^2\lambda_0^2}{m_{H_0}^4} + 40\frac{s\cdot u\lambda_0^2}{m_{H_0}^4} + 40\frac{t\cdot u\lambda_0^2}{m_{H_0}^4} + 24\frac{u^2\lambda_0^2}{m_{H_0}^4} \tag{2.4.61}$$

and

$$[\mathcal{B}_H^{U,S}]_f \quad = \quad 162\lambda_0^2 + 96\frac{\lambda_0^2 m_{Z_0}^4}{m_{H_0}^4}. \tag{2.4.62}$$

The total sum of the Boxes then satisfies

$$\varepsilon[\mathcal{B}_H^{U}]_\varepsilon \quad = \quad 108\lambda_0^2 + 144\frac{\lambda_0^2 m_{Z_0}^4}{m_{H_0}^4} \tag{2.4.63}$$

and

$$[\mathcal{B}_H^{U}]_f \quad = \quad -168\frac{\lambda_0^2 m_{Z_0}^4}{m_{H_0}^4} + 54\lambda_0^2 \ln\frac{\mu^2}{m_{H_0}^2} + 72\frac{\lambda_0^2 m_{Z_0}^4}{m_{H_0}^4}\ln\frac{\mu^2}{m_{Z_0}^2}. \tag{2.4.64}$$

In the 4-point function as well, we observe a sector by sector agreement between the R_ξ and Unitary gauges.

2.5 Renormalization

In this section we will renormalize the Abelian-Higgs model in both the R_ξ and Unitary gauges. In fact, since we will be concerned here mainly with the Z-mass and scalar potential we will be able to perform the renormalization program simultaneously for both.

One of the results of the calculation of the previous two sections is that the one-loop corrections to the Z-mass and the scalar potential have identical divergent parts in the R_ξ and Unitary gauges. This means that the two gauges have the same β-functions for the masses and quartic coupling. Now the Lagrangean in the Unitary gauge can be obtained from the R_ξ-gauge Lagrangean by dropping the gauge fixing and ghost terms and simply setting the Goldstone field to zero. Since we are interested here only in the common subsector that consists of the Z-mass term and the scalar potential, we can carry out the renormalization program on the Unitary gauge Lagrangean and only when we arrive at the stage where we analyse the finite, renormalized scalar potential where finite corrections become relevant, we may have to distinguish between the two gauges if necessary. Thus for now and until further notice, we drop the "U" superscript that denotes Unitary gauge.

2.5.1 Counter-terms

We introduce the counter-terms

$$\begin{aligned} m_0^2 &= m^2 + \delta m \\ g_0 &= g + \delta g \\ \lambda_0 &= \lambda + \delta\lambda \end{aligned} \tag{2.5.1}$$

In the Abelian-Higgs model there is a non-zero anomalous dimension for the scalar (as opposed to ϕ^4 theory and the linear sigma model) and likewise a non-zero anomalous dimension for the gauge boson. Therefore, we also introduce

$$\begin{aligned} H_0 &= \sqrt{Z_\phi}\,\phi = \sqrt{1+\delta\phi}\,\phi \\ A_0 &= \sqrt{Z_A}A = \sqrt{1+\delta A}\,A\,. \end{aligned} \tag{2.5.2}$$

Substituting the above in Eq. (2.2.1) and then expressing the Higgs in the Polar basis, we obtain

$$\mathcal{L} = \mathcal{L}^{\text{tree}} + \mathcal{L}^{\text{count.}}\,, \tag{2.5.3}$$

with $\mathcal{L}^{\text{tree}}$ the renormalized tree-level Lagrangean

$$\begin{aligned} \mathcal{L}^{\text{R,tree}} &= -\frac{1}{4}F_{\mu\nu}^2 + \frac{1}{2}\left(\partial_\mu\phi\right)\left(\partial^\mu\phi\right) + \frac{1}{2}m_Z^2 A_\mu A^\mu + g^{\mu\nu}\frac{\lambda m_Z^2}{m_H^2}A_\mu A_\nu\phi^2 \\ &+ g^{\mu\nu}\frac{m_Z^2}{m_H}\sqrt{2\lambda}\phi A_\mu A_\nu - \frac{1}{2}m_H^2\phi^2 - \sqrt{\frac{\lambda}{2}}m_H\phi^3 - \frac{\lambda}{4}\phi^4 \end{aligned} \tag{2.5.4}$$

and $\mathcal{L}^{\text{count.}}$ the counterterm Lagrangian

$$\begin{aligned} \mathcal{L}^{\text{count.}} &= \frac{1}{2}\left\{-(p^2 g_{\mu\nu} - p_\mu p_\nu - g_{\mu\nu}m_Z^2)\delta A + g_{\mu\nu}m_Z^2\delta\phi + g_{\mu\nu}\frac{2m_H m_Z}{\sqrt{2\lambda}}\delta g + \mathcal{M}_{Z,\mu\nu}\right\}A^\mu A^\nu \\ &+ g^{\mu\nu}\left\{\frac{\sqrt{2\lambda}m_Z}{m_H}\delta g + \frac{\lambda m_Z^2}{m_H^2}\delta A + \frac{\lambda m_Z^2}{m_H^2}\delta\phi + \mathcal{M}_{Z4}\right\}A_\mu A_\nu\phi^2 \\ &+ g^{\mu\nu}\left\{2m_Z\delta g + \frac{\sqrt{2\lambda}m_Z^2}{m_H}\delta A + \frac{\sqrt{2\lambda}m_Z^2}{m_H}\delta\phi + \mathcal{M}_{Z3}\right\}\phi A_\mu A_\nu \\ &+ \frac{m_H}{\sqrt{2\lambda}}\left\{-\frac{1}{2}m_H^2\delta\phi + \delta m - \frac{m_H^2}{2\lambda}\delta\lambda + \mathcal{T}_H\right\}\phi \\ &+ \frac{1}{2}\left\{(p^2 - \frac{5}{2}m_H^2)\delta\phi + \delta m - \frac{3m_H^2}{2\lambda}\delta\lambda + \mathcal{M}_H\right\}\phi^2 \\ &- \frac{m_H}{\sqrt{2\lambda}}\left\{\delta\lambda + 2\lambda\delta\phi - \frac{\sqrt{2\lambda}}{m_H}\frac{\mathcal{K}_H}{6}\right\}\phi^3 - \frac{1}{4}\left\{\delta\lambda + 2\lambda\delta\phi - \frac{\mathcal{B}_H}{6}\right\}\phi^4\,, \end{aligned} \tag{2.5.5}$$

with the computed one-loop corrections also added with appropriate factors. Corrections to interaction terms between the Higgs and the Z ($\mathcal{M}_{Z3}$ and $\mathcal{M}_{Z4}$) we have not computed but we are not concerned with those here.

The Feynman rules for the counterterms deriving from the above expression are

- Higgs 1-point function

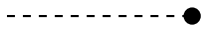

$$= i\frac{m_H}{\sqrt{2\lambda}}\left[-\frac{1}{2}m_H^2\delta\phi + \delta m - \frac{m_H^2}{2\lambda}\delta\lambda\right]$$

- Gauge boson 2-point function

$$= i\left[-(p^2 g_{\mu\nu} - p_\mu p_\nu - g_{\mu\nu}m_Z^2)\delta A + g_{\mu\nu}m_Z^2\delta\phi + g_{\mu\nu}\frac{\sqrt{2}m_H m_Z}{\sqrt{\lambda}}\delta g\right]$$

- Higgs 2-point function

$$= i\left[(p^2 - \frac{5}{2}m_H^2)\delta\phi + \delta m - \frac{3m_H^2}{2\lambda}\delta\lambda\right]$$

- For completeness, the ϕ-Z-Z counterterm vertex

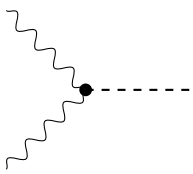

$$= ig^{\mu\nu}\left[4m_Z\delta g + 2\frac{\sqrt{2\lambda}m_Z^2}{m_H}\delta A + 2\frac{\sqrt{2\lambda}m_Z^2}{m_H}\delta\phi\right]$$

- ϕ-ϕ-ϕ vertex counterterm

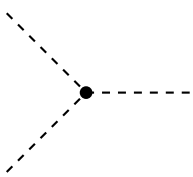

$$= -6i\frac{m_H}{\sqrt{2\lambda}}\left[\delta\lambda + 2\lambda\delta\phi\right]$$

- For completeness, the ϕ-ϕ-Z-Z vertex counterterm

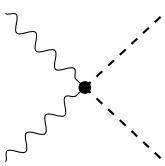

$$= ig^{\mu\nu}\left[4\frac{\sqrt{2\lambda}m_Z}{m_H}\delta g + \frac{4\lambda m_Z^2}{m_H^2}\delta A + \frac{4\lambda m_Z^2}{m_H^2}\delta\phi\right]$$

- ϕ-ϕ-ϕ-ϕ vertex counterterm

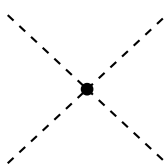

$$= -6i\left[\delta\lambda + 2\lambda\delta\phi\right]$$

The renormalization conditions are in order. All conditions are imposed at zero external momenta. Regarding the gauge boson sector, our renormalization condition is that the mass of the gauge boson be $m_Z = gv_0$. Diagrammatically this condition is

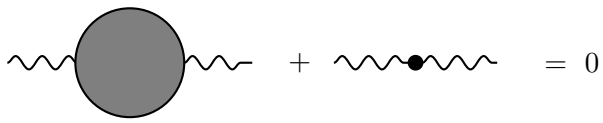

and as an equation

$$\mathcal{M}_Z - \frac{1}{3}\left(g_{\mu\nu} - \frac{p_\mu p_\nu}{p^2}\right)\left((-p^2 g_{\mu\nu} + p_\mu p_\nu + g_{\mu\nu} m_Z^2)\delta A + g_{\mu\nu} m_Z^2 \delta\phi + g_{\mu\nu}\frac{2m_H m_Z}{\sqrt{2\lambda}}\delta g\right) = 0\,. \tag{2.5.6}$$

This is an independent condition from the rest that can be directly solved for δg:

$$2v_0\delta g \;=\; \frac{\mathcal{M}_Z}{m_Z} - \left(m_Z - \frac{p^2}{m_Z}\right)\delta A - m_Z\delta\phi \tag{2.5.7}$$

At zero external momentum, this becomes

$$v_0\delta g \equiv \delta m_Z = \frac{\mu^\varepsilon}{(4\pi)^2}\left[\frac{2}{3}\frac{\lambda m_Z^3}{m_H^2}\frac{1}{\varepsilon} + \frac{1}{2}\left(\frac{\mathcal{M}_Z}{m_Z} - m_Z\delta A - m_Z\delta\phi\right)_f\right], \tag{2.5.8}$$

where we have absorbed in δg all the finite parts. Just one comment on the Higgs-Z interaction terms that we have not computed here: they become finite provided that

$$\frac{\mathcal{M}_Z}{m_Z^2} + \mathcal{M}_{Z3,Z4} = \text{ finite}\,. \tag{2.5.9}$$

Now we turn to the scalar sector. In order to avoid the tadpoles contaminating the one-loop vev for the Higgs field, we impose a vanishing tadpole condition. Diagrammatically it is

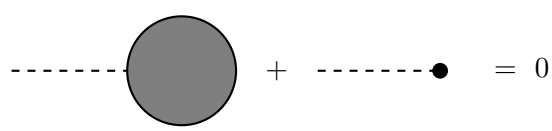

and as an equation

$$\mathcal{T}_H + \frac{m_H}{\sqrt{2\lambda}}\left(-\frac{1}{2}m_H^2\delta\phi + \delta m - \frac{m_H^2}{2\lambda}\delta\lambda\right) = 0\,. \tag{2.5.10}$$

The second condition is the requirement that the only term that remains in the quadratic part of the potential, is m_H. This means that in the quadratic term of the potential we absorb, together with the divergent part, the entire finite term as well:

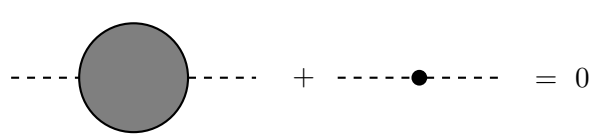

or, in equation at $p = 0$,

$$\mathcal{M}_H - \frac{5}{2}m_H^2\delta\phi + \delta m - \frac{3m_H^2}{2\lambda}\delta\lambda = 0\,. \tag{2.5.11}$$

These two conditions fix completely our freedom. The solution to the system of Eq. (2.5.10) and Eq. (2.5.11) is

$$\delta m = \frac{\mu^\varepsilon}{(4\pi)^2}\left[\frac{1}{\varepsilon}\frac{1}{2}\left(6\lambda m_H^2 - 12\lambda m_Z^2\right) + \frac{1}{2}\left(\mathcal{M}_H - m_H^2\delta\phi - 3\frac{\sqrt{2\lambda}}{m_H}\mathcal{T}_H\right)_f\right] \tag{2.5.12}$$

$$\delta\lambda = \frac{\mu^\varepsilon}{(4\pi)^2}\left[\frac{1}{\varepsilon}\left(18\lambda^2 - 24\lambda^2\frac{m_Z^2}{m_H^2} + 24\lambda^2\frac{m_Z^4}{m_H^4}\right) + \frac{\lambda}{m_H^2}\left(\mathcal{M}_H - 2m_H^2\delta\phi - \frac{\sqrt{2\lambda}}{m_H}\mathcal{T}_H\right)_f\right] \tag{2.5.13}$$

For later reference note that

$$\delta m_H = 2\delta m\,. \tag{2.5.14}$$

Divergences must cancel automatically from the rest. Absence of divergences in the cubic coupling means

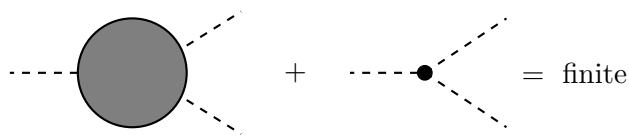

or

$$\frac{\mathcal{K}_H}{6} - \frac{m_H}{\sqrt{2\lambda}}\left(2\lambda\delta\phi + \delta\lambda\right) = \text{finite}\,. \tag{2.5.15}$$

Substituting Eq. (2.5.12) and Eq. (2.5.13) in the above, we find that the divergent part cancels as expected and we are left with the finite terms

$$C_{\phi^3} = \frac{1}{16\pi^2}\Big(\frac{\mathcal{K}_{Hf}}{6} - \frac{1}{2}\frac{\sqrt{2\lambda}}{m_H}\mathcal{M}_{Hf} + \frac{\lambda}{m_H^2}\mathcal{T}_{Hf}\Big)\,. \tag{2.5.16}$$

Absence of divergences from the quartic coupling on the other hand requires

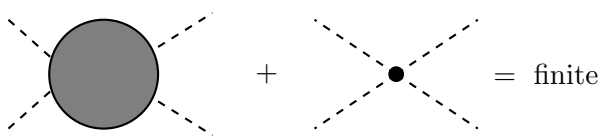

or

$$\frac{\mathcal{B}_H}{6} - \left(2\lambda\delta\phi + \delta\lambda\right) = \text{finite}\,. \tag{2.5.17}$$

Substituting again Eq. (2.5.12) and Eq. (2.5.13) in the above, we again observe the cancellation of the divergent part and we collect the finite piece

$$C_{\phi^4} = \frac{1}{16\pi^2}\Big(\frac{\mathcal{B}_{Hf}}{6} - \frac{\lambda}{m_H^2}\mathcal{M}_{Hf} + \frac{\lambda\sqrt{2\lambda}}{m_H^3}\mathcal{T}_{Hf}\Big)\,. \tag{2.5.18}$$

The subscript f in the various one-loop quantities denotes finite part, in either the R_ξ or the Unitary gauge. For example, $\mathcal{T}_{Hf} = [\mathcal{T}_H^{R_\xi}]_f + \{\mathcal{T}_H^{R_\xi}\}_f$ in the R_ξ gauge $\mathcal{T}_{Hf} = [\mathcal{T}_H^U]_f$ in the Unitary gauge.

The finite one-loop Higgs potential we are left with after renormalization is then

$$V_1(\phi) \quad = \quad \frac{1}{2}m_H^2\phi^2 + \left[\sqrt{\frac{\lambda}{2}}m_H + C_{\phi^3}\right]\phi^3 + \frac{1}{4}\left[\lambda + C_{\phi^4}\right]\phi^4 \,. \tag{2.5.19}$$

The Higgs field anomalous dimension has apparently cancelled from the renormalized potential. We are now ready to minimize this potential. There are three extrema. Our preferred "physical" solution for the global minimum is

$$\langle\phi\rangle \equiv v = 0\,, \tag{2.5.20}$$

for which the potential satisfies $V_1''(v) = m_H^2$. The quantities C_{ϕ^3} and C_{ϕ^4} are examples of the $\star$ quantities in Eq. (2.1.1) of the Introduction. Note finally that $V_1(v) = 0$.

2.5.2 Physical quantities and the β-functions

Let us denote by α_0 a generic bare coupling. Its counter-term $\delta\alpha(\mu)$ is introduced via the relation

$$\alpha_0 = \alpha(\mu) + \delta\alpha(\mu) \tag{2.5.21}$$

where $\alpha(\mu)$ is the renormalized running coupling. At one-loop the counter-term has the form

$$\delta\alpha(\mu) \quad = \quad \frac{\mu^\varepsilon}{(4\pi)^2}\left(\frac{C_\alpha}{\varepsilon} + \sum_k f_{A_0}^k \ln\frac{\mu^2}{m_k^2} + \sum_{k,i} f_{B_0}^k \int_0^1 dx \ln\left(\frac{\mu^2}{\Delta_k^i(m_k, m_i)}\right) + \sum_k f_{A_0}^k\right) . \tag{2.5.22}$$

The indices i and k are counting the fields running in the loop. The entire divergent part has been collected in the term proportional to C_a. In the notation of the previous sections, we can identify $(\mu^\varepsilon/16\pi^2)C_\alpha = \varepsilon(\delta\alpha)_\varepsilon = \varepsilon[\delta\alpha]_\varepsilon + \varepsilon\{\delta\alpha\}_\varepsilon$ and $(\delta\alpha)_f = [\delta\alpha]_f + \{\delta\alpha\}_f$ containing the finite logarithms and the non-logarithmic finite term. As already noted, in the Unitary gauge we have $\{\delta\alpha\}_\varepsilon = \{\delta\alpha\}_f = 0$ by definition.

It is useful to review the calculations of β-functions in the presence of multiple couplings. We introduce the boundary condition

$$\alpha(\mu = m_{\text{phys.}}) \equiv \alpha\,. \tag{2.5.23}$$

We also use the following standard definitions

$$\begin{aligned} \delta_\alpha \quad &\equiv \quad \frac{\delta\alpha(\mu)}{a(\mu)} \\ \beta_\alpha \quad &\equiv \quad \mu\frac{d}{d\mu}\alpha(\mu) \\ \tilde{\beta_\alpha} \quad &\equiv \quad \frac{\beta_\alpha}{\alpha} \end{aligned} \tag{2.5.24}$$

For a general coupling we recall the successive relations

$$0 \quad = \quad \mu\frac{d}{d\mu}\alpha_0 = \mu\frac{d}{d\mu}\Big\{\mu^\varepsilon\alpha(\mu)(1+\delta_\alpha)\Big\} = \mu\frac{d}{d\mu}\Big\{\mu^\varepsilon\alpha(\mu) + \mu^\varepsilon\delta\alpha(\mu)\Big\} \Leftrightarrow$$

$$
\begin{aligned}
0 &= \mu\left\{\varepsilon\alpha(1+\delta_\alpha)+(1+\delta_\alpha)\mu\frac{\partial\alpha}{\partial\mu}+\alpha\mu\frac{\partial\delta_\alpha}{\partial\mu}\right\}\Leftrightarrow \\
\beta_\alpha(1+\delta_\alpha) &= -\varepsilon\alpha(1+\delta_\alpha)-\alpha\mu\frac{\partial\delta_\alpha}{\partial\mu}\Leftrightarrow \\
\beta_\alpha &= -\varepsilon\alpha-\alpha\mu\frac{\partial\delta_\alpha}{\partial\mu}(1+\delta_\alpha)^{-1}\Leftrightarrow \\
\beta_\alpha &= -\varepsilon\alpha-\alpha\mu\frac{\partial\delta_\alpha}{\partial\mu}\Leftrightarrow, \qquad (2.5.25)
\end{aligned}
$$

where, since $\delta_\alpha \sim O(\hbar)$, we have performed an expansion in $\hbar$ in order to get rid of terms of $\mathcal{O}(\hbar^2)$ like $\delta_\alpha \cdot \frac{\partial\delta_\alpha}{\partial\mu}$. In the case of the AH model where we have three couplings, we will have a system of equations:

$$
\begin{aligned}
\beta_\lambda &= -\varepsilon\lambda-\lambda\left\{\beta_\lambda\frac{\partial\delta_\lambda}{\partial\lambda}+\beta_{m_H^2}\frac{\partial\delta_\lambda}{\partial m_H^2}+\beta_{m_Z^2}\frac{\partial\delta_\lambda}{\partial m_Z^2}\right\} \\
\beta_{m_H^2} &= -\varepsilon m_H^2-m_H^2\left\{\beta_\lambda\frac{\partial\delta_{m_H}}{\partial\lambda}+\beta_{m_H^2}\frac{\partial\delta_{m_H}}{\partial m_H^2}+\beta_{m_Z^2}\frac{\partial\delta_{m_H}}{\partial m_Z^2}\right\} \\
\beta_{m_Z^2} &= -\varepsilon m_Z^2-m_Z^2\left\{\beta_\lambda\frac{\partial\delta_{m_Z}}{\partial\lambda}+\beta_{m_H^2}\frac{\partial\delta_{m_Z}}{\partial m_H^2}+\beta_{m_Z^2}\frac{\partial\delta_{m_Z}}{\partial m_Z^2}\right\}. \qquad (2.5.26)
\end{aligned}
$$

This system can be rewritten as

$$
\begin{aligned}
\beta_\lambda(1+\frac{\partial\delta_\lambda}{\partial\lambda})+\lambda\left\{\beta_{m_H^2}\frac{\partial\delta_\lambda}{\partial m_H^2}+\beta_{m_Z^2}\frac{\partial\delta_\lambda}{\partial m_Z^2}\right\} &= -\varepsilon\lambda \\
\beta_{m_H^2}(1+\frac{\partial\delta_{m_H}}{\partial m_H^2})+m_H^2\left\{\beta_\lambda\frac{\partial\delta_{m_H}}{\partial\lambda}+\beta_{m_Z^2}\frac{\partial\delta_{m_H}}{\partial m_Z^2}\right\} &= -\varepsilon m_H^2 \\
\beta_{m_Z^2}(1+\frac{\partial\delta_{m_Z}}{\partial m_Z^2})+m_Z^2\left\{\beta_\lambda\frac{\partial\delta_{m_Z}}{\partial\lambda}+\beta_{m_H^2}\frac{\partial\delta_{m_Z}}{\partial m_H^2}\right\} &= -\varepsilon m_Z^2\,, \qquad (2.5.27)
\end{aligned}
$$

or in matrix form as

$$
\begin{pmatrix}
1+\frac{\partial\delta_\lambda}{\partial\lambda} & \lambda\frac{\partial\delta_\lambda}{\partial m_H^2} & \lambda\frac{\partial\delta_\lambda}{\partial m_Z^2} \\
m_H^2\frac{\partial\delta_{m_H}}{\partial\lambda} & 1+\frac{\partial\delta_{m_H}}{\partial m_H^2} & m_H^2\frac{\partial\delta_{m_H}}{\partial m_Z^2} \\
m_Z^2\frac{\partial\delta_{m_Z}}{\partial\lambda} & m_Z^2\frac{\partial\delta_{m_Z}}{\partial m_H^2} & 1+\frac{\partial\delta_{m_Z}}{\partial m_Z^2}
\end{pmatrix}
\cdot
\begin{pmatrix}
\beta_\lambda \\ \beta_{m_H^2} \\ \beta_{m_Z^2}
\end{pmatrix}
= -\varepsilon
\begin{pmatrix}
\lambda \\ m_H^2 \\ m_Z^2
\end{pmatrix}
\qquad (2.5.28)
$$

Inverting the matrix we obtain

$$
\begin{aligned}
16\pi^2\beta_\lambda &= \lambda^2\frac{\partial\frac{C_\lambda}{\lambda}}{\partial\lambda}+\lambda m_H^2\frac{\partial\frac{C_\lambda}{\lambda}}{\partial m_H}+\lambda m_Z^2\frac{\partial\frac{C_\lambda}{\lambda}}{\partial m_Z} \\
16\pi^2\beta_{m_H^2} &= \lambda m_H^2\frac{\partial\frac{C_{m_H^2}}{m_H^2}}{\partial\lambda}+\frac{1}{2}m_H^2\frac{\partial\frac{C_{m_H^2}}{m_H^2}}{\partial m_H}+\frac{1}{2}m_H^2\frac{\partial\frac{C_{m_H^2}}{m_H^2}}{\partial m_Z} \\
16\pi^2\beta_{m_Z^2} &= \lambda m_Z^2\frac{\partial\frac{C_{m_Z^2}}{m_Z^2}}{\partial\lambda}+\frac{1}{2}m_Z^2\frac{\partial\frac{C_{m_Z^2}}{m_Z^2}}{\partial m_H}+\frac{1}{2}m_Z^2\frac{\partial\frac{C_{m_Z^2}}{m_Z^2}}{\partial m_Z}\,. \qquad (2.5.29)
\end{aligned}
$$

Thus, all that we need to do in order to obtain the various β-functions, is to identify from the explicit form of the counterterms the quantities C_α defined in Eq.(2.5.22) and build its β-function, according to Eq.(2.5.29).

Moreover, solving the differential equation for the running coupling yields the Renormalization Group flow of the coupling α:

$$\alpha(\mu) \quad = \quad \frac{\alpha}{1+\tilde{\beta}_\alpha \, \ln\left(\frac{m_{\text{phys.}}}{\mu}\right)} \tag{2.5.30}$$

The Landau pole associated with the coupling α is

$$\mu_L^\alpha \quad = \quad m_{\text{phys.}} \, e^{\frac{\alpha}{\beta_\alpha}} \, . \tag{2.5.31}$$

In the AH model we found from our one-loop calculation that $C_{m_Z} = \frac{2}{3}\frac{\lambda m_Z^4}{m_H^2}$, $C_{m_H} = 6\lambda m_H^2 - 12\lambda m_Z^2$ and $C_\lambda = 18\lambda^2 - 24\lambda^2\frac{m_Z^2}{m_H^2} + 24\lambda^2\frac{m_Z^4}{m_H^4}$ that immediately determine

$$\begin{aligned}
\beta_{m_Z^2} &= \frac{1}{16\pi^2}\left(\frac{2}{3}\frac{\lambda m_Z^4}{m_H^2}\right) \\
\beta_{m_H^2} &= \frac{1}{16\pi^2}\left(6\lambda m_H^2 - 12\lambda m_Z^2\right) \\
\beta_\lambda &= \frac{1}{16\pi^2}\left(18\lambda^2 - 24\lambda^2\frac{m_Z^2}{m_H^2} + 24\lambda^2\frac{m_Z^4}{m_H^4}\right) \, .
\end{aligned} \tag{2.5.32}$$

The above expressions hold for both R_ξ and Unitary gauges. It is interesting to notice that these β-functions are not identically the same as those that one would compute in a Cartesian basis for the Higgs. For a comparison see the next section.

2.6 The one-loop Higgs potential

To summarize our result regarding the one-loop Higgs potential, in Eq. (2.5.19) we found that it is determined by the quantities C_{ϕ^3} and C_{ϕ^4} in Eq. (2.5.16) and in Eq. (2.5.18) respectively, yielding the finite expression

$$\begin{aligned}
V_1(\phi) \quad &= \quad \frac{1}{2}m_H^2\phi^2 + \left[\sqrt{\frac{\lambda}{2}}m_H - \frac{m_H}{16\pi^2\sqrt{2\lambda}}\left(9\lambda^2 + \frac{8\lambda^2 m_Z^4}{m_H^4}\right)\right]\phi^3 \\
&+ \quad \frac{1}{4}\left[\lambda - \frac{1}{16\pi^2}\left(\frac{32\lambda^2 m_Z^4}{m_H^4}\right)\right]\phi^4 \, .
\end{aligned} \tag{2.6.1}$$

The form of the potential is such that the ξ-independent part of its R_ξ gauge expression is the same as the Unitary gauge expression. Moreover, using the standard prescription to compute the $U_\mathcal{T}$ integral, see Eq. (2.C.2), the ξ-dependent part is made to vanish. In addition, the potential has no explicit μ-dependence. All the μ-dependence is implicit, through the dependence on μ of the renormalized quantities λ, m_H and m_Z via their RG evolution. In the following numerical analysis one can either interpret the potential in Eq. (2.6.1) as a ξ-independent R_ξ

gauge potential or simply as a Unitary gauge potential, as these are the same independently of prescriptions.

Before we proceed with the study of the gauge invariant Higgs potential Eq. (2.6.1), we recall the standard result used to extract physics from the Higgs potential. The usual method to compute the Higgs potential is in the context of the background field method, where a functional integration yields the so called Higgs effective potential. We will not review the details of this well known calculation; we assume that the reader has some familiarity with it. The derivation of an effective scalar potential via the background field method at one-loop is much simpler than computing Feynman diagrams. The simplicity is related among other reasons to the Cartesian basis representation of the Higgs field because in the Cartesian basis the Gaussian path integral involved, is almost trivial. The result of the calculation for the scalar potential in the Abelian-Higgs model (see for example [62]) with the same normalization of the mass and quartic coupling as in Eq. (2.2.1), in $\overline{\text{MS}}$ scheme with Fermi gauge fixing, is ($H_0 \to \phi/\sqrt{2}$)

$$\begin{aligned} V_{1,\text{eff.}}^{\overline{\text{MS}}} &= -\frac{1}{2}m^2\phi^2 + \frac{\lambda}{4}\phi^4 \\ &- \frac{1}{64\pi^2}\left\{3m_A^4\left(\ln\frac{\mu^2}{m_A^2}+\frac{5}{6}\right) + m_B^4\left(\ln\frac{\mu^2}{m_B^2}+\frac{3}{2}\right) + \sum_{\pm} m_{C_\pm}^4\left(\ln\frac{\mu^2}{m_{C_\pm}^2}+\frac{3}{2}\right)\right\} \end{aligned} \tag{2.6.2}$$

with

$$\begin{aligned} m_A^2 &= g^2\phi^2 \\ m_B^2 &= 3\lambda\phi^2 - m^2 \\ m_{C_\pm}^2 &= \frac{1}{2}\left[\left(\lambda\phi^2 - m^2\right) \pm \sqrt{(\lambda\phi^2-m^2)^2 - 4\xi g^2\phi^2(\lambda\phi^2-m^2)}\right] . \end{aligned} \tag{2.6.3}$$

The derivation of the β-function is also simple, provided that a separate diagram calculation has yielded the also well known result

$$16\pi^2\gamma = g^2(-3+\xi) \tag{2.6.4}$$

for the anomalous dimension γ. Then, one finds

$$\begin{aligned} 16\pi^2\beta_{m^2} &= 8\lambda m^2 - 6g^2m^2 \\ 16\pi^2\beta_\lambda &= 20\lambda^2 - 12\lambda g^2 + 6g^4 \\ 16\pi^2\beta_g &= \frac{1}{3}g^4 \end{aligned} \tag{2.6.5}$$

for the β-functions. These Cartesian basis results are not identically the same as the Polar basis results in Eq. (2.5.32). Despite however the fact that some coefficients are not the same, their physical content is similar.

In Figs. 2.1 and 2.2 we plot the RG evolution of the Higgs and the Z mass as well as that of the coupling λ, as a function of the Renormalization scale μ, as determined in Eq. (2.5.32). We do not produce separate figures for Eq. (2.6.5) because the numerical differences are quite

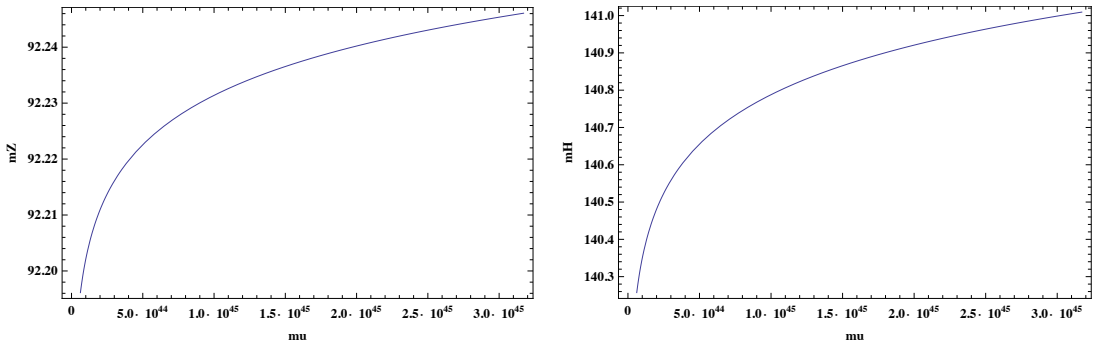

Figure 2.1: The RG evolution of the Z (left) and Higgs (right) mass.

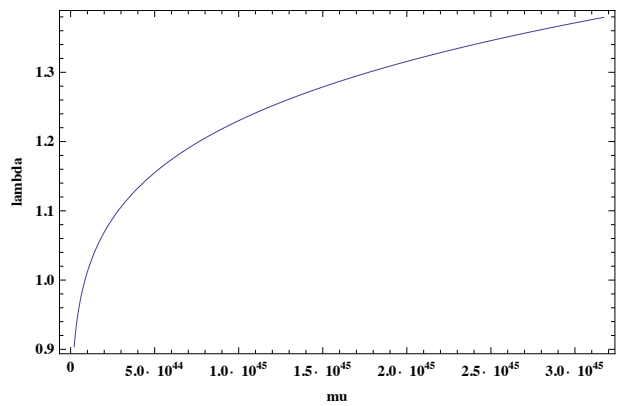

Figure 2.2: The RG evolution of λ.

small. The physical values at $\mu = 125$ GeV we use are 125 GeV for the Higgs mass, 91 GeV for the Z-mass and 0.12 for λ. We stop the evolution at a certain scale

$$\mu_I \simeq 3.03 \cdot 10^{46} \text{ GeV} \tag{2.6.6}$$

whose physical meaning will be discussed below. We observe the usual perturbative, logarithmic evolution of the couplings.

The potential in Eq. (2.6.1) is gauge invariant and the one in Eq. (2.6.2) is manifestly gauge dependent. To quantify the effect of ξ, the different basis for the Higgs and the different subtraction schemes, we compare numerically the two results. The comparison that follows should be clearly taken with a grain of salt, as the two objects are quite different. In Fig. 2.3 we plot the difference between the one-loop Higgs potential Eq. (2.6.1) and the effective potential Eq. (2.6.2) at $\mu = 125$ GeV, for $\xi = 0.001, 1, 10, 100, 100000$. The running values of m_H, m_Z and λ in the potential V_1 are determined from Eq. (2.5.32), while those of m, g and λ in $V_{1,\text{eff.}}^{\overline{\text{MS}}}$ are determined using Eq. (2.6.5). A regime around $\phi = 0$ in the plot is missing because there the effective potential is imaginary. There seem to be ways to fix this [47] but this is not our concern here. V_1 remains instead always real. What we observe is that as ξ increases, the regime where the two expressions agree shrinks. There seems to be a value of ξ for which the best agreement is achieved, which from the figure is around $\xi < O(10)$. The limit $\xi \to \infty$ of the effective potential

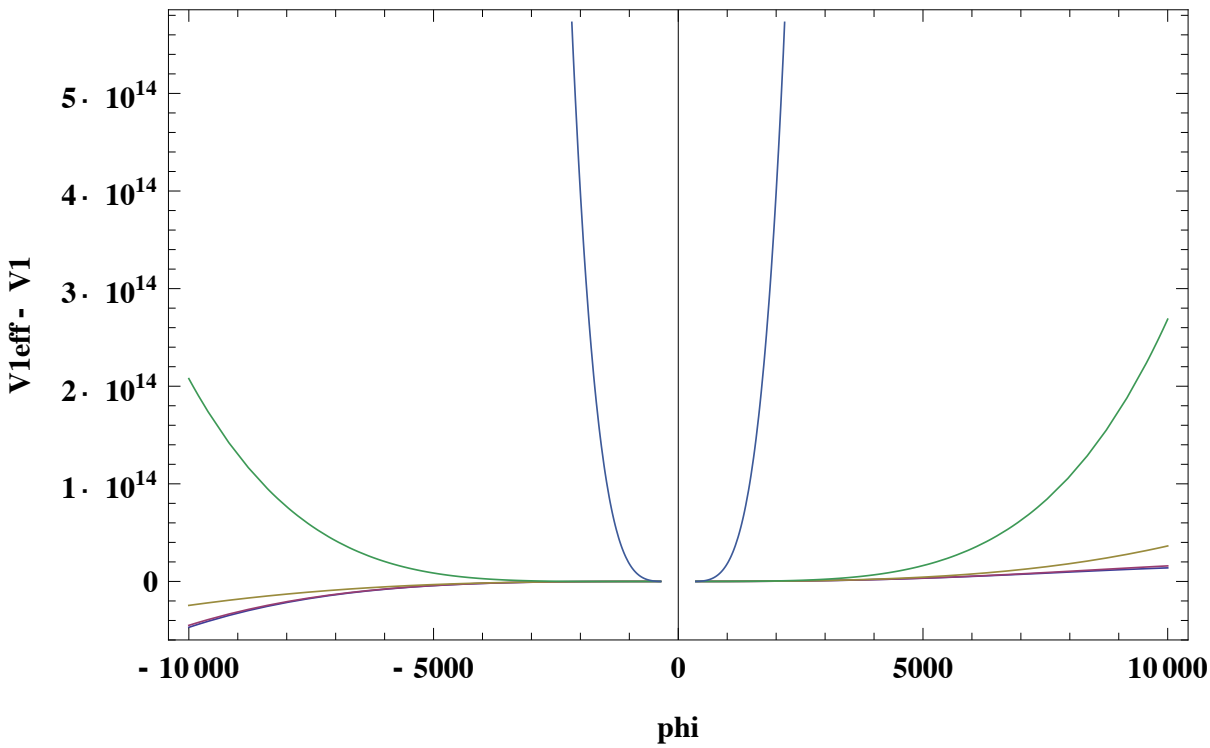

Figure 2.3: The difference $V_1(\phi) - V_{1,\text{eff.}}^{\overline{\text{MS}}}(\phi)$ between the 1-loop and effective Higgs potentials at $\mu = 125$ GeV for various values of $\xi = 10^{-3}, 1, 10, 100, 10^5$. Curves taking larger values on the vertical axis correspond to larger ξ.

is clearly singular: in Eq. (2.1.1) we have $\lim_{\xi\to\infty} g(\xi) = \infty$.

From now on we concentrate on $V_1(\phi)$ in Eq. (2.6.1) and we analyze it numerically. First, in Fig. 2.4 we plot it at the physical scale $\mu = 125$ GeV. We observe that it has two minima, of which the one at $\phi = 0$ is the global minimum, as claimed. The tilt in the mexican hat shape implies that the global Z_2 symmetry $H_0 \to -H_0$ of the classical potential has been spontaneously broken by quantum effects. The breaking is small and the vacuum in the interior of the Higgs phase is stable. Going to higher scales, we observe a big desert. To illustrate this, in Fig. 2.5 we plot the potential for $\mu = 10^{12}$ GeV and $\mu = 10^{19}$ GeV respectively. The Abelian-Higgs model does not care about 'low' intermediate scales including the Planck scale. It roams through them perturbatively to much higher scales. The first qualitative change observed is around $\mu \simeq 10^{40}$ GeV where the local minimum at negative values of ϕ becomes the global one, see the left of Fig. 2.6. For the next five or so orders of magnitude in μ, the new global minimum becomes deeper while the local one, at $\phi = 0$, becomes shallower. Nevertheless, if we zoom in near $\phi = 0$ we will see that the local minimum is still there. Just below μ_I the picture of the potential remains the same, the local minimum becomes even deeper and there is no restoration of the global Z_2 symmetry, see right of Fig. 2.6. At this scale, $\lambda \simeq 1.8$, i.e. still perturbative. In Fig. 2.7 we plot the potential just above μ_I, at $3.0 \cdot 10^{45}$ GeV; we observe that μ_I is the approximate scale where the potential develops an instability. A related question that arises is what is the

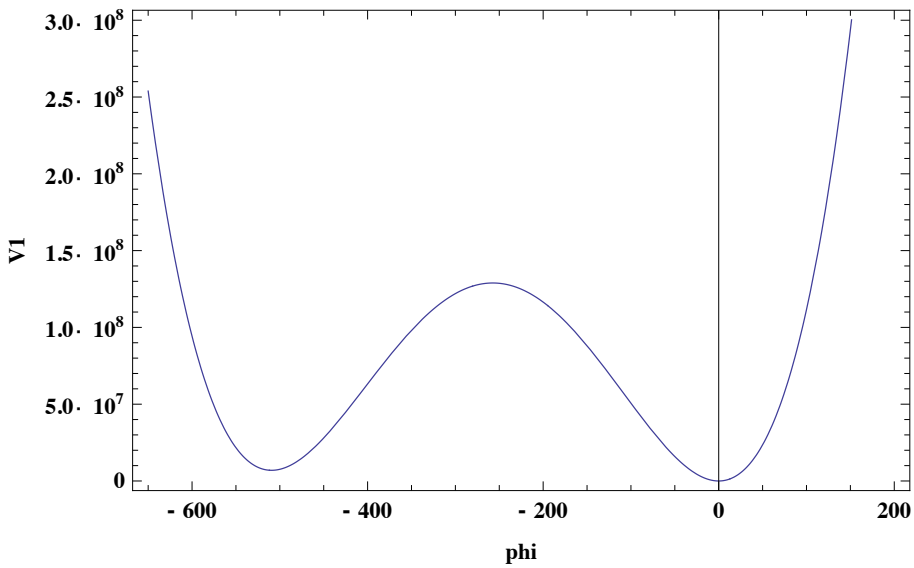

Figure 2.4: The gauge invariant 1-loop Higgs potential $V_1(\phi)$ at $\mu = 125$ GeV.

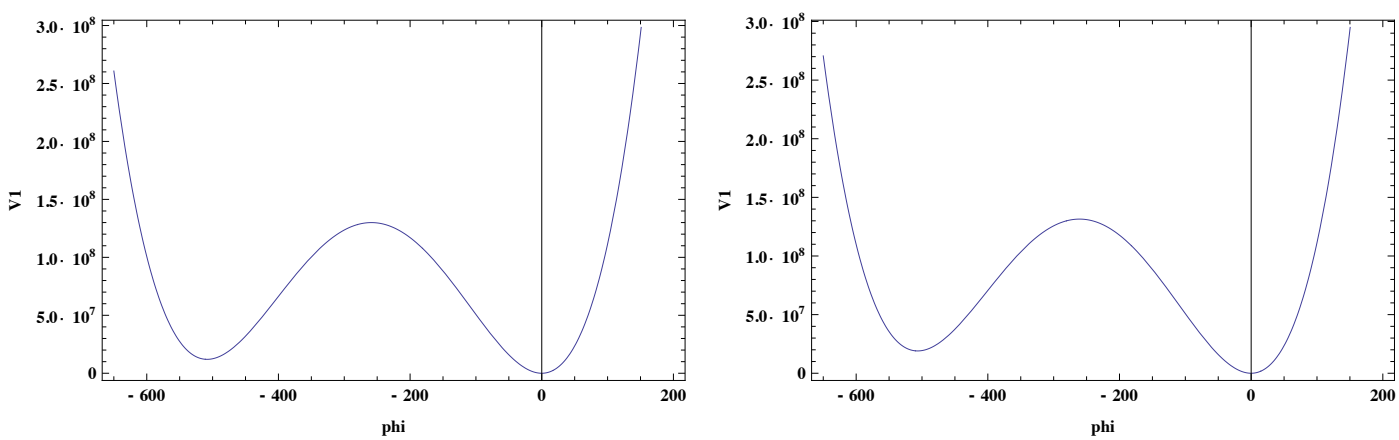

Figure 2.5: The 1-loop Higgs potential $V_1(\phi)$ at $\mu = 10^{12}$ GeV (left) and $\mu = 10^{19}$ GeV (right).

scale where perturbation theory breaks down, that is which scale produces a quartic coupling of $\lambda \simeq 4\pi$ (according to the usual perturbative argument based on the fact that each loop introduces an additional factor of $\frac{\lambda^2}{16\pi^2}$). This scale turns out to be

$$\mu_{NP} \simeq 1.5 \cdot 10^{49} \text{ GeV}\,, \tag{2.6.7}$$

a scale slightly larger than the instability scale and remarkably close to the Landau pole of λ, $\mu_L^\lambda \simeq 4.3 \cdot 10^{49}$ GeV. The three orders of magnitude in μ between μ_I and $\mu_{\rm NP}$ is just an order of magnitude or less on a logarithmic scale. In a gauge invariant cut-off regularization such as the lattice, this is typical in the vicinity of a phase transition and can be achieved by a moderate change of the bare couplings. We could say that an interval of scale evolution, long in perturbative time can be short in (cut-off) non-perturbative time. More on this in the next section.

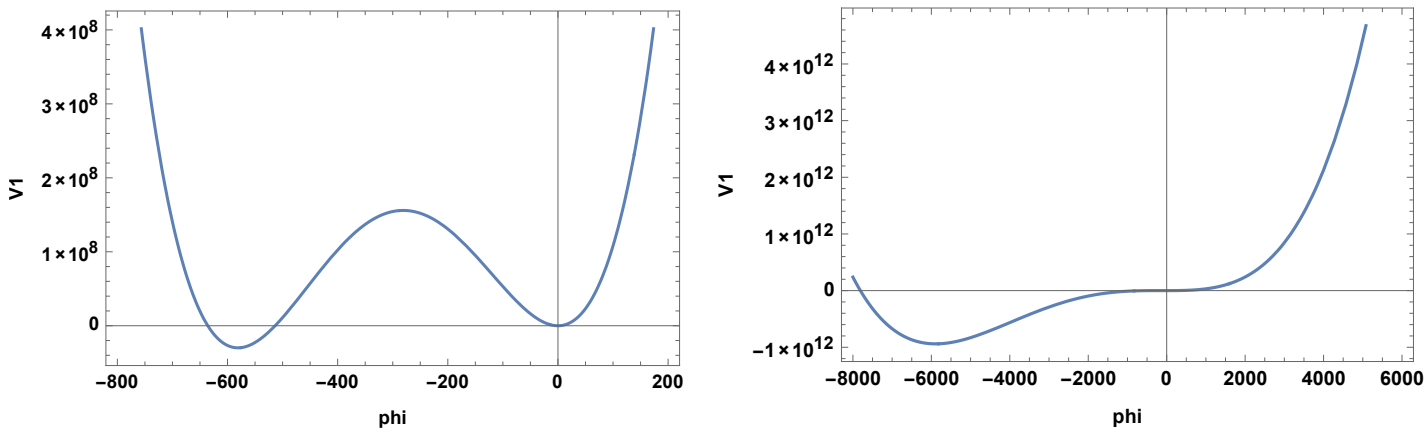

Figure 2.6: The potential $V_1(\phi)$ at $\mu \simeq 10^{40}$ GeV (left) and just below the instability scale μ_I, at $\mu \simeq 2.0 \cdot 10^{45}$ GeV (right).

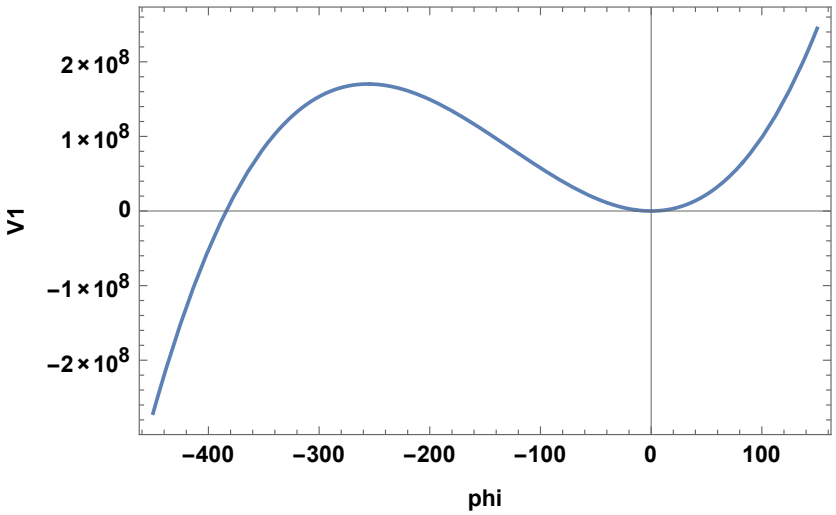

Figure 2.7: The potential $V_1(\phi)$ just above the instability scale μ_I, at $\mu \simeq 3.0 \cdot 10^{45}$GeV.

In Fig. 2.8 we plot once more the potential in the vicinity of the Landau pole. On the left, we show the global form of the potential, where we can see the flattening of the $\phi = 0$ regime. On the right, we zoom in the $\phi = 0$ regime and observe that the local minimum is still there, even though the closer one gets to the Landau pole the more one must zoom in to see it, as the flattening gets closer to forming a saddle point. Note that the gauge coupling g changes very little during these scale changes thus remains perturbative. This means that beyond the Landau pole where λ turns negative lays the Coulomb phase.

The physics that we extract from the numerical analysis is that the Abelian-Higgs model remains perturbative almost all the way to the Landau pole μ_L^λ of λ. At a scale approximately $\mu_I \simeq 7 \cdot 10^{-4}\, \mu_L^\lambda$ an instability develops, the onset of the system trying to pass from the Higgs phase into the Coulomb phase. Above μ_I there are two vacua, one is the old global minimum that has turned into a local minimum and the unstable vacuum, corresponding to the Coulomb phase. Up to the scale of $0.35\, \mu_L^\lambda$ the system is trying perturbatively to stabilize in the Coulomb

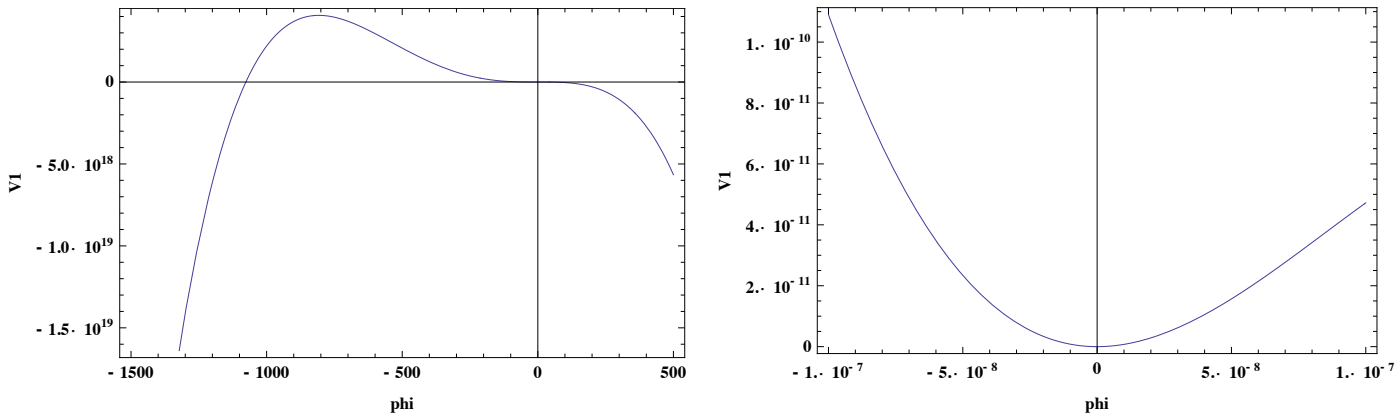

Figure 2.8: The potential $V_1(\phi)$ near the Landau pole μ_L^λ (left) and its $\phi = 0$ regime zoomed in (right).

phase and this is finally achieved at the Landau pole where in the last few tiny scale seconds, approximately between $[0.35 - 1.00] \cdot \mu_L^\lambda$, non-perturbative evolution takes over. The breadth of the unstable regime reflects perhaps the fact that the phase transition between the Higgs and the Coulomb phase is a strong first order phase transition [48]. It is likely that in a Monte Carlo simulation, as the phase transition is crossed, one would observe the system tunelling back and forth between the two vacua.

2.7 Lines of Constant Physics

The following section has a more speculative character in comparison to the previous ones in an attempt to make a connection to non-perturbative properties of the Abelian-Higgs model. In a non-perturbative approach one of the first thing one does is to map the phase diagram of a model via Monte Carlo simulations. For the Abelian-Higgs model the phase diagram is defined by three axes in the space of the three bare parameters g_0, λ_0 and m_0. For instance in a lattice regularization, the three axes can be chosen to be

$$\beta \equiv \frac{1}{g_0^2}, \qquad \kappa \equiv \frac{1 - 2\lambda_0}{1 + \frac{1}{2}a^2 m_{H_0}^2}, \qquad \lambda_0\,, \tag{2.7.1}$$

with a the lattice spacing. The β above should not be confused with a beta-function, it is the conventional notation for a lattice gauge coupling. The mapping of the phase diagram has been done for the Abelian-Higgs model to some extent in the past [48] and more recently, for $\lambda_0 = 0.15$, in [49]. It seems to depend weakly on λ_0. Here we reproduce it (semi) qualitatively:

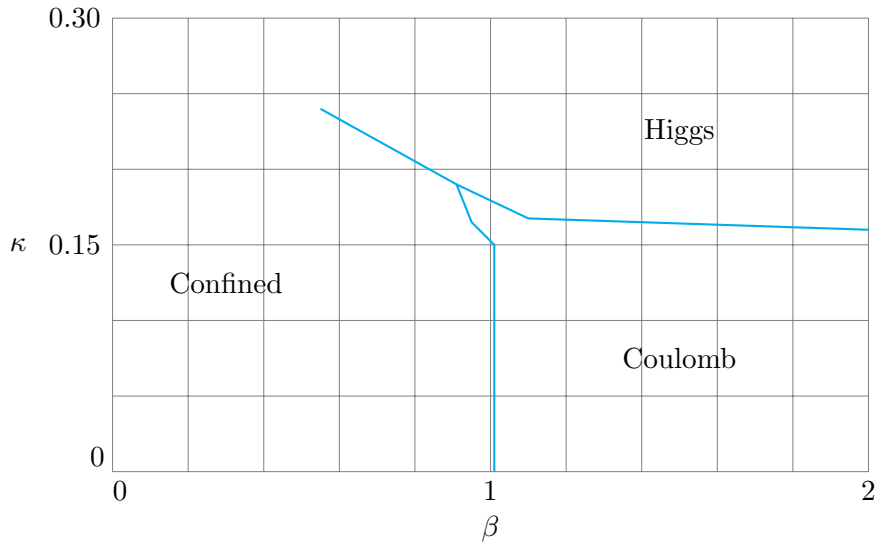

We also note that the above phase diagram has been constructed using $\kappa \equiv \frac{1-2\lambda_0}{8+a^2 m_0^2}$, a slightly different normalization for κ in Eq. (2.7.1). This just corresponds to choosing a different normalization for the bare vev parameter v_0. Here we will use the normalization of Eq. (2.7.1) and $v_0 = 246$ GeV.

A Line of Constant Physics (LCP) of the AH model is defined by the curve on its phase diagram all of whose points satisfy the constraint that m_H, m_Z and λ are some chosen constants. We can choose for example

$$m_H = 125\,\text{GeV}, \qquad m_Z = 91\,\text{GeV}, \qquad \lambda = 0.12\,, \tag{2.7.2}$$

and then the points of the LCP can be defined perturbatively to be determined by the equations

$$\begin{aligned} m_{H_0}^2(\mu) &= 125^2 + (\delta m_H)_f(m_H = 125, m_Z = 91, \lambda = 0.12; \mu) \\ m_{Z_0}^2(\mu) &= 91^2 + (\delta m_Z)_f(m_H = 125, m_Z = 91, \lambda = 0.12; \mu) \\ \lambda_0(\mu) &= 0.12 + (\delta\lambda)_f(m_H = 125, m_Z = 91, \lambda = 0.12; \mu) \end{aligned} \tag{2.7.3}$$

where

$$\begin{aligned} (\delta m_H)_f(m_H = 125, m_Z = 91, \lambda = 0.12; \mu) &= -19557.3 + 5625 \ln \frac{\mu^2}{15625} - 5962.32 \ln \frac{\mu^2}{8281} \\ (\delta\lambda)_f(m_H = 125, m_Z = 91, \lambda = 0.12; \mu) &= -0.0305 + 0.01296 \ln \frac{\mu^2}{15625} - 0.043 \ln \frac{\mu^2}{8281} \\ (\delta m_Z)_f(m_H = 125, m_Z = 91, \lambda = 0.12; \mu) &= 2537.18 + 6723.0.4 \ln \frac{\mu^2}{15625} - 52.0632 \ln \frac{\mu^2}{8281} \end{aligned} \tag{2.7.4}$$

are the finite parts of the Unitary gauge counter-terms, according to Eq. (2.5.12), Eq. (2.5.13) and Eq. (2.5.8). We recall that $m_{H_0} = 2m_0$, $m_{Z_0} = g_0 v_0$ and correspondingly $\delta m_H = 2\delta m$, $\delta m_Z = v_0 \delta g$.

We now have all the ingredients to plot a first "perturbative LCP". In Fig. 2.9 we plot the

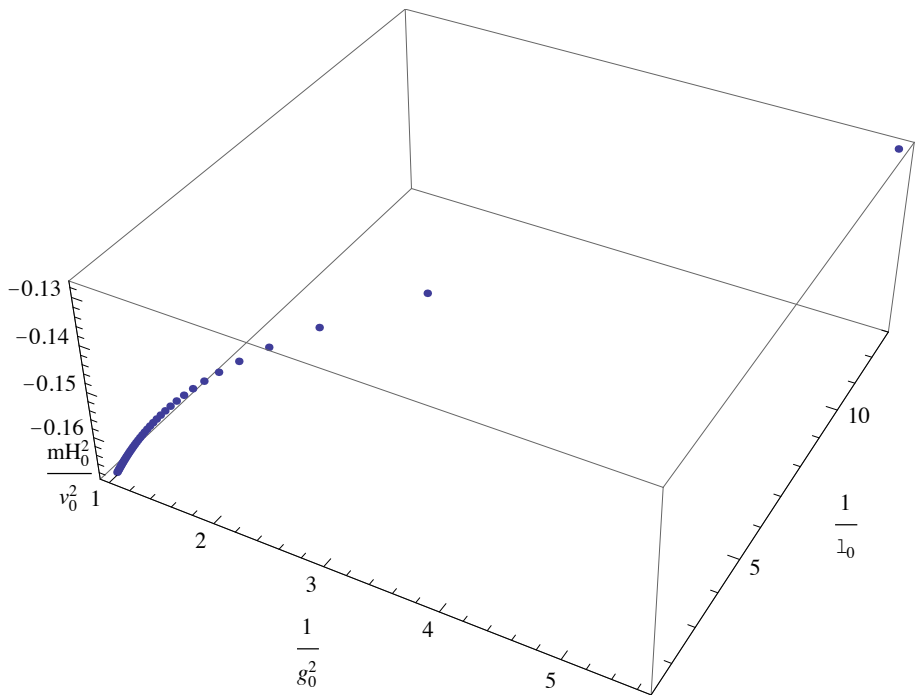

Figure 2.9: The perturbative LCP defined by Eq. (2.7.2) for $v_0 = 246$ GeV.

LCP, defined by Eq. (2.7.3) and Eq. (2.7.2) with $v_0 = 246$ GeV, for the range $\mu \in [125, 5000]$ GeV. The part (lower left) of the line where the points are denser corresponds to larger values of μ. There, the parameter $\beta = 1/g_0^2$ (that decreases quite rapidly as μ increases) approaches 1, which means that most likely we are about to enter into either the Confined or the Coulomb phase. There is potentially a non-trivial message in this so it is worth redoing it this time using Eq. (2.7.1), i.e. to try to actually put the perturbative LCP on the non-perturbative phase diagram. The only obstacle is to relate the lattice spacing to some scale parameter in the perturbative calculation. This can be quite an involved operation, depending on our desired level of precision. For a discussion of this issue, see [50]. Here we will simplify the discussion and make the naive identification $a = 1/\Lambda$ with Λ a momentum cut-off. We need to do some

Λ	β	κ	λ_0	q
125	5.6	0.45	0.07	1.7
250	3.0	0.32	0.19	3.8
375	2.4	0.25	0.26	7.3
500	2.0	0.2	0.31	12.1
625	1.9	0.15	0.35	18.3
750	1.7	0.12	0.38	25.9

Table 2.1: Scale and corresponding bare parameters of the LCP defined by $m_Z = 91$ GeV, $m_H = 125$ GeV and $\lambda = 0.12$ with the lattice spacing identified as $a = 1/\Lambda$.

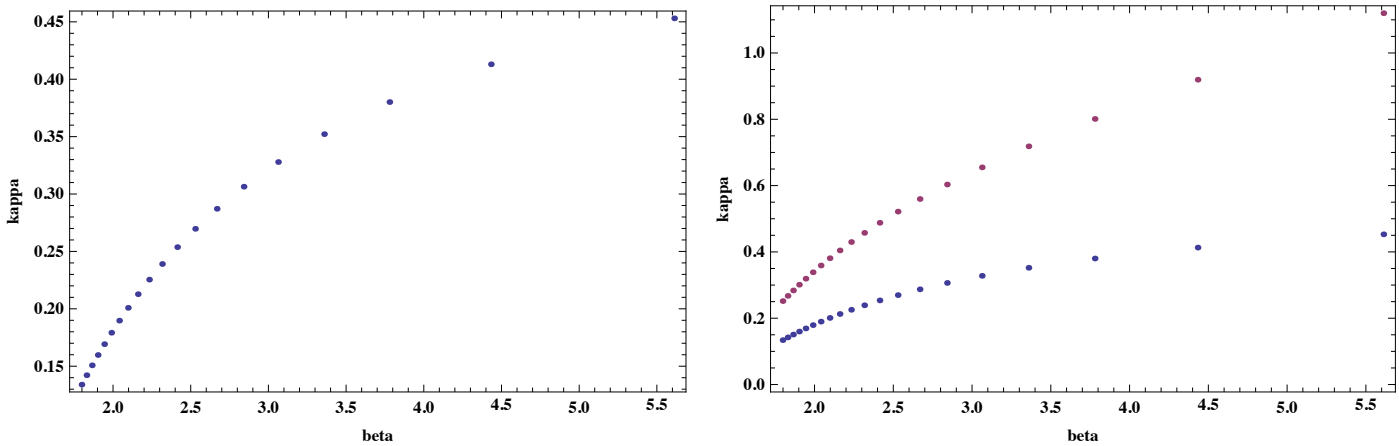

Figure 2.10: The cut-off LCP that identifies $\Lambda = 1/a$ for $v_0 = 246$ GeV projected on the $\beta - \kappa$ plane (left) and a comparison with the corresponding LCP with the identification $\mu = 1/a$ (right). The lower curve is the cut-off LCP.

extra work though, as we have to estimate δm_H in a cut-off regularization. Fortunately this is not too hard, it yields to leading order

$$m_{H_0}^2(\Lambda) = 125^2 + \frac{6\lambda}{16\pi^2}\Lambda^2 + \cdots \tag{2.7.5}$$

that should replace the first of Eq. (2.7.3) in Eq. (2.7.1). The dots stand for small corrections. For m_Z and λ on the other hand that have a logarithmic cut-off dependence we keep the same relations as before. This is not a completely well defined identification but it is good enough for the information we want to extract. We call the resulting line on the $\beta - \kappa$ plane, the "cut-off LCP". On the left of Fig. 2.10 we plot the cut-off LCP defined by Eq. (2.7.2) for $v_0 = 246$ GeV and projecting the λ_0 dependence on the $\beta - \kappa$ plane. The values of the cut-off range in $\Lambda \in [125, 700]$ GeV and they increase as we move down and left along the curve. By comparing to the Monte Carlo phase diagram we can now clearly see that around the upper limit of the Λ-range the system hits the Higgs-Coulomb phase transition. Some representative values of the parameters can be seen on Table 2.1. On the right of Fig. 2.10 we compare the cut-off LCP to the one we would have obtained by the identification $\mu = 1/a$. Some representative values of the parameters for this identification can be seen on Table 2.2. The numbers change but the conclusion remains: If we want to construct an LCP that keeps the values of the physical quantities close to their "experimentally measured values" (we are not in the Standard Model but the point we would like to make should be clear), we can not take the cut-off too high, since around 1 TeV or so we are forced to cross into the Coulomb phase. Notice that the analysis of the RG trajectories and of the potential in the previous section did not warn us about this. This has potentially consequences for the fine tuning of the Higgs mass. In Tables 2.1 and 2.2 we introduced the unsophisticated fine tuning parameter

$$q = \frac{|(\delta m_H)_f|}{m_H} \tag{2.7.6}$$

from which we can see the increase of fine tuning as the scale increases, with the $\Lambda = 1/a$

μ	β	κ	λ_0	q
125	5.6	1.11	0.07	0
250	3.0	0.65	0.19	0.0014
375	2.4	0.48	0.26	0.0023
500	2.0	0.38	0.31	0.0029
625	1.9	0.30	0.35	0.0033
750	1.7	0.23	0.38	0.0037

Table 2.2: Scale and corresponding bare parameters of the LCP defined by $m_Z = 91$ GeV, $m_H = 125$ GeV and $\lambda = 0.12$ with the lattice spacing identified as $a = 1/\mu$.

identification naturally worse. Even so though, since the cut-off stops at a maximum value of about 1 TeV, it can not take very large values.

Appendix

2.A One-loop integrals

The general form of a Feynman diagram $F_E^{G,L}$ (see Eq. (2.2.11) in the text for the explanation of the notation) is

$$(4\pi)^{d/2} F_E^{G,L} = \mu^\varepsilon \left([F_E^{G,L}]_\varepsilon + \left\{ F_E^{G,L} \right\}_\varepsilon + [F_E^{G,L}]_f + \left\{ F_E^{G,L} \right\}_f \right) . \tag{2.A.1}$$

Here we are interested in the finite part of this expression, the general form of which is

$$\frac{1}{(4\pi)^{d/2}} \left(F_E^{G,L} \right)_f = \frac{1}{(4\pi)^{d/2}} \left([F_E^{G,L}]_f + \left\{ F_E^{G,L} \right\}_f \right) = \int \frac{d^d k}{i(4\pi)^{d/2}} \sum_n \frac{\left(N^{(n)}_{F_E^{G,L}} \right)_f (k)}{D_1 D_2 \cdots D_n} , \tag{2.A.2}$$

where the range of the sum over n depends on the diagram. The n'th term of the numerator has a denominator with n factors, yields a finite result after integration over the loop momentum k and it is denoted as $\left(N^{(n)}_{F_E^{G,L}} \right)_f (k)$. It is also diagram dependent. In the Unitary gauge, even though this notation is redundant, we will still use it for extra clarity. The denominators are defined as

$$D_i(P_{i-1}, m_i) = (k + P_{i-1})^2 - m_i^2, \qquad i = 1, \cdots, n \tag{2.A.3}$$

and $P_0 \equiv 0$. Notice that the proper argument of the denominators is $D_i(P_{i-1}, m_i)$. Nevertheless, we do not always show both arguments systematically in the main text, apart from cases where otherwise their absence could cause ambiguities. Such a case is some finite diagrams, which generally have more than four denominators. In other cases where there can be no confusion, we show none, or only one of the arguments.

Feynman parametrization is implemented using

$$\frac{1}{D_1 D_2 \cdots D_n} = (n-1)! \int_0^1 \mathcal{D}^n x \frac{1}{(D_1 x_1 + D_2 x_2 + \cdots + D_n x_n)^n} , \tag{2.A.4}$$

where we defined

$$\int_0^1 dx_1 \cdots \int_0^1 dx_n \, \delta(1 - \sum_{i=1}^n x_i) \equiv \int_0^1 \mathcal{D}^n x \, . \tag{2.A.5}$$

Passing now to Dimensional Regularization, we introduce the useful shorthand notation

$$\int \frac{d^d k}{i \, (4\pi)^{d/2}} (\cdots) \equiv \langle \cdots \rangle \, . \tag{2.A.6}$$

We can then express Eq. (2.A.2) in DR as

$$\frac{1}{(4\pi)^{d/2}}\left(F_E^{G,L}\right)_f = \sum_n \Gamma(n)\int_0^1 \mathcal{D}^n x \left\langle \frac{\left(N^{(n)}_{F_E^{G,L}}\right)_f (k\to k-\sum_{i=1}^{n-1}P_i x_{i+1})}{\left(k^2-\Delta_{F_{0,n}}\right)^n}\right\rangle , \tag{2.A.7}$$

with

$$\Delta_{F_{0,n}}(x_1,\cdots,x_n) = -\sum_{i=1}^{n-1}P_i^2 x_{i+1} + \left(\sum_{i=1}^{n-1}P_i x_{i+1}\right)^2 + \sum_{i=1}^{n} x_i m_i^2 . \tag{2.A.8}$$

In a few simple cases we use the conventional notation

$$\begin{aligned}\Delta_{F_{0,2}} &\equiv \Delta_{B_0}\\ \Delta_{F_{0,3}} &\equiv \Delta_{C_0}\\ \Delta_{F_{0,4}} &\equiv \Delta_{D_0}\end{aligned} \tag{2.A.9}$$

2.B Passarino -Veltman

In this Appendix we collect some standard integrals of the Passarino-Veltman type, encountered in the text.

2.B.1 Scalars

The simplest PV integral is the scalar tadpole integral

$$A_0(m) = \int \frac{d^4k}{i\,(2\pi)^4}\frac{1}{k^2-m^2} , \tag{2.B.1}$$

naively quadratically divergent with a cut-off. In Dimensional Regularization, it can be expressed as (attaching the factor μ^ε)

$$\mu^\varepsilon A_0(m) = -\frac{\mu^\varepsilon}{(4\pi)^{d/2}}\Gamma\left(1-\frac{d}{2}\right)\frac{1}{m^{1-d/2}} \tag{2.B.2}$$

and by expanding in ε finally as

$$\mu^\varepsilon A_0(m) \quad = \quad \frac{1}{(4\pi)^2}m^2\left(\frac{2}{\varepsilon}+\ln\frac{\mu^2}{m^2}+1\right) . \tag{2.B.3}$$

The scalar, naively logarithmically diveregent PV integral is

$$B_0(P_1,m_1,m_2) = \int \frac{d^4k}{i\,(2\pi)^4}\frac{1}{D_1 D_2} . \tag{2.B.4}$$

It can be computed explicitly using the formulation of Appendix 2.A. It corresponds to $n=2$ and a numerator equal to 1. In d-dimensions, this integral is

$$B_0(P_1,m_1,m_2) \quad = \quad \int_0^1 \mathcal{D}^2 x \left\langle \frac{1}{(k^2-\Delta_{B_0})^2}\right\rangle$$

$$= \frac{1}{(4\pi)^{d/2}} \int_0^1 dx \Gamma\left(2-\frac{d}{2}\right)\left(\frac{1}{\Delta_{B_0}}\right)^{2-d/2} . \tag{2.B.5}$$

Expanding in ε we get

$$B_0(P_1, m_1, m_2) = \frac{1}{(4\pi)^2}\left(\frac{2}{\varepsilon} + \int_0^1 dx \ln \frac{4\pi e^{-\gamma_E}}{\Delta_{B_0}}\right) \tag{2.B.6}$$

and finally

$$\mu^\varepsilon B_0(P_1, m_1, m_2) = \frac{1}{(4\pi)^2}\left(\frac{2}{\varepsilon} + \int_0^1 dx \ln \frac{\mu^2}{\Delta_{B_0}}\right) . \tag{2.B.7}$$

We note that this integral is symmetric under $m_1 \leftrightarrow m_2$. An important special case is when $P_1 = 0$ in which case

$$B_0^1(m_1, m_2) \equiv B_0(P_1 = 0, m_1, m_2) = \frac{A_0(m_1) - A_0(m_2)}{m_1^2 - m_2^2} . \tag{2.B.8}$$

The finite scalar integral that appears in Triangles and Boxes is of the form

$$C_0(P_1, P_2, m_1, m_2, m_3) = \int \frac{d^4k}{i\,(2\pi)^4} \frac{1}{D_1 D_2 D_3} . \tag{2.B.9}$$

In DR, this integral becomes

$$C_0(P_1, P_2, m_1, m_2, m_3) = 2\int_0^1 \mathcal{D}^3 x \left\langle \frac{1}{(k^2 - \Delta_{C_0})^3} \right\rangle . \tag{2.B.10}$$

Expanding in ε it reduces to

$$\begin{aligned} \mu^\varepsilon C_0(P_1, P_2, m_1, m_2, m_3) &= -\frac{\mu^\varepsilon}{(4\pi)^{d/2}} \int_0^1 \mathcal{D}^3 x \frac{\Gamma\left(3-\frac{d}{2}\right)}{\Delta_{C_0}^{3-d/2}} \\ &= -\frac{\mu^\varepsilon}{16\pi^2} \int_0^1 \mathcal{D}^3 x \frac{1}{\Delta_{C_0}} . \end{aligned} \tag{2.B.11}$$

We also define some special cases of C_0 integrals that appear in the main text in various places:

$$\begin{aligned} C_0^1(p, m_{Z_0}, m_{Z_0}, m_{\chi_0}) &\equiv C_0(P_1 = p, P_2 = 0, m_{Z_0}, m_{Z_0}, m_{\chi_0}) \\ C_0^2(p, m_{Z_0}, m_{Z_0}, m_{\chi_0}) &\equiv C_0(P_1 = p, P_2 = p, m_{Z_0}, m_{Z_0}, m_{\chi_0}) \\ C_0^3(p, m_{Z_0}, m_{\chi_0}, m_{\chi_0}) &\equiv C_0(P_1 = 0, P_2 = p, m_{Z_0}, m_{\chi_0}, m_{\chi_0}) . \end{aligned} \tag{2.B.12}$$

The last scalar is the finite Box integral

$$D_0(P_1, P_2, P_3, m_1, m_2, m_3, m_4) = \int \frac{d^4k}{i\,(2\pi)^4} \frac{1}{D_1 D_2 D_3 D_4} . \tag{2.B.13}$$

The integral in d-dimensions becomes

$$\begin{aligned} \mu^\varepsilon D_0(P_1, P_2, P_3, m_1, m_2, m_3, m_4) &= 6\mu^\varepsilon \int_0^1 \mathcal{D}^4 x \left\langle \frac{1}{(k^2 - \Delta_{D_0})^4} \right\rangle \\ &= \frac{\mu^\varepsilon}{(4\pi)^{d/2}} \int_0^1 \mathcal{D}^4 x \frac{\Gamma\left(4-\frac{d}{2}\right)}{\Delta_{D_0}^{4-d/2}} \\ &= \frac{\mu^\varepsilon}{16\pi^2} \int_0^1 \mathcal{D}^4 x \frac{1}{\Delta_{D_0}^2} . \end{aligned} \tag{2.B.14}$$

2.B.2 Tensors

Standard tensor PV integrals can be algebraically reduced to scalar integrals. Actually in one-loop diagrams only contractions of tensors with the metric and external momenta occur. The tadpole integral has no standard PV extension. It has an extension of the U-type, naively quartically divergent with a cut-off and it will be computed in Appendix 2.C.

Let us introduce some shorthand notation. First, define for any P:

$$B_0(1,2) \equiv B_0(P, m_1, m_2) \tag{2.B.15}$$

and for any P_1 and P_2

$$\begin{aligned} B_0(1,3) &\equiv B_0(P_2, m_1, m_3) \\ B_0(2,3) &\equiv B_0(P_2 - P_1, m_2, m_3)\,. \end{aligned} \tag{2.B.16}$$

The simplest B-tensor is the linearly divergent

$$B^\mu(P, m_1, m_2) = \left\langle \frac{k^\mu}{(k^2 - m_1^2)((k+P)^2 - m_2^2)} \right\rangle \tag{2.B.17}$$

and it can be contracted only by a momentum

$$P_\mu B^\mu(P, m_1, m_2) = \frac{1}{2}\left(f_1(P) B_0(1,2) + A_0(m_1) - A_0(m_2)\right)\,, \tag{2.B.18}$$

where

$$f_1(P) = m_2^2 - m_1^2 - P^2\,. \tag{2.B.19}$$

The other PV tensor extension of the B-type is of the form

$$B^{\mu\nu} = \left\langle \frac{k^\mu k^\nu}{(k^2 - m_1^2)((k+P)^2 - m_2^2)} \right\rangle \tag{2.B.20}$$

and it is quadratically divergent. Its contraction with the metric is

$$g_{\mu\nu} B^{\mu\nu}(P, m_1, m_2) = m_1^2 B_0(P, m_1, m_2) + A_0(m_2) \tag{2.B.21}$$

while its contraction with $P_\mu P_\nu$ is

$$\begin{aligned} P_\mu P_\nu B^{\mu\nu}(P, m_1, m_2) &= \frac{m_2^2 - m_1^2 - P^2}{4} A_0(m_1) + \frac{m_1^2 - m_2^2 + 3P^2}{4} A_0(m_2) \\ &+ \left(\frac{m_1^4 + m_2^4 - 2m_1^2 m_2^2}{4} + \frac{P^2(2m_1^2 - 2m_2^2 + P^2)}{4} \right) B_0(P, m_1, m_2)\,. \end{aligned} \tag{2.B.22}$$

The simplest C-tensor is

$$C^\mu(P_1, P_2, m_1, m_2, m_3) = \left\langle \frac{k^\mu}{D_1 D_2 D_3} \right\rangle\,. \tag{2.B.23}$$

It contracts either as

$$R_1^{[c]} \equiv P_{1\mu} C^\mu = \frac{1}{2}\left(f_1(P_1) C_0(P_1, P_2, m_1, m_2, m_3) + B_0(1,3) - B_0(2,3)\right) \tag{2.B.24}$$

or as

$$R_2^{[c]} \equiv (P_2 - P_1)_\mu C^\mu = \frac{1}{2}\left(f_2(P_1, P_2) C_0(P_1, P_2, m_, m_2, m_3) + B_0(1,2) - B_0(1,3)\right) \tag{2.B.25}$$

where

$$f_2(P_1, P_2) = m_3^2 - m_2^2 - P_2^2 + P_1^2 \,. \tag{2.B.26}$$

The second C-tensor, logarithmically divergent, integral is

$$C^{\mu\nu}(P_1, P_2, m_1, m_2, m_3) = \left\langle \frac{k^\mu k^\nu}{D_1 D_2 D_3} \right\rangle \,. \tag{2.B.27}$$

Its contraction with the metric is

$$g_{\mu\nu} C^{\mu\nu} = m_1^2 C_0(P_1, P_2, m_1, m_2, m_3) + B_0(P_2 - P_1, m_2, m_3) \,. \tag{2.B.28}$$

There are three different momentum contractions that can appear. Following [46], we define the matrix

$$G_2^{-1} = \frac{1}{\det G_2} \begin{pmatrix} (P_2 - P_1)\cdot(P_2 - P_1) & -P_1 \cdot (P_2 - P_1) \\ -P_1 \cdot (P_2 - P_1) & P_1 \cdot P_1 \end{pmatrix}$$

and using this matrix the quantities

$$\begin{pmatrix} C_1 \\ C_2 \end{pmatrix} = G_2^{-1} \begin{pmatrix} R_1^{[c]} \\ R_2^{[c]} \end{pmatrix} . \tag{2.B.29}$$

We also define

$$\begin{aligned}
B_1(1,2) \equiv B_1(P_1, m_1, m_2) &= \frac{1}{2P_1^2}\left(f_1(P_1) B_0(1,2) + A_0(m_1) - A_0(m_2)\right) \\
B_1(1,3) \equiv B_1(P_2, m_1, m_3) &= \frac{1}{2P_2^2}\left(f_1(P_2) B_0(1,3) + A_0(m_1) - A_0(m_3)\right) \\
B_1(2,3) \equiv B_1(P_2 - P_1, m_2, m_3) &= \frac{1}{2(P_2 - P_1)^2}\left(f_1(P_2 - P_1) B_0(2,3) + A_0(m_2) - A_0(m_3)\right) \\
C_{00}(1,2,3) &= \frac{1}{2(d-2)}\left(2m_1^2 C_0 - f_2(P_2, P_1) C_2 - f_1(P_1) C_1 + B_0(2,3)\right)
\end{aligned} \tag{2.B.30}$$

out of which we construct the four quantities

$$\begin{aligned}
R_1^{[c_1]} &= \frac{1}{2}\left(f_1(P_1) C_1 + B_1(1,3) + B_0(2,3) - 2C_{00}(1,2,3)\right) \\
R_2^{[c_1]} &= \frac{1}{2}\left(f_2(P_2, P_1) C_1 + B_1(1,2) - B_1(1,3)\right) \\
R_1^{[c_2]} &= \frac{1}{2}\left(f_1(P_1) C_2 + B_1(1,3) - B_1(2,3)\right) \\
R_2^{[c_2]} &= \frac{1}{2}\left(f_2(P_2, P_1) C_2 - B_1(1,3) - 2C_{00}(1,2,3)\right) .
\end{aligned} \tag{2.B.31}$$

This data determines the quantities

$$\begin{aligned}
C_{11} &= \frac{1}{\det G_2}\Big\{(P_2-P_1)^2 R_1^{[c_1]} - P_1\cdot(P_2-P_1)R_2^{[c_1]}\Big\} \\
C_{12} &= C_{21} = \frac{1}{\det G_2}\Big\{P_1^2 R_2^{[c_1]} - P_1\cdot(P_2-P_1)R_1^{[c_1]}\Big\} \\
C_{22} &= \frac{1}{\det G_2}\Big\{P_1^2 R_2^{[c_2]} - P_1\cdot(P_2-P_1)R_1^{[c_2]}\Big\}
\end{aligned} \tag{2.B.32}$$

and in terms of these we can express $C_{\mu\nu}$ itself:

$$\begin{aligned}
C_{\mu\nu} &= \frac{g_{\mu\nu}}{2\,(d-2)}\left(2m_1^2 C_0(P_1,P_2,m_1,m_2,m_3) - f_2(P_2,P_1)C_2 - f_1(P_1)C_1 + B_0\,(2,3)\right) \\
&+ P_{1\mu}P_{1\nu}C_{11} + \left(P_{1\mu}(P_2-P_1)_\nu + (P_2-P_1)_\mu P_{1\nu}\right)C_{12} + (P_2-P_1)_\mu(P_2-P_1)_\nu C_{22}
\end{aligned} \tag{2.B.33}$$

and from the above expression it is straightforward to compute all its momentum contractions.

We sometimes encounter C-integrals with $\det[G_2]=0$. Such integrals are computed with direct Feynman parametrization and DR (i.e. without algebraic reduction). To give an example, we may stumble on

$$\begin{aligned}
C^1_{\mu\nu}(p,m_1,m_2,m_3) &\equiv C_{\mu\nu}(P_1=p,P_2=0,m_1,m_2,m_3) \\
&= \left\langle \frac{k_\mu k_\nu}{(k^2-m_1^2)((k+p)^2-m_2^2)(k^2-m_3^2)}\right\rangle \\
&= 2\int_0^1 \mathcal{D}^3x \left\langle \frac{k_\mu k_\nu + x_2 k_\mu p_\nu + x_2 k_\nu p_\nu + x_2^2 p_\mu p_\nu}{(k^2-\Delta_{C_0})^3}\right\rangle ,
\end{aligned} \tag{2.B.34}$$

which in DR, after expanding in ε, becomes

$$16\pi^2\mu^\varepsilon C^1_{\mu\nu}(d=4,\varepsilon\to 0) = \frac{g_{\mu\nu}}{4}\left\{\frac{2}{\varepsilon} + 2\int_0^1 \mathcal{D}^3x \ln\frac{\mu^2}{\Delta_{C_0}}\right\} + 2\int_0^1 \mathcal{D}^3x \frac{x_2^2 p^2}{\Delta_{C_0}} . \tag{2.B.35}$$

Let us now consider the linearly divergent rank 3 integral

$$C^{\mu\nu\alpha}(P_1,P_2,m_1,m_2,m_3) = \left\langle \frac{k^\mu k^\nu k^\alpha}{D_1 D_2 D_3}\right\rangle . \tag{2.B.36}$$

This integral could be reduced in principle algebraically, following [46]. Here, as it is only linearly divergent, we will compute it in a brute force way with Feynman parametrization. It is a case with $n=3$ and $N^{(3)}_{C^{\mu\nu\alpha}} = k^\mu k^\nu k^\alpha$ in the language of Appendix 2.A. It explicitly evaluates to

$$\begin{aligned}
16\pi^2\mu^\varepsilon C^{\mu\nu\alpha}(P_1,P_2,m_1,m_2,m_3) &= -2\frac{g^{\mu\nu}}{d}\int_0^1 \mathcal{D}^3x [P_1x_2+P_2x_3]^\alpha B_0^{K^a} \\
&- 2\frac{g^{\mu\alpha}}{d}\int_0^1 \mathcal{D}^3x [P_1x_2+P_2x_3]^\nu B_0^{K^a} \\
&- 2\frac{g^{\alpha\nu}}{d}\int_0^1 \mathcal{D}^3x [P_1x_2+P_2x_3]^\mu B_0^{K^a} \\
&+ \int_0^1 \mathcal{D}^3x \frac{[P_1x_2+P_2x_3]^\mu [P_1x_2+P_2x_3]^\nu [P_1x_2+P_2x_3]^\alpha}{\Delta_{C_0}}
\end{aligned}$$

(2.B.37)

where

$$B_0^{K^a} = \frac{2}{\varepsilon} + \ln \frac{\mu^2}{\Delta_{C_0}} \,. \tag{2.B.38}$$

It is now easy to compute any contraction of the above expression with the metric and/or momenta. A useful contraction is $C^{\mu}_{\mathcal{K}3} \equiv g_{\nu\alpha} C^{\mu\nu\alpha}$.

All Box tensor integrals are computed directly as in Appendix 2.A since they are at most logarithmically divergent. D^{μ}, $D^{\mu\nu}$, $D^{\mu\nu\alpha}$ and $D^{\mu\nu\alpha\beta}$ are computed as

$$D^{\mu,\mu\nu,\mu\nu\alpha,\mu\nu\alpha\beta} = 6 \int_0^1 \mathcal{D}^4 x \left\langle \frac{N^{(4)}_{D^{\mu,\mu\nu,\mu\nu\alpha,\mu\nu\alpha\beta}}(k - \sum_{i=1}^4 P_i x_{i+1})}{D_1 D_2 D_3 D_4} \right\rangle \,, \tag{2.B.39}$$

with $N^{(4)}_{D^{\mu}} = k^{\mu}$, $N^{(4)}_{D^{\mu\nu}} = k^{\mu}k^{\nu}$, $N^{(4)}_{D^{\mu\nu\alpha}} = k^{\mu}k^{\nu}k^{\alpha}$ and $N^{(4)}_{D^{\mu\nu\alpha\beta}} = k^{\mu}k^{\nu}k^{\alpha}k^{\beta}$. Two useful contractions are $D^{\mu\nu}_{\mathcal{B}4} \equiv g_{\alpha\beta} D^{\mu\nu\alpha\beta}$ and $D_{\mathcal{B}4} \equiv g_{\mu\nu} D^{\mu\nu}_{\mathcal{B}4}$.

2.C U-integrals

U-integrals are linearly, quadratically, cubically or quartically divergent diagrams that do not appear when the Higgs is expressed in a Cartesian basis and an R_ξ gauge fixing is performed. If either a Polar basis for the Higgs is used and/or the computation is performed in the Unitary gauge, these integrals do appear. Clearly, the standard PV reduction formulae must be extended. At each level of n-point functions we meet at least an integral of the U-type.

2.C.1 U-integrals in Tadpoles

Indeed, during the Tadpole calculation in section 2.3.1 we find the quartically divergent contraction

$$\begin{aligned}
U^{\mu\nu}_{\mathcal{T}}(m) &= \left\langle \frac{k^{\mu}k^{\nu}}{k^2 - m^2} \right\rangle = \frac{g_{\mu\nu}}{d} \left\langle \frac{k^2}{k^2 - m^2} \right\rangle \Leftrightarrow \\
U_{\mathcal{T}}(m) = g_{\mu\nu} U^{\mu\nu}_{\mathcal{T}}(m) &= \frac{d}{d} \left\langle \frac{k^2}{k^2 - m^2} \right\rangle \\
&= \left\langle \frac{m^2}{k^2 - m^2} \right\rangle + \left\langle \frac{k^2 - m^2}{k^2 - m^2} \right\rangle \\
&= m^2 A_0(m) + \mathcal{V} \,.
\end{aligned} \tag{2.C.1}$$

where $\mathcal{V}$ is the DR volume of space-time. The usual prescription is $\mathcal{V} = 0$, in which case, the tensor-Tadpole U-integral reduces to

$$U_{\mathcal{T}}(m) = m^2 A_0(m). \tag{2.C.2}$$

2.C.2 U-integrals in mass corrections

The basic U-integral with two denominators is the quartically divergent with the cut-off integral

$$U_{\mathcal{M}4}(P_1, m_1, m_2) = \left\langle \frac{k^4}{D_1 D_2(P_1)} \right\rangle \tag{2.C.3}$$

with $D_1 = k^2 - m_1^2$ and $D_2(P_1) = (k + P_1)^2 - m_2^2$ as defined in Eq. (2.A.3). We show only the momentum argument P_1 as we would like to follow it. Adding and subtracting a term, the above integral can be rewritten as

$$\begin{aligned} U_{\mathcal{M}4}(P_1, m_1, m_2) &= \left\langle \frac{(k^2 - m_1^2)k^2}{D_1 D_2(P_1)} \right\rangle + \left\langle \frac{k^2 m_1^2}{D_1 D_2(P_1)} \right\rangle \\ &= \left\langle \frac{k^2}{D_2(P_1)} \right\rangle + m_1^2 g_{\mu\nu} B^{\mu\nu}(P_1, m_1, m_2) . \end{aligned} \tag{2.C.4}$$

Now the second term is a standard PV integral, while the first term is still a U-integral (it is still quartically divergent) but we can compute it straightforwardly as

$$\begin{aligned} \left\langle \frac{k^2}{D_2(P_1)} \right\rangle &= \left\langle \frac{k^2}{D_2(0)} \right\rangle - \left\langle \frac{2P_1 \cdot k}{D_2(0)} \right\rangle + \left\langle \frac{P_1^2}{D_2(0)} \right\rangle \\ &= (m_2^2 + P_1^2) A_0(m_2) + \frac{1}{16\pi^2} m_2^4 , \end{aligned} \tag{2.C.5}$$

where we have performed the shift $k \to k - P_1$ and we have dropped the $2k \cdot P_1$ term because it is odd under $k \to -k$. Also, we have used Eq. (2.C.2) for the rational part. From (2.C.4) and (2.C.5) and using Eq.(2.B.21), we get

$$U_{\mathcal{M}4}(P_1, m_1, m_2) = \left(m_1^2 + m_2^2 + P_1^2\right) A_0(m_2) + m_1^4 B_0(P_1, m_1, m_2) . \tag{2.C.6}$$

The reduction of $U_{\mathcal{M}4}$ was carried through using at some point a loop momentum shift. We know that in DR and in the absence of fermions, momentum shifts are ok, as long as the integral is up to naively quadratically divergent with the cut-off. U-integrals are however often cubically or quartically divergent. In order to check the validity of momentum shifts, we will now re-compute $U_{\mathcal{M}4}$ without momentum shift and compare the results.

Starting with Eq. (2.C.3), by adding and subtracting terms, we construct in the numerator $D_2(P_1)$ obtaining

$$\begin{aligned} U_{\mathcal{M}4}(P_1, m_1, m_2) &= \left\langle \frac{\left((k + P_1)^2 - m_2^2\right)k^2}{D_1 D_2(P_1)} \right\rangle - 2 \left\langle \frac{k^2 P_1 \cdot k}{D_1 D_2(P_1)} \right\rangle + (m_2^2 - P_1^2) \left\langle \frac{k^2}{D_1 D_2(P_1)} \right\rangle \\ &= \left\langle \frac{k^2}{D_1} \right\rangle - 2 \left\langle \frac{k^2 P_1 \cdot k}{D_1 D_2(P_1)} \right\rangle + (m_2^2 - P_1^2) g_{\mu\nu} B^{\mu\nu}(P_1, m_1, m_2) . \end{aligned} \tag{2.C.7}$$

The second term in the last expression is

$$-2 \left\langle \frac{k^2 P_1 \cdot k}{D_1 D_2(P_1)} \right\rangle = -2 \left\langle \frac{\left((k + P_1)^2 - m_2^2\right) P_1 \cdot k}{D_1 D_2(P_1)} \right\rangle$$

$$
\begin{aligned}
&+ \quad 4\left\langle \frac{P_1\cdot k P_1\cdot k}{D_1 D_2(P_1)}\right\rangle - 2(m_2^2-P_1^2)\left\langle \frac{P_1\cdot k}{D_1 D_2(P_1)}\right\rangle \\
&= \quad -2\left\langle \frac{P_1\cdot k}{D_1}\right\rangle + 4P_{1\mu}P_{1\nu}B^{\mu\nu}\left(P_1,m_1,m_2\right) \\
&- \quad 2(m_2^2-P_1^2)P_{1\mu}B^{\mu}\left(P_1,m_1,m_2\right). \qquad (2.C.8)
\end{aligned}
$$

The first term of the above relation is zero since $P_1\cdot k$ term is odd under $k\to -k$. The third term of Eq. (2.C.7) and the second and third terms of Eq. (2.C.8) are standard PV integrals. The first term of Eq. (2.C.7) however is still a U-integral (and still quartically divergent) but we can reduce it easily as

$$
\left\langle \frac{k^2}{D_1}\right\rangle = \left\langle \frac{k^2-m_1^2}{D_1(0)}\right\rangle = m_1^2 A_0\left(m_1\right). \qquad (2.C.9)
$$

Combining Eq. (2.C.7) with Eq. (2.C.8) and Eq. (2.C.9) and using Eq. (2.B.18), Eq. (2.B.21) and Eq. (2.B.22) we obtain

$$
U_{\mathcal{M}4}(P_1,m_1,m_2) = \left(m_1^2+m_2^2+P_1^2\right)A_0(m_2)+m_1^4 B_0(P_1,m_1,m_2), \qquad (2.C.10)
$$

which is the same as Eq. (2.C.6). Clearly, we have traded loop momentum shifts in highly divergent integrals for adding and subtracting infinities, a slightly less disturbing operation. In any case, the final results will justify or not these manipulations.

2.C.3 U-integrals in Triangles

In the Triangle sector we first meet

$$
U^{\mu\nu}_{\mathcal{K}4}(P_1,P_2,m_1,m_2,m_3) = \left\langle \frac{k^2k^\mu k^\nu}{D_1D_2D_3}\right\rangle. \qquad (2.C.11)
$$

It can be reduced easily as

$$
\begin{aligned}
U^{\mu\nu}_{\mathcal{K}4}(P_1,P_2,m_1,m_2,m_3) &= \left\langle \frac{\left((k+P_2)^2-m_3^2\right)k^\mu k^\nu}{D_1D_2D_3}\right\rangle - 2P_{2\alpha}C^{\mu\nu\alpha}(P_1,P_2,m_1,m_2,m_3) \\
&+ (m_3^2-P_2^2)C^{\mu\nu}(P_1,P_2,m_1,m_2,m_3) \\
&= B^{\mu\nu}(P_1,m_1,m_2) - 2P_{2\alpha}C^{\mu\nu\alpha}(P_1,P_2,m_1,m_2,m_3) \\
&+ (m_3^2-P_2^2)C^{\mu\nu}(P_1,P_2,m_1,m_2,m_3) \qquad (2.C.12)
\end{aligned}
$$

and with PV reduction further on.

The next case is the cubically divergent

$$
U^{\mu}_{\mathcal{K}5}(P_1,P_2,m_1,m_2,m_3) = \left\langle \frac{k^4k^\mu}{D_1D_2D_3}\right\rangle. \qquad (2.C.13)
$$

Following similar steps as before

$$
U^{\mu}_{\mathcal{K}5}(P_1,P_2,m_1,m_2,m_3) = \left\langle \frac{((k+P_2)^2-m_3^2)k^2k^\mu}{D_1D_2D_3}\right\rangle - 2P_{2\nu}U^{\mu\nu}_{\mathcal{K}4}(P_1,P_2,m_1,m_2,m_3)
$$

$$
\begin{aligned}
&+ \quad (m_3^2 - P_2^2) C^{\mu}_{\mathcal{K}3}(P_1, P_2, m_1, m_2, m_3) \Leftrightarrow \\
&= \quad \left\langle \frac{k^2 k^{\mu}}{D_1 D_2} \right\rangle - 2P_{2\nu} U^{\mu\nu}_{\mathcal{K}4}(P_1, P_2, m_1, m_2, m_3) \\
&+ \quad (m_3^2 - P_2^2) C^{\mu}_{\mathcal{K}3}(P_1, P_2, m_1, m_2, m_3).
\end{aligned} \tag{2.C.14}
$$

Only the first term is new (and also a U-integral) but it is easy to compute it:

$$
\begin{aligned}
\left\langle \frac{k^2 k^{\mu}}{D_1 D_2} \right\rangle &= \left\langle \frac{(k^2 - m_1^2) k^{\mu}}{D_1 D_2} \right\rangle + m_1^2 \left\langle \frac{k^{\mu}}{D_1 D_2} \right\rangle \\
&= \left\langle \frac{k^{\mu}}{D_2(P_1)} \right\rangle + m_1^2 B^{\mu}(P_1, m_1, m_2) \\
&= \left\langle \frac{k^{\mu}}{D_2(0)} \right\rangle - P_1^{\mu} A_0(m_2) + m_1^2 B^{\mu}(P_1, m_1, m_2) \\
&= -P_1^{\mu} A_0(m_2) + m_1^2 B^{\mu}(P_1, m_1, m_2)
\end{aligned} \tag{2.C.15}
$$

where in the third line above we have shifted the loop momentum and then neglected the k-odd term, as before. It total,

$$
\begin{aligned}
U^{\mu}_{\mathcal{K}5}(P_1, P_2, m_1, m_2, m_3) &= -P_1^{\mu} A_0(m_2) + m_1^2 B^{\mu}(P_1, m_1, m_2) - 2P_{2\nu} U^{\mu\nu}_{\mathcal{K}4}(P_1, P_2, m_1, m_2, m_3) \\
&+ \quad (m_3^2 - P_2^2) C^{\mu}_{\mathcal{K}3}(P_1, P_2, m_1, m_2, m_3)\,.
\end{aligned} \tag{2.C.16}
$$

The last Triangle U-integral is quartically divergent, It is successively reduced as

$$
\begin{aligned}
U_{\mathcal{K}6}(P_1, P_2, m_1, m_2, m_3) &= \left\langle \frac{k^6}{D_1 D_2 D_3} \right\rangle \\
&= \left\langle \frac{((k + P_2)^2 - m_3^2) k^4}{D_1 D_2 D_3} \right\rangle - 2P_{2\mu} U^{\mu}_{\mathcal{K}5}(P_1, P_2, m_1, m_2, m_3) \\
&+ \quad (m_3^2 - P_2^2) U_{\mathcal{K}4}(P_1, P_2, m_1, m_2, m_3) \\
&= \left\langle \frac{k^4}{D_1 D_2} \right\rangle - 2P_{2\mu} U^{\mu}_{\mathcal{K}5}(P_1, P_2, m_1, m_2, m_3) \\
&+ \quad (m_3^2 - P_2^2) U_{\mathcal{K}4}(P_1, P_2, m_1, m_2, m_3) \\
&= \quad U_{\mathcal{M}4}(P_1, m_1, m_2) - 2P_{2\mu} U^{\mu}_{\mathcal{K}5}(P_1, P_2, m_1, m_2, m_3) \\
&+ \quad (m_3^2 - P_2^2) U_{\mathcal{K}4}(P_1, P_2, m_1, m_2, m_3).
\end{aligned} \tag{2.C.17}
$$

where we have defined $U_{\mathcal{K}4} = g_{\mu\nu} U^{\mu\nu}_{\mathcal{K}4}$.

2.C.4 U-integrals in Boxes

The lowest Box U-integrals have five momenta in their numerator. One is

$$
\begin{aligned}
U^{\mu}_{\mathcal{B}5}(P_1, P_2, P_3, m_1, m_2, m_3, m_4) &= \left\langle \frac{k^4 k^{\mu}}{D_1 D_2 D_3 D_4} \right\rangle \\
&= C^{\mu}_{\mathcal{K}3}(P_1, P_2, m_1, m_2, m_3) - 2P_{3\nu} D^{\mu\nu}_{\mathcal{B}4}(P_1, P_2, P_3, m_1, m_2, m_3, m_4) \\
&+ \quad (m_4^2 - P_3^2) g_{\nu\alpha} D^{\mu\nu\alpha}(P_1, P_2, P_3, m_1, m_2, m_3, m_4)
\end{aligned}
$$

(2.C.18)

and the other is

$$\begin{aligned} U^{\mu\nu\alpha}_{\mathcal{B}5}(P_1,P_2,P_3,m_1,m_2,m_3,m_4) &= \left\langle \frac{k^2 k^\mu k^\nu k^\alpha}{D_1 D_2 D_3 D_4} \right\rangle \\ &= C^{\mu\nu\alpha}(P_1,P_2,m_1,m_2,m_3) - 2P_{3\beta} D^{\mu\nu\alpha\beta}(P_1,P_2,P_3,m_1,m_2,m_3,m_4) \\ &+ (m_4^2 - P_3^2) D^{\mu\nu\alpha}(P_1,P_2,P_3,m_1,m_2,m_3,m_4)\,. \end{aligned} \tag{2.C.19}$$

The pattern should start becoming obvious by now. For example, we have

$$\begin{aligned} U^{\mu\nu}_{\mathcal{B}6}(P_1,P_2,P_3,m_1,m_2,m_3,m_4) &= \left\langle \frac{k^4 k^\mu k^\nu}{D_1 D_2 D_3 D_4} \right\rangle \\ &= U^{\mu\nu}_{\mathcal{K}4}(P_1,P_2,m_1,m_2,m_3) \\ &- 2P_{3\alpha} U^{\mu\nu\alpha}_{\mathcal{B}5}(P_1,P_2,P_3,m_1,m_2,m_3,m_4) \\ &+ (m_4^2 - P_3^2) D^{\mu\nu}_{\mathcal{B}4}(P_1,P_2,P_3,m_1,m_2,m_3,m_4) \end{aligned} \tag{2.C.20}$$

and its contracted version $U_{\mathcal{B}6} \equiv g_{\mu\nu} U^{\mu\nu}_{\mathcal{B}6}$. The cubically divergent Box U-integral is

$$\begin{aligned} U^{\mu}_{\mathcal{B}7}(P_1,P_2,P_3,m_1,m_2,m_3,m_4) &= \left\langle \frac{k^6 k^\mu}{D_1 D_2 D_3 D_4} \right\rangle \\ &= U^{\mu}_{\mathcal{K}5}(P_1,P_2,m_1,m_2,m_3) \\ &- 2P_{3\nu} U^{\mu\nu}_{\mathcal{B}6}(P_1,P_2,P_3,m_1,m_2,m_3,m_4) \\ &+ (m_4^2 - P_3^2) U^{\mu}_{\mathcal{B}5}(P_1,P_2,P_3,m_1,m_2,m_3,m_4)\,. \end{aligned} \tag{2.C.21}$$

Finally we have the quartically divergent

$$\begin{aligned} U_{\mathcal{B}8}(P_1,P_2,P_3,m_1,m_2,m_3,m_4) &= \left\langle \frac{k^8}{D_1 D_2 D_3 D_4} \right\rangle \\ &= U_{\mathcal{K}6}(P_1,P_2,m_1,m_2,m_3) \\ &- 2P_{3\mu} U^{\mu}_{\mathcal{B}7}(P_1,P_2,P_3,m_1,m_2,m_3,m_4) \\ &+ (m_4^2 - P_3^2) U_{\mathcal{B}6}(P_1,P_2,P_3,m_1,m_2,m_3,m_4)\,. \end{aligned} \tag{2.C.22}$$

2.D Explicit calculation of the diagrams

In this Appendix we present the explicit calculation of the one-loop Feynman diagrams, concentrating on the Tadpole and the two-point function categories, in both R_ξ and Unitary gauges. The Triangle and Box contributions can be straightforwardly computed following similar steps, therefore there is no need to calculate them explicitly here.

2.D.1 R_ξ-diagrams

In order to be synchronised with our main text, we start form the first set of diagrams which corresponds to the one-point functions. The first such diagram is

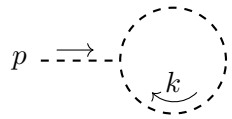

$$= i\mathcal{T}_H^{R_\xi,\phi}$$

and analytically evaluates to

$$i\mathcal{T}_H^{R_\xi,\phi} = -6\mathcal{S}_T^1\sqrt{\frac{\lambda_0}{2}}m_{H_0}\int\frac{d^4k}{(2\pi)^4}\frac{-i}{\left(k^2-m_{H_0}^2\right)}\,. \tag{2.D.1}$$

The symmetry factor is $\mathcal{S}_T^1=\frac{1}{2}$ since $(n_O,n_l,\ell_1,v_1)=(3,1,3,1)$. In DR this integral takes the form

$$\mathcal{T}_H^{R_\xi,\phi} = 3\sqrt{\frac{\lambda_0}{2}}m_{H_0}\mu^\varepsilon A_0(m_{H_0})\,. \tag{2.D.2}$$

The "tadpole integral" A_0 is defined in Appendix 2.B. It has mass dimension 2 and it is (external) momentum independent.

The next tadpole comes with a gauge boson loop:

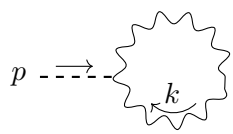

$$= i\mathcal{T}_H^{R_\xi,Z}$$

It is equal to

$$\begin{aligned}\mathcal{T}_H^{R_\xi,Z} &= d\frac{m_{Z_0}^2}{m_{H_0}}\sqrt{2\lambda_0}\int\frac{d^4k}{(2\pi)^4}\frac{-i}{k^2-m_{Z_0}^2}\\ &+ (1-\xi)\frac{m_{Z_0}^2}{m_{H_0}}\sqrt{2\lambda_0}g_{\mu\nu}\int\frac{d^4k}{(2\pi)^4}\frac{ik^\mu k^\nu}{\left(k^2-m_{Z_0}^2\right)\left(k^2-\xi m_{Z_0}^2\right)}\end{aligned} \tag{2.D.3}$$

with symmetry factor $\mathcal{S}_T^2=\frac{1}{2}$ since $(n_O,n_l,\ell_1,v_1)=(1,1,2,1)$. Using the relation $k^\mu k^\nu=\frac{g_{\mu\nu}}{d}k^2$ under the intergral it simplifies to

$$\mathcal{T}_H^{R_\xi,Z} = \frac{m_{Z_0}^2}{m_{H_0}}\sqrt{2\lambda_0}\mu^\varepsilon\left\{4A_0(m_{Z_0})-(1-\xi)A_0(\sqrt{\xi}m_{Z_0})-(1-\xi)m_{Z_0}^2B_0^1(m_{Z_0},\sqrt{\xi}m_{Z_0})\right\}, \tag{2.D.4}$$

where the B_0 scalar integral appears at $p^2=0$ and we call it B_0^1. Using Eq.(2.B.8) the gauge tadpole becomes

$$\mathcal{T}_H^{R_\xi,Z} = \frac{m_{Z_0}^2}{m_{H_0}}\sqrt{2\lambda_0}\mu^\varepsilon\left\{3A_0(m_{Z_0})+\xi A_0(\sqrt{\xi}m_{Z_0})\right\}. \tag{2.D.5}$$

The last tadpole has a Goldstone loop:

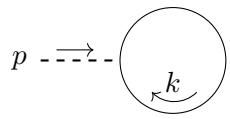

$$= i\mathcal{T}_H^{R_\xi,\chi}$$

It is equal to

$$\mathcal{T}_H^{R_\xi,\chi} = -\frac{\sqrt{2\lambda_0}}{m_{H_0}}\int\frac{d^4k}{(2\pi)^4}\frac{-ik^2}{\left(k^2-m_{\chi_0}^2\right)}\,, \tag{2.D.6}$$

with $\mathcal{S}_T^3=\frac{1}{2}$ as $(n_O,n_l,\ell_1,v_1)=(1,1,2,1)$. Notice that the integral in Eq. (2.D.6) is a U-integral (called $U_\mathcal{T}$), the first in the class of highly divergent integrals that we will often encounter in the Unitary gauge. As already mentioned, the origin of such integrals emerging also in the R_ξ gauge can be traced to our Polar basis choice to represent the Higgs field. Using Eq.(2.C.2) to calculate $U_\mathcal{T}(m_{\chi_0})$ we obtain that in DR,

$$\mathcal{T}_H^{R_\xi,\chi} = -\frac{\sqrt{2\lambda_0}}{m_{H_0}}\mu^\varepsilon m_{\chi_0}^2 A_0(m_{\chi_0})\,. \tag{2.D.7}$$

Finally, the total tadpole value is the sum of the above three contributions:

$$\mathcal{T}_H^{R_\xi} = \mu^\varepsilon\left(3\sqrt{\frac{\lambda_0}{2}}m_{H_0}A_0(m_H)+3\frac{\sqrt{2\lambda_0}m_{Z_0}^2}{m_{H_0}}A_0(m_Z)\right). \tag{2.D.8}$$

Next we have the Z 2-point function. A gauge-boson vacuum polarization amplitude can be Lorentz-covariantly split into a transverse and a longitudinal part

$$\mathcal{M}_{Z,\mu\nu} = \left(-g_{\mu\nu}+\frac{p_\mu p_\nu}{p^2}\right)\Pi^T(p^2)+\frac{p_\mu p_\nu}{p^2}\Pi^L(p^2). \tag{2.D.9}$$

Contracting with $p^\mu p^\nu$ both sides fixes

$$\Pi^L(p^2) = \frac{p^\mu p^\nu}{p^2}\mathcal{M}_{Z,\mu\nu}. \tag{2.D.10}$$

Contracting with $g^{\mu\nu}$ gives on the other hand

$$g^{\mu\nu}\mathcal{M}_{Z,\mu\nu} = -(d-1)\Pi^T+\Pi^L \tag{2.D.11}$$

that can be easily solved for the transverse part in $d=4$

$$\Pi^T = \frac{1}{3}\left(-g_{\mu\nu}+\frac{p_\mu p_\nu}{p^2}\right)\mathcal{M}_Z^{\mu\nu}\,. \tag{2.D.12}$$

Now, the Schwinger-Dyson equation that the dressed Z-propagator

$$G_{\mu\nu} = -g_{\mu\nu}G(p^2)+\frac{p_\mu p_\nu}{m_{Z_0}^2}L(p^2) \tag{2.D.13}$$

obeys is written as

$$G_{\mu\nu} = G_{\mu\nu}+D_{\mu\rho}\mathcal{M}_Z^{\rho\sigma}G_{\sigma\nu} \tag{2.D.14}$$

with $D_{\mu\rho}$ the tree level gauge boson propagator

$$D_{\mu\rho} = \frac{\left(-g_{\mu\rho} + \frac{p_\mu p_\rho}{m_{Z_0}^2}\right)}{p^2 - m_{Z_0}^2}. \tag{2.D.15}$$

So, performing the contractions the Schwinger-Dyson equation becomes

$$-g_{\mu\nu}G + \frac{p_\mu p_\nu}{m_{Z_0}^2}L = \frac{\left(-g_{\mu\nu} + \frac{p_\mu p_\nu}{m_{Z_0}^2}\right)}{p^2 - m_{Z_0}^2} + \frac{\left(-g_{\mu\nu} + \frac{p_\mu p_\nu}{p^2}\right)}{p^2 - m_{Z_0}^2}\Pi^T G. \tag{2.D.16}$$

Contracting again with $p^\mu p^\nu$ we have that

$$-G + \frac{p^2}{m_{Z_0}^2}L = \frac{1}{m_{Z_0}^2}\left[1 - \Pi^L(G - L)\right] \tag{2.D.17}$$

while contracting with the metric gives

$$-dG + \frac{p^2}{m_{Z_0}^2}L = \frac{-d + \frac{p^2}{m_{Z_0}^2}}{p^2 - m_{Z_0}^2} + \frac{-d+1}{p^2 - m_{Z_0}^2}\Pi^T G - \frac{1}{m_{Z_0}^2}\Pi^L(G - L). \tag{2.D.18}$$

The solution of the above equation is

$$\begin{aligned} G(p^2) &= \frac{1}{p^2 - m_{Z_0}^2 - \Pi^T(p^2)} \\ L(p^2) &= G(p^2)\left[1 - \frac{\Pi^T}{p^2 - \Pi^L}\right]. \end{aligned} \tag{2.D.19}$$

The quantity that enters in the renormalization of the mass of the Z gauge boson is therefore

$$\mathcal{M}_Z = -\frac{1}{3}\left(g_{\mu\nu} - \frac{p_\mu p_\nu}{p^2}\right)\mathcal{M}_Z^{\mu\nu}(p)\,. \tag{2.D.20}$$

We now start computing the one-loop Feynman diagrams contributing to $\mathcal{M}_{Z,\mu\nu}^{R_\xi}$.

The first contributing diagram has a Higgs running in the loop:

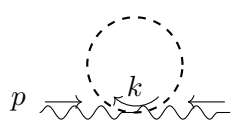

$$= i\mathcal{M}_{Z,\mu\nu}^{R_\xi,\phi}$$

and it is equal to

$$\mathcal{M}_{Z,\mu\nu}^{R_\xi,\phi} = -2g_{\mu\nu}\frac{m_{Z_0}^2}{m_{H_0}^2}\lambda_0 \int \frac{d^4k}{(2\pi)^4}\frac{-i}{k^2 - m_{H_0}^2}\,, \tag{2.D.21}$$

where we used that $\mathcal{S}_g^1 = \frac{1}{2}$ because $(n_O, n_l, \ell_1, \ell_2, v_1) = (2, 1, 2, 2, 1)$. In DR this integral is

$$\mathcal{M}_{Z,\mu\nu}^{R_\xi,\phi} = -2g_{\mu\nu}\frac{m_{Z_0}^2}{m_{H_0}^2}\lambda_0\mu^\varepsilon A_0(m_{H_0})\,. \tag{2.D.22}$$

Next we meet a couple of "sunset" diagrams. The first is

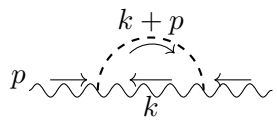

$$= i\mathcal{M}^{R_\xi,\phi Z}_{Z,\mu\nu}$$

that evaluates to

$$\begin{aligned}\mathcal{M}^{R_\xi,\phi Z}_{Z,\mu\nu} &= -8g_{\mu\alpha}g_{\nu\beta}\frac{m^4_{Z_0}}{m^2_{H_0}}\lambda_0\int\frac{d^4k}{(2\pi)^4}\frac{-ig^{\alpha\beta}}{\left(k^2-m^2_{Z_0}\right)\left((k+p)^2-m^2_{H_0}\right)}\\ &- 8g_{\mu\alpha}g_{\nu\beta}\frac{m^4_{Z_0}}{m^2_{H_0}}\lambda_0\int\frac{d^4k}{(2\pi)^4}\frac{i(1-\xi)k^\alpha k^\beta}{\left(k^2-m^2_{Z_0}\right)\left((k+p)^2-m^2_{H_0}\right)\left(k^2-m^2_{\chi_0}\right)}\end{aligned} \tag{2.D.23}$$

with $(n_O, n_l, \ell_1, \ell_2, v_1) = (2\times 2\times 2, 1, 2, 2, 2)$ and $\mathcal{S}_g^2 = 1$. In DR and using Eq. (2.B.35), it can be expressed as

$$\mathcal{M}^{R_\xi,\phi Z}_{Z,\mu\nu} = 8\frac{m^4_{Z_0}}{m^2_{H_0}}\lambda_0\mu^\varepsilon\left\{-g_{\mu\nu}B_0(p,m_{Z_0},m_{H_0}) + (1-\xi)C^1_{\mu\nu}(p,m_{Z_0},m_{H_0},m_{\chi_0})\right\}.$$

Notice that the C-type integral above is a special PV case, computed in Appendix 2.B as well.

The next sunset diagram is the last that contributes to the one-loop correction of the gauge boson propagator:

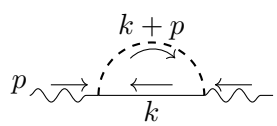

$$= i\mathcal{M}^{R_\xi,\chi\phi}_{Z,\mu\nu}$$

It is equal to

$$\mathcal{M}^{R_\xi,\chi\phi}_{Z,\mu\nu} = 8\frac{m^2_{Z_0}}{m^2_{H_0}}\lambda_0\int\frac{d^4k}{(2\pi)^4}\frac{-ik_\mu k_\nu}{(k^2-m^2_{\chi_0})((k+p)^2-m^2_{H_0})} \tag{2.D.24}$$

with $\mathcal{S}_g^3 = 1$ from $(n_O, n_l, \ell_1, \ell_2, v_1) = (1\times 1\times 2, 1, 1, 1, 2)$. In DR it is

$$\mathcal{M}^{R_\xi,\chi\phi}_{Z,\mu\nu} = 8\frac{m^2_{Z_0}}{m^2_{H_0}}\lambda_0\mu^\varepsilon B_{\mu\nu}(p,m_{\chi_0},m_{H_0})\,. \tag{2.D.25}$$

Adding up all contributions we obtain

$$\begin{aligned}\mathcal{M}^{R_\xi}_{Z,\mu\nu} &= \frac{m^2_{Z_0}}{m^2_{H_0}}\lambda_0\mu^\varepsilon\Big\{-2g_{\mu\nu}A_0(m_{H_0}) - 8g_{\mu\nu}m^2_{Z_0}B_0(p,m_{Z_0},m_{H_0})\\ &+ 8(1-\xi)m^2_{Z_0}C^1_{\mu\nu}(m_{Z_0},m_{H_0},m_{\chi_0}) + 8B_{\mu\nu}(p,m_{\chi_0},m_{H_0})\Big\}.\end{aligned} \tag{2.D.26}$$

Next, we consider the one-loop contributions to the Higgs propagator. The first diagram here is

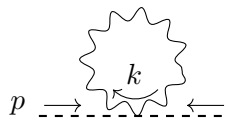

$$= i\mathcal{M}_H^{R_\xi,Z}$$

that is,

$$\begin{aligned}\mathcal{M}_H^{R_\xi,Z} &= 2d\frac{m_{Z_0}^2}{m_{H_0}^2}\lambda_0\int\frac{d^4k}{(2\pi)^4}\frac{-i}{k^2-m_{Z_0}^2} \\ &+ \frac{2(1-\xi)m_{Z_0}^2}{m_{H_0}^2}\lambda_0 g_{\mu\nu}\int\frac{d^4k}{(2\pi)^4}\frac{ik^\mu k^\nu}{\left(k^2-m_{Z_0}^2\right)\left(k^2-\xi m_{Z_0}^2\right)}\end{aligned} \tag{2.D.27}$$

with $\mathcal{S}^1_{\mathcal{M}_H}=\frac{1}{2}$ from $(n_O,n_l,\ell_1,\ell_2,v_1)=(2,1,2,2,1)$. In DR it can be written as

$$\begin{aligned}\mathcal{M}_H^{R_\xi,Z} &= \mu^\varepsilon\left\{2d\frac{m_{Z_0}^2}{m_{H_0}^2}\lambda_0 A_0(m_{Z_0})-2(1-\xi)\frac{m_{Z_0}^2}{m_{H_0}^2}\lambda_0 g_{\mu\nu}B^{\mu\nu}(0,m_{Z_0},\sqrt{\xi}m_{Z_0})\right\} \\ &= \frac{m_{Z_0}^2}{m_{H_0}^2}\lambda_0\mu^\varepsilon\left\{8A_0(m_{Z_0})-2(1-\xi)A_0(\sqrt{\xi}m_{Z_0})-2(1-\xi)m_{Z_0}^2B_0^1(m_{Z_0},\sqrt{\xi}m_{Z_0})\right\}\end{aligned} \tag{2.D.28}$$

and after reductions finally as

$$\mathcal{M}_H^{R_\xi,Z} = \frac{m_{Z_0}^2}{m_{H_0}^2}\lambda_0\mu^\varepsilon\left\{6A_0(m_{Z_0})+2\xi A_0(m_{\chi_0})\right\}. \tag{2.D.29}$$

The next contribution comes from the diagram

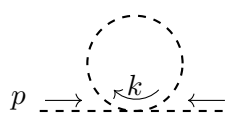

$$= i\mathcal{M}_H^{R_\xi,\phi}$$

with explicit form

$$\mathcal{M}_H^{R_\xi,\phi} = 3\lambda_0\int\frac{d^4k}{(2\pi)^4}\frac{-i}{k^2-m_{H_0}^2} \tag{2.D.30}$$

with $(n_O,n_l,\ell_1,v_1)=(4\times 3,1,4,1)$ and $\mathcal{S}^2_{\mathcal{M}_H}=\frac{1}{2}$. This is just

$$\mathcal{M}_H^{R_\xi,\phi}=3\lambda_0\mu^\varepsilon A_0(m_{H_0}) \tag{2.D.31}$$

in DR.

Next comes the Goldstone loop

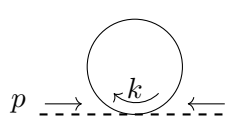

$$= i\mathcal{M}_H^{R_\xi,\chi}$$

that is equal to

$$\mathcal{M}_H^{R_\xi,\chi} = -2\frac{\lambda_0}{m_{H_0}^2}\int\frac{d^4k}{(2\pi)^4}\frac{-ik^2}{k^2-m_{\chi_0}^2} \tag{2.D.32}$$

with $(n_O, n_l, \ell_1, \ell_2, v_1) = (2, 1, 2, 2, 1)$ and $\mathcal{S}^3_{\mathcal{M}_H} = \frac{1}{2}$. This is

$$\mathcal{M}_H^{R_\xi,\chi} = -\frac{2\lambda_0}{m_{H_0}^2}\mu^\varepsilon m_{\chi_0}^2 A_0(m_{\chi_0})\,. \tag{2.D.33}$$

A few vacum polarization diagrams are in order. The first is

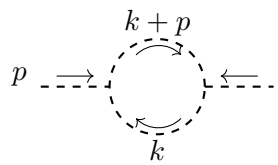

$$= i\mathcal{M}_H^{R_\xi,\phi\phi}$$

and it is equal to

$$\mathcal{M}_H^{R_\xi,\phi\phi} = 9\lambda_0 m_{H_0}^2\int\frac{d^4k}{(2\pi)^4}\frac{-i}{\left(k^2-m_{H_0}^2\right)\left((k+p)^2-m_{H_0}^2\right)} \tag{2.D.34}$$

and finally in DR to

$$\mathcal{M}_H^{R_\xi,\phi\phi} = 9\lambda_0 m_{H_0}^2\mu^\varepsilon B_0(p, m_{H_0}, m_{H_0})\,, \tag{2.D.35}$$

where $(n_O, n_l, \ell_1, \ell_2, v_1) = (3\times 3\times 2, 2, 3, 3, 2)$ and $\mathcal{S}^4_{\mathcal{M}_H} = \frac{1}{2}$.

The Goldstone loop contribution

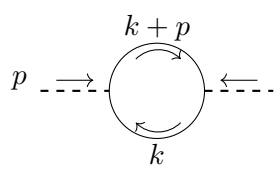

$$= i\mathcal{M}_H^{R_\xi,\chi\chi}$$

is equal to

$$\mathcal{M}_H^{R_\xi,\chi\chi} = -8\mathcal{S}^5_{\mathcal{M}_H}\frac{\lambda_0}{m_{H_0}^2}\int\frac{d^4k}{(2\pi)^4}\frac{i(k^4+2k^2k\cdot p+(p\cdot k)^2)}{\left(k^2-m_{\chi_0}^2\right)\left((k+p)^2-m_{\chi_0}^2\right)} \tag{2.D.36}$$

with symmetry factor $\mathcal{S}^5_{\mathcal{M}_H} = \frac{1}{2}$ from $(n_O, n_l, \ell_1, \ell_2, v_1) = (2\times 1, 2, 2, 2, 2)$. In DR it becomes

$$\mathcal{M}_H^{R_\xi,\chi\chi} = 4\frac{\lambda_0}{m_{H_0}^2}\mu^\varepsilon\left\{m_{\chi_0}^2 A_0(m_{\chi_0}) + (m_{\chi_0}^2-p^2)g_{\mu\nu}B^{\mu\nu}(p, m_{\chi_0}, m_{\chi_0}) + p_\mu p_\nu B^{\mu\nu}(p, m_{\chi_0}, m_{\chi_0})\right\}. \tag{2.D.37}$$

Slightly more complicated is the gauge boson loop

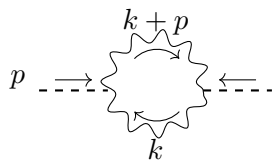

$$= i\mathcal{M}_H^{R_\xi,ZZ}$$

evaluating to

$$\mathcal{M}_H^{R_\xi,ZZ} = 4g^{\mu\nu}g^{\alpha\beta}\frac{m_{Z_0}^4}{m_{H_0}^2}\lambda_0\int\frac{d^4k}{(2\pi)^4}\frac{-i\left(-g_{\mu\alpha}+\frac{(1-\xi)k_\mu k_\alpha}{k^2-\xi m_{Z_0}^2}\right)}{\left(k^2-m_{Z_0}^2\right)}\frac{\left(-g_{\nu\beta}+\frac{(1-\xi)(k+p)_\nu(k+p)_\beta}{(k+p)^2-\xi m_{Z_0}^2}\right)}{\left((k+p)^2-m_{Z_0}^2\right)} \tag{2.D.38}$$

with $(n_O, n_l, \ell_1, \ell_2, v_1) = (2\times 1, 2, 2, 2, 2)$ and $\mathcal{S}^6_{\mathcal{M}_H} = \frac{1}{2}$. The numerator of this diagram can be expanded as

$$\begin{aligned} N &= g^{\mu\nu}g^{\alpha\beta}\left(-g_{\mu\alpha}+\frac{(1-\xi)k_\mu k_\alpha}{k^2-\xi m_{Z_0}^2}\right)\left(-g_{\nu\beta}+\frac{(1-\xi)\,(k+p)_\nu(k+p)_\beta}{(k+p)^2-\xi m_{Z_0}^2}\right) \\ &= d-(1-\xi)\left(\frac{k^2}{k^2-\xi m_{Z_0}^2}+\frac{k^2+2k\cdot p+p^2}{(k+p)^2-\xi m_{Z_0}^2}\right) \\ &+ (1-\xi)^2\left(\frac{k^4+2k^2k\cdot p+(k\cdot p)^2}{(k^2-\xi m_{Z_0}^2)((k+p)^2-\xi m_{Z_0}^2)}\right) \end{aligned} \tag{2.D.39}$$

and then it is a standard step to express it in terms of PV integrals as

$$\begin{aligned} \mathcal{M}_H^{R_\xi,ZZ} &= 4\frac{m_{Z_0}^4}{m_{H_0}^2}\lambda_0\mu^\varepsilon\Big\{dB_0(p,m_{Z_0},m_{Z_0})-(1-\xi)\Big\{g_{\mu\nu}C^{1\mu\nu}(p,m_{Z_0},m_{Z_0},m_{\chi_0}) \\ &+ g_{\mu\nu}C^{\mu\nu}(p,p,m_{Z_0},m_{Z_0},m_{\chi_0})\Big\} \\ &+ (1-\xi)^2\Big\{g_{\mu\nu}C^{1\mu\nu}(p,m_{Z_0},m_{Z_0},m_{\chi_0}) \\ &+ (m_{Z_0}^2-p^2)g_{\mu\nu}D^{\mu\nu}(p,m_{Z_0},m_{Z_0},m_{\chi_0},m_{\chi_0})+p_\mu p_\nu D^{\mu\nu}(p,m_{Z_0},m_{Z_0},m_{\chi_0},m_{\chi_0})\,,\Big\}\Big\} \end{aligned} \tag{2.D.40}$$

where the $a = 1, 2, 3$ superscripts on the C_0-integrals correspond to the different combinations of the denominators according to Eq. (2.B.12) of Appendix 2.B. The $D^{\mu\nu}$ integrals are defined in Eq. (2.B.39).

Finally, the last contribution to the one-loop correction of the Higgs mass comes from the sunset

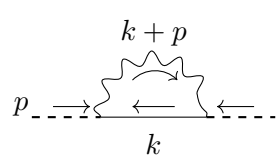

$$= i\mathcal{M}_H^{R_\xi,\chi Z}$$

with explicit form

$$\begin{aligned}
\mathcal{M}_H^{R_\xi,\chi Z} &= -8\lambda_0 \frac{m_{Z_0}^2}{m_{H_0}^2} \int \frac{d^4k}{(2\pi)^4} \frac{ik^\mu k^\nu}{k^2 - m_{\chi_0}^2} \frac{\left(-g_{\mu\nu} + \frac{(1-\xi)(k+p)_\mu (k+p)_\nu}{(k+p)^2 - \xi m_{Z_0}^2}\right)}{\left((k+p)^2 - m_{Z_0}^2\right)} \\
&= -8\lambda_0 \frac{m_{Z_0}^2}{m_{H_0}^2} g_{\mu\nu} B^{\mu\nu}(p, m_{\chi_0}, m_{Z_0}) \\
&+ 8(1-\xi)\lambda_0 \frac{m_{Z_0}^2}{m_{H_0}^2} \int \frac{d^4k}{(2\pi)^4} \frac{-i\left(k^4 + 2k^2 k\cdot p + (k\cdot p)^2\right)}{\left(k^2 - m_{\chi_0}^2\right)\left((k+p)^2 - m_{Z_0}^2\right)\left((k+p)^2 - m_{\chi_0}^2\right)}
\end{aligned} \tag{2.D.41}$$

where $(n_O, n_l, \ell_1, \ell_2, v_1) = (2\times 1, 1, 1, 1, 2)$ and $\mathcal{S}^7_{\mathcal{M}_H} = 1$. Standard steps allow us to write this as

$$\begin{aligned}
\mathcal{M}_H^{R_\xi,\chi Z} &= 8\lambda_0 \frac{m_{Z_0}^2}{m_{H_0}^2} \mu^\varepsilon \Big\{ -g_{\mu\nu} B^{\mu\nu}(p, m_{\chi_0}, m_{Z_0}) \\
&+ (1-\xi)\Big\{ g_{\mu\nu} B^{\mu\nu}(p, m_{\chi_0}, m_{\chi_0}) + (m_{Z_0}^2 - p^2) g_{\mu\nu} C^{1\mu\nu}(p, m_{Z_0}, m_{\chi_0}, m_{Z_0}) \\
&+ p_\mu p_\nu C^{1\mu\nu}(p, m_{\chi_0}, m_{Z_0}, m_{\chi_0}) \Big\} \Big\},
\end{aligned} \tag{2.D.42}$$

where $C^1_{\mu\nu}$ is defined in Eq. (2.B.34) in Appendix 2.B.

2.D.2 Unitary gauge diagrams

Similarly with the previous subsection, we consider first the Higgs tadpoles starting from

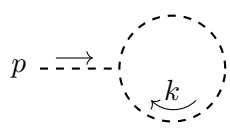

$$= i\mathcal{T}_H^{U,\phi}$$

$$\mathcal{T}_H^{U,\phi} = -6\frac{1}{2}\sqrt{\frac{\lambda_0}{2}} m_{H_0} \int \frac{d^4k}{(2\pi)^4} \frac{i}{\left(k^2 - m_{H_0}^2\right)} \tag{2.D.43}$$

and in DR is

$$\mathcal{T}_H^{U,\phi} = 3\frac{\sqrt{\frac{\lambda_0}{2}} m_{H_0} \mu^\varepsilon}{(4\pi)^{d/2}} \int \frac{d^dk}{i\pi^{d/2}} \frac{1}{\left(k^2 - m_{H_0}^2\right)}$$

or simply

$$\mathcal{T}_H^{U,\phi} = 3\sqrt{\frac{\lambda_0}{2}} m_{H_0} \mu^\varepsilon A_0(m_{H_0}). \tag{2.D.44}$$

Next is the gauge tadpole is

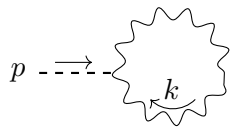

$$= i\mathcal{T}_H^{U,Z}$$

$$\mathcal{T}_H^{U,Z} = d\frac{\sqrt{2\lambda_0}m_{Z_0}^2}{m_{H_0}}\int\frac{d^4k}{(2\pi)^4}\frac{-i}{k^2-m_{Z_0}^2} + \frac{\sqrt{2\lambda_0}}{m_{H_0}}\int\frac{d^4k}{(2\pi)^4}\frac{ik^2}{k^2-m_{Z_0}^2} \tag{2.D.45}$$

where we have expanded the numerator, used that $g_{\mu\nu}g^{\mu\nu} = d$ and that under the integral $k^\mu k^\nu = \frac{g_{\mu\nu}}{d}k^2$. In DR

$$\mathcal{T}_H^{U,Z} = \mu^\varepsilon\left(d\frac{\sqrt{2\lambda_0}m_{Z_0}^2}{m_{H_0}}A_0(m_{Z_0}) - \frac{\sqrt{2\lambda_0}}{m_{H_0}}U_{\mathcal{T}}(m_{Z_0})\right). \tag{2.D.46}$$

Using Eq.(2.C.2) to calculate $U_{\mathcal{T}}(m_{Z_0})$, this becomes

$$\mathcal{T}_H^{U} = \mu^\varepsilon\left(3\sqrt{\frac{\lambda_0}{2}}m_{H_0}A_0(m_{H_0}) + 3\frac{\sqrt{2\lambda_0}m_{Z_0}^2}{m_{H_0}}A_0(m_{Z_0})\right). \tag{2.D.47}$$

Next, we present the explicit calculation of the one-loop Z boson mass corrections starting from,

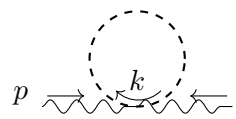

$$= i\mathcal{M}_{Z,\mu\nu}^{U,\phi}$$

$$\mathcal{M}_{Z,\mu\nu}^{U,\phi} = -2g_{\mu\nu}\frac{m_{Z_0}^2}{m_{H_0}^2}\lambda_0\int\frac{d^4k}{(2\pi)^4}\frac{-i}{k^2-m_{H_0}^2} \tag{2.D.48}$$

which is equal to

$$\mathcal{M}_{Z,\mu\nu}^{U,\phi} = -2g_{\mu\nu}\frac{m_{Z_0}^2}{m_{H_0}^2}\lambda_0\mu^\varepsilon A_0(m_{H_0}). \tag{2.D.49}$$

Next is the Higgs sunset

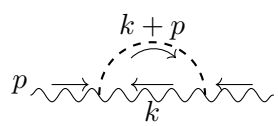

$$= i\mathcal{M}_{Z,\mu\nu}^{U,\phi Z}$$

$$\mathcal{M}_{Z,\mu\nu}^{U,\phi Z} = -8g_{\mu\alpha}g_{\nu\beta}\frac{m_{Z_0}^4}{m_{H_0}^2}\lambda_0\int\frac{d^4k}{(2\pi)^4}\frac{i}{(k+p)^2-m_{H_0}^2}\frac{-g^{\alpha\beta}+\frac{k^\alpha k^\beta}{m_{Z_0}^2}}{\left(k^2-m_{Z_0}^2\right)} \tag{2.D.50}$$

translating in DR to

$$\mathcal{M}_{Z,\mu\nu}^{U,\phi Z} = -8g_{\mu\nu}\frac{m_{Z_0}^4}{m_{H_0}^2}\lambda_0\mu^\varepsilon B_0(p,m_{Z_0},m_{H_0}) + 8\frac{m_{Z_0}^2}{m_{H_0}^2}\lambda_0\mu^\varepsilon B_{\mu\nu}(p,m_{Z_0},m_{H_0}). \tag{2.D.51}$$

The sum of these two corrections is

$$\begin{aligned}\mathcal{M}^{U}_{Z,\mu\nu} &= \frac{m^2_{Z_0}}{m^2_{H_0}}\lambda_0\mu^{\varepsilon}\Big\{-8g_{\mu\nu}m^2_{Z_0}B_0(p,m_{Z_0},m_{H_0})-2g_{\mu\nu}A_0(m_{H_0})\\ &+ 8B_{\mu\nu}(p,m_{Z_0},m_{H_0})\Big\}. \end{aligned} \tag{2.D.52}$$

Now, we deal with the one-loop corrections of the Higgs mass in Unitary gauge. The first comes from

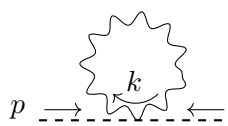

$$= i\mathcal{M}^{U,Z}_{H}$$

$$\mathcal{M}^{U,Z}_{H} = \frac{1}{2}4d\frac{\lambda_0 m^2_{Z_0}}{m^2_{H_0}}\int\frac{d^4k}{(2\pi)^4}\frac{-i}{k^2-m^2_{Z_0}}+\frac{1}{2}4\frac{\frac{\lambda_0 m^2_{Z_0}}{m^2_{H_0}}}{m^2_{Z_0}}\int\frac{d^4k}{(2\pi)^4}\frac{ik^2}{k^2-m^2_{Z_0}}. \tag{2.D.53}$$

In DR it becomes

$$\begin{aligned}\mathcal{M}^{U,Z}_{H} &= \mu^{\varepsilon}\Big\{2d\frac{\lambda_0 m^2_{Z_0}}{m^2_{H_0}}A_0(m_{Z_0})-2\frac{\lambda_0}{m^2_{H_0}}U_{\mathcal{T}}(1,m_{Z_0})\Big\}\\ &= \mu^{\varepsilon}6\frac{\lambda_0 m^2_{Z_0}}{m^2_{H_0}}A_0(m_{Z_0})\,. \end{aligned} \tag{2.D.54}$$

Next is

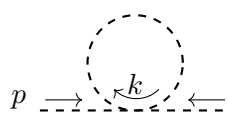

$$= i\mathcal{M}^{U,\phi}_{H}$$

$$\mathcal{M}^{U,\phi}_{H} = \frac{1}{2}6\lambda_0\int\frac{d^4k}{(2\pi)^4}\frac{-i}{k^2-m^2_{H_0}}. \tag{2.D.55}$$

In DR,

$$\mathcal{M}^{U,\phi}_{H} = 3\lambda_0\mu^{\varepsilon}A_0(m_{H_0}). \tag{2.D.56}$$

The Higgs vacuum polarization diagram

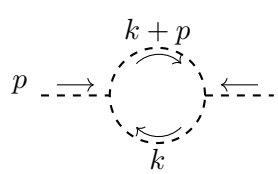

$$= i\mathcal{M}^{U,\phi\phi}_{H}$$

$$\mathcal{M}_H^{U,\phi\phi} = \frac{1}{2}18\lambda m_{H_0}^2 \int \frac{d^4k}{(2\pi)^4} \frac{-i}{\left(k^2 - m_{H_0}^2\right)\left((k+p)^2 - m_{H_0}^2\right)} \tag{2.D.57}$$

in DR is equal to

$$\mathcal{M}_H^{U,\phi\phi} = 9\lambda_0 m_{H_0}^2 \mu^\varepsilon B_0(p, m_{H_0}, m_{H_0})\,. \tag{2.D.58}$$

The corresponding gauge loop is

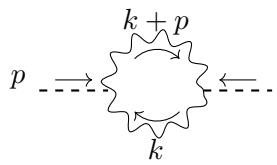

$$= i\mathcal{M}_H^{U,ZZ}$$

$$\mathcal{M}_H^{U,ZZ} = \frac{1}{2}8g^{\mu\nu}g^{\alpha\beta}\frac{\lambda_0 m_{Z_0}^4}{m_{H_0}^2}\int \frac{d^4k}{(2\pi)^4}\frac{-i\left(-g_{\mu\alpha} + \frac{k_\mu k_\alpha}{m_{Z_0}^2}\right)}{\left(k^2 - m_{Z_0}^2\right)}\frac{\left(-g_{\nu\beta} + \frac{(k+p)_\nu (k+p)_\beta}{m_{Z_0}^2}\right)}{\left((k+p)^2 - m_{Z_0}^2\right)} \tag{2.D.59}$$

Expanding the numerator it becomes

$$\begin{aligned}
\mathcal{M}_H^{U,ZZ} &= d\frac{\lambda_0 m_{Z_0}^4}{m_{H_0}^2}\int \frac{d^4k}{(2\pi)^4}\frac{-4i}{\left(k^2 - m_{Z_0}^2\right)\left((k+p)^2 - m_{Z_0}^2\right)} \\
&+ 4\frac{\lambda_0 m_{Z_0}^2}{m_{H_0}^2}\int \frac{d^4k}{(2\pi)^4}\frac{ik^2}{\left(k^2 - m_{Z_0}^2\right)\left((k+p)^2 - m_{Z_0}^2\right)} \\
&+ 4\frac{\lambda_0 m_{Z_0}^2}{m_{H_0}^2}\int \frac{d^4k}{(2\pi)^4}\frac{i(k+p)^2}{\left(k^2 - m_{Z_0}^2\right)\left((k+p)^2 - m_{Z_0}^2\right)} \\
&- 4\frac{\lambda_0}{m_{H_0}^2}\int \frac{d^4k}{(2\pi)^4}\frac{ik^2(k+p)^2}{\left(k^2 - m_{Z_0}^2\right)\left((k+p)^2 - m_{Z_0}^2\right)} \\
&+ 4\frac{\lambda_0}{m_{H_0}^2}\int \frac{d^4k}{(2\pi)^4}\frac{ip^2k^2}{\left(k^2 - m_{Z_0}^2\right)\left((k+p)^2 - m_{Z_0}^2\right)} \\
&- 4\frac{\lambda_0}{m_{H_0}^2}\int \frac{d^4k}{(2\pi)^4}\frac{i(k\cdot p)^2}{\left(k^2 - m_{Z_0}^2\right)\left((k+p)^2 - m_{Z_0}^2\right)}
\end{aligned} \tag{2.D.60}$$

and in DR

$$\begin{aligned}
\mathcal{M}_H^{U,ZZ} &= \mu^\varepsilon\Bigg\{4d\frac{\lambda_0 m_{Z_0}^4}{m_{H_0}^2}B_0(p, m_{Z_0}, m_{Z_0}) \\
&- 4\frac{\lambda_0 m_{Z_0}^2}{m_{H_0}^2}g_{\mu\nu}B_{k+p}^{\mu\nu}(p, m_{Z_0}, m_{Z_0}) + 4\frac{\lambda_0}{m_{H_0}^2}m_{Z_0}^2 A_0(m_{Z_0}) + 4\frac{\lambda_0}{m_{H_0}^2}m_{Z_0}^4 \\
&- 4\frac{\lambda_0}{m_{H_0}^2}p^2 g_{\mu\nu}B^{\mu\nu}(p, m_{Z_0}, m_{Z_0}) + 4\frac{\lambda_0}{m_{H_0}^2}p_\mu p_\nu B^{\mu\nu}(p, m_{Z_0}, m_{Z_0})\Bigg\}\,,
\end{aligned} \tag{2.D.61}$$

where we have defined

$$g_{\mu\nu}B^{\mu\nu}_{k+p}(p,m_{Z_0},m_{Z_0}) = \int \frac{d^4k}{(2\pi)^4}\frac{-i(k+p)^2}{\left(k^2-m^2_{Z_0}\right)\left((k+p)^2-m^2_{Z_0}\right)}\,. \tag{2.D.62}$$

Adding up Eq. (2.D.54), Eq. (2.D.56), Eq. (2.D.58) and Eq. (2.D.61) we obtain

$$\begin{aligned}
\mathcal{M}^U_H(p) &= \mu^\varepsilon\Bigg\{6\frac{\lambda m^2_{Z_0}}{m^2_{H_0}}A_0(m_{Z_0}) + \frac{2\lambda m^4_{Z_0}}{m^2_{H_0}} + 3\lambda_0 A_0(m_{H_0}) \\
&+ 9\lambda_0 m^2_{H_0}B_0(p,m_{H_0},m_{H_0}) + \frac{\lambda_0 m^2_{Z_0}}{m^2_{H_0}}\Big\{4dm^2_{Z_0}B_0(p,m_{Z_0},m_{Z_0}) \\
&- 4g_{\mu\nu}B^{\mu\nu}_{k+p}(p,m_{Z_0},m_{Z_0}) + 4A_0(m_{Z_0}) - 4\frac{p^2}{m^2_{Z_0}}g_{\mu\nu}B^{\mu\nu}(p,m_{Z_0},m_{Z_0}) \\
&+ 4m^2_{Z_0} + 4\frac{p_\mu p_\nu}{m^2_{Z_0}}B^{\mu\nu}(p,m_{Z_0},m_{Z_0})\Big\}\Bigg\}.
\end{aligned} \tag{2.D.63}$$

2.E Finite parts

In this Appendix we present the explicit form of the finite diagrams along with the finite parts of the divergent ones, in both R_ξ and Unitary gauges. Since the corresponding expressions are quite long, we use for simplicity some shorthand notation. In particular, for the arguments of integrals, we define

$$D4 \equiv (D_1, D_2, D_3, D_4). \tag{2.E.1}$$

In addition, in agreement with our notation in Appendix 2.A, we define the following integrals

$$\begin{aligned}
E^{\mu,\mu\nu,\mu\nu\alpha,\mu\nu\alpha\beta} &= 4!\int_0^1 \mathcal{D}^5x\left\langle\frac{N^{(5)}_{E^{\mu,\mu\nu,\mu\nu\alpha,\mu\nu\alpha\beta}}(k-\sum_{i=1}^5 P_ix_{i+1})}{D_1D_2D_3D_4D_5}\right\rangle \\
F^{\mu,\mu\nu,\mu\nu\alpha,\mu\nu\alpha\beta,\mu\nu\alpha\beta\gamma\delta} &= 5!\int_0^1 \mathcal{D}^6x\left\langle\frac{N^{(6)}_{F^{\mu,\mu\nu,\mu\nu\alpha,\mu\nu\alpha\beta,\mu\nu\alpha\beta\gamma\delta}}(k-\sum_{i=1}^6 P_ix_{i+1})}{D_1D_2D_3D_4D_5D_6}\right\rangle \\
G^{\mu,\mu\nu,\mu\nu\alpha,\mu\nu\alpha\beta,\mu\nu\alpha\beta\gamma\delta,\mu\nu\alpha\beta\gamma\delta\epsilon} &= 6!\int_0^1 \mathcal{D}^7x\left\langle\frac{N^{(7)}_{G^{\mu,\mu\nu,\mu\nu\alpha,\mu\nu\alpha\beta,\mu\nu\alpha\beta\gamma\delta,\mu\nu\alpha\beta\gamma\delta\epsilon}}(k-\sum_{i=1}^7 P_ix_{i+1})}{D_1D_2D_3D_4D_5D_7}\right\rangle \\
H^{\mu,\mu\nu,\mu\nu\alpha,\mu\nu\alpha\beta,\mu\nu\alpha\beta\gamma\delta,\mu\nu\alpha\beta\gamma\delta\epsilon,\mu\nu\alpha\beta\gamma\delta\epsilon\theta} &= 7!\int_0^1 \mathcal{D}^8x\left\langle\frac{N^{(8)}_{H^{\mu,\mu\nu,\mu\nu\alpha,\mu\nu\alpha\beta,\mu\nu\alpha\beta\gamma\delta\epsilon\theta}}(k-\sum_{i=1}^8 P_ix_{i+1})}{D_1D_2D_3D_4D_5D_8}\right\rangle
\end{aligned} \tag{2.E.2}$$

2.E.1 R_ξ gauge

In the R_ξ gauge we have the following finite parts:

Finite parts of the Triangle diagrams

$$(K_H^{R_\xi,ZZZ})_f = 16\sqrt{2}\frac{m^6_{Z_0}\lambda_0^{3/2}}{m^3_{H_0}}\mu^\varepsilon\Bigg\{(4-\varepsilon)C_0(P_1,m_{Z_0},m_{Z_0},m_{Z_0})$$

$$
\begin{aligned}
&- \quad (1-\xi)\Big\{ g_{\mu\nu} D^{\mu\nu}(P_1, P_2, m_{Z_0}, m_{Z_0}, m_{Z_0}, m_{\chi_0}) \\
&+ \quad g_{\mu\nu} D^{\mu\nu}(P_1, P_2, m_{Z_0}, m_{Z_0}, m_{Z_0}, m_{\chi_0}) \\
&+ \quad g_{\mu\nu} D^{\mu\nu}(P_1, P_2, m_{Z_0}, m_{Z_0}, m_{Z_0}, m_{\chi_0}) + 2P_1^{\mu} D^{\mu}(P_1, P_2, m_{Z_0}, m_{Z_0}, m_{Z_0}, m_{\chi_0}) \\
&+ \quad 2P_2^{\mu} D^{\mu}(P_1, P_2, m_{Z_0}, m_{Z_0}, m_{Z_0}, m_{\chi_0}) + P_1^2 D_0(P_1, P_2, m_{Z_0}, m_{Z_0}, m_{Z_0}, m_{\chi_0}) \\
&+ \quad P_2^2 D_0(P_1, P_2, m_{Z_0}, m_{Z_0}, m_{Z_0}, m_{\chi_0}) \Big\} \\
&+ \quad (1-\xi)^2 \Big\{ E_4(D4, D_5(0, m_{\chi_0})) + E_4(D4, D_5(P_1, m_{\chi_0})) \\
&+ \quad E_4(D_1, D_2, D_3, D_4(0, m_{\chi_0}), D_5(P_1, m_{\chi_0})) \\
&+ \quad 2P_{1\mu} E_3^{\mu}(D4, D_5(0, m_{\chi_0})) + 2P_{1\mu} E_3^{\mu}(D_1, D_2, D_3, D_4(0, m_{\chi_0}), D_5(P_1, m_{\chi_0})) \\
&+ \quad 2P_{2\mu} E_3^{\mu}(D4, D_5(P_1, m_{\chi_0})) + 2P_{2\mu} E_3^{\mu}(D_1, D_2, D_3, D_4(0, m_{\chi_0}), D_5(P_1, m_{\chi_0})) \\
&+ \quad 2P_{1\mu} P_{2\nu} E_2^{\mu\nu}(D_1, D_2, D_3, D_4(0, m_{\chi_0}), D_5(P_1, m_{\chi_0})) \\
&+ \quad P_{2\mu} P_{2\nu} E_2^{\mu\nu}(D4, D_5(P_1, m_{\chi_0})) \\
&+ \quad P_{2\mu} P_{2\nu} E_2^{\mu\nu}(D_1, D_2, D_3, D_4(0, m_{\chi_0}), D_5(P_1, m_{\chi_0})) \\
&+ \quad 2P_1 \cdot P_2 E_2(D_1, D_2, D_3, D_4(0, m_{\chi_0}), D_5(P_1, m_{\chi_0})) \\
&+ \quad 2P_1 \cdot P_2 (P_1 + P_2)_{\mu} E_1^{\mu}(D_1, D_2, D_3, D_4(0, m_{\chi_0}), D_5(P_1, m_{\chi_0})) \\
&+ \quad (P_1 \cdot P_2)^2 E_0(D_1, D_2, D_3, D_4(0, m_{\chi_0}), D_5(P_1, m_{\chi_0})) \Big\} \\
&- \quad (1-\xi)^3 \Big\{ F_6(D4, D_5(0, m_{\chi_0}, D_6(P_1, m_{\chi_0})) \\
&+ \quad 2(P_1 + P_2)_{\mu} F_5^{\mu}(D4, D_5(0, m_{\chi_0}, D_6(P_1, m_{\chi_0})) \\
&+ \quad (P_{1\mu} P_{1\nu} + 3P_{1\mu} P_{2\nu} + P_{2\mu} P_{2\nu}) F_4^{\mu\nu}(D4, D_5(0, m_{\chi_0}, D_6(P_1, m_{\chi_0})) \\
&+ \quad (P_{1\mu} P_{1\nu} P_{2\alpha} + P_{2\mu} P_{2\nu} P_{1\alpha}) F_3^{\mu\nu\alpha}(D4, D_5(0, m_{\chi_0}, D_6(P_1, m_{\chi_0})) \\
&+ \quad P_1 \cdot P_2 (P_1 + P_2)_{\mu} F_3^{\mu}(D4, D_5(0, m_{\chi_0}, D_6(P_1, m_{\chi_0})) \\
&+ \quad P_1 \cdot P_2 P_{1\mu} P_{2\nu} F_2^{\mu\nu}(D4, D_5(0, m_{\chi_0}, D_6(P_1, m_{\chi_0})) \\
&+ \quad P_1 \cdot P_2 F_4(D4, D_5(0, m_{\chi_0}, D_6(P_1, m_{\chi_0})) \Big\} \Big\}
\end{aligned}
\tag{2.E.3}
$$

Finite parts of the Box diagrams

$$
\begin{aligned}
(B_H^{R_\xi, ZZZZ})_f \quad &= \quad 64 \frac{m_{Z_0}^8 \lambda_0^2}{m_{H_0}^4} \mu^{\varepsilon} \Big\{ dD_0(D_1, D_2, D_3, D_4) \\
&- \quad (1-\xi) \Big(E_2(D4, D_5(0, m_{\chi_0})) + E_2(D4, D_5(P_1, m_{\chi_0})) \\
&+ \quad E_2(D4, D_5(P_2, m_{\chi_0})) + E_2(D4, D_5(P_3, m_{\chi_0})) \\
&+ \quad 2P_{1,\mu} E_1^{\mu}(D4, D_5(P_1, m_{\chi_0})) + 2P_{2,\mu} E_1^{\mu}(D4, D_5(P_2, m_{\chi_0})) \\
&+ \quad 2P_{3,\mu} E_1^{\mu}(D4, D_5(P_1, m_{\chi_0})) + P_1^2 E_0(D4, D_5(P_1, m_{\chi_0})) \\
&+ \quad P_2^2 E_0(D4, D_5(P_2, m_{\chi_0})) + P_2^2 E_0(D4, D_5(P_3, m_{\chi_0})) \Big) \\
&+ \quad (1-\xi)^2 \Big(F_4(D4, D_5(0, m_{\chi_0}), D_6(P_1, m_{\chi_0})) + F_4(D4, D_5(0, m_{\chi_0}), D_6(P_2, m_{\chi_0}))
\end{aligned}
$$

$$
\begin{aligned}
&+ \quad F_4(D4, D_5(P_1, m_{\chi_0}), D_6(P_2, m_{\chi_0})) + F_4(D4, D_5(P_1, m_{\chi_0}), D_6(P_3, m_{\chi_0})) \\
&+ \quad F_4(D4, D_5(0, m_{\chi_0}), D_6(P_3, m_{\chi_0})) + 2P_{1,\mu}F_3^{\mu}(D4, D_5(0, m_{\chi_0}), D_6(P_3, m_{\chi_0})) \\
&+ \quad 2P_{1,\mu}F_3^{\mu}(D4, D_5(P_1, m_{\chi_0}), D_6(P_3, m_{\chi_0})) + 2P_{2,\mu}F_3^{\mu}(D4, D_5(0, m_{\chi_0}), D_6(P_2, m_{\chi_0})) \\
&+ \quad 2P_{2,\mu}F_3^{\mu}(D4, D_5(P_1, m_{\chi_0}), D_6(P_3, m_{\chi_0})) + 2P_{1,\mu}F_3^{\mu}(D4, D_5(P_1, m_{\chi_0}), D_6(P_2, m_{\chi_0})) \\
&+ \quad 2P_{2,\mu}F_3^{\mu}(D4, D_5(P_2, m_{\chi_0}), D_6(P_3, m_{\chi_0})) + 2P_{3,\mu}F_3^{\mu}(D4, D_5(0, m_{\chi_0}), D_6(P_3, m_{\chi_0})) \\
&+ \quad 2P_{3,\mu}F_3^{\mu}(D4, D_5(P_1, m_{\chi_0}), D_6(P_3, m_{\chi_0})) + 2P_{3,\mu}F_3^{\mu}(D4, D_5(P_2, m_{\chi_0}), D_6(P_3, m_{\chi_0})) \\
&+ \quad P_{1,\mu}P_{1,\nu}\Big\{F_2^{\mu\nu}(D4, D_5(0, m_{\chi_0}), D_6(P_1, m_{\chi_0})) + F_2^{\mu\nu}(D4, D_5(P_1, m_{\chi_0}), D_6(P_2, m_{\chi_0})) \\
&+ \quad F_2^{\mu\nu}(D4, D_5(P_1, m_{\chi_0}), D_6(P_3, m_{\chi_0}))\Big\} + 2P_{1,\mu}P_{2,\nu}F_2^{\mu\nu}(D4, D_5(0, m_{\chi_0}), D_6(P_1, m_{\chi_0})) \\
&+ \quad P_{2,\mu}P_{2,\nu}\Big\{F_2^{\mu\nu}(D4, D_5(0, m_{\chi_0}), D_6(P_1, m_{\chi_0})) + F_2^{\mu\nu}(D4, D_5(P_1, m_{\chi_0}), D_6(P_2, m_{\chi_0})) \\
&+ \quad F_2^{\mu\nu}(D4, D_5(P_1, m_{\chi_0}), D_6(P_3, m_{\chi_0}))\Big\} \\
&+ \quad P_{3,\mu}P_{3,\nu}\Big\{F_2^{\mu\nu}(D4, D_5(0, m_{\chi_0}), D_6(P_1, m_{\chi_0})) + F_2^{\mu\nu}(D4, D_5(P_1, m_{\chi_0}), D_6(P_2, m_{\chi_0})) \\
&+ \quad F_2^{\mu\nu}(D4, D_5(P_1, m_{\chi_0}), D_6(P_3, m_{\chi_0}))\Big\} + 2P_{1,\mu}P_{2,\nu}F_2^{\mu\nu}(D4, D_5(0, m_{\chi_0}), D_6(P_1, m_{\chi_0})) \\
&+ \quad 2P_{1,\mu}P_{3,\nu}F_2^{\mu\nu}(D4, D_5(P_1, m_{\chi_0}), D_6(P_3, m_{\chi_0})) \\
&+ \quad 2P_{2,\mu}P_{3,\nu}F_2^{\mu\nu}(D4, D_5(P_2, m_{\chi_0}), D_6(P_3, m_{\chi_0})) \\
&+ \quad 2\Big\{P_1 \cdot P_2 F_2(D4, D_5(P_1, m_{\chi_0}), D_6(P_2, m_{\chi_0})) \\
&+ \quad P_1 \cdot P_3 F_2(D4, D_5(P_1, m_{\chi_0}), D_6(P_3, m_{\chi_0})) \\
&+ \quad P_2 \cdot P_3 F_2(D4, D_5(P_2, m_{\chi_0}), D_6(P_3, m_{\chi_0}))\Big\} \\
&+ \quad 2P_1 \cdot P_2\Big\{P_{1,\mu} + P_{2,\mu}\Big\}F_1^{\mu}(D4, D_5(P_1, m_{\chi_0}), D_6(P_2, m_{\chi_0})) \\
&+ \quad 2P_1 \cdot P_3\Big\{P_{1,\mu} + P_{3,\mu}\Big\}F_1^{\mu}(D4, D_5(P_1, m_{\chi_0}), D_6(P_3, m_{\chi_0})) \\
&+ \quad 2P_2 \cdot P_3\Big\{P_{2,\mu} + P_{3,\mu}\Big\}F_1^{\mu}(D4, D_5(P_2, m_{\chi_0}), D_6(P_3, m_{\chi_0})) \\
&+ \quad (P_1 \cdot P_2)^2 F_0(D4, D_5(P_1, m_{\chi_0}), D_6(P_2, m_{\chi_0})) \\
&+ \quad (P_1 \cdot P_3)^2 F_0(D4, D_5(P_1, m_{\chi_0}), D_6(P_3, m_{\chi_0})) \\
&+ \quad (P_2 \cdot P_3)^2 F_0(D4, D_5(P_2, m_{\chi_0}), D_6(P_3, m_{\chi_0}))\Bigg) \\
&- \quad (1-\xi)^3\Bigg(G_6(D4, D_5(0, m_{\chi_0}), D_6(P_1, m_{\chi_0}), D_7(P_2, m_{\chi_0})) \\
&+ \quad G_6(D4, D_5(0, m_{\chi_0}), D_6(P_1, m_{\chi_0}), D_7(P_3, m_{\chi_0})) \\
&+ \quad G_6(D4, D_5(P_1, m_{\chi_0}), D_6(P_2, m_{\chi_0}), D_7(P_3, m_{\chi_0})) \\
&+ \quad \sum_{l=1}^{3} 2P_{l,\mu}G_5^{\mu}(D4, D_5(0, m_{\chi_0}), D_6(P_1, m_{\chi_0}), D_7(P_2, m_{\chi_0})) \\
&+ \quad \sum_{l=1}^{3} 2P_{l,\mu}G_5^{\mu}(D4, D_5(0, m_{\chi_0}), D_6(P_1, m_{\chi_0}), D_7(P_3, m_{\chi_0}))
\end{aligned}
$$

$$
\begin{aligned}
&+ \sum_{l=1}^{3} 2P_{l,\mu} G_5^{\mu}(D4, D_5(P_1, m_{\chi_0}), D_6(P_2, m_{\chi_0}), D_7(P_3, m_{\chi_0})) \\
&+ \sum_{l,m=1}^{3} 2P_{l,\mu} P_{m,\nu} G_4^{\mu\nu}(D4, D_5(0, m_{\chi_0}), D_6(P_1, m_{\chi_0}), D_7(P_2, m_{\chi_0})) \\
&+ \sum_{l,m=1}^{3} 2P_{l,\mu} P_{m,\nu} G_4^{\mu\nu}(D4, D_5(0, m_{\chi_0}), D_6(P_1, m_{\chi_0}), D_7(P_3, m_{\chi_0})) \\
&+ \sum_{l,m=1}^{3} 2P_{l,\mu} P_{m,\nu} G_4^{\mu\nu}(D4, D_5(P_1, m_{\chi_0}), D_6(P_2, m_{\chi_0}), D_7(P_3, m_{\chi_0})) \\
&+ \sum_{l,m,n=1}^{3} P_{l,\mu} P_{m,\nu} P_{n,\alpha} G_3^{\mu\nu\alpha}(D4, D_5(0, m_{\chi_0}), D_6(P_1, m_{\chi_0}), D_7(P_2, m_{\chi_0})) \\
&+ \sum_{l,m,n=1}^{3} P_{l,\mu} P_{m,\nu} P_{n,\alpha} G_3^{\mu\nu\alpha}(D4, D_5(0, m_{\chi_0}), D_6(P_1, m_{\chi_0}), D_7(P_3, m_{\chi_0})) \\
&+ \sum_{l,m,n=1}^{3} P_{l,\mu} P_{m,\nu} P_{n,\alpha} G_3^{\mu\nu\alpha}(D4, D_5(P_1, m_{\chi_0}), D_6(P_2, m_{\chi_0}), D_7(P_3, m_{\chi_0})) \\
&+ \sum_{l,m=1,m\neq l}^{3} P_l \cdot P_m G_4(D4, D_5(0, m_{\chi_0}), D_6(P_1, m_{\chi_0}), D_7(P_3, m_{\chi_0})) \\
&+ \sum_{l,m=1,m\neq l}^{3} P_l \cdot P_m G_4(D4, D_5(0, m_{\chi_0}), D_6(P_2, m_{\chi_0}), D_7(P_3, m_{\chi_0})) \\
&+ \sum_{l=1}^{3} P_{l,\mu} G_3^{\mu}(D4, D_5(0, m_{\chi_0}), D_6(P_1, m_{\chi_0}), D_7(P_2, m_{\chi_0})) \\
&+ \sum_{l=1}^{3} P_{l,\mu} G_3^{\mu}(D4, D_5(0, m_{\chi_0}), D_6(P_1, m_{\chi_0}), D_7(P_3, m_{\chi_0})) \\
&+ \sum_{l=1}^{3} P_{l,\mu} G_3^{\mu}(D4, D_5(0, m_{\chi_0}), D_6(P_2, m_{\chi_0}), D_7(P_3, m_{\chi_0})) \\
&+ \sum_{l,m=1}^{3} P_l \cdot P_m P_{m,\mu} G_3^{\mu}(D4, D_5(0, m_{\chi_0}), D_6(P_1, m_{\chi_0}), D_7(P_3, m_{\chi_0})) \\
&+ \sum_{l,m=1}^{3} P_l \cdot P_m P_{m,\mu} G_3^{\mu}(D4, D_5(0, m_{\chi_0}), D_6(P_2, m_{\chi_0}), D_7(P_3, m_{\chi_0})) \\
&+ \sum_{l,m=1,m\neq l}^{3} P_l \cdot P_m P_{l,\mu} P_{m,\nu} G_2^{\mu\nu}(D4, D_5(0, m_{\chi_0}), D_6(P_1, m_{\chi_0}), D_7(P_3, m_{\chi_0})) \\
&+ \sum_{l,m=1,m\neq l}^{3} P_l \cdot P_m P_{l,\mu} P_{m,\nu} G_2^{\mu\nu}(D4, D_5(P_1, m_{\chi_0}), D_6(P_2, m_{\chi_0}), D_7(P_3, m_{\chi_0})) \\
&+ \sum_{l,m=1,m\neq l}^{3} P_l \cdot P_m P_{l,\mu} P_{m,\nu} G_2^{\mu\nu}(D4, D_5(0, m_{\chi_0}), D_6(P_1, m_{\chi_0}), D_7(P_3, m_{\chi_0}))
\end{aligned}
$$

$$
\begin{aligned}
& \Big(P_1\cdot P_2 P_2\cdot P_3 + P_2\cdot P_3 P_1\cdot P_3\Big) G_2(D4, D_5(0,m_{\chi_0}), D_6(P_1,m_{\chi_0}), D_7(P_3,m_{\chi_0})) \\
+ & \sum_{l,m,n=1,n\neq m\neq l}^{3} P_l\cdot P_m P_m\cdot P_n (P_m+P_n)_\mu G_1^\mu(D4, D_5(P_1,m_{\chi_0}), D_6(P_2,m_{\chi_0}), D_7(P_3,m_{\chi_0})) \\
+ & \sum_{l,m,n=1,n\neq m\neq l}^{3} P_l\cdot P_m P_m\cdot P_n (P_m+P_n)_\mu G_1^\mu(D4, D_5(0,m_{\chi_0}), D_6(P_1,m_{\chi_0}), D_7(P_3,m_{\chi_0})) \\
+ & \sum_{l,m=1,m\neq l}^{3} P_l\cdot P_m P_{l,\mu} P_{m,\nu} G_2^{\mu\nu}(D4, D_5(P_1,m_{\chi_0}), D_6(P_2,m_{\chi_0}), D_7(P_3,m_{\chi_0})) \\
+ & P_1\cdot P_2 P_2\cdot P_3 P_1\cdot P_3 G_0(D4, D_5(P_1,m_{\chi_0}), D_6(P_2,m_{\chi_0}), D_7(P_3,m_{\chi_0}))\Bigg) \\
+ & (1-\xi)^4\Bigg(H_8(D4, D_5(0,m_{\chi_0}), D_6(P_1,m_{\chi_0}), D_7(P_2,m_{\chi_0}), D_8(P_3,m_{\chi_0})) \\
+ & 2(P_1+P_2+P_3)_\mu H_7^\mu(D4, D_5(0,m_{\chi_0}), D_6(P_1,m_{\chi_0}), D_7(P_2,m_{\chi_0}), D_8(P_3,m_{\chi_0})) \\
+ & \Big\{P_{1\mu}P_{1\nu} + 3P_{1\mu}P_{2\nu} + P_{2\mu}P_{2\nu} \\
+ & 4P_{1\mu}P_{3\nu} + 3P_{2\mu}P_{3\nu} + P_{3\mu}P_{3\nu}\Big\}\cdot \\
& H_6^{\mu\nu}(D4, D_5(0,m_{\chi_0}), D_6(P_1,m_{\chi_0}), D_7(P_2,m_{\chi_0}), D_8(P_3,m_{\chi_0})) \\
+ & (P_1\cdot P_2 + P_2\cdot P_3) H_6(D4, D_5(0,m_{\chi_0}), D_6(P_1,m_{\chi_0}), D_7(P_2,m_{\chi_0}), D_8(P_3,m_{\chi_0})) \\
+ & \Big\{P_{1\mu}P_{1\nu}P_{2\alpha} + P_{1\mu}P_{2\nu}P_{2\alpha} + 2P_{1\mu}P_{1\nu}P_{3\alpha} + 4P_{1\mu}P_{2\nu}P_{3\alpha} \\
+ & P_{2\mu}P_{2\nu}P_{3\alpha} + 2P_{1\mu}P_{3\nu}P_{3\alpha} + P_{2\mu}P_{3\nu}P_{3\alpha}\Big\}\cdot \\
& H_5^{\mu\nu\alpha}(D4, D_5(0,m_{\chi_0}), D_6(P_1,m_{\chi_0}), D_7(P_2,m_{\chi_0}), D_8(P_3,m_{\chi_0})) \\
+ & \Big\{P_1\cdot P_2(P_1+P_2+2P_3)_\mu + P_2\cdot P_3(2P_1+P_2+P_3)_\mu\Big\}\cdot \\
& H_5^{\mu}(D4, D_5(0,m_{\chi_0}), D_6(P_1,m_{\chi_0}), D_7(P_2,m_{\chi_0}), D_8(P_3,m_{\chi_0})) \\
+ & \Big\{P_{1\mu}P_{1\nu}P_{2\alpha}P_{3\beta} + P_{1\mu}P_{2\nu}P_{2\alpha}P_{3\beta} + P_{1\mu}P_{1\nu}P_{3\alpha}P_{3\beta} + P_{1\mu}P_{2\nu}P_{3\alpha}P_{3\beta}\Big\}\cdot \\
& H_4^{\mu\nu\alpha\beta}(D4, D_5(0,m_{\chi_0}), D_6(P_1,m_{\chi_0}), D_7(P_2,m_{\chi_0}), D_8(P_3,m_{\chi_0})) \\
+ & \Big\{P_1\cdot P_2[P_{1\mu}P_{1\nu} + 2P_{1\mu}P_{3\nu} + P_{2\mu}P_{3\nu} + P_{3\mu}P_{3\nu}] \\
+ & P_2\cdot P_3[P_{1\mu}P_{1\nu} + P_{1\mu}P_{2\nu} + 2P_{1\mu}P_{3\nu} + P_{2\mu}P_{3\nu}]\Big\}\cdot \\
& H_4^{\mu\nu}(D4, D_5(0,m_{\chi_0}), D_6(P_1,m_{\chi_0}), D_7(P_2,m_{\chi_0}), D_8(P_3,m_{\chi_0})) \\
+ & (P_1\cdot P_2\times P_2\cdot P_3) H_4(D4, D_5(0,m_{\chi_0}), D_6(P_1,m_{\chi_0}), D_7(P_2,m_{\chi_0}), D_8(P_3,m_{\chi_0}))\Bigg)\Bigg\}
\end{aligned}
\tag{2.E.4}
$$

$$
\begin{aligned}
(B_H^{R_\xi,\chi ZZZ})_f &= 64\frac{m_{Z_0}^6\lambda_0^2}{m_{H_0}^4}\mu^\varepsilon\Bigg\{-C_0(D_1,D_2,D_3) - m_{Z_0}^2 D_0(D_1,D_2,D_3,D_4) \\
&+ (1-\xi)\Bigg(E_4(D4, D_5(0,m_{\chi_0})) + E_4(D4, D_5(0,m_{\chi_0})) \\
&+ E_4(D4, D_5(P_1,m_{\chi_0})) + E_4(D4, D_5(P_1,m_{\chi_0}))
\end{aligned}
$$

$$
\begin{aligned}
&+ \quad E_4(D4, D_5(0, m_{\chi_0})) + 2P_{1,\mu}E_3^{\mu}(D4, D_5(0, m_{\chi_0})) \\
&+ \quad 2P_{2,\mu}E_3^{\mu}(D4, D_5(0, m_{\chi_0})) + 2P_{3,\mu}E_3^{\mu}(D4, D_5(P_1, m_{\chi_0})) \\
&+ \quad 2P_{2,\mu}E_3^{\mu}(D4, D_5(P_2, m_{\chi_0})) + 2P_{3,\mu}E_3^{\mu}(D4, D_5(P_1, m_{\chi_0})) \\
&+ \quad P_{1,\mu}P_{1,\nu}\Big\{E_2^{\mu\nu}(D4, D_5(0, m_{\chi_0})) + 2P_{1,\mu}P_{2,\nu}E_2^{\mu\nu}(D4, D_5(0, m_{\chi_0})) \\
&+ \quad P_{2,\mu}P_{2,\nu}E_2^{\mu\nu}(D4, D_5(0, m_{\chi_0})) + E_2^{\mu\nu}(D4, D_5(P_1, m_{\chi_0})) \\
&+ \quad P_{3,\mu}P_{3,\nu}E_2^{\mu\nu}(D4, D_5(0, m_{\chi_0})) + 2P_{1,\mu}P_{2,\nu}E_2^{\mu\nu}(D4, D_5(0, m_{\chi_0}), D_6(P_1, m_{\chi_0})) \\
&+ \quad 2P_{1,\mu}P_{3,\nu}E_2^{\mu\nu}(D4, D_5(P_1, m_{\chi_0})) \\
&+ \quad 2P_1 \cdot P_2 E_2(D4, D_5(P_1, m_{\chi_0})) \\
&+ \quad 2P_1 \cdot P_2\Big\{P_{1,\mu} + P_{2,\mu}\Big\}E_1^{\mu}(D4, D_5(P_1, m_{\chi_0})) \\
&+ \quad (P_1 \cdot P_2)^2 E_0(D4, D_5(P_1, m_{\chi_0}))\Bigg) \\
&- \quad (1-\xi)^2\Bigg(F_4(D4, D_5(0, m_{\chi_0}), D_6(P_3, m_{\chi_0})) + F_4(D4, D_5(0, m_{\chi_0}), D_6(P_3, m_{\chi_0})) \\
&+ \quad F_4(D4, D_5(P_1, m_{\chi_0}), D_6(P_3, m_{\chi_0})) + F_4(D4, D_5(P_1, m_{\chi_0}), D_6(P_3, m_{\chi_0})) \\
&+ \quad F_4(D4, D_5(0, m_{\chi_0}), D_6(P_3, m_{\chi_0})) + 2P_{1,\mu}F_3^{\mu}(D4, D_5(0, m_{\chi_0}), D_6(P_3, m_{\chi_0})) \\
&+ \quad 2P_{2,\mu}F_3^{\mu}(D4, D_5(0, m_{\chi_0}), D_6(P_3, m_{\chi_0})) + 2P_{3,\mu}F_3^{\mu}(D4, D_5(P_1, m_{\chi_0})) \\
&+ \quad 2P_{2,\mu}F_3^{\mu}(D4, D_5(P_2, m_{\chi_0}), D_6(P_3, m_{\chi_0})) + 2P_{3,\mu}F_3^{\mu}(D4, D_5(P_1, m_{\chi_0}), D_6(P_3, m_{\chi_0})) \\
&+ \quad P_{1,\mu}P_{1,\nu}\Big\{F_2^{\mu\nu}(D4, D_5(0, m_{\chi_0}), D_6(P_3, m_{\chi_0})) + 2P_{1,\mu}P_{2,\nu}F_2^{\mu\nu}(D4, D_5(0, m_{\chi_0}), D_6(P_3, m_{\chi_0})) \\
&+ \quad P_{2,\mu}P_{2,\nu}F_2^{\mu\nu}(D4, D_5(0, m_{\chi_0}), D_6(P_3, m_{\chi_0})) + F_2^{\mu\nu}(D4, D_5(P_1, m_{\chi_0}), D_6(P_3, m_{\chi_0})) \\
&+ \quad P_{3,\mu}P_{3,\nu}F_2^{\mu\nu}(D4, D_5(0, m_{\chi_0}), D_6(P_3, m_{\chi_0})) + 2P_{1,\mu}P_{2,\nu}F_2^{\mu\nu}(D4, D_5(0, m_{\chi_0}), D_6(P_1, m_{\chi_0})) \\
&+ \quad 2P_{1,\mu}P_{3,\nu}F_2^{\mu\nu}(D4, D_5(P_1, m_{\chi_0}), D_6(P_3, m_{\chi_0})) \\
&+ \quad 2P_1 \cdot P_2 F_2(D4, D_5(P_1, m_{\chi_0}), D_6(P_3, m_{\chi_0})) \\
&+ \quad 2P_1 \cdot P_2\Big\{P_{1,\mu} + P_{2,\mu}\Big\}F_1^{\mu}(D4, D_5(P_1, m_{\chi_0}), D_6(P_3, m_{\chi_0})) \\
&+ \quad (P_1 \cdot P_2)^2 F_0(D4, D_5(P_1, m_{\chi_0}), D_6(P_3, m_{\chi_0}))\Bigg) \\
&+ \quad (1-\xi)^3\Bigg(G_6(D4, D_5(0, m_{\chi_0}), D_6(P_1, m_{\chi_0}), D_7(P_2, m_{\chi_0})) \\
&+ \quad G_6(D4, D_5(0, m_{\chi_0}), D_6(P_1, m_{\chi_0}), D_7(P_3, m_{\chi_0})) \\
&+ \quad G_6(D4, D_5(P_1, m_{\chi_0}), D_6(P_2, m_{\chi_0}), D_7(P_3, m_{\chi_0})) \\
&+ \quad \sum_{l=1}^{3} 2P_{l,\mu}G_5^{\mu}(D4, D_5(0, m_{\chi_0}), D_6(P_1, m_{\chi_0}), D_7(P_2, m_{\chi_0})) \\
&+ \quad \sum_{l=1}^{3} 2P_{l,\mu}G_5^{\mu}(D4, D_5(0, m_{\chi_0}), D_6(P_1, m_{\chi_0}), D_7(P_3, m_{\chi_0})) \\
&+ \quad \sum_{l=1}^{3} 2P_{l,\mu}G_5^{\mu}(D4, D_5(P_1, m_{\chi_0}), D_6(P_2, m_{\chi_0}), D_7(P_3, m_{\chi_0}))
\end{aligned}
$$

$$
\begin{aligned}
&+ \sum_{l,m=1}^{3} 2P_{l,\mu}P_{m,\nu}G_4^{\mu\nu}(D4, D_5(0, m_{\chi_0}), D_6(P_1, m_{\chi_0}), D_7(P_2, m_{\chi_0}))\\
&+ \sum_{l,m=1}^{3} 2P_{l,\mu}P_{m,\nu}G_4^{\mu\nu}(D4, D_5(0, m_{\chi_0}), D_6(P_1, m_{\chi_0}), D_7(P_3, m_{\chi_0}))\\
&+ \sum_{l,m=1}^{3} 2P_{l,\mu}P_{m,\nu}G_4^{\mu\nu}(D4, D_5(P_1, m_{\chi_0}), D_6(P_2, m_{\chi_0}), D_7(P_3, m_{\chi_0}))\\
&+ \sum_{l,m,n=1}^{3} P_{l,\mu}P_{m,\nu}P_{n,\alpha}G_3^{\mu\nu\alpha}(D4, D_5(0, m_{\chi_0}), D_6(P_1, m_{\chi_0}), D_7(P_2, m_{\chi_0}))\\
&+ \sum_{l,m,n=1}^{3} P_{l,\mu}P_{m,\nu}P_{n,\alpha}G_3^{\mu\nu\alpha}(D4, D_5(0, m_{\chi_0}), D_6(P_1, m_{\chi_0}), D_7(P_3, m_{\chi_0}))\\
&+ \sum_{l,m,n=1}^{3} P_{l,\mu}P_{m,\nu}P_{n,\alpha}G_3^{\mu\nu\alpha}(D4, D_5(P_1, m_{\chi_0}), D_6(P_2, m_{\chi_0}), D_7(P_3, m_{\chi_0}))\\
&+ \sum_{l,m=1,m\neq l}^{3} P_l \cdot P_m G_4(D4, D_5(0, m_{\chi_0}), D_6(P_1, m_{\chi_0}), D_7(P_3, m_{\chi_0}))\\
&+ \sum_{l,m=1,m\neq l}^{3} P_l \cdot P_m G_4(D4, D_5(0, m_{\chi_0}), D_6(P_2, m_{\chi_0}), D_7(P_3, m_{\chi_0}))\\
&+ \sum_{l=1}^{3} P_{l,\mu}G_3^{\mu}(D4, D_5(0, m_{\chi_0}), D_6(P_1, m_{\chi_0}), D_7(P_2, m_{\chi_0}))\\
&+ \sum_{l=1}^{3} P_{l,\mu}G_3^{\mu}(D4, D_5(0, m_{\chi_0}), D_6(P_1, m_{\chi_0}), D_7(P_3, m_{\chi_0}))\\
&+ \sum_{l=1}^{3} P_{l,\mu}G_3^{\mu}(D4, D_5(0, m_{\chi_0}), D_6(P_2, m_{\chi_0}), D_7(P_3, m_{\chi_0}))\\
&+ \sum_{l,m=1}^{3} P_l \cdot P_m P_{m,\mu}G_3^{\mu}(D4, D_5(0, m_{\chi_0}), D_6(P_1, m_{\chi_0}), D_7(P_3, m_{\chi_0}))\\
&+ \sum_{l,m=1}^{3} P_l \cdot P_m P_{m,\mu}G_3^{\mu}(D4, D_5(0, m_{\chi_0}), D_6(P_2, m_{\chi_0}), D_7(P_3, m_{\chi_0}))\\
&+ \sum_{l,m=1,m\neq l}^{3} P_l \cdot P_m P_{l,\mu}P_{m,\nu}G_2^{\mu\nu}(D4, D_5(0, m_{\chi_0}), D_6(P_1, m_{\chi_0}), D_7(P_3, m_{\chi_0}))\\
&+ \sum_{l,m=1,m\neq l}^{3} P_l \cdot P_m P_{l,\mu}P_{m,\nu}G_2^{\mu\nu}(D4, D_5(P_1, m_{\chi_0}), D_6(P_2, m_{\chi_0}), D_7(P_3, m_{\chi_0}))\\
&+ \sum_{l,m=1,m\neq l}^{3} P_l \cdot P_m P_{l,\mu}P_{m,\nu}G_2^{\mu\nu}(D4, D_5(0, m_{\chi_0}), D_6(P_1, m_{\chi_0}), D_7(P_3, m_{\chi_0}))\\
&\Big(P_1 \cdot P_2 P_2 \cdot P_3 + P_2 \cdot P_3 P_1 \cdot P_3\Big) G_2(D4, D_5(0, m_{\chi_0}), D_6(P_1, m_{\chi_0}), D_7(P_3, m_{\chi_0}))
\end{aligned}
$$

$$
\begin{aligned}
&+ \sum_{l,m,n=1,n\neq m\neq l}^{3} P_l\cdot P_m P_m\cdot P_n (P_m+P_n)_\mu G_1^\mu(D4, D_5(P_1,m_{\chi_0}), D_6(P_2,m_{\chi_0}), D_7(P_3,m_{\chi_0}))\\
&+ \sum_{l,m,n=1,n\neq m\neq l}^{3} P_l\cdot P_m P_m\cdot P_n (P_m+P_n)_\mu G_1^\mu(D4, D_5(0,m_{\chi_0}), D_6(P_1,m_{\chi_0}), D_7(P_3,m_{\chi_0}))\\
&+ \sum_{l,m=1,m\neq l}^{3} P_l\cdot P_m P_{l,\mu} P_{m,\nu} G_2^{\mu\nu}(D4, D_5(P_1,m_{\chi_0}), D_6(P_2,m_{\chi_0}), D_7(P_3,m_{\chi_0}))\\
&+ P_1\cdot P_2 P_2\cdot P_3 P_1\cdot P_3 G_0(D4, D_5(P_1,m_{\chi_0}), D_6(P_2,m_{\chi_0}), D_7(P_3,m_{\chi_0}))\Bigg)\Bigg\}
\end{aligned}
\tag{2.E.5}
$$

$$
(B_H^{R_\xi,ZZ\chi\chi})_{f,1} = 64\frac{m_{Z_0}^4\lambda_0^2}{m_{H_0}^4}\mu^\varepsilon\Bigg\{2P_{2,\mu}g_{\nu\alpha}D^{\mu\nu\alpha}(D1,D2,D3,D4) + P_{2,\mu}P_{2,\nu}D^{\mu\nu}(D1,D2,D3,D4)\Bigg\}
\tag{2.E.6}
$$

$$
\begin{aligned}
(B_H^{R_\xi,ZZ\chi\chi})_{f,2} &= 64\frac{m_{Z_0}^4\lambda_0^2}{m_{H_0}^4}\mu^\varepsilon\Bigg\{-2P_{3,\mu}E_5^\mu(D4, D_5(P_1,m_{\chi_0}))\\
&+ (m_{\chi_0}^2 - P_1^2)E_6(D4, D_5(P_1,m_{\chi_0})) + m_{\chi_0}^2 E_6(D4, D_5(0,m_{\chi_0}))\\
&+ E_4(D4, D_5(P_1,m_{\chi_0})) + E_4(D4, D_5(0,m_{\chi_0}))\\
&+ 2P_{2,\mu}E_3^\mu(D4, D_5(P_1,m_{\chi_0})) + 2P_{1,\mu}E_3^\mu(D4, D_5(0,m_{\chi_0}))\\
&+ P_{1,\mu}P_{1,\nu}E_2^{\mu\nu}(D4, D_5(0,m_{\chi_0})) + 2P_{1,\mu}P_{2,\nu}E_2^{\mu\nu}(D4, D_5(0,m_{\chi_0}))\\
&+ P_{2,\mu}P_{2,\nu}\Bigg\{E_2^{\mu\nu}(D4, D_5(0,m_{\chi_0})) + E_2^{\mu\nu}(D4, D_5(P_1,m_{\chi_0}))\Bigg\}\\
&+ P_{3,\mu}P_{3,\nu}E_2^{\mu\nu}(D4, D_5(0,m_{\chi_0})) + 2P_{1,\mu}P_{2,\nu}E_2^{\mu\nu}(D4, D_5(P_1,m_{\chi_0}))\\
&+ 2P_{1,\mu}P_{3,\nu}E_2^{\mu\nu}(D4, D_5(P_1,m_{\chi_0})) + 2P_1\cdot P_2 E_2(D4, D_5(P_1,m_{\chi_0}))\\
&+ 2P_1\cdot P_2\Bigg\{P_{1,\mu} + P_{2,\mu}\Bigg\}E_1^\mu(D4, D_5(P_1,m_{\chi_0}))\Bigg\}
\end{aligned}
\tag{2.E.7}
$$

$$
\begin{aligned}
(B_H^{R_\xi,ZZ\chi\chi})_{f,3} &= 64\frac{m_{Z_0}^4\lambda_0^2}{m_{H_0}^4}\mu^\varepsilon\Bigg\{F_4(D4, D_5(0,m_{\chi_0}), D_6(0,m_{\chi_0}))\\
&+ F_4(D4, D_5(0,m_{\chi_0}), D_6(P_2,m_{\chi_0}))\\
&+ F_4(D4, D_5(P_1,m_{\chi_0}), D_6(P_2,m_{\chi_0})) + F_4(D4, D_5(P_1,m_{\chi_0}), D_6(P_2,m_{\chi_0}))\\
&+ F_4(D4, D_5(0,m_{\chi_0}), D_6(P_2,m_{\chi_0})) + 2P_{1,\mu}F_3^\mu(D4, D_5(0,m_{\chi_0}), D_6(P_2,m_{\chi_0}))\\
&+ 2P_{2,\mu}F_3^\mu(D4, D_5(0,m_{\chi_0}), D_6(P_2,m_{\chi_0}))\\
&+ 2P_{2,\mu}F_3^\mu(D4, D_5(0,m_{\chi_0}), D_6(P_2,m_{\chi_0}))\\
&+ 2P_{2,\mu}F_3^\mu(D4, D_5(P_2,m_{\chi_0}), D_6(P_2,m_{\chi_0}))\\
&+ 2P_{2,\mu}F_3^\mu(D4, D_5(P_1,m_{\chi_0}), D_6(P_2,m_{\chi_0}))\\
&+ P_{1,\mu}P_{1,\nu}F_2^{\mu\nu}(D4, D_5(0,m_{\chi_0}), D_6(P_2,m_{\chi_0}))
\end{aligned}
$$

$$
\begin{aligned}
&+ \quad 2P_{1,\mu}P_{2,\nu}F_2^{\mu\nu}(D4, D_5(0, m_{\chi_0}), D_6(P_2, m_{\chi_0})) \\
&+ \quad P_{2,\mu}P_{2,\nu}F_2^{\mu\nu}(D4, D_5(0, m_{\chi_0}), D_6(P_2, m_{\chi_0})) \\
&+ \quad P_{2,\mu}P_{2,\nu}F_2^{\mu\nu}(D4, D_5(0, m_{\chi_0}), D_6(P_2, m_{\chi_0})) \\
&+ \quad 2P_{1,\mu}P_{2,\nu}F_2^{\mu\nu}(D4, D_5(0, m_{\chi_0}), D_6(P_1, m_{\chi_0})) \\
&+ \quad 2P_{1,\mu}P_{2,\nu}F_2^{\mu\nu}(D4, D_5(P_1, m_{\chi_0}), D_6(P_2, m_{\chi_0})) \\
&+ \quad 2P_1 \cdot P_2 F_2(D4, D_5(P_1, m_{\chi_0}), D_6(P_2, m_{\chi_0})) \\
&+ \quad 2P_1 \cdot P_2 \Big\{ P_{1,\mu} + P_{2,\mu} \Big\} F_1^{\mu}(D4, D_5(P_1, m_{\chi_0}), D_6(P_2, m_{\chi_0})) \\
&+ \quad (P_1 \cdot P_2)^2 F_0(D4, D_5(P_1, m_{\chi_0}), D_6(P_2, m_{\chi_0})) \Big\}
\end{aligned} \tag{2.E.8}
$$

$$
\begin{aligned}
(B_H^{R_\xi,\chi\chi\chi Z})_{f,1} &= 64 \frac{m_{Z_0}^2 \lambda_0^2}{m_{H_0}^4} \mu^\varepsilon \Big\{ g_{\mu\nu} D^{\mu\nu}(P_1, P_2, m_{Z_0}, m_{Z_0}, m_{Z_0}, m_{\chi_0}) \\
&+ \quad g_{\mu\nu} D^{\mu\nu}(P_1, P_2, m_{Z_0}, m_{Z_0}, m_{Z_0}, m_{\chi_0}) \\
&+ \quad g_{\mu\nu} D^{\mu\nu}(P_1, P_2, m_{Z_0}, m_{Z_0}, m_{Z_0}, m_{\chi_0}) + 2P_1^\mu D^\mu(P_1, P_2, m_{Z_0}, m_{Z_0}, m_{Z_0}, m_{\chi_0}) \\
&+ \quad 2P_2^\mu D^\mu(P_1, P_2, m_{Z_0}, m_{Z_0}, m_{Z_0}, m_{\chi_0}) + P_1^2 D_0(P_1, P_2, m_{Z_0}, m_{Z_0}, m_{Z_0}, m_{\chi_0}) \\
&+ \quad P_2^2 D_0(P_1, P_2, m_{Z_0}, m_{Z_0}, m_{Z_0}, m_{\chi_0}) \Big\}
\end{aligned} \tag{2.E.9}
$$

$$
\begin{aligned}
(B_H^{R_\xi,\chi\chi\chi Z})_{f,2} &= 64 \frac{m_{Z_0}^2 \lambda_0^2}{m_{H_0}^4} \mu^\varepsilon \Big\{ E_4(D4, D_5(0, m_{\chi_0})) + E_4(D4, D_5(P_1, m_{\chi_0})) \\
&+ \quad E_4(D_1, D_2, D_3, D_4(0, m_{\chi_0}), D_5(P_1, m_{\chi_0})) \\
&+ \quad 2P_{1\mu} E_3^\mu(D4, D_5(0, m_{\chi_0})) + 2P_{1\mu} E_3^\mu(D_1, D_2, D_3, D_4(0, m_{\chi_0}), D_5(P_1, m_{\chi_0})) \\
&+ \quad 2P_{2\mu} E_3^\mu(D4, D_5(P_1, m_{\chi_0})) + 2P_{2\mu} E_3^\mu(D_1, D_2, D_3, D_4(0, m_{\chi_0}), D_5(P_1, m_{\chi_0})) \\
&+ \quad 2P_{1\mu} P_{2\nu} E_2^{\mu\nu}(D_1, D_2, D_3, D_4(0, m_{\chi_0}), D_5(P_1, m_{\chi_0})) \\
&+ \quad P_{2\mu} P_{2\nu} E_2^{\mu\nu}(D4, D_5(P_1, m_{\chi_0})) \\
&+ \quad P_{2\mu} P_{2\nu} E_2^{\mu\nu}(D_1, D_2, D_3, D_4(0, m_{\chi_0}), D_5(P_1, m_{\chi_0})) \\
&+ \quad 2P_1 \cdot P_2 E_2(D_1, D_2, D_3, D_4(0, m_{\chi_0}), D_5(P_1, m_{\chi_0})) \\
&+ \quad 2P_1 \cdot P_2 (P_1 + P_2)_\mu E_1^\mu(D_1, D_2, D_3, D_4(0, m_{\chi_0}), D_5(P_1, m_{\chi_0})) \\
&+ \quad (P_1 \cdot P_2)^2 E_0(D_1, D_2, D_3, D_4(0, m_{\chi_0}), D_5(P_1, m_{\chi_0})) \Big\}
\end{aligned} \tag{2.E.10}
$$

2.E.2 Unitary gauge

In the Unitary gauge the finite parts are:

Finite parts of the Box diagrams

$$
(B_H^{U,ZZZZ})_{f,1} = 64 \frac{m_{Z_0}^4 \lambda_0^2}{m_{H_0}^4} \mu^\varepsilon \Big\{ 6 g_{\nu\alpha} (P_1 + P_2 + P_3)_\mu D^{\mu\nu\alpha}(P_1, P_2, m_{Z_0}, m_{Z_0}, m_{Z_0}, m_{\chi_0})
$$

$$
\begin{aligned}
&+ \Big(3P_1^\mu P_1^\nu + 2P_1^\mu P_2^\nu + 3P_2^\mu P_2^\nu \\
&+ 2P_1^\mu P_3^\nu + 2P_2^\mu P_3^\nu + 3P_3^\mu P_3^\nu \\
&+ 2(P_1\cdot P_2 + P_1\cdot P_2 + P_1\cdot P_2)g_{\mu\nu}\Big) D^{\mu\nu}(P_1,P_2,m_{Z_0},m_{Z_0},m_{Z_0},m_{\chi_0}) \\
&+ \Big(2P_1\cdot P_2(P_1^\mu + P_2^\mu) + 2P_1\cdot P_2(P_1^\mu + P_2^\mu) \\
&+ 2P_1\cdot P_2(P_1^\mu + P_2^\mu)\Big) D^{\mu\nu}(P_1,P_2,m_{Z_0},m_{Z_0},m_{Z_0},m_{\chi_0}) \\
&+ ((P_1\cdot P_2)^2 + (P_1\cdot P_3)^2 + (P_2\cdot P_3)^2) D_0(P_1,P_2,m_{Z_0},m_{Z_0},m_{Z_0},m_{\chi_0})\Bigg\}
\end{aligned}
\tag{2.E.11}
$$

$$
\begin{aligned}
(B_H^{U,ZZZZ})_{f,2} &= 64\frac{m_{Z_0}^2\lambda_0^2}{m_{H_0}^4}\mu^\varepsilon\Bigg\{\Big(2\sum_{l,m,n=1}^{3} P_{l,\mu}P_{m,\nu}P_{n,\alpha} \\
&+ \sum_{l,m,n=1,n\neq m\neq l}^{3} 2(P_l\cdot P_m \\
&+ P_l\cdot P_n + P_n\cdot P_m)(P_l + P_m + P_n)_\mu\Big) D^{\mu\nu\alpha}(P_1,P_2,m_{Z_0},m_{Z_0},m_{Z_0},m_{\chi_0}) \\
&+ P_1\cdot P_2 \sum_{l,m=1} P_{l,\mu}P_{m,\nu} D^{\mu\nu}(P_1,P_2,m_{Z_0},m_{Z_0},m_{Z_0},m_{\chi_0}) \\
&+ P_2\cdot P_3 \sum_{l,m=1} P_{l,\mu}P_{m,\nu} D^{\mu\nu}(P_1,P_2,m_{Z_0},m_{Z_0},m_{Z_0},m_{\chi_0}) \\
&+ \sum_{l,m,n=1,n\neq m\neq l} P_l\cdot P_m P_l\cdot P_n g_{\mu\nu} D^{\mu\nu}(P_1,P_2,m_{Z_0},m_{Z_0},m_{Z_0},m_{\chi_0}) \\
&+ (P_1\cdot P_2 P_2\cdot P_3(P_1+P_3)_\mu \\
&+ P_1\cdot P_3 P_2\cdot P_3(P_1+P_3)_\mu) D^\mu(P_1,P_2,m_{Z_0},m_{Z_0},m_{Z_0},m_{\chi_0}) \\
&+ P_1\cdot P_2 P_1\cdot P_3 P_2\cdot P_3 D_0(P_1,P_2,m_{Z_0},m_{Z_0},m_{Z_0},m_{\chi_0})\Bigg\}
\end{aligned}
\tag{2.E.12}
$$

$$
\begin{aligned}
(B_H^{U,ZZZZ})_{f,3} &= 64\frac{\lambda_0^2}{m_{H_0}^4}\mu^\varepsilon\Bigg\{\Big(P_1\cdot P_2(P_{1,\mu}P_{2,\nu}P_{3,\alpha} + P_{1,\mu}P_{3,\nu}P_{3,\alpha}) + P_2\cdot P_3(P_{1,\mu}P_{1,\nu}P_{3,\alpha} \\
&+ P_{1,\mu}P_{2,\nu}P_{3,\alpha}) + P_1\cdot P_2 g_{\mu\nu}(P_1+P_3)_\mu\Big) D^{\mu\nu\alpha}(P_1,P_2,m_{Z_0},m_{Z_0},m_{Z_0},m_{\chi_0}) \\
&+ P_1\cdot P_2 P_2\cdot P_3 P_{1,\mu}P_{3,\nu} D^{\mu\nu}(P_1,P_2,m_{Z_0},m_{Z_0},m_{Z_0},m_{\chi_0})\Bigg\}
\end{aligned}
\tag{2.E.13}
$$

2.F On-shell results

For completeness, in this Appendix we demonstrate the results for the divergent parts of the two- three- and four-point one-loop functions calculated on-shell, in both R_ξ and Unitary gauges. We start with the case of R_ξ gauge where we will demonstrate the results for the two-, three-

and four-point functions calculated at on-shell, i.e. at $p^2 = m_Z^2$ for the Z-mass and at $p_i^2 = m_H^2$ for everything else. Tadpoles are external momentum independent objects.

- Vacuum polarization of the Z-boson

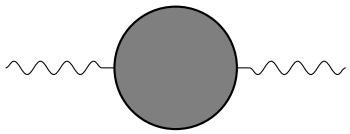

$$= [\mathcal{M}_Z^{R_\xi}]_\varepsilon + \left\{\mathcal{M}_Z^{R_\xi}\right\}_\varepsilon + [\mathcal{M}_Z^{R_\xi}]_f + \left\{\mathcal{M}_Z^{R_\xi}\right\}_f$$

with

$$\varepsilon[\mathcal{M}_Z^{R_\xi}]_\varepsilon = \frac{40}{3}\frac{\lambda_0 m_{Z_0}^4}{m_{H_0}^2}, \qquad \left\{\mathcal{M}_Z^{R_\xi}\right\}_\varepsilon = 0 \tag{2.F.1}$$

and

$$\varepsilon[\delta A^{R_\xi}]_\varepsilon = \frac{4}{3}\lambda_0\frac{m_{Z_0}^2}{m_{H_0}^2}, \qquad \left\{\delta A^{R_\xi}\right\}_\varepsilon = 0\,. \tag{2.F.2}$$

- One-loop corrections to the Higgs propagator

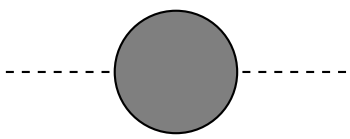

$$= [\mathcal{M}_H^{R_\xi}]_\varepsilon + \left\{\mathcal{M}_H^{R_\xi}\right\}_\varepsilon + [\mathcal{M}_H^{R_\xi}]_f + \left\{\mathcal{M}_H^{R_\xi}\right\}_f$$

with

$$\varepsilon[\mathcal{M}_H^{R_\xi}]_\varepsilon = 26\lambda_0 m_{H_0}^2 - 12\lambda_0 m_{Z_0}^2 + 36\frac{\lambda_0 m_{Z_0}^4}{m_{H_0}^2}, \qquad \varepsilon\left\{\mathcal{M}_H^{R_\xi}\right\}_\varepsilon = 12\frac{\lambda_0 m_{Z_0}^4}{m_{H_0}^2}\xi^2 \tag{2.F.3}$$

and

$$\varepsilon[\delta\phi^{R_\xi}]_\varepsilon = -4\lambda_0 + 12\lambda_0\frac{m_{Z_0}^2}{m_{H_0}^2}, \qquad \left\{\delta\phi^{R_\xi}\right\}_\varepsilon = 0 \tag{2.F.4}$$

- One-loop corrections to the Higgs three-point vertex

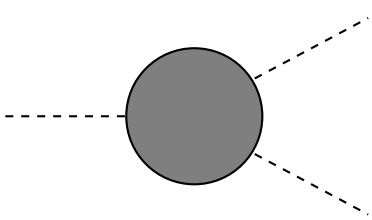

$$= [\mathcal{K}_H^{R_\xi}]_\varepsilon + \left\{\mathcal{K}_H^{R_\xi}\right\}_\varepsilon + [\mathcal{K}_H^{R_\xi}]_f + \left\{\mathcal{K}_H^{R_\xi}\right\}_f$$

where

$$\begin{aligned}
\varepsilon[\mathcal{K}_H^{R_\xi}]_\varepsilon &= \varepsilon[\mathcal{K}_H^{R_\xi,\text{red.}} + \mathcal{K}_{R_\xi}^{R_\xi,\text{irred.}}]_\varepsilon = \frac{m_{H_0}}{\sqrt{2\lambda_0}}\left(84\lambda_0^2 + 144\frac{\lambda_0^2 m_{Z_0}^4}{m_{H_0}^4}\right) \\
\left\{\mathcal{K}_H^{R_\xi}\right\}_\varepsilon &= \left\{\mathcal{K}_H^{R_\xi,\text{red.}} + \mathcal{K}_H^{R_\xi,\text{irred.}}\right\}_\varepsilon = 0.
\end{aligned} \tag{2.F.5}$$

- One-loop corrections to Higgs quartic coupling

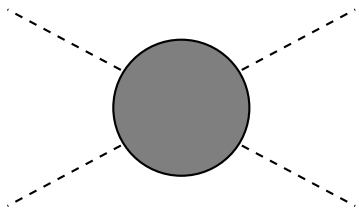

$$= [\mathcal{B}_H^{R_\xi}]_\varepsilon + \left\{\mathcal{B}_H^{R_\xi}\right\}_\varepsilon + [\mathcal{B}_H^{R_\xi}]_f + \left\{\mathcal{B}_H^{R_\xi}\right\}_f$$

with

$$\varepsilon[\mathcal{B}_H^{R_\xi}]_\varepsilon = 252\lambda_0^2 + 144\frac{\lambda_0^2 m_{Z_0}^4}{m_{H_0}^4}, \qquad \left\{\mathcal{B}_H^{R_\xi}\right\}_\varepsilon = 0. \tag{2.F.6}$$

Next we list on-shell results for the Unitary gauge.

- Vacuum polarization of the Z-boson

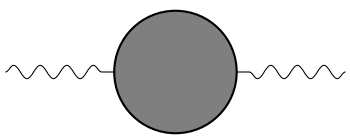

$$= [\mathcal{M}_Z^U]_\varepsilon + \left\{\mathcal{M}_Z^U\right\}_\varepsilon + [\mathcal{M}_Z^U]_f + \left\{\mathcal{M}_Z^U\right\}_f$$

with

$$\varepsilon[\mathcal{M}_Z^U]_\varepsilon = \frac{40}{3}\frac{\lambda_0 m_{Z_0}^4}{m_{H_0}^2}, \qquad \left\{\mathcal{M}_U^Z\right\}_\varepsilon = 0 \tag{2.F.7}$$

and

$$\varepsilon[\delta A^U]_\varepsilon = \frac{4}{3}\lambda_0\frac{m_{Z_0}^2}{m_{H_0}^2}, \qquad \left\{\delta A^U\right\}_\varepsilon = 0 \tag{2.F.8}$$

- One-loop corrections to the Higgs propagator

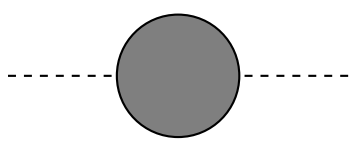

$$= [\mathcal{M}_H^U]_\varepsilon + \left\{\mathcal{M}_H^U\right\}_\varepsilon + [\mathcal{M}_H^U]_f + \left\{\mathcal{M}_H^U\right\}_f$$

with

$$\varepsilon[\mathcal{M}_H^U]_\varepsilon = 26\lambda_0 m_{H_0}^2 - 12\lambda_0 m_{Z_0}^2 + 36\frac{\lambda_0 m_{Z_0}^4}{m_{H_0}^2}, \qquad \left\{\mathcal{M}_H^U\right\}_\varepsilon = 12\frac{\lambda_0 m_{Z_0}^4}{m_{H_0}^2}\xi^2 \tag{2.F.9}$$

and

$$\varepsilon[\delta\phi^U]_\varepsilon = -4\lambda_0 + 12\lambda_0\frac{m_{Z_0}^2}{m_{H_0}^2}, \qquad \left\{\delta\phi^U\right\}_\varepsilon = 0 \tag{2.F.10}$$

- One-loop corrections to the Higgs three-point vertex

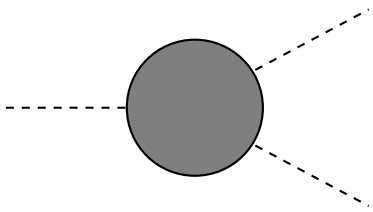

$$= [\mathcal{K}_H^U]_\varepsilon + \left\{\mathcal{K}_H^U\right\}_\varepsilon + [\mathcal{K}_H^U]_f + \left\{\mathcal{K}_H^U\right\}_f$$

where

$$\begin{aligned}
\varepsilon[\mathcal{K}_H^U]_\varepsilon &= \varepsilon[\mathcal{K}_H^{U,\text{red.}} + \mathcal{K}_H^{U,\text{irred.}}]_\varepsilon = \frac{m_{H_0}}{\sqrt{2\lambda_0}}\left(84\lambda_0^2 + 144\frac{\lambda_0^2 m_{Z_0}^4}{m_{H_0}^4}\right) \\
\left\{\mathcal{K}_H^U\right\}_\varepsilon &= \left\{\mathcal{K}_H^{U,\text{red.}} + \mathcal{K}_{H,U}^{U,\text{irred.}}\right\}_\varepsilon = 0.
\end{aligned} \tag{2.F.11}$$

- One-loop corrections to Higgs quartic coupling

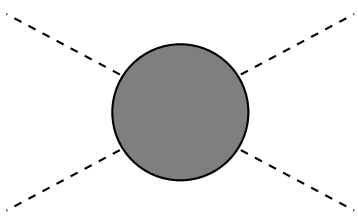

$$= [\mathcal{B}_H^U]_\varepsilon + \left\{\mathcal{B}_H^U\right\}_\varepsilon + [\mathcal{B}_H^U]_f + \left\{\mathcal{B}_H^U\right\}_f$$

with

$$\varepsilon[\mathcal{B}_H^U]_\varepsilon = 252\lambda_0^2 + 144\frac{\lambda_0^2 m_{Z_0}^4}{m_{H_0}^4}, \qquad \left\{\mathcal{B}_H^U\right\}_\varepsilon = 0\,. \tag{2.F.12}$$

We observe that the results of the one-loop diagrams in R_ξ and in the Unitary gauge are the same.

Chapter 3

Is the leading order truncation enough to develop a Higgs mechanism?

3.1 Introduction

As it is mentioned in Chapter 4.1, here we have computed the RG flows in a theory that is defined by the quantization of the truncated in the lattice spacings expansion of a five-dimensional $SU(2)$ orbifold lattice model. In this first part of the work we have truncated the expansion to the leading non-trivial order where the boundary (a massless, free 4d SQED model) decouples from the bulk (a 5d $SU(2)$ gauge theory) and the two can be studied separately. The computational tool we used was the ε-expansion. On the boundary there is a Gaussian fixed point where the theory becomes a CFT. In the bulk where in infinite volume the phase diagram is two-dimensional there is a curve of WF fixed points. The resulting phase diagram agrees qualitatively with the non-perturbative phase diagram, if we identify the WF curve with the curve of quantum phase transitions extracted from Monte Carlo simulations. RG flow lines starting from the Gaussian fixed point can end on the WF curve where classically marginal operators become relevant. There is a special point on the phase diagram, the one at $(\beta_4, \beta_5) = (\infty, 0)$, which is seen from the Coulomb phase as a WF fixed point and from the Confined phase as a Gaussian fixed point. The RG flow lines (lines labelled by A and B on Fig. 3.5) that end on that point can be correlated. This is possible because in this regime the Confined phase becomes 4d-layered along the fifth dimension.

Throughout our discussion we have tried to interpret the results from the ε-expansion as physical. This has led us to a notion of Weak Asymptotic Safety, as the WF fixed points by construction are associated with a vanishing β-function which, if generalized to all orders, implies a continuum limit that we know not to exist in this model by Monte Carlo simulations. Instead, the Weak Asymptotic Safety point of view is that the fixed loop-order vanishing of

the β-function is not a signal of exact scale invariance but an indication of the tendency of the system to become approximately scale invariant as a first order quantum phase transition is approached, from either side. Under such a perspective the WF curve of the ε-expansion can be perhaps related to the first order quantum phase transition seen by the lattice. We have given several arguments to support this picture. A consequence of these arguments is that near the phase transition an alternative way to describe the quantum theory is possibly via a radiatively broken CFT.

A shortcoming in our analysis is the complete decoupling of the boundary from the bulk. A result of the decoupling is the absence of a Higgs phase that we know however to exist non-perturbatively in the model and it is the reason why we call the model one of Non-Perturbative Gauge-Higgs Unification. This absence is due to the leading order truncation of the lattice spacing expansion that generates our classical action. Truncating the lattice spacing expansion at higher order amounts to allowing classically irrelevant operators in the action. Quantizing this action will keep the boundary coupled to the bulk and may generate large enough anomalous dimensions to change some of the irrelevant operators to relevant ones. Then if at least one of these operators generates a mass term for the boundary scalar and another generates a mass term for the gauge field, we will have a purely bosonic and quantum version of the Higgs mechanism. This next step justifies the detailed exposition of the classical lattice spacing expansions, Feynman rules, diagram computations, renormalization etc. presented here, as in the next stage no already existing results (for β-functions and anomalous dimensions) can be used without explicit new calculations. The construction of the RG flow lines itself and a matching of the kind we performed for the lines A and B in Fig. 3.5 is expected to reveal non-trivial information about the Higgs phase and as we will see it offers an alternative resolution to the Higgs hierarchy problem. This will be the topic of Chapter 5.

3.2 The classical continuum action from the lattice action

We define our classical, continuum action as the truncated expansion in a small lattice spacing of the orbifold lattice action defined in [4, 5, 6, 7], which we briefly review here. We start by considering a Euclidean five-dimensional (5d) periodic hypercubic lattice, with an $SU(2)$ gauge symmetry. Then, the circle of the fifth dimension is projected by the discrete group $\mathbb{Z}_2$. This projection identifies the upper semicircle with the lower semicircle and turns the circle into an (discretized) interval. The projection is also embedded non-trivially into the Lie group so that at the endpoints of the interval only a $U(1)$ subgroup and a complex scalar from the 5d components of the $SU(2)$ gauge field survive. Thus, we obtain an orbifold lattice with an $SU(2)$ symmetry in the bulk and with the degrees of freedom of an Abelian-Higgs system living on the 4d boundaries.

In the following we use capital Latin letters $M, N, \cdots = 0, 1, 2, 3, 5$ to denote the five-dimensional Euclidean or Minkowski index and small Greek letters $\mu, \nu, \cdots = 0, 1, 2, 3$ to denote the four-dimensional part. We define the lattice coordinates as $n_M = (n_\mu, n_5)$ with $n_\mu = 1, \cdots, L$

and $n_5 = 0, 1, \cdots, N_5$. The values $n_5 = 0, N_5$ correspond to the orbifold's fixed points. The lattice gauge variables consist of the links $U(n_M, N) \in SU(2)$

$$U(n_M, N) = e^{ia_N g_5 \mathbf{A}_N(n_M)} \tag{3.2.1}$$

located at n_M and pointing in the direction N. The a_N corresponds to the lattice spacing in the direction N. We will take $a_\mu = a_4$ for all μ but generically $a_5 \neq a_4$. g_5 is the 5d dimensionful continuum gauge coupling with mass dimension $[g_5] = -1/2$ and $\mathbf{A}_M \equiv A_M^A T^A$ is the Lie algebra valued gauge potential carrying the adjoint index A. The normalization of the generators is the usual $\mathrm{tr}\{T^A T^B\} = \frac{1}{2}\delta^{AB}$. We will take L practically infinite and allow the numbers of lattice nodes $N_5 = \frac{\pi R}{a_5}$ in the fifth direction (R is the radius of the projected parent circle) to be either finite or infinite. To the order we are working here R does not appear anywhere so we can think of it being infinite.

The orbifold condition on the links

$$(1 - \Gamma)U(n_M, N) = 0, \quad \Gamma \equiv \mathcal{R}\mathcal{T}_g\,, \tag{3.2.2}$$

is implemented on the periodic lattice by the reflection operator $\mathcal{R}$ and the group conjugation operator $\mathcal{T}_g$. The combined projector satisfies $\Gamma^2 = 1$ and is a $\mathbb{Z}_2$ element. The reflection operation acts on the nodes as

$$\mathcal{R}n_M = \bar{n}_M \equiv (n_\mu, -n_5) \tag{3.2.3}$$

and on the gauge links as

$$\begin{aligned} \mathcal{R}U(n_M, \nu) &= U(\bar{n}_M, \nu) \\ \mathcal{R}U(n_M, 5) &= U(\bar{n}_M - a_5\hat{\bar{5}}, 5) \end{aligned} \tag{3.2.4}$$

while the conjugation operator acts only on the gauge links, as

$$\mathcal{T}_g U(n_M, N) = gU(n_M, N)g^{-1} \tag{3.2.5}$$

where g^2 is an element of the centre of $SU(2)$. We shall take $g = -i\sigma^3$. In order to ensure that $\Gamma^2 = 1$ these operators must satisfy $[\mathcal{R}, \mathcal{T}_g] = 0$ and $\mathcal{R}^2 = \mathcal{T}_g^2 = 1$.

The orbifold lattice has a mirror symmetry around the central point in the fifth dimension, therefore it is sufficient to restrict ourselves on half of the lattice. Thus, we will deal with only one of the boundaries, and specifically the one at the $n_5 = 0$ fixed point. On the boundary, the action of the reflection operator on the coordinates is trivial,

$$\mathcal{R}(n_\mu, 0) = \bar{n}_M \equiv (n_\mu, 0)\,, \tag{3.2.6}$$

so that the orbifold condition Eq. (3.2.2) reads

$$U((n_\mu, 0), \nu) = \mathcal{T}_g U((n_\mu, 0), \nu) = gU((n_\mu, 0), \nu)g^{-1}. \tag{3.2.7}$$

It is clear that generally the above constraints break a bulk gauge group $SU(N_C)$ with generators T^A to a subgroup $\mathcal{H}$ on the boundary. Denoting the unbroken generators's index by α and those of broken by $\hat{\alpha}$, Eq. (3.2.7) implies that $[T^\alpha, g] = 0$. For $SU(2)$ which has the three generators $T^A = \frac{1}{2}\sigma^A, A = 1, 2, 3$ with σ^A the Pauli matrices we see that g commutes only with $T^{\alpha=3}$, thus at the boundary we are left with a $U(1)$ gauge symmetry. The two remaining generators $T^{\hat{\alpha}=1,2}$ are broken.

We take for our lattice action the simple Wilson plaquette action, appropriately generalized to implement the structure of the orbifold lattice [4, 5, 6, 7]. We denote by $U_{\mu\nu}^{U(1)}$ the 4d boundary plaquettes, constructed from links lying on the boundary and by $U_{\mu 5}^{H}$ the so called Hybrid plaquettes, with two links along the fifth dimension with one end at a fixed point and the other in the bulk. We denote by $U_{\mu\nu}^{SU(2)} \equiv U_{\mu\nu}$ and $U_{\mu 5}^{SU(2)} \equiv U_{\mu 5}$ the bulk plaquettes with their links lying only in the bulk. Therefore, the anisotropic orbifold Wilson action can be separated into two parts, one that contains the boundary and hybrid plaquettes and one that contains the bulk plaquettes, according to

$$S_{S^1/\mathbb{Z}_2} = S_{S^1/\mathbb{Z}_2}^{\text{b-H}} + S_{S^1/\mathbb{Z}_2}^{\text{bulk}} \tag{3.2.8}$$

with

$$S_{S^1/\mathbb{Z}_2}^{\text{b-H}} = \frac{1}{2N_C} \sum_{n_\mu} \left[\beta_4 \sum_{\mu<\nu} \frac{1}{2} \text{tr}\left\{1 - U_{\mu\nu}^{U(1)}(n_\mu, 0)\right\} + \beta_5 \sum_{\mu} \text{tr}\left\{1 - U_{\mu 5}^{H}(n_\mu, 0)\right\} \right] \tag{3.2.9}$$

and

$$S_{S^1/\mathbb{Z}_2}^{\text{bulk}} = \frac{1}{2N_C} \sum_{n_\mu, n_5} \left[\beta_4 \sum_{\mu<\nu} \text{tr}\left\{1 - U_{\mu\nu}(n_\mu, n_5)\right\} + \beta_5 \sum_{\mu} \text{tr}\left\{1 - U_{\mu 5}(n_\mu, n_5)\right\} \right] \tag{3.2.10}$$

where β_4 and β_5 are dimensionless lattice couplings. Note here that a factor of $\frac{1}{2}$ in Eq. (3.2.9), will be cancelled by an extra factor of 2 due to the folding of the lattice about the midpoint of the extra dimension. In the following we will often combine β_4 and β_5 and use an equivalent pair of couplings β and γ determined as

$$\begin{aligned} \beta_4 &= \frac{2N_C a_5}{g_5^2} = \frac{\beta}{\gamma} \\ \beta_5 &= \frac{2N_C a_4^2}{a_5 g_5^2} = \beta\gamma \end{aligned} \tag{3.2.11}$$

for $SU(N_C)$. Even though we will mostly be concerned with $N_C = 2$, when possible we will present expressions for general N_C. The alternative parametrization introduces the anisotropy parameter $\gamma = \sqrt{\beta_5/\beta_4}$ (whose classical value is $\gamma = \frac{a_4}{a_5}$ as already mentioned) and the lattice coupling $\beta = \sqrt{\beta_5\beta_4} = \frac{2N_C a_4}{g_5^2}$.[1] Finally we stress that in Eq. (3.2.8) and Eq. (3.2.10) there are

[1] A warning concerning the lattice versus continuum notation: the anisotropy parameter γ should not be confused with the anomalous dimension of fields and operators, also denoted by γ. Also, the various lattice couplings denoted traditionally by β should not be confused with the notation for the continuum β-functions. To reduce the possibility of confusion we will denote β-functions with the bold character $\boldsymbol{\beta}$ and anomalous dimensions with $\boldsymbol{\gamma}$. For example, in the next sections we will meet $\boldsymbol{\beta}_{\beta_{4,5}}$, the beta function of the lattice coupling $\beta_{4,5}$ etc.

three kinds of gauge links: $U(1)$ boundary links, $SU(2)$ bulk links and hybrid links with one end on the boundary and the other in the bulk, with the unconventional gauge transformation $U \to \Omega^{U(1)} U \Omega^{\dagger SU(2)}$ from where their name originates.

The next step is to expand Eq. (3.2.9) and Eq. (3.2.10) for small lattice spacings which after a truncation to the leading non-trivial order will lead us to a continuum classical action. Some of the following steps are standard in 4d lattice gauge theories but we review them anyway because eventually particularities of our 5d lattice will appear.

3.2.1 Boundary-Hybrid action

$S^{\mathrm{b-H}}_{S^1/\mathbb{Z}_2}$ in Eq. (3.2.9) can be split further into a boundary part and a hybrid part as

$$S^{\mathrm{b-H}}_{S^1/\mathbb{Z}_2} = S^b + S^H \tag{3.2.12}$$

with

$$S^b = \frac{\beta_4}{2N_C} \sum_{n_\mu} \sum_{\mu<\nu} \frac{1}{2} \mathrm{tr}\left\{1 - U^{U(1)}_{\mu\nu}(n_\mu, 0)\right\} \tag{3.2.13}$$

and

$$S^H = \frac{\beta_5}{2N_C} \sum_{n_\mu} \sum_{\mu} \mathrm{tr}\left\{1 - U^{H}_{\mu 5}(n_\mu, 0)\right\}. \tag{3.2.14}$$

Let us first consider Eq. (3.2.13) that contains links $U((n_\mu, 0), \nu) \equiv U(n_\mu, \nu) = e^{ia_4 g_5 \mathbf{A}_\nu(n_\mu)}$ with $\mathbf{A}_\mu \equiv A^\alpha_\mu T^\alpha = A^3_\mu T^3$ and plaquettes of the form

$$\begin{aligned} U^{U(1)}_{\mu\nu}(n_\mu) &= U(n_\mu, \mu) U(n_\mu + a_4\hat{\mu}, \nu) U^\dagger(n_\mu + a_4\hat{\nu}, \mu) U^\dagger(n_\mu, \nu) \\ &= e^{ia_4 g_5 \mathbf{A}_\mu(n_\mu)} e^{ia_4 g_5 \mathbf{A}_\nu(n_\mu + a_4\hat{\mu})} e^{-ia_4 g_5 \mathbf{A}_\mu(n_\mu + a_4\hat{\nu})} e^{-ia_4 g_5 \mathbf{A}_\nu(n_\mu)}. \end{aligned} \tag{3.2.15}$$

Using the Campbell-Baker-Housdorff formula we first obtain

$$\begin{aligned} U^{U(1)}_{\mu\nu}(n_\mu) &= \exp\Bigg[ig_5 a_4 \Big\{ \mathbf{A}_\mu(n_\mu) + \mathbf{A}_\nu(n_\mu + a_4\hat{\mu}) - \mathbf{A}_\mu(n_\mu + a_4\hat{\nu}) - \mathbf{A}_\nu(n_\mu) \Big\} \\ &- \frac{a_4^2 g_5^2}{2} \Big\{ [\mathbf{A}_\mu(n_\mu), \mathbf{A}_\nu(n_\mu + a_4\hat{\mu})] + [\mathbf{A}_\mu(n_\mu), -\mathbf{A}_\mu(n_\mu + a_4\hat{\nu})] \\ &+ [\mathbf{A}_\mu(n_\mu), -\mathbf{A}_\nu(n_\mu)] + [\mathbf{A}_\nu(n_\mu + a_4\hat{\mu}), -\mathbf{A}_\mu(n_\mu + a_4\hat{\nu})] \\ &+ [\mathbf{A}_\nu(n_\mu + a_4\hat{\mu}), -\mathbf{A}_\nu(n_\mu)] + [\mathbf{A}_\mu(n_\mu + a_4\hat{\nu}), \mathbf{A}_\nu(n_\mu)] \Big\} \Bigg], \end{aligned} \tag{3.2.16}$$

which for small a_4 expands as

$$\begin{aligned} U^{U(1)}_{\mu\nu}(n_\mu) &= \exp\Bigg[ig_5 a_4 \Big\{ \mathbf{A}_\mu(n_\mu) + \mathbf{A}_\nu(n_\mu) + a_4 \hat{\Delta}_\mu \mathbf{A}_\nu(n_\mu) - \mathbf{A}_\mu(n_\mu) \\ &- a_4 \hat{\Delta}_\nu \mathbf{A}_\mu(n_\mu) - \mathbf{A}_\nu(n_\mu) \Big\} \end{aligned}$$

$$
\begin{aligned}
&- \frac{a_4^2 g_5^2}{2}\Big\{[\mathbf{A}_\mu(n_\mu),\mathbf{A}_\nu(n_\mu)]+[\mathbf{A}_\mu(n_\mu),-\mathbf{A}_\mu(n_\mu)] \\
&+ [\mathbf{A}_\mu(n_\mu),-\mathbf{A}_\nu(n_\mu)]+[\mathbf{A}_\nu(n_\mu),-\mathbf{A}_\mu(n_\mu)] \\
&+ [\mathbf{A}_\nu(n_\mu),-\mathbf{A}_\nu(n_\mu)]+[\mathbf{A}_\mu(n_\mu),\mathbf{A}_\nu(n_\mu)]\Big\}+O(a_4^2)\Bigg] \\
&= \exp\left[ig_5 a_4^2\Big\{\hat{\Delta}_\mu\mathbf{A}_\nu(n_\mu)-\hat{\Delta}_\nu\mathbf{A}_\mu(n_\mu)\Big\}-a_4^2 g_5^2[\mathbf{A}_\mu(n_\mu),\mathbf{A}_\nu(n_\mu)]+O(a_4^3)\right] \\
&= \exp\left[ig_5 a_4^2\Big\{\hat{\Delta}_\mu\mathbf{A}_\nu(n_\mu)-\hat{\Delta}_\nu\mathbf{A}_\mu(n_\mu)\Big\}+O(a_4^3)\right]. \qquad (3.2.17)
\end{aligned}
$$

In the above we used that $\mathbf{A}_\nu(n_\mu+a\hat{\mu})\equiv\mathbf{A}_\nu(n_\mu)+a\hat{\Delta}_\mu\mathbf{A}_\nu(n_\mu)$ with $\hat{\Delta}_\mu\mathbf{A}_\nu(n_\mu)=\frac{1}{a}[\mathbf{A}_\nu(n_\mu+a\hat{\mu})-\mathbf{A}_\nu(n_\mu)]$ a discrete derivative and that $[A_\mu^3T^3,A_\nu^3T^3]=0$. Keeping only terms that are second order in a_4, Eq. (3.2.17) becomes

$$
U_{\mu\nu}^{U(1)}(n_\mu)=e^{ig_5a_4^2\mathbf{F}_{\mu\nu}(n_\mu)} \qquad (3.2.18)
$$

with $\mathbf{F}_{\mu\nu}=\hat{\Delta}_\mu\mathbf{A}_\nu(n_\mu)-\hat{\Delta}_\nu\mathbf{A}_\mu(n_\mu)$, where $\mathbf{F}_{\mu\nu}=F_{\mu\nu}^3T^3$. Substituting Eq. (3.2.18) into Eq. (3.2.13) and expanding once more in small a_4 we obtain (after the folding that cancels a factor of 2)

$$
S^b=\sum_{n_\mu}\sum_{\mu<\nu}\frac{\beta_4}{2N_C}\mathrm{tr}\left\{-ig_5a_4^2\mathbf{F}_{\mu\nu}+\frac{g_5^2a_4^4}{2}\mathbf{F}_{\mu\nu}^{\mathbf{2}}+O(a_4^8)+\cdots\right\}. \qquad (3.2.19)
$$

After the trace and using Eq. (3.2.11) the action Eq. (3.2.13) becomes

$$
S^b=\sum_{n_\mu}a_4^4\sum_{\mu,\nu}\frac{a_5}{4}F_{\mu\nu}^3F_{\mu\nu}^3. \qquad (3.2.20)
$$

In the limit $a_4\to 0$ the sum $\sum_{n_\mu}a_4^4\to\int d^4x$ and up to the multiplicative a_5 factor we have a usual 4d continuum $U(1)$ gauge field action in infinite volume.

The procedure for S^H is similar, with a difference originating from the definition of the links that it contains. In particular, a hybrid plaquette contains one $U(1)$ link (we denote the corresponding potential as $\mathbf{A}_\mu^{\mathbf{a}}$ below), one $SU(2)$ link and two hybrid (also $SU(2)$ valued) links:

$$
\begin{aligned}
U_{\mu5}^H &= e^{ia_4g_5\mathbf{A}_\mu^{\mathbf{a}}(n_\mu,0)}e^{ia_5g_5\mathbf{A}_5(n_\mu+a_4\hat{\mu},0)}e^{-ia_4g_5\mathbf{A}_\mu(n_\mu,a_5\hat{5})}e^{-ia_5g_5\mathbf{A}_5(n_\mu,0)} \\
&= \exp\Bigg[ia_5g_5\Big\{\gamma\mathbf{A}_\mu^{\mathbf{a}}(n_\mu,0)+\mathbf{A}_5(n_\mu+a_4\hat{\mu},0)-\gamma\mathbf{A}_\mu(n_\mu,a_5\hat{5})-\mathbf{A}_5(n_\mu,0)\Big\} \\
&- \frac{g_5}{2}\Big\{[a_4\mathbf{A}_\mu^{\mathbf{a}}(n_\mu,0),a_5\mathbf{A}_5(n_\mu+a_4\hat{\mu},0)]+[a_4\mathbf{A}_\mu^{\mathbf{a}}(n_\mu,0),-a_4\mathbf{A}_\mu(n_\mu,a_5\hat{5})] \\
&+ [a_4\mathbf{A}_\mu^{\mathbf{a}}(n_\mu,0),-a_5\mathbf{A}_5(n_\mu,0)]+[a_5\mathbf{A}_5(n_\mu+a_4\hat{\mu},0),-a_4\mathbf{A}_\mu(n_\mu,a_5\hat{5})] \\
&+ [a_5\mathbf{A}_5(n_\mu+a_4\hat{\mu},0),-a_5\mathbf{A}_5(n_\mu,0)]+[a_4\mathbf{A}_\mu(n_\mu,a_5\hat{5}),a_5\mathbf{A}_5(n_\mu,0)]\Big\}\Bigg]. \qquad (3.2.21)
\end{aligned}
$$

As before, displaced fields are expanded as

$$
\mathbf{A}_5(n_\mu+a_4\hat{\mu},0)\to\mathbf{A}_5(n_\mu,0)+a_4\hat{\Delta}_\mu\mathbf{A}_5(n_\mu,0),
$$

$$\mathbf{A}_\mu(n_\mu, a_5\hat{5}) \to \mathbf{A}_\mu(n_\mu, 0) + a_5\hat{\Delta}_5\mathbf{A}_\mu(n_\mu, 0)\,. \tag{3.2.22}$$

To complete this calculation we have to express Eq. (3.2.7) at the gauge field level. By doing so, we obtain (we follow the notation of [57])

$$\begin{aligned}
\mathcal{R}\mathbf{A}_\mu &\equiv \alpha_\mu A^A_\mu T^A = \alpha_\mu \eta^A A^A_\mu T^A \Leftrightarrow \\
A^A_\mu T^A &= \alpha_\mu \eta^A A^A_\mu T^A\,, \\
\mathcal{R}\mathbf{A_5} &\equiv \alpha_5 A^A_5 T^A = \alpha_5 \eta^A A^A_5 T^A \Leftrightarrow \\
A^A_5 T^A &= \alpha_5 \eta^A A^A_5 T^A
\end{aligned} \tag{3.2.23}$$

where $\alpha_\mu = +1$, $\alpha_5 = -1$ are the parities of the A_μ and A_5 fields respectively. Moreover, we have used the relation $gT^Ag^{-1} = \eta^A T^A$ (no sum on A) where $\eta^A = \pm 1$ is the parity of the generators with $\eta^a = 1$ and $\eta^{\hat{a}} = -1$. Thus, the Dirichlet boundary conditions Eq. (3.2.23) imply that on the boundary

$$A^{1,2}_\mu = 0 \quad \text{and} \quad A^3_5 = 0. \tag{3.2.24}$$

We also obtain the Neumann boundary conditions

$$\hat{\Delta}_5 A^3_\mu = 0,\ \hat{\Delta}_5 A^{1,2}_5 = 0 \tag{3.2.25}$$

and now Eq. (3.2.22) becomes

$$\begin{aligned}
A^A_5(n_\mu + a_4\hat{\mu}, 0) &\to A^{1,2}_5(n_\mu, 0) + a_4\hat{\Delta}_\mu A^{1,2}_5(n_\mu, 0)\,, \\
A^A_\mu(n_\mu, a_5\hat{5}) &\to A^3_\mu(n_\mu, 0)\,.
\end{aligned} \tag{3.2.26}$$

Substituting these into Eq. (3.2.21) and keeping only terms of order $O(a_4a_5)$, we get

$$U^H_{\mu 5} = e^{ia_4a_5g_5\sum_{\hat{\alpha}} F^{\hat{\alpha}}_{\mu 5}T^{\hat{\alpha}}} \tag{3.2.27}$$

with $F^{1,2}_{\mu 5}T^{1,2} = \hat{\Delta}_\mu A^{1,2}_5 T^{1,2} + ig_5[A^3_\mu T^3, A^{1,2}_5 T^{1,2}]$. Defining a complex scalar field as $\phi = \frac{1}{\sqrt{2}}(A^1_5 + iA^2_5)$ we get that

$$\mathrm{tr}\sum_{\hat{\alpha}} F^{\hat{\alpha}}_{\mu 5}T^{\hat{\alpha}}F^{\hat{\alpha}}_{\mu 5}T^{\hat{\alpha}} \equiv |\hat{D}_\mu\phi|^2\,, \qquad \hat{D}_\mu = \hat{\Delta}_\mu + ig_5A^3_\mu\,. \tag{3.2.28}$$

Setting the above relations into the action Eq. (3.2.14), using Eq. (3.2.11) and keeping terms of order $O(a_4a_5)$, the Hybrid action becomes

$$\begin{aligned}
S^H &= \sum_{n_\mu}\frac{\beta_5}{2N_C}\sum_\mu a_4^2a_5^2g_5^2|\hat{D}_\mu\phi|^2 \Leftrightarrow \\
S^H &= \sum_{n_\mu} a_4^4\sum_\mu a_5|\hat{D}_\mu\phi|^2\,.
\end{aligned} \tag{3.2.29}$$

The Hybrid action, similarly to Eq. (3.2.20), contains an extra multiplicative, dimensionful a_5 factor. Adding Eq. (3.2.20) and Eq. (3.2.29), the boundary-hybrid action $S^{\mathrm{b-H}}_{S^1/\mathbb{Z}_2}$ takes the final form

$$S^{\mathrm{b-H}}_{S^1/\mathbb{Z}_2} = \sum_{n_\mu} a_4^4a_5\left[\frac{1}{4}\sum_{\mu,\nu}F^3_{\mu\nu}F^3_{\mu\nu} + \sum_\mu|\hat{D}_\mu\phi|^2\right],$$

to leading order in the lattice spacing expansion. Note that the 4d scalar field ϕ, which is a combination of the components of the 5d gauge field A_M, plays the role of a Higgs-like field for a boundary observer. In fact, the above action is just the massless, free scalar QED (SQED) in 4d. Clearly, in the absence of a potential for ϕ there is no Higgs mechanism at the classical level.

Finally, notice that $S^{\text{b-H}}_{S^1/\mathbb{Z}_2}$ contains both a_4 and a_5. As we have already mentioned, in the limit $a_4 \to 0$ the sum $\sum_{n_\mu} a_4^4 \to \int d^4x$. On the other hand, there is no summation over n_5. Since at the expansion level that we work here bulk and boundary are decoupled, we can replace a_5 in $S^{\text{b-H}}_{S^1/\mathbb{Z}_2}$ by $a_5 = \frac{\pi R}{N_5}$, independently of the bulk action. Recall also that the radius of the fifth dimension is $R \to \infty$. Therefore, we can choose $N_5 \to (0, \text{finite or } \infty)$. Now, choosing $N_5 \to \infty$ indicates that $a_5 \to\ a_5^f$, where a_5^f is an arbitrary finite and non-zero constant of mass dimension $[a_5^f] = -1$. The action $S^{\text{b-H}}_{S^1/\mathbb{Z}_2}$ therefore becomes

$$S^{\text{b-H}}_{S^1/\mathbb{Z}_2} = a_5^f \sum_{n_\mu} a_4^4 \left[\frac{1}{4} \sum_{\mu,\nu} F^3_{\mu\nu} F^3_{\mu\nu} + \sum_{\mu} |\hat{D}_\mu \phi|^2 \right] . \tag{3.2.30}$$

3.2.2 Bulk action

If it were not for the anisotropy there would be no extra calculation necessary for Eq. (3.2.10) to leading order in the lattice spacing expansion. Because of the presence of the anisotropy, we have to go through a few short steps. It is easy to see that the bulk action can be separated further into a four-dimensional part and a five-dimensional part

$$S^{\text{bulk}}_{S^1/\mathbb{Z}_2} = S_{4d} + S_{5d} \tag{3.2.31}$$

with

$$S_{4d} = \frac{\beta_4}{2N_C} \sum_{n_\mu, n_5} \sum_{\mu<\nu} \text{tr}\left\{1 - U_{\mu\nu}(n_\mu, n_5)\right\} \tag{3.2.32}$$

and

$$S_{5d} = \frac{\beta_5}{2N_C} \sum_{n_\mu, n_5} \sum_{\mu} \text{tr}\left\{1 - U_{\mu 5}(n_\mu, n_5)\right\} . \tag{3.2.33}$$

The 4d part is trivial as it is just the usual Yang-Mills action in 4d, multiplied by β_4. The plaquette is then

$$U_{\mu\nu}(n_\mu, n_5) = e^{ig_5 a_4^2 \mathbf{F}_{\mu\nu}(n_\mu, n_5)} , \tag{3.2.34}$$

with $\mathbf{F}_{\mu\nu} = F^A_{\mu\nu} T^A = \hat{\Delta}_\mu \mathbf{A}_\nu(n_\mu, n_5) - \hat{\Delta}_\nu \mathbf{A}_\mu(n_\mu, n_5) + ig_5[\mathbf{A}_\mu, \mathbf{A}_\nu]$ and the action

$$S_{4d} = \frac{1}{2} \sum_{n_\mu} a_4^4 \sum_{n_5} a_5 \sum_{\mu,\nu} \frac{1}{2} F^A_{\mu\nu} F^A_{\mu\nu} . \tag{3.2.35}$$

Now in the continuum limit where the lattice spacings go to zero we obtain a five dimensional integral since $\sum_{n_\mu} a_4^4 \sum_{n_5} a_5 \to \int d^5x$.

The plaquette along the fifth dimension is

$$U_{\mu 5}(n_\mu, n_5) = e^{ia_4 g_5 \mathbf{A}_\mu(n_\mu,n_5)} e^{ia_5 g_5 \mathbf{A_5}(n_\mu + a_4\hat{\mu}, n_5)} e^{-ia_4 g_5 \mathbf{A}_\mu(n_\mu, n_5 + a_5\hat{5})} e^{-ia_5 g_5 \mathbf{A_5}(n_\mu,n_5)} ,$$

that finally leads to

$$S_{5d} = \frac{1}{2} \sum_{n_\mu} a_4^4 \sum_{n_5} a_5 \sum_\mu \frac{1}{2} F^A_{\mu 5} F^A_{\mu 5} . \tag{3.2.36}$$

As expected, the combination of Eq. (3.2.35) and Eq. (3.2.36) is 5d covariant and the sum reconstructs to leading order into a 5d bulk action

$$S^{\text{bulk}}_{S^1/\mathbb{Z}_2} = \sum_{n_\mu} a_4^4 \sum_{n_5} a_5 \sum_{M,N} \frac{1}{4} F^A_{MN} F^A_{MN} . \tag{3.2.37}$$

We note however that if there was some kind of dimensional reduction to 4d at work, we could have expressed Eq. (3.2.36) as $\frac{1}{2}(D_\mu \Phi)^A (D_\mu \Phi)^A$ with D_μ the $SU(2)$ gauge covariant derivative. Together with Eq. (3.2.35) this term could be interpreted as a 4d gauge-adjoint Higgs system, with no classical potential though.

3.2.3 The leading order continuum action

The classical scaling dimensions of the coupling and fields can be found in Appendix 3.B. Before we take the continuum limit of Eq. (3.2.30) and Eq. (3.2.37) we perform the rescaling

$$\{\mathbf{A}_\mu, \mathbf{A}_5\} \to \frac{1}{\sqrt{a_5^f}} \{\mathbf{A}_\mu, \mathbf{A}_5\} \tag{3.2.38}$$

only on the boundary-Hybrid action, and now $\{\mathbf{A}_\mu, \mathbf{A}_5\}$ have dimension $[\mathbf{A}_\mu] = [\mathbf{A}_5] = 1$ as a usual gauge field in 4d. In particular, we get that

$$(F^3_{\mu\nu})^2 \to \frac{1}{a_5^f} (F^3_{\mu\nu})^2, \qquad |\hat{D}_\mu \phi|^2 \to \frac{1}{a_5^f} |\hat{D}_\mu \phi|^2$$

where now the covariant derivative takes the form $\hat{D}_\mu = \hat{\Delta}_\mu + i \frac{g_5}{\sqrt{a_5^f}} A^3_\mu \equiv \hat{\Delta}_\mu + ig\sqrt{\gamma} A^3_\mu$ with the dimensionless coupling and the anisotropy factor

$$g = \frac{g_5}{\sqrt{a_4}} \quad \text{and} \quad \gamma = \frac{a_4}{a_5^f} , \tag{3.2.39}$$

We can then bring the rescaled $S^{\text{b-H}}_{S^1/\mathbb{Z}_2}$ action into a 5d action by

$$\begin{aligned} S^{\text{b-H}}_{S^1/\mathbb{Z}_2} &= \sum_{n_\mu} a_4^4 \mathcal{L}_{\text{bound}} \Leftrightarrow \\ &= \sum_{n_\mu} a_4^4 \sum_{n_5} \frac{a_5}{a_5} \delta(n_5) \mathcal{L}_{\text{bound}} \Leftrightarrow \end{aligned}$$

$$S^{\text{b-H}}_{S^1/\mathbb{Z}_2} = \sum_{n_\mu} a_4^4 \sum_{n_5} a_5 \delta(a_5 n_5) \mathcal{L}_{\text{bound}} \,. \tag{3.2.40}$$

As we have already mentioned the bulk action remains untouched under the above rescaling with the field strength reading

$$F^A_{MN} = \hat{\Delta}_M A_N - \hat{\Delta}_N A_M - g_5 f^{ABC} A^B_M A^C_N \,, \tag{3.2.41}$$

and the bulk action still reading

$$S^{\text{bulk}}_{S^1/\mathbb{Z}_2} = \sum_{n_\mu} a_4^4 \sum_{n_5} a_5 \sum_{M,N} \frac{1}{4} F^A_{MN} F^A_{MN} \,. \tag{3.2.42}$$

Now we are ready to take the naive continuum limit in Eq. (3.2.40) and Eq. (3.2.42) using $\sum_{n_\mu} a_4^4 \sum_{n_5} a_5 \to \int d^5x$, $\delta(a_5 n_5) \to \delta(x_5)$, $\hat{\Delta}_M \to \partial_M$, $\hat{D}_M \to D_M$ and $\hat{p}_M = \frac{2}{a} \sin \frac{a p_M}{2} \to p_M$. Switching to Minkowski space we finally obtain the five-dimensional continuum orbifold action

$$S_{S^1/\mathbb{Z}_2} = \int d^5x \left[P(x_5) \mathcal{L}_{\text{bulk}} + \delta(x_5) \mathcal{L}_{\text{bound}} \right] , \tag{3.2.43}$$

where $\mathcal{L}_{\text{bulk}} = -\frac{1}{4} F^A_{MN} F^A_{MN}$, $\mathcal{L}_{\text{bound}} = -\frac{1}{4} F^3_{\mu\nu} F^3_{\mu\nu} + |D_\mu \phi|^2$ and $P(x_5) = 1 - \delta(x_5)$. The projection operators act in such a way that for $x_5 = 0$ they allow only $\mathcal{L}_{\text{bound}}$ and in the bulk only $\mathcal{L}_{\text{bulk}}$ to survive. The classical action Eq. (3.2.43) is invariant under the global symmetries Parity (P), Charge conjugation (C) and "Stick" symmetry ($\mathcal{S}$). For the action of these symmetries see [10]. In Appendix 3.C we work out their action on the continuum fields. This is the action that we will quantize in this paper. Due to the continuum limit, at this order, the boundary action even though otherwise completely decoupled from, is suppressed with respect to the bulk action.

3.3 Quantum effects

In the following we quantize the classical action and compute the 1-loop corrections with the goal of extracting its β-functions and anomalous dimensions. We stress that we are in a 'zero temperature' context with no compact extra dimension and associated Kaluza-Klein states. The gauge fixed action, in the R_ξ gauge, is

$$\begin{aligned} S_{S^1/\mathbb{Z}_2} &= \int d^5x \Bigg[P(x_5) \left\{ -\frac{1}{4} F^A_{MN} F^A_{MN} - \frac{1}{2\xi} (\partial_M A^A_M)^2 + \partial_M \bar{c}^C D^{CB}_M c^B \right\} \\ &+ \delta(x_5) \left\{ -\frac{1}{4} F^3_{\mu\nu} F^3_{\mu\nu} + |D_\mu \phi|^2 - \frac{1}{2\xi} (\partial_\mu A^3_\mu)^2 + \partial_\mu \bar{c}^3 \partial_\mu c^3 \right\} \Bigg] \,. \end{aligned} \tag{3.3.1}$$

In the bulk, $D^{CB}_M = \delta^{CB} \partial_M + g_5 f^{CBA} A^A_M$ and c^B, $\bar{c}^C$ are the non-Abelian ghost and anti-ghost respectively. On the boundary only the third component of c^A and $\bar{c}^A$ survive since ghosts should respect the orbifold boundary conditions which read

$$c^A(x_\mu, -x_5) = \eta^A c^A(x_\mu, x_5)$$

and at the boundary, at $x_5 = 0$, they give

$$\begin{aligned} c^a(x_\mu, 0) &= +c^a(x_\mu, 0) = c^3(x_\mu, 0)\,, \\ c^{\hat{a}}(x_\mu, 0) &= -c^{\hat{a}}(x_\mu, 0) = -c^{1,2}(x_\mu, 0) = 0\,. \end{aligned} \tag{3.3.2}$$

The gauge fixing term should also respect the corresponding boundary conditions giving

$$\partial_M A^A_M(x_\mu, -x_5) \;=\; \alpha_M \alpha_M \eta^A \partial_M A^A_M(x_\mu, x_5)$$

which means that

$$\partial_\mu A^3_\mu(x_\mu, 0) \neq 0, \;\; \partial_5 A^3_\mu(x_\mu, 0) = 0\,.$$

Therefore, it is not necessary to use separate gauge fixing and ghosts for the boundary action, since $\partial_\mu A^3_\mu$ and c^3, $\bar{c}^3$ are components of the bulk gauge fixing and ghosts terms.

The Feynman rules deriving from Eq. (3.3.1) are computed in Appendix 3.D.

3.3.1 1-loop diagrams

At 1-loop level there are four sets of possible diagrams corresponding to one-, two-, three- and four-point functions named $\mathcal{T}^i_j$, $\mathcal{M}^i_j$, $\mathcal{K}^i_j$ and $\mathcal{B}^i_j$ respectively. Here, the superscript $i = A_M, G, A_\mu, \phi$ indicates the field(s) running in the loop and the subscript $j = A_M, G, A_\mu, \phi$ the external fields. Note that the label for the boundary gauge field is $A^3_\mu \equiv A_\mu$ and the label for a generic ghost is G. The notation for the loop and external momenta is $k_M = \{q_\mu, k_5\}$ and $p_M = \{l_\mu, p_5\}$ respectively. With these in mind, we present the 1-loop integrals obtained from the 5d orbifold action Eq. (3.3.1). It is convenient to separate them to a boundary and a bulk part and evaluate them separately. In particular, the bulk 1-loop integrals will be functions of the coupling g_5, while the boundary ones will contain the coupling $g\sqrt{\gamma}$. The momentum space projector that appears in the following expressions is

$$P(p_5) = 1 - \delta_{p_5,0}\,. \tag{3.3.3}$$

We perform all calculations in the $\xi = 1$ gauge.

The 1-point function (Tadpole) vanishes both in the bulk and the boundary by Lorentz and gauge invariance. The next set of one-loop diagrams are the two-point functions $\mathcal{M}^i_j$. The first diagram here is a two-leg Tadpole due to the gauge field self interaction:

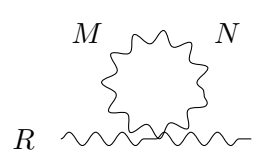

$$= i\mathcal{M}^{A_M}_{A_M,RS}\,.$$

It evaluates to

$$i\mathcal{M}^{A_M}_{A_M,RS} \;=\; ig^2\gamma \int \frac{d^5k}{(2\pi)^5} S^1_{\mathcal{M}} \Big\{ -P(k_5) K^{BCDE}_{MNRS} + 2g_{\rho\sigma}\delta_{k_5,0}\Delta_{MNRS} \Big\} \times$$

$$
\begin{aligned}
& i\Bigg\{ P(k_5)\frac{\delta^{BC}}{k^2}\Big(-g^{MN}+(1-\xi)\frac{k^M k^N}{k^2}\Big) \\
+ \quad & \frac{\delta_{k_5,0}\delta_{M,\mu}\delta_{N,\nu}}{q^2}\Big(-g^{\mu\nu}+(1-\xi)\frac{q^\mu q^\nu}{q^2}\Big)+\frac{\delta_{k_5,0}\delta_{M,5}\delta_{N,5}}{q^2}\Bigg\}, \qquad (3.3.4)
\end{aligned}
$$

where the bulk/boundary symmetry factor is given by $S^1_{\mathcal{M}} = \frac{P(k_5)}{2} + \delta_{k_5,0}$.

Taking $k_5 = 0$ (then $P(0) = 0$) projects the computation on the boundary. On the boundary there are two possible external fields, A^3_μ and ϕ, so we have two different cases. The first case corresponds to the choice $S = \sigma$, $R = \rho$, $M = 5$ and $N = 5$, giving

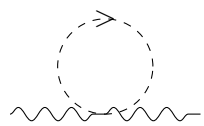

$$= i\mathcal{M}^{\phi}_{A_\mu,\rho\sigma}$$

so according to that, Eq. (3.3.4) becomes

$$\mathcal{M}^{\phi}_{A_\mu,\rho\sigma} = -2g^2\gamma g_{\rho\sigma}\int\frac{d^4q}{i(2\pi)^4}\Delta_{55\rho\sigma}\frac{1}{q^2} = -2g^2\gamma g_{\rho\sigma}\int\frac{d^4q}{i(2\pi)^4}\frac{1}{q^2} \qquad (3.3.5)$$

This is a massless Tadpole, zero in DR. Nevertheless, it is useful for the following section to convert it to a usual vacuum polarization integral. We have that

$$\mathcal{M}^{\phi}_{A_\mu,\rho\sigma} = -2g^2\gamma g_{\rho\sigma}\int\frac{d^4q}{i(2\pi)^4}\frac{q^2}{q^2(q+l)^2} = -2g^2\gamma g_{\rho\sigma}g_{\mu\nu}B^{\mu\nu}(q,q+l) \qquad (3.3.6)$$

Its contracted version

$$\mathcal{M}^{\phi}_{A_\mu} = \frac{1}{3}\Big(-g^{\rho\sigma}+\frac{l^\rho l^\sigma}{l^2}\Big)\mathcal{M}^{\phi}_{A_\mu,\rho\sigma} = 2g^2\gamma g_{\mu\nu}B^{\mu\nu}(q,q+l) \qquad (3.3.7)$$

will be also useful below. The second case corresponds to $S = 5$, $R = 5$, $M = \mu$ and $N = \nu$:

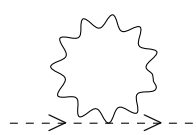

$$= i\mathcal{M}^{A_\mu}_{\phi}$$

and is equal to

$$\mathcal{M}^{A_\mu}_{\phi} = -2g^2\gamma g_{\mu\nu}\int\frac{d^4q}{i(2\pi)^4}\Delta_{\mu\nu55}\frac{-g^{\mu\nu}}{q^2} = 2dg^2\gamma\mu^{4-d}\int\frac{d^dq}{i(2\pi)^d}\frac{1}{q^2}\,. \qquad (3.3.8)$$

It is also a massless tadpole and thus zero in DR. Again, we convert it to a usual two-point function diagram

$$\mathcal{M}^{A_\mu}_{\phi} = 8g^2\gamma\int\frac{d^4q}{i(2\pi)^4}\frac{q^2}{q^2(q+l)^2} = 8g^2\gamma g_{\mu\nu}B^{\mu\nu}(q,q+l)\,. \qquad (3.3.9)$$

Next, we turn to the bulk where $k_5 \neq 0$ and $P(k_5) = 1$. The contributing diagram is

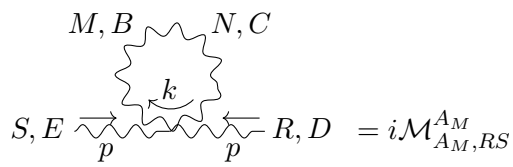

$$= i\mathcal{M}^{A_M}_{A_M,RS}$$

that evaluates to

$$\mathcal{M}^{A_M}_{A_M,RS} = -\frac{g_5^2}{2}\int \frac{d^5k}{i(2\pi)^5} K^{BCDE}_{MNRS}\frac{\delta^{BC}}{k^2} g^{MN}\,, \tag{3.3.10}$$

where here and in the following we use Eq. (3.2.39) combined with $\gamma = \frac{a_4}{a_5^f}$.
From Eq. (3.D.14) the contraction K^{BCDE}_{MNRS} with the propagator gives

$$-\delta^{BC}K^{BCDE}_{MNRS}g^{MN} = 2\mathcal{C}_A\delta^{DE}(1-d)g_{RS}$$

where we have used that $f^{ABD}f^{ABE} = \mathcal{C}_A\delta^{DE}$. So, Eq. (3.3.10) becomes

$$\mathcal{M}^{A_M}_{A_M,RS} \;=\; g_5^2\mathcal{C}_A(1-d)g_{RS}\mu^{5-d}\int\frac{d^dk}{i(2\pi)^d}\frac{\delta^{DE}}{k^2}\,. \tag{3.3.11}$$

This is a vanishing in DR massless tadpole. In other regularization schemes though it may be non-zero. To obtain a useful for such a case expression, the common trick is to multiply the integrand by $\frac{(k+p)^2}{(k+p)^2}$:

$$\begin{aligned}\mathcal{M}^{A_M}_{A_M,RS} &= g_5^2\mathcal{C}_A(1-d)g_{RS}\mu^{5-d}\int\frac{d^dk}{i(2\pi)^d}\frac{\delta^{DE}(k^2+2k\cdot p+p^2)}{k^2(k+p)^2}\\ &= g_5^2\mathcal{C}_A(1-d)g_{RS}\delta^{DE}\Big[g_{MN}B^{MN}(k,k+p)+2p_MB^M(k,k+p)+p^2B_0(k,k+p)\Big]\,.\end{aligned}$$

Then using Passarino-Veltman (PV) reduction formulae and setting $d=5$ it becomes

$$\mathcal{M}^{A_M}_{A_M,RS} \;=\; -4g_5^2\mathcal{C}_Ag_{RS}\delta^{BB'}g_{MN}B^{MN}(k,k+p)\,. \tag{3.3.12}$$

The next contribution to the two-point function is

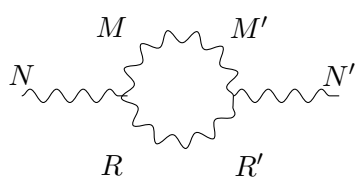

$$= i\mathcal{M}^{A_MA_M}_{A_M,NN'}$$

given by

$$\begin{aligned}i\mathcal{M}^{A_MA_M}_{A_M,NN'} &= g^2\gamma\int\frac{d^5k}{(2\pi)^5}S^2_{\mathcal{M}}\Big[P(k_5)L^{ABC}_{MNR}+i\delta_{k_5,0}Q_{MNR}\Big]\Big[P(k_5)L^{A'B'C'}_{M'N'R'}+i\delta_{k_5,0}Q_{M'N'R'}\Big]\times\\ &\quad i\Pi^{MM'}_{AA'}(k_M,q_\mu)i\Pi^{RR'}_{CC'}(k_M+p_M,q_\mu+l_\mu)\,,\end{aligned} \tag{3.3.13}$$

with $S^2_{\mathcal{M}} = \frac{P(k_5)}{2} + \delta_{k_5,0}$. It is convenient to separate at this point the boundary from the bulk.

Starting from the boundary where $P(k_5 = 0) = 0$, Eq. (3.3.13) gives

$$\mathcal{M}^{boun.}_{NN'} = g^2\gamma \int \frac{d^4q}{(2\pi)^4 i} Q_{MNR} Q_{M'N'R'} \Pi_{\mu\mu'}(q_\nu) \Pi_{\rho\rho'}(q_\nu + l_\nu)\,. \tag{3.3.14}$$

Eq. (3.3.14) corresponds to further two cases.

The first is when $(M, N, R) = (5, \nu, 5)$, $(M', N', R') = (5, \nu', 5)$, corresponding to the diagram

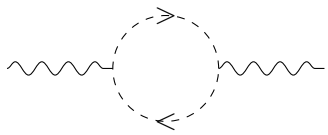

$$= i\mathcal{M}^{\phi\phi}_{A_\mu,\nu\nu'}\,.$$

This diagram is the vacuum polarization of A_μ in massless SQED and it is non-zero zero. However, this is not a quantum correction to the mass of the gauge boson but a correction to the gauge coupling. Using Eq. (3.D.13) that gives $Q_{5\nu5} = 2q_\nu + l_\nu$, $Q_{5\nu'5} = 2q_{\nu'} + l_{\nu'}$, Eq. (3.3.14) becomes

$$\mathcal{M}^{\phi\phi}_{A_\mu,\nu\nu'} = g^2\gamma \int \frac{d^4q}{(2\pi)^4 i} \frac{(2q_\nu + l_\nu)}{q^2} \frac{(2q_{\nu'} + l_{\nu'})}{(q+l)^2}\,. \tag{3.3.15}$$

This integral can be simplified by using the massless limit of standard PV formulae, see for example the Appendix of [31]. After the reduction, we obtain the expression

$$\mathcal{M}^{\phi\phi}_{A_\mu,\nu\nu'} = g^2\gamma\Big[4B_{\nu\nu'}(q, q+l) + 2l_\nu B_{\nu'}(q, q+l) + 2l_{\nu'} B_\nu(q, q+l) + l_\nu l_{\nu'} B_0(q, q+l)\Big]\,. \tag{3.3.16}$$

Finally, the contracted version of Eq. (3.3.16) is given by

$$\mathcal{M}^{\phi\phi}_{A_\mu} = \frac{1}{3}\Big(-g^{\nu\nu'} + \frac{l^\nu l^{\nu'}}{l^2}\Big)\mathcal{M}^{\phi\phi}_{A_\mu,\nu\nu'} = \frac{l^2 g^2\gamma}{3} B_0(q, q+l) - \frac{4}{3} g_{\mu\nu} B^{\mu\nu}(q, q+l)\,, \tag{3.3.17}$$

where $g_{\mu\nu}B^{\mu\nu}(q, q+l)$ corresponds to a massless tadpole integral, vanishing in DR.

The second case is when $(M, N, R) = (5, 5, \rho)$, $(M', N', R') = (5, 5, \rho)$, where now the relevant diagram is

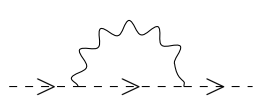

$$= i\mathcal{M}^{\phi A_\mu}_{\phi}\,.$$

Here, Eq. (3.D.13) gives $Q_{55\rho} = 2l_\rho + q_\rho$, $Q_{55\rho} = 2l_{\rho'} + q_{\rho'}$ and Eq. (3.3.14) becomes

$$\mathcal{M}^{\phi A_\mu}_{\phi} = g^2\gamma \int \frac{d^4q}{(2\pi)^4 i} \frac{-g^{\rho\rho'}}{q^2} \frac{(2l_\rho + q_\rho)(2l_{\rho'} + q_{\rho'})}{(q+l)^2}\,. \tag{3.3.18}$$

It can be reduced as

$$\begin{aligned}
\mathcal{M}_{\phi}^{\phi A_\mu} &= 4g^2\gamma\Big[-l^2 B_0(q,q+l) - l^\mu B_\mu(q,q+l) - \frac{1}{4}g^{\mu\nu}B_{\mu\nu}(q,q+l)\Big] \\
&= l^2 g^2 \gamma\Big[-2B_0(q,q+l) - g_{\mu\nu}B^{\mu\nu}(q,q+l)\Big] \\
&= l^2 g^2 \gamma M_\phi(l^2)\,,
\end{aligned} \tag{3.3.19}$$

where $M_\phi(l^2) = -2B_0(q,q+l) - g_{\mu\nu}B^{\mu\nu}(q,q+l)$ and with $g_{\mu\nu}B^{\mu\nu}(q,q+l)$ vanishing in DR. A comment before we move on is that on boundary there is no contribution from the ghost fields since they are decoupled. It is straightforward to check that the scalar field stays massless and the above correction contributes only to the anomalous dimension of ϕ.

In the bulk $P(k_5) = 1$ and there is only one diagram:

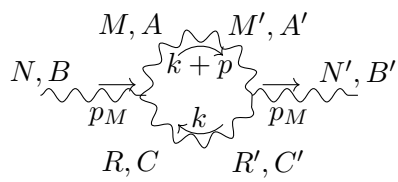

$$= \; i\mathcal{M}^{A_M A_M}_{A_M, NN'}$$

Eq. (3.3.13) in this case reads

$$\begin{aligned}
\mathcal{M}^{A_M A_M}_{A_M, NN'} &= -\frac{g_5^2}{2}\int \frac{d^5k}{(2\pi)^5 i} L^{ABC}_{NRM} L^{A'B'C'}_{N'R'M'} \Pi^{MM'}_{AA'}(k_M, q_\mu)\Pi^{RR'}_{CC'}(k_M + p_M, q_\mu + l_\mu) \\
&= -\frac{g_5^2}{2}\int \frac{d^5k}{(2\pi)^5 i} f^{ABC} f^{A'B'C'} \delta_{AA'}\delta_{CC'} G_{NRM} G_{N'R'M'} \frac{-g^{MM'}}{k^2}\frac{-g^{RR'}}{(k+p)^2}\,.
\end{aligned} \tag{3.3.20}$$

Identifying G_{MNR} from Eq. (3.D.11) for $p_{12} = p - k$, $p_{23} = 2k + p$ and $p_{31} = -k - 2p$ we have the identity

$$\begin{aligned}
G_{NRM}G_{N'R'M'}g^{MM'}g^{RR'} &= -(-6+4d)k_N k_{N'} - (-3+2d)k_N p_{N'} - (-3+2d)p_N k_{N'} \\
&- (-6+d)p_N p_{N'} - 2g_{NN'}k^2 - 2g_{NN'}k\cdot p - 5g_{NN'}p^2
\end{aligned}$$

and by following the reduction program Eq. (3.3.20) takes the final form

$$\begin{aligned}
\mathcal{M}^{A_M A_M}_{A_M, NN'} &= \frac{g_5^2}{2}\mathcal{C}_A \delta^{BB'}\Big[(-6+4d)B_{NN'}(k,k+p) + (-3+2d)p_{N'}B_N(k,k+p) \\
&+ (-3+2d)p_N B_{N'}(k,k+p) + (-6+d)p_N p_{N'}B_0(k,k+p) + 2g_{NN'}g_{AB}B^{AB}(k,k+p) \\
&+ 2g_{NN'}p_M B^M(k,k+p) + 5g_{NN'}p^2 B_0(k,k+p)\Big]\,,
\end{aligned} \tag{3.3.21}$$

where again we have used that $f^{ABC}f^{A'B'C'}\delta_{AA'}\delta_{CC'} = \mathcal{C}_A\delta^{BB'}$. Of course, the vacuum polarization diagrams of the bulk are not yet complete since they admit contributions from the ghost fields. The ghost contribution to the vacuum polarization is

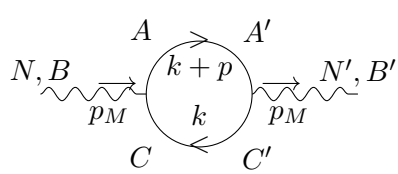

$$= \; i\mathcal{M}^{GG}_{A_M, NN'}$$

and it evaluates to

$$i\mathcal{M}^{GG}_{A_M,NN'} = (-1)g_5^2 f^{BAC} f^{B'C'A'} \int \frac{d^5k}{(2\pi)^5} S^3_{\mathcal{M}} \frac{ik_N \delta_{AA'}}{k^2} \frac{i(k+p)_{N'}\delta_{CC'}}{(k+p)^2}\,, \tag{3.3.22}$$

where the (-1) factor comes from the fact that ghosts are anti-commuting fields. Notice here that the symmetry factor is $S^3_{\mathcal{M}} = 1$ for $k_5 \neq 0$ and that $f^{BAC} f^{B'C'A'} \delta_{AA'}\delta_{CC'} = f^{BAC} f^{B'CA} = -f^{BAC} f^{B'AC} = -\mathcal{C}_A \delta^{BB'}$. The final form of the above integral is

$$\mathcal{M}^{GG}_{A_M,NN'} = -g_5^2 \mathcal{C}_A \delta^{BB'} \Big[B_{NN'}(k,k+p) + p_{N'} B_N(k,k+p) \Big]\,. \tag{3.3.23}$$

The complete vacuum polarization in the bulk is given by the sum of Eq. (3.3.12), Eq. (3.3.21) and Eq. (3.3.23):

$$\begin{aligned}
\mathcal{M}_{A,MN} &= g_5^2 \mathcal{C}_A \delta^{AB} \Big[(-4+2d) B_{MN}(k,k+p) + \frac{(-5+2d)}{2} p_N B_M(k,k+p) \\
&+ \frac{(-3+2d)}{2} p_M B_N(k,k+p) + \frac{(-6+d)}{2} p_M p_N B_0(k,k+p) + 5 g_{MN} g_{AB} B^{AB}(k,k+p) \\
&+ g_{MN} p_A B^A(k,k+p) + \frac{5}{2} g_{MN} p^2 B_0(k,k+p) \Big]
\end{aligned} \tag{3.3.24}$$

which for $d = 5$ becomes

$$\begin{aligned}
\mathcal{M}_{A,MN} &= g_5^2 \mathcal{C}_A \delta^{AB} \Big[6 B_{MN}(k,k+p) + \frac{5}{2} p_N B_M(k,k+p) \\
&+ \frac{7}{2} p_M B_N(k,k+p) - \frac{1}{2} p_M p_N B_0(k,k+p) + 5 g_{MN} g_{AB} B^{AB}(k,k+p) \\
&+ g_{MN} p_A B^A(k,k+p) + \frac{5}{2} g_{MN} p^2 B_0(k,k+p) \Big]\,.
\end{aligned} \tag{3.3.25}$$

The last one-loop two-point function diagram in the bulk corresponds to the vacuum polarization of the ghost propagator given by

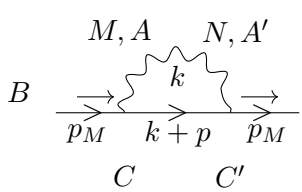

$$= i\mathcal{M}^{GA_M}_G\,.$$

Of course ghosts are not physical degrees of freedom nevertheless this contribution will play a role in the renormalization program of the bulk Lagrangian, performed in the next section. This diagram evaluates to

$$i\mathcal{M}^{GA_M}_G = g_5^2 f^{ABC} f^{A'B'C'} \int \frac{d^5k}{(2\pi)^5} S^4_{\mathcal{M}} p_M (k+p)_N \frac{-ig^{MN}\delta_{AA'}}{k^2} \frac{i\delta_{CC'}}{(k+p)^2}\,, \tag{3.3.26}$$

with symmetry factor $S^4_{\mathcal{M}} = 1$ for $k_5 \neq 0$. Finally, the above integral admits the reduced form

$$\mathcal{M}^{GA_M}_G = g_5^2 \mathcal{C}_A \delta^{BB'} \frac{p^2}{2} B_0(k,k+p)\,. \tag{3.3.27}$$

With this contribution the calculation of the $\mathcal{M}^i_j$ diagram set ends.

Now, let us move on to the $\mathcal{K}^i_j$ one-loop diagrams which correct the cubic vertices of the boundary and the bulk. In general there are two types, corresponding to reducible and irreducible diagrams called Triangles. The two types have the form

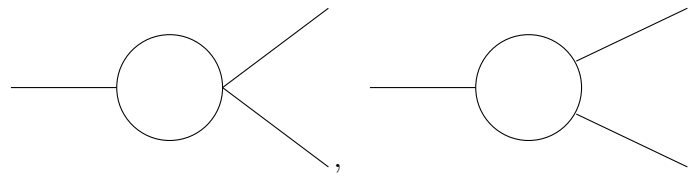

Let us first discuss the boundary. Diagrams with three A^3_μ external fields should be all zero by gauge invariance. We have checked that this is indeed the case. Another important case on the boundary is when we have Triangle diagrams with three external ϕ fields. Such a diagram, if non-zero, would be a quantum contribution to the Higgs potential that is absent at the classical level. Appendix 3.D shows that there is no possible way to connect the Feynman rules so as to obtain a Triangle diagram contributing to a scalar cubic vertex. Actually, this was expected since the existence of a vertex with three complex scalars as external legs, would violate charge conservation.

There are two non-zero Triangle diagrams on the boundary correcting the gauge-ϕ vertex. The first one is given by

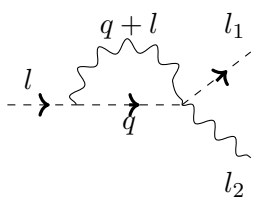

$$= i\mathcal{K}^{\phi A}_{\phi A\phi,\mu} \ ,$$

where $l + l_1 + l_2 = 0$. It is equal to

$$i\mathcal{K}^{\phi A}_{\phi A\phi,\mu} \quad = \quad 2ig^3\gamma^{3/2} ig^{\mu\nu} \int \frac{d^4q}{(2\pi)^4} i \frac{2l_{\nu'} + q_{\nu'}}{q^2} \frac{-ig_{\nu\nu'}}{(q+l)^2} \, . \tag{3.3.28}$$

Following the appropriate reduction formulae it can be written as

$$\mathcal{K}^{\phi A}_{\phi A\phi,\mu} \quad = \quad -3g^3\gamma^{3/2} l_\mu B_0(q, q+l) \, . \tag{3.3.29}$$

The second Triangle diagram correcting the gauge-scalar vertex is given by

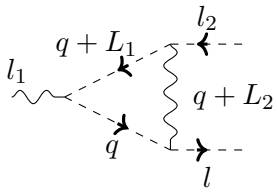

$$= i\mathcal{K}^{\phi A\phi}_{\phi A\phi,\mu} \ ,$$

where $l_1 + l_2 + l = 0$ and $L_1 = l_1$, $L_2 = l_1 + l_2$. Its explicit expression is

$$i\mathcal{K}^{A\phi\phi}_{A\phi\phi,\mu} \quad = \quad -ig^3\gamma^{3/2} \int \frac{d^4q}{(2\pi)^4} i \frac{(2q+l_1)_\mu}{q^2} \frac{(q+l_1+l_2)_\nu}{(q+L_1)^2} \frac{(q+l)_\rho}{(q+L_2)^2} g^{\nu\rho} \, .$$

$$(3.3.30)$$

Using momentum conservation to simplify the calculation its reduced form is

$$\mathcal{K}^{A\phi\phi}_{A\phi\phi,\mu} = g^3\gamma^{3/2}\Big[l_\mu B_0(q,q+l_2) - 2l^2 C_\mu(q,q+L1,q+L_2) - l_{1,\mu}l^2 C_0(q,q+L1,q+L_2)\Big]\,. \tag{3.3.31}$$

The total correction to the gauge-scalar vertex is given by the sum of Eq. (3.3.29) and Eq. (3.3.31):

$$\begin{aligned}\mathcal{K}_{A\phi\phi,\mu} &= g^3\gamma^{3/2}\Big[-3l_\mu B_0(q,q+l) + l_\mu B_0(q,q+l_2)\\ &- 2l^2 C_\mu(q,q+L1,q+L_2) - l_{1,\mu}l^2 C_0(q,q+L1,q+L_2)\Big]\,.\end{aligned} \tag{3.3.32}$$

Next we discuss the bulk, where things are quite different. In particular, recall that in the bulk lies a non-Abelian gauge theory, so there is a non-trivial classical cubic gauge-field vertex. Likewise there are Triangle diagrams with external gauge fields which are non-zero and correct this vertex. Notice also that all the vertices of the bulk action Eq. (3.3.1) contain a single coupling constant. Therefore, the renormalization program of the bulk can be done by evaluating only the Triangle diagrams that contribute as quantum corrections to the gauge-ghost vertex. This is technically simpler and 1-loop corrections come only from two irreducible diagrams. For loop momenta, we adopt the notation of [31] where $P_1 = p_1$, $P_2 = p_1 + p_2$ and $p_1 + p_2 + p = 0$. The first diagram

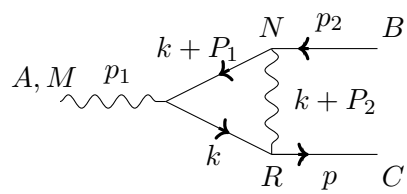

$$= i\mathcal{K}^{GAG}_{AGG,M}$$

is equal to

$$\begin{aligned}i\mathcal{K}^{GAG}_{AGG,M} &= -g_5^3 f^{AED} f^{BB'F} f^{CC'F'} \int \frac{d^5k}{(2\pi)^5} k_M (k+P_1)_N p_R \frac{i\delta^{EB'}}{k^2}\frac{i\delta^{DC'}}{(k+P_1)^2}\frac{i\delta^{FF'}}{(k+P_2)^2} g^{NR} \Rightarrow\\ \mathcal{K}^{GAG}_{AGG,M} &= g_5^3 \frac{\mathcal{C}_A}{2} f^{ABC} \int \frac{d^5k}{(2\pi)^5 i}\frac{k_M(k\cdot p + p\cdot p_1)}{k^2(k+P_1)^2(k+P_2)^2}\,,\end{aligned} \tag{3.3.33}$$

where we have used the identity $if^{AB'D} if^{BB'F} if^{CDF} = i\frac{\mathcal{C}_A}{2} f^{ABC}$. Using the usual reduction formula the above integral takes the final form

$$\mathcal{K}^{GAG}_{AGG,M} = g_5^3 \frac{\mathcal{C}_A}{2} f^{ABC}\Big[p^N C_{MN}(k,P_1,P_2) + p\cdot p_1 C_M(k,P_1,P_2)\Big]\,. \tag{3.3.34}$$

The other diagram that corrects the gauge-ghost vertex is

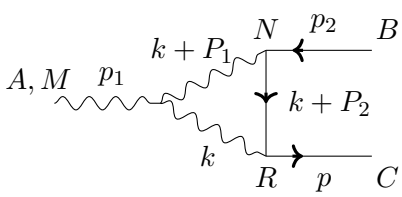

$$= i\mathcal{K}^{AGA}_{AGG,M}\,,$$

and its explicit form is

$$
\begin{aligned}
i\mathcal{K}^{AGA}_{AGG,M} &= g_5^3 f^{AED} f^{BD'F} f^{CE'F'} \int \frac{d^5k}{(2\pi)^5} G_{MNR}(k-p)_{N'} p_{R'} \frac{-ig^{RR'}\delta^{EE'}}{k^2} \\
&\times \frac{-ig^{NN'}\delta^{DD'}}{(k+P_1)^2} \frac{i\delta^{FF'}}{(k+P_2)^2} \Rightarrow \\
\mathcal{K}^{AGA}_{AGG,M} &= -g_5^3 \frac{\mathcal{C}_A}{2} f^{ABC} \int \frac{d^5k}{(2\pi)^5 i} \frac{G_{MNR}(k-p)^N p^R}{k^2(k+P_1)^2(k+P_2)^2}\,,
\end{aligned}
\tag{3.3.35}
$$

where here G_{MNR} is given in Eq. (3.D.11) for $p_{12} = p_1 - k$, $p_{23} = 2k + p_1$ and $p_{31} = -2p_1 - k$. Its reduced form is

$$
\begin{aligned}
\mathcal{K}^{AGA}_{AGG,M} &= -g_5^3 \frac{\mathcal{C}_A}{2} f^{ABC} \Big[p^N C_{MN}(k,P_1,P_2) - p_M B_0(k,k+p_2) \\
&+ (p\cdot p_1 - 2p^2) C_M(k,P_1,P_2) + 2p_M(p_N - p_{1,N}) C^N(k,P_1,P_2) \\
&+ p_{1,M} p_N C^N(k,P_1,P_2) + (p\cdot p_1 p_M - p^2 p_{1,M}) C_0(k,P_1,P_2) \Big]\,.
\end{aligned}
\tag{3.3.36}
$$

The total contribution to the gauge-ghost vertex is the sum of Eq. (3.3.34) and Eq. (3.3.36):

$$
\begin{aligned}
\mathcal{K}_{AGG,M} &= g_5^3 \frac{\mathcal{C}_A}{2} f^{ABC} \Big[p_M B_0(k,k+p_2) + 2p^2 C_M(k,P_1,P_2) - 2p_M(p_N - p_{1,N}) C^N(k,P_1,P_2) \\
&- p_{1,M} p_N C^N(k,P_1,P_2) - (p\cdot p_1 p_M - p^2 p_{1,M}) C_0(k,P_1,P_2) \Big]\,.
\end{aligned}
\tag{3.3.37}
$$

Eq. (3.3.37) along with Eq. (3.3.29) and Eq. (3.3.31) are the contributions needed to carry out the renormalization program of both the boundary and bulk Lagrangians.

There are non-vanishing Box diagrams both on the boundary and in the bulk. The role of these boxes can be quite subtle in some cases and for this reason we compute them explicitly on the boundary, in a separate Appendix 3.F. We will make some related comments in the following.

3.3.2 Renormalization, β-functions and anomalous dimensions

Boundary and bulk are decoupled to the order that we are working and renormalization can be carried out separately for the two sectors. The process needs some care in both cases because on the boundary we have a massless, free SQED and in the bulk a 5d $SU(2)$ gauge theory which is perturbatively non-renormalizable. In particular for the latter an issue is that Gamma functions have no poles in odd dimensions which makes dimensional regularization delicate. A way around this is to perform the calculations in $d = 4 - \varepsilon$ dimensions and set $\varepsilon = -1$ in the end. This version of DR is called ε-expansion, whose validity is not always guaranteed. What makes this approach interesting is that we know from lattice Monte Carlo simulations the phase diagram of the bulk theory [20] so we have a robust check. On the other hand, massive, free SQED has issues of renormalizability due to the divergent Box diagrams that we compute in Appendix 3.F. In the massive case we do not know of a smooth resolution to the problem of absorbing these divergences in counter-terms, except from the ad hoc counter-term proposed by Salam in [58]. For the massless limit however that is realized on the orbifold's boundary the dangerous

integrals are scaleless of the 0/0 type, whose limit is regularizable. We define this limit so that the resulting renormalized theory coincides with the massless, free limit of the gauge invariant 1-loop Abelian-Higgs model presented in [31].

Having assumed that the anisotropy parameter γ does not get renormalized at this order, for both the boundary and the bulk actions we have to renormalize only one coupling and the corresponding fields. In the following to simplify some expressions, following [55], we will use the auxiliary dimensionless couplings[2]

$$\alpha_{4,0} \equiv \frac{1}{(4\pi)^2}\mu^{d-4}g_0^2 \tag{3.3.38}$$

on the boundary and

$$\alpha_{5,0} \equiv \frac{2N_C}{(4\pi)^2}\mu^{d-4}g_{5,0}^2 \tag{3.3.39}$$

in the bulk. We introduce the counterterm

$$\begin{aligned} g_0 &= g + \delta g \Rightarrow \\ g_0 &= g(1+\frac{\delta g}{g}) = (1+\delta_g)g = Z_g g \end{aligned} \tag{3.3.40}$$

for the boundary gauge coupling and

$$\begin{aligned} g_{5,0} &= g_5 + \delta g_5 \Rightarrow \\ g_{5,0} &= g_5(1+\frac{\delta g_5}{g_5}) = (1+\delta_{g_5})g_5 = Z_{g_5}g_5\,, \end{aligned} \tag{3.3.41}$$

for the bulk gauge coupling. In d-dimensions the scale independence relations of the bare couplings

$$\begin{aligned} \mu\frac{dg_0}{d\mu} &= \mu\frac{d(4\pi\mu^{\frac{4-d}{2}}\sqrt{\alpha_{4,0}})}{d\mu} = 0 \\ \mu\frac{dg_{5,0}}{d\mu} &= \mu\frac{d(4\pi\mu^{\frac{4-d}{2}}\sqrt{\frac{\alpha_{5,0}}{2N_C}})}{d\mu} = 0 \end{aligned} \tag{3.3.42}$$

generate the β-function equations. Finally, for the anomalous dimensions of the fields we define

$$\phi_0 = \sqrt{Z_\phi}\phi = \sqrt{1+\delta_\phi}\phi \tag{3.3.43}$$

$$A_{\mu,0} = \sqrt{Z_{A_\mu}}A_\mu = \sqrt{1+\delta_{A_\mu}}A_\mu \tag{3.3.44}$$

$$A_{M,0} = \sqrt{Z_{A_M}}A_M = \sqrt{1+\delta_{A_M}}A_M \tag{3.3.45}$$

$$c_0^A = \sqrt{Z_{c^A}}c^A = \sqrt{1+\delta_{c^A}}c^A \tag{3.3.46}$$

$$\bar{c}_0^A = \sqrt{Z_{c^A}}\bar{c}^A = \sqrt{1+\delta_{c^A}}\bar{c}^A \tag{3.3.47}$$

where the subscript 0 indicates bare quantities.

[2] From this point on several old and new (not necessarily independent) couplings will appear. To facilitate the reader we list them in Appendix 3.A.

Let us start from the bare boundary Lagrangian given by

$$\begin{aligned}\mathcal{L}_{\text{bound},0} &= -\frac{1}{4}F^3_{\mu\nu,0}F^3_{\mu\nu,0} + \partial_\mu\bar{\phi}_0\partial_\mu\phi_0 - \frac{1}{2}(\partial_\mu A^3_{\mu,0})^2 + \partial_\mu\bar{c}^3_0\partial_\mu c^3_0 \\ &+ ig_0\sqrt{\gamma}A^3_{\mu,0}\Big(\phi_0\partial_\mu\bar{\phi}_0 - \bar{\phi}_0\partial_\mu\phi_0\Big) + g_0^2\gamma(A^3_{\mu,0})^2\bar{\phi}_0\phi_0 \end{aligned} \tag{3.3.48}$$

where substituting Eq. (3.3.40), Eq. (3.3.43) and Eq. (3.3.44) we obtain

$$\mathcal{L}_{\text{bound},0} = \mathcal{L}_R + \mathcal{L}_{\text{count.}}$$

with $\mathcal{L}_R$ the renormalized Lagrangian

$$\begin{aligned}\mathcal{L}_R &= -\frac{1}{4}F^3_{\mu\nu}F^3_{\mu\nu} + \partial_\mu\bar{\phi}\partial_\mu\phi - \frac{1}{2}(\partial_\mu A^3_\mu)^2 + \partial_\mu\bar{c}^3\partial_\mu c^3 \\ &+ ig\sqrt{\gamma}A^3_\mu\Big(\phi\partial_\mu\bar{\phi} - \bar{\phi}\partial_\mu\phi\Big) + g^2\gamma(A^3_\mu)^2\bar{\phi}\phi\,, \end{aligned} \tag{3.3.49}$$

and $\mathcal{L}_{\text{count.}}$ the counter-term Lagrangian

$$\begin{aligned}\mathcal{L}_{\text{count.}} &= \frac{1}{2}\Big\{-\delta_{A_\mu}g_{\mu\nu}l^2 + \mathcal{M}^{\phi\phi}_{A_\mu,\mu\nu}\Big\}A^{3,\mu}A^{3,\nu} + \Big\{\delta_\phi l^2 + \mathcal{M}^{\phi A_\mu}_{\phi}\Big\}\phi\bar{\phi} \\ &+ \Big\{g\sqrt{\gamma}\delta_3 l_\mu + \mathcal{K}_{A\phi\phi,\mu}\Big\}A^3_\mu\phi\bar{\phi} + \Big\{\delta_4 g^2\gamma + \mathcal{B}_{A\phi A\phi}\Big\}(A^3_\mu)^2\phi\bar{\phi}\,. \end{aligned} \tag{3.3.50}$$

For the gauge-scalar three- and four-point vertices the following relations hold:

$$\begin{aligned} Z_3 &= Z_g Z_\phi\sqrt{Z_{A_\mu}} \Rightarrow \\ 1+\delta_3 &= (1+\delta_g)(1+\delta_\phi)(1+\frac{1}{2}\delta_{A_\mu}) \Rightarrow \\ \delta_3 &= \delta_g + \delta_\phi + \frac{1}{2}\delta_{A_\mu} \end{aligned} \tag{3.3.51}$$

and

$$\begin{aligned} Z_4 &= Z_g^2 Z_\phi Z_{A_\mu} \Rightarrow \\ 1+\delta_4 &= (1+2\delta_g)(1+\delta_\phi)(1+\delta_{A_\mu}) \Rightarrow \\ \delta_4 &= 2\delta_g + \delta_\phi + \delta_{A_\mu} \end{aligned} \tag{3.3.52}$$

respectively. Ghosts are completely decoupled in SQED, thus there is no need to renormalize them. The Feynman rules for the counter-terms deriving from Eq. (3.3.50) are

- Gauge boson 2-point function

$$= -i\delta_{A_\mu}g_{\mu\nu}l^2$$

- Scalar 2-point function

$$= i\delta_\phi l^2$$

- The A_μ-ϕ-$\bar{\phi}$ counterterm vertex

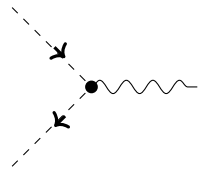

$$= ig\sqrt{\gamma}\delta_3 l_\mu$$

- The A_μ-A_ν-ϕ-$\bar{\phi}$ vertex counterterm

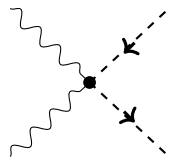

$$= 2ig_{\mu\nu}\delta_4 g^2\gamma \ .$$

The renormalization conditions needed to make the theory finite at 1-loop are in order. For the gauge boson propagator, diagrammatically, we have that

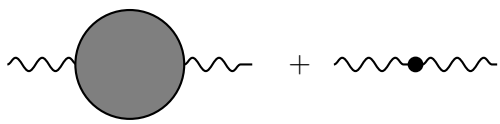

$$= 0$$

This implies that the contracted gauge propagator satisfies

$$-\frac{1}{3}\left(g_{\mu\nu} - \frac{l_\mu l_\nu}{l^2}\right)(-\delta_{A_\mu} g_{\mu\nu} l^2) + \mathcal{M}^{\phi\phi}_{A_\mu} = 0\,. \tag{3.3.53}$$

The second condition demands that

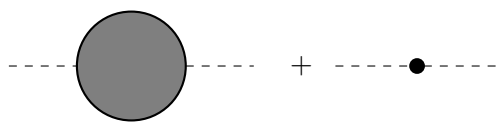

$$= 0$$

which, as equation, reads

$$\delta_\phi l^2 + \mathcal{M}^{\phi A_\mu}_{\phi} = 0\,. \tag{3.3.54}$$

Finally, the condition for the three-point vertex demands

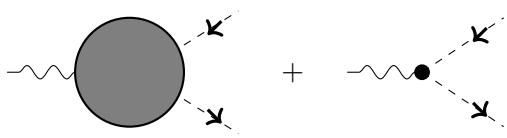

$$= 0$$

or

$$g\sqrt{\gamma}\delta_3 l_\mu + \mathcal{K}_{A\phi\phi,\mu} = 0\,. \tag{3.3.55}$$

Regarding the bulk, following similar arguments as for the boundary, we have the bare bulk Lagrangian

$$\mathcal{L}_{\text{bulk},0} \;=\; -\frac{1}{4}\Big(\partial_M A^A_{N,0} - \partial_N A^A_{M,0}\Big)^2 - \frac{1}{2}(\partial_M A^A_{M,0})^2 + \partial_M \bar{c}^B_0 \partial_M c^B_0$$

$$
\begin{aligned}
&- \quad g_{5,0} f^{ABC} \partial_M A^A_{N,0} A^B_{M,0} A^C_{N,0} - \frac{1}{4} g_{5,0}^2 \gamma (f^{ABC} A^B_{M,0} A^C_{N,0})(f^{ADE} A^D_{M,0} A^E_{N,0}) \\
&+ \quad g_{5,0} f^{CBA} \partial_M \bar{c}^C_0 c^B_0 A^A_{M,0} \, . \qquad (3.3.56)
\end{aligned}
$$

Substituting Eq. (3.3.41), Eq. (3.3.45), Eq. (3.3.46) and Eq. (3.3.47) we get that

$$
\mathcal{L}_{\text{bulk},0} \quad = \quad \mathcal{L}_R + \mathcal{L}_{\text{count.}}
$$

with $\mathcal{L}_R$ given by

$$
\begin{aligned}
\mathcal{L}_R \quad &= \quad -\frac{1}{4}\Big(\partial_M A^A_N - \partial_N A^A_M\Big)^2 - \frac{1}{2}(\partial_M A^A_M)^2 + \Lambda_5 \partial_M \bar{c}^B \partial_M c^B \\
&- \quad g_5 f^{ABC} \partial_M A^A_N A^B_M A^C_N - \frac{1}{4} g_5^2 (f^{ABC} A^B_M A^C_N)(f^{ADE} A^D_M A^E_N) \\
&+ \quad g_{5,0} f^{CBA} \partial_M \bar{c}^C c^B A^A_M \qquad (3.3.57)
\end{aligned}
$$

and $\mathcal{L}_{\text{count.}}$ by

$$
\begin{aligned}
\mathcal{L}_{\text{count.}} \quad &= \quad \frac{1}{2}\Big\{-\delta^{AB} g_{MN} p^2 \delta_{A_M} + \mathcal{M}_{A,MN}\Big\} A^A_M A^B_N + \Big\{-\delta^{AB} p^2 \delta_{c^A} + \mathcal{M}^{GA_M}_G\Big\} c^A \bar{c}^B \\
&+ \quad \Big\{-g_5 p_M f^{ABC} \delta_{A_3} + \mathcal{K}_{A_M,M}\Big\} A^A_N A^B_M A^C_N \\
&+ \quad \Big\{-g_5^2 g_{MN} g_{RS} f^{ABC} f^{ADE} \delta_{A_4} + \mathcal{B}_{A_M,MNRS}\Big\} (A^B_M A^C_N)(A^D_R A^E_S) \\
&+ \quad \Big\{-i g_5 f^{ABC} p_M \delta_1 + \mathcal{K}_{AGG,M}\Big\} c^A \bar{c}^B A_M \, , \qquad (3.3.58)
\end{aligned}
$$

where we have defined

$$
\begin{aligned}
Z_1 \quad &= \quad Z_{g_5} Z_{c^A} \sqrt{Z_{A_M}} \Rightarrow \\
1 + \delta_1 \quad &= \quad (1 + \delta_{g_5})(1 + \delta_{c^A})(1 + \frac{1}{2}\delta_{A_M}) \Rightarrow \\
\delta_1 \quad &= \quad \delta_{g_5} + \delta_{c^A} + \frac{1}{2}\delta_{A_M} \qquad (3.3.59)
\end{aligned}
$$

and $\delta_{A_3} = \frac{3}{2}\delta_{A_M}$, $\delta_{A_4} = 2\delta_{A_M}$. In order to renormalize the above Lagrangian we need three renormalization conditions. The Feynman rules for the counter-terms are

- Gauge boson 2-point function

$$= -i\delta^{AB} g_{MN} p^2 \delta_{A_M}$$

- Ghost 2-point function

$$= -i\delta^{AB} p^2 \delta_{c^A}$$

- The A_M-c-$\bar{c}$ counterterm vertex

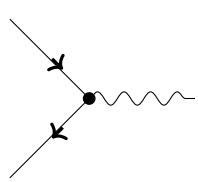

$$= g_5 \delta_1 f^{ABC} p_M \, .$$

The renormalization conditions for the bulk Lagrangian are next in order. For the gauge boson propagator, diagrammatically, we have

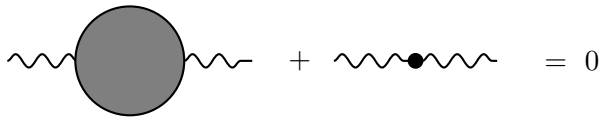

which yields

$$-\frac{1}{d-1}\left(g_{MN}-\frac{p_M p_N}{p^2}\right)\left[-\delta^{AB}g_{MN}p^2\delta_{A_M}+\mathcal{M}_{A,MN}\right]=0\,. \tag{3.3.60}$$

The second condition demands that

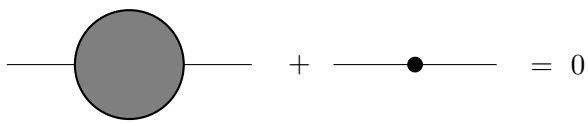

which, in equation form is

$$-\delta^{AB}p^2\delta_{c^A}+\mathcal{M}_G^{GA_M}=0\,. \tag{3.3.61}$$

The third condition involves the three-point vertex and requires

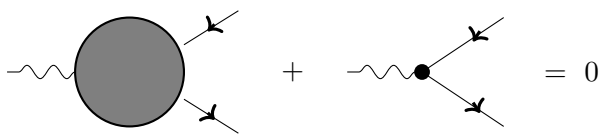

translating into

$$g_5 f^{ABC}p_M\delta_1+\mathcal{K}_{AGG,M}=0\,. \tag{3.3.62}$$

Next we evaluate the 1-loop integrals in Dimensional Regularization.

Let us start with the boundary where things are more straightforward. There, the corresponding diagrams are four-dimensional PV scalar and tensor integrals and their values in DR is standard. The complete vacuum polarization diagram is given by Eq. (3.3.17) and in DR by

$$\begin{aligned}\mathcal{M}_{A_\mu}^{\phi\phi} &= \frac{l^2g^2\gamma}{3}B_0(q,q+l)\\ &= \frac{1}{16\pi^2}\left[\frac{2l^2g^2\gamma}{3}\frac{1}{\varepsilon}\right]+(\mathcal{M}_{A_\mu}^{\phi\phi})_f\,,\end{aligned} \tag{3.3.63}$$

where $(\mathcal{M}_{A_\mu}^{\phi\phi})_f$ corresponds to the finite part. Recall that on the boundary lies a massless SQED so the pole of the propagators is at $l^2=0$. In the on-shell renormalization scheme we demand that the external momenta are equal to zero and also that the subtraction point is at $\mu=0$. Therefore the finite parts of the one-loop diagrams, proportional to $\ln\frac{\mu^2}{l^2}$ can be made to vanish in the on-shell limit. Substituting Eq. (3.3.63) in the condition of the gauge field renormalization, Eq. (3.3.53), we obtain

$$\delta_{A_\mu}l^2 = -\mathcal{M}_{A_\mu}^{\phi\phi}\Rightarrow$$

$$\delta_{A_\mu} = \frac{1}{16\pi^2}\Big[-\frac{2g^2\gamma}{3}\frac{1}{\varepsilon}\Big]. \tag{3.3.64}$$

The scalar propagator is given by Eq. (3.3.19), which in DR reads

$$\begin{aligned}\mathcal{M}_\phi^{\phi A_\mu} &= -2l^2g^2B_0(q,q+l)\\ &= \frac{1}{16\pi^2}\Big[-4l^2g^2\gamma\frac{1}{\varepsilon}\Big] + (\mathcal{M}_\phi^{\phi A_\mu})_f\,. \end{aligned}\tag{3.3.65}$$

Substituting this in the condition Eq. (3.3.54) we obtain

$$\begin{aligned}\delta_\phi l^2 &= -\mathcal{M}_\phi^{\phi A_\mu} \Rightarrow\\ \delta_\phi &= \frac{1}{16\pi^2}\Big[4g^2\gamma\frac{1}{\varepsilon}\Big]. \end{aligned}\tag{3.3.66}$$

Finally, the one-loop contribution to the three-point vertex is given by Eq. (3.3.37) and specifically in DR it is

$$\begin{aligned}\mathcal{K}_{A\phi\phi,\mu} &= g^3\gamma^{3/2}\Big[-3l_\mu B_0(q,q+l) + l_\mu B_0(q,q+l_2)\\ &- 2l^2C_\mu(q,q+L1,q+L_2) - l_{1,\mu}l^2C_0(q,q+L1,q+L_2)\Big] \Rightarrow\\ \mathcal{K}_{A\phi\phi,\mu} &= \frac{1}{16\pi^2}\Big[-4g^3\gamma^{3/2}l_\mu\frac{1}{\varepsilon}\Big] + (\mathcal{K}_{A\phi\phi,\mu})_f\,. \end{aligned}\tag{3.3.67}$$

Substituting in the vertex condition, Eq. (3.3.55), we get

$$\begin{aligned}g\sqrt{\gamma}\delta_3 l_\mu &= -\mathcal{K}_{A\phi\phi,\mu} \Rightarrow\\ \delta_3 &= \frac{1}{16\pi^2}\Big[4g^2\gamma\frac{1}{\varepsilon}\Big] - \frac{1}{g\sqrt{\gamma}}(\mathcal{K}_{A\phi\phi,\mu})_f\,. \end{aligned}\tag{3.3.68}$$

Using the result $\delta_3 = \delta_\phi$ along with Eq. (5.2.49) we have

$$\begin{aligned}\delta_g &= -\frac{1}{2}\delta_{A_\mu} - \frac{1}{g\sqrt{\gamma}}(\mathcal{K}_{A\phi\phi,\mu})_f \Rightarrow\\ \delta_g &= \frac{1}{16\pi^2}\Big[\frac{g^2\gamma}{3}\frac{1}{\varepsilon}\Big] - \frac{1}{g\sqrt{\gamma}}(\mathcal{K}_{A\phi\phi,\mu})_f \Rightarrow\\ \delta g &= \frac{1}{16\pi^2}\Big[\frac{g^3\gamma}{3}\frac{1}{\varepsilon}\Big] - \frac{1}{\sqrt{\gamma}}(\mathcal{K}_{A\phi\phi,\mu})_f \end{aligned}\tag{3.3.69}$$

and we see that the renormalization of the coupling comes only through the renormalization of the gauge field. Thus, we need only one counter-term for the A_μ and g renormalizations. Finally, knowing δ_g, δ_ϕ and δ_{A_μ} we can fix from Eq. (5.2.50) the four-vertex counter-term:

$$\delta_4 = \frac{1}{16\pi^2}\Big[4g^2\gamma\frac{1}{\varepsilon}\Big] + (\mathcal{B}_{A\phi A\phi})_f\,, \tag{3.3.70}$$

which is equal to δ_ϕ and δ_3 at the divergent part level. Now we can write down the renormalized boundary Lagrangian in the on-shell scheme:

$$\mathcal{L}_{\text{bound}} = -\frac{1}{4}F^3_{\mu\nu}F^3_{\mu\nu} + \partial_\mu\bar{\phi}\partial_\mu\phi - \frac{1}{2\xi}(\partial_\mu A^3_\mu)^2 + \partial_\mu\bar{c}^3\partial_\mu c^3$$

$$+ \quad ig\sqrt{\gamma}A^3_\mu\Big(\phi\partial_\mu\bar{\phi} - \bar{\phi}\partial_\mu\phi\Big) + g^2\gamma(A^3_\mu)^2\bar{\phi}\phi\,. \tag{3.3.71}$$

The 1-loop corrected action still has a vanishing potential after renormalization after regularizing the finite parts to zero. In addition we are able to determine the β-function of the gauge coupling. We need Eq. (3.3.40) and Eq. (3.3.38) which in DR and around four-dimensions, imply that

$$\boldsymbol{\beta}_{\alpha_4} \equiv \mu\frac{d\alpha_4(\mu)}{d\mu} = -\varepsilon\alpha_4 + \frac{2\gamma}{3}\alpha_4^2\,, \tag{3.3.72}$$

where the first and the second term correspond to the classical and the quantum parts of the β-function. The classical contribution vanishing in 4d, the solution of the above RG equation is

$$\alpha_4(\mu) = \frac{3}{\gamma\ln\frac{\mu^2_{L4}}{\mu^2}}\,. \tag{3.3.73}$$

Here,

$$\mu_{L4} = me^{\frac{3}{2\gamma\alpha_{4,m}}} \tag{3.3.74}$$

is the Landau pole of the boundary gauge coupling with m a reference mass scale where $\alpha_4(m) = \alpha_{4,m}$. Finally, notice that from Eq. (3.3.38) it holds that

$$\begin{aligned}\frac{1}{g\mu^{-\frac{\varepsilon}{2}}}\boldsymbol{\beta}_{g\mu^{-\frac{\varepsilon}{2}}} &= \frac{1}{2\alpha_4}\boldsymbol{\beta}_{\alpha_4} \Rightarrow \\ \boldsymbol{\beta}_{g\mu^{-\frac{\varepsilon}{2}}} &= -\frac{\varepsilon}{2}g\mu^{\frac{-\varepsilon}{2}} + \frac{1}{16\pi^2}\frac{g^3\gamma\mu^{\frac{-3\varepsilon}{2}}}{3}\,.\end{aligned} \tag{3.3.75}$$

We now move to the bulk where the computation in DR and the associated renormalization program are done in the ε-expansion. In particular for $d = 5$, we expand the theory around $d = 4 - \varepsilon$ and after renormalization we set $\varepsilon = -1$. In fact, in the bulk we have a 5d $SU(2)$ theory whose corresponding β-functions and anomalous dimensions are known in the ε-expansion since a long time (up to the ε factor they are identical to the $d = 4$ data) and in principle we could give directly those results. For future use however we go through some of the standard steps. Starting from the vacuum polarization of the gauge field Eq. (3.3.24) and performing the Feynman parameterization on its contracted version we have in DR

$$\begin{aligned}\mathcal{M}_A &= \frac{1}{3}(-g^{MN} + \frac{p^M p^N}{p^2})\mathcal{M}_{A,MN} \\ &= \frac{p^2 g_5^2\mathcal{C}_A\delta^{AB}}{16\pi^2}\Big[-\frac{10}{3}\frac{1}{\varepsilon}\Big] + (\mathcal{M}_A)^{DR}_f\,,\end{aligned} \tag{3.3.76}$$

where $(\mathcal{M}_A)^{DR}_f$ is the finite part and it is proportional to $\ln\frac{\mu^2}{p^2}$. Notice here that we have performed the contraction of $\mathcal{M}_A$ in 4-dimensions even though the bulk is five-dimensional. Next follows the correction to the ghost propagator given by Eq. (3.3.27). This contribution reads

$$\mathcal{M}_G^{GA_M} = \frac{p^2 g_5^2\mathcal{C}_A\delta^{AB}}{16\pi^2}\Big[\frac{1}{\varepsilon}\Big] + (\mathcal{M}_G^{GA_M})^{DR}_f\,, \tag{3.3.77}$$

where $(\mathcal{M}_G^{GA_M})_f^{DR}$ is proportional to $\ln\frac{\mu^2}{p^2}$. Finally, the correction to the gauge-ghost vertex given by Eq. (3.3.37) is equal to

$$\mathcal{K}_{AGG} = \frac{p_M g_5^3 \mathcal{C}_A f^{ABC}}{16\pi^2}\left[\frac{1}{\varepsilon}\right] + (\mathcal{K}_{AGG})_f^{DR}\,, \tag{3.3.78}$$

where $(\mathcal{K}_{AGG})_f^{DR}$ is the finite part. We can now use these results in the bulk renormalization conditions in Sect.3.3.2. In the on-shell scheme where $p^2 = 0$ (and where the finite parts of Eq. (3.3.76) and Eq. (3.3.77) are zero) the first condition Eq. (3.3.60) gives

$$\begin{aligned} \delta^{AB} p^2 \delta_{A_M} &= -\mathcal{M}_A \Rightarrow \\ \delta_{A_M} &= \frac{g_5^2 \mathcal{C}_A}{16\pi^2}\left[\frac{10}{3}\frac{1}{\varepsilon}\right]. \end{aligned} \tag{3.3.79}$$

The second condition corresponding to the ghost propagator is given by Eq. (3.3.61) and reads

$$\begin{aligned} -\delta^{AB} p^2 \delta_{c^A} &= -\mathcal{M}_G^{GA_M} \Rightarrow \\ \delta_{c^A} &= \frac{g_5^2 \mathcal{C}_A}{16\pi^2}\left[\frac{1}{\varepsilon}\right]. \end{aligned} \tag{3.3.80}$$

Finally, the third renormalization condition Eq. (3.3.62) combined with Eq. (3.3.78) gives

$$\begin{aligned} g_5 f^{ABC} p_M \delta_1 &= -\mathcal{K}_{AGG,M} \Rightarrow \\ \delta_1 &= \frac{g_5^2 \mathcal{C}_A}{16\pi^2}\left[-\frac{1}{\varepsilon}\right] + \frac{(\mathcal{K}_{AGG})_f}{g_5}\,. \end{aligned} \tag{3.3.81}$$

Then the counter-term of the gauge coupling from Eq. (3.3.59) is

$$\begin{aligned} \delta_{g_5} &= \frac{g_5^2 \mathcal{C}_A}{16\pi^2}\left[-\frac{11}{3}\frac{1}{\varepsilon}\right] - \frac{(\mathcal{K}_{AGG})_f}{g_5} \Rightarrow \\ \delta g_5 &= \frac{g_5^3 \mathcal{C}_A}{16\pi^2}\left[-\frac{11}{3}\frac{1}{\varepsilon}\right] - (\mathcal{K}_{AGG})_f\,. \end{aligned} \tag{3.3.82}$$

All the counterterms of the bulk theory are now fixed and we can write down the renormalized bulk Lagrangian:

$$\begin{aligned} \mathcal{L}_{\text{bulk}} &= -\frac{1}{4}\Big(\partial_M A_N^A - \partial_N A_M^A\Big)^2 + \partial_M \bar{c}^B \partial_M c^B \\ &- g_5 f^{ABC}(\partial_M A_N^A) A_M^B A_N^C - \frac{1}{4} g_5^2 (f^{ABC} A_M^B A_N^C)(f^{ADE} A_M^D A_N^E) \\ &+ g_5 f^{CBA}(\partial_M \bar{c}^C) c^B A_M^A\,. \end{aligned} \tag{3.3.83}$$

The β-function can be determined from Eq. (3.3.41), Eq. (3.3.39) and Eq. (3.3.42) that in the ε-expansion give

$$\boldsymbol{\beta}_{\alpha_5} \equiv \mu \frac{d\alpha_5(\mu)}{d\mu} = -\varepsilon\alpha_5 - \frac{11\mathcal{C}_A \alpha_5^2}{3N_C}\,. \tag{3.3.84}$$

Notice that $\boldsymbol{\beta}_{\alpha_5}$ consists of a classical and a quantum part, where the latter corresponds to the usual one-loop β-function of an $SU(N)$ gauge theory in $d = 4$, originally calculated in [53]. We can also form a dimensionless in d-dimensions coupling, $g_5\mu^{-\frac{\varepsilon}{2}}$, whose β-function is

$$\frac{1}{g_5\mu^{-\frac{\varepsilon}{2}}}\boldsymbol{\beta}_{g_5\mu^{-\frac{\varepsilon}{2}}} = \frac{1}{2\alpha_5}\boldsymbol{\beta}_{\alpha_5} \Rightarrow$$

$$\boldsymbol{\beta}_{g_5\mu^{-\frac{\varepsilon}{2}}} = -\frac{\varepsilon}{2}g_5\mu^{\frac{-\varepsilon}{2}} - \frac{1}{16\pi^2}\frac{11\mathcal{C}_A}{3}g_5^3\mu^{\frac{-3\varepsilon}{2}} . \tag{3.3.85}$$

The solution of the RG equation Eq. (3.3.84) then is

$$\alpha_5(\mu) = \frac{3N_C\varepsilon M^\varepsilon}{11\mathcal{C}_A\alpha_{5,M}(\mu^\varepsilon - M^\varepsilon) + 3N_C\varepsilon\mu^\varepsilon}\alpha_{5,M} \tag{3.3.86}$$

that satisfies $\alpha_5(M) = \alpha_{5,M}$ at some reference mass scale M. There is a potential Landau pole to this equation, at the scale μ_{L5} where the denominator vanishes:

$$\mu_{L5} = M\left(\frac{11\mathcal{C}_A\alpha_{5,M}}{11\mathcal{C}_A\alpha_{5,M} + 3N_C\varepsilon}\right)^{1/\varepsilon} . \tag{3.3.87}$$

The Landau pole above is real and positive when $\alpha_{5,M} > -\frac{3N_C}{11\mathcal{C}_A}\varepsilon$. For $SU(2)$ ($\mathcal{C}_A = 2$ and $N_C = 2$) in $d = 5$ this is $\alpha_{5,M} > 3/11$. Then,

$$\mu_{L5} = M\frac{11\alpha_{5,M} - 3}{11\alpha_{5,M}} . \tag{3.3.88}$$

Suppose now that we pick a reference scale such that $\alpha_{5,M} < -\frac{3N_C}{11\mathcal{C}_A}\varepsilon$. The RG equation tells us that with this choice there can not be a Landau pole, as long as the value $\alpha_{5*} = -\frac{3N_C}{11\mathcal{C}_A}\varepsilon$ is not crossed. In fact, as we will see in the next section this is precisely the value of the coupling on the non-trivial fixed point, where $\mu_* = \infty$ and there is a continuum limit.[3] Thus, the Landau branch is disconnected from the branch with the continuum limit where $\alpha < \alpha_{5*}$. Finally if $\alpha_{5,M} = -\frac{3N_C}{11\mathcal{C}_A}\varepsilon$, then Eq. (3.3.86) indicates that the coupling freezes at μ_* and does not run.

3.4 RG Flows and the Phase Diagram

We now apply the above formalism to the boundary and bulk couplings and operators. The couplings and their associated operators of interest here are g and $\mathcal{O}_{A\phi\bar{\phi}} = A_\mu\phi\partial_\mu\bar{\phi}$ on the boundary and g_5 and $\mathcal{O}_{AAA} = (\partial_M A_N)A_M A_N$ in the bulk.

3.4.1 Boundary

On the boundary there is a massless, free SQED with a β-function given by Eq. (3.3.72). In terms of g, and using Eq. (3.3.75) we can rewrite the β-function according to Eq. (3.B.11) as

$$\begin{aligned}\boldsymbol{\beta}_{g\mu^{-\frac{\varepsilon}{2}}} &= (d - \frac{\varepsilon}{2} - d)g\mu^{\frac{-\varepsilon}{2}} + \frac{1}{16\pi^2}\frac{g^3\gamma\mu^{\frac{-3\varepsilon}{2}}}{3} \\ &= (d_{\mathcal{O}_{A\phi\bar{\phi}}} - d)g\mu^{\frac{-\varepsilon}{2}} + \boldsymbol{\beta}_g^1 ,\end{aligned} \tag{3.4.1}$$

with $d_{\mathcal{O}_{A\phi\bar{\phi}}} = d - \frac{\varepsilon}{2}$ and $\boldsymbol{\beta}_g^1 = \frac{1}{16\pi^2}\left[\frac{g^3\gamma\mu^{\frac{-3\varepsilon}{2}}}{3}\right]$. The anomalous dimensions of A_μ and ϕ are given by

$$\boldsymbol{\gamma}_{A_\mu} = \frac{1}{16\pi^2}\frac{2g^2\gamma\mu^{-\varepsilon}}{3} = \frac{2}{3}\alpha_4\gamma , \tag{3.4.2}$$

[3] When we say here and in the following "continuum limit", we really mean "continuum limit to 1-loop in the ε-expansion", as explained in the Introduction.

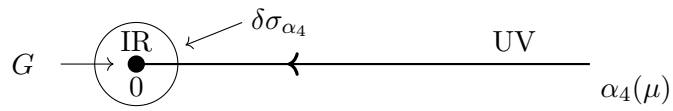

Figure 3.1: The RG flow for the marginally irrelevant boundary coupling, $\alpha_4(\mu)$. G is the IR Gaussian fixed point where $\alpha_4 = 0$ and $\delta\sigma_{\alpha_4}$ is a small region around G.

$$\boldsymbol{\gamma}_\phi \quad = \quad -\frac{1}{16\pi^2}4g^2\gamma\mu^{-\varepsilon} = -4\alpha_4\gamma \tag{3.4.3}$$

respectively. The DR here is for $d = 4$ which corresponds to $\varepsilon = 0$. The classical dimension of the marginal operator is $d_{\mathcal{O}_{A\phi\bar{\phi}}} = 4 = d$ and Eq. (3.4.1) becomes

$$\boldsymbol{\beta}_{g\mu^{\frac{-\varepsilon}{2}}} \quad = \quad \frac{1}{16\pi^2}\frac{g^3\gamma}{3}\,. \tag{3.4.4}$$

The β-function vanishes for $g = 0$ where a Gaussian, IR fixed point G is located. At the Gaussian fixed point the anomalous dimensions $\boldsymbol{\gamma}_{A_\mu}$ and $\boldsymbol{\gamma}_\phi$ vanish and according to Eq. (3.B.14), $\Delta_{g\mathcal{O}_{A\phi\bar{\phi}}} = d_{\mathcal{O}_{A\phi\bar{\phi}}}$. Now Eq. (3.B.16) tells us that g (or α_4) is marginal. From Eq. (3.3.73) we see that $\alpha_4(\mu) \to 0$ as $\mu \to 0$, i.e. it inherits the triviality of the 5d gauge coupling and becomes along with $g\mathcal{O}_{A\phi\bar{\phi}}$ marginally irrelevant in the IR.

We conclude that the boundary theory flows from the UV to the IR and reaches G, where the theory becomes non-interacting and without a mass-gap: the massless, free SQED breaks down to a free Maxwell theory and a free, massless scalar theory, both 4d CFT's. A qualitative picture showing the one-dimensional direction of RG flow for the boundary coupling $\alpha_4(\mu)$ is given in Fig. 3.1.

At this stage the boundary theory's quantum behaviour on (near) G should better be analyzed by exact (softly deformed) CFT techniques.

3.4.2 Bulk

In d-dimensions $\boldsymbol{\beta}_{\alpha_5}$ (or equivalently $\boldsymbol{\beta}_{g_5\mu^{\frac{-\varepsilon}{2}}}$), is given by Eq. (3.3.84) (or by Eq. (3.3.85)). According to Eq. (3.B.11) we have

$$\begin{aligned}\boldsymbol{\beta}_{g_5\mu^{\frac{-\varepsilon}{2}}} \quad &= \quad (d - \frac{\varepsilon}{2} - d)g_5\mu^{\frac{-\varepsilon}{2}} - \frac{11\mathcal{C}_A}{3}\frac{g_5^3\mu^{\frac{-3\varepsilon}{2}}}{16\pi^2} \\ &= \quad (d_{\mathcal{O}_{AAA}} - d)g_5\mu^{\frac{-\varepsilon}{2}} + \boldsymbol{\beta}^1_{g_5}(g_5)\,,\end{aligned} \tag{3.4.5}$$

with $d_{\mathcal{O}_{AAA}} = d - \frac{\varepsilon}{2}$ and $\boldsymbol{\beta}^1_{g_5}(g_5) = -\frac{11\mathcal{C}_A}{3}\frac{g_5^3\mu^{\frac{-3\varepsilon}{2}}}{16\pi^2}$. The anomalous dimension of the gauge field A_M is given by

$$\boldsymbol{\gamma}_{A_M} = -\frac{1}{16\pi^2}\frac{10\mathcal{C}_A g_5^2\mu^{-\varepsilon}}{3} = -\frac{10\mathcal{C}_A\alpha_5}{6N_C}\,. \tag{3.4.6}$$

Setting $\boldsymbol{\beta}_{g_5\mu^{\frac{-\varepsilon}{2}}} = 0$ we obtain a Gaussian fixed point G at $g_5 = 0$ but also a Wilson-Fisher fixed point WF at $g_{5*} = 4\pi\sqrt{\frac{-3\varepsilon}{22\mathcal{C}_A}}\mu^{\frac{\varepsilon}{2}}$ or equivalently at $\alpha_5 = 0$ and

$$\alpha_{5*} = \frac{3N_C}{11\mathcal{C}_A}(-\varepsilon) \tag{3.4.7}$$

(that can be also obtained directly from Eq. (3.3.84)) respectively, in agreement with [54]. On G the anomalous dimension of A_M vanishes while on WF Eq. (3.4.6) gives

$$\gamma_{A_M*} = \frac{5}{11}\varepsilon = 0.45\varepsilon\,. \tag{3.4.8}$$

For a five-dimensional bulk $d = 5$ and $\varepsilon = -1$ which gives $d_{\mathcal{O}_{AAA}} = 5.5$, $\gamma_{A_M*} = -0.45$ and for the WF fixed point $g_{5*} = 4\pi\sqrt{\frac{3}{22\mathcal{C}_A}}\mu^{-\frac{1}{2}}$ and $\alpha_{5*} = \frac{3N_C}{11\mathcal{C}_A}$. An important quantity is the mass scale where the bulk coupling reaches WF. This scale is denoted by μ_* and its value is determined by demanding that $g_5(\mu_*) = g_{5*}$ or $\alpha_5(\mu_*) = \alpha_{5*}$. The latter, together with Eq. (3.3.86) for $\varepsilon = -1$ determines

$$\mu_* = \frac{\alpha_{5*}}{\alpha_{5,M}}\frac{\left(11\mathcal{C}_A\alpha_{5,M} - 3N_C\right)}{\left(11\mathcal{C}_A\alpha_{5*} - 3N_C\right)}M\,. \tag{3.4.9}$$

Inserting the α_{5*} determined above into Eq. (3.4.9) and if $\alpha_{5,M} \neq \alpha_{5*}$, the denominator vanishes and then $\mu_* = \infty$. If $\alpha_{5,M} = \alpha_{5*}$ then there is a 0/0 limit to be taken indicating that $\mu_* = C_{\mu_*}M$, with C_{μ_*} some constant. In the continuum branch where $\alpha_{5,M} < \alpha_{5*}$, when the coupling reaches the WF point the theory becomes (1-loop) scale invariant, $\alpha_5(\mu)$ stops running and obtains its maximum value, α_{5*}. In the Landau branch on the other hand where $\alpha_{5,M} > \alpha_{5*}$ the running stops at $\mu = \mu_{5L}$ given by Eq. (3.3.88). The RG flow of the coupling $\alpha_5(\mu)$ is qualitatively shown in the left of Fig. 3.2. Regarding the Landau branch one can see that it has a negative β-function which means that it describes the RG flow beyond the WF point. Now there are two possibilities: one is that the WF point coincides with a phase transition. We will see that in such a case beyond the WF can only be a Confined phase in which case the 1-loop computations is not valid to begin. The other case is that the WF does not coincide with a phase transition, it just signals some qualitative change in the behaviour of the coupling inside the Coulomb phase and the appearance of the Confined phase a bit further. In this case the Landau branch, viewed from beyond the WF point, is disconnected from the Gaussian fixed point which is the starting point of the RG flow as determined by the ε-expansion. Also, according to the RG equation and the negative sign β-function in this branch, the system tends to become less scale invariant as it approaches the phase transition. This is a too exotic scenario to accept it at face value because among other things a higher loop analysis could easily change it, so from now on we concentrate only on the continuum branch.

Let us deal more thoroughly with the two fixed points of g_5. On the Gaussian fixed point we have $\gamma_{A_M} = 0$ indicating that $\Delta_{\mathcal{O}_{AAA}} = d_{\mathcal{O}_{AAA}} = 5.5$. Then $\Delta_{\mathcal{O}_{AAA}} - d = 0.5 > 0$ and from Eq. (3.B.16) for a small deformation $\delta\sigma_{g_5}$ of the coupling around the fixed point we have that

$$\delta\sigma_{g_5}(\mu) = \left(\frac{\mu}{M}\right)^{0.5}\delta\sigma_{g_5}(M) \tag{3.4.10}$$

with M some fixed reference mass scale. This shows that for the Gaussian fixed point $\delta\sigma_{g_5}(\mu) \to 0$ as $\mu \to 0$, implying that the small area around it decreases as μ decreases. Since G is an IR fixed point, we conclude that g_5 is an IR irrelevant coupling flowing towards G, an IR attractive fixed point. Correspondingly, $g_5\mathcal{O}_{AAA}$ is marginally irrelevant in the IR.

When the coupling reaches the non-trivial UV fixed point on the other hand, a non-zero anomalous dimension develops. According to Eq. (3.B.15) we have

$$\gamma_{\mathcal{O}_{AAA^*}} = \partial_{g_5}\beta^1_{g_5}(g_{5*}) = -1.5 \tag{3.4.11}$$

and then

$$\Delta_{\mathcal{O}_{AAA^*}} = d_{\mathcal{O}_{AAA}} + \gamma_{\mathcal{O}_{AAA^*}} = 5.5 - 1.5 = 4 < d = 5\,, \tag{3.4.12}$$

showing that g_5 is a relevant coupling in the vicinity of the WF fixed point. Notice that $3\gamma_{A_{M^*}} = 3\cdot(-0.45) = -1.35$ which is a bit larger than $\gamma_{\mathcal{O}_{AAA^*}} = -1.5$. From Eq. (3.B.16) we also have that

$$\delta\sigma_{g_5}(\mu) = \Big(\frac{M}{\mu}\Big)\delta\sigma_{g_5}(M)\,, \tag{3.4.13}$$

which means that regarding WF, $\delta\sigma_{g_5}(\mu) \to 0\,(\infty)$ as $\mu \to \infty\,(0)$, indicating that the small area around it decreases (increases) as μ increases (decreases). In other words, $g_5\mathcal{O}_{AAA}$ is indeed a relevant operator in the UV and the WF point is attractive at $g_5 = g_{5*}$. The above for $\gamma = 1$ reproduces earlier results that can be found for example in [55, 56]. A qualitative picture of the bulk β-function and the direction of RG flow including the corresponding fixed points, in the limit where the bulk is decoupled from the boundary, is shown on the right of Fig. 3.2. We keep in mind for later that according to the ε-expansion itself the RG flow of Fig. 3.2 lies effectively on a one-dimensional phase diagram parametrized by α_5 because we have assumed that γ is a classical quantity. From the point of view of the non-perturbative phase diagram parametrized by β_4 and β_5 we can think of our calculations projecting us on constant γ trajectories.

To have a more quantitative picture of the behaviour of the theory near and on the fixed points we evaluate the critical exponents ν and η connected with the correlation length ξ as the WF fixed point is approached and the power law behaviour of a 2-point correlation function on the WF point. To evaluate the first critical exponent we use the linearized version of $\boldsymbol{\beta}_{g_5\mu^{\frac{-\varepsilon}{2}}}$ around the WF fixed point according to Eq. (3.B.13)

$$g_5(\mu) = \Big(\frac{M}{\mu}\Big)^{\Delta_{\mathcal{O}_{AAA}}-d} g_5(M)\,. \tag{3.4.14}$$

Recalling from statistical physics that the characteristic range of correlations is given by $\xi \propto 1/\mu$ as $\mu \to \mu_*$ and combining with Eq. (3.4.14) we obtain

$$\begin{aligned} \xi \;&\propto\; \frac{1}{\mu} = \left[\frac{g_5(\mu)}{g_5(M)}\right]^{\frac{1}{\Delta_{\mathcal{O}_{AAA}}-d}} M^{-1} \Rightarrow \\ \xi \;&\propto\; g_5(\mu)^{\frac{1}{\Delta_{\mathcal{O}_{AAA}}-d}} = g_5(\mu)^{-\nu} \end{aligned} \tag{3.4.15}$$

which fixes the critical exponent to $\nu = \frac{1}{d-\Delta_{\mathcal{O}_{AAA}}} = 1$ for the five-dimensional bulk in agreement, to leading order, with the result obtained in Eq. (2.13) of [55]. Including corrections up to 4 loops, changes the exponent by approximately 30%, without changing the qualitative picture. Regarding η, the universal form of a two-point correlation function of a field Φ in d-dimensions follows the relation

$$\langle \Phi(x)\Phi(0)\rangle \sim \frac{1}{x^{d-2+\eta}}\,. \tag{3.4.16}$$

On the other hand, at the fixed point from CFT arguments it is also valid to express the 2-point correlation function as

$$\langle \Phi(x)\Phi(0)\rangle \sim \frac{1}{x^{2\Delta_\Phi}} = \frac{1}{x^{2d_\Phi+2\boldsymbol{\gamma}_{\Phi*}}}\,, \tag{3.4.17}$$

where d_Φ and $\boldsymbol{\gamma}_\Phi$ are the classical and anomalous dimensions for the field Φ respectively. In our case we are interested in the 2-point function of the gauge field which, according to Appendix 3.B, has classical dimension $d_{A_M} = \frac{d-2}{2}$ and an anomalous dimension given by Eq. (3.4.8). Combining these relations we obtain

$$d-2+\eta = 2d_{A_M} + 2\boldsymbol{\gamma}_{A_M*} \Rightarrow \eta = -0.9\,. \tag{3.4.18}$$

Matching to the non-perturbative phase diagram

We would like to see now if there is a connection between the WF fixed points that the ε-expansion produces and the non-perturbative phase diagram that lattice simulations see. The non-perturbative phase diagram for the bulk, reproduced on the left in Fig. 3.3, has been determined in [20]. It is constructed in the space of (β_4, β_5) couplings, multiplying the 4d and extra dimensional plaquettes respectively. It exhibits two phases, a Coulomb and a Confined phase, separated by a line of first order phase transitions. The most interesting aspect of the role of γ is that in the regime $\gamma < 1$ and in the Confined phase, the 5d space becomes layered along the fifth dimension. The same approximately happens in the Coulomb phase near the phase transition. In order to construct the phase diagram of the bulk theory from the ε-expansion and be able to compare it to the non-perturbative one, we should connect the bulk couplings g_5 (or β) and γ to the lattice couplings β_4 and β_5. We have already seen that the order to which we have truncated the naive lattice spacing expansion, among others, projected us onto RG trajectories of constant γ. There is one conclusion that we can already draw if we bring γ in the game, namely that we expect the curve of WF fixed points on the $\beta_4 - \beta_5$ plane to be a parabola, qualitatively the same as in Fig. 3.3. Conversely, if the non-perturbative phase diagram is a good fit to a parabola the anisotropy parameter is not expected to be renormalized by much.[4] This means that it is sufficient to concentrate on the RG flow of β_4, the one of β_5 being determined by the relation $\beta_5 = \gamma^2\beta_4$.

[4] This seems to imply that finite temperature phase transitions along the fifth dimension that are governed by N_5 but also by γ are tied to a significant renormalization of γ for given N_5.

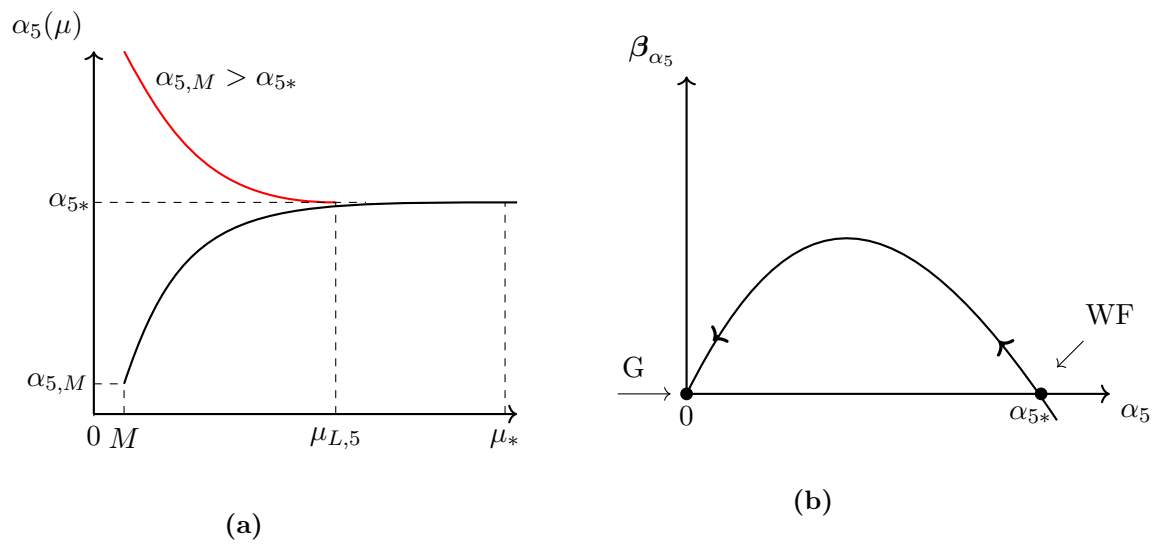

Figure 3.2: (a): The RG flow of $\alpha_5(\mu)$ as a function of the mass scale μ. There is a reference scale M where $\alpha_5(M) = \alpha_{5,M}$. The black (lower) curve corresponds to $\alpha_{5,M} < \alpha_{5*}$ where the system has a continuum limit at $\mu_* = \infty$ and the coupling reaches a WF fixed point, α_{5*}. The red (upper) curve corresponds to $\alpha_{5,M} > \alpha_{5*}$ where the theory has a Landau pole at $\mu = \mu_{L,5}$, with $\mu_{L,5} < \mu_*$, and there is no continuum limit. This is the Landau branch. The value of α_{5*} is independent of γ. (b): The RG flow direction of $\boldsymbol{\beta}_{\alpha_5}$ as a function of α_5. There is an IR Gaussian fixed point (G) at $\alpha_5 = 0$ and a non-trivial UV fixed point (WF) at $\alpha_{5*} = \frac{3N_C}{11C_A}$.

For a more detailed comparison there is a price to be paid. Recall the definition of $\beta_4 = \frac{2N_C a_5}{g_5^2}$ and notice the appearance of a_5. On the lattice a_4 and a_5 are independent quantities. Now recall also that in order to derive a classical, continuum action from the lattice spacing expansion we took the continuum limit in a_4. This is why a_4 had disappeared from the Lagrangians that we quantized. Quantization however re-introduces a scale μ that can be thought of as a scale proportional to a cut-off, a role that the lattice spacings had on the lattice, to begin. So in the context of the ε-expansion we are in a basis where the dynamical scale is μ and there is a classical parameter γ, while non-perturbatively we have the two dynamical scales a_4 and a_5 or a_4 and γ. If we assume that γ is not renormalized, in both cases $\gamma = a_4/a_5 = \text{const}$. Therefore if we want to relate the two pictures we need a relation between a_4 and μ. It turns out that all we need to specify is

$$\mu = \frac{F(\beta_4, \beta_5)}{a_4} \,. \tag{3.4.19}$$

To justify Eq. (3.4.19) beyond the naive dimensional analysis which is obviously correct, we note that F could be a complicated, unknown dimensionless function of the couplings. In any case we can expand it around the WF point:

$$\mu = \frac{1}{a_4}\big[F(\beta_{4*}, \beta_{5*}) + O(a_4, a_5))\big] \tag{3.4.20}$$

and notice that the series near the WF curve can be safely truncated to the first term in the

expansion, $f \equiv F(\beta_{4*}, \beta_{5*})$, with f a (possibly d-dependent) non-zero constant.[5] Under this assumption we can set $a_5 = \frac{1}{\gamma}\frac{f}{\mu}$ and the rest is simple algebra. For example we can express β_4 as a function of the bulk coupling α_5 and from that determine its β-function and RG flows. We have

$$\beta_4 = \frac{N_C^2}{4\pi^2}\frac{\mu^{-\varepsilon}}{\alpha_5}a_5 = \frac{N_C^2}{4\pi^2}\frac{f\mu^{-(\varepsilon+1)}}{\gamma\alpha_5} \tag{3.4.21}$$

and inserting into Eq. (3.3.84) we obtain the RG equation and the β-function of β_4

$$\boldsymbol{\beta}_{\beta_4} \equiv \mu\frac{d\beta_4}{d\mu} = \varepsilon\beta_4 + \frac{11\mathcal{C}_A N_C}{12\pi^2}\frac{f}{\gamma}\mu^{-(\varepsilon+1)}\,. \tag{3.4.22}$$

Regarding the fixed points of β_4, for the Gaussian fixed point situated at $g_5 = 0$ we get that $\beta_4 = \infty$. For the WF point we set $\boldsymbol{\beta}_{\beta_4} = 0$ and we get

$$\beta_{4*} = \frac{11\mathcal{C}_A N_C}{12\pi^2}\frac{f}{-\varepsilon\gamma}\mu^{-(\varepsilon+1)}\,. \tag{3.4.23}$$

Notice that substituting directly $g_{5*} = 4\pi\sqrt{\frac{-3\varepsilon}{22\mathcal{C}_A}}\mu^{\frac{\varepsilon}{2}}$ into β_4 gives the same result. Solving the RGE gives for the running coupling $\beta_4(\mu)$

$$\beta_4(\mu) \;=\; \Big(\frac{11\mathcal{C}_A N_C}{12\pi^2}\frac{f}{\gamma\varepsilon}\mu^{-(\varepsilon+1)} + \beta_{4,M}\Big)\frac{\mu^\varepsilon}{M^\varepsilon} - \frac{11\mathcal{C}_A N_C}{12\pi^2}\frac{f}{\gamma\varepsilon}\mu^{-(\varepsilon+1)}\quad. \tag{3.4.24}$$

Here we have defined a reference scale M where $\beta_4(M) = \beta_{4,M}$, which is the same scale where $\alpha_5(M) = \alpha_{5,M}$. Recall that the maximum value of α_5 in the continuum branch is α_{5*} with $\alpha_{5,M} < \alpha_{5*}$, while now β_{4*} corresponds to the minimum value of β_4 and $\beta_{4,M} > \beta_{4*}$ in the continuum branch. The running of β_5 is obtained by simply substituting $f/\gamma \to f\gamma$ in Eq. (3.4.24). Specifying to $\varepsilon = -1$, $N_C = 2$ and $\mathcal{C}_A = 2$ we have

$$\beta_{4*} = \frac{11}{3\pi^2}\frac{f}{\gamma}\,, \qquad \beta_{5*} = \frac{11}{3\pi^2}f\gamma \tag{3.4.25}$$

while the RGE of Eq. (3.4.24) gives

$$\begin{aligned}\beta_4(\mu) &= \Big(-\frac{11}{3\pi^2}\frac{f}{\gamma} + \beta_{4,M}\Big)\frac{M}{\mu} + \frac{11}{3\pi^2}\frac{f}{\gamma}\\ \beta_5(\mu) &= \Big(-\frac{11}{3\pi^2}f\gamma + \beta_{5,M}\Big)\frac{M}{\mu} + \frac{11}{3\pi^2}f\gamma\,.\end{aligned} \tag{3.4.26}$$

As G is approached, $\mu \to 0$ and $\beta_4 \to \infty$ and when $\mu \to \mu_* = \infty$, $\beta_4 \to \beta_{4*}$. Eq. (3.4.25) yields a phase diagram of the form on the left of Fig. 3.3, as anticipated. A numerical plot of Eq. (3.4.25) and the curve of fixed points that it generates can be seen (it is the blue curve) in Fig. 3.5. The qualitative behaviour of β_4 as a function of μ can be seen on the right of Fig. 3.3.

One thing to keep in mind is that β_4, thus β_5 as well, decreases as the WF line is approached along constant γ trajectories and that the critical value of β_4 increases as γ decreases. These are all generic features of the non-perturbative phase diagram. We can perform a quantitative

[5] The assumption $f \neq 0$ can be justified if we keep $a_5 =$ const. and take in the number of lattice nodes $L = l/a_4$, the physical size l of the box very large. Then $F = f + O(1/L)$ and $\mu = f/a_4 + O(1/l)$. This is equivalent to saying that to obtain the classical continuum action we have taken both $a_4 \to 0$ and $l \to \infty$. Then quantum effects effectively re-introduce a scale in an infinitely sized box.

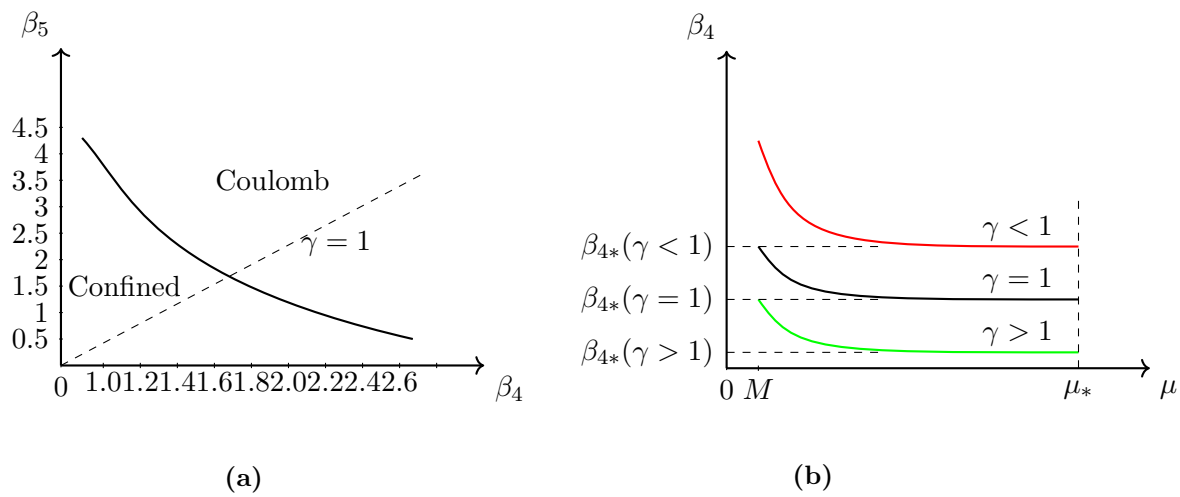

Figure 3.3: (a): The phase diagram of an anisotropic 5d $SU(2)$ Yang-Mills theory, according to lattice Monte Carlo simulations, reproduced qualitatively from [20]. The thick line indicates first order quantum phase transitions. Its upward concavity suggests a mildly renormalized anisotropy factor. The dashed line shows the isotropic lattice where $\beta_{4*} = \beta_{5*} \simeq 1.65$. (b): The RG flow of $\beta_4(\mu)$ as a function of the mass scale μ for different values of anisotropy parameter γ in the continuum branch. There is a reference scale M where $\beta_4(M) = \beta_{4,M}$. Here are depicted the WF fixed points, $\beta_{4*}(\gamma)$ for $\gamma < 1$, $\gamma = 1$ and $\gamma > 1$, when $\mu = \mu_* = \infty$. In this basis $\beta_4(M) > \beta_{4*}(\gamma)$. The behaviour of $\beta_5(\mu)$ is similar but with the γ-dependence reversed.

comparison of the phase diagrams if we fix the constant f. For this we can use the knowledge of the value $\beta_{5*} = \beta_{4*} = \beta_* = 1.65$ for the $SU(2)$ coupling that determines the phase transition on the isotropic lattice [20, 59] and the corresponding value of the coupling on the phase transition for any d [60] in the Mean-Field approximation

$$\beta_* = \frac{6.704840}{d-1}\,. \tag{3.4.27}$$

From the above and Eq. (3.4.25) for $\gamma = 1$ we can fix

$$f = \frac{d-4}{d-1}\frac{6.704840}{0.371} \simeq 4.51\,. \tag{3.4.28}$$

In our numerical analysis, we will use the value $f = 4.44$ that reproduces better the Monte Carlo rather than the Mean-Field data. In $d = 5$ and for $SU(2)$ the β-functions of β_4 and β_5 are

$$\begin{aligned} \boldsymbol{\beta}_{\beta_4} &= -\beta_4 + \frac{11}{3\pi^2}\frac{f}{\gamma} \\ \boldsymbol{\beta}_{\beta_5} &= -\beta_5 + \frac{11}{3\pi^2} f\gamma\,. \end{aligned} \tag{3.4.29}$$

The behaviour of $\boldsymbol{\beta}_{\beta_4}$ as a function of β_4 is plotted on the left of Fig. 3.4 for various values of γ. The behaviour of $\boldsymbol{\beta}_{\beta_5}$ is similar. Indeed, as the WF line is approached from the side of the Coulomb phase, the system tends towards scale invariance as the vanishing of $\boldsymbol{\beta}_{\beta_4}$ (thus also of $\boldsymbol{\beta}_{\beta_5}$) shows.

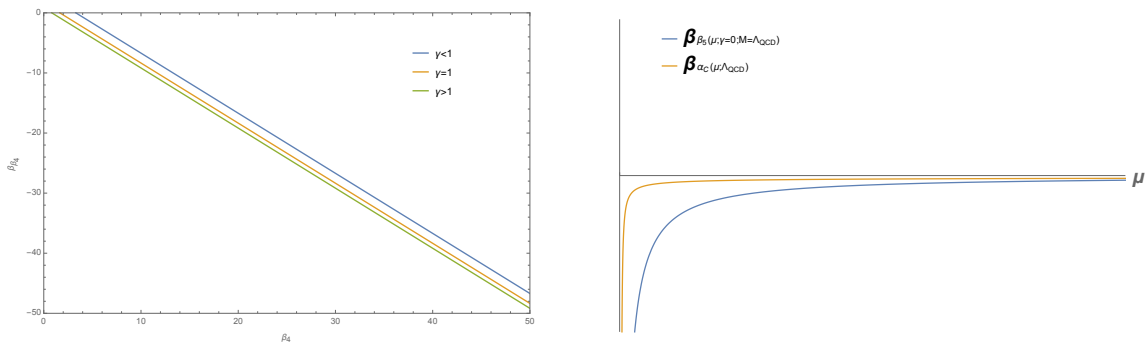

Figure 3.4: Left: The RG flow of $\boldsymbol{\beta}_{\beta_4}$ as a function of β_4 for various γ in the Coulomb phase according to Eq. (3.4.29). At G, $\beta_4(0) = \infty$ and $\boldsymbol{\beta}_{\beta_4} \to -\infty$. At WF $\beta_4(\mu_*) = \beta_{4*}$ and $\boldsymbol{\beta}_{\beta_4} \to 0$. As boundary conditions we have chosen $M = \Lambda_{4d} \simeq 200MeV$ and $\beta_{4,M} = 4\beta_{4*}$. Right: Plot of $\boldsymbol{\beta}_{\beta_5}(\mu; \gamma = 0; M = \Lambda_{4d}) = -\beta_{5,\Lambda_{4d}} \frac{\Lambda_{4d}}{\mu}$ from Eq. (3.4.26) lower (blue) curve and of $\boldsymbol{\beta}_{\alpha_C}(\mu; \Lambda_{4d})$ from Eq. (3.4.30) upper (yellow) curve as functions of μ. These illustrate that as $\mu \to \infty$ both go to zero from negative values, showing the tendency of the system becoming scale invariant from both sides along the RG flows A and B of Fig. 3.5.

Whether it is possible to derive the RG flows in a general 5d Confined phase using the ε-expansion is not clear. In the special case where the 5d space breaks into approximately independently fluctuating 4d planes though, called the Confined-layered phase, it is. We will assume that the layering is perfect in which case we have in the bulk an array of non-interacting 4d $SU(2)$ gauge theories. This can be made exact by setting $\beta_5 = 0$ that makes the contribution of plaquettes in the lattice having links along the fifth dimension, vanish. Then indeed the lattice decomposes into 4d sublattices and only the coupling β_4 survives. In this regime, with the boundary naturally decoupled from the bulk, our truncated to marginal operators classical Lagrangian is a good approximation. The $4d$ Yang-Mills β-function is known up to several loops. To 1-loop we can extract (and verify) the β-function of the Confined phase coupling from our computation. Replacing $g_5 \mu^{\frac{-\varepsilon}{2}} \to g_C$ in the bulk expression Eq. (3.3.85) gives

$$\boldsymbol{\beta}_{g_C} = -\frac{22}{3} \frac{g_C^3}{16\pi^2} \tag{3.4.30}$$

or equivalently $\boldsymbol{\beta}_{\alpha_C} = -\frac{44}{3}\alpha_C^2$ with g_C (α_C) identified as the dimensionless coupling of the 4d $SU(2)$ theory on each 4d plane (we added a subscript C to quantities to remind that it is their value in the Confined-layered phase). The only fixed point is the Gaussian fixed point $g_C = 0$ ($\alpha_C = 0$) which in terms of the 5d couplings is at $\beta_5 = 0$ and $\beta_4 = \infty$, or at $\gamma = 0$ and $\beta_C = \infty$ (here β_C is the coupling β defined in Eq. (3.2.11) evaluated in the Confined phase). It is easy to see that $\beta_C = 2N_C/g_C^2$. At this point of the 5d phase diagram the WF fixed point from the point of view of the Coulomb phase coincides with the Gaussian fixed point from the point of view of the Confined phase. It is useful to look also at β_C. Its β-function for $N_C = 2$ is

$$\begin{aligned} \mu \frac{d\beta_C}{d\mu} &= -\frac{8}{g_C^3} \mu \frac{dg_C}{d\mu} \Rightarrow \\ \boldsymbol{\beta}_{\beta_C} &= \mu \frac{d\beta_C}{d\mu} = -\frac{8}{g_C^3} \boldsymbol{\beta}_{g_C} = \frac{11}{3\pi^2} \end{aligned} \tag{3.4.31}$$

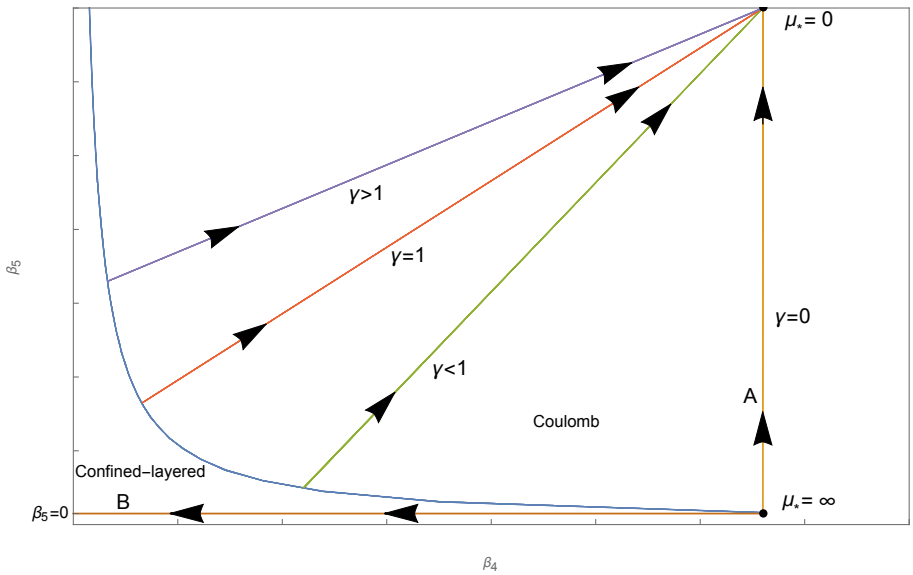

Figure 3.5: The phase diagram and RG flows in the bulk according to the ε-expansion. The (blue) curve represents WF fixed points. The straight lines are $\gamma = \text{const.}$ RG flows. The flows labelled by A and B are correlated according to Eq. (3.4.33).

which has the solution

$$\beta_C(\mu) = \beta_{C,\Lambda_{4d}} + \frac{11}{3\pi^2} \ln \frac{\mu}{\Lambda_{4d}} + \cdots \tag{3.4.32}$$

with $\beta_{C,\Lambda_{4d}} = \beta_C(\mu = \Lambda_{4d})$ an integration constant and the dots representing higher loop corrections. On the right of Fig. 3.4 we pick the RG flow line in the Coulomb phase for $\gamma = 0$ from Eq. (3.4.26) and the corresponding RG flow line in the Confined-layered phase from Eq. (3.4.32) and we plot their μ-dependence. We can clearly see the tendency of the system becoming scale invariant as the fixed point where $\mu_* = \infty$ is approached from either side.

A related observation is that the scale μ in Eq. (3.4.32) sweeps through the same values as the μ that enters in the $\gamma = 0$ Coulomb phase RGE. This is because they originate from the fluctuations of the same lattice and in the vicinity of the UV fixed point each value of μ in one phase corresponds to a point on the other side of the phase transition with the same value of μ. We can then solve Eq. (3.4.32) for μ and substitute it into the RGE of β_5. Choosing $M = \Lambda_{4d}$ we obtain

$$\beta_5(\mu) = \beta_{5,\Lambda_{4d}} e^{-\frac{3\pi^2}{11}\beta_C(\mu)} \tag{3.4.33}$$

a relation that correlates the running of the couplings on the two sides of the phase transition. This is just one example of a generic property that the runnings of couplings on opposite sides of quantum phase transitions seem to have [14, 15]. Notice for example that if the Landau branch were physical, the existence of a Landau pole from one side of the phase transition would impose a maximum cut-off on the other side. We actually expect to see a behaviour along these lines near a first order phase transition. On Fig. 3.5 we summarize our findings for the RG flows on the bulk phase diagram according to the ε-expansion and in particular for the lines A and B

under the assumption explained below Eq. (3.4.19).

3.5 Scale invariance and the Stress-Energy Tensor

The easiest way to establish a connection between results from the ε-expansion and scale invariance is via the Stress-Energy (S-E) tensor. In fact, in many cases scale invariance leads to conformal invariance. There is a known relation between scale and conformal invariance [63], which we will use here in order to show that the fixed points that the ε-expansion sees may correspond to CFTs. Our analysis here is preliminary, as it does not take into account possible subtleties with unitarity, the gauge fixing and ghost contributions etc., but we plan to return to all these issues in greater detail in the future.

According to the prescription the first step is to evaluate the dilatation current by performing scale transformations of the fields. For a given field Φ_i, the variation under dilatation transformations is

$$\delta_D \Phi_i = (x \cdot \partial + d_{\Phi_i})\Phi_i \,, \tag{3.5.1}$$

where the subscript D stands for dilatation and d_{Φ_i} is the classical dimension of Φ_i. Applying the above variation to a Lagrangian, $\mathcal{L}(\Phi_i, \partial\Phi_i)$, the dilatation current $\mathcal{D}^\mu$ is given by

$$\mathcal{D}^\mu = x_\nu \Theta_c^{\mu\nu} + \frac{\partial \mathcal{L}(\Phi_i, \partial\Phi_i)}{\partial(\partial^\mu \Phi_i)} d_{\Phi_i} \Phi_i \,, \tag{3.5.2}$$

where $\Theta_c^{\mu\nu}$ is the canonical S-E tensor. This and all the following S-E tensors are assumed to be conserved. In addition, we can insert the symmetric Belinfante S-E tensor, $\Theta_B^{\mu\nu}$, defined by[6]

$$\Theta_B^{\mu\nu} = \Theta_c^{\mu\nu} + \partial_\rho X^{\rho\mu\nu}$$

in Eq. (3.5.2) in order to obtain the expression

$$\mathcal{D}^\mu = x_\nu \Theta_B^{\mu\nu} + V^\mu \,, \tag{3.5.3}$$

where V^μ is the virial field. We now recall the two conditions which should be fulfilled by a conformally invariant theory. The first condition is that the virial field should be a total derivative

$$V^\mu = \partial_\beta \Sigma^{\mu\beta}$$

and the second is that the divergence of the dilatation current should vanish. These conditions suggest the definition of an improved S-E tensor $T^{\mu\nu}$ via the relation

$$\mathcal{D}^\mu = x_\nu T^{\mu\nu} \,. \tag{3.5.4}$$

An easy way to calculate this S-E tensor is to consider a general manifold with metric $g_{\mu\nu}$ and then take the functional derivative of the action with respect to the metric evaluated in the flat limit, i.e.

$$T^{\mu\nu} = -\frac{2}{\sqrt{\mathcal{G}}} \frac{\delta(\sqrt{\mathcal{G}}\mathcal{L})}{\delta g_{\mu\nu}}\Big|_{g_{\mu\nu}\to\eta_{\mu\nu}} \tag{3.5.5}$$

[6] $X^{\rho\mu\nu}$ is antisymmetric in $\rho\mu$ so that $\Theta_B^{\mu\nu}$ is conserved.

where $\mathcal{G} = \det g_{\mu\nu}$.
According to the above discussion if the divergence of Eq. (3.5.4), given by

$$\partial_\mu \mathcal{D}^\mu = T^\mu_\mu \,, \tag{3.5.6}$$

vanishes then the theory is conformally invariant. The above arguments obviously hold both at the classical and quantum levels. In what follows we obtain the classical and renormalized improved S-E tensors for the boundary and the bulk and then we evaluate their trace. On the fixed points we expect that the trace of the renormalized S-E tensor vanishes indicating that both theories may become CFTs at the quantum level. The discussion has to be necessarily carried out though order by order in the ε-expansion so when we speak of a CFT we really mean "conformally invariant at 1-loop in the ε-expansion". For the Gaussian fixed points this could be presumably generalized to all orders but it is not clear to us if this is the case also for fixed points of the WF type. This is of course consistent with the spirit of Weak Asymptotic Safety as described in the Introduction. We note that in the following evaluation of the stress-energy tensors contributions from the gauge fixing term and the Faddeev-Popov ghost fields have been neglected.

3.5.1 Boundary

Using Eq. (3.3.38) the boundary Lagrangian can be written as

$$\mathcal{L}_{\text{bound},0} = -\frac{(4\pi)^2}{4\alpha_{4,0}\gamma} F_0^{3,\mu\nu} F^3_{0,\mu\nu} + |D_\mu \phi_0|^2 \,, \tag{3.5.7}$$

The classical, improved S-E tensor then reads

$$\begin{aligned} T^{\mu\nu}_{\text{bound},0} &= -\frac{2}{\sqrt{\mathcal{G}}} \frac{\delta(\sqrt{\mathcal{G}}\mathcal{L}_{\text{bound},0})}{\delta g_{\mu\nu}}\Big|_{g_{\mu\nu}\to\eta_{\mu\nu}} \\ &= \frac{\eta^{\mu\nu}(4\pi)^2}{4\alpha_{4,0}\gamma} F_0^{3,\rho\sigma} F^3_{0,\rho\sigma} - \frac{(4\pi)^2}{\alpha_{4,0}\gamma} F_0^{3,\mu\sigma} F^{3,\nu}_{0,\sigma} - \eta^{\mu\nu} \left(D^\rho \phi_0\right)^* D_\rho \phi_0 + 2 \left(D^\mu \phi_0\right)^* D^\nu \phi_0 \,, \end{aligned} \tag{3.5.8}$$

whose trace is

$$\begin{aligned} \eta_{\mu\nu} T^{\mu\nu}_{\text{bound},0} &= (4\pi)^2 \frac{4}{4\alpha_{4,0}\gamma} F_0^{3,\rho\sigma} F^3_{0,\rho\sigma} - \frac{(4\pi)^2}{\alpha_{4,0}\gamma} F_0^{3,\rho\sigma} F^3_{0,\rho\sigma} - 4 \left(D^\rho \phi_0\right)^* D_\rho \phi_0 + 2 \left(D^\rho \phi_0\right)^* D_\rho \phi_0 \Rightarrow \\ T_{b,0} &= -2 \left(D^\rho \phi_0\right)^* D_\rho \phi_0 = 0 \,, \end{aligned} \tag{3.5.9}$$

where in the last step we used the equation of motion of the scalar field and defined $T_{b,0} \equiv \eta_{\mu\nu} T^{\mu\nu}_{\text{bound},0}$. Eq. (3.5.6) combined with the above relation indicates that for the 4d SQED at the classical level the divergence of the dilatation current vanishes and the theory is conformally invariant.

To extend the statement to the quantum level we must renormalize the trace of the S-E tensor. The trace of Eq. (3.5.8) in d-dimensions (using the equation of motion of ϕ) reads

$$T_{b,0} = \frac{d-4}{4} \frac{(4\pi)^2}{\alpha_{4,0}\gamma\mu^\varepsilon} F_0^{3,\rho\sigma} F^3_{0,\rho\sigma} \,. \tag{3.5.10}$$

Using the results of Section 3.3.2 its quantum version in the ε-expansion can be defined through

$$T_{b,0} \quad = \quad \frac{d-4}{4}\frac{(4\pi)^2}{\alpha_4\gamma\mu^{4-d}}Z_{\alpha_4}^{-1}Z_{A_\mu}F^{3,\rho\sigma}F^3_{\rho\sigma} \tag{3.5.11}$$

by separating the finite, renormalized part T_b from the rest, $\langle T_b\rangle$:

$$T_{b,0} \quad = \quad T_b + \langle T_b\rangle\,. \tag{3.5.12}$$

Thus,

$$T_b \quad = \quad \frac{d-4}{4}\frac{(4\pi)^2}{\alpha_4\gamma\mu^{\varepsilon}}F^{3,\rho\sigma}F^3_{\rho\sigma} = \frac{-\varepsilon}{4}\frac{(4\pi)^2}{\alpha_4\gamma\mu^{\varepsilon}}F^{3,\rho\sigma}F^3_{\rho\sigma}\,. \tag{3.5.13}$$

Now notice that in d-dimensions the renormalized part of Eq. (3.5.7) is

$$\mathcal{L}_{\text{bound}} = -\frac{(4\pi)^2}{4\alpha_4\gamma\mu^{\varepsilon}}F^{3,\mu\nu}F^3_{\mu\nu} + |D_\mu\phi|^2\,,$$

so that Eq. (3.5.13) can be rewritten in terms of $\mathcal{L}_{\text{bound}}$ as

$$T_b \quad = \quad -\mu\frac{d\mathcal{L}_{\text{bound}}}{d\mu} = -\boldsymbol{\beta}_{\alpha_4}\frac{d\mathcal{L}_{\text{bound}}}{d\alpha_4} \tag{3.5.14}$$

with $\boldsymbol{\beta}_{\alpha_4}$ the β-function of the boundary coupling α_4. The above relation is known as the trace anomaly preventing the theory from being conformally invariant at the quantum level. Nevertheless at the Gaussian point G where $\boldsymbol{\beta}_{\alpha_4} = 0$, T_b vanishes. Therefore, Eq. (3.5.6) implies that the divergence of the dilatation current is zero and as a consequence the boundary theory is a CFT on G.

3.5.2 Bulk

In the bulk, using Eq. (3.3.39) we start with the classical Lagrangian

$$\mathcal{L}_{\text{bulk},0} = -\frac{1}{4\alpha_{5,0}\mu^{-1}\Omega}F_0^{A,MN}F^A_{0,MN} \tag{3.5.15}$$

where $\Omega = 2N_C/(4\pi)^2$ and the S-E tensor

$$T^{MN}_{\text{bulk},0} = -\frac{2}{\sqrt{\mathcal{G}}}\frac{\delta(\sqrt{\mathcal{G}}\mathcal{L}_{\text{bulk},0})}{\delta g_{\mu\nu}}\Big|_{g_{\mu\nu}\to\eta_{\mu\nu}} = \frac{\eta^{MN}}{4\alpha_{5,0}\mu^{-1}\Omega}F_0^{A,RS}F^A_{0,RS} - \frac{1}{\alpha_{5,0}\mu^{-1}\Omega}F_0^{A,MS}F^{A,N}_{0,S} \tag{3.5.16}$$

whose trace is

$$\begin{aligned} T_{B,0} \equiv \eta_{MN}T^{MN}_{\text{bulk},0} \quad &= \quad \frac{5}{4\alpha_{5,0}\mu^{-1}\Omega}F_0^{A,RS}F^A_{0,RS} - \frac{1}{\alpha_{5,0}\mu^{-1}\Omega}F_0^{A,RS}F^A_{0,RS} \\ &= \quad \frac{1}{4\alpha_{5,0}\mu^{-1}\Omega}F_0^{A,RS}F^A_{0,RS}\,, \end{aligned} \tag{3.5.17}$$

which is non-zero. This means that the 5d $SU(2)$ theory is neither scale nor conformally invariant at the classical level.

Now let us renormalize $T_{B,0}$. In d-dimensions it reads

$$T_{B,0} = \frac{d-4}{4\alpha_{5,0}\mu^{4-d}\Omega} F_0^{A,RS} F_{0,RS}^A \tag{3.5.18}$$

and its renormalized version, according to Section 3.3.2, can be extracted from

$$T_{B,0} = \frac{d-4}{4\alpha_5\mu^{4-d}\Omega} Z_{\alpha_5}^{-1} Z_{A_M} F^{A,RS} F_{RS}^A = T_B + \langle T_B \rangle \tag{3.5.19}$$

where

$$T_B = \frac{d-4}{4\alpha_5\mu^{4-d}\Omega} F^{A,RS} F_{RS}^A = \frac{-\varepsilon}{4\alpha_5\mu^{\varepsilon}\Omega} F^{A,RS} F_{RS}^A \,. \tag{3.5.20}$$

Combining this with the renormalized part of Eq. (3.5.15)

$$\mathcal{L}_{\text{bulk}} = -\frac{1}{4\alpha_5\mu^{\varepsilon}\Omega} F^{A,MN} F_{MN}^A \,,$$

we end up with

$$T_B = -\boldsymbol{\beta}_{\alpha_5} \frac{d\mathcal{L}_{\text{bulk}}}{d\alpha_5} \,, \tag{3.5.21}$$

where $\boldsymbol{\beta}_{\alpha_5}$ is the β-function of the bulk coupling defined in Eq. (3.3.84). For the bulk $SU(2)$ gauge theory we found a Gaussian fixed point and a WF fixed point, located at $\alpha_5 = 0$ and $\alpha_{5*} = \frac{3}{11}(-\varepsilon)$ respectively, where $\boldsymbol{\beta}_{\alpha_5}$ vanishes. Then Eq. (3.5.6) implies that on those points the theory becomes conformally invariant. This is an interesting result since, even though classically the bulk theory is generically not a CFT, it flows to a CFT at the fixed points.

Appendix

3.A Couplings

There are several dimensionless couplings that can form from the dimensionful parameters of the classical 5d $SU(N_C)$ theory a_4, a_5 and g_5 and the extra parameter μ that appears in the quantum theory. They are not all independent of course but one may be more convenient to use than another in specific cases. Below we summarize the various couplings in the order they appear in the text with a pointer to their definition.

Coupling	Value	Equation
β_4	$\frac{2N_C a_5}{g_5^2}$	*Eq.* (3.2.11)
β_5	$\frac{2N_C a_4^2}{a_5 g_5^2}$	*Eq.* (3.2.11)
γ	$\sqrt{\beta_5/\beta_4} = \frac{a_4}{a_5}$	below *Eq.* (3.2.11)
β	$\sqrt{\beta_5\beta_4} = \frac{2N_C a_4}{g_5^2}$	below *Eq.* (3.2.11)
g	$\frac{g_5}{\sqrt{a_4}}$	*Eq.* (3.2.39)
α_4	$\frac{1}{(4\pi)^2}\mu^{d-4}g^2$	*Eq.* (3.3.38)
α_5	$\frac{2N_C}{(4\pi)^2}\mu^{d-4}g_5^2$	*Eq.* (3.3.39)

3.B Dimensional analysis

In this Appendix we review some well known facts about the dimensional analysis involved in RG flows in QFT's. The notation $[\Phi] = d_\Phi$ is used for the mass dimension of the field Φ. The gauge link

$$U_M = e^{iag_5\mathbf{A}_M} \tag{3.B.1}$$

is dimensionless which implies that

$$[a] + [g_5] + [\mathbf{A}_M] = 0\,. \tag{3.B.2}$$

Using that $[a] = [a_4] = [a_5] = -1$ and $[g_5] = -\frac{1}{2}$ we have $[\mathbf{A}_M] = [\mathbf{A}_\mu] = [\mathbf{A}_5] = \frac{3}{2}$. Moreover, since $[\hat{\Delta}_M] = 1$ it is easy to see that $[\mathbf{F}_{MN}] = [\mathbf{F}_{\mu\nu}] = [\mathbf{F}_{\mu 5}] = \frac{5}{2}$.

Dimensional analysis is relevant for the quantum behaviour of operators. We first determine the classical dimensions that are needed in Section 3.4.1 and Section 3.4.2 to be compared with the corresponding anomalous dimensions. Starting with the boundary part of Eq. (3.3.1) we have that in d-dimensions

$$\mathcal{S}^{\text{bound.}} \propto \int d^d x \Big[(\partial_\mu A_\nu)^2 + (\partial_\mu \phi)^2 + g\sqrt{\gamma} A_\mu \phi \partial_\mu \bar{\phi} + g^2 \gamma (A_\mu)^2 \phi \bar{\phi} \Big] \,, \tag{3.B.3}$$

from which we infer that the operator of interest is $g\sqrt{\gamma}\mathcal{O}_{A\phi\bar{\phi}}$ where $\mathcal{O}_{A\phi\bar{\phi}} = A_\mu \phi \partial_\mu \bar{\phi}$. From the kinetic terms of the gauge field we see that $-d + 2[\partial_\mu] + 2d_{A_\mu} = 0$, determining

$$d_{A_\mu} = \frac{d-2}{2} \tag{3.B.4}$$

and from the kinetic term of the scalar that $-d + 2[\partial_\mu] + 2d_\phi = 0$, determining

$$d_\phi = \frac{d-2}{2} \,. \tag{3.B.5}$$

From the interaction term $g\sqrt{\gamma} A_\mu \phi \partial_\mu \bar{\phi}$ we get that $d_g + d_{A_\mu} + 1 + 2d_\phi = d$ thus

$$d_g = \frac{4-d}{2} \,. \tag{3.B.6}$$

For $d = 4$ we have that $d_{A_\mu} = 1$, $d_\phi = 1$ while the boundary coupling is dimensionless. For the bulk part of Eq. (3.3.1) recall that there is no need to perform any rescaling and therefore, the bulk action in d-dimensions reads

$$\mathcal{S}^{\text{bulk}} \propto \int d^d x \Big[(\partial_M A_N)^2 + g_5 (\partial_M A_N) A_M A_N + g_5^2 A_M A_N A_M A_N \Big] \,. \tag{3.B.7}$$

From the kinetic term we obtain again that

$$d_{A_M} = \frac{d-2}{2} \,. \tag{3.B.8}$$

Here, the operator of interest is $g_5 \mathcal{O}_{AAA}$ with $\mathcal{O}_{AAA} = (\partial_M A_N) A_M A_N$ that determines

$$d_{g_5} = \frac{4-d}{2} \,. \tag{3.B.9}$$

In $d = 5$, $d_{A_M} = \frac{3}{2}$ and $d_{g_5} = -\frac{1}{2}$.

For a dimensionless in d-dimensions coupling $G_{i,0} = \mu^{d_{g_i}} g_{i,0} = \mu^{d_{g_i}} (g_i + \delta g_i)$ holds the RG equation

$$\begin{aligned} \mu \frac{dG_{i,0}}{d\mu} &= \mu \frac{d[\mu^{d_{g_i}} (g_i + \delta g_i)]}{d\mu} = 0 \Rightarrow \\ \boldsymbol{\beta}_{g_i}(g_i) &\equiv \mu \frac{dg_i}{d\mu} = -d_{g_i}(g_i + \delta g_i) + d_{g_i} g_i \partial_{g_i} \delta g_i \,, \end{aligned} \tag{3.B.10}$$

with d_{g_i} the mass dimension of g_i. Equivalently, the above relation can be modified to

$$\boldsymbol{\beta}_{g_i}(g_i) = (d_{\mathcal{O}_i} - d) g_i + \boldsymbol{\beta}^1_{g_i}(g_i) \,, \tag{3.B.11}$$

where $d_{\mathcal{O}_i} + d_{g_i} = d$. $d_{\mathcal{O}_i}$ is the classical mass dimension of the operator associated with g_i, while

$$\boldsymbol{\beta}^1_{g_i} = -d_{g_i}\delta g_i + d_{g_i} g_i \partial_{g_i}\delta g_i \tag{3.B.12}$$

is the one-loop part of the corresponding β-function. The above relations indicate the existence of a set of couplings, g_{i*} for which $\boldsymbol{\beta}_{g_i}$ is zero. The points on a phase diagram where this happens may indicate fixed points. An important implication of the fixed points is that they can show us if the couplings g_i under discussion and their associated operators, are relevant, marginal or irrelevant. To see this choose a fixed point $g_i = g_{i*}$ and define a small area around it, $\delta\sigma_i$ so that $g = g_{i*} + \delta\sigma_i$. The β-function then deforms as $\boldsymbol{\beta}_{g_i}(g_{i*} + \delta\sigma_i)$. Performing an expansion around g_{i*} to linear order in $\delta\sigma_i$ we have that

$$\begin{aligned}
\mu\frac{d(g_{i*} + \delta\sigma_i)}{d\mu} &= (d_{\mathcal{O}_i} - d)(g_{i*} + \delta\sigma) + \boldsymbol{\beta}^1_{g_i}(g_{i*} + \delta\sigma) \Rightarrow \\
\mu\frac{d\delta\sigma_i}{d\mu} &= \Big[(d_{\mathcal{O}_i} - d)g_{i*} + \boldsymbol{\beta}^1_{g_i}(g_{i*})\Big] + \Big[(d_{\mathcal{O}_i} - d) + \partial_{g_i}\boldsymbol{\beta}^1_{g_i}(g_{i*})\Big]\delta\sigma_i + \mathcal{O}(\delta\sigma_i^2) \Rightarrow \\
\mu\frac{d\delta\sigma_i}{d\mu} &= (\Delta_{\mathcal{O}_i} - d)\delta\sigma_i + \mathcal{O}(\delta\sigma_i^2)\,,
\end{aligned} \tag{3.B.13}$$

where we used that by definition $(d_{\mathcal{O}_i} - d)g_{i*} + \boldsymbol{\beta}^1_{g_i}(g_{i*}) = \boldsymbol{\beta}_{g_i}(g_{i*}) = 0$ and

$$\Delta_{\mathcal{O}_i} = d_{\mathcal{O}_i} + \boldsymbol{\gamma}_{\mathcal{O}_i}\,, \tag{3.B.14}$$

is the quantum scaling dimension of the operator $\mathcal{O}_i$ associated with g_i and the anomalous dimension of the operator $\mathcal{O}_i$ is defined as

$$\boldsymbol{\gamma}_{\mathcal{O}_i} = \partial_{g_i}\boldsymbol{\beta}^1_{g_i}(g_{i*})\,. \tag{3.B.15}$$

At a Gaussian fixed point G where $g_i = 0$ the anomalous dimensions vanish and $\Delta_{\mathcal{O}_i} = d_{\mathcal{O}_i}$.

Solving Eq. (3.B.13) we obtain

$$\delta\sigma_i(\mu) = \Big(\frac{\mu}{M}\Big)^{\Delta_{\mathcal{O}_i} - d}\delta\sigma_i(M)\,, \tag{3.B.16}$$

with M an arbitrary mass scale, which shows that for $\Delta_{\mathcal{O}_i} < d$, $\delta\sigma_i(\mu) >> (<<) 1$ as $\mu \to 0\,(\infty)$, for $\Delta_{\mathcal{O}_i} > d$, $\delta\sigma_i(\mu) << (>>) 1$ as $\mu \to 0\,(\infty)$ while for $\Delta_{\mathcal{O}_i} = d$, $\delta\sigma_i(\mu) = \delta\sigma_i(M)$. The above cases correspond to an IR relevant (UV irrelevant), an IR irrelevant (UV relevant) and a marginal coupling g_i, respectively. The same terminology is used for the operator $g_i\mathcal{O}_i$.

Finally, the anomalous dimension of the field Φ is defined by the Callan-Symanzik equation of a renormalized n-point Green function of a field Φ and a coupling g, reading

$$\Big(\mu\frac{\partial}{\partial\mu} + \beta(g)\frac{\partial}{\partial g} + \frac{n}{2}\boldsymbol{\gamma}_\Phi\Big)G^{(n)}(p_1, \cdots, p_n) = 0\,, \tag{3.B.17}$$

where

$$\boldsymbol{\gamma}_\Phi = \frac{\mu}{Z_\Phi}\frac{dZ_\Phi}{d\mu} \tag{3.B.18}$$

The sum of the anomalous dimensions of the fields contained in an operator is not equal in general to the anomalous dimension of the operator.

3.C Global symmetries

In this Appendix we discuss the global symmetries involved in the construction. At the level of the lattice formulation the global symmetries were identified in [**?**]. Here we extend the discussion by considering the action of the global symmetries Parity (P), charge conjugation (C) and Stick symmetry ($\mathcal{S}$) on the continuum fields.

3.C.1 Parity P

The Parity transformation acts on the lattice coordinates and the links as [**?**]

$$Pn_M = P(n_0, \vec{n}, n_5) = (n_0, -\vec{n}, n_5) \equiv \bar{n}_M$$

and

$$PU(n_M, i) = U^\dagger(\bar{n}_M - \hat{i}, i),\ PU(n_M, 0) = U(\bar{n}_M, 0),\ PU(n_M, 5) = U(\bar{n}_M, 5)$$

respectively. In the lattice space expansion this gives

$$\begin{aligned} PU(n_M, i) &= P\Big[1 + iag_5\mathbf{A}_i(n_M) + O(a^2) + \cdots\Big] \\ PU(n_M, \{0,5\}) &= P\Big[1 + iag_5\mathbf{A}_{\{0,5\}}(n_M) + O(a^2) + \cdots\Big] \end{aligned} \tag{3.C.1}$$

where $\mathbf{A}_M \equiv A^A_M T^A$. This implies an action on the continuum fields

$$\begin{aligned} P : A^A_i(x) &\to -A^A_i(\bar{x}) \\ P : A^A_{\{0,5\}}(x) &\to A^A_{\{0,5\}}(\bar{x})\,. \end{aligned} \tag{3.C.2}$$

Scalars and ghosts that do not carry a space-time index are invariant under P. The boundary and bulk actions are both invariant under P.

3.C.2 Charge conjugation C

The action of charge conjugation on the gauge links is given by

$$CU(n_M, N) = U^*(n_M, N)\,. \tag{3.C.3}$$

In the lattice spacing expansion we have

$$CU(n_M, N) = C\Big[1 + iag_5\mathbf{A}_N(n_M) + O(a^2) + \cdots\Big]$$

from which we extract that

$$C\mathbf{A}_M(x) = -(\mathbf{A}_M(x))^*\,, \tag{3.C.4}$$

which implies the action $CT^A = -(T^A)^*$ at the level of the Lie algebra. For $SU(2)$ and transferring the action on the fields, we have

$$C : A^1_M \to -A^1_M$$

$$
\begin{aligned}
C : A^2_M &\rightarrow A^2_M \\
C : A^3_M &\rightarrow -A^3_M
\end{aligned}
\tag{3.C.5}
$$

Regarding the boundary complex scalar $\phi = 1/\sqrt{2}(A^1_5 + iA^2_5)$ the above determines the transformation

$$
C : \phi \rightarrow -\phi^* \tag{3.C.6}
$$

Ghosts transform as in Eq. (3.C.5) according to their gauge index. The boundary and bulk actions are both invariant under C.

3.C.3 Stick symmetry $\mathcal{S}$

The stick symmetry $\mathcal{S}$ is a global symmetry particular to the lattice orbifold [61]. In [**?**] it was identified as the symmetry governing the Higgs mechanism, therefore it is of special importance. The stick transformation acts only on the boundary and hybrid links. In particular, restricting to the left boundary of the orbifold lattice, its action is

$$
U((n_\mu, 0), 5) \rightarrow g_{\mathcal{S}}^{-1} U_5((n_\mu, 0), 5), \quad U((n_\mu, 0), \mu) \rightarrow g_{\mathcal{S}}^{-1} U((n_\mu, 0), \mu) g_{\mathcal{S}}\,, \tag{3.C.7}
$$

where the above relation shows clearly that the hybrid links transform as matter fields under stick transformations. Without loss of generality we can take $g_{\mathcal{S}} = -i\sigma^2$. For the boundary links we therefore have

$$
\mathcal{S}\, U((n_\mu, 0), \mu) \;=\; g_{\mathcal{S}}^{-1}\Big[1 + i a_4 g_5 A^3_\mu(n_\mu, 0))T^3 + O(a_4^2) + \cdots\Big] g_{\mathcal{S}} \tag{3.C.8}
$$

while for hybrid links

$$
\mathcal{S}\, U((n_\mu, 0), 5) \;=\; g_{\mathcal{S}}^{-1}\Big[1 + i a_5 g_5 \sum_{\hat{\alpha}=1,2} A^{\hat{\alpha}}_5(n_\mu, 0))T^{\hat{\alpha}} + O(a_5^2) + \cdots\Big]\,. \tag{3.C.9}
$$

This implies that

$$
\mathcal{S} : A^3_\mu \;\rightarrow\; -A^3_\mu\,. \tag{3.C.10}
$$

The action on ϕ is a non-trivial rotation

$$
\mathcal{S} : \begin{pmatrix} 0 & -\phi^* \\ \phi & 0 \end{pmatrix} \longrightarrow \begin{pmatrix} \phi & 0 \\ 0 & -\phi^* \end{pmatrix} \tag{3.C.11}
$$

such that the kinetic term of ϕ is invariant.

3.D Feynman rules

Here we follow the usual procedure in order to evaluate the Feynman rules of the continuum orbifold action Eq. (3.3.1). We split the action into bulk and boundary parts as follows:

$$
S_{S^1/\mathbb{Z}_2} = S^1 + S^2
$$

with

$$S^1 = \int d^5x P(x_5)\left[-\frac{1}{4}F^A_{MN}F^A_{MN} - \frac{1}{2\xi}(\partial_M A^A_M)^2 + \partial_M \bar{c}^C D^{CB}_M c^B\right] \tag{3.D.1}$$

and

$$S^2 = \int d^5x \delta(x_5)\left\{\mathcal{L}_{\text{bound}} - \frac{1}{2\xi}(\partial_\mu A^3_\mu)^2 + \partial_\mu \bar{c}^3 \partial_\mu c^3\right\}. \tag{3.D.2}$$

Starting with the bulk action Eq. (3.D.1) and expanding the field strength and the covariant derivative we have

$$\begin{aligned}
S^1 &= \int d^5x P(x_5)\left[-\frac{1}{4}\left\{\partial_M A^A_N - \partial_N A^A_M - g_5 f^{ABC} A^B_M A^C_N\right\}^2 - \frac{1}{2\xi}(\partial_M A^A_M)^2 + \partial_M \bar{c}^B \partial_M c^B\right. \\
&+ \left. g_5 f^{CBA}\partial_M \bar{c}^C c^B A^A_M\right] \Leftrightarrow \\
&= \int d^5x P(x_5)\left[-\frac{1}{4}\Big(\partial_M A^A_N - \partial_N A^A_M\Big)^2 - \frac{1}{2\xi}(\partial_M A^A_M)^2 + \frac{g_5}{2}\Big(\partial_M A^A_N - \partial_N A^A_M\Big) f^{ABC} A^B_M A^C_N\right. \\
&- \left. \frac{g_5^2}{4}(f^{ABC}A^B_M A^C_N)(f^{ADE}A^D_M A^E_N) + \partial_M \bar{c}^B \partial_M c^B + g_5 f^{CBA}\partial_M \bar{c}^C c^B A^A_M\right]. \qquad (3.D.3)
\end{aligned}$$

Massaging the kinetic part gives

$$\begin{aligned}
S^1_{kin} &= \int d^5x d^5y \delta(x-y)\delta_{AB}\left[\frac{1}{2}P(x_5)A^A_M(x)\Big\{g^{MN}\Box_y + \Big(\frac{1}{\xi}-1\Big)\partial_M\partial_{N,y}\Big\}A^B_N(y)\right. \\
&- \left. \bar{c}^A \Box c^B\right] \\
&= \int d^5x d^5y \delta(x-y)\delta_{AB}\left[\frac{1}{2}P(x_5)A^A_M(x)\Big\{g^{MN}\Box_y + \Big(\frac{1}{\xi}-1\Big)\partial_M\partial_{N,y}\Big\}P^{-1}(y_5)P(y_5)A^B_N(y)\right. \\
&- \left. \bar{c}^A \Box c^B\right] \Leftrightarrow \\
S^1_{kin} &= \int d^5x d^5y \delta_{xy}\delta_{AB}\left[\frac{1}{2}A'^A_M(x)\Big\{g^{MN}\Box_y + \Big(\frac{1}{\xi}-1\Big)\partial_M\partial_{N,y}\Big\}P^{-1}(y_5)A'^B_N(y) - \bar{c}^A\Box c^B\right]
\end{aligned}$$

where $\delta(x-y) = \delta_{xy}$ and we have defined the projected gauge field $A'^A_M(x) = P(x_5)A^A_M(x)$. We Fourier transform to momentum space using

$$A'^A_M(x) = \int \frac{d^5p}{(2\pi)^5} A'^A_M(p) e^{-ip\cdot x}$$

and then S^1_{kin} becomes

$$S^1_{kin} = \int d^5x d^5y \frac{d^5p}{(2\pi)^5}\frac{d^5q}{(2\pi)^5}\frac{\delta_{xy}\delta_{AB}}{2}A'^A_M(p)e^{-ip\cdot x}\Big\{g^{MN}\Box_y + \Big(\frac{1}{\xi}-1\Big)\partial_M\partial_{N,y}\Big\}e^{-iq\cdot y}P^{-1}(q_5)A'^B_N(q)$$

$$
\begin{aligned}
&+ \quad ghosts \\
&= \quad \int \frac{d^5p}{(2\pi)^5}\frac{d^5q}{(2\pi)^5}(2\pi)^5\delta(p+q)\frac{\delta_{AB}}{2}A'^A_M(p)\Big\{-g^{MN}q^2-\Big(\frac{1}{\xi}-1\Big)q_Mq_N\Big\}P^{-1}(q_5)A'^B_N(q)+ghosts
\end{aligned}
$$

where we have used that $\int d^5x d^5y \delta_{xy} e^{-ip\cdot x}e^{-iq\cdot y} = \int d^5x e^{-i(p+q)\cdot x} = (2\pi)^5\delta^{(5)}(p+q)$. Using the δ-function to eliminate the q-integral and setting $q=-p$ we get

$$
S^1_{kin} = \int \frac{d^5p}{(2\pi)^5}\frac{1}{2}A'^A_M(p)M^{MN}_{AB}A'^B_N(-p)+ghosts \tag{3.D.4}
$$

with $M^{MN}_{AB} = \delta_{AB}\left(-g^{MN}p^2+\left(1-\frac{1}{\xi}\right)p^Mp^N\right)P^{-1}(-p_5)$. Inverting the matrix we obtain the gauge boson propagator that respects $M^{MN}_{AB}\Pi^{BC}_{NR} = \delta^{AC}\delta_{MR}$:

$$
\Pi^{AB}_{MN} \quad = \quad P(p_5)\frac{\delta^{AB}}{p^2}\left(-g_{MN}+(1-\xi)\frac{p_Mp_N}{p^2}\right). \tag{3.D.5}
$$

Following similar arguments for the ghost part, we obtain the ghost propagator

$$
G^{AB} = P(p_5)\frac{\delta^{AB}}{p^2}\,. \tag{3.D.6}
$$

From the rest of Eq. (3.D.1) we read off the interaction vertices which contain two self-interacting gauge boson vertices and one ghost-gauge boson vertex. These interactions corresponds to the terms $\partial_M A'^A_N A'^B_M A'^C_N$, $A'^B_M A'^C_N A'^D_M A'^E_N$ and $\partial_M \bar{c}^C c^B A'^A_M$.

The procedure for the boundary action Eq. (3.D.2) is analogous. We have

$$
\begin{aligned}
S^2 \quad &= \quad \int d^5x\delta(x_5)\Big\{-\frac{1}{4}F^3_{\mu\nu}F^3_{\mu\nu}+\partial_\mu\bar{\phi}\partial_\mu\phi-\frac{1}{2\xi}(\partial_\mu A^3_\mu)^2+\partial_\mu\bar{c}^3\partial_\mu c^3 \\
&+ \quad ig\sqrt{\gamma}A^3_\mu\Big(\phi\partial_\mu\bar{\phi}-\bar{\phi}\partial_\mu\phi\Big)+g^2\gamma(A^3_\mu)^2\bar{\phi}\phi\Big\}
\end{aligned} \tag{3.D.7}
$$

so that the propagator of A^3_μ is

$$
\Pi^3_{\mu\nu} = \frac{\delta_{p_5,0}}{p^2}\left(-g_{\mu\nu}+(1-\xi)\frac{p_\mu p_\mu}{p^2}\right), \tag{3.D.8}
$$

the propagator of the scalar field, ϕ is

$$
\Pi^\phi = \frac{\delta_{p_5,0}}{p^2}\,, \tag{3.D.9}
$$

and the propagator of the ghost, c^3 is

$$
\Pi^\phi = \frac{\delta_{p_5,0}}{p^2} \tag{3.D.10}
$$

The boundary vertices are determined by the interaction terms $A^3_\mu\Big(\partial_\mu\bar{\phi}\phi-\bar{\phi}\partial_\mu\phi\Big)$ and $(A^3_\mu)^2\bar{\phi}\phi$.

We summarize the Feynman rules below:

- Gauge boson Propagator

$$= \quad i\Pi^{AB}_{MN}(p_M, q_\mu) = iP(p_5)\frac{\delta^{AB}}{p^2}\left(-g_{MN} + (1-\xi)\frac{p_M p_N}{p^2}\right)$$
$$+i\frac{\delta_{p_5,0}\delta_{M,\mu}\delta_{N,\nu}}{q^2}\left(-g_{\mu\nu} + (1-\xi)\frac{q_\mu q_\nu}{q^2}\right) + i\frac{\delta_{p_5,0}\delta_{M,5}\delta_{N,5}}{q^2}$$

- Ghost Propagator

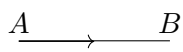

$$= iP(p_5)\frac{\delta^{AB}}{p^2} + i\frac{\delta^{A3}\delta^{B3}\delta_{p_5,0}}{q^2}$$

- three-point self interaction vertex

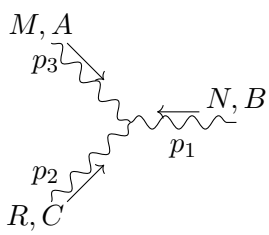

$$= P(p_5)g\sqrt{\gamma}f^{ABC}G_{NRM}$$
$$+i\delta_{p_5,0}g\sqrt{\gamma}Q_{NRM}$$

- four-point self interaction vertex

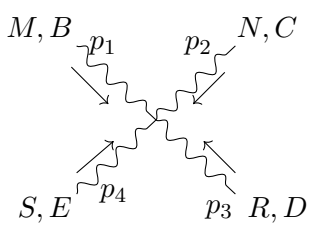

$$= -iP(p_5)g^2\gamma K^{BCDE}_{MNRS}$$
$$+2i\delta_{p_5,0}g^2\gamma g_{\mu\nu}\Delta_{MNRS}$$

- Ghost-gauge boson vertex

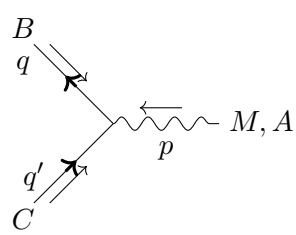

$$= -P(p_5)g\sqrt{\gamma}f^{ABC}q_M \ ,$$

where we have defined that

$$\begin{aligned} G_{NRM} &\equiv G_{NRM}(p_{12}, p_{23}, p_{31}) = g_{NR}(p_1 - p_2)_M + g_{RM}(p_2 - p_3)_N \\ &+ g_{MN}(p_3 - p_1)_R \end{aligned} \tag{3.D.11}$$

$$
\begin{aligned}
L^{ABC}_{NRM} &= f^{ABC} G_{NRM} && (3.D.12)\\
Q_{MNR} &= (q_2 - q_1)_\mu (\delta_{M,5}\delta_{N,5}\delta_{R,\rho} + \delta_{N,5}\delta_{R,5}\delta_{M,\mu} + \delta_{R,5}\delta_{M,5}\delta_{N,\nu}) && (3.D.13)\\
K^{BCDE}_{MNRS} &= f^{ABC} f^{AED} (g_{MS} g_{NR} - g_{MR} g_{NS}) + f^{ABE} f^{ACD} (g_{MN} g_{SR} - g_{MR} g_{NS}) \\
&+ f^{ABD} f^{ACE} (g_{MN} g_{SR} - g_{MS} g_{NR}) && (3.D.14)\\
\Delta_{MNRS} &= (\delta_{M,\mu}\delta_{N,\nu}\delta_{S,5}\delta_{R,5} + \delta_{M,5}\delta_{N,5}\delta_{S,\sigma}\delta_{R,\rho}) && (3.D.15)
\end{aligned}
$$

with $p_{ij} = p_i - p_j$.

3.E Looking at the scaleless integrals

Here we present a discussion which affects both the boundary and the bulk renormalization procedure. In particular, recall that in both cases the fields are massless and as a consequence the one-loop diagrams, involve massless integrals. On-shell, both the external momenta and the masses go to zero. These integrals are called scaleless and their general form is

$$
\mathcal{FD} = \int \frac{d^4k}{(2\pi)^4} \frac{1}{k^{2a}} \,, \tag{3.E.1}
$$

with a an integer. In d-dimensions the above integral becomes

$$
\mathcal{FD} = \int \frac{d^dk}{(2\pi)^d} \frac{1}{k^{2a}} \equiv \int_{-\infty}^{\infty} dk k^{d-(1+2a)} \tag{3.E.2}
$$

and in DR it is zero. The simplest example of this type [62] is $B_0(q,q)$, which is of the form

$$
B_0(q,q) = \int \frac{d^4q}{(2\pi)^4} \frac{1}{q^4}
$$

and in DR it does not converge in any dimension, in fact it has both IR and UV divergences. The way to regularize it is by separating the IR from the UV divergent part. $B_0(q,q)$ in Euclidean space becomes

$$
\begin{aligned}
\int \frac{d^4q}{(2\pi)^4} \frac{1}{q^4} &\equiv \int d^dq_E \frac{1}{q_E^4} \Rightarrow \\
\int \frac{d^4q}{(2\pi)^4} \frac{1}{q^4} &\equiv \Omega_d \int_0^M dq_E q_E^{d-5} + \Omega_d \int_M^\infty dq_E q_E^{d-5} \Rightarrow \\
\int \frac{d^4q}{(2\pi)^4} \frac{1}{q^4} &\equiv \Omega_d \Big(\ln M - \frac{1}{\varepsilon_{IR}} \Big) + \Omega_d \Big(-\ln M + \frac{1}{\varepsilon_{UV}} \Big) && (3.E.3)
\end{aligned}
$$

which shows that only if we consider $\varepsilon_{IR} = \varepsilon_{UV}$, $B_0(q,q)$ really goes to zero. Here M is an arbitrary scale. When we are interested only in the UV case we can extract from the above scaleless integral the ε_{UV} part obtaining that

$$
B_0(q,q) = \Big[\int \frac{d^dq}{(2\pi)^d} \frac{1}{q^4} \Big]_{UV} = \frac{1}{16\pi^2} \frac{2}{\varepsilon_{UV}} \,. \tag{3.E.4}
$$

The same arguments hold also for the scaleless tensor B-integrals and for the massless $B_0(q, q+l)$ integrals.

Now, let us deal with two more examples of scaleless integrals, corresponding to the massless limit of scalar integrals C_0 and D_0. The general form of these massless integrals is

$$C_0(q, q+L_1, q+L_2) \quad = \quad \int \frac{d^4q}{(2\pi)^4} \frac{1}{q^2(q+L_1)^2(q+L_2)^2}$$

and

$$D_0(q, q+L_a, q+L_b, q+L_c) \quad = \quad \int \frac{d^4q}{(2\pi)^4} \frac{1}{q^2(q+L_a)^2(q+L_b)^2(q+L_c)^2}$$

for a triangle and a square loop respectively. In order to evaluate them it is useful to separate them into two regions, regarding the loop and the external momentum, obtaining the following cases ($i = 1, 2$ and $j = a, b, c$):

- Case $q >> L_i, L_j$. In this limit C_0 becomes

  $$C_0(q, q+L_1, q+L_2) \equiv \int \frac{d^4q}{(2\pi)^4} \frac{1}{q^6}$$

  while D_0 becomes

  $$D_0(q, q+L_a, q+L_b, q+L_c) \equiv \int \frac{d^4q}{(2\pi)^4} \frac{1}{q^8}\,.$$

  The above integrals correspond to Eq. (3.E.1), for $a = 3, 4$ respectively, thus they should vanish in DR.

- Case $L_i, L_j >> q$. In this limit C_0 reads

  $$C_0(q, q+L_1, q+L_2) \equiv \frac{1}{L_1^2 L_2^2} \int \frac{d^4q}{(2\pi)^4} \frac{1}{q^2}$$

  and D_0

  $$D_0(q, q+L_a, q+L_b, q+L_c) \equiv \frac{1}{L_a^2 L_b^2 L_c^2} \int \frac{d^4q}{(2\pi)^4} \frac{1}{q^2}\,.$$

  Therefore, according again to Eq. (3.E.1) for $a = 1$ these integrals superficially vanish in DR.

A comment regarding the second case is that in the on-shell scheme, which coincides with the zero-momentum scheme in a massless theory, then $l_i^2, l_j^2 \to 0$ and $\frac{1}{L_1^2 L_2^2}, \frac{1}{L_a^2 L_b^2 L_c^2} \to \frac{1}{0}$. As a consequence, both C_0 and D_0 have a $\frac{0}{0}$ form so they can be rendered to be equal to

$$C_0(q, q+L_1, q+L_2) \equiv C_s\,, \tag{3.E.5}$$

and

$$D_0(q, q+L_a, q+L_b, q+L_c) \equiv D_s \tag{3.E.6}$$

with C_s, D_s undetermined constants. The arguments presented above hold also for the massless tensor C- and D-integrals.

3.F Box Diagrams on the Boundary

The boundary theory contains at one-loop level also contributions to the $4A_\mu$ and 4ϕ vertices. These diagrams are divergent and here we present their calculation. Let us first make a qualitative study of the possible one-loop contributions to the four point function, usually called Boxes. Box diagrams, denoted collectively as $\mathcal{B}^i_j$, are separated into reducible and irreducible Boxes and there are three possible categories, of the form

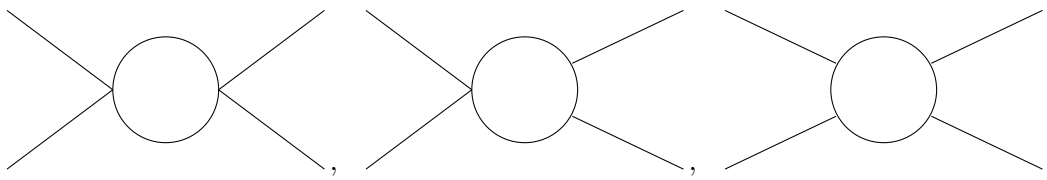

corresponding to *C-Boxes* (or *Candies*), *T-Boxes* and *S-Boxes* respectively [31]. Since the boundary theory at this order is just a massless and free SQED (no non-zero 4-vertex at the classical level) the above diagrams will contribute as quantum corrections to three processes. The first set of one-loop four-point functions corrects the A_μ-A_μ-ϕ-ϕ vertex and is given by the following diagrams:

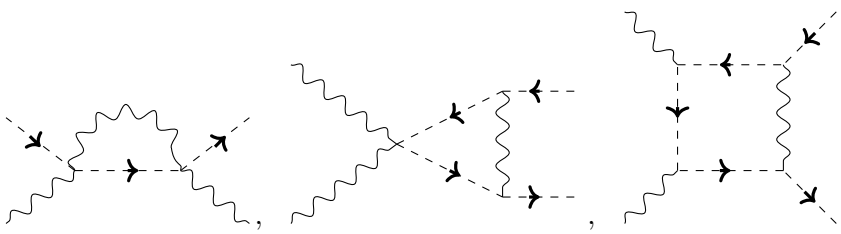

Note that for $\mathcal{B}^C_{A\phi A\phi}$ and $\mathcal{B}^T_{A\phi A\phi}$ there are two possible channels, while for $\mathcal{B}^S_{A\phi A\phi}$ there is only one. Apart from that, all of them are divergent and thus they have a non-trivial contribution to the renormalization procedure. Nevertheless, there is no need to calculate them explicitly here. The reason is that the renormalization of the theory allows us to fix the counter-term of the four-vertex in terms of counter-terms of lower dimensional vertices (by Ward identities).

It is legitimate to ask whether there are Box diagrams that contribute to the four-photon scattering similarly to the spinor QED. For the boundary theory the Feynman rules show that indeed such diagrams exist and they are of the form

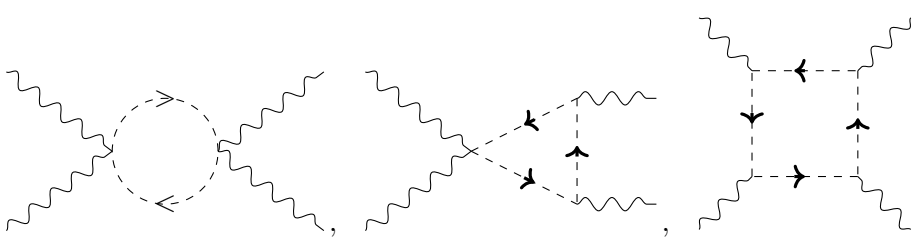

(3.F.1)

The explicit form of the four-photon scattering amplitudes is given below. There are two main differences between this case and the spinor QED. The first one is that here there are three classes of four-photon diagrams, while in spinor QED only one, the $\mathcal{B}^S_{4ph.,\mu\nu\alpha\beta}$. The second is

that $\mathcal{B}^S_{4ph.,\mu\nu\alpha\beta}$ is finite in spinor QED, while in SQED all of the above diagrams are divergent. Actually, this is a severe problem since SQED is an Abelian gauge theory and there is no $4-A_\mu$ vertex to be renormalized in order to absorb the corresponding divergences.

An analogous question concerns the boundary 1-loop diagrams that could contribute a ϕ^4 term to the scalar potential (we remind that terms proportional to ϕ or ϕ^3 are prohibited for various reasons). Such diagrams indeed exist (they do not break any symmetry) and are of the form

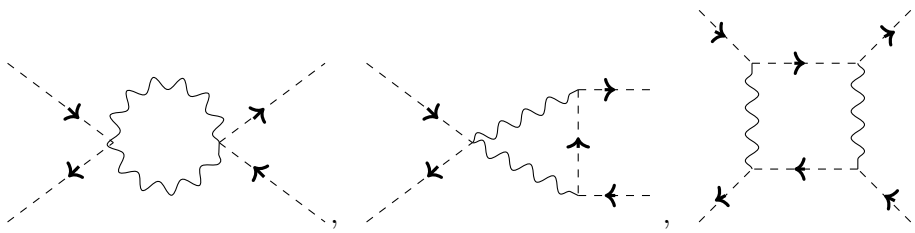

(3.F.2)

Their explicit form is given in Sect. 3.F.2. For the $\mathcal{B}^C_{4\phi}$ and $\mathcal{B}^T_{4\phi}$ diagrams there are two possible channels, while for $\mathcal{B}^S_{4\phi}$ there is only one. Now notice that even though the boundary theory does not contain a scalar potential at the classical level, this seems to imply that at the 1-loop level a ϕ^4 term appears. One could therefore argue that this radiative scalar potential is similar to the Coleman-Weinberg potential and a Higgs mechanism could be triggered, perhaps at two loops. As we show in Sect. 3.F.2 all of the above 4ϕ diagrams are divergent and we hit on the same issue that came up in the $4A_\mu$ case: there is no tree level ϕ^4 term to be renormalized and a corresponding counter-term to absorb the divergences, leaving only a finite term which could then play the role of a Higgs potential. So, both the 4γ and the 4ϕ diagrams seem to break the renormalizability of the massive, free SQED. As far as we know this was first noticed by Salam in [58]. In our case where we consider the massless limit we are able to deal with this problem and to keep the theory finite, as we show in the Renormalization section.

3.F.1 Four-photon Diagrams

Let us start with the one-loop diagrams contributing to the $\gamma\gamma \to \gamma\gamma$ scattering amplitude. This set contains the following diagrams

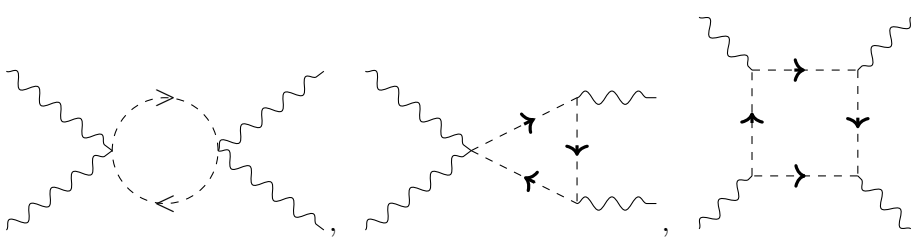

where C- and S-Boxes come in three versions, corresponding to the usual s, t and u channels, where

$$s = (l_1 + l_2)^2 \qquad t = (l_1 + l_3)^2 \qquad u = (l_1 + l_4)^2 \,, \tag{3.F.3}$$

while, the T-Boxes come in six versions since they are not invariant under a reflection with respect to the axis passing through the centre of the loop in the diagram. In particular, there are two independent topologies and each one comes with the three known channels. Here we follow the procedure and the notation of [31]. So, starting with the Candy topology notice that its generic momentum dependence is $\mathcal{B}^C(L_1)$ with $L_1 = \sqrt{s}, \sqrt{t}, \sqrt{u}$ thus for the s-channel we get that

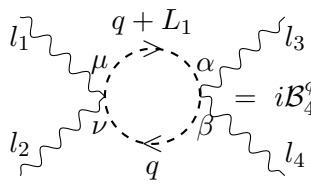

$$= i\mathcal{B}^{\phi\bar{\phi},s}_{4ph.,\mu\nu\alpha\beta}\,, \qquad S^A_{\mathcal{B}^C} = 1 \quad .$$

Using the Feynman rules from Appendix 3.D, its explicit form reads

$$\begin{aligned} i\mathcal{B}^{\phi\bar{\phi},s}_{4ph.,\mu\nu\alpha\beta} &= (2ig^2\gamma g_{\mu\nu})(2ig^2\gamma g_{\alpha\beta})\int \frac{d^4q}{(2\pi)^4}\frac{i}{q^2}\frac{i}{(q+L_1)^2} \Rightarrow \\ \mathcal{B}^{\phi\bar{\phi},s}_{4ph.,\mu\nu\alpha\beta} &= 4g^4\gamma^2 g_{\mu\nu}g_{\alpha\beta}\int \frac{d^4q}{(2\pi)^4 i}\frac{1}{q^2(q+L_1)^2}\,, \end{aligned} \tag{3.F.4}$$

where $L_1 = l_1 + l_2$. Using PV reduction formulae the above integral becomes

$$\mathcal{B}^{\phi\bar{\phi},s}_{4ph.,\mu\nu\alpha\beta} = 4g^4\gamma^2 g_{\mu\nu}g_{\alpha\beta}B_0(q, q+L_1)\,. \tag{3.F.5}$$

Adding up the three channels we get the complete C-Box contribution given by

$$\mathcal{B}^C_{4ph.,\mu\nu\alpha\beta} = 4g^4\gamma^2 g_{\mu\nu}g_{\alpha\beta}\Big[B_0(q, q+\sqrt{s}) + B_0(q, q+\sqrt{t}) + B_0(q, q+\sqrt{u})\Big]\,. \tag{3.F.6}$$

Next, we consider the T-Boxes which are determined by two linear combination of the external momenta L_1 and L_2. A consistent choice for (L_1, L_2) for the channels $T_{1,\cdots,6}$ is $T_1 : (l_1 + l_2, l_1 + l_2 + l_3)$, $T_2 : (l_1 + l_3, l_1 + l_3 + l_4)$, $T_3 : (l_1 + l_4, l_1 + l_3 + l_4)$, $T_4 : (l_2, l_1 + l_2)$, $T_5 : (l_1, l_1 + l_3)$ and $T_6 : (l_1, l_1 + l_4)$. Since the generic T-Box is of the form $\mathcal{B}^T(L_1, L_2)$ it is enough to calculate only one diagram and then take the sum over the six different pairs (L_1, L_2). Here we choose to evaluate the following s-channel diagram:

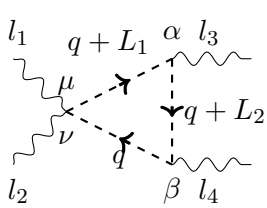

$$= i\mathcal{B}^{\phi\phi\phi}_{4ph.,\mu\nu\alpha\beta}\,, \qquad S^A_{\mathcal{B}^T} = 1 \quad .$$

It is equal to

$$i\mathcal{B}^{\phi\phi\phi,s}_{4ph.,\mu\nu\alpha\beta} = (2ig^2\gamma g_{\mu\nu})(ig\sqrt{\gamma})(ig\sqrt{\gamma})\int \frac{d^4q}{(2\pi)^4}\frac{i(2q+L_1+L_2)_\alpha}{q^2}\frac{i(2q+L_2)_\beta}{(q+L_1)^2}\frac{i}{(q+L_2)^2} \Rightarrow$$

$$\mathcal{B}^{\phi\phi\phi,s}_{4ph.,\mu\nu\alpha\beta} = -2g^4\gamma^2 g_{\mu\nu}\int\frac{d^4q}{(2\pi)^4 i}\frac{(2q+L_1+L_2)_\alpha(2q+L_2)_\beta}{q^2(q+L_1)^2(q+L_2)^2}\,, \tag{3.F.7}$$

and using PV reduction formulae it becomes

$$\begin{aligned}\mathcal{B}^{\phi\phi\phi,s}_{4ph.,\mu\nu\alpha\beta} &= -2g^4\gamma^2 g_{\mu\nu}\Big[4C_{\alpha\beta}(q,q+L_1,q+L_2)+(2L_1+4L_2)_\alpha C_\beta(q,q+L_1,q+L_2)\\ &+ L_{2,\alpha}(L_1+L_2)_\beta C_0(q,q+L_1,q+L_2)\Big]\,.\end{aligned} \tag{3.F.8}$$

Considering the sum over the six different topologies, the complete T-Box contribution is given by

$$\mathcal{B}^{T}_{4ph.,\mu\nu\alpha\beta} = \sum_{(L_1,L_2)}\mathcal{B}^{\phi\phi\phi,s}_{4ph.,\mu\nu\alpha\beta}(L_1,L_2)\,. \tag{3.F.9}$$

Regarding the four-photon scattering amplitude there is one more set of one-loop diagrams, the S-Boxes. These are determined by three linear combinations of the external momenta, (L_1,L_2,L_3) and in this case there are only three topologies corresponding to the usual s, t and u-channels. So, a proper choice for the (L_1,L_2,L_3) for the three channels $S_{1,2,3}$ is $S_1 = (l_1, l_1+l_3, l_1+l_3+l_4)$, $S_2 = (l_3, l_1+l_3, l_1+l_3+l_4)$ and $S_3 = (l_1, l_1+l_4, l_1+l_3+l_4)$. In order to take into account all the channels it is enough to calculate one of them and then take the sum over the three momenta, (L_1,L_2,L_3). Let us start by evaluating the s-channel S-Box which is given by

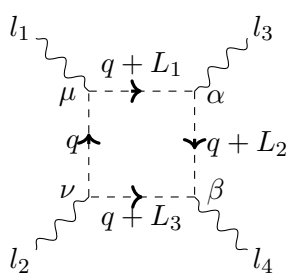

$$= i\mathcal{B}^{\phi\phi\phi\phi}_{4ph.,\mu\nu\alpha\beta}\,, \qquad S^A_{\mathcal{B}^S} = 1\,,$$

and its explicit form reads

$$\begin{aligned}i\mathcal{B}^{\phi\phi\phi\phi,s}_{4ph.,\mu\nu\alpha\beta} &= (ig\sqrt{\gamma})(ig\sqrt{\gamma})(ig\sqrt{\gamma})(ig\sqrt{\gamma})\int\frac{d^4q}{(2\pi)^4}\frac{i(2q+L_1)_\mu}{q^2}\frac{i(2q+L_1+L_2)_\alpha}{(q+L_1)^2}\\ &\times \frac{i(2q+L_2+L_3)_\beta}{(q+L_2)^2}\frac{i(2q+L_2)_\nu}{(q+L_3)^2}\Rightarrow\\ \mathcal{B}^{\phi\phi\phi\phi,s}_{4ph.,\mu\nu\alpha\beta} &= g^4\gamma^2\int\frac{d^4q}{(2\pi)^4 i}\frac{(2q+L_1)_\mu(2q+L_1+L_2)_\alpha(2q+L_2+L_3)_\beta(2q+L_3)_\nu}{q^2(q+L_1)^2(q+L_2)^2(q+L_3)^2}\,.\end{aligned} \tag{3.F.10}$$

Using the PV reduction, the above integral becomes

$$\begin{aligned}\mathcal{B}^{\phi\phi\phi\phi,s}_{4ph.,\mu\nu\alpha\beta} &= g^4\gamma^2\Big[16D_{\mu\nu\alpha\beta}(q,q+L_1,q+L_2,q+L_3)+8L_{3,\alpha}D_{\beta\mu\nu}(q,q+L_1,q+L_2,q+L_3)\\ &+ 8(L_2+L_3)_\beta D_{\mu\nu\alpha}(q,q+L_1,q+L_2,q+L_3)+8L_{1,\mu}D_{\beta\nu\alpha}(q,q+L_1,q+L_2,q+L_3)\end{aligned}$$

$$
\begin{aligned}
&+ \quad 8(L_1+L_2)_\nu D_{\beta\mu\alpha}(q,q+L_1,q+L_2,q+L_3) \\
&+ \quad 4(L_{3,\alpha}L_{3,\beta}+L_{2,\alpha}L_{3,\beta})D_{\mu\nu}(q,q+L_1,q+L_2,q+L_3) \\
&+ \quad 4(L_{1,\mu}L_{3,\alpha}+L_{1,\mu}L_{2,\alpha})D_{\nu\beta}(q,q+L_1,q+L_2,q+L_3) \\
&+ \quad 4L_{1,\mu}L_{3,\beta}D_{\alpha\nu}(q,q+L_1,q+L_2,q+L_3) \\
&+ \quad 4(L_{1,\alpha}L_{3,\nu}+L_{2,\alpha}L_{3,\nu}+L_{1,\alpha}L_{2,\nu}+L_{2,\alpha}L_{2,\nu})D_{\mu\beta}(q,q+L_1,q+L_2,q+L_3) \\
&+ \quad 4(L_{1,\nu}L_{3,\beta}+L_{2,\nu}L_{3,\beta})D_{\mu\alpha}(q,q+L_1,q+L_2,q+L_3) \\
&+ \quad 4(L_{1,\mu}L_{1,\nu}+L_{1,\mu}L_{2,\nu})D_{\alpha\beta}(q,q+L_1,q+L_2,q+L_3) \\
&+ \quad 2(L_{1,\mu}L_{2,\alpha}L_{3,\beta}+L_{1,\mu}L_{3,\beta}L_{3,\alpha})D_\nu(q,q+L_1,q+L_2,q+L_3) \\
&+ \quad 2(L_{1,\nu}L_{3,\beta}L_{3,\alpha}+L_{2,\nu}L_{3,\beta}L_{3,\alpha}+L_{1,\nu}L_{2,\alpha}L_{3,\beta}+L_{2,\alpha}L_{2,\nu}L_{3,\beta})D_\mu(q,q+L_1,q+L_2,q+L_3) \\
&+ \quad 2(L_{1,\mu}L_{1,\nu}L_{3,\alpha}+L_{1,\mu}L_{2,\nu}L_{3,\alpha}+L_{1,\mu}L_{1,\nu}L_{2,\alpha}+L_{1,\mu}L_{2,\nu}L_{2,\alpha})D_\beta(q,q+L_1,q+L_2,q+L_3) \\
&+ \quad 2(L_{1,\mu}L_{1,\nu}L_{3,\beta}+L_{1,\mu}L_{2,\nu}L_{3,\beta})D_\alpha(q,q+L_1,q+L_2,q+L_3) \\
&+ \quad L_{1,\mu}L_{3,\beta}(L_{1,\nu}L_{2,\alpha}+L_{2,\nu}L_{2,\alpha}+L_{1,\nu}L_{3,\alpha}+L_{2,\nu}L_{3,\alpha})D_0(q,q+L_1,q+L_2,q+L_3)\Big] \,. \qquad (3.F.11)
\end{aligned}
$$

The complete S-Box contribution comes by summing the three different channels and is given by

$$
\mathcal{B}^{S}_{4ph.,\mu\nu\alpha\beta} = \sum_{(L_1,L_2,L_3)} \mathcal{B}^{\phi\phi\phi\phi,s}_{4ph.,\mu\nu\alpha\beta}(L_1,L_2,L_3)\,, \qquad (3.F.12)
$$

while the full contribution to the $\gamma\gamma \to \gamma\gamma$ scattering amplitude is given by adding the C-, T- and S-Boxes and reads

$$
\mathcal{B}_{4ph.,\mu\nu\alpha\beta} = \mathcal{B}^{C}_{4ph.,\mu\nu\alpha\beta} + \mathcal{B}^{T}_{4ph.,\mu\nu\alpha\beta} + \mathcal{B}^{S}_{4ph.,\mu\nu\alpha\beta}\,. \qquad (3.F.13)
$$

3.F.2 Four-scalar Diagrams

Apart from the four-photon scattering amplitudes, the boundary action contains also a set of one-loop diagrams contributing to the $\phi\bar{\phi} \to \phi\bar{\phi}$ process. In particular, this set contains the following diagrams

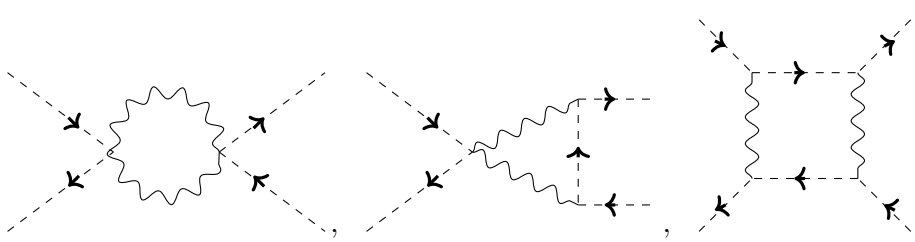

where in this case, C- and T-Boxes come in two possible channels, s and t, while the S-Boxes come in only one channel, s. The reason for this is that the external legs are particle-antiparticle pairs so they cannot be interchanged. Now, notice here that there are four T-Boxes, since they have two independent topologies and each comes with the two channels mentioned previously. Moreover, notice that also for the S-Boxes there are two independent topologies, since there are two possible ways to arrange the propagators inside the loop, while each of them comes

in one channel. So, with these in mind let us start with the s-channel of the C-Box, which diagrammatically reads

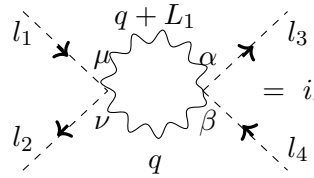

$$= \; i\mathcal{B}_{4\phi}^{AA,s}\,, \qquad S_{\mathcal{B}^C}^{\phi} = 1 \quad .$$

Its explicit form is given by

$$\begin{aligned} i\mathcal{B}_{4\phi}^{AA,s} &= (2ig^2\gamma g_{\mu\nu})(2ig^2\gamma g_{\alpha\beta})\int \frac{d^4q}{(2\pi)^4}\frac{-ig^{\mu\alpha}}{q^2}\frac{-ig^{\nu\beta}}{(q+L_1)^2} \Rightarrow \\ \mathcal{B}_{4\phi}^{AA,s} &= 4dg^4\gamma^2\int \frac{d^4q}{(2\pi)^4 i}\frac{1}{q^2(q+L_1)^2}\,, \end{aligned} \tag{3.F.14}$$

while in DR the above integral reads

$$\mathcal{B}_{4\phi}^{AA,s} = 4dg^4\gamma^2 B_0(q, q+L_1)\,. \tag{3.F.15}$$

The complete C-Box contribution comes by summing over the two channels giving

$$\mathcal{B}_{4\phi}^{C} = 4dg^4\gamma^2\Big[B_0(q, q+\sqrt{s}) + B_0(q, q+\sqrt{t})\Big]\,. \tag{3.F.16}$$

Next, we move on to the T-Boxes which, in this case, are determined by two pairs of two linear combinations of the external momenta, (L_1, L_2) and (L_A, L_B). A good choice for these pairs for the channels $T_{1,\cdots,4}$ is the following

$$\begin{aligned} T_1 &: (l_1+l_2, l_1+l_2+l_3)\,, \quad (l_1+l_2+2l_3, l_1+l_2+l_3-l_4) \\ T_2 &: (l_1+l_3, l_1+l_3+l_4)\,, \quad (l_1+l_3+2l_4, 0) \\ T_3 &: (l_2, l_1+l_2)\,, \quad (2l_2, l_2-l_1) \\ T_4 &: (l_1, l_1+l_3)\,, \quad (2l_1, l_1+l_3)\,. \end{aligned} \tag{3.F.17}$$

The first s-channel here is given by

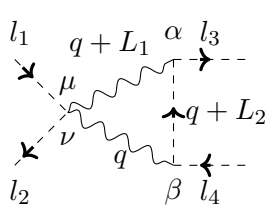

$$= \; i\mathcal{B}_{4\phi}^{AA\phi,s}\,, \qquad S_{\mathcal{B}^T}^{\phi} = 1 \quad ,$$

and it is equal to

$$i\mathcal{B}_{4\phi}^{AA\phi,s} = (2ig^2\gamma g_{\mu\nu})(ig\sqrt{\gamma})(ig\sqrt{\gamma})\int \frac{d^4q}{(2\pi)^4}\frac{-ig^{\mu\alpha}(q+L_A)_\alpha}{q^2}\frac{-ig^{\nu\beta}(q+L_B)_\beta}{(q+L_1)^2}\frac{i}{(q+L_2)^2} \Rightarrow$$

$$\mathcal{B}_{4\phi}^{AA\phi,s} = -2g^4\gamma^2 \int \frac{d^4q}{(2\pi)^4 i} \frac{(q+L_A)\cdot(q+L_B)}{q^2(q+L_1)^2(q+L_2)^2} \,. \tag{3.F.18}$$

In DR the above integral becomes

$$\begin{aligned} \mathcal{B}_{4\phi}^{AA\phi,s} &= -2g^4\gamma^2 \Big[B_0(q, q+L_2-L_1) + (L_A+l_B)_\mu C^\mu(q, q+L_1, q+L_2) \\ &+ (L_A\cdot L_B) C_0(q, q+L_1, q+L_2) \Big] \,. \end{aligned} \tag{3.F.19}$$

The complete T-Box contribution is given by

$$\mathcal{B}_{4\phi}^{T} = \sum_{(L_A,L_B)} \sum_{(L_1,L_2)} \mathcal{B}_{4\phi}^{AA\phi,s}(L_1, L_2, L_A, L_B) \,. \tag{3.F.20}$$

The last set of diagrams contains the S-Boxes. On the one hand there is only one channel and as a consequence we have a unique choice for (L_1, L_2, L_3), say $(l_1, l_1+l_3, l_1+l_3+l_4)$. On the other hand these S-Boxes are determined by four linear combinations of the external momenta, L_A, L_B, L_C and L_D. Thus, for the two possible topologies that we have here a proper choice for $L_{A,\cdots D}$ is the following

$$\begin{aligned} L_A &= 2l_1 \,, \quad -l_1 \\ L_B &= l_1 - l_3 \,, \quad l_1 \\ L_C &= l_1 + l_3 + 2l_4 \,, \quad l_1 + l_3 + l_4 \\ L_D &= l_1 + l_3 + l_4 - l_2 \,, \quad l_2 \,. \end{aligned} \tag{3.F.21}$$

So, the first diagram is

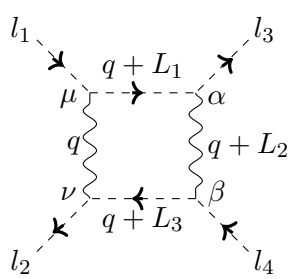

$$= i\mathcal{B}_{4\phi}^{A\phi A\phi,s} \,, \quad S_{\mathcal{B}^S}^{\phi} = 1 \,,$$

and it is equal to

$$\begin{aligned} i\mathcal{B}_{4\phi}^{A\phi A\phi,s} &= (ig\sqrt{\gamma})(ig\sqrt{\gamma})(ig\sqrt{\gamma})(ig\sqrt{\gamma}) \int \frac{d^4q}{(2\pi)^4} \frac{-ig^{\alpha\beta}(q+L_A)_\mu}{q^2} \frac{i(-q-L_B)_\alpha}{(q+L_1)^2} \\ &\times \frac{-ig^{\mu\nu}(q+L_C)_\beta}{(q+L_2)^2} \frac{i(-q-L_D)_\nu}{(q+L_3)^2} \Rightarrow \\ \mathcal{B}_{4\phi}^{A\phi A\phi,s} &= g^4\gamma^2 \int \frac{d^4q}{(2\pi)^4 i} \frac{(q+L_A)\cdot(q+L_D)(q+L_B)\cdot(q+L_C)}{q^2(q+L_1)^2(q+L_2)^2(q+L_3)^2} \,. \end{aligned} \tag{3.F.22}$$

The above integral in DR becomes

$$\mathcal{B}_{4\phi}^{A\phi A\phi,s} = g^4\gamma^2 \Big[g_{\mu\nu} g_{\alpha\beta} D^{\mu\nu\alpha\beta}(q, q+L_1, q+L_2, q+L_3)$$

$$
\begin{aligned}
&+ \quad g_{\mu\nu}(L_A + L_B + L_C + L_D)_\alpha D^{\mu\nu\alpha}(q, q+L_1, q+L_2, q+L_3) \\
&+ \quad g_{\mu\nu}(L_B \cdot L_C + L_A \cdot L_D) D^{\mu\nu}(q, q+L_1, q+L_2, q+L_3) \\
&+ \quad (L_{C,\alpha} L_{D,\beta} + L_{B,\alpha} L_{D,\beta} + L_{A,\alpha} L_{C,\beta} + L_{A,\alpha} L_{B,\beta}) D^{\alpha\beta}(q, q+L_1, q+L_2, q+L_3) \\
&+ \quad (L_B \cdot L_C L_{D,\mu} + L_A \cdot L_D L_{C,\mu} + L_A \cdot L_D L_{B,\mu} + L_B \cdot L_C L_{A,\mu}) D^{\mu}(q, q+L_1, q+L_2, q+L_3) \\
&+ \quad L_A \cdot L_D L_B \cdot L_C D_0(q, q+L_1, q+L_2, q+L_3) \Big] \,, \qquad (3.F.23)
\end{aligned}
$$

while the complete S-Box contribution is taken by considering the sum over the two possible topologies:

$$
\mathcal{B}_{4\phi}^{S} = \sum_{(L_A, L_B, L_C, L_D)} \mathcal{B}_{4\phi}^{A\phi A\phi, s}(L_A, L_B, L_C, L_D) \,. \qquad (3.F.24)
$$

The full one-loop contribution to the scalar potential is given by adding the C-, T- and S-Boxes:

$$
\mathcal{B}_{4\phi} = \mathcal{B}_{4\phi}^{C} + \mathcal{B}_{4\phi}^{T} + \mathcal{B}_{4\phi}^{S} \,. \qquad (3.F.25)
$$

Chapter 4

Generalized effective field theory: The quantum origin of the higher dimensional operators

4.1 Introduction

As far as the current Chapter is concerned, we considered the example of a scalar Generalized Effective Field Theory, which is an Effective Field Theory where the couplings associated with Higher Dimensional Operators run with the renormalization scale in an independent fashion. In particular we start with the real scalar Lagrangian

$$\mathcal{L} = -\frac{1}{2}\phi\Box\phi - \frac{1}{2}m_0^2\phi^2 - \frac{\lambda_0}{4!}\phi^4 + \cdots = \mathcal{L}^{(2)} + \mathcal{L}_{\text{int}} \tag{4.1.1}$$

which is invariant under a global $\mathbb{Z}_2$ symmetry ($\phi_0 \to -\phi_0$) and extend it using the most general basis of Higher Dimensional Operators. Such extensions are non-renormalizable, possess in general Ostrogradsky ghosts and superluminal propagation of information. Despite of all these drawbacks they can be meaningful in certain regimes of their phase diagram. A necessary condition for this is that the infinite tower of HDO can be truncated. In order to do this in a systematic way we parametrized them by inverse powers of an auxiliary scale Λ and truncated the series at fixed powers of Λ. In this context we showed how the GEFT can be made ghost-free and subsequently finite. The couplings of the HDO contribute to the β-function of the marginal coupling in GEFT which could be observable.

An interesting corner of effective field theories is the massless limit, the reason being that to the extent that the breaking of scale invariance induced by the presence of Λ is spontaneous, it is connected to the spontaneous breaking of the internal symmetry in the broken phase. Then we could have a Coleman-Weinberg like mechanism [13] where instead of gauge fields, the breaking is triggered by the HDO. Indeed, the phase diagrams that we have seen, do possess such phases.

We also extended the analysis to dimensions $d \neq 4$, exploiting the flexibility of the ε-

expansion. In this case the phase diagram has more structure as Wilson-Fisher fixed points or lines start to appear where the system becomes scale invariant or approximately scale invariant, given that our analysis was restricted to 1-loop.

4.2 GEFT β-functions and anomalous dimensions

We are interested in the evaluation of β-functions and anomalous dimensions for the Lagrangian of Eq. (1.0.1) with $n = 3, 4$. This is just the massive ϕ^4 theory extended by HDO of dimension-$(6, 8)$. The associated Wilson coefficients run independently of the marginal and relevant couplings, which determines the model as a GEFT. An operator insertion of level-w is an expectation value $\langle \cdots O^{(r_1)} \cdots O^{(r_w)} \rangle$, generated by the quantum theory, perturbatively or non-perturbatively.

In the case of only one independent operator at every mass dimension, as it is the case for the scalar theory we are interested in here, the β-function of the coupling $c^{(l)}$ associated with the operator $O^{(l)}$ ($c^{(2)} = m^2$ and $c^{(4)} = \lambda$ etc.), as obtained from the renormalization of Eq. (1.0.1), can be expressed as [70]

$$\beta_{c^{(l)}} = (d_{O^{(l)}} - d)c^{(l)} + q_{l+2}\,\Gamma_m^{l+2}\,m^2 + \Gamma_{O^{(l)}}\,c^{(l)} + \Gamma_{lrs}\,c^{(r)}c^{(s)} + \cdots\,, \tag{4.2.1}$$

with $l, r, s = 2, 4, 6, 8, \cdots$ (sum over the indices r and s is implied),

$$q_{l+2} = \begin{cases} 0 \text{ when } l = 2 \\ \frac{2}{l} \text{ otherwise} \end{cases} \tag{4.2.2}$$

The dots represent higher than level-2 insertions and 1-loop corrections. In case where there are several operators of a given dimension, the couplings and the Γ's acquire extra indices. Γ_m^{l+2} and $\Gamma_{O^{(l)}}$ are the anomalous dimensions of the operator $O^{(l)}$, induced by the relevant and marginal operators respectively. For the mass operator, when $l = 2$, the terms $\Gamma_m^{l+2}m^2$ and $\Gamma_{O^{(l)}}\,c^{(l)}$ coincide, so a coefficient q_{l+2} in front of Γ_m^{l+2} is needed to avoid double counting. Moreover, q_{l+2} protects Γ_m^{l+2} from numerical factors infiltrating from the classical dimension of $O^{(l)}$. The quantity Γ_{lrs} in the non-linear term represents the anomalous dimension associated with the level-2 operator insertion $\langle \cdots O^{(r)}O^{(s)} \rangle$, $r, s \geq 2$. For $l \leq 8$ we have only $r = s$, otherwise mixing of HDO of different mass dimensions starts to appear. Renormalization of Eq. (1.0.1) indeed gives this total structure but it is not sensitive to the entire substructure implied by the Γ-matrices. It is our intention here to reconstruct $\beta_{c^{(l)}}$ to expose this substructure, by applying the operator insertion method.

Consider the operator $O_0^{(l)}$ and its associated coupling $c_0^{(l)}$. Renormalization (with Dimensional Regularization) indicates that

$$\phi_0 = \sqrt{Z_\phi}\phi = \sqrt{(1+\delta_\phi)}\phi\,,\ c_0^{(l)} = Z_{c^{(l)}}\,c^{(l)} = (1+\delta_{c^{(l)}})c^{(l)}\,, \tag{4.2.3}$$

and introduces the regulating scale μ so that in d-dimensions $c_0^{(l)} \to c_0^{(l)} \mu^{d-d_{O^{(l)}}}$ since (denoting the dimension of an operator by $[\cdots]$)

$$[c^{(l)}\, O^{(l)}] = d_{c^{(l)}} + d_{O^{(l)}} = d \Rightarrow d_{c^{(l)}} = d - d_{O^{(l)}}\,, \tag{4.2.4}$$

where $d_{O^{(l)}}$ and $d_{c^{(l)}}$ are the classical dimensions of $O^{(l)}$ and $c^{(l)}$ respectively. Now $c^{(l)}$ is dimensionless in d dimensions. An observation here is that Eq. (4.2.3) is not the full story of renormalization since $O_0^{(l)}$ may include bare fields located at the same space-time point and this generates extra UV divergences. So Green's functions which include composite operators are divergent even in an already renormalized theory. The simplest example that demonstrates this is $O_0^{(2)}(y) = \phi_0^2(y)$ (see [19]), as then $< O_0^{(2)} >$ is

$$\langle 0|T[\phi_0^2(y)]|0\rangle \equiv \lim_{x\to y} \langle 0|T[\phi_0(x)\phi_0(y)]|0\rangle = \lim_{x\to y} \int \frac{d^4k}{(2\pi)^4 i} \frac{e^{ik(x-y)}}{k^2-m^2} = \int \frac{d^4k}{(2\pi)^4 i} \frac{1}{k^2-m^2}\,,$$

which is the known (divergent) $A_0(m^2)$ Tadpole integral. Thus, a bare operator, a product of m-fields ϕ_0, should be renormalized as

$$O_0^{(l)} = Z_\phi^{m/2}\, \overline{Z}_{O^{(l)}} O^{(l)} = Z_{O^{(l)}} O^{(l)}\,, \tag{4.2.5}$$

with

$$Z_{O^{(l)}} = Z_\phi^{m/2}\, \overline{Z}_{O^{(l)}} = 1 + \delta_{O^{(l)}} \quad \text{or} \quad (Z_{O^{(l)}})^{-1} = 1 - \delta_{O^{(l)}}\,. \tag{4.2.6}$$

Let us now recall how the anomalous dimension $\Gamma_{O^{(l)}}$ of an operator fits in the β-function (see for example [71, 73]). To this effect, let us assume for a moment that level-1 insertions are the only ones present. Acting on $c_0^{(l)} \mu^{d-d_{O^{(l)}}} = Z_{c^{(l)}} c^{(l)} \mu^{d-d_{O^{(l)}}}$ with $\mu\, d/d\mu$ on both sides we have

$$\begin{aligned}
\mu \frac{d(c_0^{(l)} \mu^{d-d_{O^{(l)}}})}{d\mu} &= \mu \frac{d(Z_{c^{(l)}} c^{(l)} \mu^{d-d_{O^{(l)}}})}{d\mu} \\
0 &= \mu \frac{dZ_{c^{(l)}}}{d\mu} c^{(l)} \mu^{d-d_{O^{(l)}}} + Z_{c^{(l)}} \left(\mu \frac{dc^{(l)}}{d\mu} \right) \mu^{d-d_{O^{(l)}}} + (d - d_{O^{(l)}}) Z_{c^{(l)}} c^{(l)} \mu^{d-d_{O^{(l)}}}
\end{aligned}$$

while acting from the left with $Z_{c^{(l)}}^{-1}$ and isolating the $\mu \frac{dc^{(l)}}{d\mu} \equiv \beta_{c^{(l)}}$ term, we obtain

$$\beta_{c^{(l)}} = (d_{O^{(l)}} - d) c^{(l)} - \left(Z_{c^{(l)}}^{-1}\, \mu \frac{dZ_{c^{(l)}}}{d\mu} \right) c^{(l)}\,. \tag{4.2.7}$$

Since $c^{(l)}$ is contained in the insertion of $c_0^{(l)} O_0^{(l)}$, the extra UV divergences that $O_0^{(l)}$ carries are cancelled when

$$Z_{c^{(l)}}^{-1} = Z_{O^{(l)}}\,. \tag{4.2.8}$$

Then Eq. (4.2.7) becomes

$$\begin{aligned}
\beta_{c^{(l)}} &= (d_{O^{(l)}} - d) c^{(l)} - \left(Z_{O^{(l)}}\, \mu \frac{d(Z_{O^{(l)}})^{-1}}{d\mu} \right) c^{(l)} \\
&= (d_{O^{(l)}} - d) c^{(l)} + (Z_{O^{(l)}})^{-1}\, \mu \frac{dZ_{O^{(l)}}}{d\mu} c^{(l)}
\end{aligned}$$

$$= \quad (d_{O^{(l)}} - d)c^{(l)} + \Gamma_{O^{(l)}} c^{(l)} \tag{4.2.9}$$

where we defined

$$\Gamma_{O^{(l)}} = (Z_{O^{(l)}})^{-1}\, \mu \frac{dZ_{O^{(l)}}}{d\mu}\,, \tag{4.2.10}$$

the anomalous dimension of the operator $O^{(l)}$. In case where the only marginal operator is $O^{(4)}$, at 1-loop, the simple formula $\Gamma_{O^{(l)}} = (d_{O^{(4)}} - d)\frac{\delta_{O^{(l)}}}{c^{(4)}}$ can be used. The contribution of the mass insertion to $\beta_{c^{(l)}}$ in Eq. (4.2.1) is analogously defined by (see Eq. (4.2.21) below)

$$\Gamma_m^{l+2} = \sum_k (Z_k^{l+2})^{-1} \mu \frac{dZ_k^{l+2}}{d\mu}\,. \tag{4.2.11}$$

Here one can use the 1-loop formula $\Gamma_m^{l+2} = \sum_k (d_{O^{(l+2)}} - d)\frac{\delta_k^{(l+2)}}{c^{(l+2)}}$, with $k = 2, 4, 6, 8 \cdots$.

This is of course just one part of Eq. (4.2.1) because higher level insertions are also generated, affecting the β-function already at 1-loop. Such a case is the level-2 insertion. Applying the OPE on the double insertion and repeating the steps above yields the contribution $\Gamma_{lrs}\, c^{(r)} c^{(s)} \in \beta_{c^{(l)}}$. The level-2 anomalous dimension for every triplet of indices is then

$$\Gamma_{lrs} = \varepsilon \delta_{lrs}\,, \tag{4.2.12}$$

where $\delta_{lrs} = Z_{lrs} - 1$ is the renormalization counter-term of the double insertion.

Now let us be more specific about the operator insertion method, according to which every operator can be considered as a deformation of the kinetic term. Let us assume for simplicity that $Z_\phi = 1$, which is true at 1-loop. The basic path integral of a pure scalar theory with action $S[\phi_0]$ and inserted operators $O_0^{(l)}$ is given by

$$\mathcal{Z}[J, J^{(l)}] = \int \mathcal{D}\phi_0\, e^{iS[\phi_0] + J\phi_0 + J^{(l)} O_0^{(l)}}\,,$$

with summation over l implied. Then the n-point Green's function is

$$\langle \phi(x_1) \cdots \phi(x_n) \rangle_0 = \frac{1}{\mathcal{Z}[J, J^{(l)}] i^n} \frac{\partial}{\partial J(x_1)} \cdots \frac{\partial}{\partial J(x_n)} \mathcal{Z}[J, J^{(l)}]\Big|_{J=J^{(l)}=0}\,. \tag{4.2.13}$$

In order to insert w times the $O_0^{(l)}$ operator we must act with $\partial^w / i^w \partial J^{(l)}(y_1) \cdots J^{(l)}(y_w)$ on the partition function. w defines the level of the insertion in the sense that $w = 1$ is a single insertion, $w = 2$ is a double insertion and so on. A single insertion for example affects the n-point function as

$$\langle \phi(x_1) \cdots \phi(x_n) O^{(l)}(y) \rangle_0 = \frac{1}{\mathcal{Z}[J, J^{(l)}] i^n} \frac{\partial}{\partial J(x_1)} \cdots \frac{\partial}{\partial J(x_n)} \frac{\partial}{i \partial J^{(l)}(y)} \mathcal{Z}[J, J^{(l)}]\Big|_{J=J^{(l)}=0}\,. \tag{4.2.14}$$

Since the functional derivatives wrt J and $J^{(l)}$ are independent, each group of derivatives should be renormalized independently. That is to say, any n-point Green's function can be affected by any operator $O_0^{(l)}$.

Now, the action depends on a Lagrangian which we split in two parts:

$$S[\phi_0] = \int d^d x \Big[\mathcal{L}_{\text{kin},0} + \mathcal{L}_{\text{int},0} \Big]\,, \tag{4.2.15}$$

with $\mathcal{L}_{\text{kin},0}$ and $\mathcal{L}_{\text{int},0}$ the kinetic and interaction parts of the Lagrangian. The former determines the propagator while the latter contains the vertices. The l.h.s of Eq. (4.2.13) is given by

$$G_0^{(n)}(x_1, \cdots, x_n) \equiv \langle \phi(x_1) \cdots \phi(x_n) \rangle_0 = \langle 0 | T[\phi_0(x_1) \cdots \phi_0(x_n)] | 0 \rangle \,, \tag{4.2.16}$$

where $T[\cdots]$ denotes time-ordering. Following [19], the expectation value in Eq. (4.2.16) is

$$\langle 0 | T[\phi_0(x_1) \cdots \phi_0(x_n)] | 0 \rangle = \mathcal{N}^{-1} \langle 0 | T[\phi_0(x_1) \cdots \phi_0(x_n) e^{i \int d^d x \mathcal{L}_{\text{int},0}}] | 0 \rangle \,, \tag{4.2.17}$$

with

$$\mathcal{N} = \langle 0 | T[e^{i \int d^d x \mathcal{L}_{\text{int},0}}] | 0 \rangle \,,$$

necessary for the cancellation of disconnected and bubble diagrams. ϕ represents the field as a quantum operator.

The algorithm is the following: start with a bare, free massless action so that any operator (including the mass term) added to the kinetic term can be viewed as an operator insertion. Since the mass term is considered as part of the operator-insertion, massless propagators will run in the loops. Then, $\mathcal{L}_{\text{int},0} = \sum_l c_0^{(l)} O_0^{(l)}(y)$ which means that

$$\langle \phi(x_1) \cdots \phi(x_n) \rangle_0 = \mathcal{N}^{-1} \langle 0 | T[\phi_0(x_1) \cdots \phi_0(x_n) e^{i \int d^d y \sum_l c_0^{(l)} O_0^{(l)}(y)}] | 0 \rangle \,. \tag{4.2.18}$$

Next, single out one operator with label l from the sum in the exponent and apply the series expansion to it [73]. The rest of the operators remain summed over in the exponent, in a reduced sum over l'. Then Eq. (4.2.18) becomes

$$\begin{aligned}
&\langle \phi(x_1) \cdots \phi(x_n) \rangle_0 = \mathcal{N}^{-1} \sum_{w=0}^{\infty} \int d^d y_1 \cdots d^d y_w \frac{(i c_0^{(l)} \mu^{d - d_{O^{(l)}}})^w}{w!} \times \\
&\langle 0 | T[\phi_0(x_1) \cdots \phi_0(x_n) O_0^{(l)}(y_1) \cdots O_0^{(l)}(y_w) e^{i \int d^d y \sum_{l'} c_0^{(l')} O_0^{(l')}(y)}] | 0 \rangle \\
= \; & \sum_{w=0}^{\infty} \int d^d y_1 \cdots d^d y_w \frac{(i c_0^{(l)} \mu^{d - d_{O^{(l)}}})^w}{w!} \langle \phi(x_1) \cdots \phi(x_n) O^{(l)}(y_1) \cdots O^{(l)}(y_w) \rangle_0 \\
= \; & \sum_{w=0}^{\infty} \int d^d y_1 \cdots d^d y_w \frac{(i c_0^{(l)} \mu^{d - d_{O^{(l)}}})^w}{w!} G_0^{(n,w)}
\end{aligned} \tag{4.2.19}$$

The correlator $G^{(n,w)}$ on the r.h.s of Eq. (4.2.19) expresses the way that the w times inserted operator $O^{(l)}$ affects the n-point Green's function, in the presence of interactions specified by the sum $\sum_{l'}$. For example, for a single insertion $w = 1$ and $G^{(n,1)}$ gives the l.h.s of Eq. (4.2.14).

Now we are ready to evaluate the different parts of Eq. (4.2.1). At level-1 of insertions, for n-external legs and operators $O^{(l)}$, there are two relevant cases:

- $n = l$
  In this case the l.h.s of Eq. (4.2.14) is

$$\langle \phi(x_1) \cdots \phi(x_n) O^{(l)}(y) \rangle_0 \equiv \langle \phi(x_1) \cdots \phi(x_l) O^{(l)}(y) \rangle_0$$

and its renormalization requires that

$$\langle \phi(x_1)\cdots\phi(x_l)O^{(l)}(y)\rangle_0 = Z_{O^{(l)}}\langle \phi(x_1)\cdots\phi(x_l)O^{(l)}(y)\rangle\,, \tag{4.2.20}$$

from which the $\Gamma_{O^{(l)}}$ part of Eq. (4.2.1) can be extracted.

- $n \neq 2$ and $l = 2$
  The above shows the way that a mass operator affects n-external legs. Then the l.h.s of Eq. (4.2.14) is given by

  $$\langle \phi(x_1)\cdots\phi(x_n)O^{(2)}(y)\rangle_0\,.$$

  After renormalization we have $n \neq 2$ but all the possible insertions, so that

  $$\langle \phi(x_1)\cdots\phi(x_n)O^{(2)}(y)\rangle_0 = \sum_k Z_k^{n+2}\langle \phi(x_1)\cdots\phi(x_n)O^{(k)}(y)\rangle\,. \tag{4.2.21}$$

  This will give us Γ_m^{n+2} of Eq. (4.2.1) through Eq. (4.2.11).

The remaining contribution to $\beta_{c^{(l)}}$ has its origin in double operator insertions and specifies the anomalous dimension Γ_{lrs}. Double insertions can be generated by acting one more time with $\partial/i\partial J^{(l)}$ on Eq. (4.2.14). Then, for n-external legs and two $O^{(l)}$ operators, we obtain the following two cases:

- $n = l$
  The relevant expectation value is

  $$\langle \phi(x_1)\cdots\phi(x_n)O^{(l)}(y)O^{(l)}(z)\rangle_0 \equiv \langle \phi(x_1)\cdots\phi(x_l)O^{(l)}(y)O^{(l)}(z)\rangle_0\,,$$

  therefore renormalization indicates that

  $$\langle \phi(x_1)\cdots\phi(x_l)O^{(l)}(y)O^{(l)}(z)\rangle_0 = Z_{lrs}\langle \phi(x_1)\cdots\phi(x_l)O^{(r)}(y)O^{(s)}(z)\rangle\,, \tag{4.2.22}$$

  where we have set $O_0^{(l)}(y)O_0^{(l)}(z) = Z_{lrs}O_0^{(r)}(y)O_0^{(s)}(z)$.

- $n \neq k'$ with k' the dimension of the inserted operators.
  In this case double insertions are just

  $$\langle \phi(x_1)\cdots\phi(x_n)O^{(k')}(y)O^{(k')}(z)\rangle_0\,,$$

  while renormalizing the above, now with $O_0^{(k')}(y)O_0^{(k')}(z) = Z_{qrs}O_0^{(r)}(y)O_0^{(s)}(z)$, we get

  $$\langle \phi(x_1)\cdots\phi(x_n)O^{(k')}(y)O^{(k')}(z)\rangle_0 = Z_{qrs}\langle \phi(x_1)\cdots\phi(x_n)O^{(r)}(y)O^{(s)}(z)\rangle\,, \tag{4.2.23}$$

  where $Z_{qrs} \equiv Z_{q_{(n,k')}rs}$. By the subscript (n, k') on q we stress the fact that the β-function can in general be affected by the level-2 insertion of a dimension-$k' \neq n$ operator into the n-point function.

From these, the non-linear contribution $\Gamma_{lrs}c^{(r)}c^{(s)}$ to $\beta_{c^{(l)}}$ can be obtained.

There are a couple of subtle points here. The first regards the possible contractions of the fields in the expectation value. When we consider double insertions there is no need to use $\mathcal{L}_{\text{int}}$ to contract fields. So couplings do not participate in the calculation. The second refers to the absorption of divergences. In particular the two sides of Eq. (4.2.23), when $l \leq 8$, give the same loop integral but the l.h.s is divergent while the r.h.s is finite. The equality of the two sides holds since Z_{lrs} is divergent, which means that the diagram at the r.h.s should be considered as a finite vertex. Finally, in the following calculations we meet only two kinds of divergent integrals. These are the scalar integrals A_0 and B_0 evaluated in Appendix 4.A. When massless propagators participate in the loop, these integrals are scaleless. When scaleless, the former is identically zero in DR, while the latter can be broken into a UV and an IR part. Depending on the situation, we keep only its UV part (operator insertion) or we consider both its UV and IR parts in which case B_0 is zero (renormalization of Eq. (1.0.1)) in DR. There are two more 1-loop integrals, a Triangle (C_0) and a Box (D_0), already mentioned in the Introduction, which are finite.

4.3 Inserting dimension-6 operators

Consider the Lagrangian $\mathcal{L} = \mathcal{L}^{(2)} + \mathcal{L}^{(4)} + \mathcal{L}^{(6)}$ which includes also the classically irrelevant HDO of dimension-6 [34, 74]. We would like to determine its RG flows and symmetry breaking patterns. There are three such operators (up to total derivatives), which respect Lorentz and $\mathbb{Z}_2$ symmetry:

$$(O_1^{(6)}, O_2^{(6)}, O_3^{(6)}) = \left(\frac{\phi^2\Box\phi^2}{\Lambda^2}, \frac{\phi\Box^2\phi}{\Lambda^2}, \frac{\phi^6}{\Lambda^2}\right) \tag{4.3.1}$$

and they introduce the respective dimensionless couplings $c_1^{(6)}$, $c_2^{(6)}$ and $c_3^{(6)}$. Nevertheless, as we will see, only one of them is independent. Λ is a cut-off scale and it is present to regulate the dimension of the inserted operators.

With this in mind we add to $\mathcal{L}^{(4)}$ in Eq. (4.1.1), the terms

$$\mathcal{L}^{(6)} = \frac{c_1^{(6)}}{4!\Lambda^2}\phi^2\Box\phi^2 + \frac{c_2^{(6)}}{2\Lambda^2}\phi\Box^2\phi + \frac{c_3^{(6)}}{6!\Lambda^2}\phi^6\,, \tag{4.3.2}$$

so that the dimension-6 GEFT Lagrangian is

$$\begin{aligned}\mathcal{L} \;=\; & -\frac{1}{2}\phi\Box\phi - \frac{1}{2}m^2\,\phi^2 - \frac{\lambda}{4!}\phi^4 \\ & + \frac{c_1^{(6)}}{4!\Lambda^2}\phi^2\Box\phi^2 + \frac{c_2^{(6)}}{2\Lambda^2}\phi\Box^2\phi + \frac{c_3^{(6)}}{6!\Lambda^2}\phi^6\end{aligned} \tag{4.3.3}$$

and defines the $O^{(2)}$-$O^{(4)}$-$O^{(6)}$ system. Let us call the set of dimension-6 operators in Eq. (4.3.2) the G-basis. Notice that upon integration by parts and dropping total derivatives, the box operator commutes with ϕ and all positions of it in the operator are equivalent. There is an obstruction to compute directly RG flows in this basis since $O_1^{(6)}$ can result in superluminal

propagation when $c_1^{(6)} < 0$ [75], in addition $O_2^{(6)}$ contains an Ostrogradsky ghost (the O-ghost) [8], as it adds an extra, ghost-like pole to the propagator. The analysis of the phase diagram is expected to be simplified and more transparent in the basis where only $O_3^{(6)}$ exists. We call this the W-basis, by analogy to the Warsaw basis of dim-6 operators in the Standard Model [67] which is ghost free.

Indeed, there is a freedom in Eq. (4.3.3) because we can perform a field redefinition that allows to eliminate any HDO we want. To see how this works, take $\mathcal{L}_0$ (the bare version of Eq. (4.3.3)), introduce the field redefinition[1]

$$\phi_0 \to \phi_0 + \frac{x}{\Lambda^2}\Box\phi_0 + \frac{y}{\Lambda^2}\phi_0^3 \tag{4.3.4}$$

and substitute it back into $\mathcal{L}_0$. Keeping consistently terms up to $\mathcal{O}(1/\Lambda^2)$, we obtain the transformed Lagrangian

$$\begin{aligned}\mathcal{L}_0 &= -\frac{1}{2}\left[1+2x\frac{m_0^2}{\Lambda^2}\right]\phi_0\Box\phi_0 - \frac{1}{2}\phi_0\, m_0^2\phi_0 - \left[\frac{\lambda_0}{4!}+\frac{ym_0^2}{\Lambda^2}\right]\phi_0^4 \\ &+ \left[\frac{c_{1,0}^{(6)} - y - \frac{x}{6}\lambda_0}{4!\Lambda^2}\right]\phi_0^2\Box\phi_0^2 + \left[\frac{c_{2,0}^{(6)} - x}{2\Lambda^2}\right]\phi_0\Box^2\phi_0 + \left[\frac{c_{3,0}^{(6)} - \frac{y\lambda_0}{6}}{6!\Lambda^2}\right]\phi_0^6\,.\end{aligned} \tag{4.3.5}$$

Perform also the extra redefinition

$$\phi_0 \to \frac{1}{\sqrt{1+2x\frac{m_0^2}{\Lambda^2}}}\,\phi_0 \tag{4.3.6}$$

in order to bring the kinetic term into a canonical form. Now we can try to eliminate some operators in favour of others. The preferred elimination is that of the ones with higher derivatives. This can be done by requiring the coefficients of those terms to vanish, which happens if $x = c_{2,0}^{(6)}$ and $y = c_{1,0}^{(6)} - (c_{2,0}^{(6)}/6)\lambda_0$. With these conditions we obtain the Lagrangian

$$\begin{aligned}\mathcal{L}_0 &= -\frac{1}{2}\phi_0\Box\phi_0 - \frac{m_0^2}{2}\left[1-\frac{2c_{2,0}^{(6)}m_0^2}{\Lambda^2}\right]\phi_0^2 + \left[-\frac{\lambda_0}{24}+\frac{m_0^2(-c_{1,0}^{(6)}+\frac{1}{3}\lambda_0 c_{2,0}^{(6)})}{\Lambda^2}\right]\phi_0^4 \\ &+ \left[\frac{c_{3,0}^{(6)} - \frac{1}{6}c_{1,0}^{(6)}\lambda_0 + \frac{1}{36}c_{2,0}^{(6)}\lambda_0^2}{\Lambda^2}\right]\phi_0^6\,,\end{aligned} \tag{4.3.7}$$

where indeed only ϕ^6 remains as the only HDO.

Unfortunately this can not be the full story since in general, field redefinitions affect the measure of the path-integral [34, 74]. To clarify this aspect we renormalize $\mathcal{L}_0$ diagrammatically in the on-shell scheme, considering the HDO as part of the classical Lagrangian and we demonstrate how ghosts can be discarded from the spectrum. Having obtained a ghost-free theory with a reduced set of operators (the W-basis), we can safely apply the operator insertion algorithm for the evaluation of the anomalous dimensions.

[1] Whether field redefinitions and renormalization commute is a fair question at this point and there are arguments that they do [76].

4.3.1 Ghosts induced by higher derivative operators

The main problem of Eq. (4.3.3) is the existence of the O-ghost, originating from $O_2^{(6)}$, which makes the model ill-defined. Consistency suggests that we must add a sector whose purpose is to cancel the pole of the O-ghost. The sector that does the job is

$$\mathcal{L}_{Rg,0} = -\frac{1}{2}\bar{\chi}_0 \,\Box\chi_0 + \frac{m_{\chi,0}^2}{2}\bar{\chi}_0\chi_0 - \frac{\lambda_{\chi,0}}{4}\,\bar{\chi}_0\chi_0\,\phi_0^2\,, \tag{4.3.8}$$

featuring the Grassmann fields χ_0 and $\bar{\chi}_0$ which we call the R-ghosts for reasons that will become clear. The total G-basis Lagrangian then becomes

$$\begin{aligned}\mathcal{L}_0 &= \mathcal{L}_0^{(4)} + \mathcal{L}_0^{(6)} + \mathcal{L}_{Rg,0} \\ &= -\frac{1}{2}\phi_0\Box\phi_0 - \frac{m_0^2}{2}\phi_0^2 - \frac{\lambda_0}{4!}\phi_0^4 + \frac{c_{1,0}^{(6)}}{4!\Lambda^2}\phi_0^2\Box\phi_0^2 + \frac{c_{2,0}^{(6)}}{2\Lambda^2}\phi_0\Box^2\phi_0 \\ &\quad + \frac{c_{3,0}^{(6)}}{6!\Lambda^2}\phi_0^6 - \frac{1}{2}\bar{\chi}_0\,\Box\chi_0 + \frac{m_{\chi,0}^2}{2}\bar{\chi}_0\chi_0 - \frac{\lambda_{\chi,0}}{4}\,\bar{\chi}_0\chi_0\phi_0^2\,.\end{aligned} \tag{4.3.9}$$

The Feynman rules that this Lagrangian generates are:

- Scalar Propagator

$$= \frac{i}{p^2 - m_0^2 + c_{2,0}^{(6)}\frac{p^4}{\Lambda^2}}$$

- Ghost Propagator

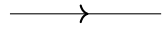

$$= \frac{i}{p^2 + m_{\chi,0}^2}$$

- Four-point self interaction vertex

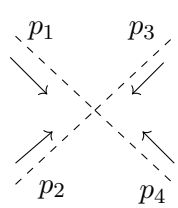

$$= -i\lambda_0 - ic_{1,0}^{(6)}\frac{p^2}{\Lambda^2}\,.$$

- Scalar-ghost vertex

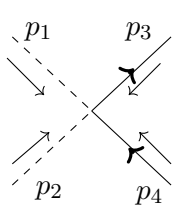

$$= -i\frac{\lambda_{\chi,0}}{2}\,.$$

- Six-point self interaction vertex

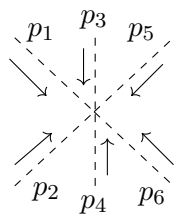

$$= i\frac{c^{(6)}_{3,0}}{\Lambda^2}\,,$$

We are about to renormalize Eq. (4.3.9) using these rules. Clearly, this is in the spirit of Eq. (1.0.1) rather than in the spirit of the operator insertions. It is a more familiar process, which is however numb to the decomposition of the β-functions in terms of the various anomalous-dimension contributions that comprise it. At the end though, we will obtain the same β-functions from both methods.

The presence of the O-ghost is manifest through the scalar propagator which now has two poles. The extra pole can be exposed if we rewrite the scalar propagator as

$$G^{(2)}_0(x_1,x_2) = \frac{i}{p^2 - m_0^2 + c^{(6)}_{2,0}\frac{p^4}{\Lambda^2}} = \frac{\Lambda^2}{c^{(6)}_{2,0}}\frac{i}{(p^2-m^2_{+,0})(p^2-m^2_{-,0})} \tag{4.3.10}$$

and breaking the denominator as

$$\begin{aligned} G^{(2)}_0(x_1,x_2) &= \frac{1}{\sqrt{1+4m_0^2\frac{c^{(6)}_{2,0}}{\Lambda^2}}}\left(\frac{i}{(p^2-m^2_{+,0})} - \frac{i}{(p^2-m^2_{-,0})}\right) \\ &= \frac{i}{b_0(p^2-m^2_{+,0})} - \frac{i}{b_0(p^2-m^2_{-,0})}\,, \end{aligned} \tag{4.3.11}$$

where

$$b_0 = \sqrt{1+4m_0^2\frac{c^{(6)}_{2,0}}{\Lambda^2}}\,. \tag{4.3.12}$$

This shows that the propagator describes two scalar fields with masses

$$m^2_{\pm,0} = \frac{\Lambda^2}{2c^{(6)}_{2,0}}\left(-1 \pm b_0\right)\,, \tag{4.3.13}$$

where $m^2_{+,0}$, $m^2_{-,0}$ correspond to the bare masses of ϕ and of the O-ghost respectively.

In order to arrive at a ghost-free and finite theory in this basis we should first deal with the extra pole and its possible connection to the R-ghosts. Our expectation is that the unphysical pole of the O-ghost somehow cancels due to the presence of the R-ghosts and this should happen order by order in the loop expansion. To fulfill this expectation we need the 1-loop part of the action, which includes the quantum corrections and the renormalized version of Eq. (4.3.9). Let us denote the 1-loop corrections to the 2-, 4- and 6-point functions of ϕ as $\mathcal{M}_{2,\phi}$, $\mathcal{B}_{4,\phi}$ and $\mathcal{B}_{6,\phi}$ respectively. The correction of χ's propagator is $\mathcal{M}_{2,\chi}$ while the ϕ-χ vertex is corrected by $\mathcal{B}_{4,\chi}$.

For the finite parts of the diagrams we use the notation $[\,]_{\rm f}$. Relating bare and renormalized quantities in the usual way, Eq. (4.3.9) gives in momentum space

$$\mathcal{L} = \mathcal{L}_R + \mathcal{L}_{\rm ct}\,, \tag{4.3.14}$$

where

$$\begin{aligned}\mathcal{L}_R &= \frac{p^2}{2}\phi^2 - \frac{m^2}{2}\phi^2 - \frac{\lambda}{4!}\phi^4 - \frac{c_1^{(6)}p^2}{4!\Lambda^2}\phi^4 + \frac{c_2^{(6)}p^4}{2\Lambda^2}\phi^2 + \frac{c_3^{(6)}}{6!\Lambda^2}\phi^6 \\ &\quad + \frac{p^2}{2}\bar\chi\chi + \frac{m_\chi^2}{2}\bar\chi\chi - \frac{\lambda_\chi}{4}\,\bar\chi\chi\phi^2\,,\end{aligned}$$

featuring the renormalized field and couplings and

$$\begin{aligned}\mathcal{L}_{\rm ct} &= \frac{\delta\phi\, p^2}{2}\phi^2 - \frac{\delta m + m^2\delta\phi}{2}\phi^2 - \frac{\delta\lambda + 2\lambda\delta\phi}{4!}\phi^4 - \frac{(\delta c_1^{(6)} + 2c_1^{(6)}\delta\phi)\,p^2}{4!\Lambda^2}\phi^4 + \frac{(\delta c_2^{(6)} + c_2^{(6)}\delta\phi)\,p^4}{2\Lambda^2}\phi^2 \\ &\quad + \frac{\delta c_3^{(6)} + 3c_3^{(6)}\delta\phi}{6!\Lambda^2}\phi^6 + \frac{\delta\chi\, p^2}{2}\bar\chi\chi + \frac{\delta m_\chi + m_\chi^2\delta\chi}{2}\bar\chi\chi - \frac{\delta\lambda_\chi + \lambda_\chi(\delta\chi + \delta\phi)}{4}\,\bar\chi\chi\phi^2 \\ &\quad + \frac{\mathcal{M}_{2,\phi}}{2}\phi^2 + \frac{\mathcal{B}_{4,\phi}}{4!}\phi^4 + \frac{\mathcal{B}_{6,\phi}}{6!}\phi^6 + \frac{\mathcal{M}_{2,\chi}}{2}\bar\chi\chi + \frac{\mathcal{B}_{4,\chi}}{4}\bar\chi\chi\phi^2\end{aligned}$$

which contains the counter-terms and the 1-loop diagrams. The next step is to use the above expressions to choose the renormalization conditions which simultaneously make vertices and propagators finite and leave ϕ with a single pole. Start with the 2-point Green's function. For the scalar field the renormalized, double pole, propagator is

$$G^{(2)}(x_1, x_2) = \frac{i}{Ap^4 + Bp^2 + C}$$

with

$$\begin{aligned}A &= \frac{c_2^{(6)} + \delta c_2^{(6)} + c_2^{(6)}\delta\phi}{\Lambda^2} \\ B &= 1 + \delta\phi \\ C &= \mathcal{M}_{2,\phi} - m^2 - \delta m - m^2\delta\phi\end{aligned}$$

and the R-ghost propagator is

$$G^{(2)}_{{\rm R}g}(x_1, x_2) = \frac{i}{p^2 + m_\chi^2 + \delta m_\chi + \delta\chi(p^2 + m_\chi^2) + \mathcal{M}_{2,\chi}}\,. \tag{4.3.15}$$

Following steps analogous to Eq. (4.3.10), we break $G^{(2)}$ in two parts to obtain the renormalized version of Eq. (4.3.11) and we get

$$G^{(2)}(x_1, x_2) = \frac{i}{A[M_+ - M_-](p^2 - M_+)} - \frac{i}{A[M_+ - M_-](p^2 - M_-)} \tag{4.3.16}$$

with

$$M_\pm = \frac{B}{2A}\left[-1 \pm \sqrt{1 - 4\frac{AC}{B^2}}\right]\,. \tag{4.3.17}$$

The pole-cancelation condition that we want to impose amounts to forcing $G^{(2)}_{\rm Rg}$ to cancel the wrong-sign term in Eq. (4.3.16). In other words we need

$$A[M_+ - M_-](p^2 - M_-) = p^2 + m_\chi^2 + \delta m_\chi + \delta\chi(p^2 + m_\chi^2) + \mathcal{M}_{2,\chi}\,.$$

This contains two pole-cancellation conditions. The first is

$$\begin{aligned} p^2 &= A[M_+ - M_-]p^2 \\ &= b_0\, p^2 + \hbar \left[b_0 \frac{2m^2(\delta c_2^{(6)} + 2c_2^{(6)}\delta\phi) + c_2^{(6)}(-2\mathcal{M}_{2,\phi} + 2\delta m + \frac{\Lambda^2}{c_2^{(6)}}\delta\phi)}{c_2^{(6)}(4m^2 + \frac{\Lambda^2}{c_2^{(6)}})} \right] p^2\,, \end{aligned}$$

which, comparing the two sides order by order in $\hbar$, gives

$$\begin{aligned} b_0 &= 1 \\ 2m^2(\delta c_2^{(6)} + 2c_2^{(6)}\delta\phi) + c_2^{(6)}(-2\mathcal{M}_{2,\phi} + 2\delta m + \frac{\Lambda^2}{c_2^{(6)}}\delta\phi) &= 0\,. \end{aligned}$$

Checking back to Eq. (4.3.12) it is easy to see that the first constraint is fulfilled when $c_2^{(6)} = 0$ or when $m^2 = 0$. The former is rejected since it gets us to a basis where there are no O-ghosts from the beginning and the pole cancelation is meaningless. Therefore, we have to choose the $m^2 = 0$ solution. Substituting this in the second constraint we have

$$2\frac{c_2^{(6)}}{\Lambda^2}\left(-\mathcal{M}_{2,\phi} + \delta m\right) + \delta\phi = 0\,. \tag{4.3.18}$$

The second pole-cancellation condition is

$$-A[M_+ - M_-]M_- = m_\chi^2 + \delta m_\chi + \delta\chi(p^2 + m_\chi^2) + \mathcal{M}_{2,\chi}\,,$$

which, keeping terms up to $\mathcal{O}(\hbar)$ and using the constraints from the first condition, becomes

$$\frac{\Lambda^2}{c_2^{(6)}} + \hbar\left[3(\delta m - \mathcal{M}_{2,\phi}) - \frac{\Lambda^2}{c_2^{(6)}}\left(\frac{\delta c_2^{(6)}}{c_2^{(6)}}\right) + \frac{\Lambda^2}{c_2^{(6)}}\delta\phi\right] = m_\chi^2 + \hbar\left(\delta m_\chi + \delta\chi(p^2 + m_\chi^2) + \mathcal{M}_{2,\chi}\right)\,.$$

At $\mathcal{O}(\hbar^0)$ the constraint

$$m_\chi^2 = \frac{\Lambda^2}{c_2^{(6)}} \tag{4.3.19}$$

is obtained, a relation that connects the O- and R-ghosts and defines the mass of the latter in terms of the coupling of the former. It also implies the useful identity

$$\frac{\delta m_\chi}{m_\chi^2} = -\frac{\delta c_2^{(6)}}{c_2^{(6)}}\,. \tag{4.3.20}$$

At $\mathcal{O}(\hbar)$ level we obtain

$$3(\delta m - \mathcal{M}_{2,\phi}) - m_\chi^2\frac{\delta c_2^{(6)}}{c_2^{(6)}} + m_\chi^2\delta\phi \;=\; \delta m_\chi + \delta\chi(p^2 + m_\chi^2) + \mathcal{M}_{2,\chi} \Rightarrow$$

$$3(\delta m - \mathcal{M}_{2,\phi}) + m_\chi^2 \delta\phi \quad = \quad \delta\chi(p^2 + m_\chi^2) + \mathcal{M}_{2,\chi}\,. \tag{4.3.21}$$

Notice that even though we are forced to set the renormalized mass to zero, there is a mass counterterm δm left over, whose purpose is to absorb $\mathcal{M}_{2,\phi}$. Eq. (4.3.18) resembles the way that the single-pole propagator of a pure scalar theory gets renormalized after resummation. This behaviour is inherited by the G-basis propagator when

$$\delta m = \mathcal{M}_{2,\phi} \;\text{ and }\; \delta\phi = 0\,. \tag{4.3.22}$$

Then Eq. (4.3.21) fixes the counter-term $\delta\chi$:

$$\delta\chi = -\frac{\mathcal{M}_{2,\chi}}{p^2 + m_\chi^2}\,. \tag{4.3.23}$$

It is now easy to check that using all the constraints, the renormalized ϕ-propagator takes the form

$$G^{(2)}(x_1, x_2) = \frac{i}{p^2} - \frac{i}{p^2 + m_\chi^2}\,, \tag{4.3.24}$$

with the second term the same as the R-ghost propagator, with the opposite sign. Bringing the ϕ and χ propagators in this relative form is a necessary condition but its sufficiency is not yet obvious.

The only ingredient left at the 2-point function level is the computation of $\mathcal{M}_{2,\phi}$ and $\mathcal{M}_{2,\chi}$. Starting with the former, we consider contributions from two vertices. The first comes from the 4-point vertex given by

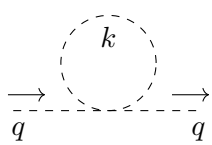

$$= i\mathcal{M}^1_{2,\phi}$$

whose evaluation gives

$$\begin{aligned}
i\mathcal{M}^1_{2,\phi} &= -i\left(\lambda + c_1^{(6)}\frac{q^2}{\Lambda^2}\right) S_{\mathcal{M}^1} \int \frac{d^4k}{(2\pi)^4}\left[\frac{i}{k^2} - \frac{i}{k^2 + m_\chi^2}\right] \Rightarrow \\
\mathcal{M}^1_{2,\phi} &= \frac{1}{2}\left(\lambda + c_1^{(6)}\frac{q^2}{\Lambda^2}\right) \int \frac{d^4k}{(2\pi)^4 i}\left[\frac{1}{k^2} - \frac{1}{k^2 + m_\chi^2}\right] \Rightarrow \\
\mathcal{M}^1_{2,\phi} &= \frac{1}{2}\left(\lambda + c_1^{(6)}\frac{q^2}{\Lambda^2}\right) \left[A_0(0) - A_0(-m_\chi^2)\right]\,,
\end{aligned} \tag{4.3.25}$$

with the symmetry factor $S_{\mathcal{M}^1} = \frac{1}{2}$ and Eq. (4.3.24) used for the scalar propagator. The second two-point contribution comes from the ϕ-χ vertex:

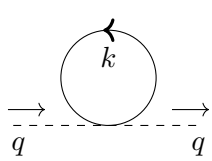

$$= i\mathcal{M}^2_{2,\phi}$$

It evaluates to

$$
\begin{aligned}
i\mathcal{M}^2_{2,\phi} &= (-1)(-i)\frac{\lambda_\chi}{2} S_{\mathcal{M}^2} \int \frac{d^4k}{(2\pi)^4} \frac{i}{k^2+m_\chi^2} \Rightarrow \\
\mathcal{M}^2_{2,\phi} &= -\frac{\lambda_\chi}{2} \int \frac{d^4k}{(2\pi)^4 i} \frac{1}{k^2+m_\chi^2} \equiv -\frac{\lambda_\chi}{2} A_0(-m_\chi^2)\,, \qquad (4.3.26)
\end{aligned}
$$

with symmetry factor $S_{\mathcal{M}^2} = 1$. Notice the extra minus sign in the above due to the anti-commuting ghost which runs in the loop. Adding Eq. (4.3.25) and Eq. (4.3.26) we get the complete 1-loop correction to the scalar two-point function

$$
\mathcal{M}_{2,\phi} = \frac{1}{2}\left(\lambda + c_1^{(6)}\frac{q^2}{\Lambda^2}\right)\left[A_0(0) - A_0(-m_\chi^2)\right] - \frac{\lambda_\chi}{2} A_0(-m_\chi^2) \qquad (4.3.27)
$$

or, in DR,

$$
\mathcal{M}_{2,\phi} = \frac{\lambda m_\chi^2}{16\pi^2\varepsilon} + \frac{c_1^{(6)}}{c_2^{(6)}}\frac{q^2}{16\pi^2\varepsilon} + \frac{\lambda_\chi m_\chi^2}{16\pi^2\varepsilon} + [\mathcal{M}_{2,\phi}]_{\rm f}\ . \qquad (4.3.28)
$$

We complete the 2-point function analysis with the correction to R-ghost's propagator. In this case only one digram contributes, coming from the ϕ-χ vertex:

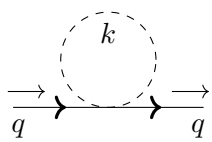

$= i\mathcal{M}_{2,\chi}$

Its explicit form is given by

$$
\begin{aligned}
i\mathcal{M}_{2,\chi} &= (-i)\frac{\lambda_\chi}{2} S_{\mathcal{M}_\chi} \int \frac{d^4k}{(2\pi)^4}\left[\frac{i}{k^2} - \frac{i}{k^2+m_\chi^2}\right] \Rightarrow \\
\mathcal{M}_{2,\chi} &= \frac{\lambda_\chi}{2} \int \frac{d^4k}{(2\pi)^4 i}\left[\frac{1}{k^2} - \frac{1}{k^2+m_\chi^2}\right] \Rightarrow \\
\mathcal{M}_{2,\chi} &= \frac{\lambda_\chi}{2}\left[A_0(0) - A_0(-m_\chi^2)\right]\,, \qquad (4.3.29)
\end{aligned}
$$

with symmetry factor $S_{\mathcal{M}_\chi} = 1$. In DR this is

$$
\mathcal{M}_{2,\chi} = \frac{\lambda_\chi m_\chi^2}{16\pi^2\varepsilon} + [\mathcal{M}_{2,\chi}]_{\rm f}\ . \qquad (4.3.30)
$$

Using these results, Eq. (4.3.22) and Eq. (4.3.23) become

$$
\begin{aligned}
\delta m &= \frac{\lambda m_\chi^2}{16\pi^2\varepsilon} + \frac{c_1^{(6)}}{c_2^{(6)}}\frac{q^2}{16\pi^2\varepsilon} + \frac{\lambda_\chi m_\chi^2}{16\pi^2\varepsilon} + [\mathcal{M}_{2,\phi}]_{\rm f} \\
\delta\chi &= \frac{-1}{p^2+m_\chi^2}\left[\frac{\lambda_\chi m_\chi^2}{16\pi^2\varepsilon} + [\mathcal{M}_{2,\chi}]_{\rm f}\right] \\
\delta\phi &= 0\,. \qquad (4.3.31)
\end{aligned}
$$

Up to this point we have managed to secure a scalar-field whose extra propagator component is of the opposite sign with respect to the propagator of the R-ghost and to renormalize these

propagators. To render the theory finite, renormalization conditions associated with the 4- and 6-point functions are also needed.

Starting with the ϕ^4 vertex, $\mathcal{L}_{\rm ct}$ indicates that

$$\begin{aligned}\delta\lambda + \delta c_1^{(6)}\frac{p^2}{\Lambda^2} + 2(\lambda + c_1^{(6)}\frac{p^2}{\Lambda^2})\delta\phi &= \mathcal{B}_{4,\phi} \Rightarrow \\ \delta\lambda + \delta c_1^{(6)}\frac{p^2}{\Lambda^2} &= \mathcal{B}_{4,\phi}\,, \end{aligned} \tag{4.3.32}$$

where we have used Eq. (4.3.22). The diagrammatic set of $\mathcal{B}_{4,\phi}$ consists of three 1-loop box diagrams. The first contribution is a pure scalar box with pinched external legs, i.e. a Candy. It has three channels given by Eq. (4.B.19). The s-channel, denoted by $\mathcal{B}^{1,s}_{4,\phi}$

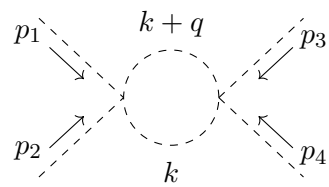

$$= i\mathcal{B}^{1,s}_{4,\phi}$$

is evaluated as

$$\begin{aligned} i\mathcal{B}^{1,s}_{4,\phi} &= (-i)(-i)\left(\lambda + c_1^{(6)}\frac{q^2}{\Lambda^2}\right)^2 S_{\mathcal{B}^1_\phi}\int\frac{d^4k}{(2\pi)^4}\left[\frac{i}{k^2}-\frac{i}{k^2+m_\chi^2}\right]\left[\frac{i}{(k+q)^2}-\frac{i}{(k+q)^2+m_\chi^2}\right] \Rightarrow \\ \mathcal{B}^{1,s}_{4,\phi} &= \frac{1}{2}\left(\lambda + c_1^{(6)}\frac{q^2}{\Lambda^2}\right)^2\int\frac{d^4k}{(2\pi)^4 i}\left[\frac{1}{k^2}-\frac{1}{k^2+m_\chi^2}\right]\left[\frac{1}{(k+q)^2}-\frac{1}{(k+q)^2+m_\chi^2}\right] \Rightarrow \\ \mathcal{B}^{1,s}_{4,\phi} &= \frac{1}{2}\left(\lambda + c_1^{(6)}\frac{q^2}{\Lambda^2}\right)^2\left[B_0(q^2,0,0) - B_0(q^2,0,-m_\chi^2) - B_0(q^2,-m_\chi^2,0) + B_0(q^2,-m_\chi^2,-m_\chi^2)\right]\,, \end{aligned}$$

where the symmetry factor is $S_{\mathcal{B}^1_\phi} = \frac{1}{2}$ and $p_1+p_2+p_3+p_4 = 0$. Including the other two channels, we obtain

$$\mathcal{B}^1_{4,\phi} = \mathcal{B}^{1,s}_{4,\phi} + \mathcal{B}^{1,t}_{4,\phi} + \mathcal{B}^{1,u}_{4,\phi} \equiv \sum_{q^2=s,t,u}\frac{1}{2}\left(\lambda + c_1^{(6)}\frac{q^2}{\Lambda^2}\right)^2 F(q^2,m_\chi^2)\,, \tag{4.3.33}$$

with

$$F(q^2,m_\chi^2) = B_0(q^2,0,0) - B_0(q^2,0,-m_\chi^2) - B_0(q^2,-m_\chi^2,0) + B_0(q^2,-m_\chi^2,-m_\chi^2)\,.$$

The next contribution to the four-point vertex comes from the ϕ-χ interaction. The diagram is another Candy whose s-channel is

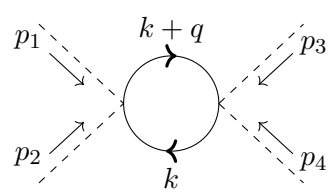

$$= i\mathcal{B}^{2,s}_{4,\phi}$$

evaluating to

$$
\begin{aligned}
i\mathcal{B}^{2,s}_{4,\phi} &= (-1)(-i)(-i)\frac{\lambda_\chi^2}{4} S_{\mathcal{B}^2_\phi} \int \frac{d^4k}{(2\pi)^4} \frac{i}{k^2+m_\chi^2} \frac{i}{(k+q)^2+m_\chi^2} \Rightarrow \\
\mathcal{B}^{2,s}_{4,\phi} &= -\frac{\lambda_\chi^2}{4} \int \frac{d^4k}{(2\pi)^4 i} \frac{1}{[k^2+m_\chi^2][(k+q)^2+m_\chi^2]} \equiv -\frac{\lambda_\chi^2}{4} B_0(q^2, -m_\chi^2, -m_\chi^2)\,, \quad (4.3.34)
\end{aligned}
$$

with symmetry factor $S_{\mathcal{B}^2_\phi} = 1$ and momentum conservation $p_1+p_2+p_3+p_4 = 0$. The complete contribution of this diagram is

$$
\mathcal{B}^2_{4,\phi} = -\frac{\lambda_\chi^2}{4} \sum_{q^2=s,t,u} B_0(q^2, -m_\chi^2, -m_\chi^2)\,. \quad (4.3.35)
$$

The third, and last, diagram which corrects the ϕ^4-vertex comes from the six-point function. The s-channel diagram is

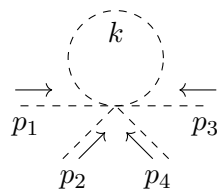

$$= i\mathcal{B}^{3,s}_{4,\phi}$$

This contribution is the same as that of Eq. (4.3.25) except from an extra vertex factor. We can then directly write

$$
\mathcal{B}^{3,s}_{4,\phi} = -\frac{c_3^{(6)}}{2\Lambda^2}\left[A_0(0) - A_0(-m_\chi^2)\right]\,. \quad (4.3.36)
$$

This diagram gives an A_0-integral which is channel-independent, so its total contribution is just three times $\mathcal{B}^{3,s}_{4,\phi}$:

$$
\mathcal{B}^3_{4,\phi} = -\frac{3c_3^{(6)}}{2\Lambda^2}\left[A_0(0) - A_0(-m_\chi^2)\right]\,. \quad (4.3.37)
$$

Adding Eq. (4.3.33), Eq. (4.3.35) and Eq. (4.3.37) we end up with the full 1-loop correction to the pure scalar 4-point vertex

$$
\begin{aligned}
\mathcal{B}_{4,\phi} &= \sum_{q^2=s,t,u} \frac{1}{2}\left(\lambda + \frac{q^2}{m_\chi^2}\frac{c_1^{(6)}}{c_2^{(6)}}\right)^2 F(q^2, m_\chi^2) - \frac{\lambda_\chi^2}{4}\sum_{q^2=s,t,u} B_0(q^2, -m_\chi^2, -m_\chi^2) \\
&- \frac{3c_3^{(6)}}{2\Lambda^2}\left[A_0(0) - A_0(-m_\chi^2)\right]\,. \quad (4.3.38)
\end{aligned}
$$

Decompressing and calculating the integrals in DR, we obtain

$$
\mathcal{B}_{4,\phi} = -\frac{3\lambda^2}{16\pi^2\varepsilon} - \frac{3\lambda_\chi^2}{32\pi^2\varepsilon} - \frac{3c_3^{(6)}}{\Lambda^2}\frac{m_\chi^2}{16\pi^2\varepsilon} + [\mathcal{B}_{4,\phi}]_{\rm f}\,, \quad (4.3.39)
$$

where we have used the identity $s+t+u=0$ and kept terms up to $\mathcal{O}(1/\Lambda^2)$.

For the ϕ-χ vertex, according to $\mathcal{L}_{\rm ct}$, we get the condition

$$
\delta\lambda_\chi + \lambda_\chi(\delta\chi + \delta\phi) = \mathcal{B}_{4,\chi} \Rightarrow
$$

$$\delta\lambda_\chi + \lambda_\chi \delta\chi = \mathcal{B}_{4,\chi}\,, \tag{4.3.40}$$

using Eq. (4.3.22). In this case the 1-loop correction comes only from one box diagram. It is again a Candy and its s-channel is

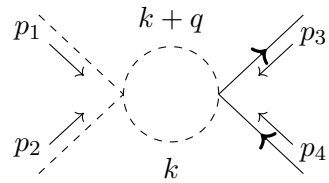

$$= i\mathcal{B}^s_{4,\chi}$$

It is of the form Eq. (4.3.33) except from the vertex factor. Thus,

$$\mathcal{B}^s_{4,\chi} = \frac{\lambda_\chi}{4}\left(\lambda + c_1^{(6)}\frac{q^2}{\Lambda^2}\right) F(q^2, m_\chi^2)\,. \tag{4.3.41}$$

Even though this diagram is a Candy with scalar fields in the loop, it has only two channels, so its total contribution is

$$\mathcal{B}_{4,\chi} = \sum_{q^2=s,t} \frac{\lambda_\chi}{4}\left(\lambda + c_1^{(6)}\frac{q^2}{\Lambda^2}\right) F(q^2, m_\chi^2)\,. \tag{4.3.42}$$

Computing in DR the integrals, we get

$$\mathcal{B}_{4,\chi} = -\frac{\lambda_\chi\,\lambda}{16\pi^2\varepsilon} + [\mathcal{B}_{4,\chi}]_{\rm f}\,, \tag{4.3.43}$$

where we have used that $s+t=0$.

The renormalization condition that ensures the finiteness of the 6-point vertex is

$$\begin{aligned}\delta c_3^{(6)} + 3c_3^{(6)}\delta\phi = -\Lambda^2\mathcal{B}_{6,\phi} \Rightarrow \\ \delta c_3^{(6)} = -\Lambda^2\mathcal{B}_{6,\phi}\,.\end{aligned} \tag{4.3.44}$$

The related diagrammatic set includes $\mathcal{K}^1_{\phi^6}$, $\mathcal{K}^2_{\phi^6}$ and $\mathcal{B}_{\phi^6}$. The first and the second come from the ϕ^4 and ϕ-χ vertices respectively, while the third is a combination of the ϕ^4 and ϕ^6 vertices. $\mathcal{K}^1_{\phi^6}$ is a triangle diagram with only one channel. It is

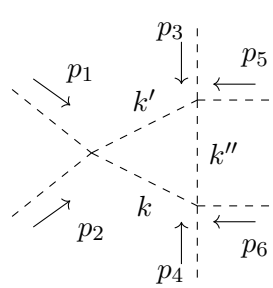

$$= i\mathcal{K}^1_{\phi^6}$$

where $k' = k + p_1 + p_2$, $k'' = k' + p_3 + p_5$. In addition, momentum conservation demands that $p_1 + p_2 + p_3 + p_4 + p_5 + p_6 = 0$. Now the propagators in the loop come from Eq. (4.3.24) so the

calculation of this diagram involves eight parts. It is useful to see how $\mathcal{K}^1_{\phi^6}$ scales as a function of the loop momentum. Each one of the contributing parts contributes as $\mathcal{K}^1_{\phi^6} \sim \int d^4k \frac{1}{k^6}$ which is just a finite correction, proportional to a C_0-integral. In other words, the above 1-loop Triangle is finite and we can write it as

$$\mathcal{K}^1_{\phi^6} \equiv \left[\mathcal{K}^1_{\phi^6}\right]_{\mathrm{f}} . \tag{4.3.45}$$

This is the diagram mentioned in the Introduction and it is in fact the only correction associated with a dimension-6 operator in the usual EFT, at 1-loop. The second diagram in the GEFT is another Triangle diagram, originating from the interaction of the scalar field with the R-ghost. It is a contribution with only one channel, given by

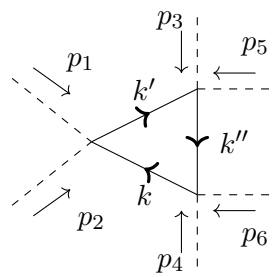

$$= i\mathcal{K}^2_{\phi^6}$$

evaluating to

$$\begin{aligned} i\mathcal{K}^2_{\phi^6} &= (-1)(-i)^3 \frac{\lambda_\chi^3}{8} S_{\mathcal{K}^2_{\phi^6}} \int \frac{d^4k}{(2\pi)^4} \frac{i^3}{[k^2+m_\chi^2][(k')^2+m_\chi^2][(k'')^2+m_\chi^2]} \Rightarrow \\ \mathcal{K}^2_{\phi^6} &= -\frac{\lambda_\chi^3}{8} \int \frac{d^4k}{(2\pi)^4 i} \frac{1}{[k^2+m_\chi^2][(k')^2+m_\chi^2][(k'')^2+m_\chi^2]} \equiv -\frac{\lambda_\chi^3}{8} C_0(P_1, P_2, -m_\chi^2, -m_\chi^2, -m_\chi^2) , \end{aligned}$$

with symmetry factor $S_{\mathcal{K}^2_{\phi^6}} = 1$ and momentum conservation $p_1 + p_2 + p_3 + p_4 + p_5 + p_6 = 0$. It also gives a finite C_0-integral which has no effect on the β-function of the corresponding coupling. So,

$$\mathcal{K}^2_{\phi^6} = \left[\mathcal{K}^2_{\phi^6}\right]_{\mathrm{f}} . \tag{4.3.46}$$

This calculation ends with one more 1-loop diagram which corrects the ϕ^6-vertex and has five channels, labelled by s_σ with $\sigma = 1, 2, 3, 4, 5$. The diagram itself is a $2 \to 4$ Candy whose first channel is

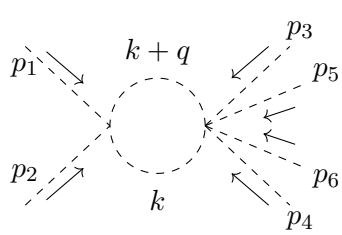

$$= i\mathcal{B}^{s_1}_{\phi^6}$$

It is equal to $\mathcal{B}^{1,s}_{4,\phi}$ barring the vertex factor. Therefore, it is equal to

$$\mathcal{B}^{s_1}_{\phi^6} = -\frac{1}{2}\left(\lambda + \frac{q^2}{m_\chi^2}\frac{c_1^{(6)}}{c_2^{(6)}}\right)\frac{c_3^{(6)}}{\Lambda^2} F(q^2, m_\chi^2) . \tag{4.3.47}$$

Adding all channels we get

$$\mathcal{B}_{\phi^6} = -\sum_{q^2=s_1,\cdots,s_5} \frac{1}{2}\left(\lambda + \frac{q^2}{m_\chi^2}\frac{c_1^{(6)}}{c_2^{(6)}}\right)\frac{c_3^{(6)}}{\Lambda^2}F(q^2,m_\chi^2)\,. \tag{4.3.48}$$

Adding Eq. (4.3.45), Eq. (4.3.46) and Eq. (4.3.48) in DR, we have

$$\begin{aligned}\Lambda^2\mathcal{B}_{6,\phi} &= \frac{5\lambda c_3^{(6)}}{16\pi^2\varepsilon} + \Lambda^2\left[\mathcal{K}^1_{\phi^6}\right]_{\rm f} + \Lambda^2\left[\mathcal{K}^2_{\phi^6}\right]_{\rm f} + \Lambda^2\left[\mathcal{B}_{\phi^6}\right]_{\rm f} \Rightarrow \\ \Lambda^2\mathcal{B}_{6,\phi} &= \frac{5\lambda c_3^{(6)}}{16\pi^2\varepsilon} + \Lambda^2\left[\mathcal{B}_{6,\phi}\right]_{\rm f}\,, \end{aligned} \tag{4.3.49}$$

where $s_1+s_2+s_3+s_4+s_5=0$ and

$$[\mathcal{B}_{6,\phi}]_{\rm f} = \left[\mathcal{K}^1_{\phi^6}\right]_{\rm f} + \left[\mathcal{K}^2_{\phi^6}\right]_{\rm f} + \left[\mathcal{B}_{\phi^6}\right]_{\rm f}\,.$$

An important comment is in order. We calculated the 1-loop diagrams using the function $F(q^2,m_\chi^2)$ that contains the scaleless version of the B_0-integral. To extract the counter-terms we use the fact that in DR this integral is zero. This seems to be in contrast with the operator insertion method where they also contributed to the renormalization but we took them to be non-zero. The reason is that here the loop integrals see momenta from IR to UV and this is why they give zero in DR. In contrast the renormalized correlation function of a composite operator has extra UV divergences that are possible to extract by separating the UV from the IR part of the scaleless B_0-integrals. The A_0 integral on the other hand does not have this flexibility because its UV and IR limits are non-separable, therefore it vanishes identically when scaleless.

Having completed the computation of the 1-loop corrections we can now determine the counter-terms of the vertices. Substituting the four-point vertex in Eq. (4.3.32) we have

$$\delta\lambda = \frac{3\lambda^2}{16\pi^2\varepsilon} + \frac{3c_3^{(6)}}{16\pi^2\varepsilon}\frac{m_\chi^2}{\Lambda^2} + [\mathcal{B}_{4,\phi}]_{\rm f} \quad\text{and}\quad \frac{p^2}{\Lambda^2}\delta c_1^{(6)} = -\frac{6\lambda^2}{16\pi^2\varepsilon} - \frac{3\lambda_\chi^2}{32\pi^2\varepsilon} - \frac{6c_3^{(6)}}{\Lambda^2}\frac{m_\chi^2}{16\pi^2\varepsilon} \tag{4.3.50}$$

where we have added $\pm 3(\lambda^2 + c_3^{(6)}\frac{m_\chi^2}{\Lambda^2})/(16\pi^2\varepsilon)$, taking advantage of the arbitrariness of $\delta c_1^{(6)}$. The ϕ-χ vertex, substituted in Eq. (4.3.40), gives the condition

$$\delta\lambda_\chi = -\frac{\lambda_\chi\,\lambda}{16\pi^2\varepsilon} + [\mathcal{B}_{4,\chi}]_{\rm f} + \frac{\lambda_\chi}{p^2+m_\chi^2}\left(\frac{\lambda_\chi m_\chi^2}{16\pi^2\varepsilon} + [\mathcal{M}_{2,\chi}]_{\rm f}\right)\,, \tag{4.3.51}$$

and the 6-point vertex substituted in Eq. (4.3.44) gives

$$\delta c_3^{(6)} = -\frac{5\lambda c_3^{(6)}}{16\pi^2\varepsilon} - \Lambda^2\left[\mathcal{B}_{6,\phi}\right]_{\rm f}\,. \tag{4.3.52}$$

Notice here that the above renormalization conditions should be enough to render the theory finite. This means that $\delta c_2^{(6)}$, or equivalently δm_χ, remains undetermined. Nevertheless it has a significant role which we will uncover soon.

Using Eq. (4.3.22), Eq. (4.3.23), Eq. (4.3.32), Eq. (4.3.40) and Eq. (4.3.44) in Eq. (4.3.14), the renormalized Lagrangian becomes

$$\mathcal{L} = \frac{1}{2}\left(p^2+m_\chi^2\right)\left(\frac{p^2}{m_\chi^2}\phi^2 + \bar\chi\,\chi\right) - \frac{1}{4!}\left(\lambda + c_1^{(6)}\frac{p^2}{\Lambda^2}\right)\phi^4 + \frac{c_3^{(6)}}{6!\Lambda^2}\phi^6$$

$$+\frac{\delta c_2^{(6)}}{2c_2^{(6)}}\left(\frac{p^4}{m_\chi^2}\phi^2 - m_\chi^2\,\bar{\chi}\,\chi\right)\,. \tag{4.3.53}$$

An observation from the above analysis is that the ϕ-χ vertex did not contribute to the pole-cancelation conditions of the scalar propagator. Recall that the ghost-like pole did not disappear through cancellation between diagrams, rather only the kinetic part of the R-ghost was used. In other words even if χ was decoupled, we would have ended up with the above, single-pole, Lagrangian. This is why in $\mathcal{L}$, without loss of generality, we have set $\lambda_\chi = 0$. However, Eq. (4.3.53) still needs refinement since the pole cancellation and renormalization left $\delta c_2^{(6)}$ undetermined in the Lagrangian. In fact, in the last term in Eq. (4.3.53) it appears as a Lagrange multiplier so we can integrate it out. By doing so we obtain

$$\bar{\chi}\,\chi = \frac{p^4}{m_\chi^4}\phi^2\,,$$

a condition that relates the R-ghost to ϕ. Substituting back into Eq. (4.3.53) and defining the composite field

$$\Phi^2 = \frac{p^2}{m_\chi^2}\left(\frac{p^2}{m_\chi^2}+1\right)\phi^2$$

the Lagrangian, in position-space, becomes

$$\mathcal{L}_\Phi = -\frac{1}{2}\Phi\left(\Box - m_\chi^2\right)\Phi - \frac{\lambda'}{4!}\Phi^4 + \frac{c_3^{(6)\prime}}{6!\Lambda^2}\Phi^6 \tag{4.3.54}$$

with

$$\lambda' = \frac{\lambda - c_1^{(6)}\frac{\Box}{\Lambda^2}}{\left[\frac{\Box}{m_\chi^2}\left(\frac{\Box}{m_\chi^2}-1\right)\right]^2} \quad \text{and} \quad c_3^{(6)\prime} = \frac{c_3^{(6)}}{\left[\frac{\Box}{m_\chi^2}\left(\frac{\Box}{m_\chi^2}-1\right)\right]^3}\,.$$

Finally, the counter-terms determine the 1-loop contributions to the β-functions (with $\lambda_\chi = 0$)

$$\begin{aligned}
\beta^q_{m^2} &= \frac{\lambda m_\chi^2}{16\pi^2} + \frac{c_1^{(6)}}{c_2^{(6)}}\frac{q^2}{16\pi^2}\\
\beta^q_{\lambda} &= \frac{3\lambda^2}{16\pi^2} + \frac{3c_3^{(6)}}{16\pi^2}\frac{m_\chi^2}{\Lambda^2}\\
\beta^q_{c_3^{(6)}} &= -\frac{5\lambda c_3^{(6)}}{16\pi^2}\,.
\end{aligned} \tag{4.3.55}$$

A few additional comments are in order. The comparison between $\mathcal{L}$ and $\mathcal{L}_\Phi$ shows that the original local theory with all the dimension-6 operators and R-ghosts present is equivalent to a non-local and ghost-free theory including only the polynomial dimension-6 operator. Moving from $\mathcal{L}$ to $\mathcal{L}_\Phi$ the pole is shifted and from the viewpoint of the non-local field Φ, is located at $-m_\chi^2$. On the other hand, even though the propagator of the original local field ϕ had a pole at $m^2 = 0$, there is a non-trivial counter-term δm. This is reminiscent of the Coleman-Weinberg model [13]. Note also that the original basis of Eq. (4.3.9) becomes consistent only after renormalization, having imposed both tree and loop level conditions. This can be considered as a hint of the quantum nature of the HDO. Note finally that the equivalence of the two Lagrangians

renders the operators $O_1^{(6)}$ and $O_2^{(6)}$ redundant since Eq. (4.3.54) contains only one dimension-6 operator, $O_3^{(6)}$.

The only nuisance is the non-local nature of Eq. (4.3.54) which makes the computation of RG flows difficult. In the next section we will show that $\mathcal{L}_\Phi$ is equivalent to a local and ghost-free theory, connected to Eq. (4.3.9) via the redefinition of Eq. (4.3.4).

4.3.2 The pure polynomial W-basis

In the previous section we showed how the non-physical degrees of freedom present in the G-basis are cancelled by the R-ghost Lagrangian, which was added though by hand. How can this structure be better motivated? Suppose that we start with the local, ghost-free Lagrangian

$$\widetilde{\mathcal{L}}_0 = -\frac{1}{2}\phi_0\Box\phi_0 - \frac{1}{2}\widetilde{m}_0^2\phi_0^2 - \frac{\widetilde{\lambda}_0}{4!}\phi_0^4 + \frac{\widetilde{c}_{3,0}^{(6)}}{6!\Lambda^2}\phi_0^6\,, \tag{4.3.56}$$

that includes only one, non-derivative dimension-6 operator. This "tilded" basis is just our previous W-basis. We have seen that the field redefinition of Eq. (4.3.4) transforms us back to G-basis but without the R-ghosts. Not to miss those one must be careful since after the field transformation a non-trivial Jacobean develops. This can be made clear if we consider the path-integral in the absence of sources

$$\mathcal{Z}[0] = \int \mathcal{D}\phi_0\, e^{i\widetilde{S}[\phi_0]}\,, \qquad \widetilde{S}[\phi_0] = \int d^4x\, \widetilde{\mathcal{L}}_0\,.$$

Now since Eq. (4.3.56) is ghost-free then the field redefinition[2]

$$\phi_0 \to \phi_0' = \phi_0 + \frac{x}{\Lambda^2}\Box\phi_0 + \frac{y}{\Lambda^2}\phi_0^3$$

should move us to another ghost-free basis without changing anything, if performed consistently. This means that if in

$$\mathcal{Z}[0] = \int \mathcal{D}\phi_0 \left|\frac{d\phi_0'}{d\phi_0}\right| e^{i\widetilde{S}[\phi_0 + \frac{x}{\Lambda^2}\Box\phi_0 + \frac{y}{\Lambda^2}\phi_0^3]} \tag{4.3.57}$$

the Jacobean of the transformation is non-trivial, it must be accounted for. Now the new degrees of freedom ϕ_0' and $(\Box\phi_0)'$ are a function of two independent functions, the field ϕ_0 and $\Box\phi_0$. Clearly since everything (both the Lagrangian and the field redefinition) is valid up to total derivatives there is an arbitrariness involved in the choice of the independent field variables. To choose a gauge in the equivalence class of the $\partial^{2n}\phi$ variables we demand that in the transformed basis a pole cancellation mechanism should be at work. This amounts to a "diagonal" or "physical" gauge where ϕ_0' is a function only of ϕ_0 and $(\Box\phi_0)'$ is a function only of $\Box\phi_0$. In the diagonal gauge the Jacobean is a diagonal matrix given by

$$\frac{d\phi_0'}{d\phi_0} = \begin{bmatrix} 1 + \frac{x}{\Lambda^2}\Box + \frac{3y}{\Lambda^2}\phi_0^2 & 0 \\ 0 & 1 + \frac{x}{\Lambda^2}\Box + \frac{3y}{\Lambda^2}\phi_0^2 \end{bmatrix}$$

[2] In the presence of sources the term $J_0\,\phi_0$ should also be properly transformed, otherwise the S-matrix can not be kept unchanged. Also, one could reduce the operator basis by using the equations of motion and dropping operators that are proportional to them. This would give the basis of reduced β-functions [68]. This can also reduce the derivative order of the HDO avoiding the O-ghost but it is not clear if it leads to an equivalent theory [34, 74].

with determinant

$$D(\phi_0) = \det\left[\frac{d\phi_0'}{d\phi_0}\right] = \left(1 + \frac{x}{\Lambda^2}\Box + \frac{3y}{\Lambda^2}\phi_0^2\right)^2 \equiv 1 + \frac{2x}{\Lambda^2}\Box + \frac{6y}{\Lambda^2}\phi_0^2\,, \tag{4.3.58}$$

keeping terms to $\mathcal{O}(1/\Lambda^2)$. Now recall that an operator depending on commuting variables, like $D(\phi_0)$, can be rewritten as a path integral of the form

$$D(\phi_0) = \int \mathcal{D}\bar{\chi}_0'\mathcal{D}\chi_0'\, e^{-i\int d^4x \bar{\chi}_0' D(\phi_0)\chi_0'}\,,$$

with $\bar{\chi}_0', \chi_0'$ two real Grassmann variables. Then the transformed path integral of Eq. (5.B.4) includes also the anti-commuting, "reparametrization" ghost-fields. It becomes

$$\mathcal{Z}[0] = \int \mathcal{D}\phi_0\mathcal{D}\bar{\chi}_0'\mathcal{D}\chi_0'\, e^{i\widetilde{S}[\phi_0 + \frac{x}{\Lambda^2}\Box\phi_0 + \frac{y}{\Lambda^2}\phi_0^3] - i\int d^4x \bar{\chi}_0' D(\phi_0)\chi_0'} \tag{4.3.59}$$

and the correct version of Eq. (4.3.56) is

$$\widetilde{\mathcal{L}}_0 = \widetilde{\mathcal{L}}_{\text{red},0} + \mathcal{L}_{\text{R}g,0} \tag{4.3.60}$$

with

$$\begin{aligned}
\widetilde{\mathcal{L}}_{\text{red},0} &= -\frac{1}{2}\left[1 + 2x\frac{\widetilde{m}_0^2}{\Lambda^2}\right]\phi_0\Box\phi_0 - \frac{1}{2}\widetilde{m}_0^2\,\phi_0^2 - \left[\frac{\widetilde{\lambda}_0}{4!} + \frac{y\,\widetilde{m}_0^2}{\Lambda^2}\right]\phi_0^4 + \left[\frac{-y - \frac{x}{6}\widetilde{\lambda}_0}{\Lambda^2}\right]\phi_0^2\Box\phi_0^2 \\
&\quad + \left[\frac{-x}{\Lambda^2}\right]\phi_0\Box^2\phi_0 + \left[\frac{\widetilde{c}_{3,0}^{(6)}}{6!\Lambda^2} - \frac{y\widetilde{\lambda}_0}{6\Lambda^2}\right]\phi_0^6\,, \\
\mathcal{L}_{\text{R}g,0} &= -\frac{2x}{\Lambda^2}\,\bar{\chi}_0'\Box\chi_0' - \bar{\chi}_0'\chi_0' - \frac{6y}{\Lambda^2}\,\bar{\chi}_0'\chi_0'\phi_0^2\,.
\end{aligned} \tag{4.3.61}$$

The kinetic term of ϕ_0 and χ_0' can be made canonical using Eq. (4.3.6) and the redefinition $(\bar{\chi}_0', \chi_0') \to \sqrt{\frac{\Lambda^2}{2x}}(\bar{\chi}_0, \chi_0)$. Then

$$\begin{aligned}
\widetilde{\mathcal{L}}_0 &= -\frac{1}{2}\phi_0\Box\phi_0 - \frac{\widetilde{m}_0^2}{2}\left[1 - 2x\frac{\widetilde{m}_0^2}{\Lambda^2}\right]\phi_0^2 + \left[-\frac{\widetilde{\lambda}_0}{4!} - \frac{y\widetilde{m}_0^2}{\Lambda^2} + \frac{x\widetilde{\lambda}_0\widetilde{m}_0^2}{6\Lambda^2}\right]\phi_0^4 \\
&\quad + \left[\frac{-y - \frac{x}{6}\widetilde{\lambda}_0}{\Lambda^2}\right]\phi_0^2\Box\phi_0^2 + \left[\frac{-x}{\Lambda^2}\right]\phi_0\Box^2\phi_0 + \left[\frac{\widetilde{c}_{3,0}^{(6)}}{6!\Lambda^2} - \frac{y\widetilde{\lambda}_0}{6\Lambda^2}\right]\phi_0^6 \\
&\quad -\bar{\chi}_0\,\Box\chi_0 - \frac{\Lambda^2}{2x}\bar{\chi}_0\chi_0 - \frac{6y}{2x}\left[1 - 2x\frac{\widetilde{m}_0^2}{\Lambda^2}\right]\bar{\chi}_0\chi_0\phi_0^2 \\
&= -\frac{1}{2}\phi_0\Box\phi_0 - \frac{m_0^2}{2}\phi_0^2 - \frac{\lambda_0}{4!}\phi_0^4 + \frac{c_{1,0}^{(6)}}{4!\Lambda^2}\phi_0^2\Box\phi_0^2 + \frac{c_{2,0}^{(6)}}{2\Lambda^2}\phi_0\Box^2\phi_0 \\
&\quad + \frac{c_{3,0}^{(6)}}{6!\Lambda^2}\phi_0^6 - \bar{\chi}_0\,\Box\chi_0 + \frac{\Lambda^2}{c_{2,0}^{(6)}}\bar{\chi}_0\chi_0 - \frac{\lambda_{\chi,0}}{2}\,\bar{\chi}_0\chi_0\phi_0^2\,,
\end{aligned} \tag{4.3.62}$$

where in the last expression we made the identifications

$$m_0^2 = \widetilde{m}_0^2\left[1 - 2x\frac{\widetilde{m}_0^2}{\Lambda^2}\right]$$

$$
\begin{aligned}
\lambda_0 &= \widetilde{\lambda}_0 + 4!\frac{\widetilde{m}_0^2}{\Lambda^2}\left(y - \frac{x}{6}\widetilde{\lambda}_0\right) \\
c_{1,0}^{(6)} &= 4!\left(-y - \frac{x}{6}\widetilde{\lambda}_0\right) \\
c_{2,0}^{(6)} &= 2\,(-x) \\
c_{3,0}^{(6)} &= \widetilde{c}_{3,0}^{(6)} - 6!\frac{y}{6}\widetilde{\lambda}_0 \\
\lambda_{\chi,0} &= \frac{6y}{x}\left[1 - 2x\frac{\widetilde{m}_0^2}{\Lambda^2}\right] .
\end{aligned}
\tag{4.3.63}
$$

As we expected, we started from a ghost-free basis and the redefinition gave us back exactly Eq. (4.3.9) (up to a harmless normalization of χ), justifying the original insertion of $\mathcal{L}_{\mathrm{R}g}$. To complete the connection between the G and W-bases we need to relate the corresponding couplings. Using the renormalized form of Eq. (4.3.63) to move from the tilded to the un-tilded Lagrangian, we got

$$
x = -\frac{1}{2}c_2^{(6)} \text{ and } y = -\frac{1}{4!}(c_1^{(6)} - 2\widetilde{\lambda}c_2^{(6)})\,. \tag{4.3.64}
$$

In addition, recall that the R-ghost decouples if $\lambda_\chi = 0$ which can be achieved when $y = 0$ or $\widetilde{m}^2 = -m_\chi^2$. The former happens if $c_1^{(6)} = 2\widetilde{\lambda}c_2^{(6)}$ and the latter ensures that $m^2 = 0$ and we need both in order to get an equivalent to Eq. (4.3.54) theory. With these constraints, we have $\lambda = -\widetilde{\lambda}$ and $c_3^{(6)} = \widetilde{c}_3^{(6)}$.

We are now ready to use directly the W-basis given by the Lagrangian Eq. (4.3.56) for the evaluation of the phase diagram and of the RG flows. For this, we return to the algorithm of Sect. 4.2. Like we considered the mass and ϕ^4 term deformations of the kinetic term, we will do the same for the ϕ^6 operator. We can fully exploit the detailed example of Sect. 4.B where the operator insertion method was applied and the notation was set up. Our Lagrangian now has the form

$$
\widetilde{\mathcal{L}} = \widetilde{\mathcal{L}}_4 + \widetilde{c}_3^{(6)}\widetilde{O}_3^{(6)}
$$

with $\widetilde{\mathcal{L}}_4$ the tilded version of Eq. (4.B.1). $\widetilde{c}^{(2)}\widetilde{O}^{(2)}$ and $\widetilde{c}^{(4)}\widetilde{O}^{(4)}$ were defined in Sect. 4.B and the new entry here is $\widetilde{O}_3^{(6)} = \phi^6/(6!\Lambda^2)$ with coupling $\widetilde{c}_3^{(6)}$. The classical dimension of the coupling is

$$
d_{\widetilde{c}_3^{(6)}} = 2(4-d) = 2\varepsilon\,, \tag{4.3.65}
$$

while the classical dimension of its associated operator, using $d_\phi = \frac{d-2}{2}$, is

$$
d_{\widetilde{O}_3^{(6)}} = 3d - 8 = 4 - 3\varepsilon\,. \tag{4.3.66}
$$

Since the extra deformation is just another polynomial term there is no new contribution to δ_ϕ which remains zero at 1-loop.

Here we admit three β-functions, since $l = 2, 4, 6$, so let us start with the determination of $\beta_{\widetilde{c}^{(2)}}$. Its general form is given by Eq. (4.B.3). Only the non-linear part is affected since, apart from $\widetilde{Z}_{222}$ and $\widetilde{Z}_{244}$, there is now one more contribution, $\widetilde{Z}_{266}$. In particular, this is given by Eq. (4.2.23) with $n = 2$, $k' = r = s = 6$ and $q_{(2,6)} = 2$ whose effect starts at 3-loop level. Hence

$\widetilde{Z}_{266}$ and $\widetilde{\Gamma}_{266}$ are trivial. Then $\beta_{\widetilde{c}^{(2)}}$ is the same as in Eq. (4.B.13) and reads

$$\beta_{\widetilde{c}^{(2)}} = -2\widetilde{m}^2 + \frac{\widetilde{\lambda}\widetilde{m}^2}{16\pi^2}\,. \tag{4.3.67}$$

Next we look at the β-function of $\widetilde{c}^{(4)}$ whose general form is

$$\beta_{\widetilde{c}^{(4)}} = -\varepsilon\widetilde{c}^{(4)} + \frac{\widetilde{m}^2}{2}\widetilde{\Gamma}^6_m + \widetilde{\Gamma}_{\widetilde{O}^{(4)}}\,\widetilde{c}^{(4)} + \widetilde{\Gamma}_{422}\,\widetilde{c}^{(2)}\widetilde{c}^{(2)} + \widetilde{\Gamma}_{444}\,\widetilde{c}^{(4)}\widetilde{c}^{(4)} + \widetilde{\Gamma}_{466}\,\widetilde{c}^{(6)}_3\widetilde{c}^{(6)}_3\,. \tag{4.3.68}$$

In this case there are two extra contributions to $\beta_{\widetilde{c}^{(4)}}$ with respect to Appendix 4.B. The first refers to $\widetilde{\Gamma}^6_m$ which is non-zero here and the second to $\widetilde{\Gamma}_{466}$.

The former is calculated using Eq. (4.2.21) for $n = 4$ and $k = 2, 4, 6$

$$\begin{aligned}\langle\phi(x_1)\phi(x_2)\phi(x_3)\phi(x_4)\widetilde{O}^{(2)}(y)\rangle_0 &= \widetilde{Z}^6_2\langle\phi(x_1)\cdots\phi(x_4)\widetilde{O}^{(2)}(y)\rangle + \widetilde{Z}^6_4\langle\phi(x_1)\cdots\phi(x_4)\widetilde{O}^{(4)}(y)\rangle \\ &+ \widetilde{Z}^6_6\langle\phi(x_1)\cdots\phi(x_4)\widetilde{O}^{(6)}_3(y)\rangle\end{aligned} \tag{4.3.69}$$

where now the bare part of the expression involves $\widetilde{\mathcal{L}}_{\text{int},0} = -\widetilde{c}^{(4)}_0\widetilde{O}^{(4)}_0 + \widetilde{c}^{(6)}_{3,0}\widetilde{O}^{(6)}_{3,0}$. Expanding the exponential in the expectation value to order $\mathcal{O}(\widetilde{c}^{(4)}_0, \widetilde{c}^{(6)}_{3,0})$, the l.h.s becomes

$$\langle\phi(x_1)\phi(x_2)\phi(x_3)\phi(x_4)\frac{\phi^2(y)}{2}\frac{-i\widetilde{\lambda}\,\phi^4(z)}{4!}\rangle_0 + \langle\phi(x_1)\phi(x_2)\phi(x_3)\phi(x_4)\frac{\phi^2(y)}{2}\frac{i\widetilde{c}^{(6)}_3\,\phi^6(z)}{6!\Lambda^2}\rangle_0$$

The first term above contributes only disconnected and bubble diagrams while the second term gives

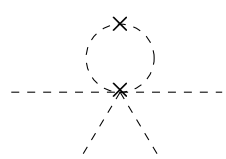

(4.3.70)

corresponding to a scaleless B_0-integral. Its explicit form is given by Eq. (4.A.9), where remember, we must now extract its UV divergent part. Apart from this, it has three channels given in Eq. (4.B.19). From the r.h.s of Eq. (4.3.69) only the second term gives a counter-term at 1-loop which can absorb the remnant divergence. This fixes $\widetilde{Z}^6_4 = 3\widetilde{c}^{(6)}_3/(16\pi^2\Lambda^2\varepsilon)$ and from the definition of Eq. (4.2.11) we get

$$\widetilde{\Gamma}^6_m = -6\frac{\widetilde{c}^{(6)}_3}{16\pi^2\Lambda^2}\,. \tag{4.3.71}$$

Next we consider the non-linear term, $\widetilde{\Gamma}_{466}$. For the evaluation of this contribution we use Eq. (4.2.23) for $n = 4$, $k' = r = s = 6$ and $q_{(4,6)} = 4$ getting back only greater than 1-loop scaleless Tadpoles. Collecting all the ingredients, the picture of $\beta_{\widetilde{c}^{(4)}}$ is complete:

$$\beta_{\widetilde{c}^{(4)}} = -\varepsilon\widetilde{\lambda} + \frac{3\widetilde{\lambda}^2}{16\pi^2} - \frac{3\widetilde{c}^{(6)}_3\widetilde{m}^2}{16\pi^2\Lambda^2}\,. \tag{4.3.72}$$

As a last step we consider Eq. (4.2.1) for $l = 6$ which gives the general form

$$\beta_{\widetilde{c}^{(6)}_3} = -2\varepsilon\widetilde{c}^{(6)}_3 + \frac{\widetilde{m}^2}{3}\widetilde{\Gamma}^8_m + \widetilde{\Gamma}_{\widetilde{O}^{(6)}_3}\,\widetilde{c}^{(6)}_3 + \widetilde{\Gamma}_{622}\,\widetilde{c}^{(2)}\widetilde{c}^{(2)} + \widetilde{\Gamma}_{644}\,\widetilde{c}^{(4)}\widetilde{c}^{(4)} + \widetilde{\Gamma}_{666}\,\widetilde{c}^{(6)}_3\widetilde{c}^{(6)}_3\,. \tag{4.3.73}$$

Since the Lagrangian does not include dim-8 operators, the second term of Eq. (4.3.73) is absent. We start with the linear part using Eq. (4.2.20) for $n = l = 6$ and the corresponding expectation value is

$$\langle \phi(x_1)\cdots\phi(x_6)\widetilde{O}_3^{(6)}(y)\rangle_0 = \widetilde{Z}_{\widetilde{O}_3^{(6)}}\langle \phi(x_1)\cdots\phi(x_6)\widetilde{O}_3^{(6)}(y)\rangle\,, \tag{4.3.74}$$

or using Eq. (4.2.6),

$$\langle \phi(x_1)\cdots\phi(x_6)\widetilde{O}_3^{(6)}(y)\rangle_0 - \widetilde{\delta}_{\widetilde{O}_3^{(6)}}\langle \phi(x_1)\cdots\phi(x_6)\widetilde{O}_3^{(6)}(y)\rangle = \langle \phi(x_1)\cdots\phi(x_6)\widetilde{O}_3^{(6)}(y)\rangle\,. \tag{4.3.75}$$

The l.h.s of this expression should be evaluated with $\widetilde{\mathcal{L}}_{\text{int},0} = -\widetilde{c}_0^{(2)}\widetilde{O}_0^{(2)} - \widetilde{c}_0^{(4)}\widetilde{O}_0^{(4)}$. Doing so, we have

$$\mathcal{N}^{-1}\langle 0|T[\phi_0(x_1)\cdots\phi_0(x_6)\frac{\phi_0^6(y)}{6!\Lambda^2}e^{-i\int d^dz\frac{\widetilde{m}_0^2}{2}\phi_0^2(z)+\frac{\widetilde{\lambda}_0}{4!}\phi_0^4(z)}]|0\rangle - \widetilde{\delta}_{\widetilde{O}_3^{(6)}}\langle \phi(x_1)\cdots\phi(x_6)\frac{\phi^6(y)}{6!\Lambda^2}\rangle$$

with disconnected and 2-loop diagrams to $\mathcal{O}(\widetilde{m}^2, \widetilde{\lambda}^0)$. On the other hand, to $\mathcal{O}((\widetilde{m}^2)^0, \widetilde{\lambda})$ it gives

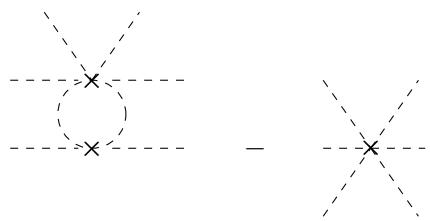

where apart from the 6 external legs, which imply 5 different channels and the coupling multiplying the diagram, it gives the same contribution as in Eq. (5.3.27). Keeping only the UV part of the scaleless integral involved, finiteness forces

$$\widetilde{\delta}_{\widetilde{O}_3^{(6)}} = -\frac{5\widetilde{\lambda}}{16\pi^2}\frac{1}{\varepsilon}\,, \tag{4.3.76}$$

while using Eq. (4.2.10) or its 1-loop version below, we get

$$\widetilde{\Gamma}_{\widetilde{O}_3^{(6)}} = \frac{5\widetilde{\lambda}}{16\pi^2}\,. \tag{4.3.77}$$

The only thing left is the evaluation of the non-linear part in Eq. (4.3.73). The first two of the three non-linear terms, $\widetilde{\Gamma}_{622}$ and $\widetilde{\Gamma}_{644}$, are determined from Eq. (4.2.23) with $n = 6$, $k' = r = s = 2$, $q_{(6,2)} = 6$ and $n = 6$, $k' = r = s = 4$, $q_{(6,4)} = 6$ respectively. Both expectation values admit disconnected (finite or 1-loop) diagrams. As a consequence, $\widetilde{\Gamma}_{622}$ and $\widetilde{\Gamma}_{644}$ vanish. The third non-linear term, $\widetilde{\Gamma}_{666}$, is given by Eq. (4.2.22) for $l = r = s = 6$ and has the same fate with the previous cases since it gives a 2-loop diagram as the lowest order contribution. Putting all the pieces together we get

$$\beta_{\widetilde{c}_3^{(6)}} = -2\varepsilon\widetilde{c}_3^{(6)} + \frac{5\widetilde{\lambda}\,\widetilde{c}_3^{(6)}}{16\pi^2}\,. \tag{4.3.78}$$

Using Eq. (4.3.67), Eq. (4.3.72) and Eq. (4.3.78) we summarize. Then the quantum parts of the β-functions are

$$\vec{\beta}^q_{\widetilde{c}^{(l)}} = \begin{bmatrix} \beta^q_{\widetilde{c}^{(2)}} \\ \beta^q_{\widetilde{c}^{(4)}} \\ \beta^q_{\widetilde{c}_3^{(6)}} \end{bmatrix} = \begin{bmatrix} \frac{\widetilde{\lambda}\widetilde{m}^2}{16\pi^2} \\ -\frac{3\widetilde{c}_3^{(6)}\widetilde{m}^2}{16\pi^2\Lambda^2} + \frac{3\widetilde{\lambda}^2}{16\pi^2} \\ \frac{5\widetilde{\lambda}\,\widetilde{c}_3^{(6)}}{16\pi^2} \end{bmatrix} \tag{4.3.79}$$

while the full 1-loop β-functions are

$$\vec{\beta}_{\widetilde{c}^{(l)}} = \begin{bmatrix} \beta_{\widetilde{c}^{(2)}} \\ \beta_{\widetilde{c}^{(4)}} \\ \beta_{\widetilde{c}_3^{(6)}} \end{bmatrix} = \begin{bmatrix} -2\widetilde{m}^2 + \frac{\widetilde{\lambda}\widetilde{m}^2}{16\pi^2} \\ -\varepsilon\widetilde{\lambda} + \frac{3\widetilde{\lambda}^2}{16\pi^2} - \frac{3\widetilde{c}_3^{(6)}\widetilde{m}^2}{16\pi^2\Lambda^2} \\ -2\varepsilon\widetilde{c}_3^{(6)} + \frac{5\widetilde{\lambda}\,\widetilde{c}_3^{(6)}}{16\pi^2} \end{bmatrix} . \tag{4.3.80}$$

Check that using the relations below Eq. (4.3.63) which connect the tilded and untilded couplings, we have arrived at the same β-functions as in Eq. (4.3.55).

One of our original goals was to search for a broken phase in the absence of an explicit mass term. Let us then take $\widetilde{m}^2 \to 0$ in Eq. (4.3.79) and Eq. (4.3.80) so that we are left with only two operator insertions, $\widetilde{O}^{(4)}$ and $\widetilde{O}_3^{(6)}$. This defines the $O^{(4)}$-$O^{(6)}$ system. Now we can finally evaluate the phase diagram of the theory in $d = 3, 4$ and 5 dimensions. Regarding the breaking of the $\mathbb{Z}_2$ internal symmetry, its fate is governed by the renormalized scalar potential

$$\widetilde{V}^{(6)} = \frac{\widetilde{\lambda}}{4!}\phi^4 - \frac{\widetilde{c}_3^{(6)}}{6!\Lambda^2}\phi^6 . \tag{4.3.81}$$

According to the signs of $\widetilde{\lambda}$ and $\widetilde{c}_3^{(6)}$, there are the following cases:

- $\widetilde{\lambda} > 0$ and $\widetilde{c}_3^{(6)} > 0$
  ϕ^6 is dominant so the overall sign of the potential is minus. As a consequence, it becomes unstable and since the relative sign of the couplings is negative there are two maxima.
- $\widetilde{\lambda} > 0$ and $\widetilde{c}_3^{(6)} < 0$
  The overall sign of the potential and the relative sign of the couplings is positive. Therefore, the potential is stable but the theory does not exhibits broken phase.
- $\widetilde{\lambda} < 0$ and $\widetilde{c}_3^{(6)} > 0$
  This case resembles the previous one with the difference that now the overall sign of the potential is negative making the system unstable.
- $\widetilde{\lambda} < 0$ and $\widetilde{c}_3^{(6)} < 0$
  The potential is stable since the dominant term, ϕ^6, has a positive sign. The relative sign of the couplings is negative and the theory has a broken phase with two minima.

In the last case the minimization of the potential inherits to the scalar field a non-trivial vev, given by

$$\widetilde{v} = \pm\sqrt{20}\sqrt{\frac{|\widetilde{\lambda}|}{|\widetilde{c}_3^{(6)}|}}\Lambda . \tag{4.3.82}$$

Observe that the vev depends explicitly on the cutoff, Λ, which in general should be considered a function of the renormalization scale. Performing now the expansion $\phi \to \phi \pm \widetilde{v}$ in Eq. (4.3.81) and looking at the extrema of the potential, we obtain the physical mass

$$\widetilde{m}_\phi^2 = \frac{|\widetilde{\lambda}|}{3}\widetilde{v}^2 , \tag{4.3.83}$$

which also depends on Λ.

We proceed by constructing the phase diagram. Following the same steps as for the $O^{(2)}$-$O^{(4)}$ system, the main ingredients are the RG equations of the couplings $\widetilde{\lambda}, \widetilde{c}_3^{(6)}$, the possible fixed points of the RG flow and the determination of the nature of the associated operators. Regarding the first of these ingredients, we need to solve the RG equations $\mu\, d\widetilde{\lambda}/d\mu = \beta_{\widetilde{\lambda}}$ and $\mu\, d\widetilde{c}_3^{(6)}/d\mu = \beta_{\widetilde{c}_3^{(6)}}$. The solution for the RG evolution of $\widetilde{\lambda}$ in $d = 4$ is

$$\widetilde{\lambda}(\mu) = \frac{\widetilde{\lambda}}{1 - \frac{3\widetilde{\lambda}^2}{16\pi^2} \ln \frac{\mu}{\mu_{\mathrm{R}}}}\,, \tag{4.3.84}$$

while in $d \neq 4$ it is

$$\widetilde{\lambda}(\mu) = \frac{\widetilde{\lambda}}{\frac{3\widetilde{\lambda}}{16\pi^2\varepsilon} + \frac{\mu^\varepsilon}{\mu_{\mathrm{R}}^\varepsilon}\left(1 - \frac{3\widetilde{\lambda}}{16\pi^2\varepsilon}\right)}\,. \tag{4.3.85}$$

The solution for $\widetilde{c}_3^{(6)}$ in $d = 4 - \varepsilon$ is

$$\widetilde{c}_3^{(6)}(\mu) = \widetilde{c}_3^{(6)} \left(\frac{\mu}{\mu_{\mathrm{R}}}\right)^{-2\varepsilon + \frac{5\widetilde{\lambda}}{16\pi^2}}\,, \tag{4.3.86}$$

with μ_{R} the usual arbitrary renormalization scale. Recalling that the RG equation of the mass in the ϕ^4 theory is given by

$$m^2(\mu) = m^2 \left(\frac{\mu}{m}\right)^{-2 + \frac{\lambda}{16\pi^2}} \tag{4.3.87}$$

and comparing it with Eq. (4.3.86) one observes that $\widetilde{c}_3^{(6)}$ acts like a mass term in $d = 3$ and as an inverse mass in $d = 5$. The above solutions allow us to combine Eq. (4.3.83) with Eq. (4.3.84) and Eq. (4.3.86), and compute the running of $\widetilde{m}_\phi^2$ as a function of μ. To be more specific, in $d = 4$ we get

$$\widetilde{m}_\phi^2(\mu) = \frac{|\widetilde{\lambda}(\mu)|}{3}\widetilde{v}^2\,, \tag{4.3.88}$$

whose running is depicted on Fig. 4.1 and shows that it sees the Landau pole in the UV.

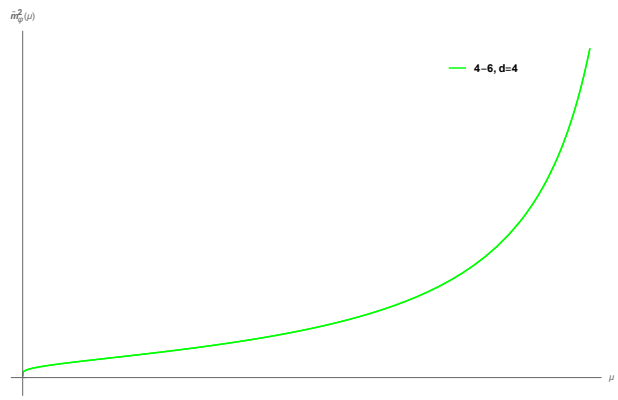

Figure 4.1: The running of the physical mass, after SSB, as a function of the renormalization scale in four dimensions. Eq. (4.3.88) shows that the running of $\widetilde{m}_\phi$ is dominated by $\widetilde{\lambda}$ which diverges when μ reaches the Landau pole. This is a representation of the naturalness problem.

The next step is to check for possible fixed points in the RG flow, which is done by demanding that the β-functions vanish for specific values of the couplings. In four dimensions $\beta_{\widetilde{\lambda}}$ vanishes only when

$$\widetilde{\lambda} = \widetilde{\lambda}_\bullet = 0 \tag{4.3.89}$$

and on that point $\beta_{\widetilde{c}_3^{(6)}}$ vanishes for any value of $\widetilde{c}_3^{(6)}$. A special case is when both couplings are zero since then, the flow reaches a trivial fixed point, $(\widetilde{\lambda}_\bullet, \widetilde{c}_{3\bullet}^{(6)})$. Regarding the $d = 4$ case, the picture therefore is that of a WF line formed by all possible values of $\widetilde{c}_3^{(6)}$, when Eq. (4.3.89) is true. This line ends on the G fixed-point where both couplings vanish simultaneously. On the other hand, in $d \neq 4$, $\beta_{\widetilde{\lambda}}$ has both $\bullet$ and $\star$ points corresponding to

$$\widetilde{\lambda}_\bullet = 0 \quad \text{and} \quad \widetilde{\lambda}_\star = \frac{16\pi^2}{3}\varepsilon\,, \tag{4.3.90}$$

while $\beta_{\widetilde{c}_3^{(6)}}$ vanishes only for vanishing $\widetilde{c}_3^{(6)}$. This is true in any dimension, except four, and indicates that $\widetilde{c}_3^{(6)}$ has only one fixed point given by

$$\widetilde{c}_{3\star}^{(6)} = \widetilde{c}_{3\bullet}^{(6)} = 0\,.$$

The last ingredient we need for the description of the phase diagram is the behaviour of the operators $\widetilde{O}^{(4)}$ and $\widetilde{O}_3^{(6)}$ with respect to the fixed points, as we move from the UV to the IR. For this we apply the rules reviewed in Appendix 4.B. In what follows we present these results for $-1 \leq \varepsilon \leq 1$.

$$\frac{\partial \beta_{\widetilde{\lambda}}}{\partial \widetilde{\lambda}} = -\varepsilon + \frac{6}{16\pi^2}\widetilde{\lambda} = \begin{cases} \bullet : -\varepsilon & \begin{cases} d = 4 : 0 \text{ (IR from Eq. (4.3.84))} \\ d = 3 : -1 < 0 \to \text{UV} \\ d = 5 : +1 > 0 \to \text{IR} \end{cases} \\ \star : +\varepsilon & \begin{cases} d = 4 : - \\ d = 3 : +1 > 0 \to \text{IR} \\ d = 5 : -1 < 0 \to \text{UV} \end{cases} \end{cases} \tag{4.3.91}$$

$$\frac{\partial \beta_{\widetilde{c}_3^{(6)}}}{\partial \widetilde{c}_3^{(6)}} = -2\varepsilon + \frac{5\widetilde{\lambda}}{16\pi^2} \begin{cases} \bullet : -2\varepsilon & \begin{cases} d=4: 0 \text{ (IR from Eq. (4.3.86) for } \varepsilon = 0) \\ d=3: -2<0 \to \text{UV} \\ d=5: +2>0 \to \text{IR} \end{cases} \\ \star : -\frac{\varepsilon}{3} & \begin{cases} d=4: - \\ d=3: -\frac{1}{3}<0 \to \text{UV} \\ d=5: \frac{1}{3}>0 \to \text{IR} \end{cases} \end{cases} \tag{4.3.92}$$

where Eq. (4.3.92) shows that $\widetilde{O}_3^{(6)}$ sees both fixed points as UV and as IR in $d=3$ and $d=5$ respectively. The way to determine the nature of the two operators is through their scaling dimensions as reviewed in Appendix 4.B. From Eq. (5.4.35) and Eq. (5.4.36) we get

$$\Delta_{\widetilde{O}^{(4)}} = 4 - 2\varepsilon + \frac{6\widetilde{\lambda}}{16\pi^2} \tag{4.3.93}$$

for $\widetilde{O}^{(4)}$, while for $\widetilde{O}_3^{(6)}$, keeping in mind Eq. (4.3.66),

$$\Delta_{\widetilde{O}_3^{(6)}} = 4 - 3\varepsilon + \frac{5\widetilde{\lambda}}{16\pi^2}\,. \tag{4.3.94}$$

Applying these expressions to the two fixed points we obtain the 1-loop exponent that determines the nature of an operator:

	$\Delta_O - d$	$\bullet$	$\star$
$\widetilde{O}^{(4)}$	$-\varepsilon + 2\frac{3\widetilde{\lambda}}{16\pi^2}$	$-\varepsilon$	ε
$\widetilde{O}_3^{(6)}$	$-2\varepsilon + \frac{5\widetilde{\lambda}}{16\pi^2}$	-2ε	$-\frac{\varepsilon}{3}$

and this fixes the following characterizations:

	$d=4$		$d=3$		$d=5$	
$\widetilde{O}^{(4)}$	$\bullet$: irrel	$\star$: $-$	$\bullet$: rel	$\star$: irrel	$\bullet$: irrel	$\star$: rel
$\widetilde{O}_3^{(6)}$	$\bullet$: irrel	$\star$: $-$	$\bullet$: rel	$\star$: rel	$\bullet$: irrel	$\star$: irrel

The construction of the phase diagram follows the rules given in the last part of Appendix 4.B.

Let us start with $d=4$ where the RG flows are determined by Eq. (4.3.84) and Eq. (4.3.86) for $\varepsilon = 0$. There are four possible combinations for the sign of the couplings, two for $\widetilde{\lambda} > 0$ and two for $\widetilde{\lambda} < 0$. In each case the theory has a Landau pole when the scale reaches $\mu_{\rm L} = \exp[16\pi^2/3\widetilde{\lambda}]\mu_{\rm R}$. Notice that the broken phase here mimics the one of $\mathcal{L}^{(4)}$ for $\lambda < 0$ in Fig. 4.B.1. In fact, when $\widetilde{\lambda} < 0$ the absolute value of the coupling $\widetilde{c}_3^{(6)}(\mu)$ increases towards the IR which indeed resembles the behaviour of a mass operator. These features are depicted in Fig. 4.2.

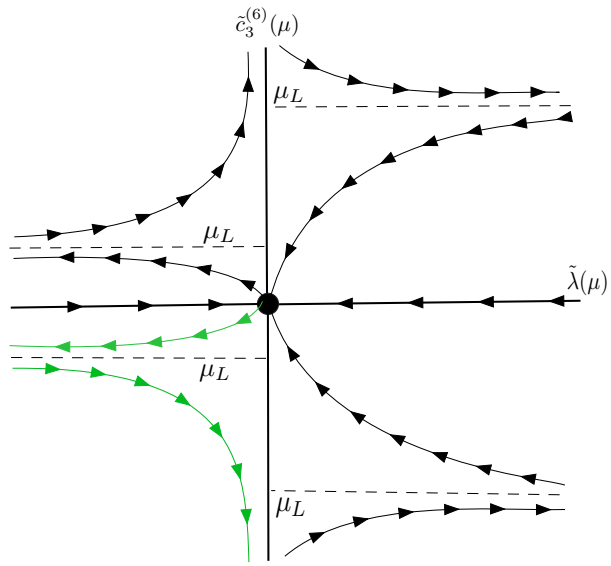

Figure 4.2: RG flows for $\widetilde{\mathcal{L}}$, in $d = 4$. The $\widetilde{\lambda}, \widetilde{c}_3^{(6)} < 0$ (green) flow corresponds to the broken phase.

Next we consider the $d = 3$ RG flows, given by Eq. (4.3.85) and Eq. (4.3.86) for $\varepsilon = 1$. The RG equation of $\widetilde{\lambda}(\mu)$ is exactly the same as that of $\lambda(\mu)$ in Appendix 4.B. Moreover, notice that for $\widetilde{\lambda} < \frac{32\pi^2}{5}$, the coupling $\widetilde{c}_3^{(6)}(\mu)$ has the same behaviour as the mass, Eq. (4.3.87). Therefore the phase diagram on the left of Fig. 4.3 is qualitatively similar to the left part of Fig. 4.B.2. The last case regards the $d = 5$ RG flows given by Eq. (4.3.85) and Eq. (4.3.86) but now for $\varepsilon = -1$. The flows are depicted on the right of Fig. 4.3. In this case the WF point is negative and we can take $\widetilde{\lambda}$ as negative we want, however we restrict ourselves here to $-\frac{32\pi^2}{5} < \widetilde{\lambda}$, to keep the exponent in the RG equation of $\widetilde{c}_3^{(6)}(\mu)$ positive. Similarly to the $d = 3$ case, we see two Landau branches, for $\widetilde{\lambda} < 0$, $\widetilde{\lambda} < \widetilde{\lambda}_\star$ and $\widetilde{\lambda} > 0$. The flow of the broken phase here starts off G in the IR where both couplings vanish and tends to a constant $\widetilde{\lambda}$ and a diverging $\widetilde{c}_3^{(6)}$ in the UV.

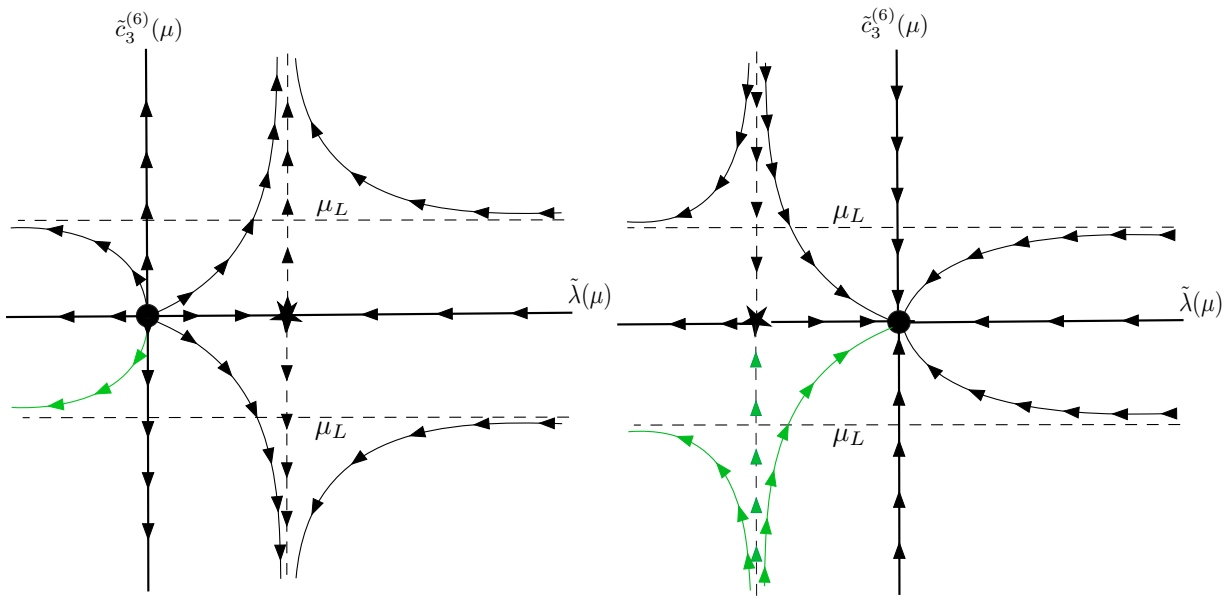

Figure 4.3: Left: RG flows for $\widetilde{\mathcal{L}}$, in $d = 3$. The $\widetilde{\lambda}, \widetilde{c}_3^{(6)} < 0$ (green) flow corresponds to the broken phase. Here, $\star$ denotes the WF fixed point where scale invariance is restored while the system is still interacting. Right: RG flows for $\widetilde{\mathcal{L}}$, in $d = 5$.

4.3.3 Filling a couple of remaining holes

We have repeatedly argued that Λ is not an external to the system scale but we have not given any quantitative argument to that effect. In DR we argued in particular that at a general point of the phase diagram Λ is a function of μ. At special points it may be easily related to specific scales like a Landau pole or a vev (which is a function of μ) but in general there is an arbitrariness in fixing this function. Let us analyze a bit one simple case here, the case $\Lambda = \mu$ and demonstrate that this choice does not affect qualitatively the phase diagrams. To see this, recall that for the construction of the phase diagrams in d-dimensions we used Eq. (4.3.85) and Eq. (4.3.86) and focus on $\widetilde{c}_3^{(6)}(\mu)$. In Eq. (4.3.86), the number in the first term of the exponent is determined by the dimensionality of $\widetilde{c}_3^{(6)}(\mu)$ and ε determines the nature of the running. Suppose now that the dimension-6 operator insertion is

$$\widetilde{c}_3^{(6)} \widetilde{O}_3^{(6)} = \widetilde{c}_3^{(6)} \frac{\phi^6}{\mu^2} \,.$$

Dimensional analysis shows that $d_{\widetilde{c}_3^{(6)}}$ is still given by Eq. (4.3.65). Therefore in this case the running of $\widetilde{c}_3^{(6)}$ follows Eq. (4.3.86), leading to the same phase diagrams.

There is another possibility, one where the inserted coupling $\widetilde{c}_3^{(6)}$ is dimensionfull, with $[\widetilde{c}_3^{(6)}] = -2$. In such scenario the β-function is given by

$$\beta_{\hat{c}_3^{(6)}} = (2 - 2\varepsilon)\hat{c}_3^{(6)} + \beta^q_{\hat{c}_3^{(6)}}$$

since in d-dimensions $\widetilde{c}_3^{(6)} = \hat{c}_3^{(6)} \mu^{d - d_{\widetilde{O}_3^{(6)}}} \equiv \hat{c}_3^{(6)} \mu^{-2(1-\varepsilon)}$, with $\hat{c}_3^{(6)}$ dimensionless. In any case,

the above leads to the RG equation

$$\begin{aligned}\hat{c}_3^{(6)}(\mu) &= \hat{c}_3^{(6)}\left(\frac{\mu}{\mu_{\rm R}}\right)^{2-2\varepsilon+\beta^q_{\hat{c}_3^{(6)}}/\hat{c}_3^{(6)}} \Rightarrow \\ \frac{\hat{c}_3^{(6)}(\mu)}{\mu^2} &= \frac{\hat{c}_3^{(6)}}{\mu_{\rm R}^2}\left(\frac{\mu}{\mu_{\rm R}}\right)^{-2\varepsilon+\beta^q_{\hat{c}_3^{(6)}}/\hat{c}_3^{(6)}} ,\end{aligned}$$

indicating that the RG equation for the dimensionfull coupling reads

$$\widetilde{c}_3^{(6)}(\mu) = \widetilde{c}_3^{(6)}\left(\frac{\mu}{\mu_{\rm R}}\right)^{-2\varepsilon+\beta^q_{\hat{c}_3^{(6)}}/\hat{c}_3^{(6)}}$$

which is equivalent to Eq. (4.3.86).

Finally, we have said nothing about unitarity in GEFT. It would be interesting to establish the unitarity bounds that the theory respects in the presence of the HDO. This is quite important since unitarity violation imposes on the theory an energy scale above which it cannot be trusted. Focusing on our case, recall that the $O^{(4)}$-$O^{(6)}$ system contains only one HDO, $O_3^{(6)}$. This operator was introduced along with Λ which regulates its strength. Therefore, connecting this scale with unitarity bounds indicates how the internal scale μ is related to the violation of unitarity. Moreover, as we have seen, both the vev and the physical mass of the scalar field depend on Λ. This means that through unitarity we can obtain bounds for the scale where SSB takes place and see how the bound affects $\widetilde{m}_\phi$. To make these arguments more concrete, we follow Appendix A of [77]. There, a general formula for placing bounds in tree-level scattering amplitudes was derived using unitarity. In our case we want to constrain the six-point vertex which in potential-form is given by

$$\widetilde{V} \sim \frac{\widetilde{c}_3^{(6)}}{6!\Lambda^2}\phi^6$$

and resembles Eq. (A.12) of [77] for $n_1 = 6$, $n_2 = \cdots = n_r = 0$ and $n = n_1 + n_2 \cdots n_r = 6$ with $\lambda_6 = \frac{\widetilde{c}_3^{(6)}}{\Lambda^2}$. Treating the 6-point vetrex as a $3 \to 3$ scattering process corresponds to the case $k_1 = \frac{n_1}{2} = 3$ hence Eq. (A.18) of [77] can be used directly leading to the optimal energy bound

$$E_3 \leq \frac{16\sqrt{6}\pi^{3/2}}{\sqrt{|\widetilde{c}_3^{(6)}|}}\Lambda \approx 218\frac{\Lambda}{\sqrt{|\widetilde{c}_3^{(6)}|}} . \tag{4.3.95}$$

Therefore, the W-basis remains unitary as long as the energy scale respects this bound.

4.4 Dimension-8 operators

Consider now the most general (up to total derivatives) dimension-8 extension of Eq. (4.3.3)

$$\mathcal{L}^{(8)} = \frac{c_1^{(8)}}{\Lambda^4}\phi^3\Box\phi^3 + \frac{c_2^{(8)}}{\Lambda^4}\phi^2\Box^2\phi^2 + \frac{c_3^{(8)}}{\Lambda^4}\phi\Box^3\phi + \frac{c_4^{(8)}}{\Lambda^4}\phi^8 . \tag{4.4.1}$$

Dropping tildes from now on, we immediately attempt to rotate onto a pure polynomial basis. The most general field redefinition up to total derivatives is

$$\phi \to \phi + \frac{x}{\Lambda^2}\Box\phi + \frac{y}{\Lambda^2}\phi^3 + \frac{z}{\Lambda^4}\Box^2\phi + \frac{u}{\Lambda^4}\phi\Box\phi^2 + \frac{w}{\Lambda^4}\phi^5 . \tag{4.4.2}$$

Then we follow steps similar to those that lead us to Eq. (4.3.7). We will not go through the analysis of operator elimination. Things should work out in an analogous, alas more complicated way. The final result is coefficients x, y, z, u, w that can be chosen[3] so that after the transformation the Lagrangian becomes

$$\mathcal{L} = -\frac{1}{2}\phi\Box\phi - \frac{1}{2}m^2\phi^2 - \frac{\lambda}{4!}\phi^4 + \frac{c_3^{(6)}}{6!\Lambda^2}\phi^6 + \frac{c_4^{(8)}}{8!\Lambda^4}\phi^8 \,. \tag{4.4.3}$$

The potential in this Lagrangian is

$$V^{(8)} = \frac{1}{2}m^2\phi^2 + \frac{\lambda}{4!}\phi^4 - \frac{c_3^{(6)}}{6!\Lambda^2}\phi^6 - \frac{c_4^{(8)}}{8!\Lambda^4}\phi^8 \,. \tag{4.4.4}$$

This is now our dimension-8 W-basis. Regarding insertions, the dimension-8 extension has the three operator insertions of Eq. (4.3.56) plus $O_4^{(8)}$ with its associated coupling $c_4^{(8)}$. The extra operator, as a function of the field, is $O_4^{(8)} = \phi^8/(8!\Lambda^4)$ and its classical dimension is

$$d_{O_4^{(8)}} = 4d - 12 = 4(1-\varepsilon)\,, \tag{4.4.5}$$

while the classical dimension of the corresponding coupling is

$$d_{c_4^{(8)}} = 3(4-d) = 3\varepsilon\,. \tag{4.4.6}$$

In this case we have $l = 2, 4, 6, 8$ in Eq. (4.2.1) while the interaction Lagrangian will always include three terms. At 1-loop ϕ^8 does not affect the one-point function and δ_ϕ stays zero. We have demonstrated in great detail how the insertion algorithm works in the previous sections, so here we will be more concise.

Starting with $\beta_{c^{(2)}}$, we have the form of Eq. (4.3.67) plus one more non-linear contribution, Γ_{288}. This is given by Eq. (4.2.23) for $n = 2$, $k' = r = s = 8$ and $q_{(2,8)} = 2$ which gives higher than 1-loop diagrams at lowest order. This means that Z_{288} and Γ_{288} are trivial. Then, the β-function of $c^{(2)}$ remains as in the dimension-6 model:

$$\beta_{c^{(2)}} = -2m^2 + \frac{\lambda m^2}{16\pi^2}\,. \tag{4.4.7}$$

The same goes for $\beta_{c^{(4)}}$ as Eq. (4.3.68) is enhanced by the non-linear term $\Gamma_{488}c_4^{(8)}c_4^{(8)}$. Eq. (4.2.23) with $n = 4$ and $k' = r = s = 8$ along with $q_{(4,8)} = 4$ generates higher than 1-loop diagrams hence,

$$\beta_{c^{(4)}} = -\varepsilon\lambda - \frac{3c_3^{(6)}m^2}{16\pi^2\Lambda^2} + \frac{3\lambda^2}{16\pi^2}\,. \tag{4.4.8}$$

The first non-trivial contribution here comes from the effect of $O_4^{(8)}$ on $O_3^{(6)}$ due to the mass operator. Eq. (4.2.1) for $l = 6$ reads

$$\beta_{c_3^{(6)}} = -2\varepsilon c_3^{(6)} + \frac{m^2}{3}\Gamma_m^8 + \Gamma_{O_3^{(6)}}\, c_3^{(6)} + \Gamma_{622}\, c^{(2)}c^{(2)} + \Gamma_{644}\, c^{(4)}c^{(4)} + \Gamma_{666}\, c_3^{(6)}c_3^{(6)} + \Gamma_{688}\, c_4^{(8)}c_4^{(8)} \tag{4.4.9}$$

[3] Even though we have explicitly calculated $x, y, z, u,$ and w eliminating the derivative operators of the redefined Lagrangian, we do not adduce their values here since they are not illuminating. However, in [33] a simple example is presented where these coefficients have a transparent form. A relevant calculation is given in Passarino's paper in [74].

where now Γ^8_m is non-zero and Γ_{688} is added. The former is evaluated using Eq. (4.2.21) for $n = 6$ and $k = 2, 4, 6, 8$

$$\begin{aligned}\langle\phi(x_1)\cdots\phi(x_6)O^{(2)}(y)\rangle_0 &= Z^8_2\langle\phi(x_1)\cdots\phi(x_6)O^{(2)}(y)\rangle + Z^8_4\langle\phi(x_1)\cdots\phi(x_6)O^{(4)}(y)\rangle \\ &+ Z^8_6\langle\phi(x_1)\cdots\phi(x_6)O^{(6)}_3(y)\rangle + Z^8_8\langle\phi(x_1)\cdots\phi(x_6)O^{(8)}_4(y)\rangle\,.\end{aligned} \tag{4.4.10}$$

Now the bare part of the above expression involves $\mathcal{L}_{\text{int},0} = -c^{(4)}_0 O^{(4)}_0 + c^{(6)}_{3,0}O^{(6)}_{3,0} + c^{(8)}_{4,0}O^{(8)}_{4,0}$. Expanding the exponential in the expectation value to order $\mathcal{O}(c^{(4)}_0, c^{(6)}_{3,0}, c^{(8)}_{4,0})$, the l.h.s becomes

$$\begin{aligned}\langle\phi(x_1)\cdots\phi(x_6)\frac{\phi^2(y)}{2}\frac{-i\lambda\,\phi^4(z)}{4!}\rangle_0 &+ \langle\phi(x_1)\cdots\phi(x_6)\frac{\phi^2(y)}{2}\frac{ic^{(6)}_3\,\phi^6(z)}{6!\Lambda^2}\rangle_0 \\ &+ \langle\phi(x_1)\cdots\phi(x_6)\frac{\phi^2(y)}{2}\frac{ic^{(8)}_4\,\phi^8(z)}{8!\Lambda^4}\rangle_0\end{aligned} \tag{4.4.11}$$

The first and second terms give only disconnected 1-loop diagrams while the third gives

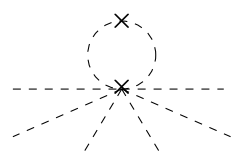

This is once more a scaleless B_0-integrals, given by Eq. (4.A.9) and we keep only its UV part. There are five independent channels. From the r.h.s of Eq. (4.4.10) only the third term gives, at 1-loop, a counter-term which absorbs the remnant divergence. Notice that on one side there is a $1/\Lambda^4$ contribution while on the other only $1/\Lambda^2$ which fixes $Z^8_6 = 5c^{(8)}_4/(16\pi^2\Lambda^2\varepsilon)$. From the definition of Eq. (4.2.11) we then get

$$\Gamma^8_m = -15\frac{c^{(8)}_4}{16\pi^2\Lambda^2}\,. \tag{4.4.12}$$

This expression generates the opposite sign term in the β-function compared to the diagrammatic calculation. The mismatch is an artifact of the operator insertion method, for level-1 insertions are defined up to an overall sign. For the determination of Γ_{688} we need Eq. (4.2.23) with $n = 6$, $k' = r = s = 8$ and $q_{(6,8)} = 6$ that involves higher loop diagrams so it does not contribute to $\beta_{c^{(6)}_3}$. Then,

$$\beta_{c^{(6)}_3} = -2\varepsilon c^{(6)}_3 - \frac{5\,c^{(8)}_4}{16\pi^2}\frac{m^2}{\Lambda^2} + \frac{5\lambda\,c^{(6)}_3}{16\pi^2}\,. \tag{4.4.13}$$

The last β-function is of the form Eq. (4.2.1) for $l = 8$:

$$\beta_{c^{(8)}_4} = -3\varepsilon c^{(8)}_4 + \frac{m^2}{4}\Gamma^{10}_m + \Gamma_{O^{(8)}_4}\,c^{(8)}_4 + \Gamma_{822}\,c^{(2)}c^{(2)} + \Gamma_{844}\,c^{(4)}c^{(4)} + \Gamma_{866}\,c^{(6)}_3c^{(6)}_3 + \Gamma_{888}\,c^{(8)}_4c^{(8)}_4\,. \tag{4.4.14}$$

There is no dim-10 operator in the action so the second term does not contribute. However, the third term is non-trivial and the same is true only for the non-linear term Γ_{866}, at 1-loop. The former is evaluated from Eq. (4.2.20) for $n = l = 8$ and the associated expectation value is

$$\langle\phi(x_1)\cdots\phi(x_8)O^{(8)}_4(y)\rangle_0 = Z_{O^{(8)}_4}\langle\phi(x_1)\cdots\phi(x_8)O^{(8)}_4(y)\rangle\,. \tag{4.4.15}$$

From Eq. (4.2.6) this is

$$\langle\phi(x_1)\cdots\phi(x_8)O_4^{(8)}(y)\rangle_0 - \delta_{O_4^{(8)}}\langle\phi(x_1)\cdots\phi(x_8)O_4^{(8)}(y)\rangle = \langle\phi(x_1)\cdots\phi(x_8)O_4^{(8)}(y)\rangle\,, \quad (4.4.16)$$

where the l.h.s involves $\mathcal{L}_{\text{int},0} = -c_0^{(2)}O_0^{(2)} - c_0^{(4)}O_0^{(4)} + c_{3,0}^{(6)}O_{3,0}^{(6)}$. Then we get

$$\mathcal{N}^{-1}\langle 0|T[\phi_0(x_1)\cdots\phi_0(x_8)\frac{\phi_0^8(y)}{8!\Lambda^4}e^{-i\int d^dz\frac{m_0^2}{2}\phi_0^2(z)+\frac{\lambda_0}{4!}\phi_0^4(z)-c_{3,0}^{(6)}\frac{\phi_0^6}{6!\Lambda^2}}]|0\rangle - \delta_{O_4^{(8)}}\langle\phi(x_1)\cdots\phi(x_8)O_4^{(8)}(y)\rangle$$

and the only non-trivial contribution comes at order $\mathcal{O}((m^2)^0,\lambda,(c_3^{(6)})^0)$:

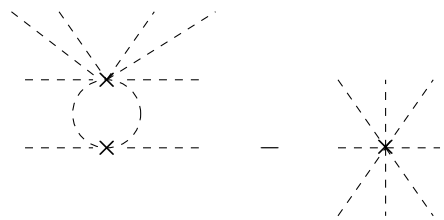

The first diagram has seven channels and belongs to the scaleless integrals of Eq. (4.A.9). The second is just a vertex multiplied with a counter-term. Keeping only the UV part, finiteness requires

$$\delta_{O_4^{(8)}} = -\frac{7\lambda}{16\pi^2}\frac{1}{\varepsilon} \quad (4.4.17)$$

and Eq. (4.2.10) (or its 1-loop version below) indicates that

$$\Gamma_{O_4^{(8)}} = \frac{7\lambda}{16\pi^2}\,. \quad (4.4.18)$$

The last step is the evaluation of Γ_{866}. We take Eq. (4.2.23) for $n=8$ and $k'=r=s=6$, with $q_{(8,6)}=8$, so that

$$\langle\phi(x_1)\cdots\phi(x_8)O_3^{(6)}(y)O_3^{(6)}(z)\rangle_0 = Z_{866}\langle\phi(x_1)\cdots\phi(x_8)O_3^{(6)}(y)O_3^{(6)}(z)\rangle\,. \quad (4.4.19)$$

The l.h.s gives the divergent diagram

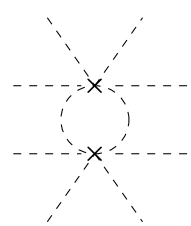

another scaleless B_0-integral with seven channels. The r.h.s of Eq. (4.4.19) gives the finite version of the above diagram. Since Z_{866} is divergent, according to the discussion below Eq. (4.2.23), the latter diagram should be thought as a finite vertex. Then the remnant divergence is absorbed by $\delta_{866} = 7/(16\pi^2\varepsilon)$ which determines

$$\Gamma_{866} = \frac{7}{16\pi^2}\,. \quad (4.4.20)$$

Assembling all parts of $\beta_{c_4^{(8)}}$, we arrive at the final expression

$$\beta_{c_4^{(8)}} = -3\varepsilon c_4^{(8)} + \frac{7\lambda\, c_4^{(8)}}{16\pi^2} + \frac{7(c_3^{(6)})^2}{16\pi^2}\,. \tag{4.4.21}$$

Let us collect for easier reference all β-functions from Eq. (4.4.7), Eq. (4.4.8), Eq. (4.4.13) and Eq. (4.4.21) into

$$\vec{\beta}_{c^{(l)}} = \begin{bmatrix} -2m^2 + \frac{\lambda m^2}{16\pi^2} \\ -\varepsilon\lambda + \frac{3\lambda^2}{16\pi^2} - \frac{3c_3^{(6)} m^2}{16\pi^2\Lambda^2} \\ -2\varepsilon c_3^{(6)} + \frac{5\lambda c_3^{(6)}}{16\pi^2} - \frac{5\, c_4^{(8)}}{16\pi^2}\frac{m^2}{\Lambda^2} \\ -3\varepsilon c_4^{(8)} + \frac{7(c_3^{(6)})^2}{16\pi^2} + \frac{7\lambda c_4^{(8)}}{16\pi^2} \end{bmatrix} \tag{4.4.22}$$

The phase diagram is a four-dimensional space and its full analysis is straightforward but quite complicated. As in the previous section we are particularly interested in the massless limit which reduces the dimensionality of the phase diagram by one unit. A further limit that can be considered is the one of vanishing quartic coupling. The resulting two-dimensional phase diagram could be just the projection on the $\lambda = 0$ plane in the three-dimensional phase diagram or it could be the phase diagram of a system that for some reason, generates only irrelevant interactions. The potentially interesting fact is that even in this drastic limit there is a non-trivial scalar potential

$$V^{(8)} = -\frac{c_3^{(6)}}{6!\Lambda^2}\phi^6 - \frac{c_4^{(8)}}{8!\Lambda^4}\phi^8\,. \tag{4.4.23}$$

The $\mathbb{Z}_2$ broken phase is the one where $c_3^{(6)} > 0$ and $c_4^{(8)} < 0$ since the dominant term, ϕ^8, has a positive sign. Then the scalar field acquires a non-trivial vev at the minimum

$$v = \pm\sqrt{42}\sqrt{\frac{c_3^{(6)}}{|c_4^{(8)}|}}\Lambda\,. \tag{4.4.24}$$

Expanding the field around its vev $\phi \to \phi \pm v$ we obtain the mass of the scalar field:

$$m_\phi^2 = \frac{7}{10}\frac{(c_3^{(6)})^2}{|c_4^{(8)}|}v^2\,, \tag{4.4.25}$$

which shows that it depends on Λ through the vev, as expected.

RG flows in this context have not been examined before to our knowledge, so let us proceed further. In the double limit the β-functions simplify to

$$\vec{\beta}_{c^{(l)}} = \begin{bmatrix} -2\varepsilon c_3^{(6)} \\ -3\varepsilon c_4^{(8)} + \frac{7(c_3^{(6)})^2}{16\pi^2} \end{bmatrix} \tag{4.4.26}$$

and according to Eq. (5.4.36) the anomalous dimensions of $O_3^{(6)}$ and $O_4^{(8)}$ are

$$\gamma_{O_3^{(6)}} = 0\,, \qquad \gamma_{O_4^{(8)}} = 0\,, \tag{4.4.27}$$

which means that the scaling dimensions of both operators coincide with the classical ones. The RG flows are determined by the solution to

$$\mu \frac{dc_3^{(6)}(\mu)}{d\mu} = \beta_{c_3^{(6)}} = -2\varepsilon c_3^{(6)} \quad \text{and} \quad \mu \frac{dc_4^{(8)}(\mu)}{d\mu} = \beta_{c_4^{(8)}} = -3\varepsilon c_4^{(8)} + \frac{7(c_3^{(6)})^2}{16\pi^2} \,. \tag{4.4.28}$$

Here we will meet behaviour of the couplings that can be quite exotic, depending on d.

In $d = 4$ the β-function of $c_3^{(6)}$ vanishes and the coupling does not run: $c_3^{(6)}(\mu) \equiv c_3^{(6)}$. The other β-function is

$$\beta_{c_4^{(8)}} = \frac{7(c_3^{(6)})^2}{16\pi^2} \,. \tag{4.4.29}$$

This distinguishes two cases:

- $c_3^{(6)} = 0$
  For $\varepsilon = 0$, $\beta_{c_4^{(8)}}$ vanishes independently of $c_4^{(8)}$. Neither $c_3^{(6)}$ nor $c_4^{(8)}$ runs and the phase diagram has a WF-line with points labelled by $c_4^{(8)}$ ending on a Gaussian fixed point where $c_{3\bullet}^{(6)} = c_{4\bullet}^{(8)} = 0$. The potential in Eq. (4.4.23) becomes

  $$V^{(8)} = -\frac{c_4^{(8)}}{8!\Lambda^4}\phi^8$$

  and determines $\mathbb{Z}_2$-symmetric phase that is stable or unstable when $c_4^{(8)} < 0$ or $c_4^{(8)} > 0$ respectively.

- $c_3^{(6)} \neq 0$
  $\beta_{c_4^{(8)}}$ is strictly non-zero. The RG flow does not move towards or away from a fixed point. Nevertheless, $c_4^{(8)}$ has a non-trivial flow at a constant distance equal to $c_3^{(6)}$ from the WF-line that forces it to vanish in the IR at some scale μ_L and to diverge in the UV. The corresponding RG equation is given by

  $$c_4^{(8)}(\mu) = c_4^{(8)} + \frac{7(c_3^{(6)})^2}{16\pi^2} \ln \frac{\mu}{\mu_{\mathrm{R}}} \tag{4.4.30}$$

  and its running is depicted in Fig. 4.4. It vanishes at the scale

  $$\mu_L = e^{-\frac{16\pi^2 c_4^{(8)}}{7(c_3^{(6)})^2}} \,,$$

  while at scales $\mu < (>)\mu_L$ it admits negative (positive) values.

We can now combine Eq. (4.4.25) with Eq. (4.4.29) and Eq. (4.4.30) to evaluate the running of m_ϕ^2 as a function of μ in $d = 4$, to obtain

$$m_\phi^2(\mu) = \frac{7}{10} \frac{(c_3^{(6)})^2}{|c_4^{(8)}(\mu)|} v^2 \,.$$

This scale dependence is depicted in Fig. 4.5. The case here is particular since the behaviour of m_ϕ^2 is the opposite to that of the mass in Fig. 4.1. Recall that in the latter case there was

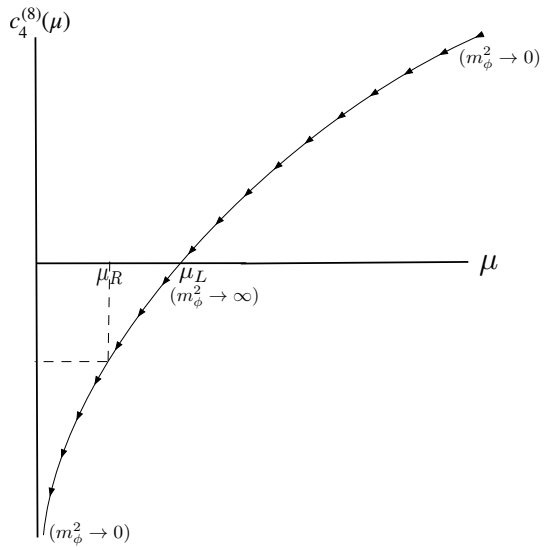

Figure 4.4: The running of $c_4^{(8)}(\mu)$ as a function of the renormalization scale μ when the physical coupling, $c_4^{(8)}$, is positive and the potential is stable. As the scale decreases, the coupling becomes less positive and at some small scale μ_L it vanishes. After that scale, $c_4^{(8)}$ flips sign and as $\mu \to 0$ it increases up to minus infinity.

a high but not infinite scale (the UV Landau pole) where $\lambda(\mu)$ and as a consequence the scalar mass, became infinite. Instead, Fig. 4.4 shows that $c_4^{(8)}(\mu)$ decreases for decreasing scale and when μ reaches a small but non-zero value the coupling vanishes and the scalar mass blows up. Therefore here we have an "inverse" or IR Landau pole. Let us now turn to $d \neq 4$ where $\beta_{c_3^{(6)}}$

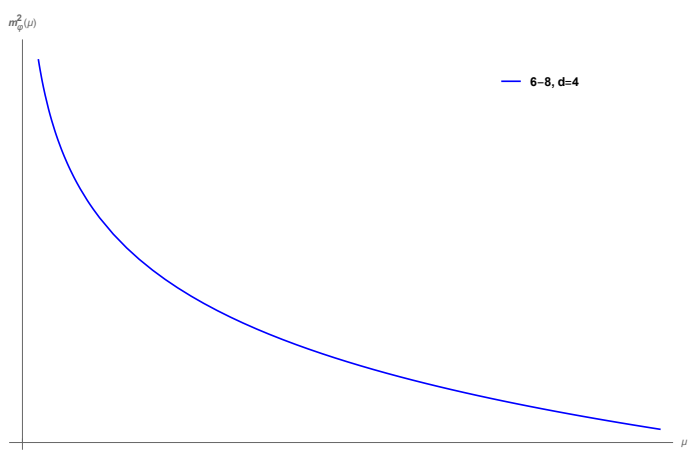

Figure 4.5: The running of the physical mass in $d = 4$, after SSB, as a function of the renormalization scale.

is not necessarily zero. Then $c_3^{(6)}$ is a function of μ and the solution to Eq. (4.4.28) admits a non-trivial RG flow given by

$$c_3^{(6)}(\mu) = c_3^{(6)} \left(\frac{\mu}{\mu_{\mathrm{R}}}\right)^{-2\varepsilon} . \tag{4.4.31}$$

Notice that the above relation matches Eq. (4.3.86) in the limit $\widetilde{\lambda} \to 0$. For the other coupling,

Eq. (4.4.28) suggests the RG flow

$$c_4^{(8)}(\mu) = c_4^{(8)}(\mu_{\rm R}) \left(\frac{\mu}{\mu_{\rm R}}\right)^{-3\varepsilon} + \frac{7(c_3^{(6)})^2}{48\pi^2\varepsilon}\left[1 - \left(\frac{\mu}{\mu_{\rm R}}\right)^{-3\varepsilon}\right] \tag{4.4.32}$$

and choosing for simplicity the renormalization prescription $c_4^{(8)}(\mu_{\rm R}) = c_4^{(8)} + \frac{7(c_3^{(6)})^2}{48\pi^2\varepsilon}$, we get

$$c_4^{(8)}(\mu) = c_4^{(8)} \left(\frac{\mu}{\mu_{\rm R}}\right)^{-3\varepsilon} + \frac{7(c_3^{(6)})^2}{48\pi^2\varepsilon}\,. \tag{4.4.33}$$

Regarding the fixed points things are simpler here than in the previous case since, the only point that eliminates both $\beta_{c_3^{(6)}}$ and $\beta_{c_4^{(8)}}$ simultaneously is

$$c_{3\bullet}^{(6)} = 0 \quad \text{and} \quad c_{4\bullet}^{(8)} = 0\,. \tag{4.4.34}$$

This means that $O^{(6)}$-$O^{(8)}$ system admits only a Gaussian fixed point. All the above information is depicted in Fig. 4.6 for $d = 4$ and in Fig. 4.7 for $d = 3, 5$. To complete the picture we look at the behaviour of the operators $O_3^{(6)}$ and $O_4^{(8)}$ with respect to the fixed points, as we move from UV to IR. We need to know also the nature of the fixed points and this is given in the following:

$$\frac{\partial \beta_{c_3^{(6)}}}{\partial c_3^{(6)}} = -2\varepsilon \begin{cases} \bullet : -2\varepsilon & \begin{cases} d = 4 : 0 \ (c_3^{(6)} \text{ does not run}) \\ d = 3 : -2 < 0 \to \text{UV} \\ d = 5 : +2 > 0 \to \text{IR} \end{cases} \\ \star : -2\varepsilon & \begin{cases} d = 4 : - \\ d = 3 : - \\ d = 5 : - \end{cases} \end{cases} \tag{4.4.35}$$

$$\frac{\partial \beta_{c_4^{(8)}}}{\partial c_4^{(8)}} = -3\varepsilon \begin{cases} \bullet : -3\varepsilon & \begin{cases} d = 4 : 0 \ (\text{ G exists only for } c_3^{(6)}, c_4^{(8)} = 0. \text{ Otherwise no fixed-points}) \\ d = 3 : -3 < 0 \to \text{UV} \\ d = 5 : +3 > 0 \to \text{IR} \end{cases} \\ \star : -3\varepsilon & \begin{cases} d = 4 : - \ (\text{ WF-line only for } c_3^{(6)} = 0 \text{ and } c_4^{(8)} \neq 0. \text{ There is no flow}) \\ d = 3 : - \\ d = 5 : - \end{cases} \end{cases} \tag{4.4.36}$$

As we have already mentioned,

$$\Delta_{O^{(6)}} = d_{O^{(6)}} = 4 - 3\varepsilon \ \text{ and } \ \Delta_{O^{(8)}} = d_{O^{(8)}} = 4 - 4\varepsilon\,. \tag{4.4.37}$$

Therefore, we have for the 1-loop exponent that determines the nature of an operator:

	$\Delta_O - d$	$\bullet$	$\star$
$O_3^{(6)}$	-2ε	-2ε	$-$
$O_4^{(8)}$	-3ε	-3ε	$-$

and this distinguishes the following cases:

	$d=4$	$d=3$		$d=5$	
$O_3^{(6)}$	truly marginal(for $c_3^{(6)} \neq 0$)	$\bullet$: rel	$\star$: $-$	$\bullet$: irrel	$\star$: $-$
$O_4^{(8)}$	irrelevant(from Eq. (4.4.30))	$\bullet$: rel	$\star$: $-$	$\bullet$: irrel	$\star$: $-$

As a last comment, recall that unitarity sets energy bounds when a HDO is inserted in the Lagrangian. Such a constraint can be calculated following [77] as in Sect. 4.3.2 and for $n_1 = 8$ and $k_1 = \frac{n_1}{2} = 4$, the bound

$$E_4 \leq \frac{16\sqrt{3}\pi^{5/4}}{\left(c_4^{(8)}\right)^{1/4}}\Lambda \approx 116\frac{\Lambda}{\left(c_4^{(8)}\right)^{1/4}} \,. \tag{4.4.38}$$

is obtained.

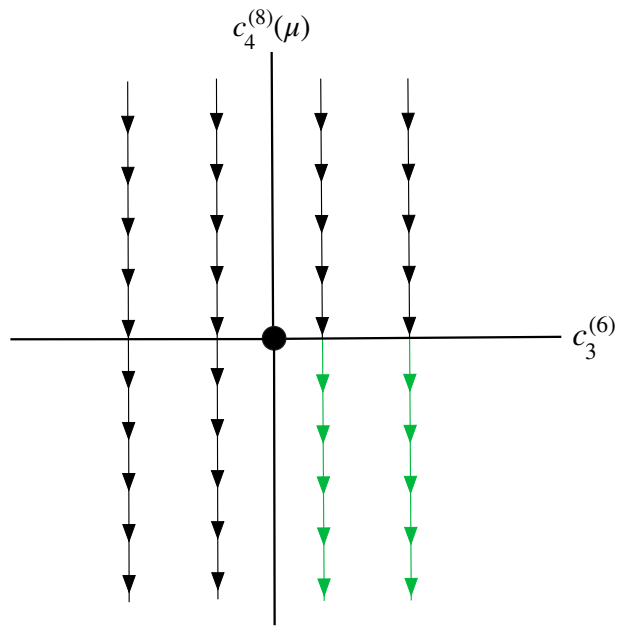

Figure 4.6: The $4d$ RG flows for $\mathcal{L}$ in Eq. (4.4.3) at $m^2 = \lambda = 0$ limit. The flow is non-trivial only when $c_3^{(6)} \neq 0$. The stable, broken branch of the flow (green lines) is for $0 < \mu < \mu_L$ with $\mu_L = \mu_R \exp[16\pi^2 v^2/10m_\phi^2]$ and $\mu_R < \mu_L$ the renormalization scale.

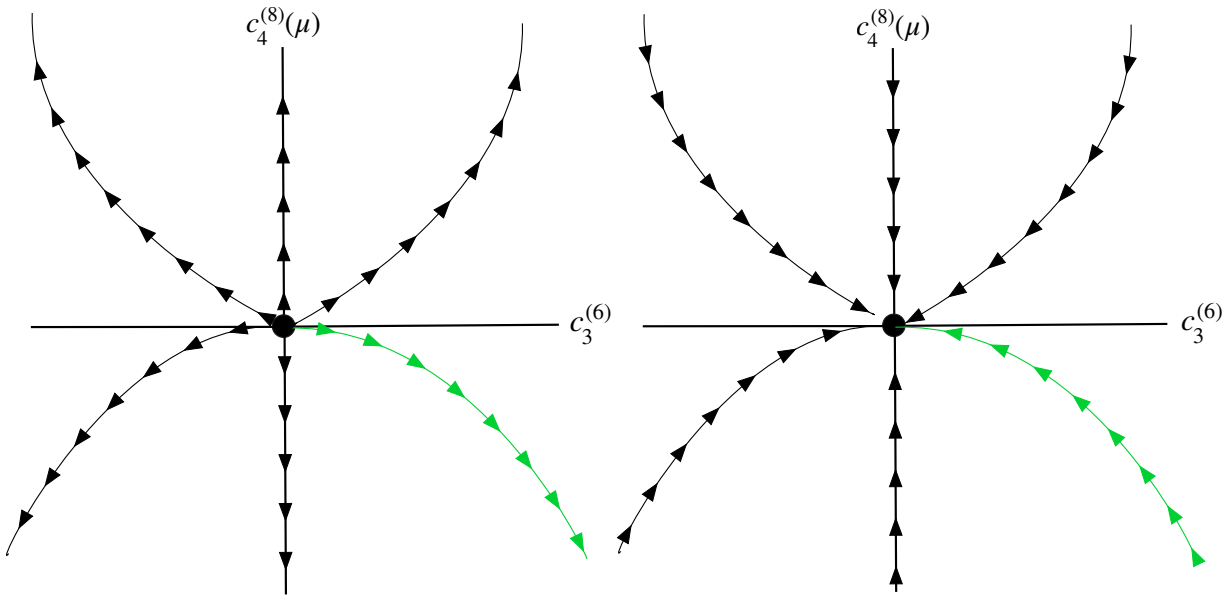

Figure 4.7: Left: RG flows for $\mathcal{L}$ in Eq. (4.4.3) at $m^2 = \lambda = 0$ limit, in $d = 3$. The phase admits a Gaussian fixed point, which is UV, while the couplings both diverge in the IR. Right: RG flows of Eq. (4.4.3) at $m^2 = \lambda = 0$ limit, in $d = 5$. The phase admits a Gaussian fixed point, which is IR, hence both couplings decrease for deceasing renormalization scale.

Appendix

4.A Scaleless integrals

Here the calculation of divergent, scaleless integrals is reviewed. Our interest is restricted to the scalar integrals A_0 and B_0.

Let as start with A_0 which comes from Tadpole diagrams. As an example consider a two-point diagram of the form

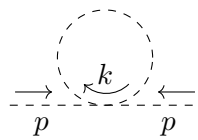

$= i\mathcal{M}^1$

with only one momentum running the loop. In addition, we assume that there is a mass scale m_0^2 that on-shell forces the external momentum to be $p^2 = m_0^2$. Then the above diagram in d-dimensions, evaluates to

$$\mathcal{M}^1 \simeq \int \frac{d^dk}{(2\pi)^d i} \frac{1}{k^2 - m_0^2} = A_0(m_0^2)\,, \tag{4.A.1}$$

which is equal to the known result in Dimensional Regularization

$$A_0(m_0^2) = m_0^2 \Big[\frac{2}{\varepsilon} + \ln \frac{\mu^2}{m_0^2} + 1 \Big]\,. \tag{4.A.2}$$

Now the question that we want to address is how the integral of Eq. (4.A.1) is calculated in the absence of a scale or, in other words, when $m_0 \to 0$. The result is a scaleless integral of the form

$$A_0(0) = \int \frac{d^dk}{(2\pi)^d i} \frac{1}{k^2}\,. \tag{4.A.3}$$

Of course if we take the $m_0^2 \to 0$ limit of Eq. (4.A.2) the integral is zero. Nevertheless, let us look at the behaviour of $A_0(0)$ performing an explicit calculation of Eq. (4.A.3). The first step is to move to Euclidean space and remove i from the above expression. Then, we get that

$$A_0(0) \quad = \quad \int \frac{d^dk_E}{(2\pi)^d} \frac{1}{k_E^2} \Rightarrow$$

$$A_0(0) \quad \sim \quad \Omega_d \int_0^\infty dk_E \frac{k_E^{d-1}}{k_E^2}\,, \tag{4.A.4}$$

where we have performed the integration in the $(d-1)$-spherical surface, extracting the solid angle

$$\Omega_d = \frac{2\pi^{\frac{d}{2}}}{\Gamma(\frac{d}{2})}\,.$$

Now, this scaleless integral gives

$$\begin{aligned} A_0(0) \quad &\sim \quad \Omega_d \int_0^\infty dk_E k_E^{d-3} \Rightarrow \\ A_0(0) \quad &\sim \quad \Omega_d \Big[\int_0^M dk_E k_E^{d-3} + \int_M^\infty dk_E k_E^{d-3}\Big]\,, \end{aligned} \tag{4.A.5}$$

and notice that it does not converge in any dimension and for that reason we inserted an arbitrary scale M to split the integral into its IR and UV parts. The next step is to calculate Eq. (4.A.5) close to 4-dimensions. To do so we take $d = 4-\varepsilon$. Here we should be careful since the way we move away from $4-d$ is different for the IR and UV limits. For the former case we define $\varepsilon_{\rm IR} < 0$ with $d = 4-\varepsilon_{\rm IR}$ and for the latter $\varepsilon \equiv \varepsilon_{\rm UV} > 0$ with $d = 4-\varepsilon_{\rm UV}$. With these in mind we obtain

$$\begin{aligned} A_0(0) \quad &\sim \quad \Omega_d \Big[\frac{M^{2-\varepsilon_{\rm IR}}}{2-\varepsilon_{\rm IR}} - \frac{M^{2-\varepsilon_{\rm UV}}}{2-\varepsilon_{\rm UV}}\Big] \Rightarrow \\ A_0(0) \quad &\sim \quad M^2\Omega_d \Big[\frac{M^{-\varepsilon_{\rm IR}}}{2-\varepsilon_{\rm IR}} - \frac{M^{-\varepsilon_{\rm UV}}}{2-\varepsilon_{\rm UV}}\Big]\,, \end{aligned}$$

and expanded for $\varepsilon_{\rm IR}, \varepsilon_{\rm UV} << 1$ the above expression becomes

$$A_0(0) \sim M^2\Omega_d \Big[\frac{\varepsilon_{\rm IR}}{2}\Big(\frac{1}{2} - \ln M\Big) - \frac{\varepsilon_{\rm UV}}{2}\Big(\frac{1}{2} - \ln M\Big)\Big]\,.$$

It is easy to check that for $\varepsilon_{\rm IR} \neq \varepsilon_{\rm UV}$, $\ln M$ is not canceled between the two parts of the parenthesis. This indicates that A_0 depends on the way that we split the integrals into an IR and a UV part which should not be the case. Therefore the only solution is $\varepsilon_{\rm IR} = \varepsilon_{\rm UV}$ when the integral is identically zero. This shows that A_0 is both IR- and UV-divergent and as a consequence

$$A_0(0) = 0\,. \tag{4.A.6}$$

Let us now turn to the scaleless integral with two propagators, the B_0-integral. Consider the two-point function diagram

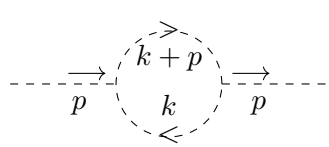

$$= i\mathcal{M}^2$$

which in d-dimensions, when the masses are non-zero, reads

$$\mathcal{M}^2 \simeq \int \frac{d^dk}{(2\pi)^d i} \frac{1}{k^2 - m_{1,0}^2} \frac{1}{(k+p)^2 - m_{2,0}^2} = B_0(p, m_{1,0}, m_{2,0})\,. \tag{4.A.7}$$

Evaluating it in DR, the known result

$$B_0(p, m_{1,0}, m_{2,0}) = \frac{2}{\varepsilon} + \int_0^1 dx \ln \frac{\mu^2}{\Delta_B}\,, \tag{4.A.8}$$

with $\Delta_B = -p^2 x(1-x) + m_{1,0}^2 + m_{2,0}^2$ is obtained. Similarly to the previous case, we want to calculate this integral in the limit $m_{0,1}, m_{0,2}^2 \to 0$. Following the same steps with the A_0 calculation, we go to Euclidean space for general d and then B_0 becomes

$$\begin{aligned}
B_0(p,0,0) &= \int \frac{d^d k_E}{(2\pi)^d} \frac{1}{k_E^4} \Rightarrow \\
B_0(p,0,0) &\sim \Omega_d \int_0^\infty dk_E \frac{k_E^{d-1}}{k_E^4} \Rightarrow \\
B_0(p,0,0) &\sim \Omega_d \int_0^M dk_E k_E^{d-5} + \Omega_d \int_M^\infty dk_E k_E^{d-5}
\end{aligned}$$

where we have extracted the solid angle Ω_d and inserted an arbitrary scale M to separate the IR from the UV divergent part. This integral does not converge in any dimension.
Close to $d = 4$ demands that $d = 4 - \varepsilon_{\rm IR}$ with $\varepsilon_{\rm IR} < 0$ and $d = 4 - \varepsilon_{\rm UV}$ with $\varepsilon_{\rm UV} > 0$. The integral then evaluates to

$$\begin{aligned}
B_0(p,0,0) &\sim \Omega_d \Big[-\frac{M^{-\varepsilon_{\rm IR}}}{\varepsilon_{\rm IR}} + \frac{M^{-\varepsilon_{\rm UV}}}{\varepsilon_{\rm UV}} \Big] \Rightarrow \\
B_0(p,0,0) &\sim \Omega_d \Big[\ln M - \frac{1}{\varepsilon_{\rm IR}} - \ln M + \frac{1}{\varepsilon_{\rm UV}} \Big] \Rightarrow \\
B_0(p,0,0) &\sim \Omega_d \Big[\frac{1}{\varepsilon_{\rm UV}} - \frac{1}{\varepsilon_{\rm IR}} \Big],
\end{aligned}$$

which is independent of the arbitrary scale M. This shows that for the above integral, IR and UV divergences can be split from each other. This is summarized in the following:

$$\Big[B_0(p,0,0)\Big]_{\rm IR} = \frac{1}{16\pi^2}\frac{2}{\varepsilon_{\rm IR}} \quad \text{and} \quad \Big[B_0(p,0,0)\Big]_{\rm UV} = \frac{1}{16\pi^2}\frac{2}{\varepsilon_{\rm UV}}\,. \tag{4.A.9}$$

We finish by a discussion of the role of these scaleless integrals in our computations. First of all, they appear in the computations involved in the operator insertion method because we chose to consider any operator, including the mass operator, as a deformation of the kinetic term. As a result the propagators in the loops are massless and the resulting integrals scaleless. Now according to our discussion about operator insertions, the method is sensitive to particular UV divergences. This means that when a scaleless integral is encountered during operator insertion operations, if possible, its UV divergent part must be extracted. We saw above that this is not possible for $A_0(0)$ which is always identically zero, but it is possible for B_0 that has a non-trivial UV divergent part. On the other hand when we renormalize Eq. (1.0.1) directly as in Sect. 4.3.1 there is no reason to split the IR from the UV part which means that in such a case we must use the exact result, that is $B_0(p,0,0) = 0$.

4.B Review of the $\mathcal{L}^{(2)} + \mathcal{L}^{(4)}$ (usual ϕ^4) theory

In this section we review the renormalizable ϕ^4-theory, rederiving textbook results [19], but using for renormalization the operator-insertion method. The Lagrangian is

$$\mathcal{L} = -\frac{1}{2}\phi\Box\phi - c^{(2)}O^{(2)} - c^{(4)}O^{(4)}\,, \tag{4.B.1}$$

where $O^{(2)} = \frac{\phi^2}{2}$ with coupling $c^{(2)} = m^2$ and $O^{(4)} = \frac{\phi^4}{4!}$ with coupling $c^{(4)} = \lambda$. The classical dimension of ϕ in $d = 4 - \varepsilon$ dimensions is $[\phi] = d_\phi = \frac{d-2}{2}$. The classical dimensions of the inserted operators are

$$d_{O^{(2)}} = 2 - \varepsilon \;\text{ and }\; d_{O^{(4)}} = 4 - 2\varepsilon\,. \tag{4.B.2}$$

For this model we face two β-functions which, according to Eq. (4.2.1), are given by

$$\beta_{c^{(2)}} = -2c^{(2)} + \Gamma_{O^{(2)}}\, c^{(2)} + \Gamma_{222}\, c^{(2)}c^{(2)} + \Gamma_{244}\, c^{(4)}c^{(4)} \tag{4.B.3}$$

for $l = 2$ and by

$$\beta_{c^{(4)}} = -\varepsilon c^{(4)} + \frac{m^2}{2}\Gamma^6_m + \Gamma_{O^{(4)}}\, c^{(4)} + \Gamma_{422}\, c^{(2)}c^{(2)} + \Gamma_{444}\, c^{(4)}c^{(4)} \tag{4.B.4}$$

for $l = 4$. The anomalous dimensions in the above β-functions are evaluated through the procedure described in Sect. 4.2. As a first step we consider Eq. (4.2.18) for $n = 1$ and the insertion of only one field, $\phi(y)$. Then renormalization gives

$$\langle\phi(x_1)\phi(y)\rangle_0 = Z_\phi\langle\phi(x_1)\phi(y)\rangle\,, \tag{4.B.5}$$

where $\mathcal{L}_{\text{int},0} = -c_0^{(2)}O_0^{(2)} - c_0^{(4)}O_0^{(4)}$ and Z_ϕ defined in Eq. (4.2.3). Performing the expansion of the exponential, at order $\mathcal{O}(c_0^{(2)}, c_0^{(4)})$, we get

$$\langle\phi(x_1)\phi(y)\frac{-im^2\phi^2(z)}{2}\rangle_0 + \langle\phi(x_1)\phi(y)\frac{-i\lambda\phi^4(z)}{4!}\rangle_0 = Z_\phi\langle\phi(x_1)\phi(y)\rangle\,. \tag{4.B.6}$$

The contractions on the first term on the l.h.s result in a finite propagator from x_1 to y. The second term on the same side gives the divergent diagram

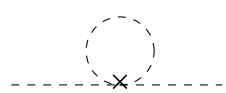

(4.B.7)

where the mark on the loop indicates the spot where the operator is inserted. This is the two-point Tadpole integral A_0 which here is scaleless, so according to Appendix 4.A it is equal to zero. Since also the r.h.s of Eq. (4.B.6) gives a finite propagator from x_1 to y, equivalence holds if $Z_\phi = 1$ which gives the known result, $\delta_\phi = 0$.

Next we focus on $\beta_{c^{(2)}}$. For its linear part the relevant Green's function is given by Eq. (4.2.20) for $n = l = 2$:

$$\langle\phi(x_1)\phi(x_2)O^{(2)}(y)\rangle_0 = Z_{O^{(2)}}\langle\phi(x_1)\phi(x_2)O^{(2)}(y)\rangle\,, \tag{4.B.8}$$

with $Z_{O^{(2)}}$ given by Eq. (4.2.6). It can be rewritten as

$$\langle\phi(x_1)\phi(x_2)O^{(2)}(y)\rangle_0 - \delta_{O^{(2)}}\langle\phi(x_1)\phi(x_2)O^{(2)}(y)\rangle = \langle\phi(x_1)\phi(x_2)O^{(2)}(y)\rangle\,. \tag{4.B.9}$$

According to the discussion below Eq. (4.2.19), $\mathcal{L}_{\text{int},0} = -c_0^{(4)}O_0^{(4)}$, therefore the l.h.s is

$$\mathcal{N}^{-1}\langle 0|T[\phi_0(x_1)\phi_0(x_2)\frac{\phi_0^2(y)}{2}e^{i\int d^dz\frac{-\lambda_0}{4!}\phi_0^4(z)}]|0\rangle - \delta_{O^{(2)}}\langle\phi(x_1)\phi(x_2)\frac{\phi_0^2(y)}{2}\rangle\,. \tag{4.B.10}$$

Expanding the exponential to $\mathcal{O}(\lambda_0)$ and performing contractions we get, at 1-loop, the diagrams

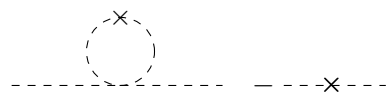

The first diagram looks like a usual scalar tadpole but it is in fact a three-point function contributing to $G^{(2)}(x_1, x_2)$. The second diagram corresponds to a counter-term insertion. Again, the mark on the loop indicates the spot where the operator is inserted. Now recall that the propagators in the loop are massless, so the first diagram is a scaleless B_0-integral given by Eq. (4.A.9). Extracting only its UV part, finiteness requires

$$\delta_{O^{(2)}} = -\frac{\lambda}{16\pi^2}\frac{1}{\varepsilon}\,, \tag{4.B.11}$$

while using Eq. (4.2.10) or its 1-loop version below, we get

$$\Gamma_{O^{(2)}} = \frac{\lambda}{16\pi^2}\,. \tag{4.B.12}$$

For the non-linear part of Eq. (4.B.3) there are two possible contributions. The first will determine Γ_{222} and corresponds to $l = r = s = 2$ in Eq. (4.2.22). The second gives Γ_{244} using Eq. (4.2.23) for $n = 2$ and $k' = r = s = 4$ with $q_{(2,4)} = 2$. Both anomalous dimensions vanish in this case. With each part of $\beta_{c^{(2)}}$ determined, Eq. (4.B.3) takes the form

$$\beta_{c^{(2)}} = -2c^{(2)} + \frac{\lambda}{16\pi^2}c^{(2)} \equiv -2m^2 + \frac{\lambda m^2}{16\pi^2}\,. \tag{4.B.13}$$

Let us now move on to $\beta_{c^{(4)}}$. Since the Lagrangian does not include a dim-6 operator, the second term of Eq. (4.B.4) is absent. The linear part on the other hand, is evaluated through Eq. (4.2.20) for $n = l = 4$ and the corresponding expectation value is

$$\langle\phi(x_1)\phi(x_2)\phi(x_3)\phi(x_4)O^{(4)}(y)\rangle_0 = Z_{O^{(4)}}\langle\phi(x_1)\phi(x_2)\phi(x_3)\phi(x_4)O^{(4)}(y)\rangle\,, \tag{4.B.14}$$

or using Eq. (4.2.6),

$$\langle\phi(x_1)\phi(x_2)\phi(x_3)\phi(x_4)O^{(4)}(y)\rangle_0 - \delta_{O^{(4)}}\langle\phi(x_1)\cdots\phi(x_4)O^{(4)}(y)\rangle = \langle\phi(x_1)\cdots\phi(x_4)O^{(4)}(y)\rangle\,. \tag{4.B.15}$$

Now the bare part of the above expression involves $\mathcal{L}_{\text{int},0} = -c_0^{(2)}O_0^{(2)}$. Then the l.h.s gives

$$\mathcal{N}^{-1}\langle 0|T[\phi_0(x_1)\cdots\phi_0(x_4)\frac{\phi_0^4(y)}{4!}e^{i\int d^dz\frac{-m_0^2}{2}\phi_0^2(z)}]|0\rangle - \delta_{O^{(4)}}\langle\phi(x_1)\cdots\phi(x_4)\frac{\phi^4(y)}{4!}\rangle$$

with the first term contributing only bubble and disconnected diagrams and the second giving a 4-point vertex. Thus, at 1-loop, there is no non-vanishing contribution to $Z_{O^{(4)}}$ which means that $\delta_{O^{(4)}} = 0$. Using Eq. (4.2.10) the anomalous dimension of $O^{(4)}$ is

$$\Gamma_{O^{(4)}} = 0\,. \tag{4.B.16}$$

The last step here is the evaluation of the non-linear part in Eq. (4.B.4). The first of the two non-linear terms, Γ_{422}, is determined using the formula of Eq. (4.2.23) for $n = 4$ and $k' = r = s = 2$ along with $q_{(4,2)} = 4$. This admits only disconnected propagators and then, Z_{422} is trivial and as a consequence Γ_{422} vanishes. For the the second non-linear term, Γ_{444}, we have a non-vanishing contribution. The relevant expectation value follows from Eq. (4.2.22) for $l = r = s = 4$:

$$\langle\phi(x_1)\phi(x_2)\phi(x_3)\phi(x_4)O^{(4)}(y)O^{(4)}(z)\rangle_0 = Z_{444}\langle\phi(x_1)\phi(x_2)\phi(x_3)\phi(x_4)O^{(4)}(y)O^{(4)}(z)\rangle\,. \tag{4.B.17}$$

With the level-2 inserted operator $O^{(4)} = \phi^4/4!$, this is

$$\langle\phi(x_1)\cdots\phi(x_4)\frac{\phi^4(y)}{4!}\frac{\phi^4(z)}{4!}\rangle_0 - \delta_{444}\langle\phi(x_1)\cdots\phi(x_4)\frac{\phi^4(y)}{4!}\frac{\phi^4(z)}{4!}\rangle = \langle\phi(x_1)\cdots\phi(x_4)\frac{\phi^4(y)}{4!}\frac{\phi^4(z)}{4!}\rangle\,. \tag{4.B.18}$$

The bare part after the contractions gives the known 1-loop diagram

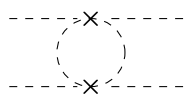

$= \mathcal{M}^{44}$

without any coupling included. The diagram has three possible channels, s, t and u, given by

$$s = (p_1 + p_2)^2 \qquad t = (p_1 + p_3)^2 \qquad u = (p_1 + p_4)^2\,, \tag{4.B.19}$$

with each channel contributing a scaleless B_0 integral. Separating only the UV part of Eq. (4.A.9) and adding the three channels we get

$$\mathcal{M}^{44} = (-i)\frac{3}{16\pi^2}\frac{1}{\varepsilon} + \text{finite}\,, \tag{4.B.20}$$

The renormalized term on the l.h.s of Eq. (4.B.18) gives exactly the same diagram, multiplied by δ_{444}, but now this is finite. Notice that both sides of Eq. (4.B.18) include the extra $(-i)$ factor. According to the discussion below Eq. (4.2.23), such expectation values should be considered as finite vertices so that the corresponding counter-term absorbs any remnant divergence. In other words finiteness requires $\delta_{444} = \frac{3}{16\pi^2}\frac{1}{\varepsilon}$ determining

$$\Gamma_{444} = \frac{3}{16\pi^2}\,. \tag{4.B.21}$$

Putting all the pieces together we can reconstruct $\beta_{c^{(4)}}$:

$$\beta_{c^{(4)}} = -\varepsilon c^{(4)} + \frac{3}{16\pi^2}(c^{(4)})^2 \equiv -\varepsilon\lambda + \frac{3}{16\pi^2}\lambda^2\,. \tag{4.B.22}$$

With Eq. (4.B.13) and Eq. (4.B.22) in hand, the quantum parts of the β-functions are

$$\vec{\beta}^{q}_{c^{(l)}} = \begin{bmatrix} \beta^{q}_{c^{(2)}} \\ \beta^{q}_{c^{(4)}} \end{bmatrix} = \begin{bmatrix} \frac{\lambda m^2}{16\pi^2} \\ \frac{3\lambda^2}{16\pi^2} \end{bmatrix} \tag{4.B.23}$$

and the full 1-loop β-functions are

$$\vec{\beta}_{c^{(l)}} = \begin{bmatrix} -2m^2 + \frac{\lambda m^2}{16\pi^2} \\ -\varepsilon\lambda + \frac{3\lambda^2}{16\pi^2} \end{bmatrix} .$$

As mentioned, these are the right expressions expected from standard treatments. Based on these β-functions we review the properties of the phase diagrams for $d = 4, 3, 5$. On Figs. 4.B.1 and 4.B.2 we plot the corresponding renormalization group (RG) flows according to the following conventions:

- We denote by $\bullet$ the Gaussian fixed points and by $\star$ the Wilson-Fisher fixed points.
- μ_L is the Landau pole.
- The arrow on an RG flow line points towards the IR. This means that it points to the direction of an increasing mass, when the mass is non-zero. For a flow line where the mass remains constant, the arrow indicates the flow of λ towards the IR.
- We keep in mind that when $\lambda < 0$, an instability eventually develops for large field values.
- We also consider flows with $\lambda > |\lambda_\star|$ and $\lambda < -|\lambda_\star|$ even though they may lie beyond the validity of the ε expansion.
- The green flows are the regions on the phase diagram where a stable mechanism of spontaneous breaking of $\mathbb{Z}_2$ is at work.

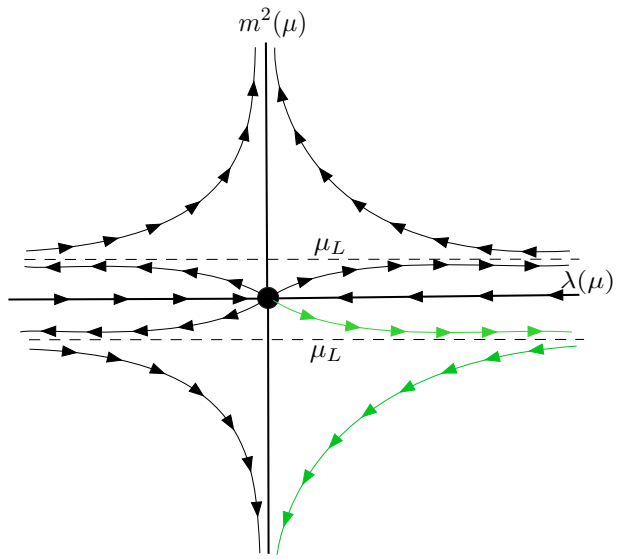

Figure 4.B.1: RG flows for Eq. (4.B.1), in $d = 4$. The $\lambda > 0, m^2 < 0$ (green) flow corresponds to the $\mathbb{Z}_2$ broken phase.

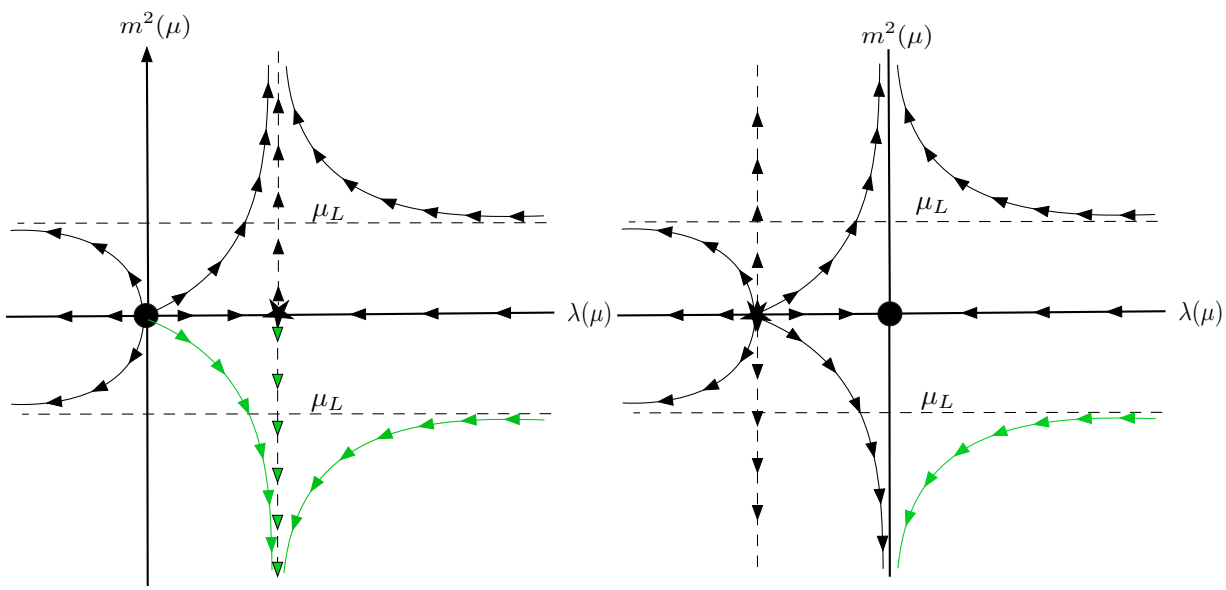

Figure 4.B.2: Left: RG flows for Eq. (4.B.1), in $d = 3$. The $\lambda > 0, m^2 < 0$ (green) flow corresponds to the broken phase. Here, $\star$ denotes the WF fixed point where scale invariance is restored while the system is still interacting. Right: RG flows for Eq. (4.B.1), in $d = 5$. The broken phase has a Landau pole brach where λ diverges as μ reaches μ_L, similarly to the $\varepsilon = 0$ case.

Let us summarize the features of the phase diagrams. Each fixed point is seen by the couplings as either a UV fixed point or an IR fixed point. This is decided by the derivative of the β-function evaluated at the fixed point. In the case where the two couplings featuring in the model are m^2 and λ, we have (we consider only $\varepsilon = 0, \pm 1$):

$$\frac{\partial \beta_{m^2}}{\partial m^2} = -2 + \frac{\lambda}{16\pi^2} \begin{cases} \bullet : -2 < 0 \text{ for any } d \to \text{UV} \\ \star : \begin{cases} d = 4 : - \\ -2 + \frac{\varepsilon}{3} < 0 \text{ for any } d \neq 4 \to \text{UV} \end{cases} \end{cases} \tag{4.B.24}$$

$$\frac{\partial \beta_\lambda}{\partial \lambda} = -\varepsilon + \frac{6}{16\pi^2}\lambda = \begin{cases} \bullet : -\varepsilon & \begin{cases} d = 4 : 0 \ \to \text{IR} \\ d = 3 : -1 < 0 \to \text{UV} \\ d = 5 : +1 > 0 \to \text{IR} \end{cases} \\ \star : +\varepsilon & \begin{cases} d = 4 : - \\ d = 3 : +1 > 0 \to \text{IR} \\ d = 5 : -1 < 0 \to \text{UV} \end{cases} \end{cases} \tag{4.B.25}$$

From Eq. (4.B.24) we see that the mass feels both fixed points as UV.

The nature of an operator is decided by the quantity $\Delta_{O^{(l)}} - d$ according to:

$$\Delta_{O^{(l)}} - d : \begin{cases} < 0 \to \text{relevant} \\ > 0 \to \text{irrelevant} \\ = 0 \to \text{RG equation} \end{cases} \tag{4.B.26}$$

An appropriate definition for the scaling dimension $\Delta_{O^{(l)}}$ is needed. In general it is defined as

$$\Delta_{O^{(l)}} = d_{O^{(l)}} + \gamma_{O^{(l)}} \tag{4.B.27}$$

with $d_{O^{(l)}}$ defined in Eq. (4.2.4). The second term on the r.h.s refers to the full anomalous dimension of the associated operator and it should not be confused with $\Gamma_{O^{(l)}}$ of Eq. (4.2.10), which comes from just the linear part of $\beta_{c^{(l)}}$. Taking into account the full quantum part of the β-function, we define [72]

$$\gamma_{O^{(l)}} = \left. \frac{\partial \beta^q_{c^{(l)}}(c^{(l)})}{\partial c^{(l)}} \right|_{c^{(l)} \to c^{(l)}_\star} . \tag{4.B.28}$$

Note that $\gamma_{O^{(l)}}$ contributes to Eq. (5.4.35) only for $d \neq 4$ where a $c^{(l)}_\star$ exists, so any error in the characterization of the operators using $\gamma_{O^{(l)}}$ vs $\Gamma_{O^{(l)}}$ in the definition of the scaling dimension is invisible in $d = 4$. These results are summarized in the following tables. The nature of the fixed points in various dimensions, as determined by $\frac{\partial \beta^q_\lambda}{\partial \lambda}|_{\bullet,\star}$ are:

d	$\bullet$	$\star$
4	trivial (UV when $\lambda = 0$)	$-$
3	UV	IR
5	IR	UV

The 1-loop exponent is determined by the nature of an operator, according to Eq. (5.4.35) using Eq. (4.B.2) and Eq. 4.B.23 combined with Eq. (5.4.36). With respect to the IR, when it is

negative the operator is relevant, if it is positive then the operator is irrelevant and if it is zero it is marginal and the RG running must decide (when it applies):

	$\Delta_{O^{(l)}} - d$	$\bullet$	$\star$
$O^{(2)}$	$-2 + \frac{\lambda}{16\pi^2}$	-2	$-2 + \frac{\varepsilon}{3}$
$O^{(4)}$	$-\varepsilon + 2\frac{3\lambda}{16\pi^2}$	$-\varepsilon$ (irrel. in d $= 4$)	ε

Finally, the chracterization of operators at the fixed points according to the above is:

	$d = 4$		$d = 3$		$d = 5$	
$O^{(2)}$	$\bullet\,(\lambda = 0)$: rel	$\star$: $-$	$\bullet$: rel	$\star$: rel	$\bullet$: rel	$\star$: rel
$O^{(4)}$	$\bullet$: marg. irrel	$\star$: $-$	$\bullet$: rel	$\star$: irrel	$\bullet$: irrel	$\star$: rel

Chapter 5

A quantum, 1st order, phase Transition as the solution of the Higgs fine tuning problem

5.1 Introduction

In our final Chapter we continue the work done in Chapter 3 by truncating the lattice spacing expansion at NLO. As a consequence, we constructed again the 1-loop effective action of an $SU(2)$ gauge theory in five dimensions with boundary conditions that leave a $U(1)$-complex scalar theory on the boundary, located at the origin of a semi-infinite fifth dimension, enhanced now with HDO. At an exclusively perturbative level, the boundary theory is a version of the Coleman-Weinberg model where the quartic term is replaced by a dimension-6 derivative operator. A qualitatively similar to the CW model Higgs mechanism is at work but with different coefficients in the scalar mass and the β-functions that change things towards a more realistic direction. If in addition we impose on the effective action non-perturbative features known from the lattice, the system becomes highly constrained. The picture is that the model possesses a non-trivial phase diagram where the phases are separated by first order, quantum phase transitions located in the UV. A crucial step in our construction of a continuum effective action is relating lattice to continuum parameters. In the continuum, the boundary theory will have a dimensionless 4d coupling and at the quantum level it will develop two dimensionful scales: a regularization scale, say μ in Dimensional Regularization (DR) and a vacuum expectation value (vev) v in the Higgs phase. The structure of the phase diagram [10, 11] which is determined by two dimensionless couplings, β_4 and β_5, or equivalently by β and γ, (see Eq. (5.A.10)) will guide us in this respect and it is useful to review it in some more detail. For general γ, the model exhibits three distinct phases, separated by first-order phase transitions. These are a Higgs phase, a Hybrid phase and a Confined phase, see Fig. 5.1. We point out here certain features of this phase diagram which will have to be incorporated in, or reproduced by, the

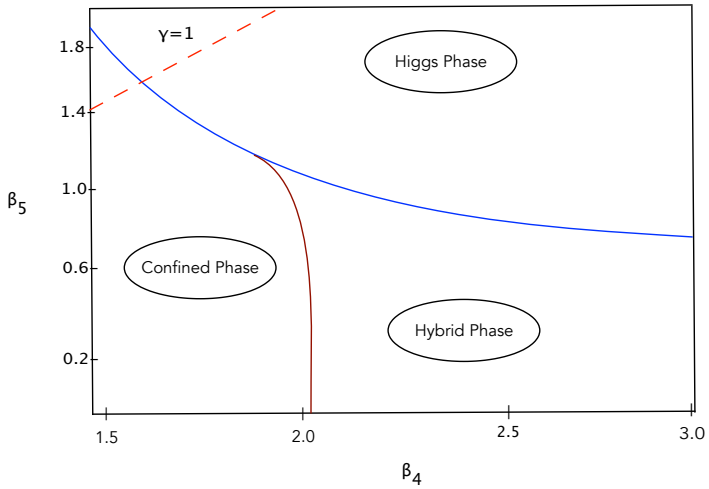

Figure 5.1: The Phase Diagram of the anisotropic orbifold lattice [10, 11]. It exhibits three distinct phases, the Confined, the Higgs and the Hybrid phase, separated by either bulk-driven (blue) or by boundary-driven (red) first-order phase transitions. The dashed line corresponds to $\gamma = 1$.

continuum effective action. Actually, the first feature will be reproduced by it while the second will have to be input, as perturbation theory seems to be blind to it. The first feature is the fact that the line that separates the Higgs from the other two phases (blue line in Fig. 5.1) is bulk driven. This just means that it is unaffected by the boundary conditions and it is present even on a fully periodic, infinite lattice. For the effective action this implies that the presence of this phase transition should be detectable by 5d equations only as it was shown in Chapter 3 using the ε-expansion. The second non-perturbative property that has been observed on the lattice is that the entire Hybrid phase, as well as the Higgs phase but only near the Higgs-Hybrid phase transition, are layered. This seems to be a fully non-perturbative property [29], not seen by the ε-expansion and it must be built in by hand in the effective action. The way to do it is to set for the $d = 4 - \varepsilon$ parameter $\varepsilon = -1$ when locating the bulk driven phase transition as a line of WF points, but use $\varepsilon = 0$ when computing the spectrum and the RG flows in the dimensionally reduced regimes. When locating the phase transition as a first order transition, we can use instead purely $d = 4$ language, which however should result in small deviations from the second order, WF line. This would imply that the first order transition is weak. The phase transition that separates the Hybrid and Confined phases on the other hand, is boundary driven. Indeed, its presence is a non-trivial consistency fact of dimensional reduction, as the boundary of the system has the degrees of freedom of an Abelian-Higgs model, where such a phase transition is indeed present (for Higgs charge 2). The 5d Confined phase will not concern us here much. Finally, there is the above mentioned link between the lattice and continuum parameters that

we need. As explained in detail in Chapter 3, this comes down to a relation of the form

$$\mu = \frac{F(\beta_4, \beta_5)}{a_4} \tag{5.1.1}$$

which relates the DR regularization scale μ to the lattice spacing a_4. In general and especially in a non-perturbative regime of a non-renormalizable, spontaneously broken theory, $F(\beta_4, \beta_5)$ may be a complicated function. Its perturbative effect will be taken into account by promoting the fixed numerical factors that lattice spacing expansion generates in front of operators to general couplings, to be determined by the renormalization process. As far as its non-perturbative effects are concerned built in the effective action, as argued in Chapter 3, near the phase transition it can be safely approximated by a constant.

It should be pointed out here that even though we carry out our analysis for a specific model, analogous considerations are expected to apply for any quantum gauge theory with boundaries of reduced gauge symmetry and a phase diagram of similar structure. This is a rather broad class of models whose zero temperature properties have not been yet sufficiently investigated. If we are interested to use the model as a cartoon of a possible origin of the Standard Model Higgs sector, then it turns out that we have to sit on, or near the interface of the phase transition that separates the Higgs phase and a layered-type of phase, the Hybrid phase. There, dimensional reduction happens via localization in both phases and the effective action must be constructed with a dynamically generated finite cut-off but also with RG flows that are correlated below and above the phase transition.

An important question is if we have provided in the context of our construction with an alternative resolution to the Higgs mass hierarchy problem. The fine tuning involved is about one part in a hundred and it is of a different type compared for example to the supersymmetric SM, being related to the choice of a "physical RG flow" on the phase diagram. More specifically what we saw is that the dynamics do not allow a high cut-off for the effective action, which indeed does ameliorate the fine tuning problem. On the other hand, in order to satisfy the constraint of a proper scale hierarchy, a considerable fine tuning of the free parameters (the initial data for the gauge coupling RG flows and the scalar vev) is necessary and this becomes more enhanced when a realistic spectrum is asked for. This essentially amounts to a fine tuning in the process of picking a physical RG flow line (equivalently of a Line of Constant Physics) out of a continuum of RG flows on the phase diagram. Once such a physical RG flow is picked, there is very little fine tuning that takes place along it.

Let us close the current introduction with the following comments: The phenomenology of models of localization is expected to be quite different from the phenomenology of models with a Kaluza-Klein spectrum. We have not performed a related analysis in the present paper, instead we leave it for a future work. On the other hand it should be possible to do several related measurements on the lattice. For example, the numerical methods of [12] could be applied to see to which extent the potential Eq. (5.3.9) agrees with the full non-perturbative potential. A question that arises here is whether on the lattice, the scalar potential is a potential for a fundamental field or a composite. Perturbation theory can not tell the difference nonetheless

the two approaches should agree on the shape of the potential. It is also most likely possible to measure numerically the quantity Λ_s in the Hybrid phase, reducing further the parameter freedom to only $\alpha_{4,R}$, $\alpha_{s,R}$ and v_*. Moreover it is possible that the above will also give some information about $\alpha_{s,R}$ and measurements of scalar Polyakov loop expectation values in the Higgs phase most likely can constrain v_*.

A well known fact is that fermions play a catalytic role in the validity of both CW-like models and the Standard Model since, when dominant, they may render the effective potentials unstable. Crucial for this to happen is the coupling of the top quark (the heaviest fermion of the SM) to the Higgs boson be stronger than both the self and the gauge-Higgs couplings. Then, beyond a critical scale the former dominates the running of the quartic coupling which then takes large and negative values. A fair question is whether such a situation could be realized in our model. In our case the starting point would be a 5d orbifold lattice with an $SU(2)$ gauge field minimally coupled to massless fermions. Even though the introduction of fermionic degrees of freedom on the lattice is non-trivial, let us assume that we have followed analogous steps as described in this work and ended up with a classical continuum Lagrangian. It is then expected that in the continuum, the boundary action will inherit extra derivative operators some of which generate fermion-scalar vertices. These extra vertices, being fermionic, will have the usual negative-sign contribution to the 1-loop effective potential and this could be the root of an instability. However, in our prescription there is only one 5d gauge coupling, g_5, which appears in the form of g_4 on the boundary for both the gauge-scalar and the fermion-scalar vertices. Due to this universality the Yukawa couplings will share the same order of magnitude and the same running properties with the gauge coupling so, their contribution to the effective potential will not be dominant and the latter will stay stable. On the other hand, under the presence of fermions there would be changes in the constraints Eq. (5.4.30) and Eq. (5.4.31) which, however, are not expected to affect the current picture drastically. Suppose finally that, for an unforeseen reason, the above scenario fails and the top quark dominates violently the running of our quartic coupling when a critical scale is reached. The SM prediction for this scale is $\mu \sim 10^{10}$ GeV and lies far beyond, say, the cut-off scale $\mu = \mu_* \simeq 209.1$ GeV of our prime example, where our boundary model exhibits a first order phase transition. In other words, the boundary action Eq. (5.2.11) enhanced with fermions will never reach the instability scale hence the potential as well as the associated SSB mechanism will remain valid.

5.2 Quantization with higher derivative operators

Here we become more specific of the action to be quantized. The starting point is the lattice orbifold action $S^{\rm orb}$ defined in [4, 6] and reproduced in Appendix 5.A:

$$S^{\rm orb} = S^{\rm b-h} + S^B \,, \tag{5.2.1}$$

with $S^{\text{b-h}}$ the Boundary-Hybrid action and S^B the bulk action, given by Eq. (5.A.8) and Eq. (5.A.9). These are

$$S^{\text{b-h}} = \frac{1}{2N}\sum_{n_\mu}\left[\frac{\beta_4}{2}\sum_{\mu<\nu}\text{tr}\left\{1-U^b_{\mu\nu}(n_\mu,0)\right\}+\beta_5\sum_{\mu}\text{tr}\left\{1-U^h_{\mu 5}(n_\mu,0)\right\}\right]$$

and

$$S^B = \frac{1}{2N}\sum_{n_\mu,n_5}\left[\beta_4\sum_{\mu<\nu}\text{tr}\left\{1-U_{\mu\nu}(n_\mu,n_5)\right\}+\beta_5\sum_{\mu}\text{tr}\left\{1-U_{\mu 5}(n_\mu,n_5)\right\}\right],$$

respectively. $N=2$ for $SU(2)$, β_4 and β_5 are the lattice couplings, n_μ, n_5 the discrete coordinates of the nodes and U_{MN} is the plaquette lying in the MN directions, with $M,N=\mu,5$. The Boundary-Hybrid action represents plaquettes lying on the boundary and plaquettes that are orthogonal to it with one of their sides only on the boundary. The Bulk action represents all other plaquettes. The lattice spacings in which the above actions are to be expanded are in the definitions

$$\beta_4 = \frac{4}{g_4^2}\,, \qquad \beta_5 = \frac{4a_4^2}{a_5^2 g_4^2} \tag{5.2.2}$$

with g_4 a dimensionless derived coupling, defined in terms of the 5d gauge coupling as $g_4^2 = g_5^2/a_5$. From these definitions it is clear that the model has three raw dimensionful parameters (a_4, a_5 and g_5), or two dimensionless (β_4 and β_5). Expanding now in small a_4 and a_5 and truncating at next to leading order in the expansion, yields

$$S^{\text{b-h}} = \sum_{n_\mu} a_4^4 \sum_{\mu}\left[\sum_{\nu}\left(\frac{1}{4}F^3_{\mu\nu}F^3_{\mu\nu}+\frac{1}{16}a_4^2(\hat{\Delta}_\mu F^3_{\mu\nu})(\hat{\Delta}_\mu F^3_{\mu\nu})\right)+|\hat{D}_\mu\phi|^2+\frac{a_4^2}{4}|\hat{D}_\mu\hat{D}_\mu\phi|^2\right] \tag{5.2.3}$$

for the Boundary-Hybrid part of the action, on which we will mainly concentrate. For the details of this step, as well as for the analogous step for the Bulk part, see Appendix 5.A.

Next, we have to take the naive continuum limit to obtain a continuum action. For that purpose we exploit Eq. (5.A.18) along with $\hat{\Delta}_\mu \to \partial_\mu$, $\hat{D}_\mu \to D_\mu$ and $\hat{p}_M = (2/a_M)\sin(a_M p_M/2) \to p_M$. Moreover we move to Minkowski space with metric $\eta_{\mu\nu} \equiv (+,-,-,-)$. These are standard operations and they are also shown in detail in Appendix 5.A. Here we only comment on the handling of the dimension 6 operators multiplied by a_4^2, for which we use Eq. (5.1.1). After these steps, we arrive at

$$S^{\text{b-h}} = \int d^4x\left[-\frac{1}{4}F^3_{\mu\nu}F^{3,\mu\nu}+|D_\mu\phi|^2+\frac{c_\alpha^{(6)}}{2\mu^2}(\partial^\mu F^3_{\mu\nu})(\partial_\mu F^{3,\mu\nu})-\frac{c_2^{(6)}}{\mu^2}|D^\mu D_\mu\phi|^2\right], \tag{5.2.4}$$

where ϕ is a complex scalar field, A^3_μ is the photon field and $F^3_{\mu\nu} = \partial_\mu A^3_\nu - \partial_\nu A^3_\mu$. The couplings $c_\alpha^{(6)}$ and $c_2^{(6)}$ are introduced for the HDO of the gauge and scalar field respectively, absorbing the unknown function F in Eq. (5.1.1). The final step before the quantization process starts is to interpret μ in Eq. (5.2.4). In principle we could leave it as it is (see [30]), however we can rewrite it in a more convenient form that resembles usual Effective Field Theory (EFT) treatments. Multiplying and dividing by a constant scale Λ^2 and absorbing Λ^2/μ^2 in the couplings, we can replace $\mu \to \Lambda$ in Eq. (5.2.4). Now Λ can be regarded as the cut-off of the EFT. In fact, we will

see that in our case Λ is not an external scale that must be introduced at this point by hand. It is rather an internal scale, given by the value of the regulating scale at the phase transition, μ_*, where it assumes its maximum value. Notice that we could have arrived at Eq. (5.2.4) directly by using gauge invariance. One reason we went through the painful process of generating it by expanding the lattice action is because of the anisotropy factor γ, hiding in the covariant derivative $D_\mu = \partial_\mu - ig_4 A^3_\mu$, where

$$g_4^2 = \frac{g_5^2}{a_5} = \frac{g_5^2}{a_4}\frac{a_4}{a_5} = \frac{g_5^2}{a_4}\gamma = g^2\gamma\,. \tag{5.2.5}$$

In the above we have used the bare value of the anisotropy originating from Eq. (5.2.2) and defined another convenient dimensionless coupling, $g^2 = g_5^2/a_4 = g_4^2/\gamma$. The presence of γ is non-trivial since it opens a second dimension in the phase diagram, where new phases and a triple point appear, among others. But there is another, equally important reason. Notice that in the presence of quadratic and quartic potential terms for the complex scalar, Eq. (5.2.4) would be just the Lee-Wick Scalar QED whose 1-loop renormalization was extensively studied in [9]. However, the above effective action does not have a scalar potential since the lattice does not produce polynomial terms for the boundary effective action at any order in the expansion in the lattice spacings. Using standard jargon, our Higher Dimensional Operators are exclusively Higher Derivative Operators. This is due to the 5d origin of the boundary theory and it is a crucial characteristic of our model which distinguishes it from other models of the sort.

5.2.1 The ghost-free basis of the gauge-fixed classical action

Now we are almost ready to renormalize the Lagrangean at 1-loop level, obtain its β-functions and through them determine the Renormalization Group (RG) flows. We have to tackle one more obstacle though, associated with the scalar HDO in Eq. (5.2.4) which contains an Ostrogradsky instability. We will deal with this immediately, but first we will fix the gauge. The gauge-fixing term for the bulk action is $\partial_M A^A_M$ while for the boundary, using the boundary conditions as in [3], it is $\partial_\mu A^3_\mu$. The same is true for the Faddeev-Popov ghosts which in the bulk are $\bar{c}^A$, c^A and on the boundary $\bar{c}^3$, c^3. In the latter case recall that the Faddeev-Popov ghosts are decoupled from the spectrum. Given the above, the gauge-fixed $S^{\rm b-h}$ reads

$$\begin{aligned} S^{\rm b-h} &= \int d^4x \Bigg[-\frac{1}{4}F^3_{\mu\nu}F^{3,\mu\nu} - \frac{1}{2\xi}(\partial^\mu A^3_\mu)^2 + |D_\mu\phi|^2 \\ &+ \frac{c^{(6)}_\alpha}{2\Lambda^2}(\partial^\mu F^3_{\mu\nu})(\partial_\mu F^{3,\mu\nu}) - \frac{c^{(6)}_2}{\Lambda^2}|D^\mu D_\mu\phi|^2 + \partial^\mu\bar{c}^3\partial_\mu c^3 \Bigg]\,. \end{aligned} \tag{5.2.6}$$

The instability is exposed by expanding the covariant derivative and rearranging terms up to total partial derivatives. By doing this, we arrive at the bare Boundary-Hybrid action

$$S_0^{\rm b-h} = \int d^4x \Bigg[-\frac{1}{4}F^3_{\mu\nu,0}F_0^{3,\mu\nu} + \frac{1}{2\xi}A^3_{\mu,0}\partial^\mu\partial_\nu A_0^{3,\nu} - \bar{\phi}_0\Box\phi_0 - \frac{c^{(6)}_{\alpha,0}}{2\Lambda^2}F^3_{\mu\nu,0}\Box F_0^{3,\mu\nu} - \frac{c^{(6)}_{2,0}}{\Lambda^2}\bar{\phi}_0\Box^2\phi_0 - \bar{c}_0^3\Box c_0^3$$

$$
\begin{aligned}
&+ \quad ig_0\sqrt{\gamma_0}A^3_{\mu,0}\left(\left\{\bar\phi_0\partial^\mu\phi_0-\phi_0\partial^\mu\bar\phi_0\right\}+\frac{c^{(6)}_{2,0}}{\Lambda^2}\left\{\Box\bar\phi_0\partial^\mu\phi_0-\Box\phi_0\partial^\mu\bar\phi_0\right\}\right)+g_0^2\gamma_0(A^3_{\mu,0})^2\bar\phi_0\phi_0\\
&+ \quad g_0^2\gamma_0\left(\frac{c^{(6)}_{2,0}}{\Lambda^2}\left\{\phi_0\Box^2\bar\phi_0+\bar\phi_0\Box^2\phi_0\right\}-\frac{c^{(6)}_{2,0}}{\Lambda^2}\partial^\mu(A^3_{\mu,0}\bar\phi_0)\partial_\mu(A^{3,\mu}_0\phi_0)\right)\\
&- \quad \frac{ig_0^3\gamma_0^{3/2}c^{(6)}_{2,0}}{\Lambda^2}(A^3_{\rho,0})^2A^3_{\mu,0}\left(\bar\phi_0\partial^\mu\phi_0-\phi_0\partial^\mu\bar\phi_0\right)-\frac{g_0^4\gamma_0^2c^{(6)}_{2,0}}{\Lambda^2}(A^3_{\rho,0})^4\bar\phi_0\phi_0\Bigg]\\
&= \quad S^{\rm b-h}_{\rm Kin,0}+S^{\rm b-h}_{\rm Int,0}\,,
\end{aligned}
\tag{5.2.7}
$$

where $S^{\rm b-h}_{\rm Kin,0}$ is the kinetic part of the action

$$
S^{\rm b-h}_{\rm Kin,0}=\int d^4x\left[-\frac{1}{4}F^3_{\mu\nu,0}F_0^{3,\mu\nu}+\frac{1}{2\xi}A^3_{\mu,0}\partial^\mu\partial_\nu A_0^{3,\nu}-\bar\phi_0\Box\phi_0-\frac{c^{(6)}_{\alpha,0}}{2\Lambda^2}F^3_{\mu\nu,0}\Box F_0^{3,\mu\nu}-\frac{c^{(6)}_{2,0}}{\Lambda^2}\bar\phi_0\Box^2\phi_0-\bar c_0^3\Box c_0^3\right]
$$

while $S^{\rm b-h}_{\rm Int,0}$ is the interaction part

$$
\begin{aligned}
S^{\rm b-h}_{\rm Int,0} \quad &= \quad \int d^4x\Bigg[ig_0\sqrt{\gamma_0}A^3_{\mu,0}\left(\left\{\bar\phi_0\partial^\mu\phi_0-\phi_0\partial^\mu\bar\phi_0\right\}+\frac{c^{(6)}_{2,0}}{\Lambda^2}\left\{\Box\bar\phi_0\partial^\mu\phi_0-\Box\phi_0\partial^\mu\bar\phi_0\right\}\right)\\
&+ \quad g_0^2\gamma_0(A^3_{\mu,0})^2\bar\phi_0\phi_0+g_0^2\gamma_0\left(\frac{c^{(6)}_{2,0}}{\Lambda^2}\left\{\phi_0\Box^2\bar\phi_0+\bar\phi_0\Box^2\phi_0\right\}-\frac{c^{(6)}_{2,0}}{\Lambda^2}\partial^\mu(A^3_{\mu,0}\bar\phi_0)\partial_\mu(A^{3,\mu}_0\phi_0)\right)\\
&- \quad \frac{ig_0^3\gamma_0^{3/2}c^{(6)}_{2,0}}{\Lambda^2}(A^3_{\rho,0})^2A^3_{\mu,0}\left(\bar\phi_0\partial^\mu\phi_0-\phi_0\partial^\mu\bar\phi_0\right)-\frac{g_0^4\gamma_0^2c^{(6)}_{2,0}}{\Lambda^2}(A^3_{\rho,0})^4\bar\phi_0\phi_0\Bigg]\,.
\end{aligned}
$$

The subscript 0 denotes the bare fields and couplings. Looking at the kinetic part we notice that each of the two higher derivative operators may impose non-physical degrees of freedom on the spectrum. These are the Ostrogradsky ghosts (the O-ghosts) [8] and a possible way to describe their effect can be found in [9]. There, these ghosts correspond to extra poles in the gauge and scalar propagators, reducing the divergence level of the loop diagrams. However, this observation is not sufficient to fully deal with them at the quantum level, since if O-ghosts remain in the spectrum, the instability remains. In [30, 33] an algorithm was developed so as to get a ghost free basis when, after a general field redefinition, the Jacobean of the transformation is properly taken into account. According to this algorithm, another ghost-field must be introduced, the Reparameterization ghost (R-ghost), which cancels the pole due to the O-ghost. Here we do not get into the details of these operations and just use the result of [30, 33] to eliminate the O-ghosts, after performing the field redefinition

$$
\begin{aligned}
\phi_0 \quad &\to \quad \hat\phi_0=\phi_0+\frac{x}{\Lambda^2}D^2\phi_0+\frac{y}{\Lambda^2}(\bar\phi_0\phi_0)\phi_0\\
\bar\phi_0 \quad &\to \quad \bar{\hat\phi}_0=\bar\phi_0+\frac{x}{\Lambda^2}\bar D^2\bar\phi_0+\frac{y}{\Lambda^2}(\bar\phi_0\phi_0)\bar\phi_0\\
A^3_{\mu,0} \quad &\to \quad \hat A^3_{\mu,0}=A^3_{\mu,0}+\frac{x_\alpha}{\Lambda^2}(\eta_{\mu\rho}\Box-\partial_\mu\partial_\rho)A_0^{3,\rho}\\
F^3_{\mu\nu,0} \quad &\to \quad \hat F^3_{\mu\nu,0}=F^3_{\mu\nu,0}+\frac{x_\alpha}{\Lambda^2}\Box F^3_{\mu\nu,0}\,,
\end{aligned}
\tag{5.2.8}
$$

with D^2 standing for $D^\mu D_\mu$. Now these field redefinitions raise two related questions. The first regards the generality of the redefinition (for example the gauge-field redefinition seems to be

incomplete, as we could have added the term $(A^3_\rho)^2 A^3_\mu/\Lambda^2)$ and the second is concerned about the fate of gauge invariance of the redefined action. Actually these questions are related and the answer to both of them is contained in the analysis of Appendix 5.B, according to which a properly redefined field should transform covariantly, in such a way that leaves gauge invariance intact. This is the case for Eq. (5.2.8) and this is made clear if we gauge transform the scalar field as $\phi_0' = e^{i\alpha(x)}\phi_0$ to get

$$\begin{aligned}
\hat{\phi}_0' &= \phi_0' + \frac{x}{\Lambda^2} D'^2 \phi_0' + \frac{y}{\Lambda^2}(\bar{\phi}_0'\phi_0')\phi_0' \\
&= e^{i\alpha(x)}\phi_0 + \frac{x}{\Lambda^2} D'^\mu (D'_\mu e^{i\alpha(x)}\phi_0) + \frac{y}{\Lambda^2}(\bar{\phi}_0 e^{-i\alpha(x)} e^{i\alpha(x)}\phi_0) e^{i\alpha(x)}\phi_0 \\
&= e^{i\alpha(x)}\{\phi_0 + \frac{x}{\Lambda^2} D^2\phi_0 + \frac{y}{\Lambda^2}(\bar{\phi}_0\phi_0)\phi_0\} \equiv e^{i\alpha(x)}\hat{\phi}_0
\end{aligned} \tag{5.2.9}$$

and the gauge field as $(A^3_{\mu,0})' = A^3_{\mu,0} + \partial_\mu \alpha(x)$ to get

$$\begin{aligned}
(\hat{A}^3_{\mu,0})' &= (A^3_{\mu,0})' + \frac{x_\alpha}{\Lambda^2}(\eta_{\mu\rho}\Box - \partial_\mu\partial_\rho)(A^{3,\rho}_0)' \\
&= A^3_{\mu,0} + \partial_\mu\alpha(x) + \frac{x_\alpha}{\Lambda^2}(\eta_{\mu\rho}\Box - \partial_\mu\partial_\rho)A^{3,\rho}_0 + \frac{x_\alpha}{\Lambda^2}\{\Box\partial_\mu\alpha(x) - \partial_\mu\partial_\rho\partial^\rho\alpha(x)\} \\
&= \{A^3_{\mu,0} + \frac{x_\alpha}{\Lambda^2}(\eta_{\mu\rho}\Box - \partial_\mu\partial_\rho)A^{3,\rho}_0\} + \partial_\mu\alpha(x) \equiv \hat{A}^3_{\mu,0} + \partial_\mu\alpha(x)\,,
\end{aligned} \tag{5.2.10}$$

with $\alpha(x)$ a gauge tranformation function and then under a gauge transformation $D_\mu\phi \to e^{i\alpha(x)}D_\mu\phi$. Note also that the R-ghosts which are inherited in the spectrum due to the field redefinitions are in accordance with Eq. (5.B.13). Hence the redefined action remains gauge invariant. Then, Eq. (5.2.7) becomes

$$\begin{aligned}
S_0^{\rm b-h} &= \int d^4x \Bigg[-\frac{1}{4}F^3_{\mu\nu,0}F_0^{3,\mu\nu} + \frac{1}{2\xi}A^3_{\mu,0}\partial^\mu\partial_\nu A_0^{3,\nu} - \bar{\phi}_0\Box\phi_0 - \frac{c^{(6)}_{\alpha,0} + x_\alpha}{2\Lambda^2}F^3_{\mu\nu,0}\Box F_0^{3,\mu\nu} \\
&- \frac{c^{(6)}_{2,0} + 2x}{\Lambda^2}\bar{\phi}_0\Box^2\phi_0 - \frac{2y}{\Lambda^2}(\bar{\phi}_0\phi_0)\bar{\phi}_0\Box\phi_0 - \bar{c}^3_0\Box c^3_0 \\
&+ ig_0\sqrt{\gamma_0}A^3_{\mu,0}\Bigg(\Big\{1 + \frac{2y(\bar{\phi}_0\phi_0)}{\Lambda^2}\Big\}\Big(\bar{\phi}_0\partial^\mu\phi_0 - \phi_0\partial^\mu\bar{\phi}_0\Big) + \frac{c^{(6)}_{2,0} + 2x}{\Lambda^2}\Big(\Box\bar{\phi}_0\partial^\mu\phi_0 - \Box\phi_0\partial^\mu\bar{\phi}_0\Big)\Bigg) \\
&+ ig_0\sqrt{\gamma_0}x_\alpha\frac{(\eta_{\mu\rho}\Box - \partial_\mu\partial_\rho)A^{3,\rho}_0}{\Lambda^2}\Big(\bar{\phi}_0\partial^\mu\phi_0 - \phi_0\partial^\mu\bar{\phi}_0\Big) + g_0^2\gamma_0(A^3_{\mu,0})^2\bar{\phi}_0\phi_0\Big(1 + \frac{2y}{\Lambda^2}\bar{\phi}_0\phi_0\Big) \\
&+ g_0^2\gamma_0\Bigg(\frac{c^{(6)}_{2,0} + 2x}{\Lambda^2}\Big\{\phi_0\Box^2\bar{\phi}_0 + \bar{\phi}_0\Box^2\phi_0\Big\} - \frac{x}{\Lambda^2}A^3_{\mu,0}\Big\{\partial^\rho(A^3_{\rho,0}\bar{\phi}_0)\partial^\mu\phi_0 + \partial^\rho(A^3_{\rho,0}\phi_0)\partial^\mu\bar{\phi}_0\Big\} \\
&- \frac{c^{(6)}_{2,0} + 2x}{\Lambda^2}\partial^\mu(A^3_{\mu,0}\bar{\phi}_0)\partial_\mu(A_0^{3,\mu}\phi_0)\Bigg) + 2g_0^2\gamma_0 x_\alpha\frac{A_0^{3,\mu}(\eta_{\mu\rho}\Box - \partial_\mu\partial_\rho)A_0^{3,\rho}}{\Lambda^2}\bar{\phi}_0\phi_0 \\
&- \frac{ig_0^3\gamma_0^{3/2}(c^{(6)}_{2,0} + 2x)}{\Lambda^2}(A^3_{\rho,0})^2A^3_{\mu,0}\Big(\bar{\phi}_0\partial^\mu\phi_0 - \phi_0\partial^\mu\bar{\phi}_0\Big) - \frac{g_0^4\gamma_0^2(c^{(6)}_{2,0} + 2x)}{\Lambda^2}(A^3_{\rho,0})^4\bar{\phi}_0\phi_0\Bigg]
\end{aligned}$$

and there is indeed extra freedom from the redefinition so as to eliminate the two higher derivative operators. In particular choosing $x_\alpha = -c^{(6)}_{\alpha,0}$, $x = -c^{(6)}_{2,0}/2$ and $2y = c^{(6)}_{1,0}/4$ the redefined bare action becomes

$$S_0^{\rm b-h} = \int d^4x \Bigg[-\frac{1}{4}F^3_{\mu\nu,0}F_0^{3,\mu\nu} + \frac{1}{2\xi}A^3_{\mu,0}\partial^\mu\partial_\nu A_0^{3,\nu} - \bar{\phi}_0\Box\phi_0 - \frac{c^{(6)}_{1,0}}{4\Lambda^2}(\bar{\phi}_0\phi_0)\bar{\phi}_0\Box\phi_0 - \bar{c}^3_0\Box c^3_0$$

$$
\begin{aligned}
&+ \quad i g_{4,0}\Big\{\eta_{\mu\rho} - \frac{\eta_{\mu\rho}\Box - \partial_\mu\partial_\rho}{\Lambda^2}\Big\} A_0^{3,\rho}\Big(\bar\phi_0\partial^\mu\phi_0 - \phi_0\partial^\mu\bar\phi_0\Big) + g_{4,0}^2 (A^3_{\mu,0})^2 \bar\phi_0\phi_0 \\
&+ \quad \frac{g_{4,0}^2}{2\Lambda^2}\Big(A^3_{\mu,0}A^3_{\rho,0}\partial^\rho\bar\phi_0\partial^\mu\phi_0 + A^3_{\mu,0}\partial^\rho A^3_{\rho,0}\partial^\mu(\bar\phi_0\phi_0)\Big) - 2g_{4,0}^2 \frac{A_0^{3,\mu}(\eta_{\mu\rho}\Box - \partial_\mu\partial_\rho)A_0^{3,\rho}}{\Lambda^2}\bar\phi_0\phi_0 \\
&+ \quad i\frac{g_{4,0}\, c_{1,0}^{(6)}}{4\Lambda^2} A^3_{\mu,0}\bar\phi_0\phi_0\Big(\bar\phi_0\partial^\mu\phi_0 - \phi_0\partial^\mu\bar\phi_0\Big) + \frac{g_{4,0}^2\, c_{1,0}^{(6)}}{4\Lambda^2}(A^3_{\mu,0})^2(\bar\phi_0\phi_0)^2\Bigg], \qquad (5.2.11)
\end{aligned}
$$

where $c_{1,0}^{(6)}$ is a dimensionless coupling which is undetermined at present. For simplicity of notation, we have turned back to our original notation $g_4 = g\sqrt{\gamma}$ and normalized the undefined couplings as $c_{2,0}^{(6)} = c_{\alpha,0}^{(6)} \equiv 1$. Notice that the gauge-fixing term is untouched since it is an arbitrary function and can be redefined to its original form. Another way to see this is that since the redefinition commutes[1] with renormalization it could have been performed before gauge fixing.

Comparing now Eq. (5.2.11) to its original form Eq. (5.2.7), the interesting point to notice is that the former includes, after the field redefinition, the scalar quartic-like term $(\bar\phi\phi)\bar\phi\Box\phi$, instead of the original higher derivative term. In fact, apart from the modified vertices, $S_0^{\text{b-h}}$ now resembles an effective version of the Coleman-Weinberg (CW) [13] model. What happened is that a term like $\bar\phi\Box^2\phi$ has dual nature since it could be both part of the kinetic Lagrangian and a mass term of the scalar field. Then performing the field redefinition we threw away the O-ghost whose nature as a mass term was left implicit in the theory through the appeared potential. The Feynman rules for Eq. (5.2.11) are given in Appendix 5.C.

5.2.2 One loop corrections

Now that a consistent basis for the Boundary-Hybrid action has been developed we are finally ready to initiate the renormalization program. We choose to work in the Feynman gauge, where $\xi = 1$. We first set some notation used in the following. The 1-loop corrections to the 2-, 3-, 4-, 5- and 6-point functions of the fields are denoted by $\mathcal{M}_F$, $\mathcal{K}_F$, $\mathcal{B}_{4,F}$, $\mathcal{B}_{5,F}$ and $\mathcal{B}_{6,F}$ respectively. The subscript F corresponds to the different combinations that ϕ, $\bar\phi$ and A^3_μ can form as external fields. As an example consider the correction to the scalar-scalar-gauge vertex which is represented by $\mathcal{K}_{\bar\phi A\phi}$ where A in the subscript represents A^3_μ. The symmetry factor which is associated with a given diagram will be denoted as $S_{\mathcal{G}}$ with $\mathcal{G} \equiv \mathcal{M}_F, \mathcal{K}_F, \mathcal{B}_{4,F}, \mathcal{B}_{5,F}, \mathcal{B}_{6,F}$. Finally if the scalar and gauge fields are external, then the notation of the momentum is p_μ and q_μ respectively. Otherwise, when they run in the loop, the vector k_μ is used. For the finite parts of the diagrams we use the notation $[\ ]_f$.

Now looking at the Feynman rules of Eq. (5.2.11) note that there is only one possible 1-leg Tadpole, a correction to the gauge field, which is however forbidden due to gauge and Lorentz symmetry. Hence the loop calculation starts with the 2-point functions of ϕ and A^3_μ. More specifically for the scalar case there are three contributions, $\mathcal{M}^1_\phi$, $\mathcal{M}^2_\phi$ and $\mathcal{M}^3_\phi$ with equal symmetry factors $S_{\mathcal{M}^1_\phi} = S_{\mathcal{M}^2_\phi} = S_{\mathcal{M}^3_\phi} = 1$. The first diagram is a two-leg Tadpole which

[1] For more details see [30] and references therein.

includes only scalar fields and is given by

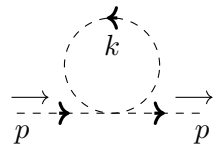

$$= i\mathcal{M}^1_\phi$$

whose evaluation gives

$$\begin{aligned} i\mathcal{M}^1_\phi &= ic_1^{(6)}\frac{p^2}{\Lambda^2}S_{\mathcal{M}^1_\phi}\int\frac{d^4k}{(2\pi)^4}\frac{i}{k^2}\Rightarrow \\ \mathcal{M}^1_\phi &= -c_1^{(6)}\frac{p^2}{\Lambda^2}\int\frac{d^4k}{(2\pi)^4 i}\frac{1}{k^2} \\ &= -c_1^{(6)}\frac{p^2}{\Lambda^2}A_0(0)\,. \end{aligned} \tag{5.2.12}$$

In the last line we have used the standard Passarino-Veltman notation, which we will be using throughout. The next diagram in line is another two-leg Tadpole with gauge contribution:

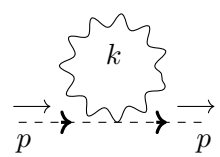

$$= i\mathcal{M}^2_\phi$$

and it is equal to

$$\begin{aligned} i\mathcal{M}^2_\phi &= 2ig_4^2 S_{\mathcal{M}^2_\phi}\int\frac{d^4k}{(2\pi)^4}\frac{-i\eta^{\mu\nu}}{k^2}Q_{\mu\nu}(p,k)\Rightarrow \\ \mathcal{M}^2_\phi &= 2g_4^2\int\frac{d^4k}{(2\pi)^4 i}\frac{\eta^{\mu\nu}}{k^2}\left[\eta_{\mu\nu}+\frac{\eta_{\mu\nu}p^2}{2\Lambda^2}+\frac{2(\eta_{\mu\nu}k^2-k_\mu k_\nu)}{\Lambda^2}\right] \\ &= 2g_4^2\int\frac{d^4k}{(2\pi)^4 i}\left[d(1+\frac{p^2}{2\Lambda^2})+\frac{2(d-1)k^2}{\Lambda^2}\right]\frac{1}{k^2} \\ &= 8g_4^2\,(1+\frac{p^2}{2\Lambda^2})A_0(0)\,, \end{aligned} \tag{5.2.13}$$

where Eq. (5.C.5) and the fact that

$$\int\frac{d^dk}{(2\pi)^d}\equiv 0$$

in DR were used. Up to now we have faced two massless tadpoles which vanish in dimensional regularization. A useful relation based on that is obtained if we convert Eq. (5.2.13) to a usual 2-point function of the form

$$\mathcal{M}^2_\phi = 8g_4^2\,(1+\frac{p^2}{2\Lambda^2})\int\frac{d^4k}{(2\pi)^4 i}\frac{k^2}{k^2(k+p)^2} = 8g_4^2\,(1+\frac{p^2}{2\Lambda^2})\eta_{\mu\nu}B^{\mu\nu}(k,k+p)\,. \tag{5.2.14}$$

Combining Eq. (5.2.13) with Eq. (5.2.14) shows that $\eta_{\mu\nu}B^{\mu\nu}$, when scaleless, is analogous to A_0 and vanishes in DR. Therefore in the following only B_0's will contribute a divergent part to the calculation, as we will see. The last contribution of the current category comes from the square of a vertex and yields

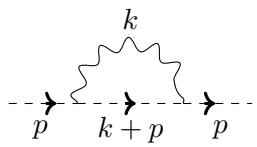

$$= i\mathcal{M}^3_\phi \ .$$

Its explicit form is given by

$$\begin{aligned}
i\mathcal{M}^3_\phi &= -g_4^2 S_{\mathcal{M}^3_\phi} \int \frac{d^4k}{(2\pi)^4} \frac{-i\eta^{\mu\nu}}{k^2} \frac{iQ_\mu(p,k)Q_\nu(p,k)}{(k+p)^2} \Rightarrow \\
\mathcal{M}^3_\phi &= -g_4^2 \int \frac{d^4k}{(2\pi)^4 i} \frac{Q_\mu(p,k)Q^\mu(p,k)}{k^2(k+p)^2} \\
&= -g_4^2 \int \frac{d^4k}{(2\pi)^4 i} \left[(2p+k)^2 + 2(2p+k)^2 \frac{k^2}{\Lambda^2} - 2\frac{(k^2+2p\cdot k)^2}{\Lambda^2} \right] \frac{1}{k^2(k+p)^2} + \mathcal{O}(\frac{1}{\Lambda^4}) \,,
\end{aligned}$$

using again Eq. (5.C.5). As indicated in the above relation there are terms of order higher than $\mathcal{O}(1/\Lambda^2)$ contributing to $\mathcal{M}^3_\phi$. Nevertheless, these cannot be renormalized unless operators with dimension higher that 6 appear in the action. Since Eq. (5.2.11) includes only dim-4 and -6 operators, in the following we neglect such contributions without loss of consistency. To move on let us clarify that our calculating algorithm is to reduce the integrals until they reach the scalar form A_0 and B_0 following the Appendix of [31], using the massless limit of the formulae. When necessary the relation

$$\int \frac{d^4k}{(2\pi)^4 i} \frac{k_\mu}{k^2} \equiv 0 \,,$$

due to the anti-symmetry under $k \to -k$, is exploited. So with the above in our hand $\mathcal{M}^3_\phi$ becomes

$$\mathcal{M}^3_\phi = -g_4^2 \left[\frac{4p^2}{\Lambda^2} A_0(0) + 2p^2(1 - \frac{p^2}{\Lambda^2}) B_0(k, k+p) + \eta_{\mu\nu} B^{\mu\nu}(k, k+p) \right] \tag{5.2.15}$$

and collectively the 1-loop correction to the scalar field propagator reads

$$\begin{aligned}
\mathcal{M}_\phi &= \mathcal{M}^1_\phi + \mathcal{M}^2_\phi + \mathcal{M}^3_\phi \\
&= -c_1^{(6)} \frac{p^2}{\Lambda^2} A_0(0) + 8g_4^2 A_0(0) - 2g_4^2 p^2 (1 - \frac{p^2}{\Lambda^2}) B_0(k, k+p) - g_4^2 \eta_{\mu\nu} B^{\mu\nu}(k, k+p) \,.
\end{aligned} \tag{5.2.16}$$

The next set of 2-point functions regards the quantum corrections to the gauge-field propagator. Here there are two possible diagrams at 1-loop level, $\mathcal{M}^1_{A,\mu\nu}$ and $\mathcal{M}^2_{A,\mu\nu}$, again with equal symmetry factors $S_{\mathcal{M}^1_A} = S_{\mathcal{M}^2_A} = 1$. The first diagram is the only two-leg Tadpole left given by

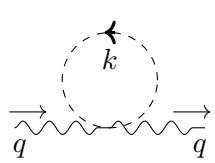

$$= i\mathcal{M}^1_{A,\mu\nu}$$

and is equal to

$$
\begin{aligned}
i\mathcal{M}^1_{A,\mu\nu} &= 2ig_4^2 S_{\mathcal{M}^1_A}\int\frac{d^4k}{(2\pi)^4}\frac{iQ_{\mu\nu}(k,q)}{k^2}\Rightarrow\\
\mathcal{M}^1_{A,\mu\nu} &= -2g_4^2\int\frac{d^4k}{(2\pi)^4 i}\frac{1}{k^2}\left[\eta_{\mu\nu}+\frac{\eta_{\mu\nu}k^2}{2\Lambda^2}+\frac{2(\eta_{\mu\nu}q^2-q_\mu q_\nu)}{\Lambda^2}\right]\\
&= -2g_4^2\left[\eta_{\mu\nu}+\frac{2(\eta_{\mu\nu}q^2-q_\mu q_\nu)}{\Lambda^2}\right]A_0(0)
\end{aligned}
\tag{5.2.17}
$$

while its contracted version gives

$$
\mathcal{M}^1_A=\frac{1}{3}\left(-\eta^{\mu\nu}+\frac{q^\mu q^\nu}{q^2}\right)\mathcal{M}^1_{A,\mu\nu}=2g_4^2\left[1+\frac{2q^2}{\Lambda^2}\right]A_0(0)\,. \tag{5.2.18}
$$

The second contribution to the gauge field propagator comes from the $\bar{\phi}$-ϕ-A^3_μ interaction and yields

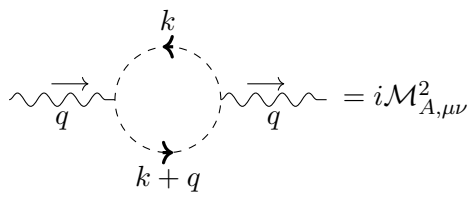

$= i\mathcal{M}^2_{A,\mu\nu}$

while its evaluation gives

$$
\begin{aligned}
i\mathcal{M}^2_{A,\mu\nu} &= -g_4^2 S_{\mathcal{M}^2_A}\int\frac{d^4k}{(2\pi)^4}\frac{iQ_\mu(k,q)}{k^2}\frac{iQ_\nu(k,q)}{(k+q)^2}\Rightarrow\\
\mathcal{M}^2_{A,\mu\nu} &= g_4^2\int\frac{d^4k}{(2\pi)^4 i}\frac{Q_\mu(k,q)Q_\nu(k,q)}{k^2(k+q)^2}\\
&= g_4^2\int\frac{d^4k}{(2\pi)^4 i}\Big[(2k+q)_\mu(2k+q)_\nu(1+\frac{2q^2}{\Lambda^2})-\frac{q_\nu q^\rho}{\Lambda^2}(2k+q)_\mu(2k+q)_\rho\\
&- \frac{q_\mu q^\rho}{\Lambda^2}(2k+q)_\nu(2k+q)_\rho\Big]\frac{1}{k^2(k+q)^2}+\mathcal{O}(\frac{1}{\Lambda^4})\,,
\end{aligned}
$$

where again terms of higher than $\mathcal{O}(1/\Lambda^2)$ are neglected. Expanding the parentheses and performing the appropriate reduction the above expression becomes

$$
\begin{aligned}
\mathcal{M}^2_{A,\mu\nu} &= g_4^2(1+\frac{2q^2}{\Lambda^2})\left[q_\mu q_\nu B_0(k,k+p)+2q_\mu B_\nu(k,k+p)+2q_\nu B_\mu(k,k+p)+4B_{\mu\nu}(k,k+p)\right]\\
&- \frac{q_\nu q^\rho}{\Lambda^2}\left[q_\mu q_\rho B_0(k,k+p)+2q_\mu B_\rho(k,k+p)+2q_\rho B_\mu(k,k+p)+4B_{\mu\rho}(k,k+p)\right]\\
&- \frac{q_\mu q^\rho}{\Lambda^2}\left[q_\nu q_\rho B_0(k,k+p)+2q_\nu B_\rho(k,k+p)+2q_\rho B_\nu(k,k+p)+4B_{\nu\rho}(k,k+p)\right]
\end{aligned}
\tag{5.2.19}
$$

and its contracted version

$$
\mathcal{M}^2_A=\frac{1}{3}\left(-\eta^{\mu\nu}+\frac{q^\mu q^\nu}{q^2}\right)\mathcal{M}^2_{A,\mu\nu}=\frac{g_4^2q^2}{3}(1+\frac{2q^2}{\Lambda^2})B_0(k,k+p)-\frac{4g_4^2}{3}(1+\frac{2q^2}{\Lambda^2})\eta_{\mu\nu}B^{\mu\nu}(k,k+p)\,. \tag{5.2.20}
$$

Finally the complete, contracted, contribution of the current set of diagrams is

$$\begin{aligned}\mathcal{M}_A &= \mathcal{M}_A^1 + \mathcal{M}_A^2 \\ &= \frac{2g_4^2}{3}(1+\frac{2q^2}{\Lambda^2})A_0(0) + \frac{g_4^2 q^2}{3}(1+\frac{2q^2}{\Lambda^2})B_0(k,k+p)\,,\end{aligned} \tag{5.2.21}$$

where we took advantage of Eq. (5.2.14). The quantum corrections of the propagators, from which the anomalous dimensions of the fields will be constructed, are now finished.

The next step is to compute the corrections to the vertices. Recall that Eq. (5.2.11) contains the couplings g_4 and $c_1^{(6)}$ whose desired running will be revealed if we correct the vertices $\bar{\phi}$-ϕ-A_μ^3 and $(\bar{\phi}\phi)\bar{\phi}\Box\phi$ respectively. Nevertheless the explicit calculation of the 3-point vertex corrections is not necessary for the model which we are looking at. In particular note that in SQED gauge invariance forces the overall counterterm of the 3-point vertex and the counterterm of the scalar field to be equal, at least at the divergent level, as it was shown in [3]. Actually this is a well known fact in both scalar and regular QED due to the universality of the electromagnetic coupling. So for the action $S^{\mathrm{b-h}}$ which is an extended, with gauge invariant HDO, version of SQED there is no reason to expect a different conclusion. Therefore, as it will be revealed in the renormalization program, the β-function of g_4 is determined only by the gauge-field counterterm. So in the following we focus on the quantum corrections of the four-scalar vertex.

Let us first perform a qualitative study of the possible one-loop contributions to the four point function, usually called Boxes. Recall that Box diagrams here are denoted collectively as $\mathcal{B}_{4,F}$ while they are separated into reducible and irreducible Boxes and there are three possible categories of the form

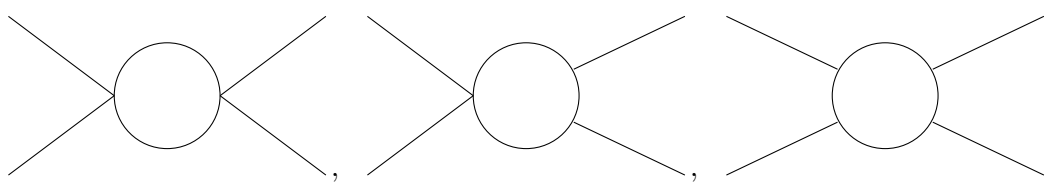

corresponding to *C-Boxes* (or *Candies*), *T-Boxes* and *S-Boxes* respectively, using the conventions in [31]. The above diagrams will contribute as quantum corrections to three processes regarding the $4A_\mu^3$ scattering, the $\bar{\phi}$-ϕ-A_μ^3-A_μ^3 vertex and the four-scalar interaction. Here we are interested in the latter case even though all the above corrections include divergencies. Actually these divergencies will be absorbed, through the renormalization procedure, from the counterterms of the lower dimensional vertices. In that sense the calculation starts with the set of C-Boxes which includes the diagrams $\mathcal{B}_{4,\phi}^{C,1}$, $\mathcal{B}_{4,\phi}^{C,2}$ and $\mathcal{B}_{4,\phi}^{C,3}$. All of them come in two channels, s and t with

$$s = (p_1+p_2)^2 \quad \text{and} \quad t = (p_1+p_3)^2\,, \tag{5.2.22}$$

while their symmetry factor is $S_{\mathcal{B}_{4,\phi}^{C,1}} = S_{\mathcal{B}_{4,\phi}^{C,2}} = S_{\mathcal{B}_{4,\phi}^{C,3}} = 1$. The reason for this is that the external legs are particle-antiparticle pairs so they cannot be interchanged. So the s-channel of the first Candy-diagram is

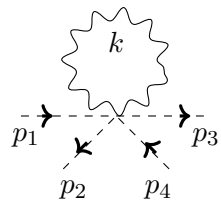

$$= i\mathcal{B}^{C,1s}_{4,\phi}$$

with momentum conservation condition $p_1 + p_2 + p_3 + p_4 = 0$. This is a four-point Tadpole coming from a dim-6 operator and its explicit expression reads

$$\begin{aligned} i\mathcal{B}^{C,1s}_{4,\phi} &= 2ig_4^2 \frac{c_1^{(6)}}{\Lambda^2} S_{\mathcal{B}^{C,1}_{4,\phi}} \int \frac{d^4k}{(2\pi)^4} \frac{-i\eta^{\mu\nu}}{k^2} \eta_{\mu\nu} \Rightarrow \\ \mathcal{B}^{C,1s}_{4,\phi} &= 2dg_4^2 \frac{c_1^{(6)}}{\Lambda^2} \int \frac{d^4k}{(2\pi)^4 i} \frac{1}{k^2} \\ &= 8g_4^2 \frac{c_1^{(6)}}{\Lambda^2} A_0(0)\,, \end{aligned} \tag{5.2.23}$$

while adding the t-channel we get

$$\mathcal{B}^{C,1}_{4,\phi} = \mathcal{B}^{C,1s}_{4,\phi} + \mathcal{B}^{C,1t}_{4,\phi} = 16g_4^2 \frac{c_1^{(6)}}{\Lambda^2} A_0(0)\,, \tag{5.2.24}$$

since the diagrams are channel-independent. Next comes the s-channel of the second Candy-diagram given by

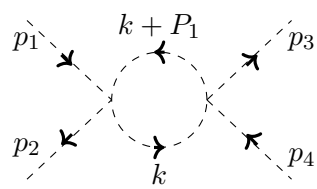

$$= i\mathcal{B}^{C,2s}_{4,\phi} \quad ,$$

with $p_1 + p_2 + p_3 + p_4 = 0$ and $P_1 = p_1 + p_2$. Its evaluation yields

$$\begin{aligned} i\mathcal{B}^{C,2s}_{4,\phi} &= -\Big(c_1^{(6)} \frac{p^2}{\Lambda^2}\Big)^2 S_{\mathcal{B}^{C,2}_{4,\phi}} \int \frac{d^4k}{(2\pi)^4} \frac{i}{k^2} \frac{i}{(k+P_1)^2} \Rightarrow \\ \mathcal{B}^{C,2s}_{4,\phi} &= \Big(c_1^{(6)} \frac{p^2}{\Lambda^2}\Big)^2 \int \frac{d^4k}{(2\pi)^4 i} \frac{1}{k^2(k+P_1)^2} \\ &= \Big(c_1^{(6)} \frac{p^2}{\Lambda^2}\Big)^2 B_0(k, k+\sqrt{s}) \end{aligned} \tag{5.2.25}$$

and collectively we get

$$\mathcal{B}^{C,2}_{4,\phi} = \mathcal{B}^{C,2s}_{4,\phi} + \mathcal{B}^{C,2t}_{4,\phi} = \Big(c_1^{(6)} \frac{p^2}{\Lambda^2}\Big)^2 B_0(k, k+\sqrt{s}) + \Big(c_1^{(6)} \frac{p^2}{\Lambda^2}\Big)^2 B_0(k, k+\sqrt{t})\,, \tag{5.2.26}$$

where now the diagrams, at least to their finite part, depend on the channels. Moreover, notice that even though the factor in front of B_0's seems that scales like $1/\Lambda^4$ it will not be neglected. The reason is that it corrects a vertex proportional to $c_1^{(6)} p^2/\Lambda^2$ and not just $c_1^{(6)}$, so throwing it away will cost us in completeness. The last contribution of this category, which originates from the $\bar{\phi}$-ϕ-A_μ^3-A_μ^3 vertex, is

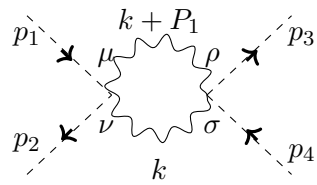

$$= i\mathcal{B}^{C,3s}_{4,\phi} \quad .$$

Again momentum conservation forces that $p_1+p_2+p_3+p_4=0$ while the s-channel of the above diagram gives

$$\begin{aligned}
i\mathcal{B}^{C,3s}_{4,\phi} &= -4g_4^4 S_{\mathcal{B}^{C,3}_{4,\phi}} \int \frac{d^4k}{(2\pi)^4} \frac{-i\eta^{\mu\rho}Q_{\mu\nu}(p,k)}{k^2} \frac{-i\eta^{\nu\sigma}Q_{\rho\sigma}(p,k)}{(k+P_1)^2} \Rightarrow \\
\mathcal{B}^{C,3s}_{4,\phi} &= 4g_4^4 \int \frac{d^4k}{(2\pi)^4 i} \left[\eta^{\mu\nu} + \frac{\eta^{\mu\nu}p_1\cdot p_2 + k^\mu(p_2-p_1)^\nu}{2\Lambda^2} + \frac{2(\eta^{\mu\nu}k^2 - k^\mu k^\nu)}{\Lambda^2}\right] \frac{1}{k^2(k+P_1)^2} \times \\
&\quad \left[\eta_{\mu\nu} + \frac{\eta_{\mu\nu}p_3\cdot p_4 + k_\mu(p_3-p_4)_\nu}{2\Lambda^2} + \frac{2(\eta_{\mu\nu}k^2 - k_\mu k_\nu)}{\Lambda^2}\right] \\
&= 4g_4^4 \left[4(1+\frac{p_1\cdot p_2 + p_3\cdot p_4}{2\Lambda^2})B_0(k,k+\sqrt{s}) + (p_1^2+p_4^2-p_3^2-p_2^2)\frac{B_0(k,k+\sqrt{s})}{4\Lambda^2} + \frac{12}{\Lambda^2}A_0(0)\right] .
\end{aligned} \tag{5.2.27}$$

The corresponding calculation for the t-channel is obtained from the above relation with the exchange $2 \leftrightarrow 3$ and $s \to t$, so collectively we get

$$\begin{aligned}
\mathcal{B}^{C,3}_{4,\phi} &= \mathcal{B}^{C,3s}_{4,\phi} + \mathcal{B}^{C,3t}_{4,\phi} \\
&= 4g_4^4\Big[4(1+\frac{p_1\cdot p_2 + p_3\cdot p_4}{2\Lambda^2})B_0(k,k+\sqrt{s}) + 4(1+\frac{p_1\cdot p_3 + p_2\cdot p_4}{2\Lambda^2})B_0(k,k+\sqrt{t}) \\
&+ (p_1^2+p_4^2-p_3^2-p_2^2)\frac{B_0(k,k+\sqrt{s})}{4\Lambda^2} + (p_1^2+p_4^2-p_3^2-p_2^2)\frac{B_0(k,k+\sqrt{t})}{4\Lambda^2} + \frac{24}{\Lambda^2}A_0(0)\Big] .
\end{aligned} \tag{5.2.28}$$

Adding Eq. (5.2.24), Eq. (5.2.26) and Eq. (5.2.28) we end up with the full contribution of the C-Boxes to the 4-point scalar vertex

$$\begin{aligned}
\mathcal{B}^{C}_{4,\phi} &= 16g_4^2\left(c_1^{(6)} + 6g_4^2\right)\frac{A_0(0)}{\Lambda^2} + \left(\frac{c_1^{(6)}p^2}{\Lambda^2}\right)^2\Big(B_0(k,k+\sqrt{s}) + B_0(k,k+\sqrt{t})\Big) \\
&+ 4g_4^4\Big[4(1+\frac{p_1\cdot p_2 + p_3\cdot p_4}{2\Lambda^2})B_0(k,k+\sqrt{s}) + 4(1+\frac{p_1\cdot p_3 + p_2\cdot p_4}{2\Lambda^2})B_0(k,k+\sqrt{t}) \\
&+ (p_1^2+p_4^2-p_3^2-p_2^2)\frac{B_0(k,k+\sqrt{s})}{4\Lambda^2} + (p_1^2+p_4^2-p_3^2-p_2^2)\frac{B_0(k,k+\sqrt{t})}{4\Lambda^2}\Big] .
\end{aligned} \tag{5.2.29}$$

The next contribution to the four-scalar vertex refers to the T-Boxes and the associated set contains the channels s and t while for each channel there are two possible topologies. Notice that the T-Boxes are determined by two pairs of two linear combinations of the external momenta, (P_1, P_2) and (P_A, P_B). A useful choice for these pairs for the channels $T_{1,\cdots,4}$ is the following

$$\begin{aligned}
T_1 &: \quad (p_1+p_2, p_1+p_2+p_3)\,, \qquad (p_1+p_2+2p_3, 0) \\
T_2 &: \quad (p_1+p_3, p_1+p_3+p_4)\,, \qquad (p_1+p_3+2p_4, 0)
\end{aligned}$$

$$
\begin{aligned}
T_3 \quad &: \quad (p_2, p_1+p_2)\,, \qquad (2p_2, p_1+p_2) \\
T_4 \quad &: \quad (p_1, p_1+p_3)\,, \qquad (2p_1, p_1+p_3)\,,
\end{aligned}
\tag{5.2.30}
$$

and the counting of the internal momenta starts always from the photon-field with assigned loop-momentum k and it is clockwise. The symmetry factor for this topology is $S_{\mathcal{B}_{4,\phi}^{T_{1,\cdots,4}}} = 1$. Here it is enough to evaluate just one channel since the summation over $T_{1,\cdots,4}$ gives the full contribution of the T-Boxes. Then the first s-channel is

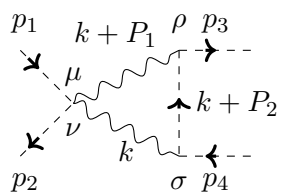

$$= \; i\mathcal{B}_{4,\phi}^{T,1s}$$

and its explicit form is given by

$$
\begin{aligned}
i\mathcal{B}_{4,\phi}^{T,1s} &= (-i)2g_4^4 \int \frac{d^4k}{(2\pi)^4} \frac{-i\eta^{\mu\rho}Q_\rho(P_j,P_l,k)}{k^2} \frac{-i\eta^{\nu\sigma}Q_\sigma(P_j,P_l,k)}{(k+P_1)^2} \frac{iQ_{\mu\nu}(P_j,P_l,k)}{(k+P_2)^2} \Rightarrow \\
\mathcal{B}_{4,\phi}^{T,1s} &= -2g_4^4 \int \frac{d^4k}{(2\pi)^4 i} \frac{Q^\mu(P_j,P_l,k)Q^\nu(P_j,P_l,k)Q_{\mu\nu}(P_j,P_l,k)}{k^2(k+P_1)^2(k+P_2)^2} \\
&= -2g_4^4 \int \frac{d^4k}{(2\pi)^4 i} \left[(k+P_A)^\mu + \frac{(k+P_A)^\mu(k+P_1)^2}{\Lambda^2} - \frac{(k+P_A)\cdot(k+P_1)\,(k+P_1)^\mu}{\Lambda^2}\right] \times \\
&\quad \left[(k+P_B)^\nu + \frac{(k+P_B)^\nu k^2}{\Lambda^2} - \frac{(k+P_B)\cdot k\, k^\nu}{\Lambda^2}\right] \frac{1}{k^2(k+P_1)^2(k+P_2)^2} \times \\
&\quad \left[\eta_{\mu\nu} + \frac{\eta_{\mu\nu}p_2\cdot p_1 + k_\mu(p_2-p_1)_\nu}{2\Lambda^2} + \frac{2(\eta_{\mu\nu}k^2 - k_\mu k_\nu)}{\Lambda^2}\right]
\end{aligned}
$$

with $j = 1,2$ and $l = A,B$. Expanding the brackets, reducing the integrals and keeping terms up to $\mathcal{O}(1/\Lambda^2)$, the above expression becomes

$$
\begin{aligned}
\mathcal{B}_{4,\phi}^{T,1s} &= -2g_4^4 \Bigg[(1+\frac{p_1\cdot p_2}{2\Lambda^2}) B_0(k,k+P_2-P_1) - \frac{P_A\cdot P_2}{2\Lambda^2} B_0(k,k+P_2) + \Big(-P_1\cdot P_2 + \frac{P_A\cdot(P_2-P_1)}{2} \\
&+ \frac{P_A\cdot(p_2-p_1)}{8} - \frac{(P_2+P_1)\cdot(p_2-p_1)}{4}\Big) \frac{B_0(k,k+P_2-P_1)}{\Lambda^2} \\
&+ 3P_B\cdot\Big(P_A - \frac{P_1}{4}\Big) \frac{B_0(k,k+P_2-P_1)}{\Lambda^2} + [\mathcal{B}_{4,\phi}^{T,1s}]_f \Bigg]\,,
\end{aligned}
\tag{5.2.31}
$$

where $[\mathcal{B}_{4,\phi}^{T,1s}]_f$ includes all the reduced and finite integrals of the C_0 and C_μ form. Then the complete contribution of the T-Boxes is given by

$$
\mathcal{B}_{4,\phi}^{T} = \sum_{(P_A,P_B)} \sum_{(P_1,P_2)} \mathcal{B}_{4,\phi}^{T,1s}(P_1,P_2,P_A,P_B)\,. \tag{5.2.32}
$$

Note that there are three terms which do not include exclusively the capital momenta, nevertheless, when we consider the t-channels the replacement $p_1\cdot p_2 \to p_1\cdot p_3$ and $(p_2-p_1) \to (p_3-p_1)$ should take place.

The last set of 1-loop diagrams, correcting the 4-scalar vertex, regards the S-Boxes. Recall that there is only one channel here which however is given in two different topologies since there are two possible ways to arrange the propagators inside the loop. In that sense the diagrams are determined by seven linear combinations of the external momenta, P_1, P_2, P_3, P_A, P_B, P_C and P_D which are defined in the following. Therefore the diagram of the first topology is given by

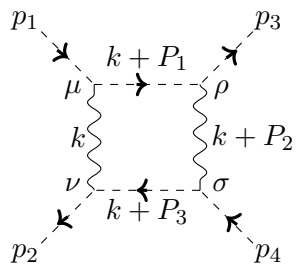

$$= i\mathcal{B}^{S,1}_{4,\phi}\,,$$

with symmetry factor $S_{\mathcal{B}^{S,1}_{4,\phi}} = 1$ and momentum conservation $p_1 + p_2 + p_3 + p_4 = 0$. Starting the counting of the loop momenta from the gauge propagator a useful choice for the P's reads

$$\begin{aligned} &P_1 = p_1, \quad P_2 = p_1 + p_3 \;\text{ and }\; P_3 = p_1 + p_3 + p_4 \\ &P_A = 2p_1, \quad P_B = 0, \quad P_C = p_1 + p_3 = P_2 \;\text{ and }\; P_D = p_1 + p_3 + 2p_4\,, \end{aligned} \tag{5.2.33}$$

then its explicit form reads

$$\begin{aligned} i\mathcal{B}^{S,1}_{4,\phi} &= g_4^4 \int \frac{d^4k}{(2\pi)^4} \frac{-i\eta^{\mu\nu} Q_\mu(P_j,P_l,k) Q_\nu(P_j,P_l,k)}{k^2} \frac{i}{(k+P_1)^2} \frac{-i\eta^{\rho\sigma} Q_\rho(P_j,P_l,k) Q_\sigma(P_j,P_l,k)}{(k+P_2)^2} \frac{i}{(k+P_3)^2} \Rightarrow \\ \mathcal{B}^{S,1}_{4,\phi} &= g_4^4 \int \frac{d^4k}{(2\pi)^4 i} \frac{\eta^{\mu\nu} Q_\mu(P_j,P_l,k) Q_\nu(P_j,P_l,k) \eta^{\rho\sigma} Q_\rho(P_j,P_l,k) Q_\sigma(P_j,P_l,k)}{k^2 (k+P_1)^2 (k+P_2)^2 (k+P_3)^2} \\ &= g_4^4 \int \frac{d^4k}{(2\pi)^4 i} \eta^{\mu\nu} \left[(k+P_A)_\mu + \frac{(k+P_A)_\mu k^2 - (k+P_A)\cdot k\, k_\mu}{\Lambda^2} \right] \frac{k_\nu}{k^2 (k+P_1)^2 (k+P_2)^2 (k+P_3)^2} \times \\ &\quad \eta^{\rho\sigma} \left[(k+P_C)_\rho + \frac{(k+P_C)_\rho (k+P_2)^2 - (k+P_C)\cdot(k+P_2)\,(k+P_2)_\rho}{\Lambda^2} \right] \times \\ &\quad \left[(k+P_D)_\sigma + \frac{(k+P_D)_\sigma (k+P_2)^2 - (k+P_D)\cdot(k+P_2)\,(k+P_2)_\sigma}{\Lambda^2} \right] \\ &= g_4^4 \int \frac{d^4k}{(2\pi)^4 i} \frac{k\cdot(k+P_A)\Big[(k+P_2)\cdot(k+P_D)\Big]}{k^2 (k+P_1)^2 (k+P_2)^2 (k+P_3)^2}\,, \end{aligned}$$

where here $j = 1,2,3$ and $l = A,B,C,D$. Notice that for this specific type of diagrams the contribution of $\mathcal{O}(1/\Lambda^2)$ terms is canceled and the result is the usual one in SQED. So performing the products and reducing the integrals we get, similarly with the Appendix of [3], that

$$\begin{aligned} \mathcal{B}^{S,1}_{4,\phi} &= g_4^4 \Big[B_0(k, k+P_3-P_2) - 2P_1^\mu C_\mu(k, k+P_2-P_1, k+P_3-P_1) \\ &+ \Big(P_D + P_2 + P_A\Big)^\mu C_\mu(k+P_1, k+P_2, k+P_3) + P_1^2 C_0(k, k+P_2-P_1, k+P_3-P_1) \\ &+ \Big(\eta^{\mu\nu} P_2\cdot P_D + P_A^\mu (P_2+P_D)^\nu\Big) D_{\mu\nu}(k, k+P_1, k+P_2, k+P_3) \\ &+ P_2\cdot P_D\, P_A^\mu D_\mu(k, k+P_1, k+P_2, k+P_3) \Big]\,. \end{aligned} \tag{5.2.34}$$

Now the diagram of the second topology is

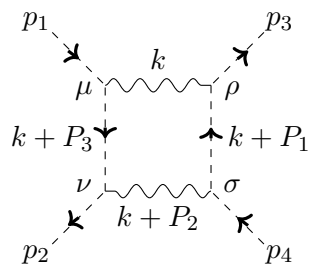

$$= \; i\mathcal{B}^{S,2}_{4,\phi}\,,$$

with symmetry factor $S_{\mathcal{B}^{S,2}_{4,\phi}} = 1$ and momentum conservation $p_1 + p_2 + p_3 + p_4 = 0$. Following our loop-momentum counting a useful choice would be

$$\begin{aligned} &P_1 = p_3, \quad P_2 = p_3 + p_4 \;\text{ and }\; P_3 = p_2 + p_3 + p_4 \\ &P_A = 0, \quad P_B = 2p_2 + p_3 + p_4, \quad P_C = 2p_3 = 2P_1 \;\text{ and }\; P_D = p_3 + p_4 = P_2 \end{aligned} \tag{5.2.35}$$

and hence the above diagram gives directly

$$\begin{aligned} \mathcal{B}^{S,2}_{4,\phi} \;=\;& g_4^4\Big[B_0(k, k+P_3-P_2) - 2P_1^\mu C_\mu(k, k+P_2-P_1, k+P_3-P_1) \\ +\;& \Big(P_C + P_2 + 2P_1\Big)^\mu C_\mu(k+P_1, k+P_2, k+P_3) + P_1^2 C_0(k, k+P_2-P_1, k+P_3-P_1) \\ +\;& \Big(\eta^{\mu\nu} P_2\cdot P_C + 2P_1^\mu (P_2+P_C)^\nu\Big) D_{\mu\nu}(k, k+P_1, k+P_2, k+P_3) \\ +\;& 2P_2\cdot P_C\, P_1^\mu D_\mu(k, k+P_1, k+P_2, k+P_3)\Big]\,. \end{aligned} \tag{5.2.36}$$

Finally, the complete S-Box contribution is given by

$$\mathcal{B}^{S}_{4,\phi} = \mathcal{B}^{S,1}_{4,\phi}(P_j, P_{j'}) + \mathcal{B}^{S,2}_{4,\phi}(P_j, P_{j'})\,, \tag{5.2.37}$$

with $j = 1, 2, 3$ and $j' = A, B, C, D$, while the full 1-loop correction to the $(\bar\phi\phi)^2$ vertex yields

$$\mathcal{B}_{4,\phi} = \mathcal{B}^{C}_{4,\phi} + \mathcal{B}^{T}_{4,\phi} + \mathcal{B}^{S}_{4,\phi}\,. \tag{5.2.38}$$

All the needed information to start the renormalization procedure for the boundary action, $S^{\mathrm{b-h}}$, is now in our hands and is contained in Eq. (5.2.16), Eq. (5.2.21) and Eq. (5.2.38). In what follows we use these equations to extract the counter-terms and the β-functions of the associated couplings.

5.2.3 Renormalization and β-functions

Regarding the Boundary-Hybrid action given in Eq. (5.2.11), there is only one step left towards the calculation of the β-functions and of the RG flows. This step refers to the renormalization procedure, according to which the divergencies cancel after inserting appropriate counter-terms in the action. An important point is the following: Recall from Section 5.2.2 that every 1-loop diagram that we faced was reduced to scaleless integrals due to the absence of explicit mass terms in the classical Lagrangian. Since our scheme is DR, these integrals in general vanish, however here we distinguish three cases following the Appendices of [3, 30]. According to those

the scalar integrals of A_0-type are forced to vanish in DR while, for the B_0-type we have the freedom to separate the UV from the IR divergence. So on our road to the β-functions A_0's will be absent and B_0's will contribute a $2/\varepsilon$ divergent term. The third case refers to the finite integrals which, when scaleless, take a $0/0$ form and they can be replaced by arbitrary constants.

We now proceed with the renormalization of the couplings $g_{4,0}$ and $c^{(6)}_{1,0}$ as well as of the fields $A^3_{\mu,0}$ and ϕ_0. The subscript 0 indicates bare quantities. Regarding the gauge coupling recall that it contains g_0 and the anisotropy factor γ_0 which in principle both get renormalized. Then their contribution will be hidden in the counter-term/β-function of $g_{4,0}$. Moreover, to simplify expressions, the alternative dimensionless in d-dimensions coupling

$$\alpha_{4,0} \equiv \frac{1}{(4\pi)^2}\mu^{d-4}g^2_{4,0} \tag{5.2.39}$$

can be considered. This and its 5d analogue will be used extensively in the following. The counter-term for the gauge coupling is given by

$$\begin{aligned} g_{4,0} &= g_4 + \delta g_4 \Rightarrow \\ g_{4,0} &= g_4(1+\frac{\delta g_4}{g_4}) = (1+\delta_{g_4})g_4 = Z_{g_4}g_4 \end{aligned} \tag{5.2.40}$$

while for the scalar self-coupling by

$$\begin{aligned} c^{(6)}_{1,0} &= c^{(6)}_1 + \delta c^{(6)}_1 \\ &= c^{(6)}_1(1+\frac{\delta c^{(6)}_1}{c^{(6)}_1}) = (1+\delta_{c^{(6)}_1})c^{(6)}_1 = Z_{c^{(6)}_1}c^{(6)}_1 \,. \end{aligned} \tag{5.2.41}$$

In d-dimensions the scale independence relations of the bare couplings

$$\mu\frac{dg_{4,0}}{d\mu} = \mu\frac{d(4\pi\mu^{\frac{4-d}{2}}\sqrt{\alpha_{4,0}})}{d\mu} = 0 \tag{5.2.42}$$

$$\mu\frac{dc^{(6)}_{1,0}}{d\mu} = 0 \tag{5.2.43}$$

generate the β-function equations. Similarly, for the anomalous dimensions of the fields we define

$$\phi_0 = \sqrt{Z_\phi}\phi = \sqrt{1+\delta_\phi}\phi \tag{5.2.44}$$

$$A^3_{\mu,0} = \sqrt{Z_A}A^3_\mu = \sqrt{1+\delta_A}A^3_\mu \,. \tag{5.2.45}$$

The next step is to apply the above relations to our Lagrangian given by

$$\begin{aligned} \mathcal{L}^{\rm b-h}_0 &= -\frac{1}{4}F^3_{\mu\nu,0}F^{3,\mu\nu}_0 + \frac{1}{2\xi}A^3_{\mu,0}\partial^\mu\partial_\nu A^{3,\nu}_0 - \bar\phi_0\Box\phi_0 - \frac{c^{(6)}_{1,0}}{4\Lambda^2}(\bar\phi_0\phi_0)\bar\phi_0\Box\phi_0 - \bar c^3_0\Box c^3_0 \\ &+ ig_{4,0}\Big\{\eta_{\mu\rho} - \frac{\eta_{\mu\rho}\Box - \partial_\mu\partial_\rho}{\Lambda^2}\Big\}A^{3,\rho}_0\Big(\bar\phi_0\partial^\mu\phi_0 - \phi_0\partial^\mu\bar\phi_0\Big) + g^2_{4,0}(A^3_{\mu,0})^2\bar\phi_0\phi_0 \\ &+ \frac{g^2_{4,0}}{2\Lambda^2}\Big(A^3_{\mu,0}A^3_{\rho,0}\partial^\rho\bar\phi_0\partial^\mu\phi_0 + A^3_{\mu,0}\partial^\rho A^3_{\rho,0}\partial^\mu(\bar\phi_0\phi_0)\Big) - 2g^2_{4,0}\frac{A^{3,\mu}_0(\eta_{\mu\rho}\Box - \partial_\mu\partial_\rho)A^{3,\rho}_0}{\Lambda^2}\bar\phi_0\phi_0 \end{aligned}$$

$$+ \quad i\frac{g_{4,0}\, c_{1,0}^{(6)}}{4\Lambda^2} A^3_{\mu,0}\bar{\phi}_0\phi_0\Big(\bar{\phi}_0\partial^\mu\phi_0 - \phi_0\partial^\mu\bar{\phi}_0\Big) + \frac{g_{4,0}^2\, c_{1,0}^{(6)}}{4\Lambda^2}(A^3_{\mu,0})^2(\bar{\phi}_0\phi_0)^2 + \mathcal{L}_l^{\rm b-h} \tag{5.2.46}$$

where $\mathcal{L}_l^{\rm b-h}$ corresponds to the 1-loop corrections. Then substituting Eq. (5.2.40), Eq. (5.2.41), Eq. (5.2.44) and Eq. (5.2.45) into Eq. (5.2.46) we obtain

$$\mathcal{L}_0^{\rm b-h} = \mathcal{L}^{\rm b-h} + \mathcal{L}^{\rm b-h}_{\rm count.} + \mathcal{L}^{\rm b-h}_{\rm correc.} \equiv \mathcal{L}^{\rm b-h} + \mathcal{L}^{\rm b-h}_{\rm 1-loop}$$

with $\mathcal{L}^{\rm b-h}$ the renormalized Lagrangian

$$\begin{aligned}
\mathcal{L}^{\rm b-h} &= -\frac{1}{4}F^3_{\mu\nu}F^{3,\mu\nu} + \frac{1}{2}A^3_\mu\partial^\mu\partial_\nu A^{3,\nu} - \bar{\phi}\Box\phi - \frac{c_1^{(6)}}{4\Lambda^2}(\bar{\phi}\phi)\bar{\phi}\Box\phi - \bar{c}^3\Box c^3 \\
&+ ig_4\Big\{\eta_{\mu\rho} - \frac{\eta_{\mu\rho}\Box - \partial_\mu\partial_\rho}{\Lambda^2}\Big\}A^{3,\rho}\Big(\bar{\phi}\partial^\mu\phi - \phi\partial^\mu\bar{\phi}\Big) + g_4^2(A^3_\mu)^2\bar{\phi}\phi \\
&+ \frac{g_4^2}{2\Lambda^2}\Big(A^3_\mu A^3_\rho\partial^\rho\bar{\phi}\partial^\mu\phi + A^3_\mu\partial^\rho A^3_\rho\partial^\mu(\bar{\phi}\phi)\Big) - 2g_4^2\frac{A^{3,\mu}(\eta_{\mu\rho}\Box - \partial_\mu\partial_\rho)A^{3,\rho}}{\Lambda^2}\bar{\phi}\phi \\
&+ i\frac{g_4\, c_1^{(6)}}{4\Lambda^2}A^3_\mu\bar{\phi}\phi\Big(\bar{\phi}\partial^\mu\phi - \phi\partial^\mu\bar{\phi}\Big) + \frac{g_4^2\, c_1^{(6)}}{4\Lambda^2}(A^3_\mu)^2(\bar{\phi}\phi)^2
\end{aligned} \tag{5.2.47}$$

and $\mathcal{L}^{\rm b-h}_{\rm 1-loop}$ the finite 1-loop Lagrangian which in momentum space becomes

$$\begin{aligned}
\mathcal{L}^{\rm b-h}_{\rm 1-loop} &= \frac{1}{2}\Big\{-\delta_A\eta^{\mu\nu}q^2 + \mathcal{M}_A^{\mu\nu}\Big\}A^3_\mu A^3_\nu + \Big\{\delta_\phi p_1^2 + \mathcal{M}_\phi\Big\}\phi\bar{\phi} + \Big\{(\delta c_1^{(6)} + 2c_1^{(6)}\delta_\phi)\frac{p^2}{\Lambda^2} - \mathcal{B}_{4,\phi}\Big\}\frac{(\bar{\phi}\phi)^2}{4} \\
&+ \Big\{g_4\delta_3\left((p_1+p_2)_\mu + \frac{(p_1+p_2)_\mu q^2 - (p_1+p_2)\cdot q\, q_\mu}{\Lambda^2}\right) + \mathcal{K}_{\bar{\phi}A\phi,\mu}\Big\}A^3_\mu\bar{\phi}\phi \\
&+ \Big\{\delta_4 g_4^2\left(\eta^{\mu\nu} + \frac{\eta^{\mu\nu}p_1\cdot p_2 + q_1^\mu(p_2-p_1)^\nu}{2\Lambda^2} + \frac{2(\eta^{\mu\nu}q_1^2 - q_1^\mu q_1^\nu)}{\Lambda^2}\right) + \mathcal{B}^{\mu\nu}_{A\bar{\phi}A\phi}\Big\}A^3_\mu A^3_\nu\phi\bar{\phi} \\
&+ \Big\{\delta_5\frac{g_4\, c_1^{(6)}}{\Lambda^2}(p_1+p_2)^\mu + \mathcal{B}^\mu_{5,A(\bar{\phi}\phi)^2}\Big\}\frac{A^3_\mu(\phi\bar{\phi})^2}{4} + \Big\{\delta_6\frac{g_4^2\, c_1^{(6)}}{\Lambda^2}\eta^{\mu\nu} + \mathcal{B}^{\mu\nu}_{6,AA(\bar{\phi}\phi)^2}\Big\}\frac{A^3_\mu A^3_\nu(\phi\bar{\phi})^2}{4}\,.
\end{aligned} \tag{5.2.48}$$

Note that there is no counter-term for the Faddeev-Popov ghosts since they are decoupled from the theory.

For the gauge-scalar three- and four-point vertices the following relations hold:

$$\begin{aligned}
Z_3 &= Z_{g_4}Z_\phi\sqrt{Z_A} \Rightarrow \\
1+\delta_3 &= (1+\delta_{g_4})(1+\delta_\phi)(1+\frac{1}{2}\delta_A) \Rightarrow \\
\delta_3 &= \delta_{g_4} + \delta_\phi + \frac{1}{2}\delta_A\,,
\end{aligned} \tag{5.2.49}$$

and

$$\begin{aligned}
Z_4 &= Z_{g_4}^2 Z_\phi Z_A \Rightarrow \\
1+\delta_4 &= (1+2\delta_{g_4})(1+\delta_\phi)(1+\delta_A) \Rightarrow \\
\delta_4 &= 2\delta_{g_4} + \delta_\phi + \delta_A
\end{aligned} \tag{5.2.50}$$

respectively, while for the five- and six-point vertices we get:

$$Z_5 = Z_{g_4}Z_{c_1^{(6)}}Z_\phi^2\sqrt{Z_A} \Rightarrow$$

$$
\begin{aligned}
1+\delta_5 &= (1+\delta_{g_4})(1+\delta_{c_1^{(6)}})(1+2\delta_\phi)(1+\frac{1}{2}\delta_A) \Rightarrow \\
\delta_5 &= \delta_{g_4}+\delta_{c_1^{(6)}}+2\delta_\phi+\frac{1}{2}\delta_A\,, \qquad (5.2.51)
\end{aligned}
$$

and

$$
\begin{aligned}
Z_6 &= Z_{g_4}^2 Z_{c_1^{(6)}} Z_\phi^2 Z_A \Rightarrow \\
1+\delta_6 &= (1+2\delta_{g_4})(1+\delta_{c_1^{(6)}})(1+2\delta_\phi)(1+\delta_A) \Rightarrow \\
\delta_6 &= 2\delta_{g_4}+\delta_{c_1^{(6)}}+2\delta_\phi+\delta_A \qquad (5.2.52)
\end{aligned}
$$

respectively. The Feynman rules for the counter-terms deriving from Eq. (5.2.48) are

- Gauge boson 2-point function

$= -i\delta_A \eta_{\mu\nu} q^2$

- Scalar 2-point function

$= i\delta_\phi p_1^2$

- The A_μ-ϕ-$\bar{\phi}$ vertex counter-term

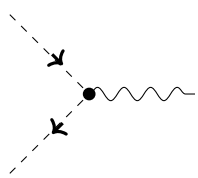

$= ig_4\delta_3 Q_\mu(p,q)$

- The $(\bar{\phi}\phi)^2$ vertex counter-term

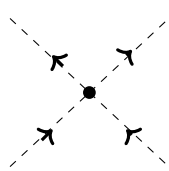

$= i(\delta c_1^{(6)} + 2c_1^{(6)}\delta_\phi)\frac{p^2}{\Lambda^2}\,.$

- The A_μ-A_ν-ϕ-$\bar{\phi}$ vertex counter-term

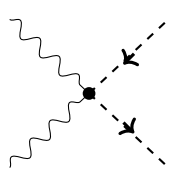

$= 2i\delta_4 g_4^2 Q_{\mu\nu}(p,q)$

- Four-scalars one-photon vertex counter-term

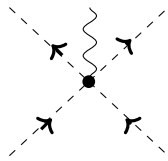

$$= \; i\delta_5 g_4 \, c_1^{(6)} \, \frac{(p_1+p_2)_\mu}{\Lambda^2} \, .$$

- Four-scalars two-photons vertex counter-term

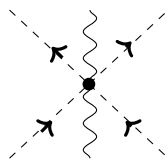

$$= \; 2i\delta_6 \, g_4^2 \frac{c_1^{(6)}}{\Lambda^2} \eta_{\mu\nu} \, .$$

The renormalization conditions needed to make the theory finite at 1-loop are in order. For the gauge boson propagator, diagrammatically, we have that

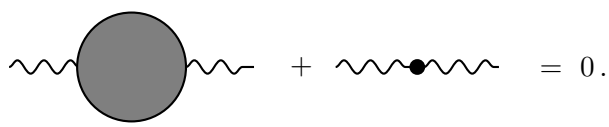

This implies that the contracted gauge propagator satisfies

$$-\frac{1}{3}\left(\eta^{\mu\nu} - \frac{q^\mu q^\nu}{q^2}\right)(-\delta_A \eta_{\mu\nu} q^2) + \mathcal{M}_A(q^2) = 0 \, . \tag{5.2.53}$$

The second condition demands that

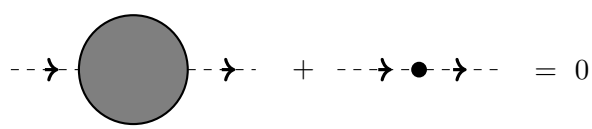

which, as equation, reads

$$\delta_\phi p_1^2 + \mathcal{M}_\phi(p_1^2) = 0 \, . \tag{5.2.54}$$

Finally, the last condition refers to the four-scalar vertex and demands that

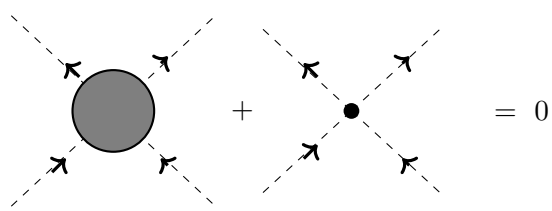

or

$$(\delta c_1^{(6)} + 2c_1^{(6)}\delta_\phi)\frac{p^2}{\Lambda^2} - \mathcal{B}_{4,\phi}(p^2) = 0 \, . \tag{5.2.55}$$

Now for the determination of the counterterms we need to evaluate the 1-loop diagrams, obtained in Section 5.2.2, which here is done with the help of dimensional regularization. Let

us start with the condition of the vacuum polarization which includes $\mathcal{M}_A$ whose complete contribution is given in Eq. (5.2.21). In DR this becomes

$$\mathcal{M}_A = \frac{1}{16\pi^2}\Big[\frac{2q^2g_4^2}{3}\frac{1}{\varepsilon} + \frac{4q^4g_4^2}{3\Lambda^2}\frac{1}{\varepsilon}\Big] + [\mathcal{M}_A]_f \tag{5.2.56}$$

and as a consequence Eq. (5.2.53) gives

$$\delta_A = \frac{1}{16\pi^2}\Big[-\frac{2g_4^2}{3}\frac{1}{\varepsilon} - \frac{4q^2g_4^2}{3\Lambda^2}\frac{1}{\varepsilon}\Big]\,. \tag{5.2.57}$$

Next consider the scalar propagator whose 1-loop correction is given in Eq. (5.2.16) and in DR reads

$$\mathcal{M}_\phi = \frac{1}{16\pi^2}\Big[-4p_1^2g_4^2(1-\frac{p_1^2}{\Lambda^2})\frac{1}{\varepsilon}+\Big] + [\mathcal{M}_\phi^{\phi A_\mu}]_f\,. \tag{5.2.58}$$

Substituting this back to the condition Eq. (5.2.54) we get

$$\delta_\phi = \frac{1}{16\pi^2}\Big[4g_4^2\frac{1}{\varepsilon} - \frac{4g_4^2p_1^2}{\Lambda^2}\frac{1}{\varepsilon}\Big]\,. \tag{5.2.59}$$

As we have already mentioned, due to gauge invariance the relation $\delta_\phi = \delta_3$ holds. So using Eq. (5.2.49) we can extract the counterterm of the gauge coupling as

$$\begin{aligned}
\delta_{g_4} &= -\frac{1}{2}\delta A \Rightarrow \\
\frac{\delta g_4}{g_4} &= \frac{1}{16\pi^2}\Big[\frac{g_4^2}{3}\frac{1}{\varepsilon} + \frac{2q^2g_4^2}{3\Lambda^2}\frac{1}{\varepsilon}\Big] \Rightarrow \\
\delta g_4 &= \frac{1}{16\pi^2}\Big[\frac{g_4^3}{3}\frac{1}{\varepsilon} + \frac{2q^2g_4^3}{3\Lambda^2}\frac{1}{\varepsilon}\Big]\,.
\end{aligned} \tag{5.2.60}$$

Finally for the last condition we need $\mathcal{B}_{4,\phi}$ which is given in Eq. (5.2.38) and in DR gives

$$\mathcal{B}_{4,\phi} = \frac{1}{16\pi^2}\Big[\frac{4(c_1^{(6)}p^2)^2}{\Lambda^4\varepsilon} + \frac{52g_4^4}{\varepsilon} + \frac{2g_4^4\{f_C(p_i)+f_T(p_i)+f_S(p_i)\}}{\Lambda^2\varepsilon}\Big] + [\mathcal{B}_{4,\phi}]_f\,, \tag{5.2.61}$$

where $i = 1,2,3,4$ and f_C, f_T and f_S are functions of the external momenta coming from the C-, T- and S-Boxes respectively. Substituting the above in the condition of Eq. (5.2.55) the counter-term of $c_1^{(6)}$, for $p^2 \equiv p_1^2$, yields

$$\delta c_1^{(6)} = \frac{1}{16\pi^2}\Big[4(c_1^{(6)})^2\frac{p_1^2}{\Lambda^2} - 8c_1^{(6)}g_4^2 + 52g_4^4\frac{\Lambda^2}{p_1^2} + \frac{8c_1^{(6)}g_4^2p_1^2}{\Lambda^2} + \frac{2g_4^4\{f_C(p_i)+f_T(p_i)+f_S(p_i)\}}{p_1^2}\Big]\frac{1}{\varepsilon}\,. \tag{5.2.62}$$

Note that δ_A, δ_ϕ and δg_4 reduce to the values of the usual SQED (see [3]) when the HDO are decoupled. As the next step should be to determine the β-function of the couplings, it is natural to choose an off-shell momentum scheme, $p^2 \neq 0$, since the classical Lagrangian lacks of explicit mass terms. This is actually necessary otherwise the calculation of $c_1^{(6)}$'s β-function is ambiguous. At this stage, it may seem that our model has two dimensionless couplings, $c_1^{(6)}$ and g_4 and three dimensionful scales μ, Λ and v in case a vev develops. On the other hand, the action Eq. (5.2.11) is a product of the orbifold lattice which, for the boundary, inherits the model only with g_4, μ and v so there is an apparent mismatch of the independent parameters. Nevertheless

this is not true because Λ and v depend on the regularization scale, as a consequence the only independent scale is μ. In addition, as we will see in the next section, the minimization condition of the scalar potential will induce a relation between $c_1^{(6)}$ and g_4, leaving us with the correct number of parameters.

The off-shell regularization scheme exploited here is choosing $p_i^2 = q_i^2 = \Lambda^2$, which together with the momentum and channel conservation relations

$$p_1 + p_2 + p_3 + p_4 = 0 \quad \text{and} \quad \{s = 4\Lambda^2, t = 0\}$$

fix

$$p_1 \cdot p_2 = p_3 \cdot p_4 = \Lambda^2, \quad \text{and} \quad p_1 \cdot p_3 = p_2 \cdot p_4 = p_1 \cdot p_4 = p_2 \cdot p_3 = -\Lambda^2 \,.$$

Using the above scheme to simplify our counter-terms, we obtain from Eq. (5.2.59), Eq. (5.2.60) and Eq. (5.2.62)

$$\begin{aligned}
\delta_\phi &= 0 && (5.2.63)\\
\delta g_4 &= \frac{1}{16\pi^2}\left[\frac{g_4^3}{\varepsilon}\right], && (5.2.64)\\
\delta c_1^{(6)} &= \frac{1}{16\pi^2}\left[4(c_1^{(6)})^2 + 34 g_4^4\right]\frac{1}{\varepsilon} && (5.2.65)
\end{aligned}$$

respectively. Now we are in position to determine the β-functions of the two couplings. For this we work in d-dimensions so we need to know the dimensionality of the couplings when $d \neq 4$. Keep in mind that the classical dimensions of the gauge and scalar fields, determined from the corresponding kinetic terms, are $d_{A^3_\mu} = \frac{d-2}{2}$ and $d_\phi = \frac{d-2}{2}$ respectively. Starting with the gauge coupling, its associated operators are $A^3_\mu \bar{\phi}\partial\phi$ and $(A^3_\mu)^2\bar{\phi}\,\phi$ and a dimensional analysis of the latter gives

$$\begin{aligned}
2d_{g_4} + 2d_{A^3_\mu} + 2d_\phi &= d \Rightarrow\\
2d_{g_4} + d - 2 + d - 2 &= d \Rightarrow\\
d_{g_4} &= \frac{4-d}{2} && (5.2.66)
\end{aligned}$$

in accordance with Eq. (5.2.42). For the scalar self-coupling there is only one associated operator, $(\bar{\phi}\phi)^2\bar{\phi}\Box\phi$ suppressed by $1/\Lambda^2$, indicating that

$$\begin{aligned}
d_{c_1^{(6)}} + 2 + 4d_\phi - 2 &= d \Rightarrow\\
d_{c_1^{(6)}} + 2(d-2) &= d \Rightarrow\\
d_{c_1^{(6)}} &= 4 - d\,. && (5.2.67)
\end{aligned}$$

These classical dimensions and since Eq. (5.2.39) and Eq. (5.2.64) determine $\delta\alpha_4 = 2\alpha_4^2/\varepsilon$, together with Eq. (5.2.42) yield the β-function of the gauge coupling

$$\beta_{\alpha_4} = -d_{\alpha_4}\,\alpha_4 + 2\alpha_4^2 \quad \text{or} \quad \beta_{g_4\mu^{\frac{-\varepsilon}{2}}} = -d_{g_4}\,g_4\mu^{\frac{-\varepsilon}{2}} + \frac{g_4^3\mu^{\frac{-3\varepsilon}{2}}}{16\pi^2} \Rightarrow$$

$$\beta_{\alpha_4} = -\varepsilon\alpha_4 + 2\alpha_4^2 \quad \text{or} \quad \beta_{g_4\mu^{\frac{-\varepsilon}{2}}} = -\frac{\varepsilon}{2}g_4\mu^{\frac{-\varepsilon}{2}} + \frac{g_4^3\mu^{\frac{-3\varepsilon}{2}}}{16\pi^2}\,.$$

For $c_1^{(6)}$, using Eq. (5.2.43), we obtain the β-function

$$\begin{aligned}\beta_{c_1^{(6)}} &= -d_{c_1^{(6)}}\, c_1^{(6)} + \frac{1}{16\pi^2}\left[4(c_1^{(6)})^2 + 34 g_4^4\right] \Rightarrow \\ \beta_{c_1^{(6)}} &= -\varepsilon c_1^{(6)} + \frac{1}{16\pi^2}\left[4(c_1^{(6)})^2 + 34 g_4^4\right].\end{aligned}$$

For completeness let us just present now the corresponding β-function of the bulk gauge coupling. There is no need for extra calculations here since the bulk lattice action, given in Eq. (5.A.37), after considering the naive continuum limit in Minkowski space, yields the Lagrangian

$$\begin{aligned}\mathcal{L}^B &= -\frac{1}{4}F^A_{\mu\nu}F^{A,\mu\nu} + \frac{1}{16\Lambda^2}(D^\mu F^A_{\mu\nu})(D_\mu F^{A,\mu\nu}) - \frac{g_5}{24\Lambda^2} f_{ABC} F^A_{\mu\nu}F^B_{\nu\rho}F^C_{\rho\mu} \\ &+ (\overline{D_\mu \Phi^A})(D^\mu \Phi^A) - \frac{1}{4\Lambda^2}(\overline{D^2\Phi^A})(D^2\Phi^A)\Bigg]. \end{aligned} \tag{5.2.68}$$

The above is a 5d version of the Lee-Wick gauge model [26, 28] from where we can extract the bulk β-functions by generalizing the results to $d = 5$. Now the Lee-Wick Lagrangian is given in [26] and it is

$$\begin{aligned}\mathcal{L} &= -\frac{1}{4}F^A_{\mu\nu}F^{A,\mu\nu} + \frac{1}{2m^2}(D^\mu F^A_{\mu\nu})(D_\mu F^{A,\mu\nu}) + \frac{k_F\, g}{2m^2} f_{ABC}F^A_{\mu\nu}F^B_{\nu\rho}F^C_{\rho\mu} + (D_\mu\phi^A)^*(D^\mu\phi^A) \\ &- \frac{1}{m^2}\left\{\delta_1 (D^2\phi^A)^*(D^2\phi^A) + ig\delta_2\,(\phi^A)^*(D_\mu F^{\mu\nu})D_\nu\phi^A + g^2\delta_3\,(\phi^B)^* F^A_{\mu\nu}F^{A,\mu\nu}\phi^B\right\}\Bigg] \end{aligned} \tag{5.2.69}$$

and the $d = 4$ β-function that derives from it, is

$$\beta(g) = -\frac{g^3}{16\pi^2}\left[\left(\frac{43}{6} - 18k_F + \frac{9}{2}k_F^2\right)C_2 - \left(\frac{\delta_1 + 6\delta_3}{3\delta_1}\right)n_\phi\right]. \tag{5.2.70}$$

C_2 is the Casimir operator in the adjoint representation, which for $SU(2)$ is $C_2 = 2$. n_ϕ is the number of scalar fields and k_F, δ_1 and δ_3 are couplings multiplying the HDO. Back to our model, the only coupling in Eq. (5.2.68) is g_5, a consequence of the lattice origin of the action, so there should be only one independent β-function which should be extracted from Eq. (5.2.70). A direct comparison of Eq. (5.2.68) and Eq. (5.2.69) can be made by setting $\delta_2 = \delta_3 = 0$ in the latter and defining $16\Lambda^2 = 2m^2$, $k_F = -2/3$ and $\delta_1 = 2$ in the former, to obtain

$$\begin{aligned}\mathcal{L}^B &= -\frac{1}{4}F^A_{\mu\nu}F^{A,\mu\nu} + \frac{1}{2m^2}(D^\mu F^A_{\mu\nu})(D_\mu F^{A,\mu\nu}) + \frac{k_F\, g_5}{2m^2} f_{ABC}F^A_{\mu\nu}F^B_{\nu\rho}F^C_{\rho\mu} \\ &+ (\overline{D_\mu\Phi^A})(D^\mu\Phi^A) - \frac{\delta_1}{m^2}(\overline{D^2\Phi^A})(D^2\Phi^A). \end{aligned} \tag{5.2.71}$$

The 1-loop part of the β-function of our bulk action, $\beta^1_{g_5}$, can be then obtained by substituting the above parameters together with $n_\phi = 1$ in $\beta(g)$. This yields

$$\beta^1_{g_5} = -\left[\frac{125}{6}\right]\frac{g_5^3}{16\pi^2}. \tag{5.2.72}$$

Finally, considering $(F^A_{\mu\nu})^3/\Lambda^2$ as the associated operator of the coupling g_5, dimensional analysis indicates that

$$d_{g_5} + 3d_{F_{\mu\nu}} - 2 = d \Rightarrow$$

$$
\begin{aligned}
d_{g_5} + 3\frac{d}{2} - 2 &= d \Rightarrow \\
d_{g_5} &= \frac{4-d}{2}
\end{aligned}
\tag{5.2.73}
$$

in d-dimensions, with $d_{F_{\mu\nu}} = d/2$. Hence including the tree level part, the complete 1-loop β-function of the gauge coupling becomes

$$
\beta_{g_5\mu^{\frac{-\varepsilon}{2}}} = -\frac{\varepsilon}{2} g_5 \mu^{\frac{-\varepsilon}{2}} - \frac{125}{6}\frac{g_5^3 \mu^{\frac{-3\varepsilon}{2}}}{16\pi^2} \quad \text{or} \quad \beta_{\alpha_5} = -\varepsilon\alpha_5 - \frac{125}{6N}\alpha_5^2
$$

where we have formed the dimensionless combination $g_5\mu^{-\varepsilon/2}$ and following our steps on the boundary, defined the dimensionless in d-dimensions gauge coupling

$$
\alpha_5 = \frac{2N\, g_5^2}{16\pi^2}\mu^{-\varepsilon}\,. \tag{5.2.74}
$$

Note that in 4-dimensions β_{α_5} is such that the coupling is asymptotically free, a well known characteristic of non-Abelian gauge theories. The contribution of the HDO affects only the numerical factor in front of the 1-loop β-function.

We collect the β-functions for the boundary and bulk couplings in $d = 4-\varepsilon$ dimensions and for $N = 2$:

$$
\beta_{\alpha_4} = -\varepsilon\alpha_4 + 2\alpha_4^2 \quad \text{or} \quad \beta_{g_4\mu^{\frac{-\varepsilon}{2}}} = -\frac{\varepsilon}{2} g_4 \mu^{\frac{-\varepsilon}{2}} + \frac{g_4^3 \mu^{\frac{-3\varepsilon}{2}}}{16\pi^2} \tag{5.2.75}
$$

$$
\beta_{c_1^{(6)}} = -\varepsilon c_1^{(6)} + \frac{1}{16\pi^2}\left[4(c_1^{(6)})^2 + 34 g_4^4\right] \tag{5.2.76}
$$

$$
\beta_{\alpha_5} = -\varepsilon\alpha_5 - \frac{125}{12}\alpha_5^2 \quad \text{or} \quad \beta_{g_5\mu^{\frac{-\varepsilon}{2}}} = -\frac{\varepsilon}{2} g_5 \mu^{\frac{-\varepsilon}{2}} - \frac{125}{6}\frac{g_5^3 \mu^{\frac{-3\varepsilon}{2}}}{16\pi^2}\,. \tag{5.2.77}
$$

5.3 The Higgs phase

The action in Eq. (5.2.11) represents a version of massless SQED, enhanced by dimension-6 operators. If instead of the dimension-6 operators a scalar, quartic polynomial self interaction term was present, it would be just the classic Coleman-Weinberg model [13]. It is natural then to ask if and in what ways the boundary theory of Section 5.2.3 is different from it. We therefore perform next such a comparison, as we analyze the Higgs phase. A short review, including all the main results of the CW model relevant to our discussion, is presented in Appendix 5.D. In the second part of this section we also consider the case where pure polynomial terms are added to our model. This would be of course inconsistent with our construction but it could be easily realized in less restricted models.

5.3.1 The scalar potential and a comparison to the Coleman-Weinberg model

This comparison is going to be very useful because not only will it show the differences between the two models but we can exploit at the same time their similarities. Let us work in momentum

space and take $d = 4$, following Appendix 5.D. First we have to construct the improved effective potential that corresponds to Eq. (5.2.46). Next comes its minimization through which we will see if there exists a non-trivial minimum and whether it imposes a relation between the couplings, as it does in Eq. (5.D.2). Then we determine the scalar and gauge field masses and from those the scalar-to-gauge mass ratio.

The starting point is the renormalized but yet unimproved potential which, up to total derivatives, is

$$\begin{aligned} V(\bar{\phi},\phi) &= -\frac{c_1^{(6)}p^2}{4\Lambda^2}(\bar{\phi}\phi)^2 \equiv -\frac{c_1^{(6)}p_1\cdot p_3}{4\Lambda^2}(\bar{\phi}\phi)^2 \Rightarrow \\ V(\bar{\phi},\phi) &= \frac{c_1^{(6)}}{4}(\bar{\phi}\phi)^2\,, \end{aligned} \tag{5.3.1}$$

where the choice $p^2 \equiv p_1 \cdot p_3 = -\Lambda^2$ comes from the off-shell scheme introduced in the previous section. Note that we used this choice so as to get rid of the unphysical overall minus sign which makes momentum space uncomfortable. One way to see the effect of the improvement is to notice that ϕ could take the place of the renormalization scale, a fact that can be seen through the definition of the effective mass. In particular this is given as the second derivative of V

$$\frac{\partial^2 V(\bar{\phi},\phi)}{\partial\bar{\phi}\partial\phi} = m^2_{\text{eff}}(\mu) = c_1^{(6)}\bar{\phi}\phi\,, \tag{5.3.2}$$

with $\bar{\phi},\phi$ the only running parameters in the r.h.s. This information can be inherited in the potential if instead of looking at the running of μ we focus on the running of ϕ, using the identifications

$$\mu^2 \to m^2_{\text{eff}}(\mu) = c_1^{(6)}\bar{\phi}\phi(\mu) \;\text{ and }\; m^2_{\text{eff}}(\mu_R) = c_1^{(6)}v^2 \tag{5.3.3}$$

with μ_R an arbitrary renormalization scale and v the vacuum expectation value (vev) of the scalar field. To make the argument clear take the fourth derivative of the full 1-loop bare potential of Eq. (5.2.46) which, in momentum space and in the same scheme as Eq. (5.3.1), is

$$\begin{aligned} V^{(4)} &\equiv \frac{\partial^2}{\partial\bar{\phi}^2}\frac{\partial^2}{\partial\phi^2}V_0(\bar{\phi},\phi) = c_1^{(6)} + \delta c_1^{(6)} + 2c_1^{(6)}\delta_\phi + \mathcal{B}_{4,\phi} \\ &\equiv c_1^{(6)} + \delta c_1^{(6)} + \mathcal{B}_{4,\phi}\,, \end{aligned} \tag{5.3.4}$$

where Eq. (5.2.63) was used. Recall that in our case the HDO made δ_ϕ vanish, which is not the case in the usual CW model (see Appendix 5.D). Essentially $V^{(4)}$ gives a reformulation of the renormalization condition in Eq. (5.2.55). Since the above relation is about a physical quantity, connected to the Green functions, it should be finite, forcing us to absorb the divergent part of $\mathcal{B}_{4,\phi}$ in the remnant counterterm. Here comes the crucial part now, since in the regularization scheme of Eq. (5.3.3) the contribution of the scaleless B_0 integrals can be rewritten as

$$B_0 \equiv \frac{2}{\varepsilon} + \ln\frac{\mu^2}{\mu_R^2} = \frac{2}{\varepsilon} + \ln\frac{m^2_{\text{eff}}(\mu)}{m^2_{\text{eff}}(\mu_R)} = \frac{2}{\varepsilon} + \ln\frac{\bar{\phi}\phi}{v^2}\,. \tag{5.3.5}$$

Substituting this into Eq. (5.3.4) (using Eq. (5.2.61)) and canceling the divergent part we get

$$V^{(4)} = c_1^{(6)} + \frac{1}{32\pi^2}\Big[4(c_1^{(6)})^2 + 34g_4^4\Big]t \equiv c_1^{(6)}(t) \;\text{ and }\; \delta c_1^{(6)} = \frac{-1}{16\pi^2}\Big[4(c_1^{(6)})^2 + 34g_4^4\Big]\frac{1}{\varepsilon}\,, \tag{5.3.6}$$

with $t = \ln(\bar{\phi}\phi/v^2)$ and the condition $V^{(4)} = c_1^{(6)}$, for $t = 0$, at work. As a side comment note that when the Callan-Symanzik operator hits on $V^{(4)}$, one obtains

$$\begin{aligned}
\left[-2\frac{\partial}{\partial t} + \beta^1_{c_1^{(6)}}\frac{\partial}{\partial c_1^{(6)}} + \beta^1_{g_4}\frac{\partial}{\partial g_4} - 2\gamma_\phi\right] V^{(4)} &= 0 \Rightarrow \\
\frac{\partial c_1^{(6)}(t)}{\partial t} &= \frac{1}{2}\beta^1_{c_1^{(6)}} \Rightarrow \\
c_1^{(6)}(t) &= c_1^{(6)} + \beta^1_{c_1^{(6)}}\frac{t}{2}\,,
\end{aligned} \tag{5.3.7}$$

where $\beta^1_{c_1^{(6)}}(\beta^1_{g_4})$ is the 1-loop part of the β-function of $c_1^{(6)}$(of g_4) while the anomalous dimension of ϕ, given by γ_ϕ, vanishes. Then comparing the above to Eq. (5.3.6) fixes $\beta^1_{c_1^{(6)}}$ to

$$\beta^1_{c_1^{(6)}} = \frac{1}{16\pi^2}\left[4(c_1^{(6)})^2 + 34g_4^4\right], \tag{5.3.8}$$

matching the loop part of Eq. (5.2.76). Notice that in the CW model, the corresponding Callan-Symanzik equation gives for the quartic coupling the β-function of Eq. (5.D.9). There, a cross term between the quartic and gauge coupling exists due to the appearance of the anomalous dimension Eq. (5.D.7). Here the presence of the HDO leads to $\gamma_\phi = 0$, hence the cross term is missing in $\beta^1_{c_1^{(6)}}$. The improved 1-loop effective potential is now easily obtained by integrating with respect to the scalar field the renormalized $V^{(4)}$, to finally arrive in momentum space at

$$V_{\text{imp.}}(\bar{\phi},\phi) = \frac{c_1^{(6)}}{4}(\bar{\phi}\phi)^2 + \left\{2(c_1^{(6)})^2 + 17g_4^4\right\}\frac{(\bar{\phi}\phi)^2}{64\pi^2}\left(\ln\frac{\bar{\phi}\phi}{v^2} - 3\right). \tag{5.3.9}$$

The corresponding effective potential from the CW analysis is given in Eq. (5.D.1) and it is apparent that taken at face value, our potential in the chosen renormalization scheme is essentially a CW potential with the HDO coupling $c_1^{(6)}$ playing the role of the quartic coupling λ. There are differences though that are quite important with the most obvious ones hiding in the numerical factors. To see an example of the effect of the different numerical factors, we proceed with the minimization of the potential. Being of the CW type, the potential is expected to be of a no-scale nature, yielding a constraint between couplings rather than determining a vev. Following [13] and defining $\bar{\phi}\phi = [(A_5^1)^2 + (A_5^2)^2]/2 \equiv \phi_r^2$, we first rewrite the potential as

$$V_{\text{imp.}}(\phi_r) = \frac{c_1^{(6)}}{4}\phi_r^4 + \left\{2(c_1^{(6)})^2 + 17g_4^4\right\}\frac{\phi_r^4}{64\pi^2}\left(\ln\frac{\phi_r^2}{v^2} - 3\right) \tag{5.3.10}$$

and then find its minimum:

$$\frac{\partial V_{\text{imp.}}(\phi_r)}{\partial\phi_r}\Big|_{\phi_r=v} = \frac{-(10(c_1^{(6)})^2 + 85g_4^4 - 32\pi^2 c_1^{(6)})v^3}{32\pi^2} = 0 \Rightarrow \tag{5.3.11}$$

$$c_1^{(6)} = \frac{85}{32\pi^2}g_4^4\,, \tag{5.3.12}$$

where $(c_1^{(6)})^2$ was neglected with respect to $c_1^{(6)}$ since the latter is approximately 32 times bigger than the former at the above relation. Substituting Eq. (5.3.12) into Eq. (5.3.9) we end up with

$$V_{\text{imp.}}(\phi_r) = \frac{17g_4^4\phi_r^4}{128\pi^2}\left(2\ln\frac{\phi_r^2}{v^2} - 1\right) + \mathcal{O}(g_4^8)\,, \tag{5.3.13}$$

which justifies our choice to neglect $(c_1^{(6)})^2$. Notice that both Eq. (5.3.12) and Eq. (5.3.13) have analogues in the CW analysis, with the corresponding results given by Eq. (5.D.2) and Eq. (5.D.3) respectively. Now, Eq. (5.3.11) indicates a non-trivial minimum at $\langle\phi_r\rangle = v$, as the shape of the potential is of the standard Mexican hat form, see Fig. 5.2.

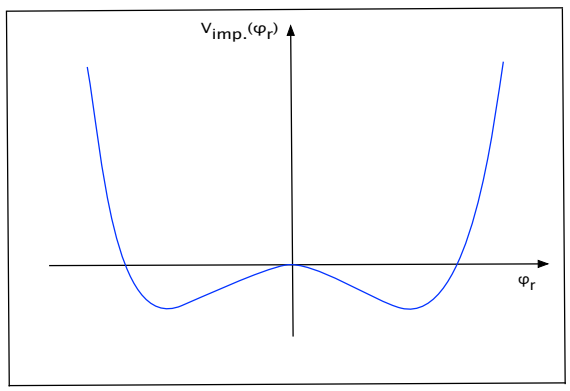

Figure 5.2: The potential in Eq. (5.3.13).

The vev triggers the spontaneous breaking of the gauge symmetry, allowing us to perform in the potential the shift $\phi_r \to h + v$ with h the physical scalar. Then,

$$m_h^2 \equiv \frac{\partial^2 V(h)}{\partial h^2}\Big|_{h=0} = \frac{210}{8\pi^2} g_4^4 v^2 \,. \tag{5.3.14}$$

Notice the difference with respect to CW numerical factor in the scalar mass. It arises due to the different overall numerical factor in Eq. (5.3.13) that affects the magnitude of the curvature of the potential at the minimum and originates from the higher derivative operator with coupling $c_1^{(6)}$. Since the gauge symmetry is broken, we expect the gauge field to develop a mass. To leading order in Λ only the operator $(A_\mu^3)^2\bar{\phi}\phi$ contributes after the shift and from that we obtain a gauge boson mass

$$m_{A_\mu^3}^2 = g_4^2 v^2 \equiv m_Z^2 \,, \tag{5.3.15}$$

the same as in the CW model. Therefore the above two expressions for the masses determine, at tree level, the scalar-to-gauge-field mass ratio

$$\begin{aligned} \frac{m_h^2}{m_Z^2} \equiv \rho_{\rm bh}^2 &= \frac{210}{8\pi^2} g_4^2 \Rightarrow \\ \rho_{\rm bh} &= \sqrt{\frac{210}{8\pi^2}}\, g_4 \simeq 1.64\, g_4 \,. \end{aligned} \tag{5.3.16}$$

In the last line we computed the numerical factor for later convenience. The corresponding CW analysis results in a scalar and gauge mass given in Eq. (5.D.4) and Eq. (5.D.5) respectively, detemining the mass ratio in Eq. (5.D.6):

$$\rho_{\rm CW} = \sqrt{\frac{3}{8\pi^2}} e \simeq 0.19\, e \,. \tag{5.3.17}$$

Let us discuss some numerics. To begin, the appearance of the anisotropy is rather important because it allows $\rho_{\rm bh}$ to reach its Standard Model value 1.38 for reasonable values of g (recall, $g_4 = g\sqrt{\gamma}$). The analogous observation from the non-perturbative point of view in [11] was that close to the Higgs-Hybrid phase transition and for $\gamma \simeq 0.50$, a $\rho_{\rm bh} \simeq 1.40$ can be measured. Away from the phase transition or in the absence of anisotropy, the mass ratio is far from this value. As an example consider the triple point in Fig. 5.1 which is reached for $\gamma \simeq 0.79$ [10]. Then, for our model, Eq. (5.3.16) gives $\rho_{\rm bh} \simeq 1.45\, g$, which for $g \simeq 0.95$ reproduces the SM value, while in the CW model we would need much larger values of e to reach the same result. Another way to see the difference is to suppose that g and e are of the same order. Then for $\gamma \simeq 0.79$ and $g \simeq e$, we get $\rho_{\rm bh} \simeq 7.60\, \rho_{\rm CW}$. Regarding the dependence of $\rho_{\rm bh}$ on g_4 in Eq. (5.3.16), forcing Eq. (5.3.16) and Eq. (5.3.17) to give the SM value, fixes $g_4 \simeq 0.84$ and $e \simeq 7.20$ respectively, indicating that the former can be consistent with perturbation theory, not so much the latter. Interestingly, this value for g_4, when substituted back into Eq. (5.3.12), gives $c_1^{(6)} \simeq 0.13$ close to the SM value for the Higgs self-coupling. Recall that $c_1^{(6)}$ plays the role of the scalar quartic coupling here so this is a non-trivial coincidence. On the other hand, setting $e \simeq 7.20$ into Eq. (5.D.2) we find $\lambda \simeq 1123.20$.

The above numerical discussion did not take into account constraints that originate from the non-perturbative dynamics. We will insert later information of this sort in the discussion and look again at the numbers but first we have to understand better the running of the various parameters involved. So, let us now look at the scale dependence of the couplings. This can be done for the two models by solving the equations

$$\mu \frac{d\, g_4(\mu)}{d\mu} = \beta_{g_4} \qquad \text{and} \qquad \mu \frac{d\, e(\mu)}{d\mu} = \beta_e \tag{5.3.18}$$

respectively, choosing as IR boundary conditions m_R, M_R, $g_4(m_R) \equiv g_{4,R}$ (or $g(m_R)\gamma(m_R) \equiv g_R\, \gamma_R$) and $e(M_R) \equiv e_R$. In order to locate the UV limit of the running in our case, recall first that the masses depend on g_4 and v only. We will choose from now on a scheme where the vev is kept frozen at a value $v = v_*$, in which case the running of the masses is determined by that of g_4 only. Both evolutions implied by Eq. (5.3.18) are not interrupted, in principle, but from a Landau pole at some extremely large UV scale. A crucial difference with respect to the CW case is that in our model the running must be halted in the UV by the quantum phase transition, way before the Landau pole is hit. Let us call this scale μ_* and see in the following section whether it can be identified more precisely.

Solving the RG equations of Eq. (5.3.18) gives

$$g_4(\mu) = \frac{g_{4,R}}{\sqrt{1 - \frac{g_{4,R}^2}{16\pi^2} \ln \frac{\mu^2}{m_R^2}}} \qquad \text{or} \qquad \alpha_4(\mu) = \frac{\alpha_{4,R}}{1 - \alpha_{4,R} \ln \frac{\mu^2}{m_R^2}} \tag{5.3.19}$$

for our boundary coupling and

$$e(\mu) = \frac{e_R}{\sqrt{1 - \frac{e_R^2}{48\pi^2} \ln \frac{\mu^2}{M_R^2}}} \tag{5.3.20}$$

for the Coleman-Weinberg case, both evaluated for $d = 4$. On Fig. 5.3 we compare the two evolutions for the case of $M_R = m_R = 91.1$ GeV, $g_{4,R} = 0.83$ and $e_R = 0.31$.

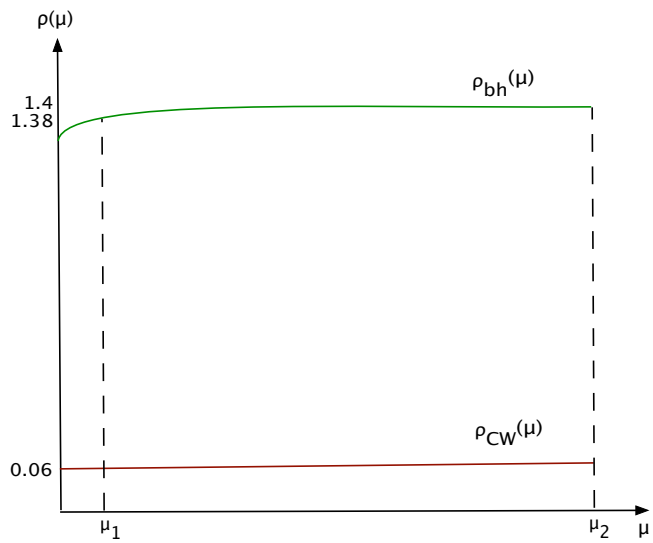

Figure 5.3: The running of the ρ-parameter with respect to the energy scale μ for the Boundary-Hybrid model (green line) and the Coleman-Weinberg model (red line). As μ increases, $\rho_{\rm bh}(\mu)$ increases and reaches the Standard Model value at μ_1. At that scale it is approximately 23 times bigger than $\rho_{\rm CW}(\mu_1) = 0.06$.

The CW evolution appears as a straight line just because the running of g_4 is 3 times faster than that of e. The running on the figure starts at $m_R = 91.1$ GeV and ends at 10^5 GeV which is an appropriate range to illustrate clearly the difference between the two models. The lower values of the ρ-parameters are $\rho_{\rm bh}(m_R) \simeq 1.36$ and $\rho_{\rm CW}(m_R) \simeq 0.06$. The running leads to a small increase from the starting values due to the logarithmic running, but the increase is relatively more substantial for $\rho_{\rm bh}$. Of course this also means that the boundary coupling g_4 could reach its Landau pole much faster compared to the CW coupling e. Numerically, the Landau pole for the g_4 gauge coupling is located at

$$\mu_{4,\rm L} = e^{\frac{8\pi^2}{g_{4,R}^2}} m_R \approx 5.3 \times 10^{51}\,\text{GeV} \tag{5.3.21}$$

and for the CW coupling at

$$\mu_{e,\rm L} = e^{\frac{24\pi^2}{e_R^2}} M_R \approx 2.6 \times 10^{1072}\,\text{GeV}\,. \tag{5.3.22}$$

There is of course a chance for $\rho_{\rm CW}(\mu)$ to also reach the SM value if $e(\mu)$ becomes large enough. This can be however realized only when μ approaches $\mu_{e,\rm L}$ where perturbation theory breaks down anyway.

Before we get into the non-trivial effects of the phase transition, let us construct the RG flow diagram on the $c_1^{(6)} - g_4$ plane, neglecting its presence. For that purpose we need the running of Eq. (5.3.19) while we evaluate $c_1^{(6)}(\mu)$ solving Eq. (5.2.43) for the β-function of Eq. (5.2.76)

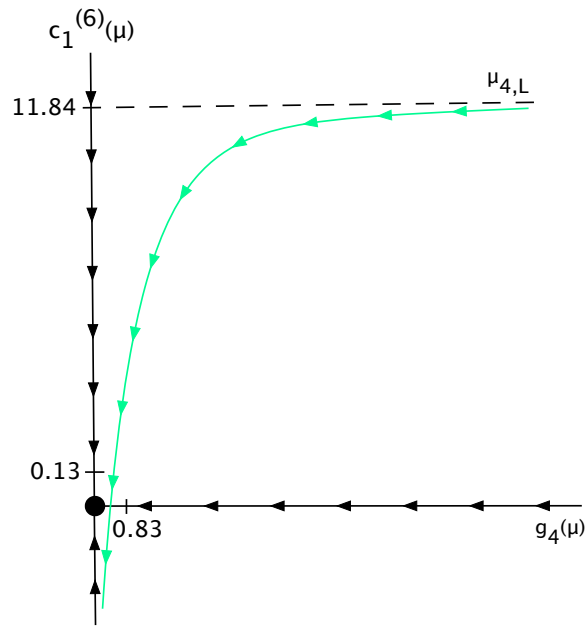

Figure 5.4: The simultaneous running of the HDO and gauge couplings $c_1^{(6)}(\mu)$ and $g_4(\mu)$. The arrows point towards the IR, so both couplings increase in the UV. As $\mu \to 0$ the Gaussian fixed point, $\bullet$, is approached and then $g_4 \to 0$ while the HDO coupling reaches $-\infty$. At the starting point of the running, $\mu = m_R$, the couplings read $(c_{1,R}^{(6)}, g_{4,R}) = (0.13, 0.83)$ while in the UV, where g_4 reaches the Landau pole $\mu_{4,\mathrm{L}}$, yield $(c_1^{(6)}(\mu_{4,\mathrm{L}}), g_4(\mu_{4,\mathrm{L}})) = (11.84, \infty)$.

(neglecting the $(c_1^{(6)})^2$ contribution). Then the RG equation reads

$$\mu \frac{dc_1^{(6)}(\mu)}{d\mu} = \beta_{c_1^{(6)}} = -\varepsilon c_1^{(6)} + 34 g_4^4 \tag{5.3.23}$$

which in $d = 4$ gives

$$c_1^{(6)}(\mu) = c_{1,R}^{(6)} + \frac{17\, g_4^4}{16\pi^2} \ln \frac{\mu^2}{m_R^2} \,. \tag{5.3.24}$$

The combined evolution of the couplings is seen in Fig. 5.4.

Below we summarize the similarities and differences between our boundary effective action (before taking into account non-perturbative dynamics) and the CW model:

- At the classical level, the CW Lagrangian contains a polynomial ϕ^4 term, a marginal in $d = 4$ operator, as the only contribution to the scalar potential. Here, due to the origin of the boundary effective action, there are only derivative terms. After field redefinitions, a dimension-6 derivative operator plays the role of the scalar potential but it also contributes to the vertices.

- In the CW model a mass counter-term is introduced from the start, despite the absence of a classical mass term. This breaks scale invariance already at the classical level. In our case we do not need such a counter-term. This is crucial if we want to assign the responsibility for the simultaneous breaking of scale and gauge symmetries to the HDO.

- Renormalization yields β_λ and $\beta_{c_1^{(6)}}$ for the CW and our case respectively. The former contains a cross term between the quartic and gauge coupling which is absent from the latter. The reason is that the effect of the HDO, for the chosen renormalization scheme, leads to the vanishing of the anomalous dimension of the scalar field. This anomalous dimension is non-zero in the CW case.

- After renormalization, both 1-loop effective potentials indicate the existence of a non-trivial minimum. Around the minimum, they differ only by a multiplicative constant. This constant affects crucially though the scalar-to-gauge boson mass ratio. The operators that appear in the effective action, determine the speed of the gauge coupling running: due to the HDO the g_4 coupling and mass ratio run 3 times faster than the corresponding quantities in the CW model.

- The running of the coupling in the CW model does not stop until the Landau pole. In our case the running of g_4 is similar but is expected to be stopped by the phase transition.

5.3.2 What if polynomial potential terms where allowed?

In contrast to the CW Lagrangian, where the potential is represented by the usual marginal operator $(\bar{\phi}\phi)^2$, here the only potential-like term

$$\frac{O_1^{(6)}}{\Lambda^2} = \frac{\bar{\phi}\phi\Box\bar{\phi}\phi}{\Lambda^2}$$

is a 6-dimensional derivative operator. In a general $U(1)$ gauge theory coupled to a complex scalar we could have other dimension-6 operators, for example

$$\left(\frac{O_1^{(6)}}{\Lambda^2}, \frac{O_2^{(6)}}{\Lambda^2}, \frac{O_3^{(6)}}{\Lambda^2}\right) = \left(\frac{\bar{\phi}\phi\Box\bar{\phi}\phi}{\Lambda^2}, \frac{\bar{\phi}\Box^2\phi}{\Lambda^2}, \frac{(\bar{\phi}\phi)^3}{\Lambda^2}\right) . \tag{5.3.25}$$

Note that we have used the usual box derivative since this analysis is supposed to be done after expanding the covariant derivatives. However, as it is demonstrated in [33, 30], after an appropriate field redefinition only one of them stays independent. In other words a Lagrangian, enhanced by the operators in Eq. (5.3.25) is in fact equivalent to a Lagrangian that contains only the polynomial term $O_3^{(6)}$. Let us call such a basis, the W-basis. The same is true if we insert also dim-8 operators and an extended W-basis can be constructed. It will contain only

$$\left(\frac{O_3^{(6)}}{\Lambda^2}, \frac{O_4^{(8)}}{\Lambda^4}\right) = \left(\frac{(\bar{\phi}\phi)^3}{\Lambda^2}, \frac{(\bar{\phi}\phi)^4}{\Lambda^4}\right) , \tag{5.3.26}$$

as HDO, which actually play the role of a non-trivial scalar potential with associated couplings $c_3^{(6)}$ and $c_4^{(8)}$. Then we would need these operators to behave like the marginal operator of the CW model. However, if only $O_3^{(6)}$ or only $O_4^{(8)}$ is present then there can be no CW mechanism in progress since neither of them contributes as a mass term through radiative corrections. To

be more specific the only possible 1-loop diagram is

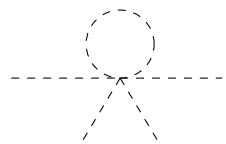

when only $O_3^{(6)}$ plays the role of the potential and

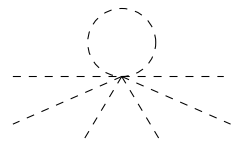

when the scalar potential is made only from $O_4^{(8)}$. In the former the radiative correction gives rise to a quartic term while in the latter to a $(\bar{\phi}\phi)^3$ term, notwithstanding both cases correspond to scaleless tadpole-integrals and vanish in DR. Another way to express this conclusion is to look at the β-functions of $c_3^{(6)}$ and $c_4^{(8)}$. These are evaluated, at 1-loop order, in [33, 30] and show that if $V \sim O_3^{(6)}$ or $V \sim O_4^{(8)}$, the associated couplings do not run. Therefore a CW analysis is meaningless. On the other hand, when both operators in Eq. (5.3.26) appear in the potential, then a non-trivial scalar potential is constructed, of the form

$$V^{(8)} \sim \frac{c_3^{(6)}}{\Lambda^2}(\bar{\phi}\phi)^3 + \frac{c_4^{(8)}}{\Lambda^4}(\bar{\phi}\phi)^4 \,,$$

whose phase diagram indeed possesses a branch with spontaneously broken internal symmetry. Nevertheless, this effect is trivial since the running of $c_4^{(8)}$ is such that it sets the phase diagram unstable. The above arguments are presented in detail in [33, 30]. Thus, another important point is that even if the W-basis of Eq. (5.3.26) were allowed we would not manage to construct a non-trivial phase diagram with SSB at work.

5.4 The effective action near the Higgs-Hybrid phase transition

The extra step we would like to take in this section is to build in the effective action certain non-perturbative features that have been observed via Monte Carlo simulations on the lattice. We start with a comment on the nature of higher dimensional operators in the effective action. We have seen above how they affect quantitatively the scalar mass and the β-functions. At a more qualitative level, one question is whether the HDO are of a classical or a quantum nature. In [30] we argued that when the suppressing scale Λ is an internal scale, they must have a quantum origin. In DR for example one can identify Λ with the regulating scale μ or alternatively with a fixed scale derived from μ, such as μ_*. We have already used this fact throughout. In addition, in [30] it was demonstrated that the (1-loop) quantization of a Lagrangean with vertices deriving from the HDO is equivalent to the quantization of a Lagrangean without HDO but taking into account all possible operator insertions. These two arguments allow us to characterize the HDO as quantum corrections which is not an unimportant detail since then, in the presence of a Higgs

mechanism, scale and internal symmetry break spontaneously and simultaneously by quantum effects.

In order to be able to build in the boundary effective action the effects of the presence of the phase transition, we now make two assumptions. The first assumption states that dimensional reduction occurs in the vicinity of the Higgs-Hybrid phase transition. Since all dimensions are infinite, the dimensional reduction must develop due to localization. This was in fact observed numerically in [11] where it was demonstrated that near the Higgs-Hybrid phase transition in the Higgs phase and in the entire Hybrid phase, the lattice becomes layered in the fifth dimension. This means in particular that the $U(1)$ gauge-scalar effective action of the boundary slice in the Higgs phase contains a 4d gauge coupling (identified as g_4) and the dynamics of a bulk slice in the Hybrid phase is to a good approximation a 4d $SU(2)$ Yang-Mills theory, associated with a 4d coupling g_s. The previous construction of the boundary effective action in the Higgs phase was of course motivated by and is consistent with this non-perturbative fact. We will also exploit the consequences of the dimensional reduction in the bulk of the Hybrid phase reflected by g_s in the following but before that, we need one more assumption. Therefore our second assumption is that the bulk-driven transition is reached by g_4 and g_s in the UV. Concrete non-perturbative evidence for the validity of this assumption we have in the Higgs phase where the masses of the gauge and scalar fields decrease in units of the lattice spacing a_4 as the phase transition is approached [11]. Regarding the behaviour of a_4 as the phase transition is approached from the side of the Hybrid phase we do not have concrete numerical evidence but we can motivate this assumption by imagining an RG flow in the Hybrid phase that starts from the phase transition that separates the 5d Confined and the Hybrid phase and approaches the Hybrid-Higgs phase transition. The evolution must be of an asymptotically free type (i.e. the evolution of g_s), monotonically flowing from the IR to the UV, where it hits the Hybrid-Higgs phase transition.

These two facts constrain the dynamics in a radical way. The most notable constraint is that then, RG flows that emanate from a given point on the Higgs-Hybrid phase transition and extend in the two phases, are necessarily correlated [15]. We will make these statements concrete below but first we have to clarify a couple of technical points. The first concerns the fact that the Higgs-Hybrid phase transition is bulk driven, which means that it is of a five-dimensional nature, independent of the boundary conditions. Its location on the phase diagram was determined in [3] using the ε-expansion and corresponds to the blue line of Fig. 5.1. Here we repeat the construction to some extent but also generalize it in several ways. One generalization is related to the renormalization of the anisotropy factor γ. In [3] it was held constant, a fact that was connected to the identification of the phase transition in the ε-expansion as a WF fixed point. This is a simplification as the phase transition is really of first order and it was consistent in [3] only because the effective action was obtained via a LO expansion in the lattice spacing and no HDO were present. Here, the effective action is computed to NLO with dimension-6 HDO induced in it and the anisotropy is free to run due to quantum corrections. The HDO must be suppressed by a scale which defines a cut-off. This cut-off must be an internal to the system scale and is necessary to define an effective action without a continuum limit, such as one

that is appropriate near a first order phase transition. Practically this means that in the present analysis the location of the phase transition will be identified by the matching of the RG flows of the effective 4d couplings g_4 and g_s rather than as a 5d WF fixed point. This is consistent with the non-perturbative picture because the first method defines a finite cut-off, while the second yields a continuum limit by construction. To put it in simple words, in the effective action a second order phase transition is seen as a 5d WF fixed point while a first order phase transition is seen as the point where 4d RG flows meet. Of course, these two methods should differ by a small amount in the UV parametrized by the effect of the HDO. The matching of the 4d RG flows, made possible by our assumptions above, encodes therefore in an indirect way the 5d nature of the phase transition. The other technical point we need to settle concerns the connection between lattice and continuum parameters mentioned in the Introduction, expressed as [3]

$$\mu = \frac{F(\beta_4, \beta_5)}{a_4} \,. \tag{5.4.1}$$

We have already used this relation in the construction of the continuum effective action from the lattice action, where the non-trivial lattice coupling dependence of F was responsible for the appearance of general couplings in front of the HDO. Now we try to make one more step in the characterization of F, using the fact that here the anisotropy runs. Let us distinguish F in the Higgs and Hybrid phases by denoting it as $F_4 \equiv F(\beta_4, \beta_5)$ and $F_s \equiv F(\beta_{4,s}, \beta_{5,s})$ respectively. Then

$$F_4 = a_4(\mu)\,\mu \tag{5.4.2}$$

for the former and

$$F_s = a_{4,s}(\mu)\,\mu \tag{5.4.3}$$

for the latter and the difference between F_4 and F_s originates from the way that the lattice spacing connects to μ in the two phases. The observation here is that since the phase transition is a line of UV points, the lattice spacing necessarily sweeps through the same values on the two sides near a point on the phase transition, that is $a_4 = a_{4,s}$, thus it is a regularization choice to take $F_4(\mu) = F_s(\mu)$. On the phase transition where RG flows from the two sides meet, they assume of course the common value $F_4(\mu_*) = F_s(\mu_*) \equiv F_*$. In [3] it was demonstrated that the choice $F_* =$ const. reproduces qualitatively well the Higgs-Hybrid phase transition in the limit that it is a line of WF fixed points, therefore here we continue using this approximation.

Moving one step further we can express these relations through the lattice spacing of the extra dimension inserting the anisotropy. Using the tree level relation $\gamma = a_4/a_5$ and then promoting to running parameters, we obtain

$$F_4 = a_5(\mu)\,\mu\,\gamma(\mu) \quad \text{and} \quad F_s = a_{5,s}(\mu)\,\mu\,\gamma_s(\mu) \tag{5.4.4}$$

in the Higgs and Hybrid phase respectively, with γ and γ_s representing the anisotropy in each phase. Then, using the above approximation, we have that

$$\frac{\gamma(\mu)}{\gamma_s(\mu)} \equiv \frac{a_{5,s}(\mu)}{a_5(\mu)} \,. \tag{5.4.5}$$

5.4.1 Matching RG flows in the Higgs and Hybrid phases

In order to match RG flows, we need to evaluate $g_s(\mu)$, the coupling in the Hybrid phase. According to [7, 10] localization holds approximately near the Hybrid-Higgs phase transition on both sides (see Fig. 5.1), while as we move deeper in the Hybrid phase the 5d space becomes more and more layered. In the limit $\beta_5 = 0$, the 5d space is exactly (and trivially) layered. This means that inside the entire Hybrid phase we see approximate 4d slices with $SU(2)$ gauge group in the bulk and a $U(1)$ theory on the boundary in either a Coulomb or a Confined phase, with the slices almost decoupled from each other. It is sufficient for our discussion to focus on one of the bulk slices. This means that we know exactly how to construct the RG flow of its gauge coupling, especially towards the UV where it becomes asymptotically free. The only point that needs care is the fact that in the bulk too, we have HDO in the effective action. Fortunately, according to the formalism developed at the end of Section 5.2.3 the corresponding β-function is that of the usual 4d Lee-Wick gauge model, [26], given in Eq. (5.2.70) which for $\delta_2 = \delta_3 = 0$, $k_F = -2/3$ and $\delta_1 = 2$ becomes

$$\beta_{\alpha_s} = -\frac{125}{12}\alpha_s^2 \quad \text{or} \quad \beta_{g_s} = -\frac{125}{6}\frac{g_s^3}{16\pi^2} \tag{5.4.6}$$

with $g_s(\alpha_s = g_s^2/16\pi^2)$ the 4d dimensionless $SU(2)$ coupling. Its running is given by

$$\begin{aligned} g_s(\mu) &= \frac{g_{s,R}}{\sqrt{1+\frac{125 g_{s,R}^2}{96\pi^2}\ln\frac{\mu^2}{m_R^2}}} \qquad \text{or} \qquad \alpha_s(\mu) = \frac{\alpha_{s,R}}{1+\frac{125\alpha_{s,R}}{6}\ln\frac{\mu^2}{m_R^2}} \Rightarrow \\ g_s(\mu) &= \frac{c_s}{\sqrt{\ln\frac{\mu}{\Lambda_s}}} \qquad \text{or} \qquad \alpha_s(\mu) = \frac{c_s'}{\ln\frac{\mu}{\Lambda_s}} \end{aligned} \tag{5.4.7}$$

with

$$\Lambda_s = e^{-\frac{c_s^2}{g_{s,R}^2}} m_R = e^{-\frac{c_s'}{\alpha_{s,R}}} m_R \tag{5.4.8}$$

and $c_s = \sqrt{48\pi^2/125}$ and $c_s' = 3/125$. If we had a general LW gauge model, Eq. (5.4.7) would suggest that the coupling has the usual asymptotically free behaviour reaching zero in the continuum limit. However here, due to the Higgs-Hybrid transition and the assumption that approaching it from either side drives the system towards the UV, the running in the Hybrid phase should be related to that of the Higgs phase. A matching of all physical observables at a generic point along RG flows is expected to be extremely hard but the matching of gauge couplings only, should be possible at the scale μ_*. There, the running of $g_s(\mu)$ stops and it never reaches the continuum limit and the model inherits a finite cut-off. This is rather unusual as it defines a 4d Yang-Mills theory with a finite UV cut-off. One should keep in mind of course that this phase is not physical from the Higgs phase boundary point of view, it just regulates the Higgs phase, where the interesting physics takes place.

To be more specific, consider the auxiliary running couplings in the Higgs and Hybrid phases, Eq. (5.3.19) and Eq. (5.4.7) respectively and invert both with respect to the regulating scale. Then the former gives that

$$\mu = \exp\Big[\frac{\alpha_4(\mu) - \alpha_{4,R}}{2\alpha_4(\mu)\,\alpha_{4,R}}\Big] m_R\,, \tag{5.4.9}$$

while in the Hybrid phase that

$$\mu = e^{\frac{c_s'}{\alpha_s(\mu)}} \Lambda_s \,. \tag{5.4.10}$$

As both move towards the UV trying to reach the phase transition at a common point where $\mu = \mu_*$, they must necessarily assume common values. Hence, equating Eq. (5.4.9) with Eq. (5.4.10) we get

$$\frac{\alpha_4(\mu) - \alpha_{4,R}}{2\alpha_4(\mu)\,\alpha_{4,R}} - \frac{c_s'}{\alpha_s(\mu)} = \ln \frac{\Lambda_s}{m_R} \,, \tag{5.4.11}$$

where m_R is not independent from Λ_s due to Eq. (5.4.8). Using this, we obtain the relation

$$\frac{\alpha_4(\mu) - \alpha_{4,R}}{2\alpha_4(\mu)\,\alpha_{4,R}} = c_s' \frac{\alpha_{s,R} - \alpha_s(\mu)}{\alpha_s(\mu)\alpha_{s,R}} \tag{5.4.12}$$

which makes the relation between the running of the couplings in the two sides of the phase transition explicit. Here comes the crucial step, since we are interested in finding the scale μ_* where the RG flows meet and the couplings coincide. This results in

$$\begin{aligned} \frac{\alpha_4(\mu_*) - \alpha_{4,R}}{2\alpha_4(\mu_*)\,\alpha_{4,R}} &= c_s' \frac{\alpha_{s,R} - \alpha_s(\mu_*)}{\alpha_s(\mu_*)\alpha_{s,R}} \Rightarrow \\ \frac{\alpha_* - \alpha_{4,R}}{2\alpha_*\,\alpha_{4,R}} &= c_s' \frac{\alpha_{s,R} - \alpha_*}{\alpha_*\alpha_{s,R}} \Rightarrow \\ \alpha_* &= \frac{\alpha_{4,R}\,\alpha_{s,R}(1+2c_s')}{\alpha_{s,R} + 2c_s'\alpha_{4,R}} \,, \end{aligned} \tag{5.4.13}$$

with $\alpha_4(\mu_*) = \alpha_s(\mu_*) = \alpha_*$, thereby the cut-off implied by Eq. (5.4.10) being equal to

$$\mu_* = e^{\frac{c_s'}{1+2c_s'}\left[\frac{1}{\alpha_{4,R}} + \frac{2c_s'}{\alpha_{s,R}}\right]} \Lambda_s \,. \tag{5.4.14}$$

The scale where the phase transition occurs as well as α_* in Eq. (5.4.13) depend, apart from the input scale Λ_s, on the arbitrary reference values $\alpha_{4,R}$ and $\alpha_{s,R}$. Similarly, m_R is fixed as soon as $\alpha_{s,R}$ is fixed from Eq. (5.4.8). We add the value of the scalar mass at the phase transition which will be needed later:

$$m_{h*} = \sqrt{\frac{210}{8\pi^2}} 16\pi^2 v_* \alpha_* \,. \tag{5.4.15}$$

How far is the cut-off μ_* from a continuum limit, equivalently how far the first order phase transition implied by the finite cut-off in Eq. (5.4.14) is from a second order phase transition? For this, let us look at the way that the bulk coupling runs, taking into account the HDO. The relevant RG equation, using the β-function of Eq. (5.2.77) for $\varepsilon = -1$ this time, yields

$$\alpha_5(\mu) = \frac{\alpha_{5,R}}{C\,\alpha_{5,R} + (1 - C\,\alpha_{5,R})\frac{M_R}{\mu}} \,, \tag{5.4.16}$$

with $C = 125/12$ and $M_R, \alpha_{5,R} \equiv \alpha_5(M_R)$ arbitrary parameters. Following [3], if we demand Eq. (5.2.77) to vanish at 1-loop order there appears both a Gaussian and a Wilson-Fisher fixed point given by[2]

$$\alpha_{5\bullet} = 0 \;\text{ and }\; \alpha_{5\star} = \frac{1}{C} = 0.096 \,, \tag{5.4.17}$$

[2]We denote the WF fixed point by a 'star', which is (slightly) different from the RG flow matching point, denoted before by an 'asterisk'.

where F, in Eq. (5.1.1), obtains a constant value[3] which reads

$$F(\beta_{4\star}, \beta_{5\star}) \equiv F_\star \simeq 1.51, \tag{5.4.18}$$

taking into account the HDO. The scale where the WF fixed point is reached is given by

$$\begin{aligned} \mu_\star &= \frac{\alpha_{5\star}}{\alpha_{5,R}} \frac{(C\,\alpha_{5,R} - 1)}{(C\,\alpha_{5\star} - 1)} M_R \Rightarrow \\ \mu_\star &\to \infty \end{aligned} \tag{5.4.19}$$

that is, in the continuum limit. Clearly the difference $\mu_\star - \mu_*$ is not a good distance measure on the phase diagram because it is always infinite. Instead, we can compute the value of $\alpha_{5*} = \alpha_5(\mu_*)$ and compare it to $\alpha_{5\star}$. Clearly the difference $\alpha_{5\star} - \alpha_{5*}$ is now finite. For example, with $M_R = m_R = 5.55$ GeV and $\alpha_{5,R} = \alpha_{s,R} = 0.014$ (these choices are justified in the following sections), we have $\alpha_{5*} = 0.083$, a value not far from Eq. (5.4.17). From this example we only keep that $\alpha_{5*} < \alpha_{5\star}$, showing that the first order phase transition is above the WF (blue) line on the phase diagram of Fig. 5.1. This means that moving from the side of the Higgs phase towards the phase transition, one hits on the first order phase transition before the continuum limit, in the form of a WF fixed point, is met. This is consistent with our main assumption that the phase transition is a UV point. The interesting fact is that for the other side of the phase transition, this behaviour does not imply the opposite, as one could naively conclude. For this, we point to Figure 2 of [3], where it was shown that the flow beyond the WF point can be characterized as a Landau branch, where the system, as it moves towards the WF fixed point from above, sees a Landau pole, thus a finite cut-off, not a continuum limit. Again, this is consistent with the assumption that the phase transition is seen as a UV point also from the other side.

The last piece of technical information we are missing is the running of the anisotropy parameter γ and γ_s for the Higgs and Hybrid phase respectively. Let us start with the former which in principle is fixed by already known results, since at the classical level $\gamma^2 = \beta_5/\beta_4$ (equivalently use the relations in Eq. (5.A.30)) and the running of β_4 and β_5 are determined through the running of α_4 and α_5. All we need is to promote Eq. (5.A.30) to running couplings, combined with Eq. (5.4.2). Then we have

$$g_4^2(\mu) = g_5^2(\mu)\,\mu \frac{\gamma(\mu)}{F_4} \tag{5.4.20}$$

or

$$\begin{aligned} 4\frac{g_4^2(\mu)}{16\pi^2} &= 4\frac{g_5^2(\mu)\,\mu}{16\pi^2}\frac{\gamma(\mu)}{F_4} \Rightarrow \\ 4\alpha_4(\mu) &= \alpha_5(\mu)\frac{\gamma(\mu)}{F_4}\,. \end{aligned}$$

Solving for $\gamma(\mu)$ and following the discussion above Eq. (5.4.5) we get

$$\gamma(\mu) = 4F_* \frac{\alpha_4(\mu)}{\alpha_5(\mu)} \tag{5.4.21}$$

[3] See the relative discussion in Sect. (4.2.1) of [3].

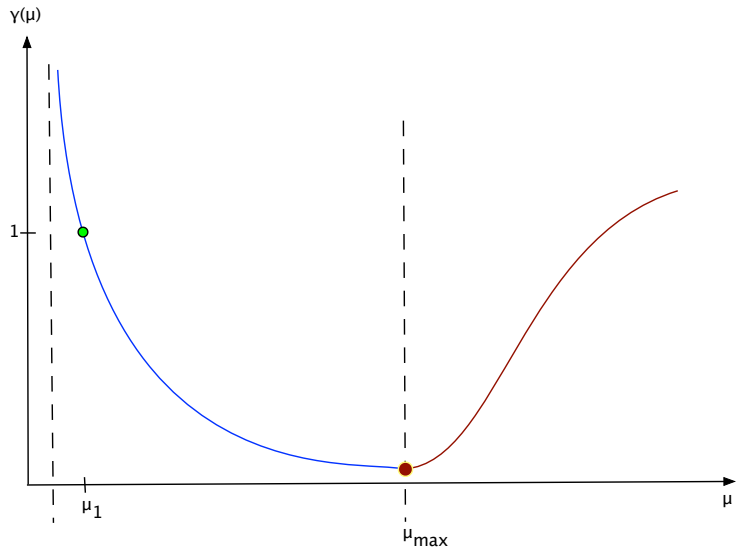

Figure 5.5: The running of the anisotropy $\gamma(\mu)$ as a function of the dynamical scale. The green bullet represent the scale μ_1 where the anisotropy becomes $\gamma(\mu_1) = 1$ while the red one shows $\gamma_{\min} \equiv \gamma(\mu_{\max})$, the minimum value of the anisotropy. The behaviour of γ between the dashed lines (blue curve) resembles the bulk-driven phase transition of Fig. 5.1. Passing towards $\mu_{\max}$ the running of the anisotropy (red line) changes its behaviour and increases with increasing μ.

and all we have to do is to combine Eq. (5.3.19) and Eq. (5.4.16) to obtain

$$\gamma(\mu) = 4F_* \frac{\alpha_{4,R}}{\alpha_{5,R}} \frac{C\,\alpha_{5,R} + (1 - C\,\alpha_{5,R})\frac{M_R}{\mu}}{1 - 2\alpha_{4,R} \ln \frac{\mu}{m_R}}\,, \tag{5.4.22}$$

with F_* given by Eq. (5.4.18) without much loss of generality since the cut-off and WF lines are very close. Computing the flow, we are lead to Fig. 5.5 which presents the running of the anisotropy parameter. According to the figure, the running of $\gamma(\mu)$, in the region between the dashed lines, resembles the line of the bulk-driven transition of Fig. 5.1. The interesting point here is that there is a minimum value, $\gamma_{\min}$, of the anisotropy or a maximum scale, $\mu_{\max}$, after which the running of γ (red line in Fig. 5.5) changes its behaviour. In particular this maximum scale is

$$\mu_{\max} = 32.5\, W_L(0.063\, e^{\frac{0.4974}{\alpha_{4,R}}}) \tag{5.4.23}$$

whose value will be useful in the next section. The function $W_L(x)$ is the product logarithm or the Lambert function. The running of γ is such that any RG flow that starts from the isotropic point $\gamma = 1$ span over values $\gamma < 1$ in the UV, which is the direction of approach of the phase transition, when the change of β_4 is mild along the RG flow.

Next we focus on the Hybrid phase and on $\gamma_s(\mu)$. For the associated running we follow an other path than the Higgs phase using the relation between lattice and continuum couplings. The needed ingredients are $\beta_4(\mu)$ and $\beta_5(\mu)$ as functions of the running couplings $\alpha_4(\mu)$ and $\alpha_s(\mu)$, given by Eq. (5.3.19) and Eq. (5.4.7) respectively. Then using also that $\gamma = \beta_5/\beta_4$ and

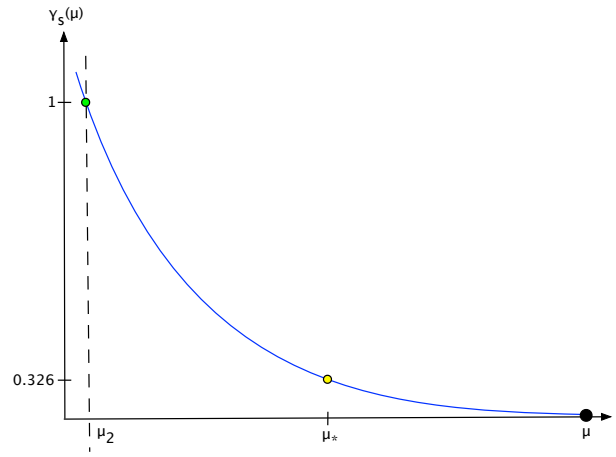

Figure 5.6: The running of the anisotropy $\gamma_s(\mu)$ as a function of the dynamical scale. The green bullet represent the scale μ_2 where the anisotropy becomes $\gamma_s(\mu_2) = 1$ while the yellow one the scale μ_* at which $\gamma_s(\mu_*) \equiv \gamma(\mu_*)$. The black bullet (Gaussian fixed point), shows the limit $\mu \to \infty$ where $\gamma_s \to 0$, corresponding to the minimum value of the anisotropy. The behaviour of γ_s stays always similar to the bulk-driven phase transition of Fig. 5.1.

$\gamma_s = \beta_{5,s}/\beta_{4,s}$ we get

$$\beta_4(\mu) = \frac{1}{4\pi^2\alpha_4(\mu)} \qquad \text{and} \qquad \beta_5(\mu) = \gamma^2(\mu)\beta_4(\mu)\,. \tag{5.4.24}$$

for the Higgs phase and

$$\beta_{4,s}(\mu) = \frac{1}{4\pi^2\alpha_s(\mu)} \qquad \beta_{5,s}(\mu) = \gamma_s^2(\mu)\beta_{4,s}(\mu) \tag{5.4.25}$$

for the Hybrid phase. Since we do not know how to compute $\gamma_s(\mu)$, we can exploit localization: Since during the evolution along a 4d slice changes little the localization property, we can safely assume that $\beta_{5,s}(\mu)$ is constant along a flow (we move along $\beta_5 = \text{const.}$ lines) in Eq. (5.4.25). Hence,

$$\begin{aligned} \beta_{5,s}(\mu) &= \gamma_s^2(\mu)\beta_{4,s}(\mu) \equiv \beta_{5,s*} \Rightarrow \\ \gamma_s(\mu) &= \sqrt{\frac{\beta_{5,s*}}{\beta_{4,s}(\mu)}} = 2\pi\sqrt{\beta_{5,s*}\,\alpha_s(\mu)} \end{aligned} \tag{5.4.26}$$

where $\beta_{5,s*}$ is the value of $\beta_{5,s}(\mu)$ on the phase transition. To be more quantitative let us choose $\alpha_{s,R} = 0.014$, $\alpha_{4,R} = 0.00435$ (these choices are justified in the following) and demand that $\gamma_s(\mu_*) \equiv \gamma(\mu_*)$. This suggests that

$$\beta_{5,s*} \simeq 0.6 \tag{5.4.27}$$

fitting to a good approximation the non-perturbative results [10, 11]. Computing the flow, with these choices, we are lead to Fig. 5.6 which presents the running of the anisotropy parameter whose form resembles the blue line of Fig. 5.1. Note that even though $\gamma(\mu_1) = \gamma_s(\mu_2) = 1$ the associated scales do not admit the same value, so $\mu_1 \neq \mu_2$.

5.4.2 Physics in the vicinity of the phase transition

Now we are ready to return to the numerical discussion and ask the sharper question of whether the RG dynamics allows realistic numbers to be generated. In order to facilitate the discussion we collect the relevant equations and simplify the notation, by defining $\alpha_{4,R} \equiv x$, $\alpha_{s,R} \equiv y$ and $c_s' \equiv c$. We have Eq. (5.4.8), Eq. (5.4.10) and Eq. (5.4.15) that read in this notation

$$m_R = \Lambda_s e^{\frac{c}{y}}, \qquad \mu_* = \Lambda_s e^{\frac{c}{\alpha_*}}, \qquad m_{h*} = \sqrt{\frac{210}{8\pi^2}} 16\pi^2 v_* \alpha_* \tag{5.4.28}$$

where $c = 3/125$ and

$$\alpha_* = (1+2c)\frac{xy}{y+2cx}\,. \tag{5.4.29}$$

If we keep Λ_s fixed, the model is parametrized by the constants x, y and v_*. A necessary condition for the validity of the effective action is that these scales obey the hierarchy

$$m_R < m_{h*} < \mu_*\,. \tag{5.4.30}$$

Beyond this constraint, we would like to see if we can generate in addition a Standard Model-like spectrum, that is

$$m_{h*} \simeq 125\,\text{GeV} \qquad \text{and} \qquad \rho_{\text{bh}} > 1 \tag{5.4.31}$$

It turns out that the window of parameters that solve Eq. (5.4.28) is small. If we focus on Eq. (5.4.30) the first restriction we get is $\alpha_* < y$ which combined with Eq. (5.4.29) suggests the condition $x < y$. Such a case is expected to be obeyed between a confined and a deconfined coupling and then we get the right hierarchy only in the range $0 < x < 0.01$ approximately, for any reasonable value of v_*, which we will assume to be $v_* \sim O(100\,\text{GeV})$. If in addition we impose Eq. (5.4.31), the solution becomes even more constrained. There are four variables, x, y, v_* and Λ_s which need care two of which can be fixed by a physical motivation. In fact, we can set $g_{s,R}$ equal to the SM strong coupling $g(m_Z) \simeq 1.5$ which fixes $y \simeq 0.014$. For Λ_s there are two interesting scenarios, $\Lambda_s \equiv \Lambda_{\text{QCD}} \simeq 200$ MeV and $\Lambda_s \equiv m_p \simeq 1000$ MeV, with the latter equal to the proton mass. We give two examples: for $\Lambda_s \simeq 200$ MeV, $x \simeq 0.00330$, $y \simeq 0.014$ and $v_* \simeq 142$ GeV, we get $m_R \simeq 1.11$ GeV, $m_{h*} \simeq 125$ GeV, $\mu_* \simeq 223.3$ GeV and $\rho_{\text{bh}} \simeq 1.2$. The value of ρ_{bh} increases towards its SM value ~ 1.38 if we use our second choice for Λ_s, which corresponds to 1000 MeV. Then the above range for x shifts by a bit and presents an alternative set of numbers: for $x \simeq 0.00435$, $y \simeq 0.014$ and $v_* \simeq 108.2$ GeV we obtain $m_R \simeq 5.55$ GeV, $m_{h*} \simeq 125.1$ GeV, $\mu_* \simeq 209.1$ GeV and $\rho_{\text{bh}} \simeq 1.373$. Note that the latter implies $m_{Z*} \simeq 91.1$ GeV for the gauge boson mass and $c_{1*}^{(6)} \simeq 0.12$ for the HDO coupling Eq. (5.3.12), therefore in this example the observables take quite Standard Model-like values. Furthermore, the obtained m_R and y justify our discussion below Eq. (5.4.19) which shows that the model reaches its first order phase transition before the continuum limit. Finally, x (or $\alpha_{4,R}$) for the above two cases when inserted in Eq. (5.3.21) gives $\mu_{4,\text{L}} \simeq 2 \times e^{60}$ GeV and $\mu_{4,\text{L}} \simeq 1 \times e^{50}$ GeV respectively. This implies that $\mu_* << \mu_{4,\text{L}}$ and hence the model remains consistent.

We are now ready to construct the perturbative phase diagram using the above numerical analysis and draw RG flow lines on it. Starting with the phase diagram what we expect is the

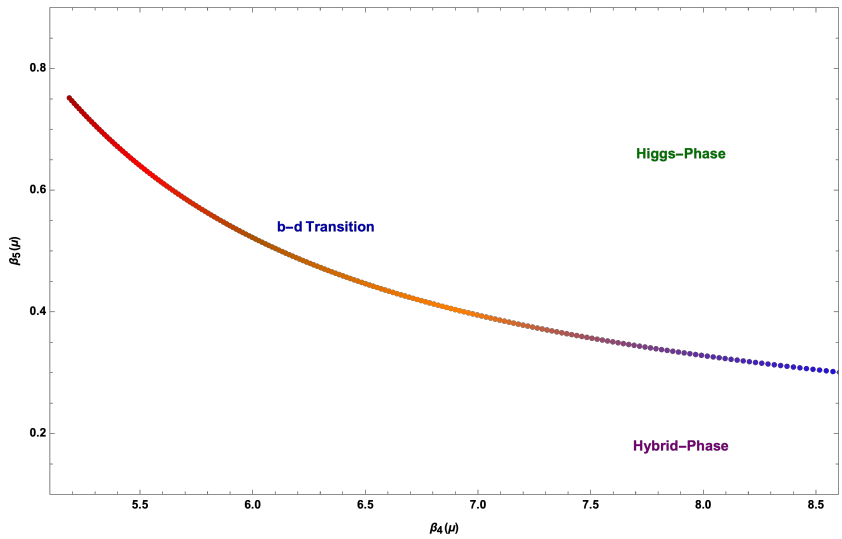

Figure 5.7: The perturbative phase diagram. The featuring phase transition is weak first order and bulk-driven (b-d Transition) separating the Higgs from the Hybrid phase. The phase line is constructed by pairs of (β_{4*}, β_{5*}) obtained at the cut-off scale μ_* by means of the matching procedure described in the text, while its colour code reflects that the cut-off scale increases from the IR (left, redder dots) to the UV (right, bluer dots).

existence of a weak, bulk-driven, first order phase transition which separates the Higgs from the Hybrid phase, deduced from the matching condition of the flows at the natural cut-off μ_*. The (re)construction of the boundary-driven transition is out of the scope of the current work.

Our construction algorithm is the following: We choose to present the phase diagram on the plane of running couplings β_4 and β_5, which is analogous to the lattice parametrization. These are connected to the perturbative $\alpha_4(\mu)$ and $\alpha_s(\mu)$ through Eq. (5.4.24) and Eq. (5.4.25) respectively. The next step is to express the couplings $\beta_4(\mu)$ and $\beta_5(\mu)$ as functions of the matching condition parameters in Eq. (5.4.28) and Eq. (5.4.29) that is in terms of Λ_s, y, v_* and x. Among them the first two are already fixed in our examples and now we choose to keep also v_* fixed and let x to run freely. Here we work with the set of parameters that gives the SM spectrum: $\Lambda_s \simeq 1000$ MeV and $y \simeq 0.014$, which combined fix also $m_R \simeq 5.55$ GeV, as well as $v_* \simeq 108.2$ GeV. Then the phase diagram is constructed by varying x and after that collecting the produced pairs $(\beta_4(\mu_*), \beta_5(\mu_*))$. As a last comment, the numerical analysis below Eq. (5.4.31) gives us the upper bound of x, $x_{\max} \simeq 0.004736$, for which Eq. (5.4.28) admits the minimum cut-off $\mu_{*,\min} \simeq 136.1$ GeV. It would be nice to also have an upper bound. Recall that our model stops generating a viable SM spectrum when $\rho_{\rm bh} \simeq 1$ which corresponds to $x_{\min} \simeq 0.002706$ and $\mu_{*,\max} \simeq 5123$ GeV. Actually this is an allowed, almost forced upper bound for our example since Eq. (5.4.23) gives for $x_{\min}$ the scale $\mu_{\max} \simeq 5751\,\text{GeV} > \mu_{*,\max}$, above which the running of γ is given by the undesired red line of Fig. 5.5. With these in our mind the perturbative phase diagram of our model is depicted in Fig. 5.7 showing indeed the existence of a first order phase transition. This bulk-driven transition (b-d Transition) is the result of a series of finite cut-offs and even though it resembles that of [3] (blue line of Fig. 5.1)

its location is slightly above the latter, so the RG flows will hit on it before reaching the WF line (see the discussion below Eq. (5.4.19)).

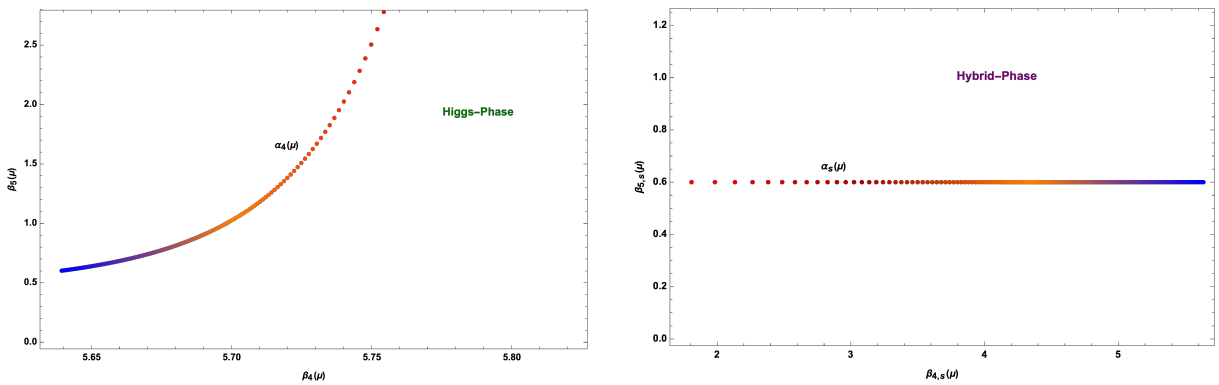

Figure 5.8: The RG flow of the running coupling $\alpha_4(\mu)$ in the Higgs phase (left) and $\alpha_s(\mu)$ in the Hybrid phase (right) depicted on the $\beta_4 - \beta_5$ and $\beta_{4,s} - \beta_{5,s}$ plane respectively. For the latter the only running parameter is $\beta_{4,s}(\mu)$ while $\beta_{5,s}(\mu)$ is kept fixed at 0.6. The colouring of the curves represents the increase of the dynamical scale from the IR (redder dots) to the UV (bluer dots) reaching eventually the cut-off, μ_*. The latter is the scale where both RG flows end hitting the same point on the line of phase transitions.

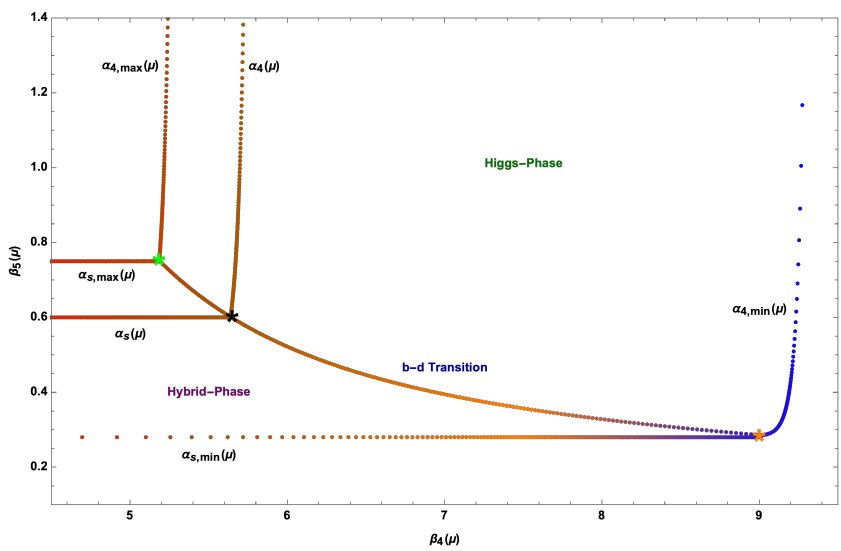

Figure 5.9: The running of the couplings $\alpha_4(\mu)$ and $\alpha_s(\mu)$ (Higgs and Hybrid phase respectively) as the RG flow moves towards the phase transition in the UV. When the cut-off scale is reached the RG flows hit the point $*$ of the phase transition. Here we show three pairs of RG flows whose end points are located at $\mu_{*,\min} \simeq 136.1$ GeV (green star), $\mu_* \simeq 209.1$ GeV (black star) and $\mu_{*,\max} \simeq 5123$ GeV (orange star) respectively. The flow whose cut-off is μ_* and whose flow ends on the black star generates the Standard Model spectrum.

For the construction of the RG flows we follow almost the same path with the previous case. As before the necessary ingredients are the couplings $\alpha_4(\mu)$ in Eq. (5.3.19) and $\alpha_s(\mu)$ in Eq. (5.4.7), as well as their counterparts Eq. (5.4.24) and Eq. (5.4.25). We choose to focus on

the RG flow corresponding to the set of parameters

$$(\Lambda_s, v_*, x, y) \equiv (1000\,\text{MeV}, 108.2\,\text{GeV}, 0.00435, 0.014) \tag{5.4.32}$$

which produced the SM-like spectrum. The difference with respect to the phase diagram algorithm is that now these are kept fixed and the only parameter which runs freely is μ. For the Higgs phase the RG flow is obtained by the simultaneous running of $\beta_4(\mu)$ and $\beta_5(\mu)$, Eq. (5.4.24). In the Hybrid phase on the other hand the only running parameter is $\beta_{4,s}(\mu)$, according to the discussion below Eq. (5.4.25), since $\beta_{5,s}$ is constant and given by Eq. (5.4.27) when the set of values in Eq. (5.4.32) is used. Collectively these arguments result in the running couplings in Fig. 5.8. Keep in mind that the RG flow in both phases, when the common cut-off scale is reached hits on the same point of the phase transition and the associated running ends, a consequence of the matching condition. In the current scenario this scale is $\mu_* \simeq 209.1$ GeV and corresponds to the point $(\beta_{4*}, \beta_{5*}) = (5.64, 0.60)$. Of course this is not the only possible choice since by changing x we get RG flows which end on different points on the phase transition, corresponding to different cut-off scales. For example for $x \equiv x_{\text{min}} = 0.002706$ and $x \equiv x_{\text{max}} = 0.004736$ we obtain $m_{h*} \simeq 78.3$ GeV, $\mu_* \simeq 5123$ GeV, $\rho_{\text{bh}} \simeq 1$ and $m_{h*} \equiv \mu_* \simeq 136.1$ GeV and $\rho_{\text{bh}} \simeq 1.43$ respectively. The associated endpoints are $(\beta_{4*}, \beta_{5*})_{\text{min}} \equiv (9.08, 0.28)$ and $(\beta_{4*}, \beta_{5*})_{\text{max}} \equiv (5.2, 0.75)$, while neither case gives a SM-like spectrum. Note that if we had changed, apart from x, also the other variables we could have come up with different RG flows which however would not refer to the phase diagram of Fig. 5.7. This is the reason why in the above examples we varied only x keeping Λ_s, y and v_* fixed. The simultaneous running of the above RG flows towards the first order phase transition is presented in Fig. 5.9. In Fig. 5.10 we

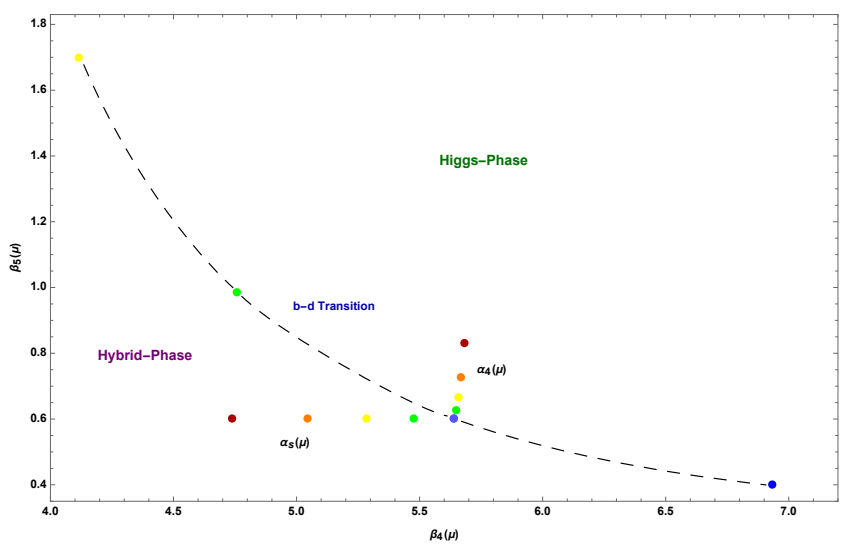

Figure 5.10: Zoom around the phase transition for the SM-like example in Eq. (5.4.32). The colour code convention regarding the scale value of each point follows light frequencies.

zoom around the phase transition for the set of parameters in Eq. (5.4.32) where we show a few points of Fig. 5.9. In this plot, the colour code is strict for all points. The colour of each point represents the value of μ that corresponds to it, with red representing the IR, blue the UV and

with intermediate frequency colours representing analogous intermediate scales. Points of same colours along the RG lines have the same μ, which illustrates explicitly the correlation of the RG flows in the two phases. The flows meet on the phase transition on the blue point where $\mu_* = 209.1$ GeV.

Up to now, we have not said much about the HDO which played the role of the potential in the boundary effective action. Let us now comment on the character of this operator using the scaling dimension, $\Delta_{O^{(l)}}$, following the notation in [30]. In our starting Lagrangian $c_1^{(6)}$, before its connection to g_4, had the role of the quartic coupling of the potential so the operator of interest is

$$O_1^{(6)} = (\bar{\phi}\phi)\Box(\bar{\phi}\phi)\,.$$

Its classical dimension is given by

$$\begin{aligned} d_{O_1^{(6)}} &= 2 + 2d - 4 \\ &= 2d - 2 \end{aligned} \tag{5.4.33}$$

and in $d = 4$ it is $d_{O_1^{(6)}} = 6$, as expected. We are interested in the way that the behaviour of this operator changes due to the quantum corrections. Following standard terminology, the nature of an operator is decided by the quantity $\Delta_{O^{(l)}} - d$ according to:

$$\Delta_{O^{(l)}} - d : \begin{cases} < 0 \to \text{relevant} \\ > 0 \to \text{irrelevant} \\ = 0 \to \text{RG equation} \end{cases} \tag{5.4.34}$$

and an appropriate definition for the scaling dimension $\Delta_{O^{(l)}}$ is

$$\Delta_{O^{(l)}} = d_{O^{(l)}} + \gamma_{O^{(l)}}\,, \tag{5.4.35}$$

with $\gamma_{O^{(l)}}$ the anomalous dimension of the operator, defined as

$$\gamma_{O^{(l)}} = \left.\frac{\partial \beta^1_{c^{(l)}}(c^{(l)})}{\partial c^{(l)}}\right|_{c^{(l)} \to c^{(l)}_*}\,, \tag{5.4.36}$$

with $c^{(l)}$ the associated to $O^{(l)}$ coupling. For example, when quantum corrections are turned off, $\gamma_{O_1^{(6)}} = 0$ and then Eq. (5.4.34) in $d = 4$ shows that

$$\Delta_{O_1^{(6)}} - 4 = 2 > 0 \tag{5.4.37}$$

exposing the irrelevant nature of $O_1^{(6)}$ near the Gaussian fixed point. On the other hand, when quantum corrections are presented we solve Eq. (5.4.36) for the coupling $c_1^{(6)}$ with the associated β-function Eq. (5.2.76). In $d = 4$ this reads

$$\gamma_{O_1^{(6)}} = \frac{c_1^{(6)}}{2\pi^2} \tag{5.4.38}$$

and on the matching point yields for $(\Lambda_s, v_*, x, y) = (200\,\text{MeV}, 142\,\text{GeV}, 0.00330, 0.014)$ and $(\Lambda_s, v_*, x, y) = (1000\,\text{MeV}, 108.2\,\text{GeV}, 0.00435, 0.014)$

$$\gamma^*_{O_1^{(6)}} = 0.022 \;\text{ and }\; \gamma^*_{O_1^{(6)}} = 0.025 \tag{5.4.39}$$

respectively, which still render $\Delta_{O_1^{(6)}} > 0$ and the associated operator irrelevant. Now this is a puzzle because the only operator in the potential is $O_1^{(6)}$ so somehow it should be able to drive the running in a relevant way. Indeed notice that it is inserted in the Lagrangian in momentum space as $\frac{p^2}{\mu_*^2}(\bar{\phi}\phi)^2$ since it is a derivative operator. This means that its effects become less (more) important when p^2 decreases with respect to (increases towards) μ_*^2. Therefore, as the coupling approaches its upper value, the operator itself

$$\frac{O_1^{(6)}}{\mu_*^2} \equiv \frac{p^2}{\mu_*^2}(\bar{\phi}\phi)^2 \longrightarrow (\bar{\phi}\phi)^2\,, \tag{5.4.40}$$

tending towards a usual quartic term. Hence, the above renders $O_1^{(6)}$ more and more marginal (or less and less irrelevant) and by taking into account the running of g_4 it can be characterized as marginally relevant.

5.4.3 Lines of Constant Physics

In our final section we construct Lines of Constant Physics[4] for the Boundary-Hybrid action, in the Higgs phase. The necessary ingredients are two observables as functions of μ, which we can take $\rho_{\text{bh}}(\mu)$ and $m_h(\mu)$. An LCP as typically constructed on the lattice is a line in the space of bare couplings along which these observables are constant, so one would also need a relation between bare and renormalized quantities. Our effective action however does not contain an explicit bare mass term so the relation between $m_{h,0}$ and m_h is undefined and the same is true also for the gauge boson mass. We must come up with a way of drawing the LCP on our phase diagram whose axes are the running and not the bare couplings. A strategy can be the following: Consider the observables mentioned above and recall from Section 5.3.1 that in our scheme the vev stays frozen at $v_* = \text{const}$. This means that when μ changes then both ρ_{bh} and m_h change only as functions of α_4. As already explained, for the example of Eq. (5.4.32) we get $m_{h*} \simeq 125.1$ GeV and $\rho_{\text{bh}_*} \simeq 1.373$ on the phase transition and we now construct our LCP for this case. In order to be able to do it, we need a relation between the observables and the lattice couplings which here is given by the first part of Eq. (5.4.24) and which evaluates on μ_* to

$$\beta_{4*} = \frac{105}{\rho_{\text{bh}}^2(\mu_*)\pi^2} \simeq 5.64\,. \tag{5.4.41}$$

Bare in mind for later use that for $\rho_{\text{bh,min}*} < \rho_{\text{bh}*}$ we get $\beta_{4,\text{max}*} > \beta_{4*}$ while $\rho_{\text{bh,max}*} > \rho_{\text{bh}*}$ gives $\beta_{4,\text{min}*} < \beta_{4*}$. Even though β_{4*} stays fixed along the LCP, this is not the case for β_5 since

[4] An LCP should not be confused with an RG flow. The latter originate from the usual RG equations which involve only the renormalized couplings while the former, in the spirit of Statistical Physics, is determined via the bare couplings. This is of course a characteristic of the lattice formulation.[7]

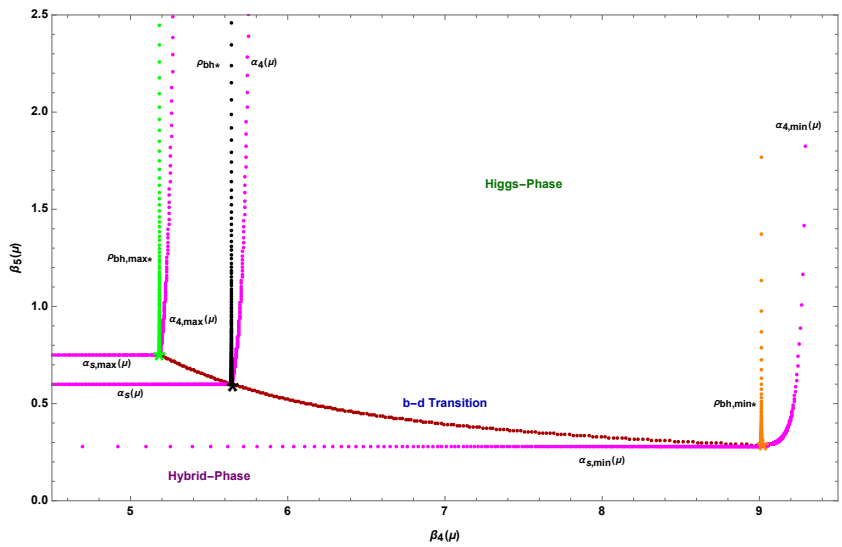

Figure 5.11: The Lines of Constant Physics (green, black and orange line) for the Boundary-Hybrid model in the Higgs phase. Along these lines the mass ratio and the scalar mass are kept fixed. However, only the curve of $\rho_{\rm bh*}$ (black line) corresponds to the Standard Model spectrum. The other two LCP refer to the cases $\rho_{\rm bh,min*} < \rho_{\rm bh*}$ (orange line) and $\rho_{\rm bh,max*} > \rho_{\rm bh*}$ (green line). The RG flows of $\alpha_4(\mu)$ and $\alpha_s(\mu)$ (magenta lines) for these three cases have also been drawn for a comparison with the LCP.

the second part of Eq. (5.4.24), given the running of the anisotropy, indicates that

$$\beta_5(\mu) = \gamma^2(\mu)\beta_{4*}\,. \tag{5.4.42}$$

As a consequence our LCP will correspond to vertical lines which start from $*$ and move into the Higgs phase, while $\rho_{\rm bh}(\mu_*)$ and $m_h(\mu_*)$ are kept fixed. The projection of the LCP on the phase diagram is depicted in Fig. 5.11 by the black line. The following comments are in order: First observe that for both the LCP and the RG running there is a lower and an upper bound. The two bounding scales (m_R and μ_* for both the Higgs and the Hybrid phase in the IR and UV respectively) ensure that the RG flow is short hence only a small amount of fine tuning, for the Higgs mass, is needed. In the same spirit, the LCP shows that the masses can stay fixed for a short scale region before a change of phase occurs, during which the masses are insensitive to changes of the dynamical scale. In this region a stable four-dimensional effective theory with a finite cut-off can be constructed. For completeness here we have considered also the cases $x \equiv x_{\rm min}$ (or $\rho_{\rm bh,min*}$) and $x \equiv x_{\rm max}$ (or $\rho_{\rm bh,max*}$), analyzed in the previous section, whose RG flows were drawn on Fig. 5.9. On the phase transition the former gives that $\beta_{4,\rm max*} \simeq 9.08$ and the latter that $\beta_{4,\rm min*} \simeq 5.2$ while the associated LCP correspond to the orange and green line of Fig. 5.11 respectively.

How much tuning is necessary in order to render our model, Eq. (5.2.11) enhanced by some non-perturbative information, a viable candidate for generating the Standard Model spectrum and at the same time give a resolution to the Higgs mass hierarchy problem? This is an important issue to discuss and we should mention that here, there are two kinds of fine tuning at work. The first type is the usual quantitative tuning associated with the cut-off, alas being realized

in a rather mild way since the presence of the phase transition as detected by perturbation theory via the matching of the RG flows, enforces systematically a low cut-off. The second type of tuning is related to the freedom of choosing the initial data $\Lambda_s, v_*, \alpha_{4,R}$ and $\alpha_{s,R}$ (the bulk parameters $\alpha_{5,R}$ and M_R are fixed by the Hybrid phase characteristics since both have the same origin. Hence, we can set $\alpha_{5,R} \equiv \alpha_{s,R}$ and $M_R = m_R$ implying that the associated RG flows have the same initial data without loss of generality), which amounts to picking the RG flow that respects the scale hierarchy constraint Eq. (5.4.30) and generates a realistic spectrum, as in Eq. (5.4.31). Clearly the picking of a special RG flow involves an infinite amount of fine tuning, but this is the case for any effective theory with a Higgs mechanism. The quantitative aspect of the choice of the initial parameters is the real fine tuning that we have to discuss in more detail. In fact, in the previous numerical analysis we were varying only $\alpha_{4,R}$ while the other three parameters were kept fixed. To get a better feel for the amount of fine tuning, let us fix the dimensionfull parameters Λ_s and v_*, let $\alpha_{4,R}$ and $\alpha_{s,R}$ vary and see how much fine tuned is a chosen RG flow line. To be concrete we take the SM-like example with $\Lambda_s \simeq 1000\,\text{MeV}$ and $v_* \simeq 108.2\,\text{GeV}$ (see below Eq. (5.4.31) for the motivation). Then, we have the following cases:

- Case I: $\alpha_{s,R} \geq \mathcal{O}(10^{-1})$. For $\alpha_{4,R} \simeq 0.00435$ we get $m_R \simeq 1.27$ GeV, $m_{h*} \simeq 126.7$ GeV, $\mu_* \simeq 195.5$ GeV and $\rho_{\text{bh}} \simeq 1.38$. This case resembles the SM spectrum, however at μ_* Eq. (5.4.16) gives $\alpha_{5*} = 0.096025$ or $\alpha_{5\star} - \alpha_{5*} < 0$ which suggests that the first order phase transition is below the WF line. This is forbidden since $\mu_\star = \infty$ while μ_* is finite.

- Case II: $\alpha_{s,R} \sim \mathcal{O}(10^{-2})$. Here there are two sub-cases. For $0.01 \leq \alpha_{s,R} \leq 0.024$ and $\alpha_{4,R} \simeq 0.00435$ we get exactly the SM spectrum, $m_{h*} \simeq 125.1$ GeV and $\rho_{\text{bh}} \simeq 1.373$, with $m_R \simeq 5.55$ GeV and $\mu_* \simeq 209.1$ GeV so both constraints, Eq. (5.4.30) and Eq. (5.4.31), are full-filled. For $0.026 \leq \alpha_{s,R} \leq 0.098$ we get a viable spectrum, again only for $\alpha_{4,R} \simeq 0.00435$, which is similar but not identical with the SM one. In both sub-cases the first order phase transition is above the WF line since $\alpha_{5\star} - \alpha_{5*} > 0$.

- Case III: $\alpha_{s,R} \leq \mathcal{O}(10^{-3})$. For $\alpha_{4,R} \simeq 0.0054$ we obtain again a viable SM spectrum, $m_{h*} \simeq 125.2$ GeV, $\mu_* \simeq 208.5$ GeV and $\rho_{\text{bh}} \simeq 1.373$ with $\alpha_{5\star} - \alpha_{5*} > 0$. Nevertheless Eq. (5.4.31) is full-filled, here we get $m_R \simeq 2.64 \times 10^{10}$ GeV which violates Eq. (5.4.30). Note that we can choose the unreasonable scale $\Lambda_s \sim 10^{-10}\,\text{GeV}$ to get the same, valid, spectrum however, the cut-off now reads $\mu_* \sim 10^{-8}$ GeV rendering also this choice problematic.

In the realistic scenario, Case II, the amount of fine tuning corresponds to forcing $\alpha_{s,R}$ to remain in the range $0.010 \leq \alpha_{s,R} \leq 0.098$, since $\alpha_{4,R} \simeq 0.00435$ stays essentially constant when Eq. (5.4.30) and Eq. (5.4.31) are satisfied. For completeness let us briefly refer to the case where $\alpha_{4,R} \simeq 0.00435$ and $\alpha_{s,R} \simeq 0.014$ are kept fixed while Λ_s and v_* are free to run. In the same spirit with the above, Eq. (5.4.30) and Eq. (5.4.31) are full-filled when Λ_s remains in the range $0.6\,\text{GeV} \leq \Lambda_s \leq 16\,\text{GeV}$ while v_* admits the value $v_* \simeq 108.2$ GeV.

In conclusion, if we imagine that Λ_s and v_* are somehow known, then the fine tuning of an RG flow that respects the physical constraints Eq. (5.4.30) and Eq. (5.4.31), is equal to or less

than $O(10^2)$. What is interesting in this way of quantifying the fine tuning is that the lattice may actually be capable of fixing these dimensionfull parameters.

Appendix

5.A Review of the NPGHU model

In part I, the Non-Perturbative Gauge-Higgs Unification model was computed at leading order in the lattice spacing expansion in [3] such that only operators of classical dimension less or equal to d were inserted in the effective action. Here we perform an extensive review of the main characteristics of this calculation and we move one step further, including next to leading order effects. We show that like this, Higher Dimensional Operators are introduced and we recalculate the extended continuum effective action.

Let us start with a short reminder of the NPGHU model. This is a non-perturbative construction whose simplest realization is a five-dimensional pure Yang–Mills gauge theory defined on a periodic hyper-cubic orbifold lattice [4, 5, 6] with an anisotropy in its fifth dimension. The four-dimensional planes, in which the lattice is infinite, have lattice spacing a_4, while the anisotropic fifth dimension, on which the orbifold boundary conditions are implemented, has lattice spacing a_5. The above discrepancy results in a geometry which has a 5d bulk and two 4d boundaries located at the endpoints of the anisotropic dimension. In its simplest realization in the bulk an $SU(2)$ gauge symmetry is embedded and the boundary conditions leave at the boundaries a $U(1)$ gauge field and a complex scalar field. At the end, the lattice can be folded about its midpoint in the extra dimension and the infinite dimensional limit can be taken. Our notation follows [3] with small exceptions.

5.A.1 The orbifold lattice action

We consider a Euclidean hyper-cubic 5d lattice which is periodic in all dimensions. The extra dimension is a circle with radius R and the orbifold lattice is constructed by projecting the circle by the discrete group $\mathbb{Z}_2$. This action identifies the upper with the lower semicircle and results in a discretized interval with two fixed points. On each of these fixed points lives a 4d slice and the produced geometry is that of $\mathbb{R}^4 \times S^1/\mathbb{Z}_2$. The projection acts also on the gauge group. If there is a 5d $SU(2)$ gauge theory in the bulk, the action of $\mathbb{Z}_2$ leaves at the endpoints of the interval a $U(1)$ subgroup and a complex scalar field. In what follows capital Latin letters M, $N, \cdots = 0, 1, 2, 3, 5$ denote the 5d Euclidean or Minkowski index while small Greek letters μ, $\nu, \cdots = 0, 1, 2, 3$ denote the four-dimensional part. Moreover, the lattice coordinates are

defined as $n_M \equiv (n_\mu, n_5)$ with $n_\mu = 1, \cdots, L_\mu$ and $n_5 = 0, \cdots, N_5$. The orbifold fixed points are located at $n_5 = 0$, N_5. Recall that the four-dimensional part of the lattice is taken infinite, a fact that is mirrored by sending $L_\mu \to \infty$. On the other hand, the extra dimension is allowed to be either finite or infinite. Since the number of lattice nodes in this direction is given by $N_5 = \pi R/a_5$, the choice $R \to \infty$ or $R \equiv$ finite determines the magnitude of the fifth dimension. The next step is the determination of the lattice gauge variables. The needed ingredients for that are the gauge links $U(n_M, N) \in SU(2)$. Their form is

$$U(n_M, N) = e^{i a_N g_5 \mathbf{A}_M(n_M)}\,, \tag{5.A.1}$$

where n_M indicates their location while N the direction in which they point. The above exponential includes the lattice spacings a_ν and a_5 given by a_N with $N = \nu$ and $N = 5$ respectively. The former is identified as $a_\nu = a_4$, for every ν, while in general $a_4 \neq a_5$. In addition we get the continuum 5d dimensionfull coupling g_5 and the Lie algebra valued gauge field (always written in bold character) $\mathbf{A}_M \equiv A_M^A T^A$ which carries the adjoint index A. The generators are normalized using $\mathrm{tr}\{T^A T^B\} = \delta^{AB}/2$. Dimensional analysis of the exponent in Eq. (5.A.1) indicates that $[\mathbf{A}_M] = 3/2$, $[a_N] = -1$ and $[g_5] = -1/2$, where $[\cdots]$ represents the classical dimension of its argument. Since the structure of the lattice and the associated gauge variables are settled down we can now consider the orbifold projection on both of them. We define the reflection operator $\mathcal{R}$ that acts as a group conjugation, $\mathcal{T}_g$, on the corresponding generators. The orbifold condition on the links is implemented on the lattice through

$$\mathcal{R} U(n_M, N) = \mathcal{T}_g U(n_M, N)\,. \tag{5.A.2}$$

Regarding the lattice nodes $n_M = (n_\mu, n_5)$, the reflection operator acts on them as

$$\mathcal{R}(n_\mu, n_5) = (n_\mu, -n_5) \equiv \bar{n}_M \tag{5.A.3}$$

while on the gauge links as

$$\mathcal{R} U(n_M, \nu) = U(\bar{n}_M, \nu) \;\text{ and }\; \mathcal{R} U(n_M, 5) = U^\dagger(\bar{n}_M - a_5 \hat{5}, 5)\,. \tag{5.A.4}$$

On the other hand, $\mathcal{T}_g$ acts solely on the gauge links and the associated action yields

$$\mathcal{T}_g\, U(n_M, N) = g U(n_M, N) g^{-1}\,, \tag{5.A.5}$$

with g^2 an element in the centre of $SU(2)$ which we can choose to be $g = -i\sigma^3$, the third Pauli matrix. Notice that $\mathcal{R}$ commutes with $\mathcal{T}_g$ and also that $\mathcal{R}^2 = \mathcal{T}_g^2 = 1$. The orbifolding becomes interesting when we look at the fixed points. As a small comment note that the orbifold has a mirror symmetry around the midpoint of the fifth dimension. Then, without loss of generality, we can fold it and consider only one of the two boundaries multiplied now with a factor of 2. Here we choose to work with the boundary located at $n_5 = 0$. Now, the reflection operation has a trivial effect on the boundary nodes, $n_M = (n_\mu, 0)$, and hence Eq. (5.A.2) becomes

$$U((n_\mu, 0), \nu) = \mathcal{T}_g\, U((n_\mu, 0), \nu) \equiv g U((n_\mu, 0), \nu) g^{-1}\,. \tag{5.A.6}$$

The above relation is satisfied only for the gauge links that commute with σ^3. Therefore on the boundary the generators of the bulk group $\mathcal{G}$ separate in T^a and $T^{\hat{a}}$. The former belong to the unbroken group $\mathcal{H}$ with $\mathcal{H} \subset \mathcal{G}$ while the latter to the broken ones. Since here $U(n_M, N)$ is an $SU(2)$ element with generators $T^A = \sigma^A/2$, the three Pauli matrices, the only acceptable choice is $a = 3$ and $\hat{a} = 1, 2$. In other words only a $U(1)$ gauge symmetry remains unbroken on the boundary. The lattice action is constructed using the Wilson plaquettes which are gauge invariant objects consisting of gauge links. The above discussion indicates that there are $U(1)$ and $SU(2)$ links on the boundary and in the bulk respectively, as well as, hybrid links which have one end on the boundary and the other in the bulk. The gauge transformation for the latter is given by $U \to \Omega^{U(1)} U (\Omega^{SU(2)})^\dagger$. With these in our hand we get the following two plaquette categories: 1) the boundary-hybrid plaquette and 2) the bulk plaquette. In 1) we define as $U^b_{\mu\nu}$ the 4d boundary plaquettes, including links lying only on the boundary, and as $U^h_{\mu 5}$ the hybrid plaquettes with two links lying on the fifth dimension with one end on the boundary and the other on the bulk. In 2) we define $U_{\mu\nu}$ and $U_{\mu 5}$ plaquettes with gauge links lying exclusively in the bulk. Hence the anisotropic orbifold Wilson action, $S_{S^1/\mathbb{Z}_2} \equiv S^{\rm orb}$, reads

$$S^{\rm orb} = S^{\rm b-h} + S^B \tag{5.A.7}$$

where orb stands for orbifold, $S^{\rm b-h}$ is the boundary-hybrid action

$$S^{\rm b-h} = \frac{1}{2N} \sum_{n_\mu} \left[\frac{\beta_4}{2} \sum_{\mu<\nu} {\rm tr} \left\{ 1 - U^b_{\mu\nu}(n_\mu, 0) \right\} + \beta_5 \sum_\mu {\rm tr} \left\{ 1 - U^h_{\mu 5}(n_\mu, 0) \right\} \right] \tag{5.A.8}$$

and S^B corresponds to the bulk action

$$S^B = \frac{1}{2N} \sum_{n_\mu, n_5} \left[\beta_4 \sum_{\mu<\nu} {\rm tr} \left\{ 1 - U_{\mu\nu}(n_\mu, n_5) \right\} + \beta_5 \sum_\mu {\rm tr} \left\{ 1 - U_{\mu 5}(n_\mu, n_5) \right\} \right]. \tag{5.A.9}$$

β_4 and β_5 are the dimensionless lattice couplings and N is the degree of the group $\mathcal{G}$. Since here $\mathcal{G} \equiv SU(2)$ then $N = 2$. Notice that we sum only over plaquettes with counterclockwise orientation.

Few comments are in order. Keep in mind that the extra 1/2 factor in the boundary lattice action will be canceled due to the folding of the orbifold around the midpoint of the fifth dimension. Moreover notice that $S^{\rm orb}$ is the same with the one developed in [3] (apart from some modifications in the notation, trivial to be synchronized). Finally the anisotropy, which at classical level is given by $\gamma = a_4/a_5$, is explicitly introduced in the above framework when we switch to the equivalent pair of dimensionless couplings:

$$\beta_4 = \frac{\beta}{\gamma}\,, \;\; \beta_5 = \beta\gamma \tag{5.A.10}$$

which holds for both the boundary and the bulk. β here should not be confused with the usual definition of a β-function. Since we know the anisotropic orbifold lattice action our next step is to construct its continuum version so we first need to explicitly compute $S^{\rm b-h}$ and S^B. Towards that direction we consider the expansion in small lattice spacing for Eq. (5.A.8) and Eq. (5.A.9)

according to the program of [3]. There the expansion was truncated to the lowest non-trivial order in a_4, a_5 which led to a disconnected boundary-bulk system[5]. Here we move a step further in our computation so that the boundary is no longer disconnected from the bulk, a property which should be mirrored in the continuum effective action. The truncation in a_4, a_5 is such that it reveals the lowest higher dimensional operators which respect the symmetries.

5.A.2 The Boundary-Hybrid action with higher order terms

Let us start our computation with the pure boundary part of Eq. (5.A.8) which we denote here as

$$S^b = \frac{1}{2N} \sum_{n_\mu} \frac{\beta_4}{2} \sum_{\mu<\nu} \mathrm{tr} \left\{ 1 - U^b_{\mu\nu}(n_\mu, 0) \right\} . \tag{5.A.11}$$

As we have already mentioned the above plaquette includes only boundary-lying gauge links and its explicit form reads

$$\begin{aligned} U^b_{\mu\nu}(n_\mu) &= U^b(n_\mu, \mu)\, U^b(n_\mu + a_4\hat{\mu}, \nu)\, (U^b(n_\mu + a_4\hat{\nu}, \mu))^\dagger\, (U^b(n_\mu, \nu))^\dagger \\ &= e^{ia_4 g_5 \mathbf{A}_\mu(n_\mu)}\, e^{ia_4 g_5 \mathbf{A}_\nu(n_\mu + a_4\hat{\mu})}\, e^{-ia_4 g_5 \mathbf{A}_\mu(n_\mu + a_4\hat{\nu})}\, e^{-ia_4 g_5 \mathbf{A}_\nu(n_\mu)} , \end{aligned} \tag{5.A.12}$$

where we have used Eq. (5.A.1) for $M, N = \mu, \nu$. For the calculation of the plaquette we use the Baker–Campbell–Housdorff (BCH) formula. To be more specific when there are four exponentials, with exponents X, Y, Z, W respectively, the complete basis for the formula is the following:

$$\begin{aligned} e^X e^Y e^Z e^W &= \exp\Big[X + Y + Z + W + \frac{1}{2}\Big([X,Y] + [X,Z] + [X,W] + [Y,Z] + [Y,W] + [Z,W] \Big) \\ &+ \frac{1}{4}\Big([X,[Z,W]] + [Y,[Z,W]] + [[X,Y],Z] + [[X,Y,],W] \Big) + \frac{1}{8}[[X,Y],[Z,W]] \Big] \end{aligned} \tag{5.A.13}$$

where here the exponents of the gauge links are represented by X, Y, Z and W. Regarding the boundary gauge field $\mathbf{A}_\mu \equiv A^3_\mu T^3$, BCH reduces to the usual product of exponentials since $[A^3_\mu T^3, A^3_\nu T^3] = 0$. As a small side note, we would like to clarify a bit more the arguments of the above exponentials. In particular, the corresponding exponents are dimensionless only if

$$[a_4] + [g_5] + [\mathbf{A}_\mu] = 0$$

which, according to the dimensional analysis of Sect. 5.A.1 gives $[\mathbf{A}_\mu] = 3/2$. This is an expected result regarding the 5d bulk but on the 4d boundary the dimensionality of the gauge field should be different. One way to overcome this obstacle, in agreement with [3], is to note that the boundary-hybrid action does not include a summation over a_5 which then becomes a free parameter. Since here we consider $R \to \infty$ and we are allowed to choose $N_5 \to \infty$ then, from $a_5 = \pi R/N_5$, we get that $a_5 \to a_{5,f}$ which is finite. Then we can define $g_5 \equiv g_4\sqrt{a_{5,f}}$, with

[5] Trailing back the computational details regarding the small lattice spacing expansion, which are presented in [3], will be a comprehensive guide for the current work.

g_4 a dimensionless coupling, and reabsorb $\sqrt{a_{5,f}}$ in the gauge field. In that sense $\sqrt{a_{5,f}}\mathbf{A}_\mu \to \mathbf{A}_\mu$ on the exponentials and now $[\mathbf{A}_\mu] = 1$ which is the usual dimension of a 4d gauge potential. Another way of seeing the above argument is that we want the fields and currents of $S^{\mathrm{b-h}}$ to be localized at the lattice boundary. This happens when the anisotropy is small, [32], which is true when $a_5 > a_4$. So since here we consider the $a_4 \to 0$ limit then a_5 cannot approach zero but it can take any finite value without losing generality. With the above in mind Eq. (5.A.12) becomes

$$U^b_{\mu\nu}(n_\mu) = e^{ia_4 g_4[\mathbf{A}_\mu(n_\mu)+\mathbf{A}_\nu(n_\mu+a_4\hat{\mu})-\mathbf{A}_\mu(n_\mu+a_4\hat{\nu})-\mathbf{A}_\nu(n_\mu)]} \tag{5.A.14}$$

and we are ready to consider the series of $\mathbf{A}_\nu(n_\mu + a_4\hat{\mu})$ and $\mathbf{A}_\mu(n_\mu + a_4\hat{\nu})$ for small a_4 while we keep terms up to order $\mathcal{O}(a_4^2)$. In other words the expansion gives

$$\begin{aligned}
\mathbf{A}_\nu(n_\mu + a_4\hat{\mu}) &\equiv \mathbf{A}_\nu(n_\mu) + a_4\hat{\Delta}_\mu\mathbf{A}_\nu(n_\mu) + \frac{a_4^2}{2}\hat{\Delta}_\mu(\hat{\Delta}_\mu\mathbf{A}_\nu(n_\mu)) \\
\mathbf{A}_\mu(n_\mu + a_4\hat{\nu}) &\equiv \mathbf{A}_\mu(n_\mu) + a_4\hat{\Delta}_\nu\mathbf{A}_\mu(n_\mu) + \frac{a_4^2}{2}\hat{\Delta}_\nu(\hat{\Delta}_\nu\mathbf{A}_\mu(n_\mu))
\end{aligned}$$

with $\hat{\Delta}_\mu\mathbf{A}_\nu(n_\mu) = (1/a)[\mathbf{A}_\nu(n_\mu + a\hat{\mu}) - \mathbf{A}_\nu(n_\mu)]$ a discretized derivative. Therefore the above plaquette yields

$$U^b_{\mu\nu}(n_\mu) = e^{ia_4^2 g_4\mathbf{F}_{\mu\nu}(n_\mu)+\frac{ia_4^3 g_4}{2}[\hat{\Delta}_\mu\mathbf{F}_{\mu\nu}(n_\mu)+(\hat{\Delta}_\mu-\hat{\Delta}_\nu)\hat{\Delta}_\nu\mathbf{A}_\mu(n_\mu)]+\mathcal{O}(a_4^4)}\,, \tag{5.A.15}$$

where we have defined that $\mathbf{F}_{\mu\nu}(n_\mu) = \hat{\Delta}_\mu\mathbf{A}_\nu(n_\mu) - \hat{\Delta}_\nu\mathbf{A}_\mu(n_\mu)$ with $\mathbf{F}_{\mu\nu} \equiv F^3_{\mu\nu}T^3$. Recall that a plaquette is designed to be a gauge and rotational (Lorentz) invariant object on the Euclidean (Minkowski) lattice. Nevertheless, due to the truncation level of the lattice-spacing expansion several terms, inconsistent with these symmetries, appear. This mismatch is an artifact of the lattice in a sense that adding higher in a_4 terms to the expansion the gauge and rotational symmetry will eventually be restored. Nevertheless, a delicate point here is the assumption that the continuum action, no matter the truncation level, should respect these symmetries. Hence, in the following we will expand all the formulae up to a specific order at the lattice-spacing and then neglect every contribution which is not gauge and rotationally invariant. Then implying Eq. (5.A.15) back to Eq. (5.A.11), performing one more expansion for small a_4 and taking the trace the boundary action becomes

$$\begin{aligned}
S^b &= 2\frac{1}{2N}\sum_{n_\mu}\frac{\beta_4}{2}\sum_{\mu<\nu}\mathrm{tr}\Big\{-ia_4^2 g_4\mathbf{F}_{\mu\nu} - i\frac{a_4^3}{2}g_4[\hat{\Delta}_\mu\mathbf{F}_{\mu\nu} + (\hat{\Delta}_\mu - \hat{\Delta}_\nu)\hat{\Delta}_\nu\mathbf{A}_\mu] \\
&+ \frac{a_4^4}{2}g_4^2\mathbf{F}^2_{\mu\nu} + \frac{a_4^5}{2}g_4^2\mathbf{F}_{\mu\nu}[\hat{\Delta}_\mu\mathbf{F}_{\mu\nu}(n_\mu) + (\hat{\Delta}_\mu - \hat{\Delta}_\nu)\hat{\Delta}_\nu\mathbf{A}_\mu] \\
&+ \frac{a_4^6}{8}g_4^2[\hat{\Delta}_\mu\mathbf{F}_{\mu\nu} + (\hat{\Delta}_\mu - \hat{\Delta}_\nu)\hat{\Delta}_\nu\mathbf{A}_\mu]^2 + i\frac{a_4^6}{6}g_4^3\mathbf{F}_{\mu\nu}\mathbf{F}_{\nu\rho}\mathbf{F}_{\rho\mu}\Big\} + \mathcal{O}(a_4^7) \\
&= \sum_{n_\mu}a_4^4\sum_{\mu<\nu}\Big\{\frac{1}{4}F^3_{\mu\nu}F^3_{\mu\nu} + \frac{a_4^2}{16}(\hat{\Delta}_\mu F^3_{\mu\nu})(\hat{\Delta}_\mu F^3_{\mu\nu})\Big\} + \mathcal{O}(a_4^7)\,,
\end{aligned} \tag{5.A.16}$$

where we added the factor of 2 in front of the sum due to the folding of the orbifold and kept operators up to dimension 6 which are gauge and rotationally invariant. To give an example the

above action originally includes the dimension-3 operators

$$\hat{\Delta}_\mu \mathbf{F}_{\mu\nu} + (\hat{\Delta}_\mu - \hat{\Delta}_\nu)\hat{\Delta}_\nu \mathbf{A}_\mu \,,$$

which are zero when the trace is taken and the dimension-5 operators

$$\mathbf{F}_{\mu\nu}\Big(\hat{\Delta}_\mu \mathbf{F}_{\mu\nu} + (\hat{\Delta}_\mu - \hat{\Delta}_\nu)\hat{\Delta}_\nu \mathbf{A}_\mu\Big)$$

which are not rotationally and gauge invariant. Note moreover that the lattice coupling is fixed by

$$\beta_4 = \frac{2N a_{5,f}}{g_5^2} = \frac{2N}{g_4^2} \,. \tag{5.A.17}$$

Let us make a small pause here and comment on the distribution of a_4's in Eq. (5.A.16). In particular considering the naive continuum limit, $a_4 \to 0$, four of them will be sacrificed so as to form the 4d integral

$$\sum_{n_0} a_4 \sum_{n_1} a_4 \sum_{n_2} a_4 \sum_{n_3} a_4 = (n_0 a_4)(n_1 a_4)(n_2 a_4)(n_3 a_4) \to \int dx_0 dx_1 dx_2 dx_3 \,. \tag{5.A.18}$$

Nevertheless the above is consistent regarding a dimension-4 operator, when the action includes HDO the situation is different. In Eq. (5.A.16) for example there is also a dimension-6 operator which comes with two a_4's extra. So the rising question is what happens to that term when the $a_4 \to 0$ limit is taken. To answer this recall that lattice-spacing works both as a definition of the lattice length and as a natural theory regulator which, in addition, respects gauge invariance. On the other hand, the same theory defined at the continuum is regularized in a gauge invariant manner using dimensional regularization. Moreover, DR introduces the intrinsic scale μ which plays a crucial role in the quantum behaviour of the theory. Matching the situation on the lattice with that of the continuum and since a_4 has a dual role, it is legal to assume that there is a non-trivial connection between the lattice-spacing and the intrinsic scale. Back to Eq. (5.A.16) the above yields that we are allowed to replace the remnant a_4 with $\mu(a_4)$ and get

$$S^b = \sum_{n_\mu} a_4^4 \sum_{\mu<\nu} \left(\frac{1}{4} F^3_{\mu\nu} F^3_{\mu\nu} + \frac{1}{16} \frac{(\hat{\Delta}_\mu F^3_{\mu\nu})(\hat{\Delta}_\mu F^3_{\mu\nu})}{\mu^2(a_4)} \right) + \mathcal{O}(a_4^7) \,. \tag{5.A.19}$$

The other part of Eq. (5.A.8) regards the hybrid action defined here as

$$S^h = \frac{1}{2N} \sum_{n_\mu} \beta_5 \sum_\mu \mathrm{tr}\left\{1 - U^h_{\mu 5}(n_\mu, 0)\right\} \tag{5.A.20}$$

and includes the hybrid plaquette $U^h_{\mu 5}$. Recall that this plaquette is constructed from a $U(1)$ gauge link, two $SU(2)$ hybrid gauge links and one $SU(2)$ gauge link. Therefore its explicit form using Eq. (5.A.1) for $M, N = \mu, 5$ reads

$$\begin{aligned} U^h_{\mu 5} &= U^b(n_\mu, \mu)\, U^h(n_\mu + a_4\hat{\mu}, \hat{5})\, (U(n_\mu + a_5\hat{5}, \mu))^\dagger\, (U^h(n_\mu, \hat{5}))^\dagger \\ &= e^{i a_4 g_4 \mathbf{A}^b_\mu(n_\mu, 0)}\, e^{i a_5 g_4 \mathbf{A}_5(n_\mu + a_4\hat{\mu}, 0)}\, e^{-i a_4 g_4 \mathbf{A}_\mu(n_\mu, a_5\hat{5})}\, e^{-i a_5 g_4 \mathbf{A}_5(n_\mu, 0)} \,, \end{aligned} \tag{5.A.21}$$

where the superscript b on the gauge field refers to the boundary. More precisely we get $\mathbf{A}_\mu^b \equiv A_\mu^3 T^3$ and $(\mathbf{A}_\mu, \mathbf{A}_5) \equiv (A_\mu^A T^A, A_5^A T^A)$. Note that here we have directly followed the arguments above Eq. (5.A.14) so the gauge potential has already mass dimension one. The hybrid plaquette has been set up and the next step is to consider the lattice-spacing expansion. For that purpose we exploit the BCH formula given in Eq. (5.A.13) for

$$X = ia_4 g_4 \mathbf{A}_\mu^b(n_\mu, 0)\,,\ Y = ia_5 g_4 \mathbf{A}_5(n_\mu + a_4\hat{\mu}, 0)\,,\ Z = -ia_4 g_4 \mathbf{A}_\mu(n_\mu, a_5\hat{5})\,,\ W = -ia_5 g_4 \mathbf{A}_5(n_\mu, 0)\,,$$

where now it will not be reduced to the usual case since the commutators are not necessarily zero. Recall that the current work deals with a higher in a_4 and a_5 order compared to [3] so in the following we will keep terms up to $\mathcal{O}(a_4^3, a_5^3)$. As a consequence, non-linear in gauge fields commutators are expected to play a crucial role in the calculation of the hybrid action. With the above in mind the desired plaquette yields

$$\begin{aligned}
U_{\mu 5}^h &= \exp\Bigg[ia_5 g_4\Big(\gamma \mathbf{A}_\mu^b(n_\mu, 0) + \mathbf{A}_5(n_\mu + a_4\hat{\mu}, 0) - \gamma \mathbf{A}_\mu(n_\mu, a_5\hat{5}) - \mathbf{A}_5(n_\mu, 0)\Big) \\
&- \frac{g_4^2}{2}\Big(a_4 a_5[\mathbf{A}_\mu^b(n_\mu, 0), \mathbf{A}_5(n_\mu + a_4\hat{\mu}, 0)] - a_4^2[\mathbf{A}_\mu^b(n_\mu, 0), \mathbf{A}_\mu(n_\mu, a_5\hat{5})] \\
&- a_4 a_5[\mathbf{A}_\mu^b(n_\mu, 0), \mathbf{A}_5(n_\mu, 0)] - a_4 a_5[\mathbf{A}_5(n_\mu + a_4\hat{\mu}, 0), \mathbf{A}_\mu(n_\mu, a_5\hat{5})] \\
&- a_5^2[\mathbf{A}_5(n_\mu + a_4\hat{\mu}, 0), \mathbf{A}_5(n_\mu, 0)] + a_4 a_5[\mathbf{A}_\mu(n_\mu, a_5\hat{5}), \mathbf{A}_5(n_\mu, 0)]\Big) \\
&- \frac{ig_4^3}{4}\Big\{a_4^2 a_5[\mathbf{A}_\mu^b(n_\mu, 0), [\mathbf{A}_\mu(n_\mu, a_5\hat{5}), \mathbf{A}_5(n_\mu, 0)]] + a_4 a_5^2[\mathbf{A}_5(n_\mu + a_4\hat{\mu}, 0), [\mathbf{A}_\mu(n_\mu, a_5\hat{5}), \mathbf{A}_5(n_\mu, 0)]] \\
&- a_4^2 a_5[[\mathbf{A}_\mu^b(n_\mu, 0), \mathbf{A}_5(n_\mu + a_4\hat{\mu}, 0)], \mathbf{A}_\mu(n_\mu, a_5\hat{5})] - a_4 a_5^2[[\mathbf{A}_\mu^b(n_\mu, 0), \mathbf{A}_5(n_\mu + a_4\hat{\mu}, 0)], \mathbf{A}_5(n_\mu, 0)]\Big\} \\
&+ \mathcal{O}(a^4)\Bigg],
\end{aligned} \tag{5.A.22}$$

where $\mathcal{O}(a^k) \equiv \mathcal{O}(a_4^{k_1}, a_5^{k_2})\ \forall\ k_1,\ k_2$ that satisfy $k_1 + k_2 = k$. Note here that the terms in the parenthesis had also been found in [3] while the ones in the curly bracket denote a new, higher order, contribution. Next we deal with the expansion of the gauge potentials for small lattice-spacing while we keep in mind that a next-to-next-to leading order truncation is needed. Then, the desired expressions yield

$$\begin{aligned}
\mathbf{A}_5(n_\mu + a_4\hat{\mu}, 0) &\equiv \mathbf{A}_5(n_\mu, 0) + a_4\hat{\Delta}_\mu \mathbf{A}_5(n_\mu, 0) + \frac{a_4^2}{2}\hat{\Delta}_\mu(\hat{\Delta}_\mu \mathbf{A}_5(n_\mu, 0)) \\
\mathbf{A}_\mu(n_\mu, a_5\hat{5}) &\equiv \mathbf{A}_\mu(n_\mu, 0) + a_5\hat{\Delta}_5 \mathbf{A}_\mu(n_\mu, 0) + \frac{a_5^2}{2}\hat{\Delta}_5(\hat{\Delta}_5 \mathbf{A}_\mu(n_\mu, 0))\,,
\end{aligned} \tag{5.A.23}$$

with $\hat{\Delta}_5$ a discretized derivative in accordance with $\hat{\Delta}_\mu$. Now the above relations should be combined with Eq. (5.A.22), an attempt that will give back a rather messy result. Nevertheless, we can avoid the undesired mess if we first consider Eq. (5.A.6), at a gauge-field level, which

will inherit our expressions with the Dirichlet and Neumann orbifold boundary conditions. To be more specific these conditions demand the following:

$$\begin{aligned}
\mathcal{R}A_\mu^{\hat{a}}T^{\hat{a}} = \alpha_\mu A_\mu^{\hat{a}}T^{\hat{a}} = \eta^{\hat{a}}A_\mu^{\hat{a}}T^{\hat{a}} \quad &\Rightarrow \quad A_\mu^{\hat{a}}T^{\hat{a}} = -A_\mu^{\hat{a}}T^{\hat{a}} \Rightarrow A_\mu^{1,2} = 0 \\
\mathcal{R}A_5^{a}T^{a} = \alpha_5 A_5^{a}T^{a} = \eta^{a}A_5^{a}T^{a} \quad &\Rightarrow \quad -A_5^{a}T^{a} = A_5^{a}T^{a} \Rightarrow A_5^{3} = 0 \\
\mathcal{R}\hat{\Delta}_5 A_\mu^{a}T^{a} = \alpha_5\alpha_\mu\hat{\Delta}_5 A_\mu^{a}T^{a} = \eta^{a}\hat{\Delta}_5 A_\mu^{a}T^{a} \quad &\Rightarrow \quad -\hat{\Delta}_5 A_\mu^{a}T^{a} = \hat{\Delta}_5 A_\mu^{a}T^{a} \Rightarrow \hat{\Delta}_5 A_\mu^{3} = 0 \\
\mathcal{R}\hat{\Delta}_5 A_5^{\hat{a}}T^{\hat{a}} = \alpha_5\alpha_5\hat{\Delta}_5 A_5^{\hat{a}}T^{\hat{a}} = \eta^{\hat{a}}\hat{\Delta}_5 A_5^{\hat{a}}T^{\hat{a}} \quad &\Rightarrow \quad \hat{\Delta}_5 A_5^{\hat{a}}T^{\hat{a}} = -\hat{\Delta}_5 A_5^{\hat{a}}T^{\hat{a}} \Rightarrow \hat{\Delta}_5 A_5^{1,2} = 0
\end{aligned}$$

where α_μ and α_5 correspond to the parity of the gauge fields $\mathbf{A}_\mu$ and $\mathbf{A}_5$ respectively, while η^A with $\eta^a = +1$ and $\eta^{\hat{a}} = -1$ is the parity of the generators coming from the relation $gT^Ag^{-1} = \eta^A T^A$. As a small comment notice that the hybrid plaquette includes also the term $\hat{\Delta}_5(\hat{\Delta}_5 A_\mu^3(n_\mu, 0))$ which survives from the Neumann boundary conditions since

$$\mathcal{R}\hat{\Delta}_5(\hat{\Delta}_5 A_\mu^a T^a) = \alpha_5\alpha_5\alpha_\mu\hat{\Delta}_5(\hat{\Delta}_5 A_\mu^a T^a) = \eta^a\hat{\Delta}_5(\hat{\Delta}_5 A_\mu^a T^a) \Rightarrow \hat{\Delta}_5(\hat{\Delta}_5 A_\mu^a T^a) \neq 0\,.$$

However, after the lattice-spacing expansion is taken all the gauge fields are defined on the boundary, which is located at $n_5 = 0$, so there is no evolution along the fifth dimension. In other words the derivative of $\hat{\Delta}_5$, of any given order, on the boundary fields should vanish. In that sense the gauge potentials become $A_5^A(n_\mu, 0) \to A_5^{1,2}(n_\mu, 0)$ and $A_\mu^A(n_\mu, 0) \to A_\mu^3(n_\mu, 0)$ so Eq. (5.A.23) now gives

$$\begin{aligned}
\mathbf{A}_5(n_\mu + a_4\hat{\mu}, 0) \quad &\to \quad \mathbf{A}_5^b(n_\mu, 0) + a_4\hat{\Delta}_\mu\mathbf{A}_5^b(n_\mu, 0) + \frac{a_4^2}{2}\hat{\Delta}_\mu(\hat{\Delta}_\mu\mathbf{A}_5^b(n_\mu, 0)) \\
\mathbf{A}_\mu(n_\mu, a_5\hat{5}) \quad &\to \quad \mathbf{A}_\mu^b(n_\mu, 0)\,,
\end{aligned} \tag{5.A.24}$$

where we have defined that $\mathbf{A}_5^b \equiv A_5^{\hat{a}}T^{\hat{a}}$. With these in hand our calculation is simplified and the hybrid palquette reads

$$\begin{aligned}
U_{\mu 5}^h \;=\; & \exp\Bigg[ig_4\Bigg(a_4a_5\hat{\Delta}_\mu\mathbf{A}_5^b(n_\mu, 0) + \frac{a_4^2a_5}{2}\hat{\Delta}_\mu(\hat{\Delta}_\mu\mathbf{A}_5^b(n_\mu, 0))\Bigg) \\
- \;& g_4^2\Bigg(a_4a_5[\mathbf{A}_\mu^b(n_\mu, 0), \mathbf{A}_5^b(n_\mu, 0)] + a_4^2a_5[\mathbf{A}_\mu^b(n_\mu, 0), \hat{\Delta}_\mu\mathbf{A}_5^b(n_\mu, 0)]\Bigg) \\
- \;& ig_4^3\Bigg\{\frac{a_4^2a_5}{2}[\mathbf{A}_\mu^b(n_\mu, 0), [\mathbf{A}_\mu^b(n_\mu, 0), \mathbf{A}_5^b(n_\mu, 0)]] + \frac{a_4a_5^2}{2}[\mathbf{A}_5^b(n_\mu, 0), [\mathbf{A}_\mu^b(n_\mu, 0), \mathbf{A}_5^b(n_\mu, 0)]]\Bigg\} + \mathcal{O}(a^4)\Bigg] \\
=\; & \exp\Bigg[ig_4\Bigg(a_4a_5\Bigg[\hat{\Delta}_\mu\mathbf{A}_5^b(n_\mu, 0) + ig_4[\mathbf{A}_\mu^b(n_\mu, 0), \mathbf{A}_5^b(n_\mu, 0)]\Bigg] \\
+ \;& \frac{a_4^2a_5}{2}\Bigg[\hat{\Delta}_\mu(\hat{\Delta}_\mu\mathbf{A}_5^b(n_\mu, 0)) + 2ig_4[\mathbf{A}_\mu^b(n_\mu, 0), \hat{\Delta}_\mu\mathbf{A}_5^b(n_\mu, 0)] - g_4^2[\mathbf{A}_\mu^b(n_\mu, 0), [\mathbf{A}_\mu^b(n_\mu, 0), \mathbf{A}_5^b(n_\mu, 0)]]\Bigg] \\
- \;& \frac{a_4a_5^2}{2}g_4^2[\mathbf{A}_5^b(n_\mu, 0), [\mathbf{A}_\mu^b(n_\mu, 0), \mathbf{A}_5^b(n_\mu, 0)]] + \mathcal{O}(a^4)\Bigg)\Bigg]\,,
\end{aligned} \tag{5.A.25}$$

and now each bracket in the last exponential includes terms of the same dimension. Actually this is not the end since there are some extra manipulations which will lead to an even more

simple relation for Eq. (5.A.25). In particular we can give up $(n_\mu, 0)$ from now on, since we are exclusively on the boundary, and do the following: The first bracket can be rewritten defining the hybrid field-strength $\mathbf{F}_{\mu 5}$ as

$$\mathbf{F}_{\mu 5} = \hat{\Delta}_\mu \mathbf{A}_5^b + i g_4 [\mathbf{A}_\mu^b, \mathbf{A}_5^b] \,.$$

Then the second bracket, after using the identity

$$\hat{\Delta}_\mu [\mathbf{A}_\mu^b, \mathbf{A}_5^b] = [\hat{\Delta}_\mu \mathbf{A}_\mu^b, \mathbf{A}_5^b] + [\mathbf{A}_\mu^b, \hat{\Delta}_\mu \mathbf{A}_5^b]$$

to rewrite one of the two $[\mathbf{A}_\mu^b, \hat{\Delta}_\mu \mathbf{A}_5^b]$ and collecting terms which form $\mathbf{F}_{\mu 5}$, reads

$$\hat{\mathbf{D}}_\mu \mathbf{F}_{\mu 5} - i g_4 [\hat{\Delta}_\mu \mathbf{A}_\mu^b, \mathbf{A}_5^b] \,,$$

with $\hat{\mathbf{D}}_\mu = \hat{\Delta}_\mu + i g_4 [\mathbf{A}_\mu^b,]$ the discretized version of the covariant derivative. In that sense Eq. (5.A.25) admits the final form

$$U_{\mu 5}^h = \exp\left[i g_4 \left(a_4 a_5 \mathbf{F}_{\mu 5} + \frac{a_4^2 a_5}{2} \hat{\mathbf{D}}_\mu \mathbf{F}_{\mu 5} - i \frac{g_4 a_4^2 a_5}{2} [\hat{\Delta}_\mu \mathbf{A}_\mu^b, \mathbf{A}_5^b] - \frac{g_4^2 a_4 a_5^2}{2} [\mathbf{A}_5^b, [\mathbf{A}_\mu^b, \mathbf{A}_5^b]] + \mathcal{O}(a^4) \right) \right] \tag{5.A.26}$$

and the next step is to insert the above relation in Eq. (5.A.20) and expand the exponential for small lattice-spacing. This is a path which needs caution since choosing to truncate the expansion at a specific order inherits the action with terms which do not respect the symmetries of the theory, in the same manner with the boundary action. In particular if we set $U_{\mu 5}^h$ back in Eq. (5.A.20), perform the trace and keep terms up to $\mathcal{O}(a^6)$, the hybrid action reads

$$\begin{aligned} S^h &= \sum_{n_\mu} a_4^4 \sum_\mu \Bigg((\overline{\hat{D}_\mu \phi}) \hat{D}_\mu \phi + \frac{a_4}{2} (\overline{\hat{D}_\mu \phi}) [\overline{\hat{D}_\mu} + \hat{D}_\mu] \hat{D}_\mu \phi + \frac{i g_4 a_4}{2} \hat{\Delta}_\mu A_\mu^3 [(\overline{\hat{D}_\mu \phi}) \phi - \bar{\phi} \hat{D}_\mu \phi] \\ &+ \frac{a_4^2}{4} (\overline{\hat{D}_\mu \hat{D}_\mu \phi}) \hat{D}_\mu \hat{D}_\mu \phi + \frac{g_4^2 a_4^2}{4} \bar{\phi} \phi (\hat{\Delta}_\mu A_\mu^3)^2 + i g 4 \frac{a_4^2}{4} \hat{\Delta}_\mu A_\mu^3 \Big[(\overline{\hat{D}_\mu \hat{D}_\mu \phi}) \phi - \bar{\phi} (\hat{D}_\mu \hat{D}_\mu \phi) \Big] \\ &+ \frac{a_5^2}{2} (\bar{\phi} \phi)^2 A_\mu^3 A_\mu^3 \Bigg) + \mathcal{O}(a^7) \,, \end{aligned} \tag{5.A.27}$$

defining first the lattice coupling $\beta_5 = 2N a_4^2 / a_5^2 g_4^2$ and in addition the complex scalar field $\phi = (A_5^1 + i A_5^2)/2$. Moreover the covariant derivative has been set as $\hat{D}_\mu = \hat{\Delta}_\mu - i g_4 A_\mu^3$. However, notice in Eq. (5.A.27) that the dimension-five and six operators, except from the case of $(\overline{\hat{D}_\mu \hat{D}_\mu \phi}) \hat{D}_\mu \hat{D}_\mu \phi$, lack of rotational and gauge invariance. Of course the situation is changed and symmetry restoration is achieved when someone keeps higher and higher order terms at the lattice-spacing expansion and the BCH formula. Nevertheless, at the expansion order of the current work these terms can be neglected without affecting the consistency of the theory. Therefore, the desired expression for the hybrid action yields

$$S^h = \sum_{n_\mu} a_4^4 \sum_\mu \left(|\hat{D}_\mu \phi|^2 + \frac{a_4^2}{4} |\hat{D}_\mu \hat{D}_\mu \phi|^2 \right) + \mathcal{O}(a^7)$$

$$= \sum_{n_\mu} a_4^4 \sum_\mu \left(|\hat{D}_\mu \phi|^2 + \frac{1}{4} \frac{|\hat{D}_\mu \hat{D}_\mu \phi|^2}{\mu^2} \right) + \mathcal{O}(a^7)\,, \tag{5.A.28}$$

where we have identified the remnant a_4 of the dim-6 operator as part of the regularization scale, $\mu \equiv \mu(a_4)$, in accordance with the pure boundary action. So now the combination of Eq. (5.A.19) and Eq. (5.A.28), according to Eq. (5.A.8), gives the boundary-hybrid action

$$S^{\mathrm{b-h}} = \sum_{n_\mu} a_4^4 \sum_\mu \left[\sum_\nu \left(\frac{1}{4} F^3_{\mu\nu} F^3_{\mu\nu} + \frac{1}{16} \frac{(\hat{\Delta}_\mu F^3_{\mu\nu})(\hat{\Delta}_\mu F^3_{\mu\nu})}{\mu^2} \right) + |\hat{D}_\mu \phi|^2 + \frac{1}{4} \frac{|\hat{D}_\mu \hat{D}_\mu \phi|^2}{\mu^2} \right], \tag{5.A.29}$$

where all the information of the anisotropy is hidden in the coupling between the fields. Recall that the boundary action includes g_4 which however is not an independent coupling since

$$g_4 = \frac{g_5}{\sqrt{a_{5,f}}} = \frac{g_5}{\sqrt{a_4}} \sqrt{\gamma} \equiv g\sqrt{\gamma} \tag{5.A.30}$$

with $g = \frac{g_5}{\sqrt{a_4}}$ a dimensionless coupling. Therefore, now the covariant derivative is expressed with the help of the new coupling as a function of the anisotropy and becomes $\hat{D}_\mu = \hat{\Delta}_\mu - ig\sqrt{\gamma} A^3_\mu$. Of course Eq. (5.A.29) is defined on the lattice and it can be useful only after considering the naive continuum limit according to Eq. (5.A.18). Nevertheless, before following this path we complete the picture constructing the bulk lattice action which will include terms coming from a higher order truncation of the lattice-spacing.

5.A.3 The Bulk action with higher order terms

Here the main ingredient is the pure bulk action, given by Eq. (5.A.9), which can be broken into a four-dimensional and a five-dimensional part. The former includes plaquettes which lie exclusively on the 4d bulk and reads

$$S^{4d} = \frac{1}{2N} \sum_{n_\mu, n_5} \beta_4 \sum_{\mu<\nu} \mathrm{tr} \left\{ 1 - U_{\mu\nu}(n_\mu, n_5) \right\}, \tag{5.A.31}$$

while the latter includes plaquettes with gauge links leaving on the full 5d bulk and reads

$$S^{5d} = \frac{1}{2N} \sum_{n_\mu, n_5} \beta_5 \sum_{\mu} \mathrm{tr} \left\{ 1 - U_{\mu 5}(n_\mu, n_5) \right\} \tag{5.A.32}$$

with $S^B = S^{4d} + S^{5d}$, $\beta_4 = 2Na_5/g_5^2$ and $\beta_5 = 2Na_4^2/a_5 g_5^2$. Notice that the two sets of couplings, $\{\beta_4', \beta_5'\}$ and $\{\beta_4, \beta_5\}$, are essentially the same except that in the bulk case a_5 is not an undetermined parameter any longer. An important difference between the boundary and bulk case is that the latter includes fields with mass dimension $[A_M] = 3/2$, with $M = \mu, 5$. This is a crucial fact regarding the calculations of the following sections. Now one of the arguments in [3] was that the actions S^{4d} and S^{5d}, at leading order, were 5d covariant so their sum reconstructed the 5d bulk action. Here the next-to-leading order is considered so there would be higher derivative terms in the action which do not allow us to expect the same conclusion regarding the covariance of Eq. (5.A.31) and Eq. (5.A.32). Actually if this is the case then the breaking

of the 5d covariance should be related with the existence of the anisotropy. Of course the above argument can be proved following the path of the previous section. For that purpose let us draw the calculation, without many details, starting from S^{4d} whose plaquette yields

$$\begin{aligned} U_{\mu\nu}(n_\mu, n_5) &= U(n_\mu, n_5; \mu)\, U(n_\mu + a_4\hat{\mu}, n_5; \nu)\, (U(n_\mu + a_4\hat{\nu}, n_5; \mu))^\dagger\, (U(n_\mu, n_5; \nu))^\dagger \\ &= e^{ia_4 g_5 \mathbf{A}_\mu(n_\mu, n_5)}\, e^{ia_4 g_5 \mathbf{A}_\nu(n_\mu + a_4\hat{\mu}, n_5)}\, e^{-ia_4 g_5 \mathbf{A}_\mu(n_\mu + a_4\hat{\nu}, n_5)}\, e^{-ia_4 g_5 \mathbf{A}_\nu(n_\mu, n_5)}\,, \end{aligned}$$

with $\mathbf{A}_\mu \equiv A^A_\mu T^A$. Then the algorithm that we follow suggests that the 4d bulk palquette is properly rewritten using the BCH formula. In particular we need Eq. (5.A.13) whose exponents here admit that

$$\begin{aligned} X &= ia_4 g_5 \mathbf{A}_\mu(n_\mu, n_5)\,,\ Y = ia_4 g_5 \mathbf{A}_\nu(n_\mu + a_4\hat{\mu}, n_5) \\ Z &= -ia_4 g_5 \mathbf{A}_\mu(n_\mu + a_4\hat{\nu}, n_5)\,,\ W = -ia_4 g_5 \mathbf{A}_\nu(n_\mu, n_5)\,. \end{aligned}$$

So now we employ the lattice-spacing expansion, at the next-to-next-to leading order in the expansion, exactly as we did for the boundary. In that sense, after collecting and massaging terms of the same dimension and keeping terms up to $\mathcal{O}(a_4^3)$, the plaquette becomes

$$\begin{aligned} U_{\mu\nu}(n_\mu, n_5) &= \exp\Bigg[ia_4^2 g_5 \mathbf{F}_{\mu\nu}(n_\mu, n_5) + \frac{ia_4^3 g_5}{2}\Big(\hat{\mathbf{D}}'_\mu \mathbf{F}_{\mu\nu}(n_\mu, n_5) + (\hat{\Delta}_\mu - \hat{\Delta}_\nu)\hat{\Delta}_\nu \mathbf{A}_\mu(n_\mu, n_5) \\ &+ ig_5[\mathbf{A}_\nu(n_\mu, n_5), \mathbf{F}_{\mu\nu}(n_\mu, n_5)] + ig_5[\mathbf{A}_\mu(n_\mu, n_5) - \mathbf{A}_\nu(n_\mu, n_5), \hat{\Delta}_\nu \mathbf{A}_\mu(n_\mu, n_5)]\Big) \\ &+ \mathcal{O}(a_4^4)\Bigg]\,, \end{aligned}$$

where we have defined

$$\mathbf{F}_{\mu\nu} \equiv F^A_{\mu\nu} T^A = \hat{\Delta}_\mu \mathbf{A}_\nu - \hat{\Delta}_\nu \mathbf{A}_\mu + ig_5[\mathbf{A}_\mu, \mathbf{A}_\nu] \ \text{ and } \ \hat{\mathbf{D}}'_\mu = \hat{\Delta}_\mu + ig_5[\mathbf{A}_\mu,]\,. \tag{5.A.33}$$

The final step of the calculation is to set $U_{\mu\nu}$ back in Eq. (5.A.31), expand, perform the trace and keep terms up to $\mathcal{O}(a_4^6)$. Keep in mind that we neglect terms which do not respect the symmetries of the theory, the lattice artifacts induced from the truncation, in the same manner with the previous section. Hence the 4d bulk action now reads[6]

$$S^{4d} = \sum_{n_\mu} a_4^4 \sum_{n_5} a_5 \sum_{\mu<\nu} \left(\frac{1}{4} F^A_{\mu\nu} F^A_{\mu\nu} + \frac{a_4^2}{16} (\hat{D}_\mu F^A_{\mu\nu})(\hat{D}_\mu F^A_{\mu\nu}) - a_4^2 \frac{g_5 f_{ABC}}{24} F^A_{\mu\nu} F^B_{\nu\rho} F^C_{\rho\mu} \right) + \mathcal{O}(a_4^7)\,, \tag{5.A.34}$$

[6]Notice that in principle the complete base of 7-dimensional terms includes also two more entries, that of $(\hat{D}_\mu F_{\nu\lambda})^2$ and $(\hat{D}_\mu F_{\mu\lambda})(\hat{D}_\nu F_{\nu\lambda})$. Nevertheless these are not independent since, using the Bianchi identity, they reduce to the already existing dim-7 terms of Eq. (5.A.34). Considering for example $(\hat{D}_\mu F_{\nu\lambda})^2$ where we can see through the Bianchi identity

$$\hat{D}_\mu F_{\nu\lambda} + \hat{D}_\nu F_{\lambda\mu} + \hat{D}_\lambda F_{\mu\nu} = 0$$

and the relation $[\hat{D}_\mu, \hat{D}_\nu] \equiv F_{\mu\nu}$ that

$$(\hat{D}_\mu F_{\nu\lambda})^2 \sim (\hat{D}_\mu F_{\mu\nu})^2 - F_{\mu\nu} F_{\nu\rho} F_{\rho\mu}\,.$$

This is the reason why the action that we get after the lattice spacing expansion does not include these redundant terms.

where a_4^2 has not been identified as the regulator μ^2 yet for reasons which will become clear in the following. The evaluation of the full bulk action ends with the determination of S^{5d}, which is given in Eq. (5.A.32). For that purpose the explicit form of the corresponding plaquette, $U_{\mu 5}$, is exploited and reads

$$\begin{aligned} U_{\mu 5}(n_\mu, n_5) &= U(n_\mu, n_5; \mu)\, U(n_\mu + a_4\hat{\mu}, n_5; 5)\, (U(n_\mu, n_5 + a_5\hat{5}; \mu))^\dagger\, (U(n_\mu, n_5; 5))^\dagger \\ &= e^{ia_4 g_5 \mathbf{A}_\mu(n_\mu, n_5)}\, e^{ia_5 g_5 \mathbf{A}_5(n_\mu + a_4\hat{\mu}, n_5)}\, e^{-ia_4 g_5 \mathbf{A}_\mu(n_\mu, n_5 + a_5\hat{5})}\, e^{-ia_5 g_5 \mathbf{A}_5(n_\mu, n_5)}\,, \end{aligned} \tag{5.A.35}$$

with the Lie element $\mathbf{A}_5 \equiv A_5^A T^A$. Similarly with the previous case the above relation can be rewritten using Eq. (5.A.13) but now for

$$\begin{aligned} X &= ia_4 g_5 \mathbf{A}_\mu(n_\mu, n_5)\,,\ Y = ia_5 g_5 \mathbf{A}_5(n_\mu + a_4\hat{\mu}, n_5) \\ Z &= -ia_4 g_5 \mathbf{A}_\mu(n_\mu, n_5 + a_5\hat{5})\,,\ W = -ia_5 g_5 \mathbf{A}_5(n_\mu, n_5)\,. \end{aligned}$$

Before we perform the lattice-spacing expansion and present the results for the action let us make a short comment. To begin note that $U_{\mu 5}$ is similar with the hybrid plaquette, given in Eq. (5.A.21), which was used in the boundary action. Nevertheless, this is a delicate point since the information that each of the two plaquettes includes is completely different and so we expect that the corresponding actions will not match. In particular $U_{\mu 5}$ includes only bulk fields whose mass dimension is different than the boundary fields, as we have already explained. In addition there is no need to respect any boundary conditions here since the corresponding gauge links live exclusively on the bulk and no dimensional reduction is implemented. Therefore Eq. (5.A.35) will contain terms which are forbidden on the boundary. With these in mind and after the expansion of the lattice spacings the desired plaquette becomes

$$\begin{aligned} U_{\mu 5}(n_\mu, n_5) &= \exp\Bigg[ia_4 a_5 g_5 \mathbf{F}_{\mu 5}(n_\mu, n_5) - ia_4 a_5 g_5 \hat{\mathbf{D}}_5 \mathbf{A}_\mu(n_\mu, n_5) - a_4 a_5 g_5^2 [\mathbf{A}_5(n_\mu, n_5), \mathbf{A}_\mu(n_\mu, n_5)] \\ &+ \frac{ia_4^2 a_5 g_5}{2} \hat{\mathbf{D}}'_\mu \mathbf{F}_{\mu 5}(n_\mu, n_5) + \frac{a_4^2 a_5 g_5^2}{2} [\hat{\Delta}_\mu \mathbf{A}_\mu(n_\mu, n_5), \mathbf{A}_5(n_\mu, n_5)] \\ &- \frac{ia_4 a_5^2 g_5}{2} \hat{\mathbf{D}}_5 (\hat{\mathbf{D}}_5 \mathbf{A}_\mu(n_\mu, n_5)) - \frac{a_4 a_5^2 g_5^2}{2} [\hat{\Delta}_5 \mathbf{A}_5(n_\mu, n_5), \mathbf{A}_\mu(n_\mu, n_5)] + \mathcal{O}(a^4)\Bigg]\,, \end{aligned}$$

where we have collected and massaged terms of the same dimension. In addition we kept terms up to $\mathcal{O}(a^3) \equiv \mathcal{O}(a_4^3, a_5^3)$, as we did for the hybrid action, while we defined that

$$\mathbf{F}_{\mu 5} = \hat{\Delta}_\mu \mathbf{A}_5 + ig_5[\mathbf{A}_\mu, \mathbf{A}_5] \ \text{ and } \ \hat{\mathbf{D}}_5 = \hat{\Delta}_5 + ig_5[\mathbf{A}_5,]\,.$$

Finally the last step is to set $U_{\mu 5}$ back to Eq. (5.A.32) which, after considering the trace, reads

$$S^{5d} = \sum_{n_\mu} a_4^4 \sum_{n_5} a_5 \sum_\mu \left(\frac{1}{4} F_{\mu 5}^A F_{\mu 5}^A + \frac{a_4^2}{16} (\hat{D}_\mu F_{\mu 5}^A)(\hat{D}_\mu F_{\mu 5}^A) - ia_4 a_5 \frac{g_5}{6} \mathrm{tr}\,\{F_{\mu 5}^3\} \right) + \mathcal{O}(a^7)\,, \tag{5.A.36}$$

where only terms up to dimension 7 have been kept while we neglected as usual those which do not respect the symmetries of the theory. The calculation of the bulk action is almost done

since the only thing left is to add S^{4d} and S^{5d} so as to form S^B. Nevertheless there is a tricky point here which should be clarified. To be more specific both Eq. (5.A.34) and Eq. (5.A.36) lack of regularization scale in contrast with the boundary case. In the latter recall that the leftover lattice-spacing for each higher-order term was the only available physical scale, a_4, which regularized the theory. On the other hand S^B is defined on the full 5d orbifold lattice and because of the anisotropy there are two physical scales, a_4 and a_5, which both participate in the regularization game. Nevertheless, these two scales depend upon each other through the anisotropy factor γ so there is some freedom left to choose one of them so as to regularize both actions. Hence if a_4 is chosen then both S^{4d} and S^{5d} inherit the scale $\mu \equiv \mu(a_4)$ while the anisotropy enters only in the latter action. With the above in our mind S^{4d} and S^{5d} become

$$S^{4d} = \sum_{n_\mu} a_4^4 \sum_{n_5} a_5 \sum_{\mu<\nu} \left(\frac{1}{4} F^A_{\mu\nu} F^A_{\mu\nu} + \frac{1}{16} \frac{(\hat{D}_\mu F^A_{\mu\nu})(\hat{D}_\mu F^A_{\mu\nu})}{\mu^2} - \frac{g_5 f_{ABC}}{24} \frac{F^A_{\mu\nu} F^B_{\nu\rho} F^C_{\rho\mu}}{\mu^2} \right)$$

and

$$S^{5d} = \sum_{n_\mu} a_4^4 \sum_{n_5} a_5 \sum_{\mu} \left(\frac{1}{4} F^A_{\mu 5} F^A_{\mu 5} + \frac{1}{16} \frac{(\hat{D}_\mu F^A_{\mu 5})(\hat{D}_\mu F^A_{\mu 5})}{\mu^2} - i \frac{g_5}{6} \frac{\mathrm{tr}\,\{F^3_{\mu 5}\}}{\gamma \mu^2} \right)$$

respectively, with $\hat{D}_\mu$ the $SU(2)$ covariant derivative. Indeed the above reflects that due to the anisotropy the 5d covariance of the theory is broken, already at the classical level, when all the higher-order terms, at the truncation level that we work, are taken into account. In particular, responsible for the breaking are only the F^3 terms since all the rest restore the covariance in accordance with [3]. There is no clear evidence why the breaking of the 5d covariance becomes obvious only when the cubic HDO appears while this is not true regarding the quadratic one. Answering that question is beyond the scope of the current work, however there is a chance to have a glance at the solution through the quantization of the bulk action. Now there are two possible ways to describe the corresponding quantum effects. The first one is to consider S^{5d} as an adjoint-scalar action, so then S^B will correspond to a 5d cartoon-version of the Lee-Wick(LW) model[7] which has extensively been studied. The second one is to take advantage of the lattice periodicity so as to compactify the fifth dimension. This step allows us to rewrite S^{5d} introducing the Kaluza-Klein states into the spectrum. However, since the 5d covariance is broken, the most profitable way to describe the system is through the LW approach. In that sense after recalculating Eq. (5.A.36) we arrive, regarding the bulk action, at the following result

$$\begin{aligned} S^B \;=\; & \sum_{n_\mu} a_4^4 \sum_{n_5} a_5 \sum_{\mu} \Bigg[\sum_{\nu} \Big(\frac{1}{4} F^A_{\mu\nu} F^A_{\mu\nu} + \frac{1}{16\mu^2} (\hat{D}_\mu F^A_{\mu\nu})(\hat{D}_\mu F^A_{\mu\nu}) - \frac{g_5}{24\mu^2} f_{ABC} F^A_{\mu\nu} F^B_{\nu\rho} F^C_{\rho\mu} \Big) \\ & + \; (\overline{\hat{D}_\mu \Phi^A})(\hat{D}_\mu \Phi^A) + \frac{1}{4\mu^2} (\overline{\hat{D}^2 \Phi^A})(\hat{D}^2 \Phi^A) \Bigg] \end{aligned} \tag{5.A.37}$$

where the capital Φ^A corresponds to a scalar doublet given by

$$\Phi^A = \begin{pmatrix} \frac{A^1_5 + i A^2_5}{2} \\ \frac{A^3_5}{2} \end{pmatrix} \equiv \begin{pmatrix} \phi \\ \phi^0 \end{pmatrix} \tag{5.A.38}$$

[7] An extensive analysis of higher-derivative Yang-Mills theories coupled to an adjoint-scalar or spinor matter Lagrangian can be found at [24, 25, 26, 27, 28] and references therein.

while ϕ corresponds exactly to the scalar d.o.f which leaves at the boundary. Moreover notice that the cubic term $F^3_{\mu 5}$ is absent, after considering the trace, a fact that seems to be characteristic of the Lee-Wick description which is exploited here. As a last comment we emphasize the fact that Eq. (5.A.37) is not the most general 5d LW theory which can be made. This becomes obvious looking at the interacting terms which all of them depend on the same coupling g_5. In addition, even though S^B seems like a 4d LW model and $\sum a_5$ seems irrelevant, A^A_μ and Φ^A are both functions of the anisotropic dimension, n_5. Actually this is characteristic of the 5d orbifold lattice where the fields correspond to different components of the original 5d gauge field A^A_M.

5.B Field redefinition and gauge invariance

There are several ways to perform a field redefinition but not all of them lead to an expression which respects the symmetries of the theory, especially when gauge symmetry is present. Here the derivation of the appropriate conditions so as to get a gauge invariant and consistent theory after a field redefinition is at work. Some useful and relevant comments in this respect are given in [34]. Here we present a self contained discussion of the issue with some additional comments. We focus on the Boundary-Hybrid action, Eq. (5.2.4) that corresponds to a particular version of SQED so we are concerned about the proper way to redefine the Abelian-gauge theory while respecting gauge invariance. We perform an analysis showing the criteria which the proper field redefinition should fulfill. We recall that, according to [33, 30], the Jacobean after the field redefinition plays a crucial role since renders a theory with O-ghosts consistent. This happens with the insertion of the R-ghosts in the spectrum and therefore they should also enter in a gauge-invariant manner.

Let us begin the analysis with the path-integral of Eq. (5.2.4) in the absence of sources

$$\mathcal{Z}[0] = \int \mathcal{D}A\mathcal{D}\bar{\phi}\mathcal{D}\phi\, e^{iS[A,\bar{\phi},\phi]}\,, \qquad S[A,\bar{\phi},\phi] \equiv S[A^3_\mu,\bar{\phi},\phi] = \int d^4x\, \mathcal{L}[A^3_\mu,\bar{\phi},\phi] = S^{\rm b-h}\,,$$

where A stands for the $U(1)$ gauge field A^3_μ. In the following both notations are used interchangeably. In the presence of sources the terms $J\,\phi$, $J\,\bar{\phi}$ and $J\,A^3_\mu$ should also be properly transformed, otherwise the S-matrix can not be kept unchanged. If we perform a finite gauge transformation to the path-integral through

$$\phi' = V(x)\phi\,,\;\; \bar{\phi}' = \bar{\phi}\bar{V}(x) \;\text{ and }\; A' = V(x)(A + \frac{1}{g_4}\partial)\bar{V}(x)\,, \tag{5.B.1}$$

with $V(x) = e^{i\alpha(x)}$ and $\bar{V}(x) = e^{-i\alpha(x)} = V^{-1}(x)$, then we get

$$\begin{aligned}\mathcal{Z}'[0] &= \int \mathcal{D}A'\mathcal{D}\bar{\phi}'\mathcal{D}\phi'\, e^{iS'[A',\bar{\phi}',\phi']} \\ &= \int \mathcal{D}A\mathcal{D}\bar{\phi}\mathcal{D}\phi \left|\frac{dA'}{dA}\right| \left|\frac{d\bar{\phi}'}{d\bar{\phi}}\right| \left|\frac{d\phi'}{d\phi}\right| e^{iS[A,\bar{\phi},\phi]} \\ &= \mathcal{Z}[0]\,.\end{aligned} \tag{5.B.2}$$

The action is by definition gauge invariant while the functional measure inherits the Jacobeans. For the transformation of Eq. (5.B.1) these are however trivial and the l.h.s matches the original

partition function. The question is how can this argument be combined with our intention to redefine the fields. To see this, we perform a general field redefinition of the form

$$\begin{aligned} \phi &\rightarrow \hat{\phi} = \phi + \frac{x}{\Lambda^2} F_\phi(\phi) \\ A^3_\mu &\rightarrow \hat{A}^3_\mu = A^3_\mu + \frac{x_\alpha}{\Lambda^2} F_{A,\mu}(A^3_\mu) \end{aligned} \tag{5.B.3}$$

and after that gauge transform the path-integral so as to see whether it will stay invariant. Let us forget for a moment about the gauge field and deal only with the complex scalar. We apply the first of Eq. (5.B.3) to the path-integral $\mathcal{Z}[0]$ to get

$$\begin{aligned} \hat{\mathcal{Z}}[0] &= \int \mathcal{D}A\mathcal{D}\bar{\hat{\phi}}\mathcal{D}\hat{\phi}\, e^{iS[A,\bar{\hat{\phi}},\hat{\phi}]} \\ &= \int \mathcal{D}A\mathcal{D}\bar{\phi}\mathcal{D}\phi \left|\frac{d\bar{\hat{\phi}}}{d\bar{\phi}}\right| \left|\frac{d\hat{\phi}}{d\phi}\right| e^{iS[A,\bar{\hat{\phi}},\hat{\phi}]}\,, \end{aligned} \tag{5.B.4}$$

where now the Jacobeans are not trivial and they must be accounted for. Since everything is valid up to total derivatives there is a freedom in the choice of the independent field variables after the redefinition. We can fix this gauge by demanding pole cancellation[8] between the O- and R-ghosts. This is the diagonal gauge so the Jacobeans are diagonal matrices with determinant

$$\begin{aligned} D(\phi) &= \det\left[\frac{d\hat{\phi}}{d\phi}\right] = \left(1 + \frac{x}{\Lambda^2}\frac{dF_\phi(\phi)}{d\phi}\right)^\beta \simeq 1 + \frac{\beta x}{\Lambda^2}\frac{dF_\phi(\phi)}{d\phi} \\ \overline{D(\phi)} &= \det\left[\frac{d\bar{\hat{\phi}}}{d\bar{\phi}}\right] = \left(1 + \frac{x}{\Lambda^2}\overline{\left[\frac{dF_\phi(\phi)}{d\phi}\right]}\right)^\beta \simeq 1 + \frac{\beta x}{\Lambda^2}\overline{\left[\frac{dF_\phi(\phi)}{d\phi}\right]} \end{aligned} \tag{5.B.5}$$

where only terms up to $\mathcal{O}(1/\Lambda^2)$ have been kept. β refers to the dimension of the Jacobean matrices. Therefore the product of the determinants in Eq. (5.B.4) would read

$$\overline{D(\phi)}D(\phi) \equiv 1 + \frac{\beta x}{\Lambda^2}\frac{dF_\phi(\phi)}{d\phi} + \frac{\beta x}{\Lambda^2}\overline{\left[\frac{dF_\phi(\phi)}{d\phi}\right]} = D(\bar{\phi},\phi)\,, \tag{5.B.6}$$

indicating that the R-ghost should be given by the path-integral of the form

$$D(\bar{\phi},\phi) = \int \mathcal{D}\bar{\chi}\mathcal{D}\chi\, e^{-i\int d^4x \bar{\chi} D(\bar{\phi},\phi)\chi}\,.$$

Combining now Eq. (5.B.4) with the above relation the resulting path-integral reads

$$\begin{aligned} \mathcal{Z}[0] &= \int \mathcal{D}A\mathcal{D}\bar{\phi}\mathcal{D}\phi\mathcal{D}\bar{\chi}\mathcal{D}\chi\, e^{iS[A,\bar{\phi}+\frac{x}{\Lambda^2}\overline{F_\phi(\phi)},\,\phi+\frac{x}{\Lambda^2}F_\phi(\phi)] - i\int d^4x\bar{\chi}D(\bar{\phi},\phi)\chi} \\ &= \int \mathcal{D}A\mathcal{D}\bar{\phi}\mathcal{D}\phi\mathcal{D}\bar{\chi}\mathcal{D}\chi\, e^{iS[A,\bar{\phi}+\frac{x}{\Lambda^2}\overline{F_\phi(\phi)},\,\phi+\frac{x}{\Lambda^2}F_\phi(\phi)] + iS_R(\bar{\chi},\chi)}\,, \end{aligned} \tag{5.B.7}$$

where we have defined the action of the scalar R-ghost through

$$S_R(\bar{\chi},\chi) = -\int d^4x \bar{\chi} D(\bar{\phi},\phi)\chi\,.$$

[8] See [30] for more details.

There are two more steps that we should take. The first is to expand the action with respect to F_ϕ, $\overline{F}_\phi$ and the second is to gauge transform the result. However, before we get into this note that for $S_R(\bar{\chi},\chi)$ to contribute to the pole cancelation, the R-ghost should be charged under the $U(1)$ group. Then after a gauge transformation also the ghost action should be invariant. As a consequence, since χ transforms as $\chi \to \chi' = V(x)\chi$, the operator $D(\bar{\phi},\phi)$ should let the transformation pass through it showing that $D'(\bar{\phi},\phi)\chi' = V(x)D(\bar{\phi},\phi)\chi$ and more importantly that F_ϕ is gauge covariant. In particular the gauge transformation of the scalar field in Eq. (5.B.3) gives that

$$F'_\phi(\phi') = V(x)F_\phi(\phi) \quad \text{and} \quad \overline{F'_\phi(\phi')} = \overline{F_\phi(\phi)}V^{-1}(x)$$

rendering, indeed, F_ϕ a covariant operator which is in the same representation with ϕ. Let us now return to our algorithm and expand the action in Eq. (5.B.7) to get

$$\mathcal{Z}[0] = \int \mathcal{D}A\mathcal{D}\bar{\phi}\mathcal{D}\phi\mathcal{D}\bar{\chi}\mathcal{D}\chi \, \exp\Big[i\sum_{m,n=0}^{\infty}\frac{x^{m+n}}{\Lambda^{2(m+n)}(m+n)!}\overline{F_\phi^m}F_\phi^n\frac{\delta^{(m+n)}S[A,\bar{\phi},\,\phi]}{(\delta\bar{\phi})^m(\delta\phi)^n} + iS_R(\bar{\chi},\chi)\Big]\,, \tag{5.B.8}$$

which then is gauge transformed to

$$\begin{aligned}\mathcal{Z}'[0] &= \int \mathcal{D}A\mathcal{D}\bar{\phi}\mathcal{D}\phi\mathcal{D}\bar{\chi}\mathcal{D}\chi \, \exp\Big[i\sum_{m,n=0}^{\infty}\frac{x^{m+n}}{\Lambda^{2(m+n)}(m+n)!}\overline{(F'_\phi)^m}(F'_\phi)^n\frac{\delta^{(m+n)}S[A,\bar{\phi},\,\phi]}{(\delta\bar{\phi}')^m(\delta\phi')^n} + iS_R(\bar{\chi},\chi)\Big] \\ &= \mathcal{Z}[0]\,.\end{aligned}$$

The actions $S[A,\bar{\phi},\,\phi]$, $S_R(\bar{\chi},\chi)$ and the functional integrals are invariant, as it was shown above, so the gauge covariance of F_ϕ makes the partition function gauge invariant. Following the same strategy for the redefinition of the gauge field leads to the same outcome indicating that the path-integral is manifestly gauge invariant under proper field redefinition. To be more specific we sketch the calculation starting with Eq. (5.B.8) where we use Eq. (5.B.3) to redefine A^3_μ. In that sense the path-integral yields

$$\begin{aligned}\mathcal{Z}[0] &= \int \mathcal{D}\hat{A}\mathcal{D}\bar{\phi}\mathcal{D}\phi\mathcal{D}\bar{\chi}\mathcal{D}\chi \, \exp\Big[i\sum_{m,n=0}^{\infty}\frac{x^{m+n}}{\Lambda^{2(m+n)}(m+n)!}\overline{F_\phi^m}F_\phi^n\frac{\delta^{(m+n)}S[\hat{A}^3_\mu,\bar{\phi},\,\phi]}{(\delta\bar{\phi})^m(\delta\phi)^n} + iS_R(\bar{\chi},\chi)\Big] \\ &= \int \mathcal{D}A\left|\frac{d\hat{A}}{dA}\right|\mathcal{D}\bar{\phi}\mathcal{D}\phi\mathcal{D}\bar{\chi}\mathcal{D}\chi \, \exp\Big[i\sum_{m,n=0}^{\infty}\frac{x^{m+n}}{\Lambda^{2(m+n)}(m+n)!}\overline{F_\phi^m}F_\phi^n\frac{\delta^{(m+n)}S[A^3_\mu + \frac{x_\alpha}{\Lambda^2}F_{A,\mu},\bar{\phi},\,\phi]}{(\delta\bar{\phi})^m(\delta\phi)^n} \\ &+ iS_R(\bar{\chi},\chi)\Big]\end{aligned} \tag{5.B.9}$$

and the Jacobean, keeping in mind the pole cancelation condition also for the gauge field, is a diagonal matrix with determinant

$$D^{\mu\nu}(A^3_\mu) = \det\left[\frac{d\hat{A}^3_\mu}{dA^3_\nu}\right] = \left(\delta^{\mu\nu} + \frac{x_\alpha}{\Lambda^2}\frac{dF_{A,\mu}(A^3_\mu)}{dA^3_\nu}\right)^{\beta'} \equiv \delta^{\mu\nu} + \frac{\beta' x_\alpha}{\Lambda^2}\frac{dF_{A,\mu}(A^3_\mu)}{dA^3_\nu}\,, \tag{5.B.10}$$

where β' indicates the dimension of the Jacobean matrix. Again we have kept terms up to $\mathcal{O}(1/\Lambda^2)$. The generated R-ghost for A^3_μ is defined as $B \equiv B^3_\mu$ and it is inserted in the path-integral by the relation

$$D^{\mu\nu}(A^3_\mu) = \int \mathcal{D}B\, e^{-i\int d^4x B^3_\mu D^{\mu\nu}(A^3_\mu)B^3_\nu}$$

leading to

$$\begin{aligned}\mathcal{Z}[0] &= \int \mathcal{D}A\mathcal{D}\bar{\phi}\mathcal{D}\phi\mathcal{D}\bar{\chi}\mathcal{D}\chi\mathcal{D}B\,\exp\Big[i\sum_{m,n=0}^{\infty}\frac{x^{m+n}}{\Lambda^{2(m+n)}(m+n)!}\overline{F_\phi^m}F_\phi^n\frac{\delta^{(m+n)}S[A_\mu^3+\frac{x_\alpha}{\Lambda^2}F_{A,\mu},\bar{\phi},\,\phi]}{(\delta\bar{\phi})^m(\delta\phi)^n}\\ &+ iS_R(\bar{\chi},\chi)+iS_R(B)\Big]\,, \end{aligned}\tag{5.B.11}$$

with

$$S_R(B) = -\int d^4x B_\mu^3 D^{\mu\nu}(A)B_\nu^3 \equiv \int d^4x B_{\mu\nu}B^{\mu\nu}\,.$$

Here $S_R(B)$ as well as $D^{\mu\nu}(A_\mu^3)$ should be invariant under gauge transformations which is also true for $F_{A,\mu}(A_\mu^3)$ since the gauge field is Abelian. If the gauge group is non-Abelian then the corresponding $F_{A,\mu}$ should be a gauge covariant operator in the same representation with the associated gauge field. Finally we expand around A_μ^3 and gauge transform Eq. (5.B.11) to get

$$\begin{aligned}\mathcal{Z}'[0] &= \int \mathcal{D}A\mathcal{D}\bar{\phi}\mathcal{D}\phi\mathcal{D}\bar{\chi}\mathcal{D}\chi\mathcal{D}B\,\exp\Big[i\sum_{m,n,p=0}^{\infty}\frac{x^{m+n}x_\alpha^p}{\Lambda^{2(m+n+p)}(m+n+p)!}\overline{F_\phi^m}F_\phi^n(F_A')^p\frac{\delta^{(m+n+p)}S[A,\bar{\phi},\,\phi]}{(\delta\bar{\phi})^m(\delta\phi)^n(\delta A')^p}\\ &+ iS_R(\bar{\chi},\chi)+iS_R(B)\Big]\\ &= \mathcal{Z}[0]\end{aligned}$$

which shows that using the proper field redefinitions a gauge invariant and, due to the pole cancelation at work, O-ghost-free path-integral can be constructed yielding

$$\mathcal{Z}[0] = \int \mathcal{D}A\mathcal{D}\bar{\phi}\mathcal{D}\phi\mathcal{D}\bar{\chi}\mathcal{D}\chi\mathcal{D}B\,e^{iS[\hat{A},\hat{\bar{\phi}},\hat{\phi}]+iS_R(\bar{\chi},\chi)+iS_R(B)}\,.\tag{5.B.12}$$

Note that specifically for our case an appropriate choice, regarding F_ϕ and $F_{A,\mu}$, is the following

$$F_\phi(\phi) = \frac{x}{\Lambda^2}D^\mu D_\mu\phi + \frac{y}{\Lambda^2}(\bar{\phi}\phi)\phi \quad\text{and}\quad F_{A,\mu}(A_\mu^3) = \frac{x_\alpha}{\Lambda^2}(\eta_{\mu\nu}\Box - \partial_\mu\partial_\nu)A^{3,\nu}\,,\tag{5.B.13}$$

with D_μ the usual covariant derivative and x, y, x_α yet undefined parameters.

5.C Feynman Rules for the Boundary-Hybrid action

In this Appendix the derivation of the Feynman rules for the field-redefined Boundary-Hybrid action, Eq. (5.2.11), is in order. The procedure that we follow is the usual one keeping in mind that we split the action into its kinetic and interaction part. Let us start with the former which after the redefinition reads

$$S_{\text{Kin},0}^{\text{b-h}} = \int d^4x\left[-\frac{1}{4}F_{\mu\nu,0}^3F_0^{3,\mu\nu} + \frac{1}{2\xi}A_{\mu,0}^3\partial^\mu\partial_\nu A_0^{3,\nu} - \bar{\phi}_0\Box\phi_0 - \bar{c}_0^3\Box c_0^3\right]\tag{5.C.1}$$

while using the fact that $F_{\mu\nu,0}^3 = \partial_\mu A_{\mu,0}^3 - \partial_\nu A_{\nu,0}^3$ and performing some massaging becomes

$$S_{\text{Kin},0}^{\text{b-h}} = \int d^4x\left[-\frac{1}{4}\Big(\partial_\mu A_{\nu,0}^3 - \partial_\nu A_{\mu,0}^3\Big)\Big(\partial^\mu A_0^{3,\nu} - \partial^\nu A_0^{3,\mu}\Big) + \frac{1}{2\xi}A_{\mu,0}^3\partial^\mu\partial_\nu A_0^{3,\nu} - \bar{\phi}_0\Box\phi_0 - \bar{c}_0^3\Box c_0^3\right]$$

$$
\begin{aligned}
&= \int d^4x \int d^4y \delta_{xy} \Bigg[-\frac{1}{4}\Big(\partial_\mu A^3_{\nu,0}(x) - \partial_\nu A^3_{\mu,0}(x)\Big)\Big(\partial^\mu A_0^{3,\nu}(y) - \partial^\nu A_0^{3,\mu}(y)\Big) + \frac{1}{2\xi} A^3_{\mu,0}(x)\partial^\mu \partial_\nu A_0^{3,\nu}(y) \\
&- \bar{\phi}_0(x)\Box\phi_0(y) - \bar{c}^3_0(x)\Box c^3_0(y)\Bigg] \\
&= \int d^4x \int d^4y \delta_{xy} \Bigg[\frac{1}{2} A^3_{\mu,0}(x)\Big(\eta^{\mu\nu}\Box_y + (\frac{1}{\xi} - 1)\partial^\mu_y \partial^\nu_y\Big) A^3_{\nu,0}(y) - \bar{\phi}_0(x)\Box_y \phi_0(y) - \bar{c}^3_0(x)\Box_y c^3_0(y)\Bigg] .
\end{aligned}
\tag{5.C.2}
$$

The next step is to Fourier transform to momentum space using that

$$
A^3_\mu(x) = \int \frac{d^4p}{(2\pi)^4} A^3_\mu(p) e^{-ip\cdot x} \,, \quad \phi_0(x) = \int \frac{d^4p}{(2\pi)^4} \phi_0(p) e^{-ip\cdot x} \tag{5.C.3}
$$

so the above equation returns the following

$$
\begin{aligned}
S^{\text{b-h}}_{\text{Kin},0} &= \int d^4x \int d^4y \frac{d^4p}{(2\pi)^4}\frac{d^4q}{(2\pi)^4} \delta_{xy} e^{-ip\cdot x} \Bigg[\frac{1}{2} A^3_{\mu,0}(p)\Big(\eta^{\mu\nu}\Box_y + (\frac{1}{\xi} - 1)\partial^\mu_y \partial^\nu_y\Big) e^{-iq\cdot y} A^3_{\nu,0}(q) \\
&- \bar{\phi}_0(p)\Box_y e^{-iq\cdot y}\phi_0(q) - \bar{c}^3_0(p)\Box_y e^{-iq\cdot y} c^3_0(q)\Bigg] \\
&= \int \frac{d^4p}{(2\pi)^4} \Bigg[\frac{1}{2} A^3_{\mu,0}(p)\Big(-\eta^{\mu\nu}p^2 + (1 - \frac{1}{\xi})p^\mu p^\nu\Big) A^3_{\nu,0}(-p) + \bar{\phi}_0(p) p^2 \phi_0(-p) - \bar{c}^3_0(p) p^2 c^3_0(-p)\Bigg] \\
&= \int \frac{d^4p}{(2\pi)^4} \Bigg[\frac{1}{2} A^3_{\mu,0}(p) M_A^{\mu\nu} A^3_{\nu,0}(-p) + \bar{\phi}_0(p) M_\phi \phi_0(-p) - \bar{c}^3_0(p) M_c c^3_0(-p)\Bigg]
\end{aligned}
\tag{5.C.4}
$$

where we have used that $\int d^4x \int d^4y \delta_{xy} e^{-ip\cdot x} e^{-iq\cdot y} = \int d^4x e^{-i(p+q)\cdot x} = (2\pi)^4 \int d^4x \delta(p+q)$. Then we used the δ-function to eliminate the q-integral setting $q = -p$ and defined the matrices $M_A^{\mu\nu} = -\eta^{\mu\nu}p^2 + (1 - \frac{1}{\xi})p^\mu p^\nu$, $M_\phi = p^2$ and $M_c = p^2$. So inverting the above matrices we end up with the corresponding propagators. Finally the Feynman rules for the interaction part of Eq. (5.2.11) will be in our hand after performing the Fourier transform given in Eq. (5.C.3) and calculating the various partial derivatives. Hence, collectively, the Feynman rules that S^{b-h} generates are:

- Gauge Propagator

$$
= \frac{i}{q^2}\Big(-\eta_{\mu\nu} + (1-\xi)\frac{q_\mu q_\nu}{q^2}\Big)
$$

- Scalar Propagator

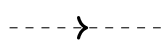

$$
= \frac{i}{p^2}
$$

- Scalar-Scalar-gauge vertex

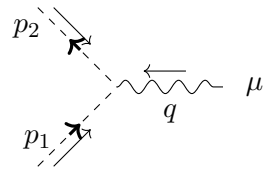

$$= ig_{4,0} Q_\mu(p,q)\,.$$

- Four-point self interaction vertex

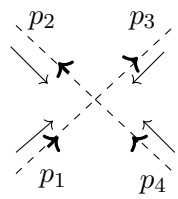

$$= ic^{(6)}_{1,0}\frac{p^2}{\Lambda^2}\,.$$

- Scalar-Scalar-gauge-gauge vertex

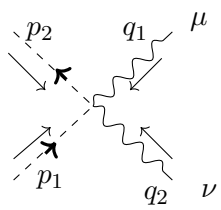

$$= \quad 2ig^2_{4,0} Q_{\mu\nu}(p,q)\,.$$

- Four-scalars one-photon vertex

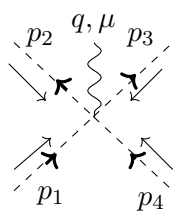

$$= ig_{4,0}\, c^{(6)}_{1,0}\frac{(p_1+p_2)_\mu}{\Lambda^2}\,.$$

- Four-scalars two-photons vertex

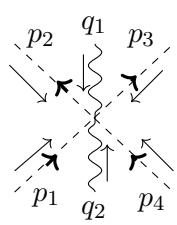

$$= 2ig^2_{4,0}\frac{c^{(6)}_{1,0}}{\Lambda^2}\eta_{\mu\nu}\,,$$

where we have used the p's and q's for the scalar-field and the gauge-field momenta respectively and in particular p_1 corresponds to ϕ while p_2 to $\bar{\phi}$. Moreover we have define the functions

$$\begin{aligned} Q_\mu(p,q) &= (\eta_{\mu\nu} + \frac{\eta_{\mu\nu}q^2 - q_\mu q_\nu}{\Lambda^2})(p_1+p_2)^\nu \\ Q_{\mu\nu}(p,q) &= \eta_{\mu\nu} + \frac{\eta_{\mu\nu}p_1\cdot p_2 + q_{1,\mu}(p_{2,\nu}-p_{1,\nu})}{2\Lambda^2} + \frac{2(\eta_{\mu\nu}q_1^2 - q_{1,\mu}q_{1,\nu})}{\Lambda^2} \end{aligned} \tag{5.C.5}$$

while notice that the propagator of the Faddeev-Popov ghosts is absent here since they are completely decoupled from the theory. A final comment is that the diagram which includes four scalar-fields and one photon-field will not contribute at the 1-loop renormalization of the theory.

5.D Review of the Coleman-Weinberg model

This part of the Appendix works as a short review of the main characteristics of the Coleman-Weinberg model [13]. The way that it is constructed follows the calculation conducted at Section 5.3.1 so as to elucidate the differences between the physical results of the Boundary-Hybrid model, Eq. (5.2.11), and that of the CW model. The analysis here is interested in the part of [13] which refers to the mSQED whose effective potential and scalar-to-gauge mass ratio have been analytically evaluated.

Let us start with the fact that all the calculations along with the regularization of the CW model are performed exclusively at $d = 4$ dimensions. On the other hand, recall that our strategy here is to keep the dimensions arbitrary and specify only when this is necessary.

Regarding the renormalization program notice that in [13], even though the model of interest is massless, a counter-term for both the mass term and the scalar-field is in use. According to the authors this is a legal step since there is no symmetry preventing the production of a bare mass in the limit of vanishing renormalized mass. Actually, as they mention, there is scale symmetry at work but they do not pay much attention to that since, in general, it could be anomalous. Therefore they brake it already at the classical level using their mass counter-term. Recall that this was not the path that we followed here where we introduced a counterterm for the scalar field but not for the mass term. The reason for that is hidden behind our intention to show how the breaking of scale invariance, inserting the HDO at quantum level, is connected with the spontaneous breaking of the internal symmetry.

Now the loop calculation of the CW model is done, at 1-loop level, through the effective action which led to the determination of the effective potential. In particular the renormalization of the model using the above arguments gives the effective potential

$$V_{CW} = \frac{\lambda}{4!}\phi_c^4 + \Big(\frac{5\lambda^2}{1152\pi^2} + \frac{3e^4}{64\pi^2}\Big)\phi_c^4\Big(\ln\frac{\phi_c^2}{M^2} - \frac{25}{6}\Big)\,, \tag{5.D.1}$$

where $\phi_c^2 \equiv \bar{\phi}\phi$ while λ and e correspond to the quartic and gauge coupling respectively. According to [13] this effective potential has a local minimum away from the origin which is made clear by supposing that λ and e^4 share the same order of magnitude. This claim, connecting the two couplings, seems a little bit suspicious at the CW analysis while it follows as a natural implementation regarding the Boundary-Hybrid model developed here. Notice however that the authors show the validity of the SSB through radiative corrections for arbitrary, but still small, couplings.

Then, the minimization condition of Eq. (5.D.1), neglecting the terms proportional to λ^2, indicates that

$$\lambda = \frac{33}{8\pi^2}e^4 \tag{5.D.2}$$

and therefore the effective potential now becomes

$$V_{CW} = \frac{3e^4}{64\pi^2}\,\phi_c^4\Big(\ln\frac{\phi_c^2}{\langle\phi\rangle^2} - \frac{1}{2}\Big)\,, \tag{5.D.3}$$

with $\langle\phi\rangle$ the vacuum expectation value of ϕ_c. Keep in mind that during the above procedure the number of the independent parameters stays fixed. In particular the explicit form of V_{CW} depends on two parameters, λ and e, which is also true for the potential of Eq. (5.D.3) but now the parameters are e and $\langle\phi\rangle$. This was defined by the authors as dimensional transmutation.

Since SSB does occur the authors sift the field ϕ_c around its vev which inherits the scalar field with the mass

$$m^2(S) = \frac{3}{8\pi^2} e^4 \langle\phi\rangle^2 \tag{5.D.4}$$

and the gauge field with the mass

$$m^2(V) = e^2 \langle\phi\rangle^2 \tag{5.D.5}$$

at leading loop order. Then the scalar-to-gauge mass ration is constructed and given by

$$\begin{aligned} \frac{m^2(S)}{m^2(V)} \equiv \rho_{CW}^2 &= \frac{3}{8\pi^2} e^2 \Rightarrow \\ \rho_{CW} &= \sqrt{\frac{3}{8\pi^2}} e \,. \end{aligned} \tag{5.D.6}$$

Finally, notice that in [13] the authors act with the Callan-Symanzik equation on the fourth derivative of the effective potential Eq. (5.D.1) and on the wave function renormalization. Then a system of equations is constructed through which the scalar-field anomalous dimension and the β-functions of e and λ are evaluated and give

$$\gamma = \frac{3e^2}{16\pi^2} \tag{5.D.7}$$

$$\beta_e = \frac{e^3}{48\pi^2} \quad \text{or} \quad \beta_{\alpha_e} = \frac{2\alpha_e^2}{3} \tag{5.D.8}$$

$$\beta_\lambda = \frac{\frac{10}{3}\lambda^2 - 12\lambda e^2 + 36 e^4}{16\pi^2} \tag{5.D.9}$$

respectively. Recall that the calculations are performed in $d = 4$, so the above results represent the loop-part of the corresponding β-functions.

Bibliography

[1] F. Englert and R. Brout, Phys. Rev. Lett. **13** (1964) 321-323.
P. W. Higgs, Phys. Lett. **12** (1964) 132-133.

[2] P. W. Higgs, Phys. Rev. Lett. **13** (1964) 508-509.

[3] N. Irges and F. Koutroulis, Nucl. Phys. B **937** (2018) 135-195.

[4] N. Irges, F. Knechtli, Nucl. Phys. B **719** (2005) 12.

[5] N. Irges, F. Knechtli, arXiv:hep-lat/0604006.

[6] N. Irges, F. Knechtli, Nucl. Phys. B **775** (2007) 283.

[7] N. Irges, F. Knechtli and K. Yoneyama Nucl. Phys. B **722** (2013) 378-383.

[8] M. Ostrogradsky, Mem. Ac. St. Petersb. VI **4** (1850) 385; R.P. Woodard, Scholarpedia **10** (8) (2015) 32243.

[9] R. S. Chivukula, A. Farzinnia, R. Foadi and E. H. Simmons, Phys. Rev. D **82** (2010) 035015.

[10] N. Irges and F. Knechtli, JHEP **06** (2014) 070.

[11] M. Alberti, N. Irges, F. Knechtli and G. Moir, JHEP **09** (2015) 159.

[12] M. Günter, R. Höllwieser and F. Knechtli, Comput. Phys. Commun. 254 (2020), 107192.

[13] S. R. Coleman, E. J. Weinberg, Phys. Rev. D **7** (1973) 1888-1910.

[14] N. Irges, PoS CORFU2016 (2016), 039.

[15] N. Irges, PoS CORFU2017 (2018), 080.

[16] Recent works include H. Patel and M. J. R-Musolf, JHEP, **1107** (2011) 029.
J. E. Miro, J. R. Espinosa, G. F. Guidice, G. Isidori and A. Riotto, Phys. Lett. B **709** (2012) 222-228.
G. Degrassi, J. E. Miro, J. R. Espinosa, G. F. Guidice, G. Isidori, A. Strumia, JHEP 1208 (2012) 098, arXiv:1205.6497.
J. R. Espinosa, M. Garny and A. Riotto, arXiv:1608.06765.
D. Buttazzo, G. Degrassi, P. P. Giardino, G. F. Guidice, A. Salvio and A. Strumia, JHEP,

1312 (2013) 089.
L. Di Luzio and L. Mihaila, JHEP, **1406** (2014) 079.
Z. Lalak, M. Lewicky and P. Olszewski, Phys. Rev. D **94** (2016) 085028.B. W. Lynn and G. D. Starkman, arXiv:1509.06471.
O. Gungor, B. W. Lynn and G. D. Starkman, arXiv:1701.05949.

[17] A. Andreassen, W. Frost and M. D. Schwartz, Phys. Rev. D **91** (2015) 121604, arXiv: 1408.0287.

[18] S. Weinberg, Phys. Rev. Lett. **27** (1971) 1688-1691.

[19] A nice example is the renormalization of the linear sigma model in M. E. Peskin and D. V. Schroeder *An Introduction to Quantum Field Theory*, Reading, USA: Addison-Wesley (1995) 842p.

[20] S. Ejiri, J. Kubo and M. Murata, Phys. Rev. D **62** (2000) 105025. S. Ejiri, S. Fujimoto and J. Kubo, Phys. Rev. D **66** (2002) 036002. P. de Forcrand, A. Kurkela and M. Panero, JHEP **1006** (2010) 050. K. Farakos and S. Vrentzos, Nucl. Phys. B **862** (2012) 633-649. F. Knechtli, M. Luz and A. Rago, Nucl. Phys. B **856** (2012) 74-94. F. Knechtli and E. Rinaldi, Int. J. Mod. Phys. A **31** (2016) no.22, 1643002.

[21] P. Weisz, Nucl. Phys. B **212** (1983) 1-17.

[22] M. Luscher, P. Weisz, Commim. Math. Phys. **97** (1985) 59-77.

[23] Nikos Irges, Fotis Koutroulis and Dimosthenis Theofilopoulos, arXiv: 2001.07171 [hep-th]

[24] E. Fradkin and A. Tseytlin, Phys. Lett. B **104** (1981) no. 5, 377-381.

[25] B. Grinstein, D. O'Connell and M. B. Wise, Phys. Rev. D **77** (2008) 025012.

[26] B. Grinstein and D. O'Connell, Phys. Rev. D **78** (2008) 105005.

[27] T. Schuster, http://qft.physik.hu-berlin.de.

[28] L. Casarin, arXiv: 1710.08021 [hep-th].

[29] Y. Fu, H. B. Nielsen, Nucl. Phys. B **236** (1984) 167.

[30] N. Irges and F. Koutroulis, Nucl. Phys. B **950** (2020) 114833.

[31] N. Irges and F. Koutroulis, Nucl. Phys. B **924** (2017) 178.

[32] E. Itou, K. Kashiwa and N. Nakamoto, arXiv:1403.6277v1 [hep-lat].

[33] N. Irges and F. Koutroulis, Phys. Rev. D **100**, 065004 (2019).

[34] J. C. Criado, M. Perez-Victoria, JHEP **03** (2019) 038

[35] S. H. Tye and Y. Vtorov-Karevsky, Int. J. Mod. Phys. A **13** (1998) 173-182.

[36] Benjamin W. Lee, Phys. Rev. D **5** (1972) 823.

[37] C. Becchi, A. Rouet, R. Stora, Commun.Math.Phys. **42** (1975) 127-162.

[38] W. J. Marciano, C. Zhang and S. Willenbrock, Phys. Rev. D **85** (2012) 013002.

[39] F. Jegerlehner, arXiv:1110.0869.

[40] A. Dedes and K. Suxho, Adv. High Energy Phys. 2013 (2013) 631841.

[41] T. T. Wu and S. L. Wu, Nucl. Phys. B **914** (2017) 421-445.

[42] H. Sonoda, hep-th/0108217.

[43] For example see the thesis: A. Rodigast, Dipl. Phys. Humboldt U. Berlin, 2007.

[44] G. 't Hooft and M. J. G. Veltman, Nucl. Phys. B **44** (1972) 189-213.

[45] G. Passarino and M. J. G. Veltman, Nucl. Phys. B **160** (1979) 151-207.

[46] R. K. Ellis, Z. Kunszt, K. Melnikov and G. Zanderighi, arXiv:1105.4319v4.

[47] S. P. Martin, Phys. Rev. D **90** (2014) 016013.

[48] E. H. Fradkin and S. H. Shenker, Phys. Rev. D **19** (1979) 3682-3697.
D. J. E. Callaway and L. J. Carson, Phys. Rev. D **25** (1982) 531-537.
H. G. Evertz, V. Grosch, K. Jansen, J. Jersak, H. A. Kastrup and T. Neuhaus, Nucl. Phys. B **285** (1987) 559.

[49] S. Khodayari, Master's Thesis, U. Wuppertal, Oct. 2016.

[50] M. Lüscher and P. Weisz, Phys. Lett. B **349** (1995) 165-169.

[51] M. Alberti, N. Irges, F. Knechtli and G. Moir, JHEP **1509** (2015) 159.

[52] Y. Fu and H. B. Nielsen, Nucl. Phys. B **236** (1984) 167.

[53] D. J. Gross, F. Wilczek, Phys. Rev. Lett. **30** (1973) 1343-1346. H. D. Politzer, Phys. Rev. Lett. **30** 1346 (1973).

[54] M. E. Peskin, Phys. Lett. B **94** (1980) 161.

[55] T. R. Morris, JHEP **0501** (2005) 002.

[56] There is an extensive literature on this. For gauge theories in higher dimensions see for example:

H. Gies, Phys. Rev. D **68** (2003) 085015. D. I. Kazakov, JHEP **0303** (2003) 020. A. Codello, K. LangYble, D. F. Litim and F. Sannino, JHEP **1607** (2016) 118 and references therein.

[57] G. von Gersdorff, N. Irges and M. Quiros, Nucl. Phys. B **635** (2002) 127-157.

[58] A. Salam, Phys. Rev. **86** (1952) 5.

[59] M. Creutz, Phys. Rev. Lett. **43** (1979) 553-556, Erratum: Phys. Rev. Lett. **43** (1979) 890.

[60] N. Irges, G. Koutsoumbas and K. Ntrekis, Phys. Rev. D **92** (2015) no.9, 094506.

[61] K. Ishiyama, M. Murata and H. So, Prog. Theor. Phys. **123** (2010) 257-269.

[62] M. Schwartz, Cambridge University Press, 2014.

[63] S. Coleman and R. Jackiw, Annals of Physics **67**, 552-598 (1971).

[64] N. Irges, F. Knechtli and K. Yoneyama, Nucl. Phys. B **865** (2012) 541-567. N. Irges, F. Knechtli and K. Yoneyama, Phys. Lett. B **722** (2013) 378-383.

[65] S. Elitzur, Phys. Rev. D **12** (1975), 3978

[66] T. J. Hollowood, *Renormalization Group and Fixed Points in Quantum Filed Theory*

[67] W. Buchmuller, D. Wyler, Nucl. Phys. B **268** (1986) 621-653. B. Grzadkowski, M. Iskrzynski, M. Misiak, J. Rosiek, JHEP 10 (2010) 085.

[68] M. B. Einhorn and J. Wudka, JHEP **08**, (2001), 025

[69] M. Buchler and G. Colangelo, Eur. Phys. J. C **32**,(2004), 427-442. E.E. Jenkins, A.V. Manohar, M. Trott JHEP **10**, (2013), 087. E. E. Jenkins, A. V. Manohar, and M. Trott, [hep-ph/1310.4838]. R. Alonso, E.E. Jenkins, A.V. Manohar, M. Trott JHEP **04**, (2014), 159. I. Brivio and M. Trott, JHEP **07**, (2017), 148. A. Dedes, W. Materkowska, M. Paraskevas, J. Rosiek, K. Suxho JHEP **06**, (2017), 143. A. Dedes, M. Paraskevas, J. Rosiek, K. Suxho and L. Trifyllis, JHEP **08**, (2018), 103. A. Dedes, K. Suxho and L. Trifyllis, JHEP **06**, (2019), 115

[70] see for example A. V. Manohar, [hep-ph/1804.05863].

[71] see for example M. Neubert, [hep-ph/1901.06573v1].

[72] T. J. Hollowood, Springer Briefs in Physics, (2013).

[73] A. Bilal, Lecture notes, Brussels (2014). M. Serone, SISSA via Bonomea 265, I-34136, Trieste, Italy (2017).

[74] G. 't Hooft, M.J.G. Veltman, NATO Sci.Ser. B**4** (1974), 177-322. A. R. Chowdhury and T. Roy, Phys. Rev. D**15** (1977) no8, 2186. K. Hagiwara, S. Ishihara, R. Szalapski, D. Zeppenfeld, Phys. Rev. D**48** (1993) 2182-2203. C. Arzt, Phys. Lett. B **342** (1995) 189. F. Goertz, Phys. Rev. D**94**, (2016) 015013. S. Nagy, J. Polonyi and I. Steib, Phys. Rev. D**97** (2018), 085002. M. Safari and G. P. Vacca, Phys. Rev. D**97** (2018) no4, 041701. G. Passarino, [hep-ph/1901.04177]. R. Trinchero, [hep-th/1904.01616].

[75] A. Adams, N. A-Hamed, S. Dubovsky, A. Nicolis, R. Rattazzi, JHEP **0610**, (2006) 014.

[76] D. Anselmi, Eur. Phys. J. C **73**, (2013) 2338.

[77] S. Chang and M. A. Luty, [hep-ph/1902.05556v1].